

Chemical Abundances for 855 Giants in the Globular Cluster Omega Centauri (NGC 5139)

Christian I. Johnson^{1,2,3} and Catherine A. Pilachowski^{1,3}

ABSTRACT

We present elemental abundances for 855 red giant branch (RGB) stars in the globular cluster Omega Centauri (ω Cen) from spectra obtained with the Blanco 4m telescope and Hydra multifiber spectrograph. The sample includes nearly all RGB stars brighter than $V=13.5$, and spans ω Cen's full metallicity range. The heavy α elements (Si, Ca, and Ti) are generally enhanced by $\sim+0.3$ dex, and exhibit a metallicity dependent morphology that may be attributed to mass and metallicity dependent Type II supernova (SN) yields. The heavy α and Fe–peak abundances suggest minimal contributions from Type Ia SNe. The light elements (O, Na, and Al) exhibit >0.5 dex abundance dispersions at all metallicities, and a majority of stars with $[Fe/H]>-1.6$ have $[O/Fe]$, $[Na/Fe]$, and $[Al/Fe]$ abundances similar to those in monometallic globular clusters, as well as O–Na, O–Al anticorrelations and the Na–Al correlation in all but the most metal-rich stars. A combination of pollution from intermediate mass asymptotic giant branch (AGB) stars and *in situ* mixing may explain the light element abundance patterns. A large fraction (27%) of ω Cen stars are O–poor ($[O/Fe]<0$) and are preferentially located within $5\text{--}10'$ of the cluster center. The O–poor giants are spatially similar, located in the same metallicity range, and are present in nearly equal proportions to blue main sequence stars. This suggests the O–poor giants and blue main sequence stars may share a common origin. $[La/Fe]$ increases sharply at $[Fe/H]\gtrsim-1.6$, and the $[La/Eu]$ ratios indicate the increase is due to almost pure s–process production.

Subject headings: stars: abundances, globular clusters: general, globular clusters: individual (ω Centauri, NGC 5139), stars: Population II

¹Department of Astronomy, Indiana University, Swain West 319, 727 East Third Street, Bloomington, IN 47405–7105, USA; cijohnson@astro.ucla.edu; catyp@astro.indiana.edu

²Department of Physics and Astronomy, University of California, Los Angeles, 430 Portola Plaza, Box 951547, Los Angeles, CA 90095–1547, USA

³Visiting astronomer, Cerro Tololo Inter–American Observatory, National Optical Astronomy Observatory, which are operated by the Association of Universities for Research in Astronomy, under contract with the National Science Foundation.

1. INTRODUCTION

For many years, globular clusters were regarded as prototypical simple stellar populations. However, recent observations have revealed that several of the most massive known globular clusters contain multiple main sequence, subgiant, and/or red giant branch (RGB) populations (Piotto et al. 2007; Marino et al. 2008; Milone et al. 2008; Anderson et al. 2009; Moretti et al. 2009; Piotto 2009; Milone et al. 2010). These data, combined with the well-known and pervasive light element abundance correlations and anticorrelations that appear to be unique to the globular cluster environment, suggest that many, if not all, globular clusters undergo at least some degree of self-enrichment (e.g., Carretta et al. 2009a). While nearly all of these clusters exhibit small ($\lesssim 0.1$ dex) star-to-star metallicity variations (e.g., see review by Gratton et al. 2004), Omega Centauri (ω Cen) has long been known to exhibit both a complex color-magnitude diagram and a metallicity spread of more than a factor of ten.

Early color-magnitude diagrams of ω Cen indicated that it hosts an unusually broad RGB (e.g., Woolley 1966; Cannon & Stobie 1973). Subsequent photometric surveys have discovered that this trend continues into both the main sequence and subgiant branch regions as well (Anderson et al. 1997; Lee et al. 1999; Hilker & Richtler 2000; Hughes & Wallerstein et al. 2000; Pancino et al. 2000; van Leeuwen et al. 2000; Bedin et al. 2004; Ferraro et al. 2004; Rey et al. 2004; Sollima et al. 2005; Castellani et al. 2007; Sollima et al. 2007; Villanova et al. 2007; Bellini et al. 2009a; Calamida et al. 2009). Additionally, detailed photometric and spectroscopic analyses have shown that at least 4–5 discrete populations are present in the cluster (Norris et al. 1996; Lee et al. 1999; Hilker & Richtler 2000; Pancino et al. 2000; Bedin et al. 2004; Rey et al. 2004; Sollima et al. 2005; Castellani et al. 2007; Villanova et al. 2007; Johnson et al. 2008; Bellini et al. 2009a,b; Calamida et al. 2009; Johnson et al. 2009; Marino et al. 2010). These individual populations span a metallicity range from $[Fe/H]^1 \approx -2.2$ to -0.5 . However, few stars are found with $[Fe/H] < -2$, and more than half of ω Cen’s stars reside in a population peaked near $[Fe/H] \approx -1.7$ (Norris & Da Costa 1995; Suntzeff & Kraft 1996; Hilker & Richtler 2000; Smith et al. 2000; Cunha et al. 2002; Sollima et al. 2005; Kayser et al. 2006; Stanford et al. 2006; Villanova et al. 2007; Johnson et al. 2008; Calamida et al. 2009; Johnson et al. 2009; Marino et al. 2010). The rest of the stars reside in the intermediate metallicity populations, and a minority ($\lesssim 5\%$) of stars are found to lie along the “anomalous”, metal-rich sequence (Lee et al. 1999; Pancino et al. 2000; Ferraro et al. 2004; Sollima et al. 2005; Villanova et al. 2007).

¹We make use of the standard spectroscopic notations where $[A/B] \equiv \log(N_A/N_B)_{\text{star}} - \log(N_A/N_B)_{\odot}$ and $\log \epsilon(A) \equiv \log(N_A/N_H) + 12.0$ for elements A and B.

The large metallicity spread in ω Cen is commonly believed to be due to significant self-enrichment induced by multiple star formation episodes (e.g., Ikuta & Arimoto 2000; Tsujimoto & Shigeyama 2003; Marcolini et al. 2007; Romano et al. 2007, 2010). Despite being the most massive known cluster in the Galaxy, with an estimated mass of $\sim 2\text{--}7 \times 10^6 M_\odot$ (Mandushev et al. 1991; Richer et al. 1991; Meylan et al. 1995; van de Ven et al. 2006), Gnedin et al. (2002) showed that ω Cen does not currently possess an abnormally deep gravitational potential well. Additionally, the cluster’s Galactic orbit indicates that it should pass through the disk at least every $1\text{--}2 \times 10^8$ years (Dinescu et al. 1999). This makes it hard to believe that ω Cen could have experienced the 2–4 Gyr period of star formation that seems required to fit observations of the main sequence turnoff (e.g., Stanford et al. 2006). However, the cluster’s retrograde motion through the Galaxy (Dinescu et al. 1999) suggests that it may be a captured system and therefore could have been more massive in the past. In fact, the most popular scenario is that ω Cen, and perhaps several other globular clusters containing multiple populations, are the remnant cores of tidally disrupted dwarf galaxies (e.g., Dinescu et al. 1999; Majewski et al. 2000; Smith et al. 2000; Gnedin et al. 2002; McWilliam & Smecker-Hane 2005; Bekki & Norris 2006). This is now favored over an accretion or merger scenario because the individual stellar populations within ω Cen all exhibit the same proper motion, rotation, and average radial velocity (e.g., Pancino et al. 2007; Bellini et al. 2009a).

Although the observed evolutionary sequences have now been mostly matched to the different populations derived from spectroscopy, one of the remaining puzzles is how these populations relate to ω Cen’s bifurcated main sequence. The discovery that ω Cen’s main sequence splits into a red and blue sequence over a span of at least two magnitudes (e.g., Anderson 1997; Bedin et al. 2004) is difficult to explain because the blue main sequence is more metal-rich than the red main sequence (Piotto et al. 2005). A possible explanation for this is that the blue main sequence stars are selectively enhanced in helium at $Y \sim 0.38$ (e.g., Norris 2004; Piotto et al. 2005). While the source of the proposed helium enrichment is not clear, the leading candidate appears to be intermediate mass ($\sim 3\text{--}8 M_\odot$) asymptotic giant branch (AGB) stars with perhaps some contribution from massive, rapidly rotating main sequence stars (e.g., Renzini 2008; Romano et al. 2010). Interestingly, the blue main sequence stars appear to be preferentially located near the cluster core (Sollima et al. 2007; Bellini et al. 2009b), which is an indication that He-rich material may have collected there at some point in the cluster’s evolution. A similar radial segregation near the core has been found for stars with $[\text{Fe}/\text{H}] \gtrsim -1.2$, but the more metal-poor stars appear to be rather uniformly distributed across the cluster (Suntzeff & Kraft 1996; Norris et al. 1997; Hilker & Richtler 2000; Pancino 2000; Rey 2004; Johnson et al. 2008; Bellini et al. 2009b; Johnson et al. 2009). It is worth noting that helium enrichment may also play a role in determining the

chemical composition of stars in monometallic globular clusters (e.g., Bragaglia et al. 2010).

ω Cen shows clear signs of extended star formation and chemical self-enrichment, and the large abundance dispersion is not limited to just the Fe-peak elements. Instead, the [X/H] ratios for all elements analyzed so far are found to vary by at least a factor of ten as well (e.g., Cohen 1981; Paltoglou & Norris 1989; Norris & Da Costa 1995; Smith et al. 2000; Cunha et al. 2002; Johnson et al. 2009; Villanova et al. 2009; Cunha et al. 2010; Stanford et al. 2010). Despite the current interpretation that ω Cen may be the surviving core of a disrupted dwarf galaxy, the [X/Fe] abundance ratios for the light elements (O, Na, Mg, and Al) and heavy α elements (Si, Ca, and Ti) more closely resemble the patterns found in individual globular clusters. These patterns include the O–Na, O–Al, and Mg–Al anticorrelations concurrent with the Na–Al correlation and consistently supersolar [α /Fe] ratios (e.g., Norris & Da Costa 1995; Smith et al. 2000; Johnson et al. 2009). This suggests that both Type II supernovae (SNe) and the products of proton–capture nucleosynthesis have played a significant role in shaping ω Cen’s chemical enrichment. However, the abundance patterns of neutron–capture elements in ω Cen stars with $[Fe/H] \gtrsim -1.5$ indicate that the slow neutron–capture process (s–process) was also a dominant production mechanism. This strongly contradicts the trends found in other globular clusters, and is instead more similar to observations of dwarf galaxies (e.g., see reviews by Venn et al. 2004; Geisler et al. 2007). While dwarf galaxies also contain many s–process enhanced stars, the low [X/Fe] ratios for the light and especially α elements suggests a significant contribution from Type Ia SNe. In contrast, the enhanced [α /Fe] ratios, high [Na/Fe] and [Al/Fe] abundances, and low [Cu/Fe] ratios seem to indicate that Type Ia SNe have played only a minimal role in ω Cen. However, Type Ia SNe may have contributed in the most metal–rich stars, as is evidenced by a potential downturn in [α /Fe] and rise in [Cu/Fe] at $[Fe/H] > -1$ (Pancino et al. 2002; Origlia et al. 2003; but see also Cunha et al. 2002).

In this paper we have obtained a nearly complete sample that includes 855 RGB stars and covers ω Cen’s full metallicity range down to $V=13.5$. We present new chemical abundance measurements of several light odd-Z, α , Fe-peak, and neutron–capture elements, and compare these results with abundance trends found in the Galactic disk, halo, bulge, globular cluster, and nearby dwarf galaxy populations. We also compare the abundance patterns found for the different ω Cen populations in an effort to understand the cluster’s formation and chemical enrichment history.

2. OBSERVATIONS AND REDUCTIONS

The observations for this project were taken at the Cerro Tololo Inter-American Observatory (CTIO) using the Blanco 4m telescope equipped with the Hydra multifiber positioner and bench spectrograph. We obtained all of the spectra in two separate runs spanning 24–28 March 2008 and 6–8 March 2009. We employed two different wavelength setups encompassing \sim 6135–6365 and \sim 6500–6800 Å with wavelength centers near 6250 and 6670 Å, respectively. This required the use of two separate order blocking filters for each echelle spectrograph setup. The red setup centered near 6670 Å used the echelle filter #6 (E6757); however, neither the echelle filter #7 nor #8 provides sufficient transmissivity over the bluer region spanning 6135–6365 Å. Since a primary goal of this project is to obtain both oxygen and sodium abundances from the 6300 Å [O I] line and 6154/6160 Å Na I lines, we purchased a new, single-piece echelle filter (E6257²) that provides >75% transmissivity from \sim 6135–6365 Å and allowed for the simultaneous observation of both the oxygen and sodium lines. For both setups, the “large” 300 μ m (2'') fibers combined with the 400 mm Bench Schmidt Camera and 316 line mm⁻¹ echelle grating to yield a resolving power of $R(\lambda/\Delta\lambda)\approx 18,000$ (0.35 Å FWHM). A summary of the Hydra observations is provided in Table 1.

Photometry, coordinates, and membership probabilities for all stars were taken from the proper motion study by van Leeuwen et al. (2000). We targeted stars with $V\leq 13.5$ and $0.70\leq B-V\leq 1.85$ while excluding those with membership probabilities below 70%. Field stars located along ω Cen’s line-of-sight are easily removed due to the cluster’s comparatively large radial velocity and small velocity dispersion ($\langle V_R \rangle \sim 232$ km s⁻¹; $\sigma \sim 10$ km s⁻¹; e.g., Reijns et al. 2006; Sollima et al. 2009). The magnitude and color restrictions provide a balance between maximizing the signal-to-noise ratio (S/N) of observations and limiting the number of required Hydra configurations. At $V=13.5$, one can obtain a $S/N\approx 100$ after three hours of integration. This luminosity cutoff also allows for the observation of all giant branches in ω Cen, and is at least 1 mag. below the RGB tip of the most metal-rich stellar population (see Figure 1).

In order to limit the number of repeat observations, stars were given a low priority in the Hydra assignment code following their inclusion into a Hydra configuration, and stars were completely removed from the fiber assignment process if incorporated into two Hydra configurations. The total number of fibers assigned to objects ranged from 50–110, and the co-added S/N ratio for almost all stars extended from about 100 to more than 350. The full sample obtained for this project is shown in Figure 1 along with the non-repeat stars from our previous papers on the cluster.

²This filter is on long-term loan at CTIO and available for public use.

The complexity of ω Cen’s color–magnitude diagram requires a large sample of stars to fully interpret its chemical history. Therefore, we have obtained a nearly 100% complete sample of RGB members with $V \leq 13.0$ and achieved more than 75% completion for $V \leq 13.5$. Since ω Cen exhibits a moderate radial metallicity gradient (Norris et al. 1996; Suntzeff & Kraft 1996; Norris et al. 1997; Hilker & Richtler 2000; Pancino et al. 2000; Rey et al. 2004; Johnson et al. 2008; Bellini et al. 2009b; Johnson et al. 2009), we targeted stars spanning a wide range of cluster radii. Figure 2 shows the observed completion fraction in terms of V magnitude, $B-V$ color, and distance from the cluster center, and Figure 3 illustrates the spatial location of our sample relative to the cluster center. For $V \leq 13.0$, $B-V > 1.1$, and $10' < D < 24'$, the completion fraction exceeds 0.90. However, the completion fraction for the inner $10'$ of the cluster ranges from 0.52–0.90. The decrease is due to both stellar crowding near the cluster core and physical limitations on fiber placement. Despite the large sample size, a modest evolutionary selection effect is present because the most metal–rich stars have both lower V magnitudes and tend to be located closer to the cluster center. Therefore, we have only observed stars along the most metal–rich giant branch that are within ~ 1 mag. of the RGB tip.

Data reduction was handled using the necessary tasks provided in standard IRAF³ packages. We used *ccdproc* to trim the overscan region and apply the bias level correction. However, the majority of the data reduction process was carried out with the *dohydra* package, which was used to trace the fiber locations on the detector, remove scattered light, apply the flat–field correction, identify lines in the ThAr comparison spectrum, apply the wavelength calibration, remove cosmic rays, subtract the background sky spectra, and extract the one–dimensional spectra. The reduction processes were identical for both the 6250 and 6750 Å data with the exception of the wavelength calibration. A problem with the calibration lamp during the 6750 Å observations meant that we had to use a high S/N, daylight solar spectrum for wavelength calibration instead of the ThAr comparison source.

Following completion of the *dohydra* task, the data were continuum fit and normalized before being corrected for telluric contamination. We obtained high S/N spectra of multiple bright, rapidly rotating B–stars spanning air masses ranging from 1.05 to 1.75. These spectra were used as the templates for removing the telluric features in the 6270–6350 Å window. Fortunately, the cluster’s radial velocity corresponds to a wavelength shift of roughly +4.8 Å. This moves the 6300 Å [O I] stellar absorption line away from the telluric emission feature at 6300 Å, and places it cleanly between the 6302 and 6306 Å telluric absorption doublets. After

³IRAF is distributed by the National Optical Astronomy Observatories, which are operated by the Association of Universities for Research in Astronomy, Inc., under cooperative agreement with the National Science Foundation.

applying the telluric correction, the spectra were then co-added to remove any remaining cosmic rays and increase the S/N.

3. Analysis

3.1. Model Stellar Atmospheres

Effective temperatures (T_{eff}) were determined via the empirical V–K color–temperature relation from Alonso et al. (1999, 2001; their equations 8 & 9), which is based on the infrared flux method (Blackwell & Shallis 1977). The V magnitudes were taken from van Leeuwen et al. (2000) and the K magnitudes were taken from the Two Micron All Sky Survey (2MASS; Skrutskie et al. 2006) database⁴. All photometry was corrected for interstellar reddening and extinction using the recommended values of $E(B-V)=0.12$ (Harris 1996) and $E(V-K)/E(B-V)=2.70$ (McCall 2004). While there is some evidence for minor differential reddening near the cluster’s core (Cannon & Strobie 1973; Calamida et al. 2005; van Loon et al. 2007; McDonald et al. 2009), the well-defined evolutionary sequences observed in the photometry by Villanova et al. (2007) seem to suggest that differential reddening is not a major issue. Therefore, we have applied a uniform reddening correction that is independent of a star’s location in the cluster. Although our data set did not contain enough Fe I lines of varying excitation potential to strongly constrain T_{eff} via excitation equilibrium, we did not find any strong, systematic trends in plots of Fe I abundance versus excitation potential. It is likely that our photometric temperatures are accurate to within the roughly 25–50 K uncertainty range given by the Alonso et al. (1999) empirical fits.

Surface gravity ($\log g$) estimates were obtained using the photometric temperatures and absolute bolometric magnitudes (M_{bol}). The bolometric corrections were taken from Alonso et al. (1999; their equations 17 and 18) and applied to the absolute visual magnitudes (M_V), which assumed a distance modulus of $(m-M)_V=13.7$ (van de Ven et al. 2006). Final surface gravity values were calculated with the standard relation,

$$\log(g_*) = 0.40(M_{\text{bol}} - M_{\text{bol},\odot}) + \log(g_\odot) + 4[\log(T/T_\odot)] + \log(M/M_\odot), \quad (1)$$

and assumed stellar mass of $0.80 M_\odot$. However, the likely age spread of $\sim 2\text{--}4$ Gyr (e.g., Stanford et al. 2006) among the stars in different populations means that a mass spread among RGB stars undoubtedly exists as well. This is further complicated by the inferred existence of a helium-rich population (Bedin et al. 2004; Norris 2004; Piotto et al. 2005) in

⁴The 2MASS catalog can be accessed online at: <http://irsa.ipac.caltech.edu/applications/Gator/>.

which stars will evolve more rapidly. When one also includes “contamination” of first ascent RGB stars with AGB stars, which could account for as much as 20–40% of the RGB above the horizontal branch (e.g., Norris et al. 1996), it is not unreasonable to assume ω Cen giants will have a mass range spanning $\sim 0.60\text{--}0.80 M_{\odot}$. Fortunately, the surface gravity estimates scale with $\log(M)$ and are thus relatively insensitive to small changes in the assumed stellar mass. We estimate that the uncertainty introduced into our surface gravity values due to the inherent mass range on ω Cen’s RGB does not exceed $\Delta \log g = 0.15$. Comparison between the abundances of elements in different ionization states seems to substantiate this with $\langle [\text{FeI}/\text{H}] - [\text{FeII}/\text{H}] \rangle = -0.09$ ($\sigma = 0.10$) and $\langle [\text{ScI}/\text{Fe}] - [\text{ScII}/\text{Fe}] \rangle = -0.18$ ($\sigma = 0.21$). We provide a more detailed analysis regarding how surface gravity uncertainties affect abundance ratio determinations in §3.3.

In addition to effective temperature and surface gravity, metallicity and microturbulence (v_t) information are required to generate a suitable 1-D model atmosphere. For an initial metallicity estimate, we used the empirical [Ca/H] calibration provided by van Leeuwen et al. (2000; their equation 15) with the assumptions that stars with $[\text{Fe}/\text{H}] < -1$ have $[\text{Ca}/\text{Fe}] = +0.30$ and those with $[\text{Fe}/\text{H}] > -1$ decline to $[\text{Ca}/\text{Fe}] = 0$ at solar metallicity. This assumption is verified in our new [Ca/Fe] data (see §4.6). An initial microturbulence value was determined from the empirical $v_t - T_{\text{eff}}$ relation given in Johnson et al. (2008; their equation 2). The initial T_{eff} , $\log g$, $[\text{Fe}/\text{H}]$, and v_t values were used to generate the necessary model atmospheres via interpolation within the available ATLAS9⁵ grid. The final determination of all microturbulence values followed the prescription outlined by Magain (1984) in which the microturbulence was adjusted until trends of Fe I abundance versus line strength were removed. The overall model atmosphere metallicity was then adjusted to match the derived [Fe/H] abundance for each star. This value was also used to further refine the calculated effective temperature, which has a slight metallicity dependence. A full listing of star identifiers, photometry, model atmosphere parameters, and S/N ratios is provided in Table 2.

3.2. Derivation of Abundances

3.2.1. Equivalent Width Analysis

Chemical abundances for Na, Si, Ca, Sc, Ti, Fe, and Ni were determined through standard equivalent width (EW) analyses using the *abfind* driver in the LTE line analysis

⁵The model atmosphere grids can be downloaded from <http://cfaku5.cfa.harvard.edu/grids.html>.

code MOOG⁶ (Sneden 1973). Individual EWs were measured by fitting single or multiple Gaussian profiles to isolated and blended stellar absorption lines using the interactive EW fitting code developed for Johnson et al. (2008). The high resolution, high S/N solar and Arcturus atlases⁷ (Hinkle et al. 2000) were used to aid in line identification and continuum placement. The Arcturus atlas was also used as a reference for selecting suitable spectral lines. However, the atomic log gf values were determined by an inverse solar analysis in which the EWs measured in the Sun were forced to match the photospheric abundances given in Anders & Grevesse (1989)⁸. When comparing our derived log gf values to those given in the NIST⁹ (Ralchenko et al. 2008), Thevenin (1990), and VALD¹⁰ (Kupka et al. 2000) compilations, we find very good agreement such that $\langle \log g f_{\text{ours}} - \log g f_{\text{lit.}} \rangle = -0.02$ ($\sigma=0.08$).

While most abundances were determined through a straight-forward EW analysis, the odd-Z Fe-peak and neutron-capture elements have line profiles that may be affected by hyperfine structure. For the purposes of this study, this includes the elements Sc, La, and Eu. Prochaska & McWilliam (2000) give hyperfine log gf values for the 6245 Å Sc II line, but unfortunately their work does not include the 6309 Å Sc II nor the 6210 and 6305 Sc I lines used here. Similarly, the Zhang et al. (2008) analysis of solar Sc abundances only includes the 6245 Å line as well. However, the error introduced by ignoring hyperfine structure increases as a function of EW, and the small Sc EWs in our sample ($\langle \text{EW} \rangle = 42 \text{ mÅ}$, $\sigma = 26 \text{ mÅ}$) lead us to believe a standard EW abundance analysis is a reasonable approach for this element.

For abundance determinations of the neutron-capture elements La and Eu, we have employed the hyperfine structure linelists available in Lawler et al. (2001a) for the 6262 Å La II line and Lawler et al. (2001b) for the 6645 Å Eu II line. However, the La abundances were determined by spectrum synthesis and are described in §3.2.2. Eu abundance determinations are more complicated than those for most elements because the line profiles are both affected by hyperfine splitting and Eu has two stable, naturally occurring isotopes (^{151}Eu and ^{153}Eu) with solar system isotopic fractions of 47.8% and 52.2%, respectively (Lawler et al. 2001b). The Eu EWs were measured using the same interactive fitting code mentioned previously, and the EWs were combined with the Eu linelist and isotope fractions as inputs into the MOOG *blends* driver to obtain the final abundances.

⁶The MOOG code can be downloaded at: <http://www.as.utexas.edu/~chris/moog.html>.

⁷These are available online from the NOAO Data Archives at: <http://www.noao.edu/archives.html>.

⁸The solar log $\epsilon(\text{Fe})$ abundance was assumed to be 7.52 (Sneden et al. 1991a).

⁹The NIST Atomic Line Database can be accessed at: <http://www.nist.gov/physlab/data/asd.cfm>.

¹⁰The VALD linelist can be accessed at: <http://www.astro.uu.se/~vald/php/vald.php>.

All EWs measured for this project and the atomic linelists are provided in Tables 3a–3b for Fe and Tables 4a–4b for all other elements. Similarly, the chemical abundance ratios for all elements are given in Table 5, and the number of lines measured for each element per star along with the σ/\sqrt{N} values are available in Tables 6a–6b. The log gf values listed for La and Eu in Table 4b represent the *total* gf values instead of an individual hyperfine component. The interested reader can find the full linelists for these elements in the references given above.

3.2.2. Spectrum Synthesis Analysis

The abundances of O, Al, and La were determined by spectrum synthesis rather than the EW fitting method described in §3.2.1. The primary motivation for using synthesis instead of an EW analysis for these elements is that the available lines suffer from varying degrees of contamination with either nearby metal lines or molecular CN. The 6300.31 Å [O I] line is blended with the nearby 6300.70 Sc II feature, and is also moderately sensitive to the C+N abundance. Similarly, the 6696/6698 Å Al I lines are both moderately blended with nearby Fe I and CN features, and the 6262 Å La II line is lightly blended with both CN and a Co I line at 6262.81 Å.

Spectrum synthesis modeling was carried out using the *synth* driver in MOOG. The atomic linelist was generated primarily from the Kurucz online database¹¹ with updated log gf values provided by C. Sneden (2008, private communication). The atomic linelist was merged with a molecular CN linelist that was created through a combination of the Kurucz molecular linelist¹² and one provided by B. Plez (2007, private communication; see also Hill et al. 2002). Individual log gf values for lines of interest were verified through spectrum synthesis of both the solar and Arcturus atlases. As was mentioned in §3.2.1, the La II hyperfine structure linelist was taken from Lawler et al. (2001a).

Since most stars in our sample do not have published [C/Fe], [N/Fe], and/or $^{12}\text{C}/^{13}\text{C}$ ratios, we set [C/Fe]=−0.5, $^{12}\text{C}/^{13}\text{C}$ =4, and treated the N abundance as a free parameter to fit the available CN features. Previous work on evolved RGB stars in ω Cen (e.g., Norris & Da Costa 1995; Smith et al. 2002; Origlia et al. 2003; Stanford et al. 2010) has shown that our set values for [C/Fe] and $^{12}\text{C}/^{13}\text{C}$ are a reasonable approximation given that all of the stars in our sample will have already undergone first dredge-up and are above the

¹¹The online database can be found at: <http://kurucz.harvard.edu/LINELISTS/GF100/>

¹²The molecular linelist can be found at: <http://kurucz.harvard.edu/LINELISTS/LINESMOL/>

RGB luminosity bump. With these assumptions, values of $+0.80 \lesssim [\text{N}/\text{Fe}] \lesssim +1.50$ tended to provide the best fits to the CN lines.

Figure 4 shows sample spectra of four moderately metal-poor ($[\text{Fe}/\text{H}] \approx -1.45$) program stars along with synthetic spectrum fits to the O, La, and Al regions. The bottom panels of Figure 4 indicate the uncertainty introduced when the abundances of CN and other nearby, blended metals are altered by ± 0.50 dex. In warmer stars and those that are moderately metal-poor, the CN contamination does not provide a significant change in the derived abundance. However, cooler and more metal-rich stars have O, La, and Al abundances that can deviate by at least 0.10–0.20 dex compared to an analysis that does not properly account for molecular blends. For the Al lines, the nearby Fe lines are generally not much of an issue in cool giants because the Fe transitions have excitation potentials $\gtrsim 5$ eV. The O and La lines are also not significantly affected by blends from neighboring Fe-peak element features unless the $[\text{Fe-peak}/\text{Fe}]$ abundance exceeds roughly $+0.3$ dex. However, the O and Sc lines are blended strongly enough at this resolution to warrant spectrum synthesis regardless of the $[\text{Sc}/\text{Fe}]$ abundance.

3.2.3. Comparison to Other Studies

As described in §1, the chemical composition of ω Cen has been extensively studied using a variety of abundance indicators. However, there are only four high resolution spectroscopic studies for which we have more than five stars in common: Norris & Da Costa (1995; 35 stars), Smith et al. (2000; 7 stars), Johnson et al. (2008; 171 stars), and Johnson et al. (2009; 59 stars). Figure 5 illustrates the differences between our adopted model atmosphere parameters and those found in the literature. The average differences in T_{eff} , $\log g$, $[\text{Fe}/\text{H}]$, and v_t , in the sense present minus literature values, are 0 K ($\sigma=61$ K), -0.02 cgs ($\sigma=0.09$), -0.03 dex ($\sigma=0.17$ dex), and 0.02 km s $^{-1}$ ($\sigma=0.24$ km s $^{-1}$), respectively. We conclude from these results that there are no strong systematic offsets among the studies with regard to the adopted model atmosphere parameters. This conclusion is in agreement with the $[\text{X}/\text{Fe}]$ abundances comparisons shown in Figure 6. The average differences in the chemical abundances between this study and those in the literature tend to be < 0.10 dex ($\sigma \lesssim 0.20$ dex).

The paucity of Al and Eu comparisons shown in Figure 6 is due to two effects: (1) we only obtained about $\sim 40\%$ as many spectra in the spectral region that contains the Al and Eu lines and (2) we purposely chose to observe stars in the Al/Eu region for which Al and/or Eu abundances were not already available in the literature. Further examination of Figure 6 indicates that La is the only element showing a systematic abundance offset. We

tend to find systematically lower [La/Fe] ratios, especially at $[\text{Fe}/\text{H}] \gtrsim -1.7$, because of our inclusion of hyperfine structure for the 6262 Å La II line. Norris & Da Costa (1995), Smith et al. (2000), and Johnson et al. (2009) base all or part of their La abundances on the 6774 Å La II line, which suffers from hyperfine broadening. However, there are no hyperfine linelists available in the literature for this transition. Since our present data, combined with that from Johnson et al. (2009), include both the 6262 and 6774 Å lines, we have derived an empirical hyperfine structure correction factor for the 6774 Å line that is described in Appendix A.

In addition to the studies mentioned above, we also have five stars in common (ROA 211, 300, 371, WFI 618854, and WFI 222068) with the Pancino et al. (2002) work that measured $[\text{Fe}/\text{H}]$, $[\text{Si}/\text{Fe}]$, $[\text{Ca}/\text{Fe}]$, and $[\text{Cu}/\text{Fe}]$ in six relatively metal-rich ($[\text{Fe}/\text{H}] \geq -1.2$) ω Cen giants. However, despite sharing small differences in our derived T_{eff} , $\log g$, $[\text{Fe}/\text{H}]$, and v_t values, we find noticeably different $[\alpha/\text{Fe}]$ abundances for two of the most metal-rich stars (ROA 300 and WFI 222068). This is important because the Pancino et al. (2002) result is one of the primary studies suggesting that Type Ia SNe may have significantly affected ω Cen’s chemical enrichment. Origlia et al. (2003) also find a decrease in $[\alpha/\text{Fe}]$ at $[\text{Fe}/\text{H}] > -1$, and we note similar discrepancies in our derived abundances for the most metal-rich stars. However, their abundances are based on low resolution, infrared spectra and may be subject to systematic offsets with our data.

For a direct comparison with the Pancino et al. (2002) data, in star ROA 300 we find Si and Ca offsets of $\Delta[\text{Si}/\text{Fe}] = +1.14$ and $\Delta[\text{Ca}/\text{Fe}] = +0.17$. Similarly, WFI 222068 exhibits differences of $\Delta[\text{Si}/\text{Fe}] = +0.60$ and $\Delta[\text{Ca}/\text{Fe}] = +0.42$. To investigate this discrepancy, we ran spectrum syntheses for the 6155 Å Si I line and 6156, 6161, and 6162 Å Ca I lines (see Figure 7). The results shown in Figure 7 indicate that the Pancino et al. (2002) $[\text{Si}/\text{Fe}]$ and $[\text{Ca}/\text{Fe}]$ abundances are too low to match the observed spectra *using our linelist and model atmospheres*. Instead, we find better agreement by using the upper limits on the error bars given by Pancino et al. (2002; their table 3), which results in increasing their $[\text{Si}/\text{Fe}]$ and $[\text{Ca}/\text{Fe}]$ abundances by $\sim +0.2$ dex.

Further inspection of Figure 7 shows that our EW-based $[\text{Si}/\text{Fe}]$ abundances may have overestimated the true $[\text{Si}/\text{Fe}]$ abundances for these two stars by $\sim +0.3$ dex. We did not find any clear reason for this discrepancy because the EW-based abundances for calcium and all other elements were in agreement with the spectrum synthesis fits, but it is possible that an unaccounted for (probably CN) blend is present near the silicon line in these very cool ($T_{\text{eff}} < 4000$ K), relatively metal-rich ($[\text{Fe}/\text{H}] \sim -0.7$) giants. It is worth noting that the $[\text{Si}/\text{Fe}]$ and $[\text{Ca}/\text{Fe}]$ abundance values are in much better agreement for two of the warmer, more metal-poor stars where the differences between EW- and synthesis-based

abundances are negligible. In the remaining star (ROA 371), the difference between our derived [Ca/Fe] abundance and that from Pancino et al. (2002) is mostly negligible, but the [Si/Fe] abundance offset is noticeably larger at $\Delta[\text{Si}/\text{Fe}] = +0.48$. However, this star was also analyzed by both Paltoglou & Norris (1989) and Norris & Da Costa (1995), and we find in agreement with those two studies that ROA 371 is Si-rich with $[\text{Si}/\text{Fe}] \gtrsim +0.5$. It seems likely that most, if not all, of the discrepancy between our derived abundance values and Pancino et al. (2002) are the result of differences in adopted log gf values, model atmospheres, and line choice.

3.3. Abundance Sensitivity to Model Atmosphere Parameters

Table 7 shows the sensitivity of our derived $\log \epsilon(\text{X})$ abundances to changes in the adopted model atmosphere parameters. The tests were conducted at $T_{\text{eff}}=4200$ K and $T_{\text{eff}}=4600$ K, values typical of stars in our sample, and metallicities ranging from $[\text{Fe}/\text{H}] = -2.0$ to -0.50 . The analyses for each test star were run by adjusting $T_{\text{eff}} \pm 100$ K, $\log g \pm 0.30$ cgs, $[\text{Fe}/\text{H}] \pm 0.30$ dex, and $v_t \pm 0.30$ km s $^{-1}$ individually while holding the other parameters constant.

We find that the chemical abundances derived from subordinate ionization state transitions (e.g., most neutral metals) are most sensitive to changes in T_{eff} . However, abundances derived from dominant ionization state transitions (e.g., neutral oxygen; singly ionized transition metals and heavy elements) are more sensitive to uncertainties in surface gravity and metallicity because of their stronger dependence on electron pressure and H $^-$ opacity. For stars with $[\text{Fe}/\text{H}] < -1$, microturbulence was found to have a negligible effect on abundances derived from all transitions except Fe I and Ca I. Abundances derived from Fe I and Ca I lines were more sensitive to microturbulence uncertainties because of their typically larger EWs than other lines at a given metallicity. In stars with $[\text{Fe}/\text{H}] > -1$, most abundances were affected at the 0.05–0.10 dex level due to the increased line strengths. Similarly, the abundances of most elements in warmer stars were less sensitive to changes in microturbulence because of the generally weaker line strengths. It seems likely that our derived $\log \epsilon(\text{X})$ abundance uncertainties do not exceed ~ 0.20 dex based on our choices of model atmosphere parameters. Additionally, the [X/Fe] abundance ratios for most elements are expected to exhibit an even weaker dependence on model atmosphere parameter uncertainties because of their similar behavior to Fe I.

In addition to the parameters shown in Table 7, we also tested the abundance uncertainties based on changes to CN and He. Since CN lines are strongest in the O-poor stars, it is possible that standard EW and spectrum synthesis analyses may not give the same

abundances for lines significantly blended with CN. However, we find that none of the lines chosen for this study that were analyzed via a standard EW approach were significantly affected by continuum suppression or blending from CN. The robust agreement between the synthesis and EW-based analyses for elements other than O, Al, and La is demonstrated in Figure 4, where the abundances of all other elements studied here were preset to those values obtained from a standard EW analysis.

Since the current interpretation of ω Cen’s blue main sequence is that stars belonging to that population are He-rich ($Y \sim 0.38$), we investigated the effects helium enrichment might have on our analyses. To test this, we ran both EW and spectrum synthesis analyses using He-normal ($Y=0.27$) and He-rich ($Y=0.35$) ATLAS9 models¹³. We find that the He-rich model does not result in a significantly different abundance ($\Delta \log \epsilon(X) < 0.1$ dex), and the effects on our derived $[X/Fe]$ ¹⁴ ratios are further mitigated for the low ionization potential metals. These results are in agreement with helium enrichment predictions by Boehm-Vitense (1979), and are consistent with similar tests on ω Cen stars in Piotto et al. (2005), Johnson et al. (2009), and Cunha et al. (2010). Furthermore, Girardi et al. (2007) conclude that increasing the He abundance to the extreme values predicted in some ω Cen stars should not significantly alter either the bolometric correction or V-K color-temperature relation. We therefore believe that our adopted atmospheric parameters are reliable even for He-rich giants.

4. RESULTS

4.1. Iron and the Metallicity Distribution Function

As discussed in §1, ω Cen’s large metallicity spread has been previously verified in many photometric and spectroscopic analyses. However, the results presented here are based on direct measurements from high resolution, high S/N spectra in a nearly complete sample of ω Cen giants with $V \leq 13.5$. These new data cover the cluster’s full metallicity regime, and are also nearly complete out to $\sim 50\%$ of the tidal radius. The data presented here, along with that from Johnson et al. (2008; 2009), yield spectroscopic $[Fe/H]$ measurements for 867 giants.

In Figure 8, we plot our derived metallicity distribution function and compare with the

¹³The He-rich models can be downloaded at <http://wwwuser.oat.ts.astro.it/castelli/grids.html>.

¹⁴Also note that the decrease in N(H) for He-rich stars will not affect abundances reported as $[X/Fe]$ ratios because $[X/H]$ and $[Fe/H]$ both increase by the same amount.

results of two other large spectroscopic surveys that spanned the upper RGB and SGB (Norris et al. 1996; Suntzeff & Kraft 1996). The general trend among all studies is that a dominant, metal-poor stellar population exists at $[Fe/H] \approx -1.7$ along with a higher metallicity tail terminating around $[Fe/H] \approx -0.5$. Our data confirm this result, and also support previous observations that found multiple peaks in the metallicity distribution function but a paucity of stars with $[Fe/H] < -2$. The full range of iron abundances in our sample extends from $[Fe/H] = -2.26$ to -0.32 , and in Figure 8 we find five peaks in the metallicity distribution function located at $[Fe/H] \approx -1.75, -1.50, -1.15, -1.05$, and -0.75 . These peaks correspond to the RGB-MP, RGB-MInt, and RGB-a populations identified by Pancino et al. (2000) and Sollima et al. (2005), and also generally agree with Strömgren photometry estimates (Hilker & Richtler 2000; Hughes & Wallerstein 2000; Calamida et al. 2009). It is difficult to accurately deblend the two populations near $[Fe/H] = -1.15$ and -1.05 because the separation is comparable to the line-to-line dispersion of Fe abundance measurements in individual stars. Instead, we will combine these two populations during further analyses. Taking this into account, the (now four) stellar populations make up roughly 61%, 27%, 10%, and 2% of our sample, respectively. For brevity, we will follow a similar naming scheme used by Sollima et al. (2005) when referring to the different metallicity populations: RGB-MP ($[Fe/H] \leq -1.6$), RGB-Int1 ($-1.6 < [Fe/H] \leq -1.3$), RGB-Int2+3 ($-1.3 < [Fe/H] \leq -0.9$), and RGB-a ($[Fe/H] > -0.9$).

The most metal-poor stars ($[Fe/H] \leq -2$) make up about 2% (17/867) of the full sample and only about 3% (17/541) of the RGB-MP stellar population. However, the RGB-a stars are slightly underrepresented because of our V magnitude cutoff. To test for any selection effects, we rebinned the data to only include stars within ~ 1 mag of each giant branch's RGB tip, which is the approximate magnitude range over which we sampled the RGB-a. We did not find any significant differences in the relative population mix, and different magnitude cutoffs only raised the RGB-a population fraction to $\sim 5\%$. These estimates are consistent with those derived from number counts in photometric analyses (Pancino et al. 2000; Sollima et al. 2005; Villanova et al. 2007; Calamida et al. 2009). It should also be noted that AGB contamination may affect the number counts of each population differently. Lee et al. (2005a) found that if the intermediate metallicity and most metal-rich stars are in fact He-rich then these stars will populate the “extreme” horizontal branch. Furthermore, D’Cruz et al. (2000) estimate that as much as 30% of the cluster’s horizontal branch population may reside on the “extreme” horizontal branch, and it is likely that these stars evolve directly to white dwarfs rather than first ascending the AGB (e.g., Sweigart et al. 1974). Since it is difficult to differentiate between RGB and AGB stars in ω Cen’s color-magnitude diagram, it is possible that the number counts for the two most metal-poor populations contain a disproportionate number of AGB stars compared to the more

metal-rich populations. However, our estimated population fractions are consistent with those found along the main sequence and subgiant branch (e.g., Villanova et al. 2007) where AGB contamination is not an issue.

In addition to the existence of multiple, discrete stellar populations in ω Cen, there is some evidence that the metal-rich stars are more centrally located than the more metal-poor populations (Norris et al. 1996; Suntzeff & Kraft 1996; Pancino et al. 2000; Hilker & Richtler 2000; Pancino et al. 2003; Rey et al. 2004; Sollima et al. 2005; Johnson et al. 2008; Bellini et al. 2009b; Johnson et al. 2009). In Figure 9, we plot our derived abundances as a function of projected distance from the cluster center. A two-sided Kolmogorov-Smirnov (K-S) test (Press et al. 1992) confirms that the metal-rich stars ($[\text{Fe}/\text{H}] > -1.3$) are more centrally located than the metal-poor stars at the 96% level¹⁵. Additionally, all of the stars with $[\text{Fe}/\text{H}] \geq -0.9$ are located within $13'$ of the cluster center, with most of those residing inside $10'$.

Further inspection of Figure 9 reveals another interesting radial distribution trend; all stars with $[\text{Fe}/\text{H}] \leq -2$ are located within $12'$ of the cluster core, and 88% (15/17) of these stars reside inside $5'$. A two-sided K-S test comparing the radial distribution of stars with $-2.0 < [\text{Fe}/\text{H}] \leq -1.60$ versus those with $[\text{Fe}/\text{H}] \leq -2$ indicates that the two distributions are drawn from different parent populations at the 99% level. Additionally, the star-to-star metallicity dispersion decreases with increasing distance from the cluster center, but this is mostly driven by the metallicity gradient and paucity of stars with $[\text{Fe}/\text{H}] \geq -1.3$ outside $\sim 15'$ from the cluster center. If one only considers stars with $[\text{Fe}/\text{H}] < -1.3$, the standard deviation in $[\text{Fe}/\text{H}]$ between $0-10'$ and $10-20'$ differs by less than 0.02 dex. This indicates that the two most metal-poor stellar populations are well mixed inside the cluster.

4.2. Oxygen

The chemical evolution of oxygen in ω Cen has previously been analyzed via high resolution spectroscopy in several studies containing sample sizes ranging from $\sim 5-40$ RGB stars (e.g., Cohen 1981; Paltoglou & Norris 1989; Brown & Wallerstein 1993; Norris & Da Costa 1995; Zucker et al. 1996; Smith et al. 2000), and more recently in a sample of ~ 200 RGB stars (Marino et al. 2010). The main results from past studies indicate that: (1) ω Cen giants exhibit large star-to-star dispersions in $[\text{O}/\text{Fe}]$ abundance, (2) many of the intermediate metallicity stars have $[\text{O}/\text{Fe}] < 0$, (3) the majority of metal-poor stars are O-rich

¹⁵We adopt the notion that the null hypothesis (i.e., that the two distributions are the same) can be rejected if the p value is “small” (< 0.05).

with $[O/Fe] \sim +0.3$, and (4) oxygen is anticorrelated with both sodium and aluminum. The results presented here add 848 new $[O/Fe]$ abundance measurements.

Figure 9 includes a plot of our derived $[O/Fe]$ abundances as a function of projected distance from the cluster center. Compared to the other elements in Figure 9, oxygen appears to exhibit a unique radial distribution. Stars with $[O/Fe] \leq 0$, and especially those with $[O/Fe] < -0.4$, are more centrally concentrated than the bulk of stars with $[O/Fe] > 0$. In our sample, 62% (145/233) of stars with $[O/Fe] \leq 0$ are located inside 5' from the core and 91% (213/233) are inside 10'. This is compared to just 42% (261/615) and 77% (472/615) for the stars with $[O/Fe] > 0$, respectively. A two-sided K-S test reveals that the O-poor stars exhibit a different spatial distribution than the O-rich stars at the 99% level. This result may have important implications regarding the origin of the blue main-sequence, and will be discussed further in §5.2.2.

Figure 10 shows the chemical evolution of $[O/Fe]$ plotted as a function of $[Fe/H]$. This plot reveals that the O-poor stars, in addition to being preferentially located near the cluster core, are also well separated from the O-rich stars over a large metallicity range. Figure 11 shows the $[O/Fe]$ data binned in 0.10 dex increments and separated into the population subclasses defined in §4.1. The resultant histograms support the existence of two subpopulations, one O-rich ($[O/Fe] > 0$) and the other O-poor ($[O/Fe] < 0$), residing inside the RGB-Int1 and RGB-Int2+3 populations. Interestingly, neither the RGB-MP nor the RGB-a populations appear to exhibit this bimodal behavior. Instead, the RGB-MP stars are predominantly O-rich with a median $[O/Fe] = +0.32$, and the RGB-a stars are moderately O-poor with a median $[O/Fe] = -0.15$. In the RGB-MP population, the percentages of O-poor and O-rich stars are 13% (71/535) and 87% (464/535), respectively. The two intermediate metallicity populations show quite different distributions, with the percentages being 46% (100/218) to 54% (118/218) in the RGB-Int1 group and 64% (47/74) to 36% (27/74) in the RGB-Int2+3 group. The relative distribution in the RGB-a stars is 71% (15/21) O-poor to 29% (6/21) O-rich, respectively.

Examining the bulk properties of the $[O/Fe]$ abundances reveals that, in all but the most metal-poor and metal-rich stars, a significant star-to-star dispersion is present with $\Delta [O/Fe] > 2$ over a large metallicity range. The full range of $[O/Fe]$ abundances found in our sample spans from $[O/Fe] = -1.30$ to $+0.80$. The stars with $[Fe/H] \leq -2$ are overwhelmingly O-rich with 94% (15/16) having $[O/Fe] > 0$ and $\langle [O/Fe] \rangle = +0.38$, and the single O-poor star is only moderately depleted at $[O/Fe] = -0.13$. The $[O/Fe]$ abundance “ceiling” decreases for stars with $[Fe/H] \gtrsim -1.3$, dropping from $[O/Fe] \approx +0.6$ at $[Fe/H] = -1.3$ to $[O/Fe] \approx +0.0$ at $[Fe/H] = -0.3$. Additionally, the super O-poor stars ($[O/Fe] \leq -0.4$) are only found in the range $-1.9 \lesssim [Fe/H] \lesssim -1.0$. When considering all stars in our sample, the relative percentages

of O-rich ($[O/Fe] > 0$), O-poor ($-0.4 < [O/Fe] \leq 0.0$), and super O-poor ($[O/Fe] \leq -0.4$) stars are 73% (615/848), 14% (118/848), and 13% (115/848), respectively. We also find that in stars with $[Fe/H] \lesssim -1$, $[O/Fe]$ is anticorrelated with both $[Na/Fe]$ and $[Al/Fe]$. The implications of these anticorrelations, along with the possible significance of the super O-poor stars, will be discussed further in §5.

4.3. Sodium

Previous sodium abundance measurements support the idea that ω Cen experienced a significantly different chemical evolutionary path than any other stellar system (Cohen 1981; Paltoglou & Norris 1989; Brown & Wallerstein 1993; Norris & Da Costa 1995; Zucker et al. 1996; Smith et al. 2000; Johnson et al. 2009; Villanova et al. 2009; Marino et al. 2010). The results from these studies have shown that: (1) $[Na/Fe]$ appears to increase as a function of increasing $[Fe/H]$, (2) $\Delta[Na/Fe] > 1$ for most values of $[Fe/H]$ in the cluster, (3) no strong $[Na/Fe]$ abundance gradient is observed, and (4) $[Na/Fe]$ is correlated with $[Al/Fe]$ and anticorrelated with $[O/Fe]$. Our new results, combined with those from Johnson et al. (2009), give $[Na/Fe]$ abundances for 848 cluster giants. Although it is likely that our derived sodium abundances suffer from moderate non-LTE (NLTE) effects, abundances derived from the 6154/6160 Å doublet used here are expected to have NLTE offsets < 0.2 dex for giants in our metallicity regime (e.g., Gratton et al. 1999; Mashonkina et al. 2000; Gehren et al. 2004). Since no standard NLTE corrections are available in the literature, the abundances reported in Table 5 and shown in the figures do not include NLTE corrections.

Inspection of Figure 11 indicates that $[Na/Fe]$ exhibits a similar bimodal abundance pattern as shown by $[O/Fe]$. That is, the most metal-poor and metal-rich stellar populations show a single primary peak in the $[Na/Fe]$ distribution function, and the two intermediate metallicity populations may be best described as having two peaks in the $[Na/Fe]$ distribution function. However, unlike the case with oxygen, we do not find an obvious centrally concentrated population that correlates with any $[Na/Fe]$ abundance range. We do find that the most Na-rich stars in our sample ($[Na/Fe] \geq +0.6$) are all found inside 13' from the cluster center, but this observation is unlikely to be significant because (1) the two most metal-rich stellar populations contain 69% (44/64) of the most Na-rich stars (see Figures 10–11) and (2) these stellar populations are already known to be centrally concentrated. This is in contrast to the O-poor radial trend that is found in stars with $-1.6 < [Fe/H] \leq -1.3$, which do not exhibit a preferred radial location. However, Figure 9 shows that a weak, declining $[Na/Fe]$ gradient may exist such that the median $[Na/Fe]$ values for 0–5', 5–10', 10–15', and 15–20' are +0.22, +0.14, +0.08, and –0.03, respectively.

Figure 10 highlights the chemical evolution of [Na/Fe] as a function of [Fe/H]. We find that a large star-to-star dispersion is present at all metallicities, and that the full range extends from [Na/Fe]=−1.02 to +1.36. Since we have many stars of the same temperature, surface gravity, and metallicity, the line strength differences confirm that the observed abundance spread is a real effect and not due to possible underlying NLTE effects. In addition to displaying a significant star-to-star dispersion, the sodium abundances also exhibit a strong metallicity dependence such that the median [Na/Fe] value increases with increasing [Fe/H]. The median [Na/Fe] value rises from +0.08 in the RGB-MP population to +0.78 in the RGB-a population. As mentioned above, the two most metal-rich populations contain the most Na-rich stars in the cluster. Despite the complex nature of sodium’s evolution in ω Cen, the O–Na anticorrelation and Na–Al correlation are present in all but the most metal-rich stars.

4.4. Aluminum

Except for iron and calcium, aluminum has been the most highly studied element in ω Cen. Previous high resolution spectroscopic work has targeted more than 200 RGB stars (Cohen 1981; Brown & Wallerstein 1993; Norris & Da Costa 1995; Zucker et al. 1996; Smith et al. 2000; Johnson et al. 2008; Johnson et al. 2009) and shown: (1) $\Delta[\text{Al}/\text{Fe}]>0.5$ at all metallicities and exceeds more than a factor of ten in the most metal-poor stars, (2) the range of observed [Al/Fe] abundances decreases at $[\text{Fe}/\text{H}]>-1.3$, (3) there is a paucity of stars with $[\text{Al}/\text{Fe}]<+0.3$ at intermediate and high metallicities, and (4) a Na–Al correlation and O–Al anticorrelation are present in most, if not all, cluster stars. In this paper we present 133 new [Al/Fe] abundance measurements, and when combined with the data from Johnson et al. (2008; 2009) provide [Al/Fe] values for 332 ω Cen giants. As with sodium (see §4.3), we have not applied any NLTE corrections to our derived aluminum abundances. However, all aluminum abundances determined here utilized the non-resonance 6696/6698 Å lines, which are not expected to have large NLTE offsets in the temperature, gravity, and metallicity range of stars in our sample (e.g., Gehren et al. 2004; Andrievsky et al. 2008).

Unlike oxygen, and to a lesser extent sodium, aluminum does not show any obvious correlation between [Al/Fe] abundance and radial location. However, aluminum does show the same bimodal abundance distribution for the RGB-Int1 and RGB-Int2+3 populations (see Figure 11). By dividing the samples at $[\text{Al}/\text{Fe}]=+0.6$, we find that the percentage of “Al-enhanced” ($[\text{Al}/\text{Fe}]\geq+0.6$) stars in the RGB-Int1 population is 50% (50/100) compared to 50% (50/100) as well for the “Al-normal” stars ($[\text{Al}/\text{Fe}]<+0.6$). Similarly, the RGB-Int2+3 stars are distributed as 69% (31/45) enhanced and 31% (14/45) normal, respectively.

Interestingly, the [Al/Fe] distribution also shows complex substructure in the RGB–MP population, which is not observed in the [O/Fe] and [Na/Fe] data. In this population, 41% (70/172) of the stars are Al–enhanced and 59% (102/172) are Al–normal. Furthermore, this is the only ω Cen population that contains a significant number of stars over the full [Al/Fe] range. For the RGB–a population, a single peak is observed at [Al/Fe]=+0.5 in the [Al/Fe] distribution function.

The full range of [Al/Fe] abundances observed here spans from −0.34 to +1.37, but only 4% (12/332) of the stars have [Al/Fe]<0. Similarly, we find that $\Delta[\text{Al}/\text{Fe}] \sim 1.5$ dex for $[\text{Fe}/\text{H}] < -1.3$. However, the star–to–star dispersion decreases noticeably at higher metallicities. Inspection of Figure 10 shows that [Al/Fe] exhibits an interesting trend as a function of [Fe/H]. The maximum value reached for stars with $[\text{Fe}/\text{H}] \lesssim -1.3$ remains steady near $[\text{Al}/\text{Fe}] \approx +1.3$, but above $[\text{Fe}/\text{H}] \sim -1.3$ the maximum abundance decreases to only $[\text{Al}/\text{Fe}] \approx +0.6$ in the RGB–a stars. Furthermore, the number of stars with $[\text{Al}/\text{Fe}] < +0.3$ strongly decreases at $[\text{Fe}/\text{H}] > -1.3$. In the RGB–MP and RGB-Int1 populations, stars with $[\text{Al}/\text{Fe}] < +0.3$ constitute 25% (69/272) of the distribution, but this decreases to only 7% (1/15) of the RGB–a population.

4.5. Silicon

Previous analyses (Cohen 1981; Paltoglou & Norris 1989; Brown & Wallerstein 1993; Norris & Da Costa 1995; Smith et al. 2000; Pancino et al. 2002; Villanova et al. 2009) have used the heavy α element (Si, Ca, and Ti) abundances to assess the dominance of Type II versus Type Ia supernovae in ω Cen and other clusters. In terms of silicon abundances, it has been shown that: (1) silicon is enhanced with $[\text{Si}/\text{Fe}] > +0.3$ in nearly all cluster stars, (2) the star–to–star dispersion in [Si/Fe] is significantly smaller than for the lighter α and odd-Z elements, and (3) the most metal–rich stars may have appreciably lower [Si/Fe] abundances compared to the more metal–poor populations. From this study, we add 821 new [Si/Fe] measurements over ω Cen’s full metallicity range.

While we find that the lighter α element oxygen shows a distinctly unique distribution versus distance from the cluster center, [Si/Fe] does not show the same trend. Figure 9 suggests that a weak [Si/Fe] gradient may be present such that the stars inside 5' have a higher average silicon abundance than those outside 5'. We find that stars inside 5' have $\langle [\text{Si}/\text{Fe}] \rangle = +0.37$, which is noticeably higher than the $\langle [\text{Si}/\text{Fe}] \rangle = +0.29$ for those at $r > 5'$. This result does not change even if we limit examination to stars only between 0–5' and 5–10'. Except near the cluster core, the average $[\text{Si}/\text{Fe}] \approx +0.3$ at all radii. It should be noted that Villanova et al. (2009) find $\langle [\text{Si}/\text{Fe}] \rangle = +0.5$ in the outer 20–30' of ω Cen, which is larger by

about 0.2 dex than we find in the same region. However, we do not presently have sufficient data to assess whether the average [Si/Fe] ratio increases at larger radii or if this merely reflects a systematic offset.

The full range of [Si/Fe] abundances in our data span from -0.30 to $+1.15$, but the average over all stars is $[\text{Si}/\text{Fe}] = +0.33$ ($\sigma = 0.17$). While we do find a few Si-poor stars ($[\text{Si}/\text{Fe}] < 0$), these stars comprise only 2% (16/821) of the total sample. Similarly, the very Si-rich stars ($[\text{Si}/\text{Fe}] > +0.6$) only represent 6% (52/821) of the total sample. Figure 10 reveals that [Si/Fe] may have a more complex morphology as a function of [Fe/H] than previously thought. The average [Si/Fe] ratio decreases from $\langle [\text{Si}/\text{Fe}] \rangle = +0.46$ ($\sigma = 0.19$) in stars with $[\text{Fe}/\text{H}] \leq -2$ to $\langle [\text{Si}/\text{Fe}] \rangle = +0.29$ ($\sigma = 0.16$) in the stars that comprise the majority of the RGB-MP population ($-2.0 < [\text{Fe}/\text{H}] \leq -1.6$). In the subsequent populations, the average [Si/Fe] abundance monotonically increases with [Fe/H] to $\langle [\text{Si}/\text{Fe}] \rangle = +0.45$ ($\sigma = 0.23$) in the RGB-a population. This is in agreement with Norris & Da Costa (1995) and Smith et al. (2000), but contrasts with the claims by Pancino et al. (2002) and Origlia et al. (2003) that stars with $[\text{Fe}/\text{H}] > -1$ have lower $[\alpha/\text{Fe}]$ abundances (see §3.2.3 for a brief discussion).

4.6. Calcium

In addition to iron, calcium abundances have been analyzed in great detail for ω Cen stars. Previous analyses have used calcium as a proxy metallicity indicator (Freeman & Rodgers 1975; Cohen 1981; Norris et al. 1996; Suntzeff & Kraft 1996; Rey et al. 2004; Sollima et al. 2005; Stanford et al. 2006; Lee et al. 2009) and as an α element tracer (Paltoglou & Norris 1989; Norris & Da Costa 1995; Smith et al. 2000; Pancino et al. 2002; Kayser et al. 2006; Villanova et al. 2007; Johnson et al. 2009; Villanova et al. 2009). These studies have shown: (1) there is a large spread of at least 1 dex in [Ca/H] with multiple peaks in the distribution function (i.e., confirms the different populations found when using [Fe/H] as a metallicity tracer), (2) nearly all stars have enhanced $[\text{Ca}/\text{Fe}] \approx +0.3$ at all metallicities, (3) the star-to-star dispersion is significantly smaller than for the lighter elements, and (4) there may be a downturn in [Ca/Fe] at $[\text{Fe}/\text{H}] > -1$. Combining our new data with that of Johnson et al. (2009), we add 857 [Ca/Fe] abundance measurements.

Unlike silicon, which provides some evidence for a weak radial abundance gradient, [Ca/Fe] does not vary ostensibly between the inner and outer regions of the cluster. When considering all stars in our sample, the majority are Ca-rich with $\langle [\text{Ca}/\text{Fe}] \rangle = +0.29$ ($\sigma = 0.12$). However, the full range of observed [Ca/Fe] abundances is smaller than for [Si/Fe], with [Ca/Fe] varying between -0.13 and $+0.65$. Figure 10 shows that [Ca/Fe] displays a similar morphology to [Si/Fe] when plotted as a function of [Fe/H]. That is, stars with $[\text{Fe}/\text{H}] \leq -$

2 tend to be more Ca-rich with $\langle [\text{Ca}/\text{Fe}] \rangle = +0.37$ ($\sigma = 0.16$) compared to the majority of stars in the RGB-MP population with $\langle [\text{Ca}/\text{Fe}] \rangle = +0.26$ ($\sigma = 0.11$). Similarly, the average [Ca/Fe] abundance rises for the RGB-Int1 and RGB-Int2+3 populations to $\langle [\text{Ca}/\text{Fe}] \rangle = +0.34$ ($\sigma = 0.11$; see also Figure 12). However, unlike the case for [Si/Fe], the average [Ca/Fe] abundance decreases for $[\text{Fe}/\text{H}] \gtrsim -1$, and the RGB-a stars have $\langle [\text{Ca}/\text{Fe}] \rangle = +0.26$ ($\sigma = 0.12$).

Further inspection of Figure 10 reveals that the distribution of [Ca/Fe] among the RGB-Int2+3 stars may be bimodal. Figure 12 also suggests that the RGB-Int2+3 stars may exhibit a bimodal distribution, and shows that the other populations appear to exhibit a mostly unimodal [Ca/Fe] distribution. Interestingly, the two RGB-Int2+3 subsets occur in nearly equal proportions with the stars peaked near $[\text{Ca}/\text{Fe}] = +0.45$ constituting 47% (36/76) of the subsample and the stars peaked near $[\text{Ca}/\text{Fe}] = +0.25$ making up 53% (40/76) of the subsample. However, a two-sided K-S test does not rule out that the [Ca/Fe] distributions for the RGB-Int1 and RGB-Int2+3 are different at more than the 95% level. While we caution the reader that the apparent bimodality may be a product of small number statistics, it would be interesting to investigate this possible trend further with additional calcium abundance indicators (e.g., HK index).

4.7. Scandium

Scandium is typically used as a tracer of Fe-peak element production in stellar populations, and Galactic halo and globular cluster stars with $[\text{Fe}/\text{H}] > -2.5$ tend to exhibit solar-scaled [Sc/Fe] abundances. Although scandium has been analyzed in only a handful of studies for ω Cen stars (Cohen 1981; Paltoglou & Norris 1989; Norris & Da Costa 1995; Zucker et al. 1996; Smith et al. 2000; Johnson et al. 2009), the results typically show that: (1) the observed star-to-star scatter in [Sc/Fe] is significantly smaller than for lighter elements and (2) $\langle [\text{Sc}/\text{Fe}] \rangle \approx 0$ at all metallicities. Combined with the results from Johnson et al. (2009), we are able to add 821 [Sc/Fe] abundance measurements.

As can be seen in Figure 9, we do not find any evidence for a radial [Sc/Fe] abundance gradient. Similarly, Figure 10 indicates that the [Sc/Fe] ratio is approximately constant over the full metallicity regime. However, a weak metallicity dependence may be present such that the average [Sc/Fe] abundance decreases from $\langle [\text{Sc}/\text{Fe}] \rangle = +0.08$ ($\sigma = 0.13$) in the RGB-MP population to $\langle [\text{Sc}/\text{Fe}] \rangle = -0.07$ ($\sigma = 0.19$) in the RGB-a stars. The full range of observed [Sc/Fe] abundances spans from -0.49 to $+0.44$, but most stars exhibit a solar-scaled [Sc/Fe] ratio. When considering the entire sample, we find $\langle [\text{Sc}/\text{Fe}] \rangle = +0.05$ ($\sigma = 0.15$).

4.8. Titanium

Titanium is generally considered either the heaviest α element or one of the lightest Fe-peak elements. Previous titanium abundance measurements for ω Cen stars (Cohen 1981; Paltoglou & Norris 1989; Brown & Wallerstein 1993; Norris & Da Costa 1995; Smith et al. 2000; Villanova et al. 2007; Johnson et al. 2009; Villanova et al. 2009) have shown: (1) the star-to-star dispersion in $[\text{Ti}/\text{Fe}]$ is comparable to that found in $[\text{Si}/\text{Fe}]$ and $[\text{Ca}/\text{Fe}]$, (2) the titanium abundance is generally enhanced at $[\text{Ti}/\text{Fe}] \sim +0.3$, and (3) there may be evidence for an increase in $[\text{Ti}/\text{Fe}]$ with increasing $[\text{Fe}/\text{H}]$. Our new results, combined with Johnson et al. (2009), provide 826 $[\text{Ti}/\text{Fe}]$ measurements.

Inspection of Figure 9 confirms that we do not find any correlation between our determined $[\text{Ti}/\text{Fe}]$ abundance and a star’s radial location. In a similar fashion to the behavior of silicon and calcium, Figure 10 shows that titanium also exhibits a metallicity dependent morphology. The average $[\text{Ti}/\text{Fe}]$ ratio is roughly constant across the RGB-MP population’s full metallicity range ($[\text{Fe}/\text{H}] \leq -1.6$) at $\langle [\text{Ti}/\text{Fe}] \rangle = +0.13$ ($\sigma = 0.12$), which is ~ 0.2 dex lower than the $[\text{Si}/\text{Fe}]$ and $[\text{Ca}/\text{Fe}]$ ratios in those same stars. However, the average $[\text{Ti}/\text{Fe}]$ abundance rises monotonically to $\langle [\text{Ti}/\text{Fe}] \rangle = +0.34$ ($\sigma = 0.25$) in the RGB-a population (see also Figure 12). The full range of abundances in our sample spans from $[\text{Ti}/\text{Fe}] = -0.42$ to $+0.85$, but most stars are at least moderately Ti-enhanced with $\langle [\text{Ti}/\text{Fe}] \rangle = +0.18$ ($\sigma = 0.16$).

4.9. Nickel

Aside from iron, nickel is the only other “true” Fe-peak element analyzed here. The chemical evolution of nickel in a stellar population often tracks very closely to iron, and ω Cen appears to follow that trend (Cohen 1981; Paltoglou & Norris 1989; Norris & Da Costa 1995; Smith et al. 2000; Johnson et al. 2009; Villanova et al. 2009). Previous studies agree that: (1) the derived $[\text{Ni}/\text{Fe}]$ abundances show the smallest intrinsic dispersion of any element and (2) the average $[\text{Ni}/\text{Fe}]$ abundance is nearly solar at all metallicities and locations in the cluster. We add to these results 806 new $[\text{Ni}/\text{Fe}]$ abundance determinations.

Figure 9 shows that, like the other transition metals, $[\text{Ni}/\text{Fe}]$ abundances do not exhibit any signs of a radial gradient. Similarly, Figure 10 indicates that the distribution of $[\text{Ni}/\text{Fe}]$ is essentially constant as a function of $[\text{Fe}/\text{H}]$ with a small intrinsic scatter, but there may be a slight decrease in $[\text{Ni}/\text{Fe}]$ at $[\text{Fe}/\text{H}] \gtrsim -1.3$. The full spread of $[\text{Ni}/\text{Fe}]$ values found in our sample ranges from -0.48 to $+0.69$, and the cluster as a whole gives $\langle [\text{Ni}/\text{Fe}] \rangle = -0.03$ ($\sigma = 0.12$).

4.10. Lanthanum

The heavy element lanthanum is often used as a tracer of the slow neutron-capture process (s-process), and its evolution has proved to be particularly interesting in ω Cen. Previous analyses (Cohen 1981; Paltoglou & Norris 1989; Norris & Da Costa 1995; Smith et al. 2000; Johnson et al. 2009; Marino et al. 2010) have examined the [La/Fe] ratios in ~ 100 RGB stars and found: (1) the most metal-poor stars tend to have [La/Fe] abundances consistent with those found in monometallic globular clusters, (2) a large increase in [La/Fe] is seen between $[\text{Fe}/\text{H}] \approx -1.7$ and -1.4 , (3) the intermediate metallicity stars are almost exclusively La-rich, and (4) the average [La/Fe] ratio remains super-solar in the most metal-rich stars. When combined with the data from Johnson et al. 2009, we add to these past results 810 new [La/Fe] abundances.

As can be seen in Figure 9, we find no evidence supporting the existence of a radial [La/Fe] gradient, and the star-to-star dispersion remains approximately constant across all radii sampled here. On the other hand, our data shown in Figure 10 support previous claims that [La/Fe] abundances exhibit an unusual morphology when plotted as a function of [Fe/H]. There is a strong increase in [La/Fe] for stars with $[\text{Fe}/\text{H}] \gtrsim -1.7$, and a large intrinsic scatter of $\Delta[\text{La}/\text{Fe}] \geq 1$ is present at nearly all metallicities. Furthermore, the average [La/Fe] abundance monotonically increases from $+0.05$ in the RGB-MP population to $+0.49$ in the RGB-Int2+3 population (see also Figure 12). However, the RGB-a stars have $\langle [\text{La}/\text{Fe}] \rangle = +0.43$, which suggests either a leveling off or slight decline in [La/Fe] at $[\text{Fe}/\text{H}] \gtrsim -1$.

The full range of [La/Fe] abundances observed here spans from -0.78 to $+1.17$, and it is worth noting that the proper accounting of hyperfine structure in the [La/Fe] derivations has decreased the maximum abundance values found in Johnson et al. (2009) from $[\text{La}/\text{Fe}] \sim +2$ to $[\text{La}/\text{Fe}] \sim +1.2$. These lower abundance ratios suggest that a large fraction of binary transfer systems may not be required to account for the significant lanthanum enhancements. However, we still find that only 29% (232/810) of the stars in our sample have $[\text{La}/\text{Fe}] < 0$, and 94% (217/232) of those stars reside in the RGB-MP population. Interestingly, the stars with $[\text{Fe}/\text{H}] \leq -2$ tend to exhibit rather high [La/Fe] abundances. These stars have $\langle [\text{La}/\text{Fe}] \rangle = +0.19$, which is distinctly larger than the $\langle [\text{La}/\text{Fe}] \rangle = +0.05$ found for the full sample of RGB-MP stars. Unfortunately, a two-sided K-S test indicates that the data are insufficient to reject the null hypothesis with more than 94% confidence.

4.11. Europium

In an analogous fashion to lanthanum, the heavy element europium is often used as an indicator of the rapid neutron–capture process (r–process). However, europium has been analyzed in far fewer stars than lanthanum (Norris & Da Costa 1995; Zucker et al. 1996; Smith et al. 2000; Johnson et al. 2009). The primary results from these studies are: (1) $[\text{Eu}/\text{Fe}]$ tends to be somewhat underabundant relative to monometallic globular clusters of similar metallicity, (2) a significant intrinsic scatter is observed, but it is smaller than that found in $[\text{La}/\text{Fe}]$, and (3) $[\text{Eu}/\text{Fe}]$ remains relatively constant as a function of $[\text{Fe}/\text{H}]$. Combined with the data from Johnson et al. (2009), we provide $[\text{Eu}/\text{Fe}]$ abundances for 194 stars.

Given the significantly smaller sample for europium compared to the other elements analyzed here, it is difficult to assess whether any true radial trends exist. Figure 9 provides weak evidence that the average $[\text{Eu}/\text{Fe}]$ abundance may increase away from the cluster center. The available data support this by showing an increase from $\langle [\text{Eu}/\text{Fe}] \rangle = +0.12$ for stars between $0\text{--}5'$ to $\langle [\text{Eu}/\text{Fe}] \rangle = +0.23$ for stars between $5\text{--}10'$ from the core. Unfortunately, the sample size becomes too small outside $\sim 10'$ to conclude whether this trend continues.

Figure 10 reveals that $[\text{Eu}/\text{Fe}]$ exhibits a significantly different behavior than $[\text{La}/\text{Fe}]$ when plotted as a function of $[\text{Fe}/\text{H}]$. The full range is somewhat smaller with $[\text{Eu}/\text{Fe}]$ spanning -0.46 to $+0.83$, and the average $[\text{Eu}/\text{Fe}]$ abundance appears to *decrease* in the metallicity range where $[\text{La}/\text{Fe}]$ shows its greatest *increase*. While the intermediate metallicity populations generally contain the lowest $[\text{Eu}/\text{Fe}]$ abundances, the average $[\text{Eu}/\text{Fe}]$ ratios differ by only $\sim +0.1$ dex among the different stellar populations.

5. DISCUSSION

The results of our analyses support previous observations that ω Cen hosts multiple stellar populations exhibiting a complex history of chemical enrichment. To briefly summarize, we have confirmed five peaks in the metallicity distribution function located at $[\text{Fe}/\text{H}] \approx -1.75, -1.50, -1.15, -1.05$, and -0.75 ; however, for discussion purposes the $[\text{Fe}/\text{H}] = -1.15$ and -1.05 populations are treated as a single group. The RGB–MP, RGB–Int1, RGB–Int2+3, and RGB–a populations constitute 61%, 27%, 10%, and 2% of stars in our sample, respectively. We also find large intrinsic abundance dispersions for O, Na, and Al, and, except for perhaps in the most metal–rich stars, these elements exhibit the well–known abundance correlations and anticorrelations found in “normal” globular clusters. Additionally, the O–poor ($[\text{O}/\text{Fe}] \leq 0$) stars are located almost exclusively within $\sim 5\text{--}10'$ of the cluster center, but the

O-rich ($[O/Fe] \sim +0.3$) stars are rather evenly distributed at all cluster radii. The heavier α elements Si, Ca, and Ti exhibit smaller star-to-star dispersions than the lighter elements and are generally enhanced by about a factor of two. The average $[\alpha/Fe]$ ratio tends to increase with metallicity up to $[Fe/H] \approx -1$, and above this metallicity the average $[Ca/Fe]$ ratio begins to decline while the average $[Si/Fe]$ and $[Ti/Fe]$ abundances remain roughly constant. The two Fe-peak elements scandium and nickel exhibit little star-to-star dispersion and their $[X/Fe]$ ratios are nearly constant as a function of metallicity. We find a strong increase in the $[La/Fe]$ abundances when comparing stars in the RGB-MP and RGB-Int1 populations, but the average $[La/Fe]$ ratios for stars in the RGB-Int2+3 and RGB-a populations remain roughly the same. In contrast, $[Eu/Fe]$ does not vary strongly with metallicity and is only modestly enhanced. We now aim to interpret what these results reveal about ω Cen’s complex evolutionary history.

5.1. Supernova Nucleosynthesis: Evidence from Heavy α and Fe-peak Elements

The standard theory of Galactic chemical evolution suggests that massive stars ($\gtrsim 10 M_\odot$) produce the majority of elements up to the Fe-peak during various hydrostatic and/or explosive burning stages, and return the newly synthesized material to the interstellar medium (ISM) primarily through Type II SN explosions (e.g., Arnett & Thielemann 1985; Thielemann & Arnett 1985; Woosley & Weaver 1995; Nomoto et al. 2006). Theoretical yields indicate that stellar populations where Type II SNe have played the dominant role in polluting the ISM should produce future generations of stars with $[\alpha/Fe]$ ratios that are about 0.3–0.5 dex larger than the solar-scaled value, and exhibit abundance ratios in the range $-0.5 \lesssim [X/Fe] \lesssim +0.3$ for other elements lighter than about zinc. The massive stars provide chemical enrichment on time scales of $\sim 2 \times 10^7$ years or less, and are believed to be the dominant production sources of most elements in the Galactic halo and disk up to $[Fe/H] \approx -1$ (e.g., Timmes et al. 1995; Samland 1998). In contrast, Type Ia SNe primarily produce Fe-peak elements, and can contribute to a stellar population’s ISM about 5×10^8 to 3×10^9 years after the onset of star formation (e.g., Yoshii et al. 1996; Nomoto et al. 1997). Significant contributions from Type Ia SNe are believed to drive the observed decrease in the Galactic $[\alpha/Fe]$ abundance trend at $[Fe/H] > -1$.

Figure 13 shows our measured $[X/Fe]$ ratios as a function of $[Fe/H]$, and overplots the expected abundance trends if (1) Type II SNe are responsible for all of ω Cen’s chemical enrichment and (2) Type Ia ejecta are mixed with Type II ejecta in a 75/25% ratio. For consistency, we show only the supernova yields from Nomoto et al. (1997; Type Ia) and

Nomoto et al. (2006; Type II), but the theoretical yields from other groups (e.g., Woosley & Weaver 1995) follow approximately the same trends. We find that the α and Fe-peak abundance distributions are generally well described by pollution from Type II SNe. However, Figures 10 and 13 indicate that the behavior of [Si/Fe], [Ca/Fe], and [Ti/Fe] as a function of increasing [Fe/H] is more complex than for [Sc/Fe] and [Ni/Fe]. For all three α elements, the average [α /Fe] abundance noticeably increases between the most metal-poor and intermediate metallicity populations. Additionally, the stars with [Fe/H]<-2 tend to exhibit larger [Si,Ca/Fe] ratios than the rest of the RGB-MP stars, but the [Ti/Fe] abundances are mostly uniform across the full RGB-MP metallicity range.

Some of this behavior may be at least qualitatively explained by examining the mass and/or metallicity dependent yields of massive stars. In Figure 14, we plot the predicted production factors from Woosley & Weaver (1995) for various elements as a function of progenitor mass. The increase in the average [Si/Fe] and [Ca/Fe] abundances for ω Cen stars at [Fe/H]>-1.6 may be explained by the metallicity dependence of the Si and Ca yields, especially for stars more massive than about $18\text{--}20 M_{\odot}$. As can be seen in Figure 14, the most massive stars are predicted to produce higher yields as the metallicity increases from [Fe/H]=-2 to -1, but the *difference* between the Si and Ca yields are expected to remain roughly constant. This means that as long as ω Cen was able to retain and mix the ejecta of $\gtrsim 18 M_{\odot}$ stars, we should expect (1) that the average [Si/Fe] and [Ca/Fe] abundances should increase with [Fe/H] and (2) that both Si and Ca should exhibit the same general morphology until at least [Fe/H] ≈ -1 . Both of these predictions are seen in Figures 10 and 13. However, the similar increase found for [Ti/Fe] may not be due to Type II SNe. The theoretical yields do not predict a significant increase in [Ti/Fe] as a function of either progenitor mass or metallicity, and the situation does not improve if $>25 M_{\odot}$ stars are included (e.g., McWilliam 1997). Instead, it seems likely that titanium has additional production sources. We should note that this all follows the assumption that the observed abundances trace ^{48}Ti , in addition to ^{28}Si and ^{40}Ca , but an increase in the production of other stable isotopes could alter this scenario.

Mass dependent yields may also be responsible for explaining the discrepancy in [Si,Ca/Fe] between the stars with [Fe/H]<-2 and the rest of the RGB-MP population. As noted in §4, the average [Si/Fe] and [Ca/Fe] abundances are 0.17 and 0.11 dex larger for the [Fe/H]<-2 stars. This trend can be reconciled if the most metal-poor stars in the cluster, which represent only 3% of the RGB-MP population, preferentially formed from the ejecta of $\gtrsim 20 M_{\odot}$ stars. However, this would require very rapid enrichment of the early ω Cen environment because $>20 M_{\odot}$ stars live $\lesssim 10^7$ years (e.g., Schaller et al. 1992). Note that this scenario is compatible with the observation that the [Fe/H]<-2 stars have the same mean [Ti/Fe] abundance as the rest of the RGB-MP population because, as mentioned above, the titanium

yields from $>20 M_{\odot}$ stars are comparable to those of lower mass stars. Additionally, if a monotonic relationship between [Fe/H] and formation time exists for at least the RGB–MP stars, then the mass dependent yields may also explain the apparent decrease in [Si,Ca/Fe] as [Fe/H] increases from ~ -2 to -1.6 , as well as, the steeper decline for [Si/Fe] compared to [Ca/Fe]. As indicated by Figure 14, the decline in Si yield is a stronger function of progenitor mass between 18 – $25 M_{\odot}$ than for Ca. Therefore, forming stars from gas polluted by progressively less massive SNe should qualitatively reproduce the observed trend. The sudden increase in [Si,Ca/Fe] in the RGB–Int1 population would then make sense if a new round of star formation began with $>20 M_{\odot}$ stars contributing once again.

5.1.1. Are Type Ia SNe Required?

Since previous analyses have estimated that the age spread among the various ω Cen populations is ~ 2 – 4 Gyr (e.g., Stanford et al. 2006), it would seem reasonable to assume that Type Ia SNe could have contributed to the cluster’s chemical enrichment. However, the consistently elevated $[\alpha/\text{Fe}]$ ratios observed for nearly all stars in the cluster suggests that Type Ia enrichment has been limited. Pancino et al. (2002) and Origlia et al. (2003) found in a small sample of ω Cen giants that the RGB–a stars had noticeably lower $[\alpha/\text{Fe}]$ and higher $[\text{Cu}/\text{Fe}]$ abundances than the lower metallicity stars, and attributed these trends to the onset of Type Ia SNe at $[\text{Fe}/\text{H}] > -1$. On the other hand, Cunha et al. (2002) analyzed $[\text{Cu}/\text{Fe}]$ abundances in a larger sample spanning $[\text{Fe}/\text{H}] \sim -2$ to -0.8 , and did not find evidence for an increase in $[\text{Cu}/\text{Fe}]$. Similarly, Norris & Da Costa (1995) and Smith et al. (2000) did not find evidence for a decrease in $[\alpha/\text{Fe}]$ or an increase in $[\text{Cu}/\text{Fe}]$.

While the primary production source of Cu is uncertain (e.g., Sneden et al. 1991b; Matteucci et al. 1993), it is clear that ambiguity remains regarding the significance of Type Ia SNe to ω Cen’s chemical evolution. Our data are generally inconsistent with the rather extreme 75% Type Ia to 25% Type II mixture plotted in Figure 13, especially at $[\text{Fe}/\text{H}] < -1$. Although we find a slight decrease in $[\text{Ca}/\text{Fe}]$ at $[\text{Fe}/\text{H}] > -0.7$, at least part of this decrease may be explained by a reduction in calcium yields from more metal-rich Type II SNe (e.g., see Figures 13–14). Interestingly, the $[\text{Si}/\text{Fe}]$ and $[\text{Ti}/\text{Fe}]$ ratios do not exhibit similar decreases at $[\text{Fe}/\text{H}] > -0.7$. However, the larger measurement error for silicon compared to calcium may be masking any subtle trends, and although titanium is often enhanced like other α elements in globular cluster stars its dominant isotope ^{48}Ti is not an α isotope. Additionally, analyzing different mixtures of Type II versus Ia ejecta requires inherent assumptions about the massive star IMF and the source of Type Ia SNe, which in Figure 13 is the “standard” white dwarf deflagration model. The model values shown in Figure 13 could easily be changed by using

different assumptions and adjusting the aforementioned parameters.

A more empirical approach is to compare the evolution of α and Fe–peak elements with other stellar populations exhibiting different levels of Type Ia enrichment. In Figures 15–17 we plot our derived abundances for ω Cen stars as a function of [Fe/H], and compare with data from the literature tracing the chemical evolution of other globular clusters, the Galactic thin/thick disk, halo, bulge, and nearby dwarf galaxies (see Table 8 for literature references). Focusing on the heavy α and Fe–peak elements at the metal–rich end of the distribution shows that, at least for stars with $[{\rm Fe}/{\rm H}] < -0.7$, ω Cen generally follows a morphology similar to that found in monometallic globular clusters, the Galactic halo, and the Galactic bulge. In contrast, the most metal–rich ω Cen stars ($[{\rm Fe}/{\rm H}] > -0.7$) exhibit [Ca/Fe] ratios that are more similar to those found in Galactic thick disk stars (e.g., see Brewer & Carney 2006). Additionally, the most metal–rich ω Cen stars tend to exhibit [Ca/Fe] ratios that are, on average, at least 0.1–0.2 dex lower than those found in the more metal–poor stars. This may indicate that the level of Type Ia enrichment in the most metal–rich ω Cen stars and the thick disk were comparable. However, at $[{\rm Fe}/{\rm H}] > -0.7$ the [Ni/Fe] ratios are noticeably low in the ω Cen stars, and as mentioned previously the [Si/Fe] and [Ti/Fe] data do not exhibit similar abundance decreases in concert with [Ca/Fe]. Although ω Cen is widely believed to be the remnant core of a dwarf spheroidal galaxy, the heavy α elements are enhanced in ω Cen stars by a factor of 2–3 compared with other dwarf galaxies, at least for $[{\rm Fe}/{\rm H}] \gtrsim -1.5$.

In addition to the heavy α and Fe–peak elements, the lighter elements O, Na, and Al are also inconsistent with significant contributions from Type Ia SNe. Figure 13 shows that nearly all of the stars with $[{\rm Fe}/{\rm H}] > -1$ have [Na/Fe] and [Al/Fe] abundances that are well above even the levels predicted by Type II SNe, but [O/Fe] is abnormally low. The abundance patterns expected from Type Ia production should lead to an overall decrease in the average abundance of all three elements as [Fe/H] increases. However, these elements can be altered by either *in situ* mixing or pollution from other sources, and therefore may not be reliable indicators of a star’s original composition. While the heavy α element data, in particular [Ca/Fe], provide some evidence for Type Ia SN contributions in the most metal–rich stars, the light element data are in better agreement with a Type II SN pollution model that includes an additional proton–capture production mechanism. The apparent suppression of Type Ia SNe in ω Cen remains an open problem, but it may be at least partially tied to the cluster’s several Gyr relaxation time scale (e.g., van de Ven et al. 2006) and low (~ 3 –4%) binary frequency (Mayor et al. 1996).

5.2. Proton–Capture Processing: Light Element Variations

The light elements oxygen through aluminum provide sensitive diagnostics for determining the chemical enrichment history of stellar populations. These elements are primarily produced in the hydrostatic helium, carbon, and/or neon burning stages of massive ($\gtrsim 10 M_{\odot}$) stars (e.g., Arnett & Thielemann 1985; Thielemann & Arnett 1985; Woosley & Weaver 1995). Stars forming out of gas that has been primarily polluted by Type II SNe should have $[O/Fe] \sim +0.4$ and exhibit increasing $[Na/Fe]$ and $[Al/Fe]$ abundances with increasing metallicity. However, these elements can also be produced (or destroyed) in lower mass stars that reach internal temperatures high enough to activate the proton–capture ON, NeNa, and MgAl cycles. If this processed material is mixed to the surface, then some stars may return gas to the ISM that is O–poor and Na/Al–rich compared to the material ejected by Type II SNe. This scenario is believed to occur in the RGB and AGB phases of low and intermediate mass ($\lesssim 8 M_{\odot}$) stars (e.g., Sweigart & Mengel 1979; Cottrell & Da Costa 1981; Denisenkov & Denisenkova 1990; Langer et al. 1993; Ventura & D’Antona 2009; Karakas 2010), but also in the cores of massive, rapidly rotating main sequence stars (e.g., Decressin et al. 2007).

Figures 15–18 highlight the distinct light element abundance patterns found in several different stellar populations. Examination of these trends indicates that although ω Cen shares some abundance patterns with other globular cluster, Galactic disk, halo, bulge, and nearby dwarf galaxy stars, it differs from all of these both in the extent of its star-to-star abundance variations and its individual abundance ratios. Approximately half of the RGB–MP stars have O, Na, and Al abundances that are consistent with those found in similar metallicity halo, and to a lesser extent, dwarf galaxy stars. The chemical composition of these stars is believed to be primarily a result of Type II SN enrichment, and the chemical similarities among these populations is not unexpected. It seems likely that ω Cen would have had considerable interaction with the primordial gas that formed the Galactic halo, and it has been shown that reproducing the cluster’s metallicity distribution function is only possible in an open box scenario (e.g., Ikuta & Arimoto 2000; Romano et al. 2007). However, the remaining RGB–MP stars exhibit $[O/Fe]$, $[Na/Fe]$, and $[Al/Fe]$ abundances that are significantly different than those found in metal–poor halo and dwarf galaxy stars. In particular, the “enhanced” RGB–MP stars are O–poor and Na/Al–rich. Similar chemical compositions are only found in some monometallic globular cluster stars (e.g., see reviews by Kraft 1994; Gratton et al. 2004). Interestingly, the number of stars in ω Cen that are O–poor and Na/Al–rich increases to 60–95% at higher metallicities. The RGB–Int2+3, and especially the RGB–a, stars have $[O/Fe]$, $[Na/Fe]$, and $[Al/Fe]$ ratios that differ significantly even from individual globular clusters by at least a factor of two. Figure 18 shows that this is true even when considering $[O/Na]$, $[O/Al]$, and $[Na/Al]$ ratios instead of $[X/Fe]$. Our data indicate that the ω Cen stars at $[Fe/H] \gtrsim -1.3$ experienced an additional enrichment process

that is not observed in any other stellar system studied so far, but the combined populations of M54 and the Sagittarius dwarf galaxy may share some similar trends (Carretta et al. 2010).

The light element abundance patterns in other globular clusters are typically believed to be the result of high temperature proton–capture nucleosynthesis operating in an environment where a combination of the ON, NeNa, and MgAl cycles are or were active. Material that has been processed through these proton–capture cycles is expected to exhibit a deficiency in [O/Fe] concurrent with supersolar [Na/Fe] and [Al/Fe] ratios, which should naturally lead to O–Na and O–Al anticorrelations along with a Na–Al correlation. In Figures 19–21, we plot [O/Fe], [Na/Fe], and [Al/Fe] against each other for the major ω Cen populations described in §4.1. We find that the O, Na, and Al abundance relations found in the RGB–MP, RGB–Int1, and RGB–Int2+3 populations are consistent with the abundance patterns that are characteristic of high temperature proton–capture processing. Furthermore, the impact of proton–capture nucleosynthesis appears to increase as a function of increasing metallicity. Both the extent of the light element variations and the percentage of stars that are O–poor and Na/Al–rich increases monotonically with [Fe/H]. However, the same O–Na, O–Al, and Na–Al relations are not observed in the RGB–a population. Instead, the RGB–a, as well as a few RGB–Int2+3, stars exhibit a rather uniform composition that is moderately O–poor ($[O/Fe] \sim -0.15$), very Na–rich ($[Na/Fe] \sim +0.78$), and is unlike any of the more metal–poor ω Cen stars.

A common interpretation of the light element abundance trends in monometallic globular clusters is that the O–rich, Na/Al–poor stars represent the first generation of stars formed from the ejecta of Type II SNe, and the O–poor, Na/Al–rich stars represent a subsequent generation formed from gas that had been chemically enriched by intermediate mass AGB stars or some other polluting source in which the ON, NeNa, and/or MgAl cycles were active (e.g., D’Ercole et al. 2008; Carretta et al. 2009b). The first generation stars are often referred to as “primordial” stars, and the enriched populations are referred to as either “intermediate” or “extreme”, depending on the level of O–depletion and Na–enrichment (e.g., Carretta et al. 2009a; but see also Lee 2010 for a different interpretation).

The ω Cen data can be divided into similar subpopulations. Here we follow a similar definition to that used in Carretta et al. (2009a) where the primordial component is defined as having $[O/Fe] \geq 0$ and $[Na/Fe] \leq +0.1$, the intermediate component includes stars with $[O/Fe]$ ratios satisfying the relation $[O/Fe] \geq [0.62([Na/Fe]) - 0.65]$, and the extreme component consists of the remaining most O–poor stars. Monometallic globular clusters typically consist of $\sim 20\text{--}40\%$ of stars belonging to the primordial component, $\sim 30\text{--}80\%$ in the intermediate component, and $\lesssim 20\%$ in the extreme component (e.g., Carretta et al. 2009a). As can be

seen in Figures 19–21, the RGB–MP stars follow the general trend observed in monometallic globular clusters with a primordial:intermediate:extreme distribution of 50%:43%:7%, respectively. The RGB–Int1 population contains roughly an equal proportion of primordial, intermediate, and extreme abundance stars with a distribution of 30%:32%:38%. However, the RGB–Int2+3 and RGB–a stars contain far more extreme abundance stars than are found in any globular cluster with distributions of 11%:15%:74% and 5%:14%:81%, respectively. The large number of intermediate and extreme abundance stars indicates that ω Cen likely experienced a similar enrichment process to that in monometallic globular clusters during each round of star formation, and it is interesting to note that the populations expected to be He-rich exhibit the largest fraction of extreme abundance stars. While there is a clear delay in the onset of whichever mechanism drives the O-poor, Na/Al-rich abundance phenomenon, it is worth noting that we find a very low incidence of carbon stars¹⁶ (<2%; see Figure 1) despite the large population of O-poor stars. Unfortunately, we cannot distinguish between *in situ* carbon stars and those formed from mass transfer, but the frequency of carbon stars on the giant branch is consistent with the expected binary fraction of \sim 3–4% (Mayor et al. 1996).

5.2.1. Enrichment by Pollution and *in situ* Processing

Although we have identified the major light element abundance trends for ω Cen, the information so far has only led us to conclude that proton–capture nucleosynthesis has likely played a significant role in the cluster’s chemical enrichment. Further examination is required in order to understand the possible location(s) where these processes are or were active. The comparatively small star-to-star dispersion in [X/Fe] exhibited by the heavy α and Fe-peak elements (see Figure 10) indicates that the >1 dex variations observed for [O/Fe], [Na/Fe], and [Al/Fe] are not due to incomplete mixing of SN ejecta, as is suspected for [Fe/H]<−3 halo stars (e.g., McWilliam 1997). Previous studies have found that many of the light element abundance patterns exhibited by monometallic globular cluster stars, which are subsequently shared by many ω Cen stars, may be best explained by proton–capture nucleosynthesis operating at temperatures near 70×10^6 K (e.g., Langer et al. 1997; Prantzos et al. 2007). If at least part of the abundance patterns found in ω Cen and other

¹⁶While we do not provide explicit carbon abundance measurements in this paper, the possible carbon stars listed in Figure 1, Figure 3, and Table 2 were identified by visual inspection of their spectra. However, all three of the possible carbon stars identified here that also overlap with the van Loon et al. (2007) survey (LEID 32059, 41071, and 52030) are confirmed carbon stars based on the presence of strong C₂ bands in their spectra.

globular cluster stars are due to pollution from external sources, then the currently favored production mechanisms are: (1) hot bottom burning in $>5 M_{\odot}$ AGB stars (e.g., Ventura & D'Antona 2009; Karakas 2010), (2) hydrogen shell burning in now extinct but slightly more massive RGB stars (Denissenkov & Weiss 2004), and (3) core hydrogen burning in rapidly rotating massive stars (Decressin et al. 2007).

While massive, rapidly rotating stars and extinct $\sim 0.9\text{--}2 M_{\odot}$ RGB stars may also reproduce many of the observed light element trends, presently there are no detailed theoretical yields spanning a fine grid of metallicities similar to those available for intermediate mass AGB stars. Furthermore, the time scale of pollution from extinct low mass RGB stars is at least 2–3 times longer than the estimated age spread among the different ω Cen populations, but this does not rule out possible mass transfer pollution from these objects. Additionally, the massive, rapidly rotating star scenario is expected to produce a continuum of polluted stars with varying He abundances (Renzini 2008), which is inconsistent with the singular $Y=0.38$ value that seems required to fit the blue main sequence (e.g., Piotto et al. 2005). Romano et al. (2010) also point out that if the winds from massive main sequence stars are also responsible for the anomalous light element abundance variations in the current generations of ω Cen stars, it is not clear why the He enrichment was delayed until higher metallicities. However, Renzini (2008) and Romano et al. (2010) find that intermediate mass AGB stars may provide a reasonable explanation for the high He content in some stars, in addition to the *average* behavior of [Na/Fe], and to a lesser extent [O/Fe], in ω Cen. Therefore, we will only consider the AGB pollution scenario here, but we caution the reader that several qualitative and quantitative hurdles remain in order for AGB pollution to be a viable explanation of light element variations in globular clusters (e.g., Denissenkov & Herwig 2004; Denissenkov & Weiss 2004; Fenner et al. 2004; Ventura & D'Antona 2005; Bekki et al. 2007; Izzard et al. 2007; Choi & Yi 2008).

In Figure 22, we plot our derived O, Na, and Al abundances as a function of [Fe/H], and overplot the metallicity dependent theoretical yields from Type II SNe, as well as, $3\text{--}6 M_{\odot}$ AGB stars. While the ω Cen stars with chemical compositions similar to the Galactic disk and halo appear well bounded by production from Type II SNe, the enhanced stars at least qualitatively follow the general trends predicted by production from $>5 M_{\odot}$ AGB stars. In particular, the depletion of oxygen concurrent with the rise in sodium and decline in the *maximum* [Al/Fe] ratio with increasing metallicity are all consistent with the predicted patterns exhibited by material that has been processed via hot bottom burning in $>5 M_{\odot}$ AGB stars. However, the theoretical AGB yield curves shown in Figure 22 do not include lifetime estimates for the polluting AGB stars, and one could envision sliding the various curves along the abscissa to account for age differences among the different populations. In other words, plots similar to Figure 22 lend insight into whether the abundance trends

are possibly consistent with AGB pollution, but numerical chemical evolution models are required to fully constrain which mass ranges have contributed to the chemical composition of stars in a given population.

Despite this limitation, we can use Figure 22 to elicit some constraints. We find that while $5\text{--}6 M_{\odot}$ AGB ejecta are generally consistent with the abundance trends observed at all metallicities, $3\text{--}4 M_{\odot}$ AGB stars likely did not contribute significantly to ω Cen’s chemical enrichment until about $[\text{Fe}/\text{H}] = -1.3$. This is most evident by examining the $[\text{O}/\text{Al}]$ and $[\text{Na}/\text{Al}]$ ratios in Figure 22. The $<5 M_{\odot}$ AGB stars produce $[\text{O}/\text{Fe}]$ and $[\text{Na}/\text{Fe}]$ ratios that are too high and $[\text{Al}/\text{Fe}]$ ratios that are too low to fit the data, even when diluted with SN or $>5 M_{\odot}$ AGB ejecta. Figures 19–21 also support the rejection of $3\text{--}4 M_{\odot}$ AGB ejecta, *which originate from AGB stars of comparable metallicity*, from contributing significantly to the chemical composition of stars with $[\text{Fe}/\text{H}] < -1.3$. However, Figures 19–22 do not rule out that $<5 M_{\odot}$ AGB stars with $[\text{Fe}/\text{H}] \lesssim -1.5$ impacted enrichment of the RGB–Int2+3 and RGB–a populations. The $[\text{Na}/\text{Fe}]$ and $[\text{Al}/\text{Fe}]$ yields from metal–poor AGB stars are mostly consistent with the trends observed in the intermediate and most metal–rich ω Cen giants, but it seems that an additional mechanism may be required to explain the $[\text{O}/\text{Fe}]$ abundances. Note that our conclusions are not drastically altered if we adopt the theoretical AGB yields from Karakas (2010)¹⁷, which uses mixing length theory for convection, instead of the Ventura & D’Antona (2009) yields, which use the full spectrum of turbulence theory for convection and are shown in Figures 19–22. Unfortunately, Karakas (2010) does not provide yield information for metallicities between $[\text{Fe}/\text{H}] = -2.3$ and -0.7 , which makes direct comparison with ω Cen difficult because most stars fall in the missing range.

One of the most puzzling aspects concerning the abundance patterns of light elements in ω Cen is the strongly bimodal distribution at intermediate metallicities (see Figure 11). If ISM pollution was driven by AGB stars, then it is unclear why (1) only the RGB–MP stars exhibit a continuous distribution of $[\text{O}/\text{Fe}]$, $[\text{Na}/\text{Fe}]$, and $[\text{Al}/\text{Fe}]$ abundances and (2) more than 70% of the more metal–rich stars have envelope material that has experienced significant proton–capture processing. As can be seen in Figures 19–22, the $[\text{O}/\text{Fe}]$ yields from AGB stars are by far the most inconsistent with our data, but the full mass range of AGB stars may reproduce the $[\text{Na}/\text{Fe}]$ and $[\text{Al}/\text{Fe}]$ abundances at nearly all metallicities. Depleting the oxygen abundance from $[\text{O}/\text{Fe}] = +0.4$ to $[\text{O}/\text{Fe}] < -0.4$ via hot bottom burning in AGB stars is generally not achieved for any mass or metallicity range. However, D’Ercole et al. (2010) showed that including the ejecta of “super–AGB” ($>6.5 M_{\odot}$) stars may reproduce the super O–poor ($[\text{O}/\text{Fe}] < -0.4$) abundances found in some globular clusters under the

¹⁷This statement is based on using the average mass fraction data from Tables A2–A6 in Karakas (2010).

assumption that the massive AGB stars deplete to $[O/Fe] \approx -1$. Despite this, it is unlikely that more massive AGB stars are the culprits behind the large contingent of super O-poor ω Cen stars because one would have to assume an IMF strongly weighted toward $\sim 5\text{--}9 M_\odot$ stars in order to produce so many super O-poor stars. Note that this is not as much of a problem in monometallic globular clusters because the number of super O-poor stars is $< 20\%$ (e.g., Carretta et al. 2009a). It seems that invoking some degree of *in situ* proton-capture processing is required to explain the observed abundance patterns of ω Cen stars with $[Fe/H] \gtrsim -1.6$, in order to avoid unrealistic requirements such as IMFs strongly weighted toward intermediate mass stars or forming a majority of the RGB-Int1, RGB-Int2+3, and RGB-a stars almost entirely out of a narrow mass range of AGB stars.

A key assumption when considering *in situ* processing in low mass RGB stars is that the material being enriched near the hydrogen burning shell must be able to mix into the convective envelope and be brought to the surface. In stars with normal helium abundances, it is not believed that this can occur until the hydrogen burning shell erases the molecular weight barrier left behind by the convective envelope after first dredge-up (e.g., see review by Salaris et al. 2002). However, some or all of the intermediate metallicity stars in ω Cen are thought to be quite He-rich, and D’Antona & Ventura (2007) found that stars with $Y=0.35\text{--}0.40$ should contain a much more shallow molecular weight gradient that might not inhibit deep mixing. Instead, deep mixing in He-rich stars might be active over a wide range of luminosities on the giant branch, which would be consistent with our observation that the degree of light element enrichment is not strongly correlated with luminosity. These authors also find that reproducing the abundance patterns exhibited by the super O-poor stars can be achieved by *in situ* mixing if the RGB stars are already polluted by the ejecta of intermediate mass AGB stars. In their scenario, *in situ* mixing should decrease the envelope $[O/Fe]$ ratio by up to a factor of 10 while only increasing the $[Na/Fe]$ ratio by about 0.2 dex. While the evolution of $[Al/Fe]$ is not reported by D’Antona & Ventura (2007), we can speculate that the enhancement in $[Al/Fe]$ is smaller than that experienced by $[Na/Fe]$ given the higher temperatures required to convert Mg to Al.

As mentioned above, the proposed deep mixing scenario only works if the intermediate metallicity RGB stars in ω Cen formed from material that was already enriched by hot bottom burning in intermediate mass AGB stars. Our current data set does not provide direct evidence of this, but we may look to the behavior of silicon as a proxy indicator because ^{28}Si can be produced through leakage from the MgAl cycle at temperatures $> 65 \times 10^6$ K (e.g., Yong et al. 2005; Carretta et al. 2009b). In Figure 23, we plot our $[X/Fe]$ abundances as a function of $[Fe/H]$ color coded by the primordial, intermediate, and extreme abundance components described above. While most of the α and Fe-peak elements do not display any particular dependence on light element abundance, the RGB-MP and RGB-Int1 extreme

component stars exhibit silicon enhancements of nearly 0.3 dex compared to the primordial and intermediate component stars. Furthermore, in Figure 24 we plot [O/Fe], [Na/Fe], and [Al/Fe] versus [Si/Fe], [Ca/Fe], and [Ti/Fe] and find that only silicon shows any semblance of a correlation with O, Na, and Al, as is indicated by the respective Pearson correlation coefficients shown in Figure 24. This suggests that silicon may have undergone an additional production process not experienced by the heavier α elements. The existence of an Al–Si correlation concurrent with an O–Si anticorrelation suggests that the O–poor stars were likely polluted by material that had been processed at temperatures exceeding $\sim 65 \times 10^6$ K. These conditions are reached during hot bottom burning in intermediate mass AGB stars, but not in the hydrogen burning shells of low mass RGB stars.

Since the ω Cen stars likely satisfy the prerequisites needed for *in situ* mixing to occur, we may attribute a large portion of the [O/Fe], and to a lesser extent the [Na/Fe], variations to this process. The relatively small number of RGB–MP stars that are super O–poor suggests that the helium content had not yet been significantly increased in the cluster to allow the formation of He–rich stars. In fact, there are very few super O–poor stars at $[Fe/H] < -1.7$. The radial segregation of O–poor stars (see Figure 9) is also consistent with the idea that additional time was needed to increase the cluster He content, and may indicate that He–rich gas was preferentially funneled into the cluster core, as is suggested in the models by D’Ercole et al. (2008). We find that the light element abundance trends in the intermediate metallicity and RGB–a stars are consistent with an AGB pollution plus *in situ* mixing scenario. In these stars, the high [Na/Fe] and [Al/Fe] abundances are consistent with production in comparable metallicity or more metal–poor AGB stars because *in situ* mixing is not expected to significantly increase [Na/Fe] or [Al/Fe] in He–rich RGB stars that are already O–poor and Na/Al–rich (D’Antona & Ventura 2007). Additionally, the increasing minimum [O/Fe] abundance at $[Fe/H] \gtrsim -1$ is consistent both with the increase in the [O/Fe] yields for $> 5 M_\odot$ AGB stars and the fact that *in situ* mixing should produce less advanced proton–capture processing at higher metallicities. This is due primarily to the lower temperatures achieved in the interiors of more metal–rich stars, but may also occur if the He mass fraction in the RGB–a stars is smaller than in the RGB–Int2+3 stars, which could lead to more shallow mixing. Lastly, we note that because the [Na/Fe] and [Al/Fe] abundances do not share the same correlation as [O/Fe] with radial location, it may be the case that some stars producing high Na and Al yields do not necessarily produce large He yields.

One of the most important effects of including *in situ* mixing in the chemical enrichment picture is that it reduces the necessity for AGB stars to account for all abundance patterns, and also increases the mass range of available AGB polluters to more than just those with favorable yields. The inferred high He–content of the blue main sequence population and the

observed large increase in s-process enrichment in this cluster indicate that the large degree of ISM pollution required for the above scenario to work is not unreasonable. A detailed comparison of the ^{24}Mg , ^{25}Mg , and ^{26}Mg isotopes may be particularly illuminating in order to investigate whether hot bottom burning, *in situ* processing, or both played an active role in shaping the abundance patterns of ω Cen giants. Note that fluorine is also expected to be strongly depleted in the proposed deep mixing scenario. Furthermore, a large sample spectroscopic abundance analysis of stars at lower luminosities could provide an interesting test for the impact of *in situ* mixing.

5.2.2. Oxygen Abundances and a Possible Connection to the Blue Main Sequence

The discovery and subsequent detailed analyses of ω Cen’s blue main sequence (Anderson 1997, 2002; Bedin et al. 2004; Norris 2004; Piotto et al. 2005; Sollima et al. 2007; Bellini et al. 2009b) have revealed that this population represents $\sim 30\%$ of all main sequence stars, is preferentially located near the cluster center, and perhaps most importantly is more metal-rich than the dominant red main sequence. As mentioned in §1, the commonly accepted reason for the existence of the blue main sequence is that these stars are significantly more He-rich than the dominant population of more metal-poor stars. In fact, Norris (2004) and Piotto et al. (2005) find that the blue main sequence is best fit with an extreme helium abundance of $Y \approx 0.38$. One of the most interesting characteristics of the blue main sequence is that it is well detached from the red main sequence in color, and almost no stars are found in between the two sequences (e.g., see Bedin et al. 2004; their Figure 1). From this and the information above, we might expect the current RGB stars that were once part of the blue main sequence to be chemically conspicuous, preferentially located near the cluster center, and more metal-rich than the dominant stellar population.

Examination of the abundance patterns in the RGB-Int1 and RGB-Int2+3 stars reveals that the [O/Fe] ratio stands out as a possible indicator of which stars once belonged to the blue main sequence. At intermediate metallicities, a majority of the stars have $[\text{O}/\text{Fe}] \leq 0$, and the radial distribution of these stars shows that more than 90% are located inside $10'$ from the cluster center while only 70% of those with $[\text{O}/\text{Fe}] > 0$ are located in the same range (see Figure 9). However, in order for the [O/Fe] abundance to be considered as a chemical tracer of the blue main sequence it must qualitatively and quantitatively agree with the observed trends of blue main sequence stars. In Figure 25, we plot the number ratio of O-poor to O-rich stars out to $\sim 15'$, and also plot the measured number ratios of blue to red main sequence stars from Bellini et al. (2009b). Although we are plotting an indirect measurement of the ratio of blue to red main sequence stars with $N_{\text{O-poor}}/N_{\text{O-rich}}$ and the

Bellini et al. (2009b) data represent direct measurements, we find that the two trends are in reasonable agreement. Both data sets indicate that the majority of O-poor (blue main sequence) stars are inside $\sim 5'$ of the cluster center, and the *relative* ratio of O-poor/O-rich (blue/red main sequence) stars decreases at larger radii. Note that Sollima et al. (2007) come to a similar conclusion when considering stars located at $\sim 7\text{--}23'$ from the cluster center.

Since the relative ratios of O-poor to O-rich stars follow those observed for the blue and red main sequences, we may expect the absolute number of O-poor stars to also be consistent with that of the blue main sequence stars due to our high completion percentage (see Figure 2). As mentioned previously, it is estimated that the blue main sequence constitutes $\sim 25\text{--}35\%$ of all main sequence stars, and we find in agreement with this estimate that 27% of all RGB stars in our sample are O-poor. Additionally, Piotto et al. (2005) showed that the blue main sequence is best fit by a metallicity similar to that of the RGB-Int1 and RGB-Int2+3 populations. We find that at least 65% of the O-poor stars in our sample are located in the appropriate metallicity range. This percentage may in fact be somewhat larger if we consider that (1) very few O-poor stars are found at $[\text{Fe}/\text{H}] < -1.7$, (2) the average $[\text{Fe}/\text{H}]$ abundance error is roughly ± 0.1 dex, and (3) the boundary between the RGB-MP and RGB-Int1 populations is not uniquely defined. However, we would still find that $\sim 20\text{--}30\%$ of intermediate metallicity stars are O-rich. Note that a significant number of O-rich, intermediate metallicity stars (i.e., stars in the correct metallicity range that would not lie on the blue main sequence) would be consistent with the observation by Sollima et al. (2006) that many RR Lyrae stars with $[\text{Fe}/\text{H}] \sim -1.2$ have standard helium abundances.

In any case, we have demonstrated that the O-poor giants are spatially similar, found mostly in the same metallicity range, and are present in nearly identical proportions to those found on the blue main sequence. It is not entirely clear why the $[\text{O}/\text{Fe}]$ ratio in the giants shares a similar sensitivity to radial location and metallicity with the blue main sequence stars, but we speculate that the oxygen deficient stars are connected with the blue main sequence through helium enrichment. That is, the He-rich main sequence stars are pushed blueward on the color-magnitude diagram, and the He-rich giants experience *in situ* mixing that strongly depletes oxygen without similarly large increases in sodium and aluminum. Comparison between the 7770 Å oxygen triplet line strengths in blue and red main sequence stars would provide a direct confirmation of our hypothesis. Although we have invoked *in situ* mixing to explain the very large O-depletion in these stars, note again that the scenario proposed by D'Antona & Ventura (2007) requires that these star were already somewhat O-poor.

5.3. Neutron-Capture Processing

While the isotopes of most elements lighter than about zinc are produced primarily through charged particle reactions, the isotopes of elements beyond the Fe-peak are mostly produced through neutron-capture reactions. Neutron-capture nucleosynthesis is believed to proceed through two main channels: (1) the s-process where the neutron-capture rate is slow compared to the β -decay rate of unstable nuclei and (2) the r-process where the neutron-capture rate is fast compared to the β -decay rate of unstable nuclei (e.g., see recent review by Sneden et al. 2008). The large difference in neutron fluxes required for the two processes points to different operational environments. The main component of the s-process is widely believed to be active in thermally pulsing low and intermediate mass AGB stars, but theoretical models indicate that most of the s-process element production is probably constrained to stars in the range $\sim 1.3\text{--}3 M_{\odot}$ (e.g., Busso et al. 1999; Herwig 2005; Straniero et al. 2006). AGB stars $\lesssim 1.3 M_{\odot}$ have envelope masses that are too small for third dredge-up to occur, and more massive AGB stars are only believed to experience a few third dredge-up episodes. Conversely, the exact location(s) where the r-process operates is (are) not well defined, but significant circumstantial evidence suggests an explosive origin associated with core collapse SNe (e.g., Mathews & Cowan 1990; Cowan et al. 1991; Wheeler et al. 1998; Arnould et al. 2007; Sneden et al. 2008).

The solar system abundances indicate that $\sim 70\text{--}75\%$ of lanthanum is produced via the s-process and more than 95% of europium is produced by the r-process (e.g., Sneden et al. 1996; Bisterzo et al. 2010). Therefore, we adopt lanthanum as an s-process indicator and europium as an r-process indicator. As can clearly be seen in Figure 17, the average [La/Fe] ratio increases by more than a factor of three between the RGB-MP and intermediate metallicity populations. Similar increases are not found for any other elements in our sample. This indicates that the s-process has played a significant role in the chemical evolution of ω Cen, and is a dominant process at $[Fe/H] \gtrsim -1.6$. Comparison with the other stellar populations plotted in Figure 17 shows that the level of s-process enrichment was far greater in ω Cen. It is interesting to note that the [La/Fe] ratio does not continue to increase beyond $[Fe/H] \geq -1.5$ despite the fact that s-process production appears to peak in the metallicity range $-1.5 \lesssim [Fe/H] \lesssim -0.8$, at least for the “standard” ^{13}C pocket (e.g., see Bisterzo et al. 2010, their Figure 8). This may indicate that a large fraction of the gas was swept out of the cluster through interaction with the Galaxy before low mass AGB stars with $[Fe/H] \gtrsim -1.5$ had a chance to contribute to ω Cen’s chemical enrichment. Comparison between the RGB-Int2+3 and RGB-a stars shows that the average [La/Fe] ratio decreases by ~ 0.2 dex (see Figure 12) for higher metallicities, but is still significantly enhanced compared to the Galactic disk and bulge trends. This suggests that s-process production still continued at high metallicities, but the rate of production did not exceed that of iron.

For the RGB–MP stars, the average [Eu/Fe] abundances are similar to those found in halo, dwarf galaxy, and individual globular cluster stars. At higher metallicities, the average [Eu/Fe] abundance of ω Cen stars actually decreases while the average [La/Fe] abundance shows a significant increase. In fact, many intermediate metallicity ω Cen stars have [Eu/Fe] abundances that are lower than those found in halo and dwarf galaxy stars, and are especially Eu-deficient compared to globular cluster stars. However, the average [Eu/Fe] abundance increases again at $[Fe/H] \gtrsim -1.2$ toward values similar to those found in the Galactic disk and bulge. The cause of the decrease in [Eu/Fe] at intermediate metallicities, and the low [Eu/Fe] abundances in general, is not entirely clear. It is believed that $\sim 8\text{--}10 M_{\odot}$ SNe may produce a large portion of the r-process elements (e.g., Mathews & Cowan 1990), but other processes such as neutron star and black hole mergers may be important as well (e.g., see review by Sneden et al. 2008 and references therein). It may be the case that either the IMF did not favor a large number of stars in the $8\text{--}10 M_{\odot}$ range or that one or more of the typical r-process production mechanisms was not active at “normal” levels in the intermediate metallicity range. Interestingly, the metallicity range at which the [Eu/Fe] abundance is lowest is also where Cunha et al. (2002; 2010) find low [Mn/Fe] and [Cu/Fe] values. Since Cunha et al. (2010) attributes the low [Cu/Fe] and [Mn/Fe] abundances to metallicity dependent SN yields, we can speculate that the low [Eu/Fe] values might also be due to a related effect. Although manganese and europium are produced through different processes, their production may be tied to similar progenitor objects and/or environments.

Despite the obvious differences in [La/Fe] and [Eu/Fe] abundances for ω Cen stars compared to those in other populations, the ratio of these elements provides a better diagnostic for analyzing the impact of the s- and r-processes. In the Galactic disk and halo, the [La/Eu] ratio slowly increases with metallicity, and this is believed to be primarily due to the longer time scales required for low and intermediate mass stars to evolve into AGB stars (e.g., Simmerer et al. 2004). Dwarf galaxies also tend to exhibit an increase in s-process elements at higher metallicities, but are typically more s-process enhanced than similar metallicity halo and disk stars (e.g., Geisler et al. 2007). In contrast, most globular clusters follow the disk/halo trend and are generally r-process rich (e.g., Gratton et al. 2004). Figure 18 plots the [La/Eu] ratio as a function of [Fe/H] for these populations and also illustrates the relatively rapid transition in ω Cen from being r-process to s-process dominated. Many stars in the RGB–MP population exhibit [La/Eu] ratios that are identical to those found in halo, dwarf galaxy, and globular cluster stars. However, almost all of the more metal-rich stars have $[La/Eu] > 0$, and many of these stars have [La/Eu] ratios matching those expected for pure s-process production. Note that proper accounting of hyperfine structure for both the La and Eu lines has revised our [La/Eu] ratios downward, at least for the most La-rich stars, from those found in Johnson et al. (2009). The new results are consistent with the

more metal-rich stars forming from gas that was already heavily polluted with s-process elements, but does not require surface pollution from mass transfer. This is in agreement with the results from Stanford et al. (2010), which suggest that the strontium abundances (a light s-process element) in several ω Cen stars are the result of primordial pollution rather than surface accretion.

Although AGB stars of about $1.3\text{--}8 M_{\odot}$ may be able to produce s-process elements, Smith et al. (2000) used the [Rb/Zr] ratio to show that AGB stars between $\sim 1.5\text{--}3 M_{\odot}$ were likely the dominant s-process enrichment sources in ω Cen. Since these stars have lifetimes of $3 \times 10^8\text{--}2 \times 10^9$ years, the time delay between the formation of RGB-MP stars and subsequent generations had to be at least this long. This delay is consistent with the estimated 2–4 Gyr age range of ω Cen stars (e.g., Stanford et al. 2006), and is also consistent with the time required for $>4\text{--}5 M_{\odot}$ AGB stars to have polluted the ISM, as seems required to explain at least part of the light element abundance trends.

In addition to analyzing the behavior of elements produced exclusively through neutron-capture processes, we can also examine how neutron-capture nucleosynthesis may have affected the abundances of lighter elements. In Figure 26, we plot multiple elements as a function of lanthanum abundance. As expected, the [Ni/Fe] and [Eu/Fe] ratios do not exhibit any correlation with [La/Fe]. This confirms our assumption that europium is produced almost exclusively through the r-process, and that nickel, along with other Fe-peak elements, is not significantly affected by the s-process. Additionally, we find that all other elements exhibit a mild correlation with [La/Fe]. Given the strong enhancement in lanthanum, it is not surprising that the lighter elements might also be mildly affected. Unfortunately, it is difficult to disentangle the production of these elements from other sources. We suspect that much of the correlation between the heavy α elements and lanthanum may be due to the combined effects of Type II SN and AGB s-process production overlapping in the same metallicity regime. In particular, the largest increase in [La/Fe] occurs at the transition between the RGB-MP and RGB-Int1 populations. The elevated [Si/Fe] and [Ca/Fe] ratios concurrent with an increase in [Fe/H] strongly suggests that Type II SNe were the major producers of these elements. As mentioned in §5.1, the increase in Si and Ca abundances may be the result of metallicity dependent Type II SN yields rather than additional production from the s-process. At present, we do not have a definitive explanation for the increase in [Ti/Fe] or its correlation with [La/Fe]. However, we point out that the stable isotope ^{50}Ti is a neutron magic nucleus, and it has been predicted that the helium shell of thermally pulsing AGB stars may exhibit a large $^{50}\text{Ti}/^{48}\text{Ti}$ ratio (e.g., Gallino et al. 1994). If at least some AGB stars that eject large amounts of s-process elements also eject material with a high $^{50}\text{Ti}/^{48}\text{Ti}$ ratio, then this may provide an explanation for the Ti-La correlation.

It is interesting to note that while the O-rich stars exhibit a correlation with [La/Fe], the same relation appears to be mostly absent from the O-poor stars. This supports the idea that the depletion of oxygen is driven by an additional process, such as *in situ* mixing, that does not alter the [La/Fe] ratio. Although we find that nearly all of the O-poor stars also have $[\text{La}/\text{Fe}] > -0.2$, we point out that this may be mostly related to the fact that the O-poor (He-rich?) stars formed at a time when the average lanthanum abundance was already becoming significantly enhanced in the cluster ISM. Also note that we do not find any correlation between lanthanum abundance and radial location in the cluster, which does not match the observed trend for the O-poor stars (see Figure 9). We therefore conclude that the simultaneous rise in the number of O-poor and La-rich stars are not due to the exact same mechanisms. However, we believe that both phenomena are at least in some way related to pollution from low and/or intermediate mass AGB stars.

5.4. Final Remarks

The data presented here and in previous analyses indicate that ω Cen experienced a unique chemical enrichment history. The occurrence of at least 4–5 discrete star formation episodes spanning $>1\text{--}2 \times 10^9$ years seems required to rectify the breadth of the main sequence turnoff, the metallicity distribution function, and the large enhancement of s-process elements. Despite ω Cen’s rather extensive chemical enrichment, the most metal-poor stars ($[\text{Fe}/\text{H}] < -2$) exhibit abundance patterns and star-to-star dispersions that are nearly identical to those found in similar metallicity halo and dwarf galaxy stars. These signatures strongly suggest a rapid enrichment time scale in which only massive stars had time to contribute to ω Cen’s chemical composition. Additionally, at least half of the RGB-MP stars exhibit abundance trends that are consistent with the metal-poor halo, and the heavy α element trends seem to indicate that the initial chemical enrichment occurred on a time scale that was sensitive to Type II SNe of different masses. However, a significant portion of the RGB-MP stars have $[\text{O}/\text{Fe}]$, $[\text{Na}/\text{Fe}]$, and $[\text{Al}/\text{Fe}]$ abundances that are unlike stars found in the halo, and are instead more similar to those found in monometallic globular clusters. A clear delay in the presence of O-poor, Na/Al-rich stars until $[\text{Fe}/\text{H}] \sim -1.7$ suggests that new generations significantly polluted by the ejecta of $\lesssim 8 M_\odot$ stars did not form until about the same time as the second major episode of star formation. Furthermore, the neutron-capture data indicate that at least 1 Gyr had to have elapsed between the formation of the RGB-MP and RGB-Int1 populations.

Since a majority of RGB-MP stars have abundance patterns matching those predicted for Type II SN pollution, it seems likely that ω Cen was able to retain and mix a significant

percentage of SN ejecta at early times in the cluster’s evolution. However, at intermediate metallicities ω Cen’s overall chemistry experienced a dramatic shift that strongly deviates from trends observed in the Galactic halo and most dwarf galaxies. The products of proton– and neutron–capture nucleosynthesis began to dominate the chemical composition of progressively more metal–rich stars, despite obvious contributions from Type II SNe. The significant pollution of intermediate metallicity stars by O–poor (He–rich?), Na/Al–rich, and s–process enhanced gas is undoubtedly the result of the RGB–MP stars evolving and enriching the cluster ISM. In order for pollution to occur at the levels observed in ω Cen, the cluster must not have strongly interacted with the Galaxy until after at least the formation of the RGB–Int1 population. Otherwise, it is likely that the gas would have been removed by ram pressure stripping. The radial concentration of the RGB–Int2+3 and RGB–a stars near the cluster core indicates that enriched gas was funneled toward the cluster center and/or the central region was the only location where the escape velocity was large enough to retain gas ejected by SNe or AGB stars. The rapid decline in the relative number of “primordial” composition stars in the RGB–Int2+3 and RGB–a populations may be evidence that ω Cen began to lose mass at $[Fe/H] \gtrsim -1.3$. Significant mass loss from the cluster may also help explain the minimal impact Type Ia SNe have played in ω Cen’s chemical enrichment.

6. SUMMARY

We have measured chemical abundances of O, Na, Al, Si, Ca, Sc, Ti, Fe, Ni, La, and Eu for 855 RGB stars in the globular cluster ω Cen. The abundances were obtained using moderate resolution ($R \approx 18,000$), high S/N (> 100) spectra obtained with the Hydra multifiber spectrograph on the Blanco 4m telescope at CTIO. The data set covers more than 80% of stars with $V \leq 13.5$, more than 90% of stars with $V \leq 13.0$, and samples the full breadth of the giant branch to include the most metal–poor and most metal–rich stars in the cluster. Similarly, we have achieved a completion fraction of $\sim 50\text{--}100\%$ at radii extending out to $\sim 24'$ from the cluster center. All abundances were determined using either equivalent width or spectrum synthesis analyses along with the inclusion of blended molecular lines, hyperfine structure, and/or isotope broadening when appropriate. An empirical hyperfine structure correction for the 6774 Å La II line is also provided.

We find in agreement with past photometric and spectroscopic studies that ω Cen contains multiple, discrete stellar populations with large star–to–star abundance variations for all elements. The metallicity distribution function contains five peaks centered at $[Fe/H] = -1.75$, -1.50 , -1.15 , -1.05 , and -0.75 . However, for the analysis we have combined the $[Fe/H] = -1.15$ and -1.05 peaks into a single population. The (now four) stellar populations

are identified as the RGB-MP ($[Fe/H] \leq -1.6$), RGB-Int1 ($-1.6 < [Fe/H] \leq -1.3$), RGB-Int2+3 ($-1.3 < [Fe/H] \leq -0.9$), and RGB-a ($[Fe/H] > -0.9$, which constitute 61%, 27%, 10%, and 2% of our sample, respectively. The metallicity distribution function also exhibits a sharp cutoff at the metal-poor end such that only 2% of the stars in our sample have $[Fe/H] < -2$. The RGB-MP and RGB-Int1 populations appear to be uniformly mixed in the cluster, but the RGB-Int2+3 and RGB-a stars are preferentially located near the cluster core. Additionally, almost 90% of the most metal-poor stars ($[Fe/H] < -2$) reside within 5' of the cluster center.

The abundance trends exhibited by the heavy α (Si, Ca, and Ti) and Fe-peak elements (Sc and Ni) are generally well described by production from Type II SNe at all metallicities. That is, the α elements are typically enhanced at $[\alpha/Fe] \approx +0.3$ and $[Sc,Ni/Fe] \approx 0$. While the Fe-peak element $[X/Fe]$ ratios and star-to-star variations remain mostly constant over ω Cen's full metallicity range, the heavy α elements show a more complicated morphology. Over the metallicity range spanned by the RGB-MP, there is a noticeable decrease in the average $[Si/Fe]$ and $[Ca/Fe]$ abundances with increasing $[Fe/H]$, but the average $[Ti/Fe]$ abundance remains essentially constant. However, the decrease in $[Si/Fe]$ is a stronger function of $[Fe/H]$ than for $[Ca/Fe]$. The average $[X/Fe]$ ratios for all three heavy α elements increase with metallicity between the RGB-MP and RGB-Int1 populations and remains mostly enhanced at higher metallicities. It seems that many of these abundance trends may be driven by mass and/or metallicity dependent Type II SN yields and a new round of star formation creating the RGB-Int1 and subsequent populations. The simultaneous rise in $[Ti/Fe]$ at $[Fe/H] \gtrsim -1.6$ may be driven by a different production mechanism because theoretical Type II SN yields do not predict a large increase in titanium with either progenitor mass or metallicity.

Although some previous analyses have suggested that Type Ia SNe may have become significant contributors to ω Cen's chemical enrichment at $[Fe/H] > -1$, we do not find particularly strong evidence supporting this claim. In the more metal-rich RGB-Int2+3 and RGB-a populations, we find that the average $[\alpha/Fe]$ abundances remain elevated above the level found in disk and dwarf galaxy stars of similar metallicity. While there does appear to be a decrease in $[Ca/Fe]$ at $[Fe/H] > -1$, this may be attributed to metallicity dependent Type II SN yields. Additionally, the strong rise in the average $[Na/Fe]$ ratio for the RGB-Int2+3 and RGB-a stars seems inconsistent with Type Ia SNe production. The maximum $[O/Fe]$ abundance also begins to decrease at $[Fe/H] \gtrsim -1.2$; however, this element, as well as Na and Al, may be altered by *in situ* mixing or pollution from sources other than Type II or Ia SNe. Therefore, the $[X/Fe]$ ratios for these light elements may not directly trace SN production or even reflect a star's original composition. We cannot explicitly rule out that Type Ia SNe have contributed to ω Cen's chemical enrichment, but it seems that their involvement has been mostly limited.

Unlike the heavy α and Fe-peak elements, the light elements (O, Na, and Al) exhibit >0.5 dex star-to-star abundance variations at all metallicities. Although roughly half of the RGB-MP stars exhibit light element abundance patterns that are consistent with those found in similar metallicity halo and dwarf galaxy stars, the remaining RGB-MP stars, as well as $>70\%$ of more metal-rich stars, show light element abundance patterns that are more similar to those found in individual globular clusters (i.e., O-poor and Na/Al-rich). Interestingly, the presence of these stars is a strong function of metallicity, and the [X/Fe] distribution functions are bimodal at intermediate metallicities. While very few O-poor, Na/Al-rich stars are found at $[Fe/H] < -1.7$, the majority of stars in the RGB-Int1 and subsequent populations exhibit these characteristics. We find that many of the metallicity dependent light element trends can be at least qualitatively reproduced by hot bottom burning in intermediate mass AGB stars. This is evidenced by the pervasive O-Na and O-Al anticorrelations and concurrent Na-Al correlation present in all stars with $[Fe/H] \lesssim -1$. Interestingly, the RGB-a stars no longer exhibit the light element relations and instead appear to have a roughly uniform composition. In any case, the light element trends in stars with $[Fe/H] \lesssim -1$ are similar to what is found in monometallic globular clusters, but the relative fraction of O-poor, Na/Al-rich stars in ω Cen at $[Fe/H] > -1.6$ is significantly larger than those found in other globular clusters. Since a wide mass range of AGB stars seem able to reproduce the observed [Na/Fe] and [Al/Fe] trends but only a narrow range eject O-poor material, we conclude that the [Na/Fe] and [Al/Fe] ratios in the “enhanced” ω Cen stars may be explained solely by pollution from intermediate mass AGB stars. However, the strongly depleted [O/Fe] ratios in many stars appear to require an additional process. Interestingly, we find a low incidence of carbon stars ($< 2\%$) in our sample despite the large population of O-poor giants.

It seems that some degree of *in situ* processing must be invoked in order to interpret the large population of O-poor stars. We find an interesting parallel between O-poor giants and blue main sequence stars that may explain at least part of this phenomenon. The two populations share strikingly similar radial locations, metallicities, and number fractions. In particular, the O-poor and blue main sequence stars are both predominantly found inside $\sim 10'$ from the cluster center, are mostly found at intermediate metallicities, and constitute $\sim 30\%$ of the RGB and main sequence by number. Since the blue main sequence stars are believed to be He-rich, it seems likely that the O-poor stars may also be He-rich. Previous theoretical analyses of He-rich, globular cluster RGB stars predict that significant *in situ* mixing can occur more easily in He-rich compared to He-normal stars. Furthermore, it is predicted that the surface [O/Fe] abundance may be significantly depleted, but [Na/Fe] (and presumably [Al/Fe]) should be mostly unaffected. However, this scenario assumes that the O-poor, Na/Al-rich stars were already polluted by material that was moderately

processed by proton–capture nucleosynthesis before ascending the RGB. The observed O–Si anticorrelation and Al–Si correlation may support this scenario. These relations can naturally arise due to leakage from the MgAl cycle at temperatures exceeding $\sim 65 \times 10^6$ K; temperatures this high are achieved in hot bottom burning conditions but not in the interiors of low mass RGB stars. If we assume that the observed O–poor stars are also He–rich and therefore more apt to experience *in situ* deep mixing, then this may explain why only the [O/Fe] ratio is correlated with radial location. Since the Na and Al abundances do not strongly correlate with radial location like O, this may be an indication that the stars responsible for producing the high Na and Al abundances do not necessarily produce high He yields as well.

A majority of RGB–MP stars have [La/Fe], [Eu/Fe], and [La/Eu] ratios indicating that the r–process was the primary production mechanism early in ω Cen’s history. This is similar to what is found in metal–poor halo, globular cluster, and dwarf galaxy stars, and is consistent with a rapid formation time scale of the RGB–MP population. However, the [La/Fe], [Eu/Fe], and [La/Eu] abundance patterns indicate that the s–process became the dominant neutron–capture production mechanism at $[Fe/H] > -1.6$, and was active at a level above that observed in any other stellar population to date. In fact, almost no stars with $[Fe/H] > -1.6$ have $[La/Fe] < 0$, and many stars in the intermediate metallicity populations exhibit [La/Eu] ratios suggesting pure s–process production. However, proper accounting of hyperfine structure in determining both La and Eu abundances has revised our [La/Eu] ratios downward from those in Johnson et al. (2009), and we now find that surface pollution from mass transfer is not generally required to explain the stars with large [La/Eu] ratios. Interestingly, the typical [Eu/Fe] abundances in the RGB–Int1 and RGB–Int2+3 stars are well below those observed in similar metallicity halo and globular cluster stars. This suggests that typical r–process production mechanisms may have been suppressed in ω Cen.

While we find that both the [Ni/Fe] and [Eu/Fe] ratios are independent of a star’s [La/Fe] abundance, all other elements exhibit a mild correlation with [La/Fe]. Since the $< 3 M_\odot$ AGB stars believed to produce most of the s–process elements in ω Cen are also predicted to produce some light elements, the correlation with La is not entirely unexpected. Interestingly, the O–rich stars show a correlation with [La/Fe], but the O–poor stars do not. This suggests that the O–depletion phenomenon is driven by an additional process, such as *in situ* mixing, that does not alter the envelope [La/Fe] ratio. With regard to the heavy α elements, we suspect that the correlation with La may be due to the combined effects of Type II SNe producing α elements and low/intermediate–mass AGB stars producing s–process elements at approximately the same time. This is supported by the observation that the rise in s–process and α elements occurs in the same metallicity range. We do not have a definitive explanation for the correlation between [Ti/Fe] and [La/Fe] because the [Ti/Fe]

ratio is not believed to be significantly enhanced in Type II SNe. However, we point out that the stable isotope ^{50}Ti is a neutron magic nucleus and that the He shell of thermally pulsing AGB stars are predicted to exhibit large $^{50}\text{Ti}/^{48}\text{Ti}$ ratios. Therefore, if at least some AGB stars that eject large amounts of s-process elements also eject material with a high $^{50}\text{Ti}/^{48}\text{Ti}$ ratio, this may explain both the rise $[\text{Ti}/\text{Fe}]$ at $[\text{Fe}/\text{H}] \gtrsim -1.6$ and the Ti-La correlation.

This publication makes use of data products from the Two Micron All Sky Survey, which is a joint project of the University of Massachusetts and the Infrared Processing and Analysis Center/California Institute of Technology, funded by the National Aeronautics and Space Administration and the National Science Foundation. This research has made use of NASA's Astrophysics Data System Bibliographic Services. Support of the College of Arts and Sciences and the Daniel Kirkwood fund at Indiana University Bloomington for CIJ and CAP is gratefully acknowledged. We would like to thank Bob Kraft and Chris Sneden for many helpful discussions, Katia Cunha for sending an electronic version of her paper in advance of publication, and TalaWanda Monroe for her assistance in obtaining these observations. We would also like to thank Frank and Janet Winkler and the CTIO staff for their generous hospitality. We also thank the referee for his/her careful reading and thoughtful comments that led to improvement of the manuscript.

A. Empirical Lanthanum 6774 Å Hyperfine Broadening Correction

The 6774 Å La II line is often measurable in the spectra of $[\text{Fe}/\text{H}] \gtrsim -2$ RGB and AGB stars, but accurate La abundance determinations from this line can be hampered by hyperfine broadening if the EW exceeds ~ 50 mÅ. Unfortunately, we are not aware of any publicly available linelists that include log gf values for the individual hyperfine components of the 6774 Å line. However, the spectra used here and in Johnson et al. (2009) provide EW measurements of the 6774 Å line and spectrum synthesis abundance determinations from the 6262 Å line in 85 giants. Since the 6262 Å abundance determinations properly account for hyperfine broadening, we can use these data to derive an empirical correction factor for EW-based abundance measurements that use the 6774 Å line. In Figure 27, we plot $[\text{La}/\text{Fe}]_{\text{syn}} - [\text{La}/\text{Fe}]_{\text{EW}}$ ($\Delta[\text{La}/\text{Fe}]_{\text{EW}}$) as a function of EW. The least-squares fit to the data gives the empirical correction factor as,

$$\Delta[\text{La}/\text{Fe}]_{\text{EW}} = [(5.0 \times 10^{-6})(\text{EW}^2)] - [(0.0068)(\text{EW})] + 0.1084 (\sigma = 0.07), \quad (\text{A1})$$

where the EW is measured in units of mÅ. This relation is qualitatively expected because it shows that a straight-forward EW analysis will overestimate the La abundance by an

increasingly larger amount as one moves up the curve-of-growth to larger EWs. Since this is an empirical correction, it is difficult to predict how the relation might change outside the T_{eff} (3800–5000 K), $\log g$ ($\lesssim 2$), and metallicity ($-2.5 \lesssim [\text{Fe}/\text{H}] \lesssim -0.5$) regime of our sample.

Facilities: CTIO

REFERENCES

- Alonso, A., Arribas, S., & Martínez-Roger, C. 1999, *A&AS*, 140, 261
- Alonso, A., Arribas, S., & Martínez-Roger, C. 2001, *A&A*, 376, 1039
- Anders, E., & Grevesse, N. 1989, *Geochim. Cosmochim. Acta*, 53, 197
- Anderson, A. J. 1997, Ph.D. Thesis
- Anderson, J. 2002, *Omega Centauri, A Unique Window into Astrophysics*, 265, 87
- Anderson, J., Piotto, G., King, I. R., Bedin, L. R., & Guhathakurta, P. 2009, *ApJ*, 697, L58
- Andrievsky, S. M., Spite, M., Korotin, S. A., Spite, F., Bonifacio, P., Cayrel, R., Hill, V., & François, P. 2008, *A&A*, 481, 481
- Arnett, W. D., & Thielemann, F.-K. 1985, *ApJ*, 295, 589
- Arnould, M., Goriely, S., & Takahashi, K. 2007, *Phys. Rep.*, 450, 97
- Barbuy, B. 1988, *A&A*, 191, 121
- Bedin, L. R., Piotto, G., Anderson, J., Cassisi, S., King, I. R., Momany, Y., & Carraro, G. 2004, *ApJ*, 605, L125
- Bekki, K., & Norris, J. E. 2006, *ApJ*, 637, L109
- Bekki, K., Campbell, S. W., Lattanzio, J. C., & Norris, J. E. 2007, *MNRAS*, 377, 335
- Bellini, A., et al. 2009a, *A&A*, 493, 959
- Bellini, A., Piotto, G., Bedin, L. R., King, I. R., Anderson, J., Milone, A. P., & Momany, Y. 2009b, *A&A*, 507, 1393
- Bensby, T., Feltzing, S., & Lundström, I. 2003, *A&A*, 410, 527
- Bensby, T., Feltzing, S., Lundström, I., & Ilyin, I. 2005, *A&A*, 433, 185

- Bisterzo, S., Gallino, R., Straniero, O., Cristallo, S., Kappeler, F. 2010, MNRAS, 404, 1529
- Blackwell, D. E., & Shallis, M. J. 1977, MNRAS, 180, 177
- Boehm-Vitense, E. 1979, ApJ, 234, 521
- Bragaglia, A., Carretta, E., Gratton, R., D’Orazi, V., Cassisi, S., & Lucatello, S. 2010, arXiv:1005.2659
- Brewer, M.-M., & Carney, B. W. 2006, AJ, 131, 431
- Brown, J. A., & Wallerstein, G. 1993, AJ, 106, 133
- Busso, M., Gallino, R., & Wasserburg, G. J. 1999, ARA&A, 37, 239
- Calamida, A., et al. 2005, ApJ, 634, L69
- Calamida, A., et al. 2009, ApJ, 706, 1277
- Cannon, R. D., & Stobie, R. S. 1973, MNRAS, 162, 207
- Carretta, E., et al. 2009a, A&A, 505, 117
- Carretta, E., Bragaglia, A., Gratton, R., & Lucatello, S. 2009b, A&A, 505, 139
- Carretta, E., et al. 2010, ApJ, 714, L7
- Castellani, V., et al. 2007, ApJ, 663, 1021
- Castelli, F., Gratton, R. G., & Kurucz, R. L. 1997, A&A, 318, 841
- Cavallo, R. M., Suntzeff, N. B., & Pilachowski, C. A. 2004, AJ, 127, 3411
- Charbonnel, C., Brown, J. A., & Wallerstein, G. 1998, A&A, 332, 204
- Choi, E., & Yi, S. K. 2008, MNRAS, 386, 1332
- Cohen, J. G. 1981, ApJ, 247, 869
- Cottrell, P. L., & Da Costa, G. S. 1981, ApJ, 245, L79
- Cowan, J. J., Thielemann, F.-K., & Truran, J. W. 1991, Phys. Rep., 208, 267
- Cunha, K., Smith, V. V., Suntzeff, N. B., Norris, J. E., Da Costa, G. S., & Plez, B. 2002, AJ, 124, 379

- Cunha, K., Smith, V. V., Bergemann, M., Suntzeff, N. B., & Lambert, D. L. 2010, ApJ, 717, 333
- D'Antona, F., & Ventura, P. 2007, MNRAS, 379, 1431
- D'Cruz, N. L., et al. 2000, ApJ, 530, 352
- D'Ercole, A., Vesperini, E., D'Antona, F., McMillan, S. L. W., & Recchi, S. 2008, MNRAS, 391, 825
- D'Ercole, A., D'Antona, F., Ventura, P., Vesperini, E., & McMillan, S. L. W. 2010, MNRAS, 999
- Decressin, T., Meynet, G., Charbonnel, C., Prantzos, N., & Ekström, S. 2007, A&A, 464, 1029
- Denisenkov, P. A., & Denisenkova, S. N. 1990, Soviet Astronomy Letters, 16, 275
- Denissenkov, P. A., & Herwig, F. 2004, ApJ, 612, 1081
- Denissenkov, P. A., & Weiss, A. 2004, ApJ, 603, 119
- Dinescu, D. I., Girard, T. M., & van Altena, W. F. 1999, AJ, 117, 1792
- Edvardsson, B., Andersen, J., Gustafsson, B., Lambert, D. L., Nissen, P. E., & Tomkin, J. 1993, A&A, 275, 101
- Fenner, Y., Campbell, S., Karakas, A. I., Lattanzio, J. C., & Gibson, B. K. 2004, MNRAS, 353, 789
- Ferraro, F. R., Sollima, A., Pancino, E., Bellazzini, M., Straniero, O., Origlia, L., & Cool, A. M. 2004, ApJ, 603, L81
- Freeman, K. C., & Rodgers, A. W. 1975, ApJ, 201, L71
- Fulbright, J. P. 2000, AJ, 120, 1841
- Fulbright, J. P., McWilliam, A., & Rich, R. M. 2007, ApJ, 661, 1152
- Gallino, R., Raiteri, C. M., Busso, M., & Matteucci, F. 1994, ApJ, 430, 858
- Gehren, T., Liang, Y. C., Shi, J. R., Zhang, H. W., & Zhao, G. 2004, A&A, 413, 1045
- Geisler, D., Wallerstein, G., Smith, V. V., & Casetti-Dinescu, D. I. 2007, PASP, 119, 939

- Girardi, L., Castelli, F., Bertelli, G., & Nasi, E. 2007, A&A, 468, 657
- Gnedin, O. Y., Zhao, H., Pringle, J. E., Fall, S. M., Livio, M., & Meylan, G. 2002, ApJ, 568, L23
- Gratton, R. G., Carretta, E., Eriksson, K., & Gustafsson, B. 1999, A&A, 350, 955
- Gratton, R., Sneden, C., & Carretta, E. 2004, ARA&A, 42, 385
- Harris, W. E. 1996, AJ, 112, 1487
- Herwig, F. 2005, ARA&A, 43, 435
- Hilker, M., & Richtler, T. 2000, A&A, 362, 895
- Hill, V., et al. 2002, A&A, 387, 560
- Hinkle, K., Wallace, L., Valenti, J., & Harmer, D. 2000, Visible and Near Infrared Atlas of the Arcturus Spectrum 3727-9300 Å ed. Kenneth Hinkle, Lloyd Wallace, Jeff Valenti, and Dianne Harmer. (San Francisco: ASP) ISBN: 1-58381-037-4
- Hughes, J., & Wallerstein, G. 2000, AJ, 119, 1225
- Ikuta, C., & Arimoto, N. 2000, A&A, 358, 535
- Ivans, I. I., Sneden, C., Kraft, R. P., Suntzeff, N. B., Smith, V. V., Langer, G. E., & Fulbright, J. P. 1999, AJ, 118, 1273
- Ivans, I. I., Kraft, R. P., Sneden, C., Smith, G. H., Rich, R. M., & Shetrone, M. 2001, AJ, 122, 1438
- Izzard, R. G., Lugaro, M., Karakas, A. I., Iliadis, C., & van Raai, M. 2007, A&A, 466, 641
- Johnson, C. I., Kraft, R. P., Pilachowski, C. A., Sneden, C., Ivans, I. I., & Benman, G. 2005, PASP, 117, 1308
- Johnson, C. I., Pilachowski, C. A., Simmerer, J., & Schwenk, D. 2008, ApJ, 681, 1505
- Johnson, C. I., Pilachowski, C. A., Michael Rich, R., & Fulbright, J. P. 2009, ApJ, 698, 2048
- Karakas, A. I. 2010, MNRAS, 403, 1413
- Kayser, A., Hilker, M., Richtler, T., & Willemse, P. G. 2006, A&A, 458, 777
- Kraft, R. P. 1994, PASP, 106, 553

- Kupka, F. G., Ryabchikova, T. A., Piskunov, N. E., Stempels, H. C., & Weiss, W. W. 2000, Baltic Astronomy, 9, 590
- Langer, G. E., Hoffman, R., & Sneden, C. 1993, PASP, 105, 301
- Langer, G. E., Hoffman, R. E., & Zaidins, C. S. 1997, PASP, 109, 244
- Lawler, J. E., Bonvallet, G., & Sneden, C. 2001a, ApJ, 556, 452
- Lawler, J. E., Wickliffe, M. E., den Hartog, E. A., & Sneden, C. 2001b, ApJ, 563, 1075
- Lecureur, A., Hill, V., Zoccali, M., Barbuy, B., Gómez, A., Minniti, D., Ortolani, S., & Renzini, A. 2007, A&A, 465, 799
- Lee, Y.-W., Joo, J.-M., Sohn, Y.-J., Rey, S.-C., Lee, H.-C., & Walker, A. R. 1999, Nature, 402, 55
- Lee, Y.-W., et al. 2005a, ApJ, 621, L57
- Lee, J.-W., Carney, B. W., & Habgood, M. J. 2005b, AJ, 129, 251
- Lee, J.-W., Kang, Y.-W., Lee, J., & Lee, Y.-W. 2009, Nature, 462, 480
- Lee, J.-W. 2010, MNRAS, 405, L36
- Magain, P. 1984, A&A, 134, 189
- Majewski, S. R., Ostheimer, J. C., Kunkel, W. E., & Patterson, R. J. 2000, AJ, 120, 2550
- Mandushev, G., Staneva, A., & Spasova, N. 1991, A&A, 252, 94
- Marcolini, A., Sollima, A., D’Ercole, A., Gibson, B. K., & Ferraro, F. R. 2007, MNRAS, 382, 443
- Marino, A. F., Villanova, S., Piotto, G., Milone, A. P., Momany, Y., Bedin, L. R., & Medling, A. M. 2008, A&A, 490, 625
- Marino, A. F., Piotto, G., Gratton, R., Milone, A. P., Zoccali, M., Bedin, L. R., Villanova, S., & Bellini, A. 2010, IAU Symposium, 268, 183
- Mashonkina, L. I., Shimanskii, V. V., & Sakhibullin, N. A. 2000, Astronomy Reports, 44, 790
- Mathews, G. J., & Cowan, J. J. 1990, Nature, 345, 491

- Matteucci, F., Raiteri, C. M., Busson, M., Gallino, R., & Gratton, R. 1993, A&A, 272, 421
- Mayor, M., Duquennoy, A., Udry, S., Andersen, J., & Nordstrom, B. 1996, The Origins, Evolution, and Destinies of Binary Stars in Clusters, 90, 190
- McCall, M. L. 2004, AJ, 128, 2144
- McDonald, I., van Loon, J. T., Decin, L., Boyer, M. L., Dupree, A. K., Evans, A., Gehrzi, R. D., & Woodward, C. E. 2009, MNRAS, 394, 831
- McWilliam, A., & Rich, R. M. 1994, ApJS, 91, 749
- McWilliam, A. 1997, ARA&A, 35, 503
- McWilliam, A., & Smecker-Hane, T. A. 2005, ApJ, 622, L29
- Meylan, G., Mayor, M., Duquennoy, A., & Dubath, P. 1995, A&A, 303, 761
- Milone, A. P., et al. 2008, ApJ, 673, 241
- Milone, A. P., et al. 2010, ApJ, 709, 1183
- Moretti, A., et al. 2009, A&A, 493, 539
- Nomoto, K., Iwamoto, K., Nakasato, N., Thielemann, F.-K., Brachwitz, F., Tsujimoto, T., Kubo, Y., & Kishimoto, N. 1997, Nuclear Physics A, 621, 467
- Nomoto, K., Tominaga, N., Umeda, H., Kobayashi, C., & Maeda, K. 2006, Nuclear Physics A, 777, 424
- Norris, J. E., & Da Costa, G. S. 1995, ApJ, 447, 680
- Norris, J. E., Freeman, K. C., & Mighell, K. J. 1996, ApJ, 462, 241
- Norris, J. E., Freeman, K. C., Mayor, M., & Seitzer, P. 1997, ApJ, 487, L187
- Norris, J. E. 2004, ApJ, 612, L25
- Origlia, L., Ferraro, F. R., Bellazzini, M., & Pancino, E. 2003, ApJ, 591, 916
- Paltoglou, G., & Norris, J. E. 1989, ApJ, 336, 185
- Pancino, E., Ferraro, F. R., Bellazzini, M., Piotto, G., & Zoccali, M. 2000, ApJ, 534, L83
- Pancino, E., Pasquini, L., Hill, V., Ferraro, F. R., & Bellazzini, M. 2002, ApJ, 568, L101

- Pancino, E., Seleznev, A., Ferraro, F. R., Bellazzini, M., & Piotto, G. 2003, MNRAS, 345, 683
- Pancino, E., Galfo, A., Ferraro, F. R., & Bellazzini, M. 2007, ApJ, 661, L155
- Piotto, G., et al. 2005, ApJ, 621, 777
- Piotto, G., et al. 2007, ApJ, 661, L53
- Piotto, G. 2009, arXiv:0902.1422
- Prantzos, N., Charbonnel, C., & Iliadis, C. 2007, A&A, 470, 179
- Press, W. H., Teukolsky, S. A., Vetterling, W. T., & Flannery, B. P. 1992, Cambridge: University Press, —c1992, 2nd ed.,
- Prochaska, J. X., & McWilliam, A. 2000, ApJ, 537, L57
- Ralchenko, Y., Kramida, A.E., Reader, J., and NIST ASD Team (2008). *NIST Atomic Spectra Database* (version 3.1.5). National Institute of Standards and Technology, Gaithersburg, MD.
- Ramírez, S. V., & Cohen, J. G. 2002, AJ, 123, 3277
- Reddy, B. E., Tomkin, J., Lambert, D. L., & Allende Prieto, C. 2003, MNRAS, 340, 304
- Reddy, B. E., Lambert, D. L., & Allende Prieto, C. 2006, MNRAS, 367, 1329
- Reijns, R. A., Seitzer, P., Arnold, R., Freeman, K. C., Ingerson, T., van den Bosch, R. C. E., van de Ven, G., & de Zeeuw, P. T. 2006, A&A, 445, 503
- Renzini, A. 2008, MNRAS, 391, 354
- Rey, S.-C., Lee, Y.-W., Ree, C. H., Joo, J.-M., Sohn, Y.-J., & Walker, A. R. 2004, AJ, 127, 958
- Richer, H. B., Fahlman, G. G., Buonanno, R., Fusi Pecci, F., Searle, L., & Thompson, I. B. 1991, ApJ, 381, 147
- Romano, D., Matteucci, F., Tosi, M., Pancino, E., Bellazzini, M., Ferraro, F. R., Limongi, M., & Sollima, A. 2007, MNRAS, 376, 405
- Romano, D., Tosi, M., Cignoni, M., Matteucci, F., Pancino, E., & Bellazzini, M. 2010, MNRAS, 401, 2490

- Salaris, M., Cassisi, S., & Weiss, A. 2002, PASP, 114, 375
- Samland, M. 1998, ApJ, 496, 155
- Sbordone, L., Bonifacio, P., Buonanno, R., Marconi, G., Monaco, L., & Zaggia, S. 2007, A&A, 465, 815
- Schaller, G., Schaerer, D., Meynet, G., & Maeder, A. 1992, A&AS, 96, 269
- Shetrone, M. D., & Keane, M. J. 2000, AJ, 119, 840
- Shetrone, M. D., Côté, P., & Sargent, W. L. W. 2001, ApJ, 548, 592
- Shetrone, M., Venn, K. A., Tolstoy, E., Primas, F., Hill, V., & Kaufer, A. 2003, AJ, 125, 684
- Simmerer, J., Sneden, C., Cowan, J. J., Collier, J., Woolf, V. M., & Lawler, J. E. 2004, ApJ, 617, 1091
- Skrutskie, M. F., et al. 2006, AJ, 131, 1163
- Smith, V. V., Suntzeff, N. B., Cunha, K., Gallino, R., Busso, M., Lambert, D. L., & Straniero, O. 2000, AJ, 119, 1239
- Smith, V. V., Terndrup, D. M., & Suntzeff, N. B. 2002, ApJ, 579, 832
- Sneden, C. 1973, ApJ, 184, 839
- Sneden, C., Kraft, R. P., Prosser, C. F., & Langer, G. E. 1991a, AJ, 102, 2001
- Sneden, C., Gratton, R. G., & Crocker, D. A. 1991b, A&A, 246, 354
- Sneden, C., McWilliam, A., Preston, G. W., Cowan, J. J., Burris, D. L., & Armosky, B. J. 1996, ApJ, 467, 819
- Sneden, C., Kraft, R. P., Shetrone, M. D., Smith, G. H., Langer, G. E., & Prosser, C. F. 1997, AJ, 114, 1964
- Sneden, C., Kraft, R. P., Guhathakurta, P., Peterson, R. C., & Fulbright, J. P. 2004, AJ, 127, 2162
- Sneden, C., Cowan, J. J., & Gallino, R. 2008, ARA&A, 46, 241
- Sollima, A., Ferraro, F. R., Pancino, E., & Bellazzini, M. 2005, MNRAS, 357, 265
- Sollima, A., Borissova, J., Catelan, M., Smith, H. A., Minniti, D., Cacciari, C., & Ferraro, F. R. 2006, ApJ, 640, L43

- Sollima, A., Ferraro, F. R., Bellazzini, M., Origlia, L., Straniero, O., & Pancino, E. 2007, ApJ, 654, 915
- Sollima, A., Bellazzini, M., Smart, R. L., Correnti, M., Pancino, E., Ferraro, F. R., & Romano, D. 2009, MNRAS, 396, 2183
- Stanford, L. M., Da Costa, G. S., Norris, J. E., & Cannon, R. D. 2006, ApJ, 647, 1075
- Stanford, L. M., Da Costa, G. S., & Norris, J. E. 2010, ApJ, 714, 1001
- Straniero, O., Gallino, R., & Cristallo, S. 2006, Nuclear Physics A, 777, 311
- Suntzeff, N. B., & Kraft, R. P. 1996, AJ, 111, 1913
- Sweigart, A. V., Mengel, J. G., & Demarque, P. 1974, A&A, 30, 13
- Sweigart, A. V., & Mengel, J. G. 1979, ApJ, 229, 624
- Thevenin, F. 1990, A&AS, 82, 179
- Thielemann, F. K., & Arnett, W. D. 1985, ApJ, 295, 604
- Timmes, F. X., Woosley, S. E., & Weaver, T. A. 1995, ApJS, 98, 617
- Tomkin, J., Lemke, M., Lambert, D. L., & Sneden, C. 1992, AJ, 104, 1568
- Tsujimoto, T., & Shigeyama, T. 2003, ApJ, 590, 803
- van de Ven, G., van den Bosch, R. C. E., Verolme, E. K., & de Zeeuw, P. T. 2006, A&A, 445, 513
- van Leeuwen, F., Le Poole, R. S., Reijns, R. A., Freeman, K. C., & de Zeeuw, P. T. 2000, A&A, 360, 472
- van Loon, J. T., van Leeuwen, F., Smalley, B., Smith, A. W., Lyons, N. A., McDonald, I., & Boyer, M. L. 2007, MNRAS, 382, 1353
- Venn, K. A., Irwin, M., Shetrone, M. D., Tout, C. A., Hill, V., & Tolstoy, E. 2004, AJ, 128, 1177
- Ventura, P., & D'Antona, F. 2005, A&A, 431, 279
- Ventura, P., & D'Antona, F. 2009, A&A, 499, 835
- Villanova, S., et al. 2007, ApJ, 663, 296

- Villanova, S., Carraro, G., Scarpa, R., & Marconi, G. 2010, New A, 15, 520
- Wheeler, J. C., Cowan, J. J., & Hillebrandt, W. 1998, ApJ, 493, L101
- Woolley, R. R. 1966, Royal Observatory Annals, 2, 1
- Woosley, S. E., & Weaver, T. A. 1995, ApJS, 101, 181
- Yong, D., Grundahl, F., Nissen, P. E., Jensen, H. R., & Lambert, D. L. 2005, A&A, 438, 875
- Yoshii, Y., Tsujimoto, T., & Nomoto, K. 1996, ApJ, 462, 266
- Zhang, H. W., Gehren, T., & Zhao, G. 2008, A&A, 481, 489
- Zucker, D., Wallerstein, G., & Brown, J. A. 1996, PASP, 108, 911

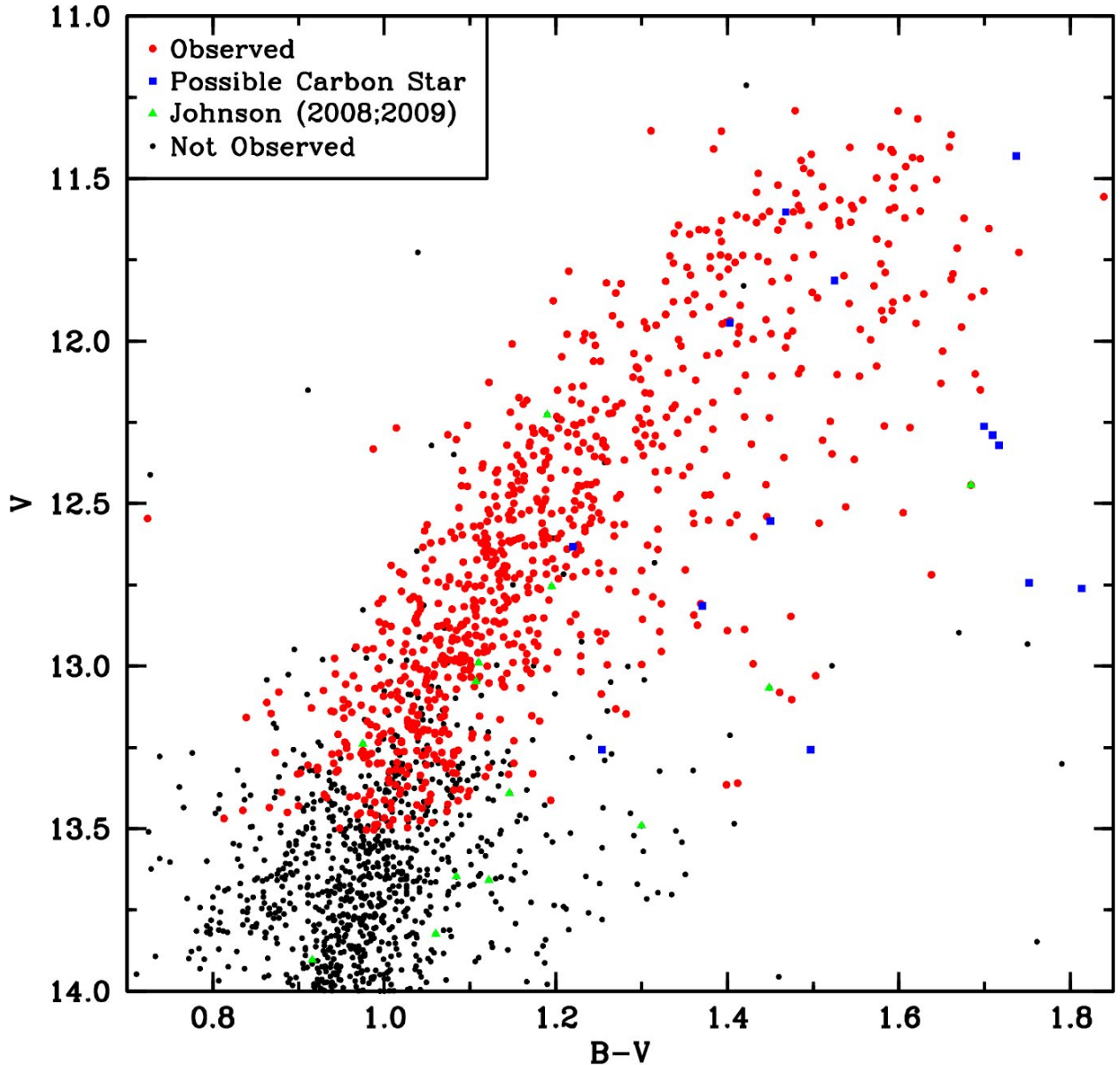


Fig. 1.— A color-magnitude diagram of ω Cen’s RGB with photometry taken from van Leeuwen et al. (2000). The filled red circles represent the stars observed for this study. The filled blue squares indicate possible carbon stars. Note that the identifiers for the carbon stars are provided in Table 2. The filled green triangles show stars that were observed for Johnson et al. (2008; 2009), but do not overlap with the current sample. The complete sample from van Leeuwen et al. is represented by the small black circles.

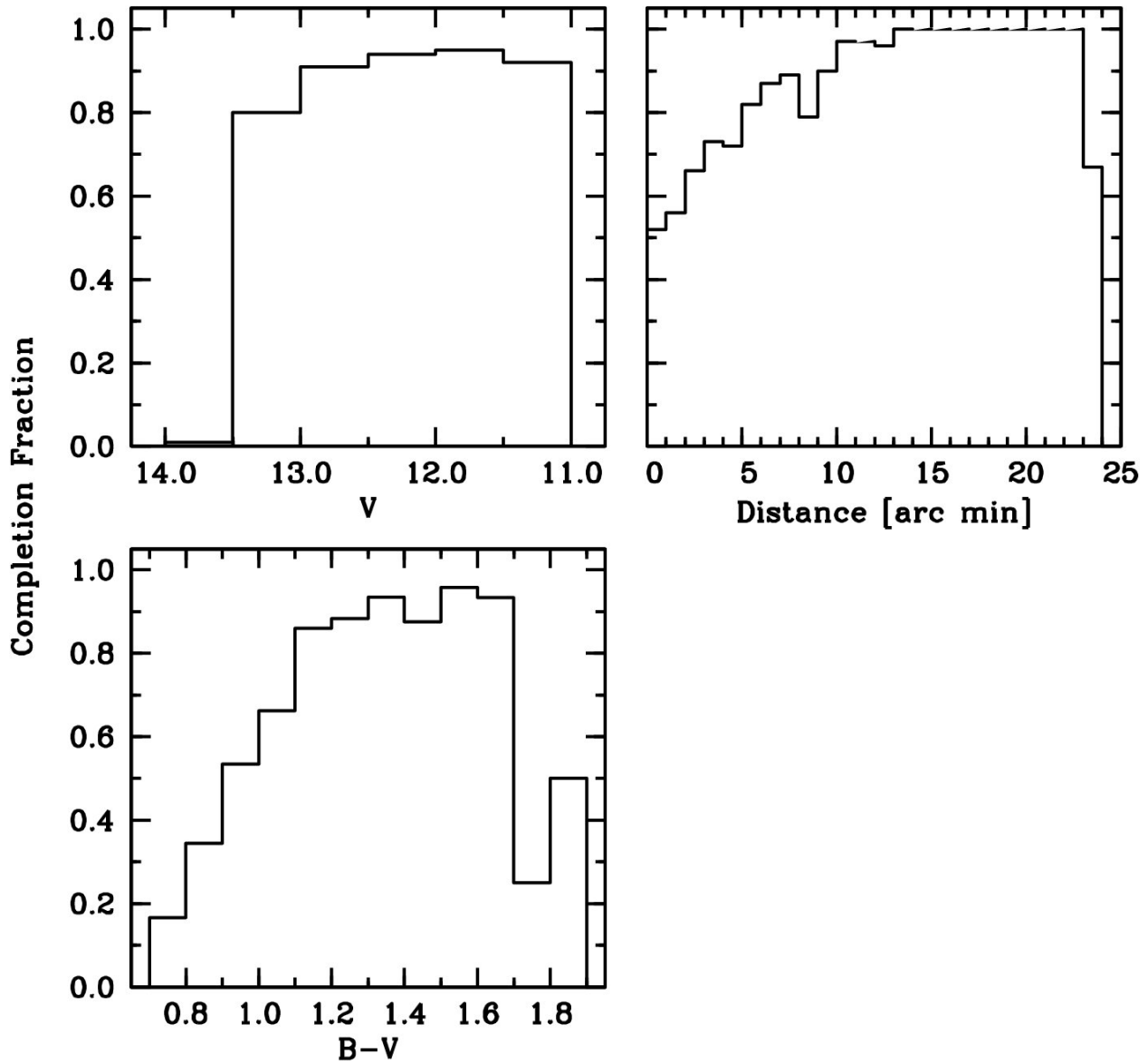


Fig. 2.— The three panels illustrate the observed completion fraction of our sample in terms of V magnitude, B-V color, and distance from the cluster center relative to the van Leeuwen et al. (2000) observations. For the bottom left and top right panels, the completion fraction only includes stars with $V \leq 13.5$, as discussed in §2.

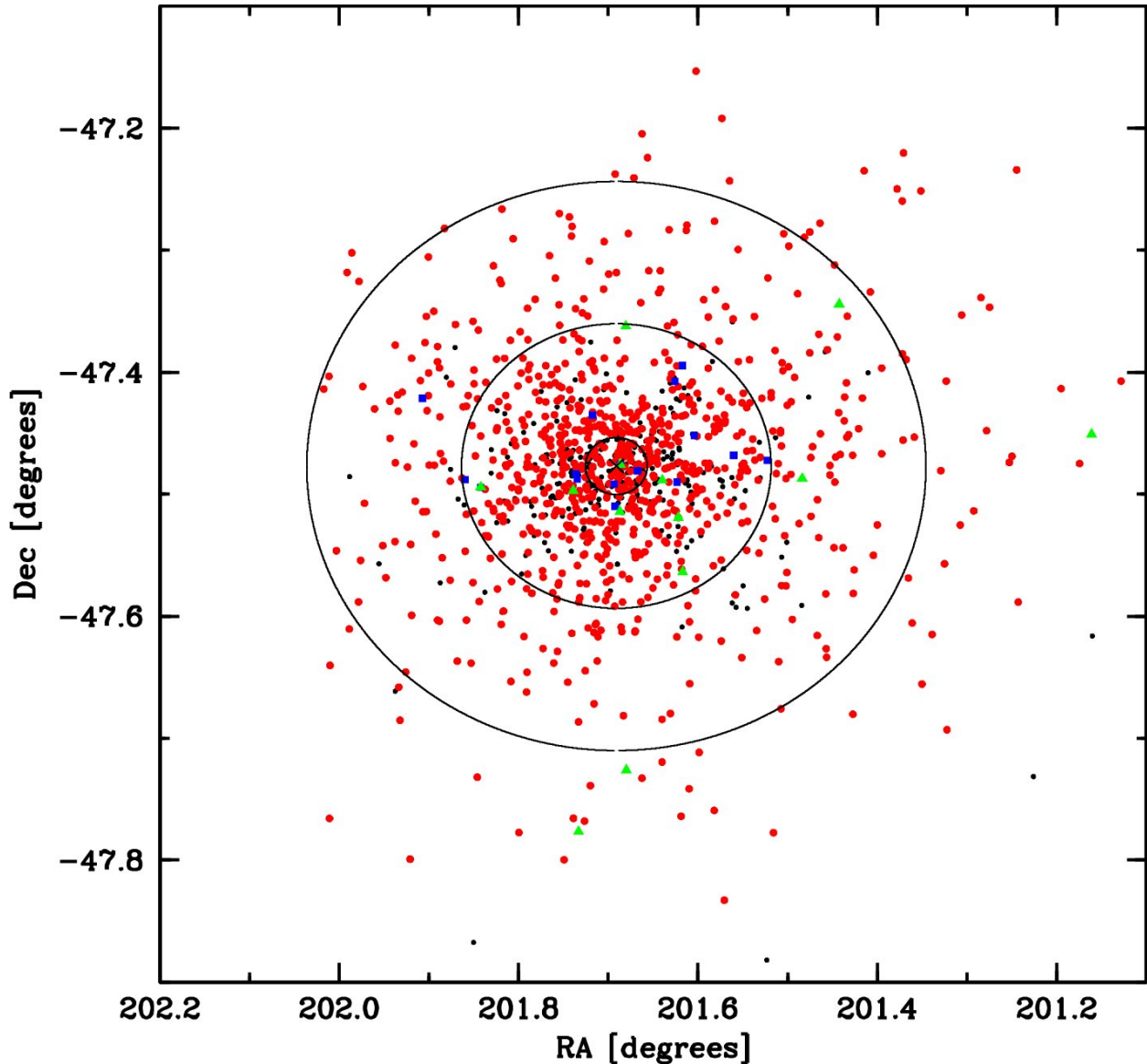


Fig. 3.— This figure shows the coordinate positions of our sample. The cross indicates the cluster center defined by van Leeuwen et al. (2000) as 201.691° , -47.4769° (J2000; $13^{\text{h}}26^{\text{m}}45.9^{\text{s}}$, $-47^{\circ}28'37.0''$). The ellipses represent 1, 5, and 10 times the core radius of $1.40'$ (Harris et al. 1996). The symbols are the same as those in Figure 1, and the van Leeuwen et al. data only represent stars with $V \leq 13.5$ and a membership probability $\geq 70\%$.

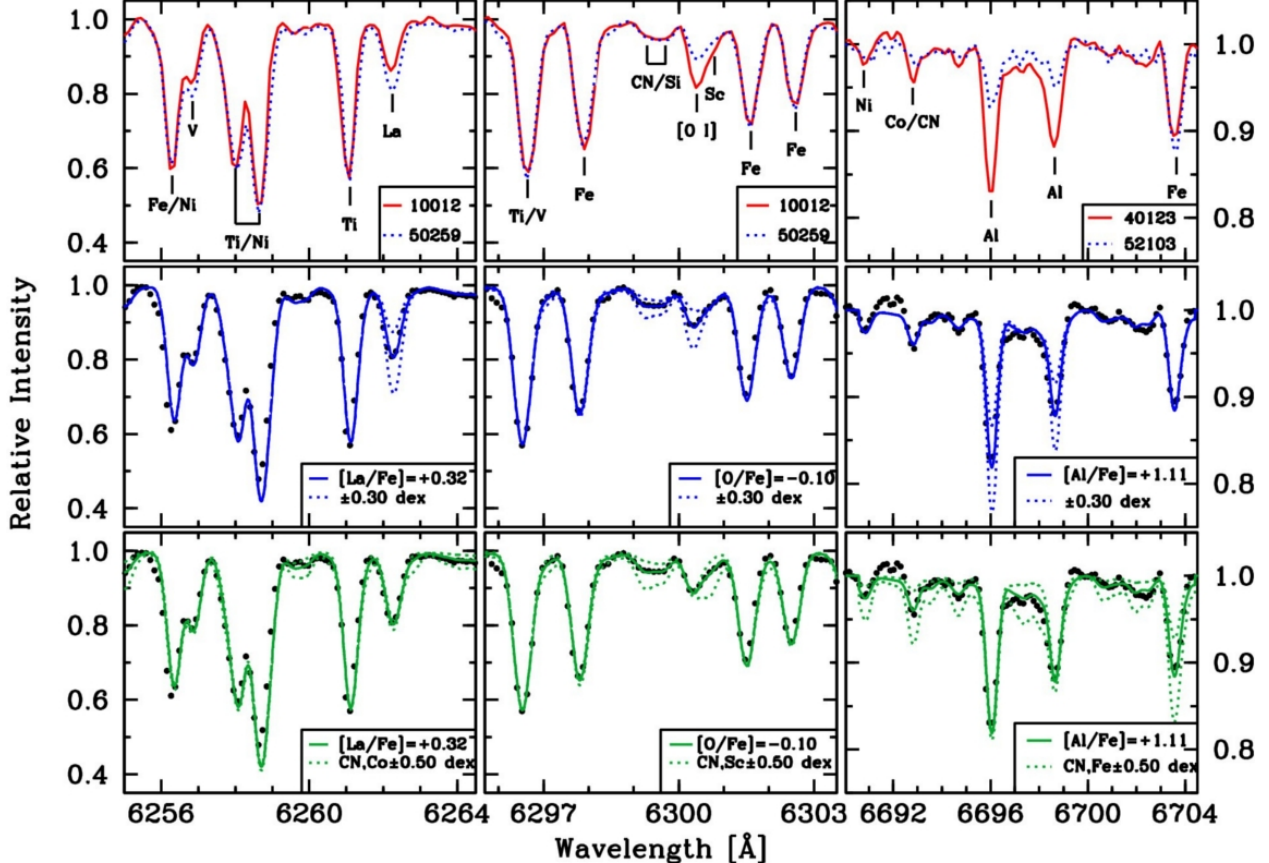


Fig. 4.— The top three panels overplot sample spectra with nearly identical atmospheric parameters and metallicity, but which exhibit significant differences in their derived [La/Fe], [O/Fe], and [Al/Fe] abundances. The middle set of panels show sample spectrum syntheses of La and O for star 50259 in the left and middle panels and Al for star 40123 in the right panel. In all three of the middle panels the solid line indicates the best fit to the spectra and the dotted lines indicate changes of ± 0.30 dex for the indicated elements. The bottom set of panels show sample spectrum syntheses, but the dotted lines in these cases illustrate changes to the synthetic spectra when the blended features of CN, Co, Sc, or Fe are altered by ± 0.50 dex. Note that the right panels have a different intensity scale than the left and middle panels.

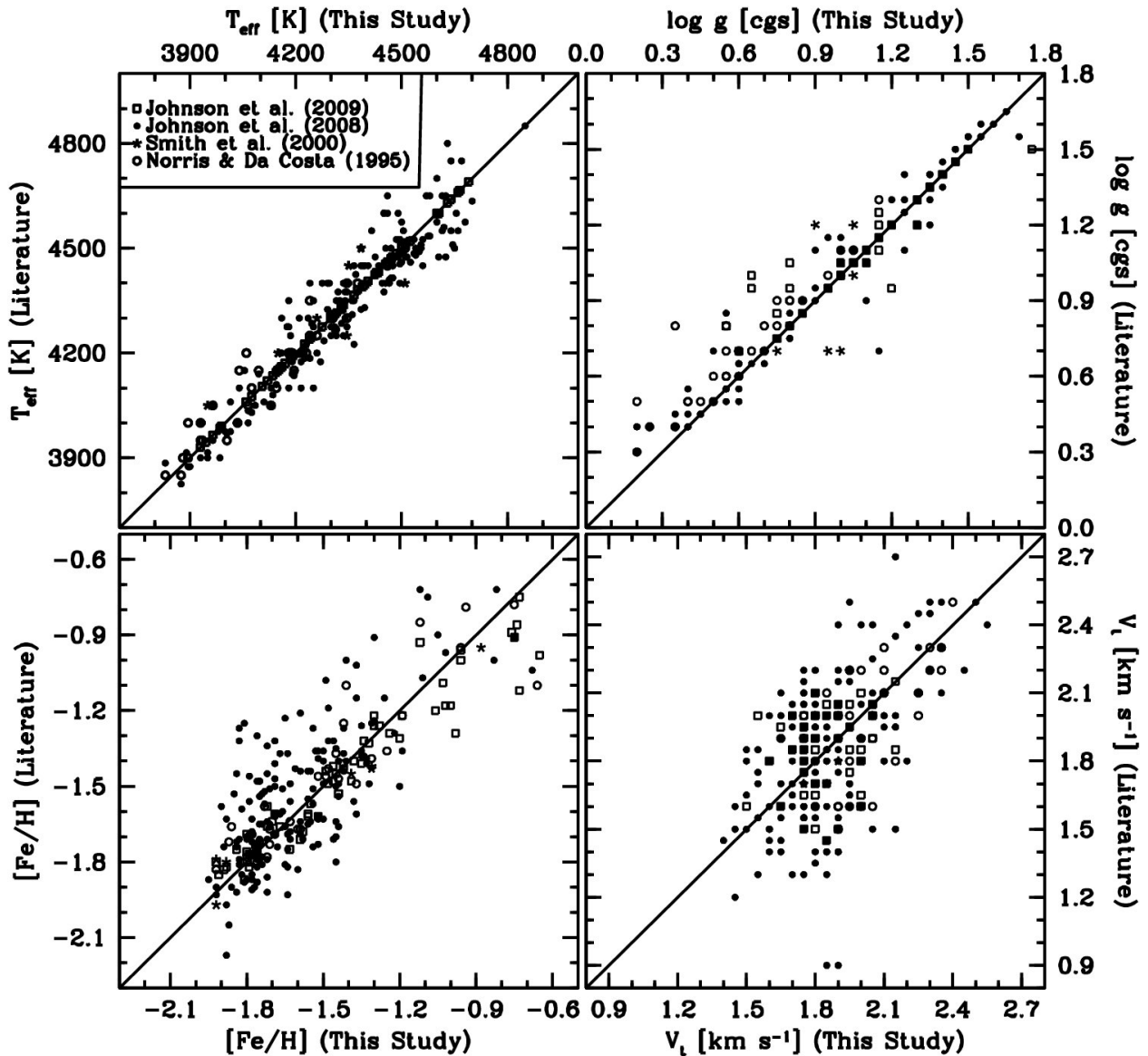


Fig. 5.— The four panels show comparisons of our adopted model atmosphere parameters versus those in the literature. In all panels the solid straight line indicates perfect agreement.

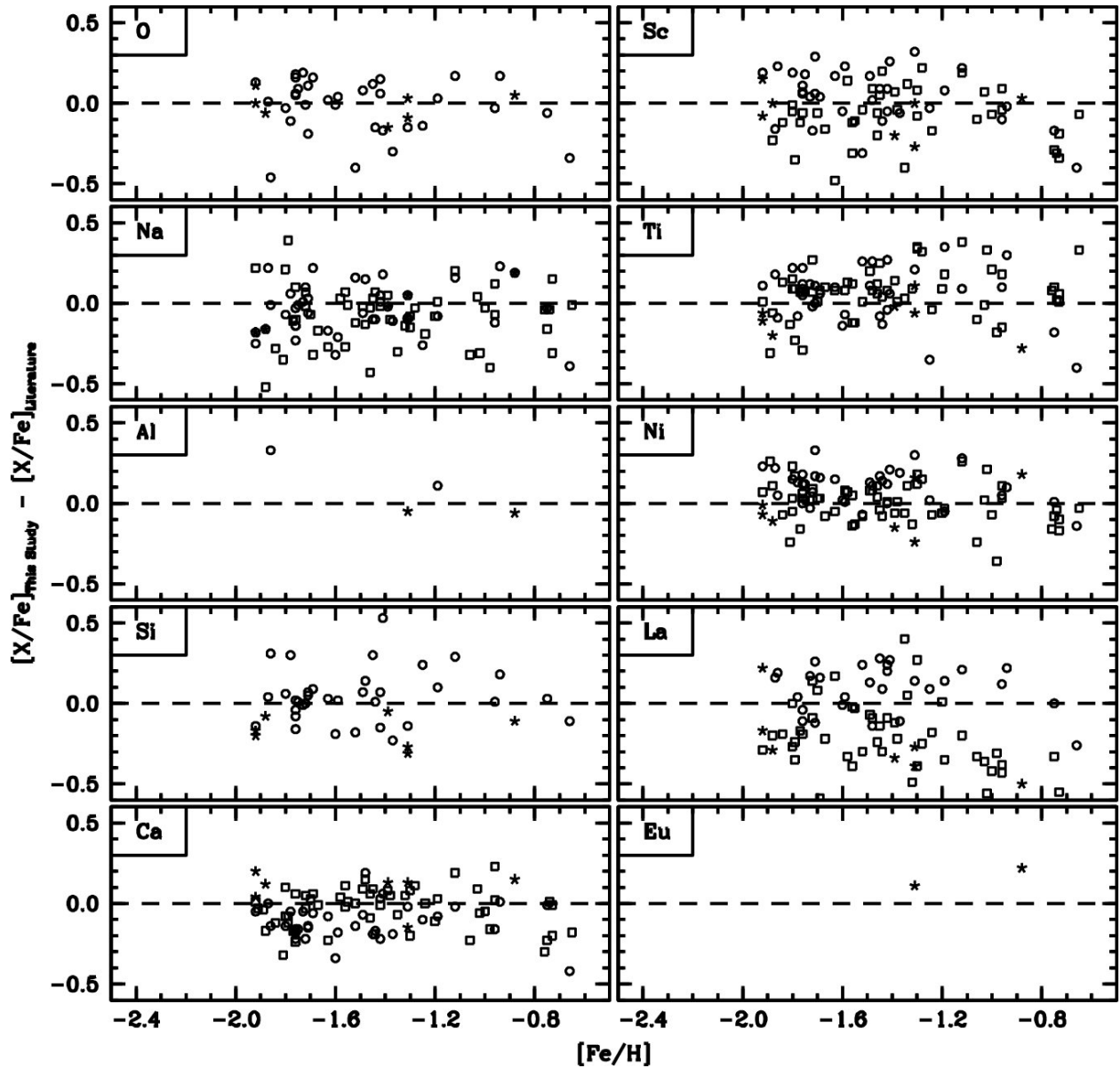


Fig. 6.— The different panels show the $[X/\text{Fe}]$ abundance comparisons between this study and those in the literature. The dashed line indicates perfect agreement, and the symbols are the same as those in Figure 5.

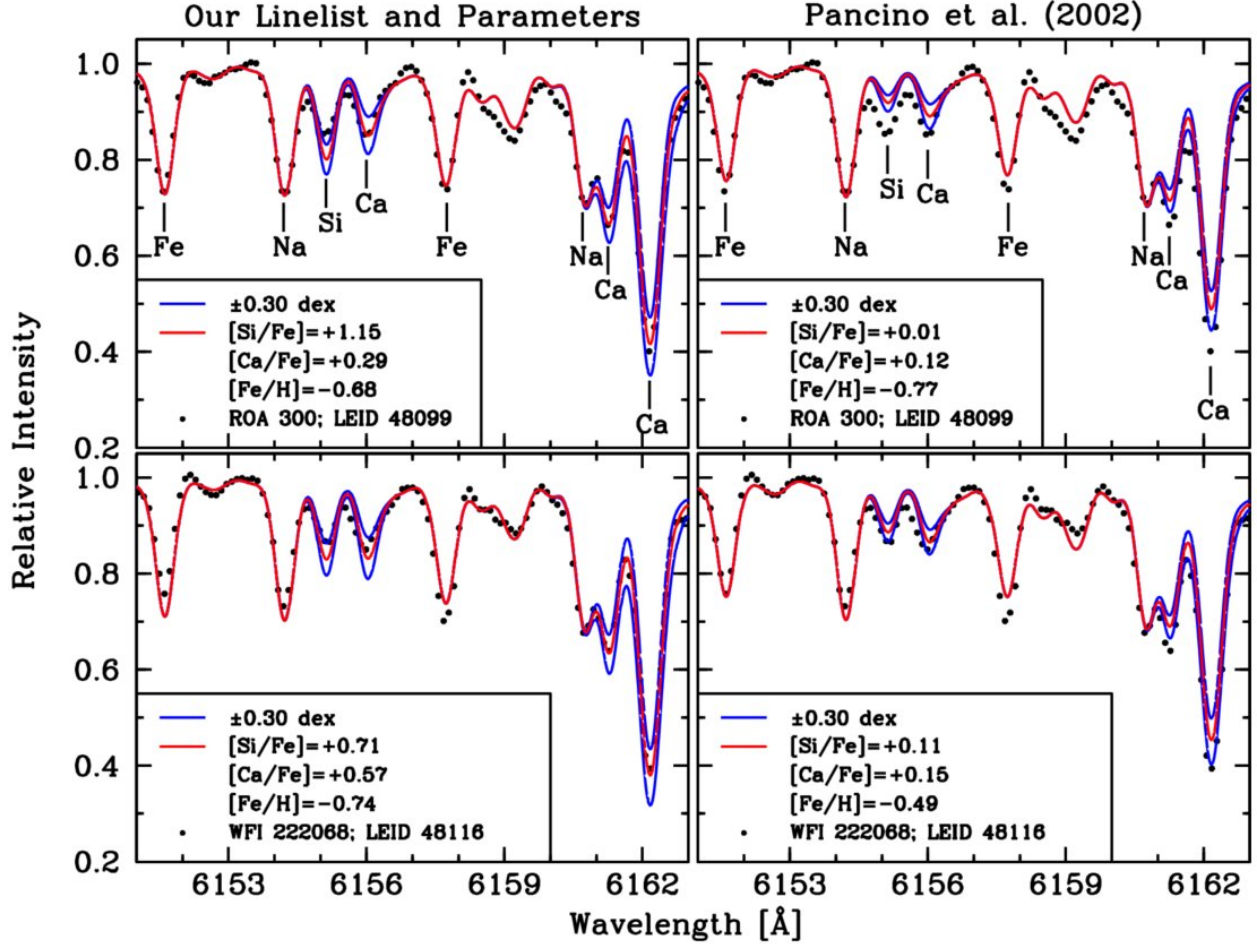


Fig. 7.— Spectrum synthesis fits to the RGB-a stars LEID 48099 (ROA 300) and LEID 48116 (WFI 222068). The two left panels show the synthetic spectrum fits using our measured abundances, model atmosphere parameters, and linelist. The two right panels show the synthetic spectrum fits using the Pancino et al. (2002) abundances and model atmosphere parameters *but our linelist*. In all panels, the solid red line shows the synthesis results using the predetermined abundances, and the solid blue lines show changes of ± 0.3 dex to $[\text{Si}/\text{Fe}]$ and $[\text{Ca}/\text{Fe}]$. Note that the abundances of elements other than silicon and calcium were set to the values listed in Table 5.

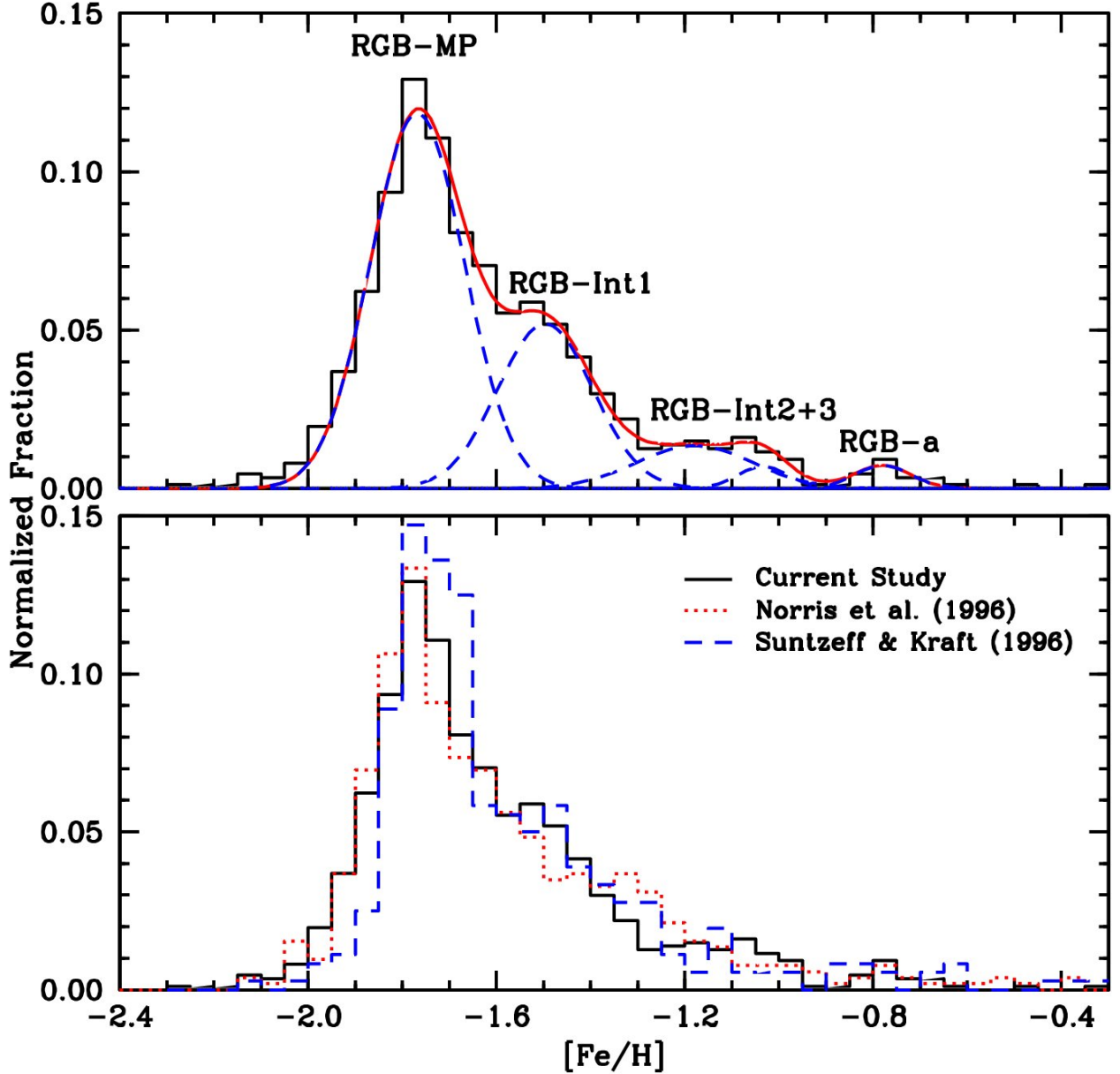


Fig. 8.— The top panel shows the metallicity distribution function for our complete sample, including data from Johnson et al. (2008; 2009). For this panel, the solid red line shows a least-squares fit to the distribution using five Gaussian profiles, and the dashed blue lines illustrate the individual Gaussian component fits. The bottom panel compares our distribution function (solid black line) to those of Norris et al. (1996; dotted red line) and Suntzeff & Kraft (1996; dashed blue line).

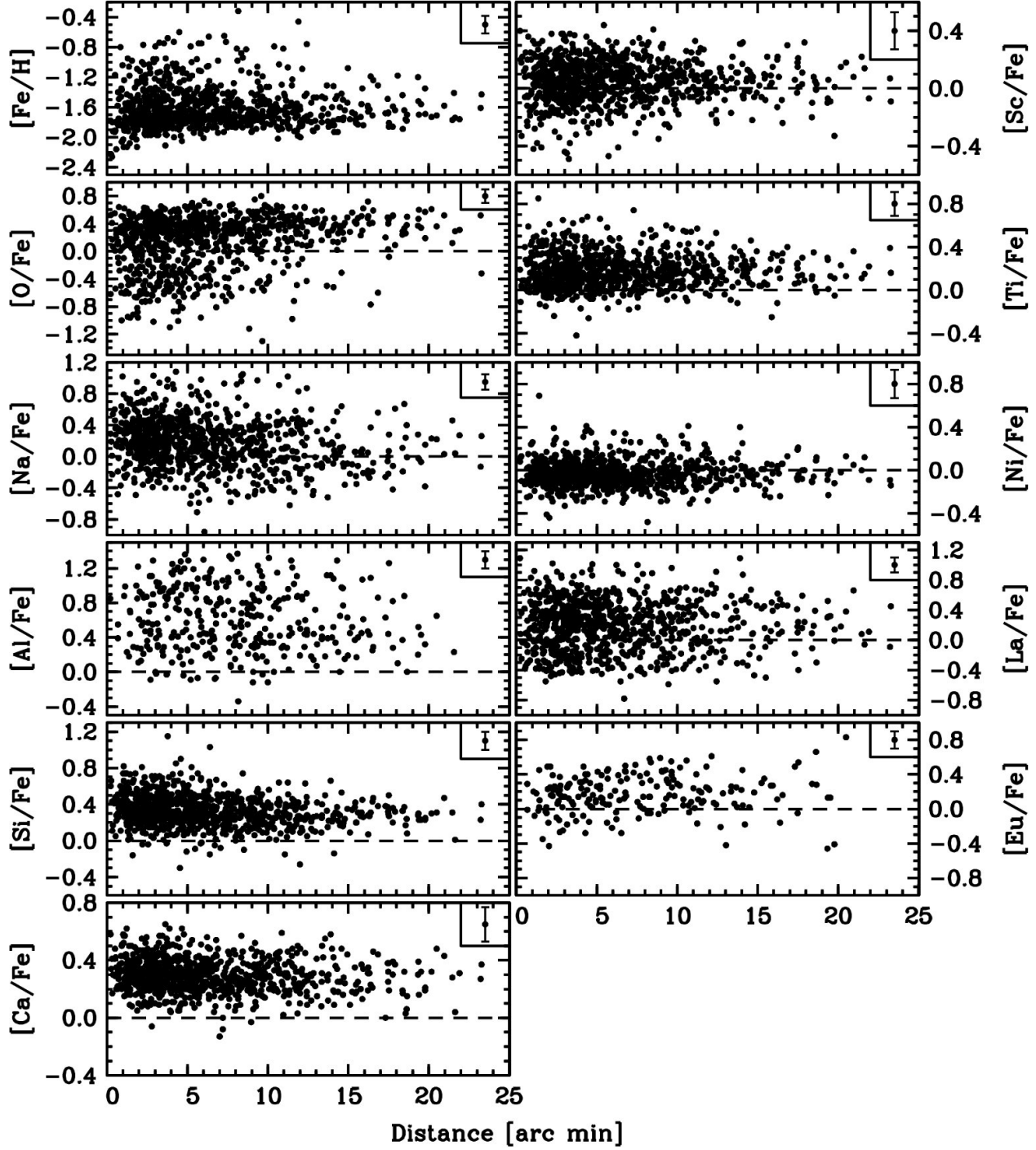


Fig. 9.— Chemical abundance ratios of all elements are plotted as a function of distance from the cluster center. The defined cluster center is the same as that used in Figure 3. The plotted abundances contain the results from this study and Johnson et al. (2008; 2009). In all panels, the black dashed line indicates the solar-scaled abundance values.

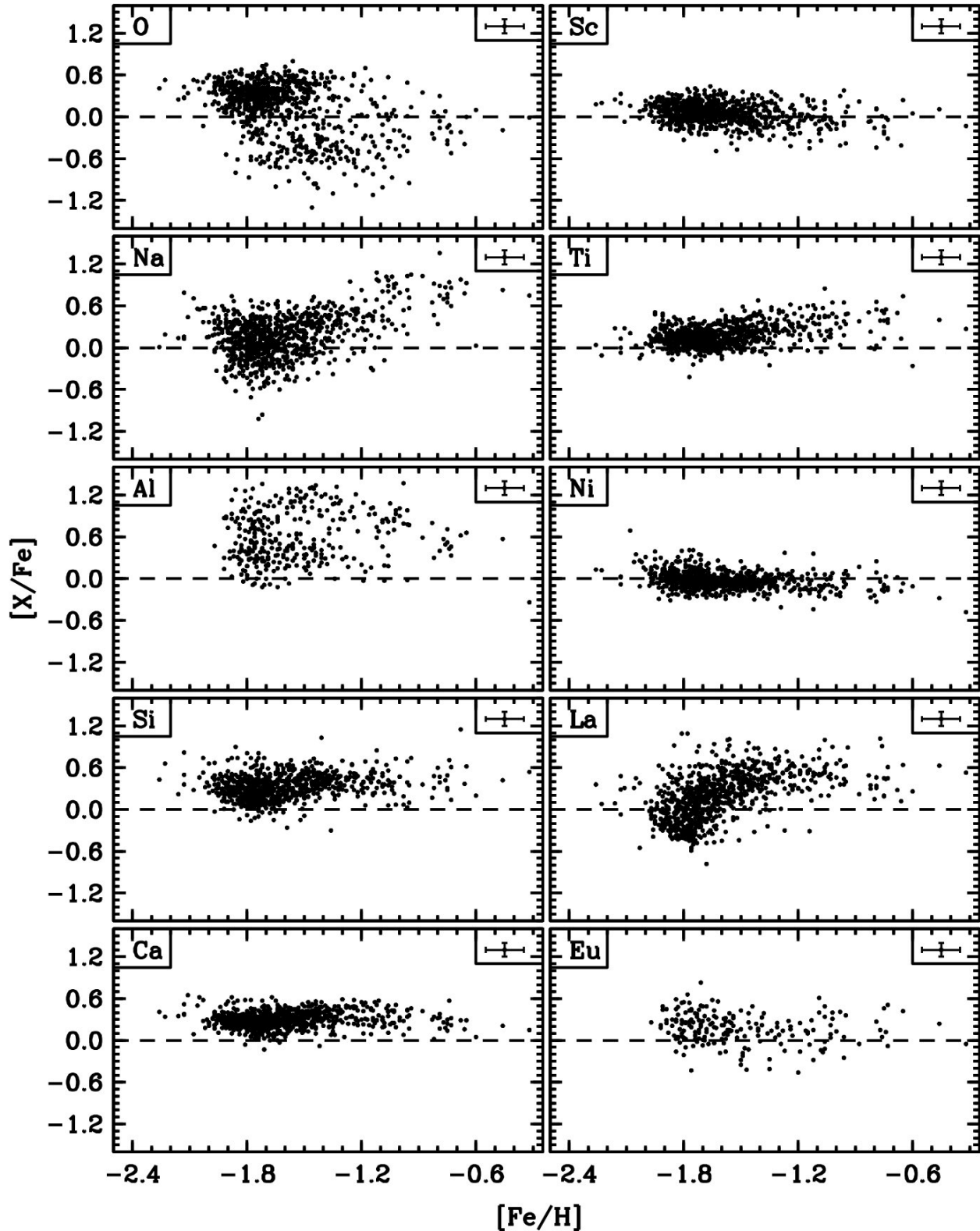


Fig. 10.— $[X/\text{Fe}]$ abundances are plotted as a function of $[\text{Fe}/\text{H}]$ for all elements analyzed in this study, including non-repeat stars from Johnson et al. (2008; 2009). The ordinate axis in all panels spans the same range, and the dashed line indicates the solar-scaled abundance values.

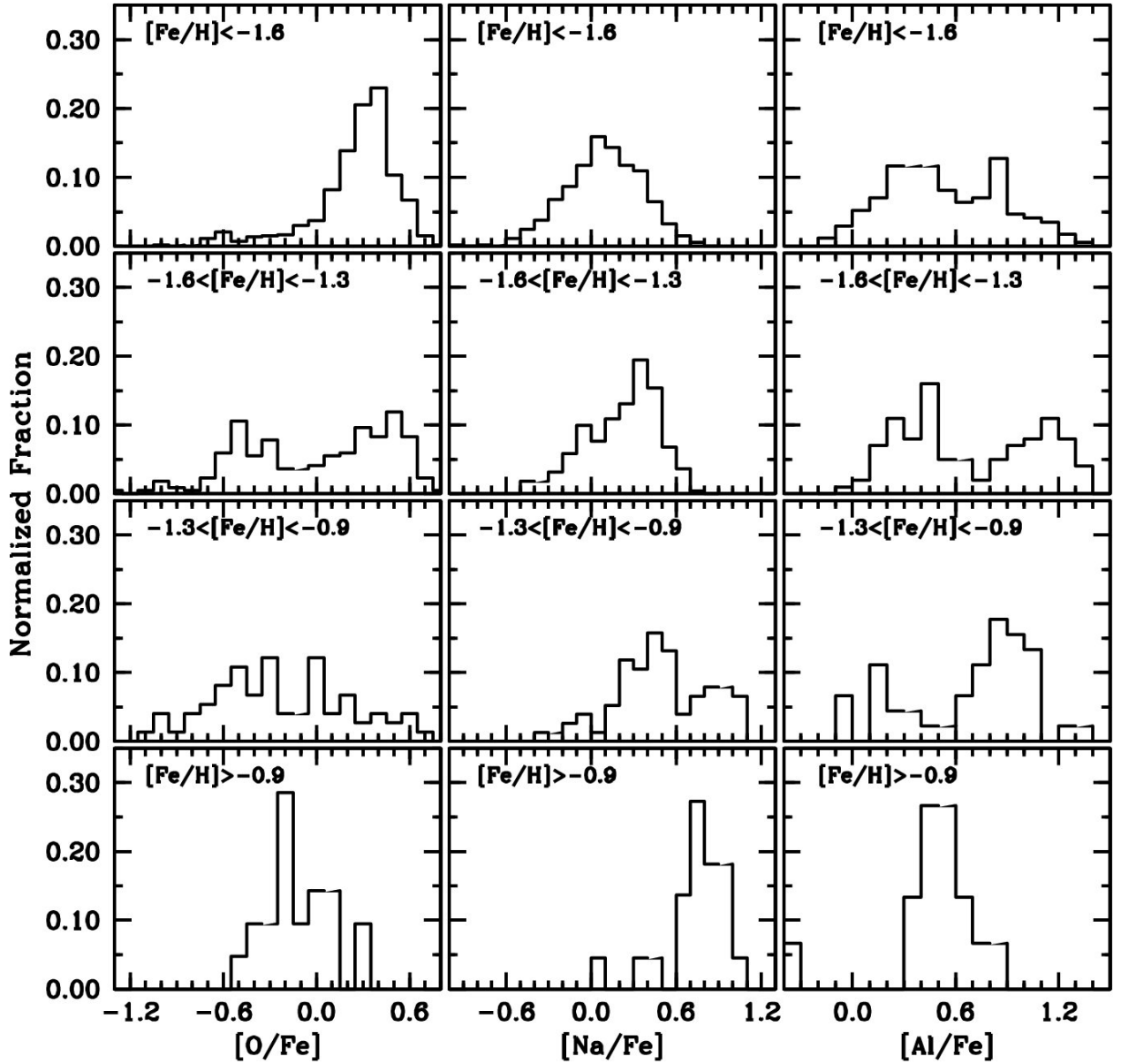


Fig. 11.— Histograms showing the abundance distributions of $[O/Fe]$, $[Na/Fe]$, and $[Al/Fe]$. Each histogram is binned in 0.10 dex increments, and the panels are broken down by the metallicity subclasses described in §4.1.

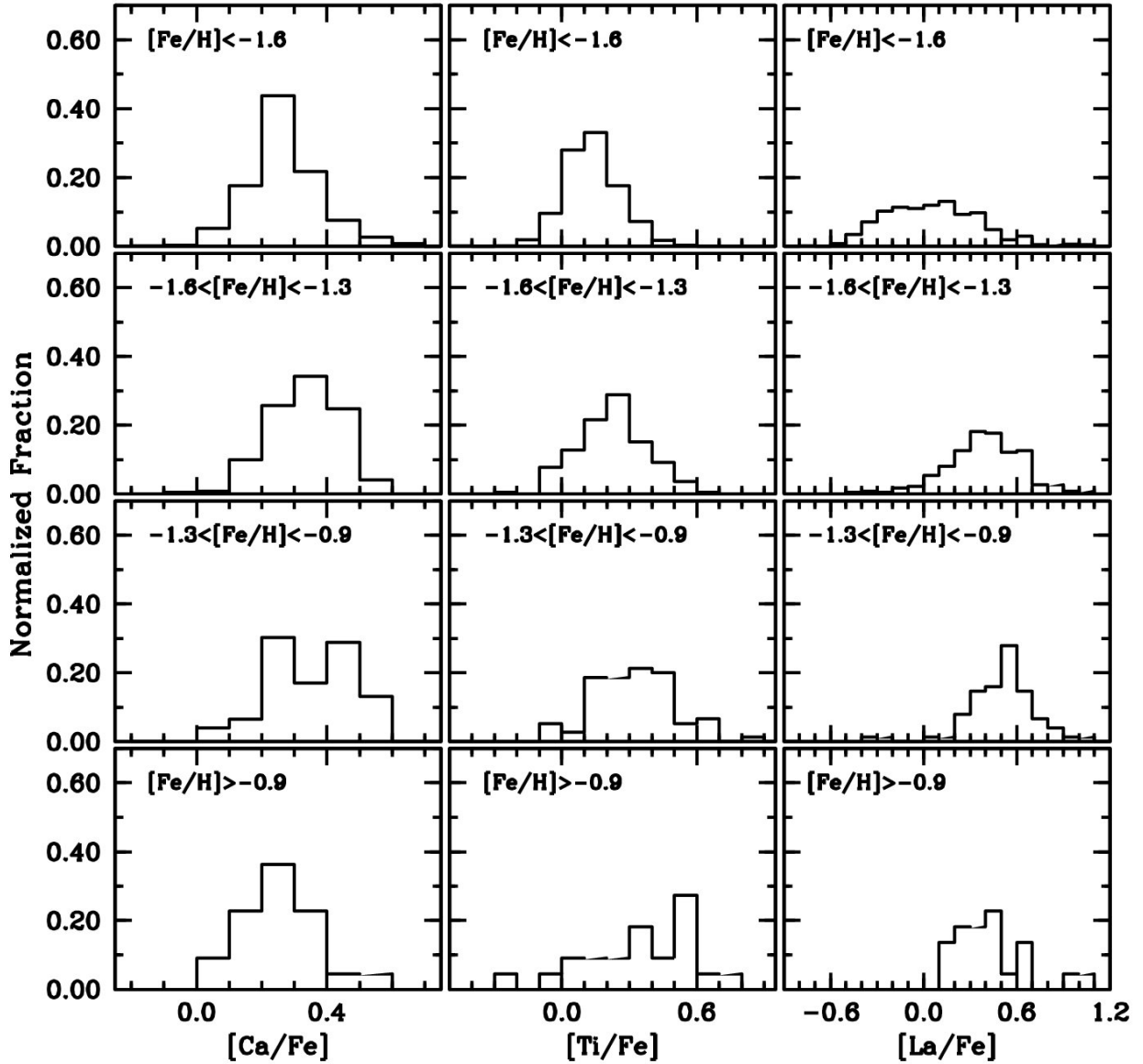


Fig. 12.— Histograms showing the abundance distributions of $[\text{Ca}/\text{Fe}]$, $[\text{Ti}/\text{Fe}]$, and $[\text{La}/\text{Fe}]$. Each histogram is binned in 0.10 dex increments, and the panels are broken down by the metallicity subclasses described in §4.1.

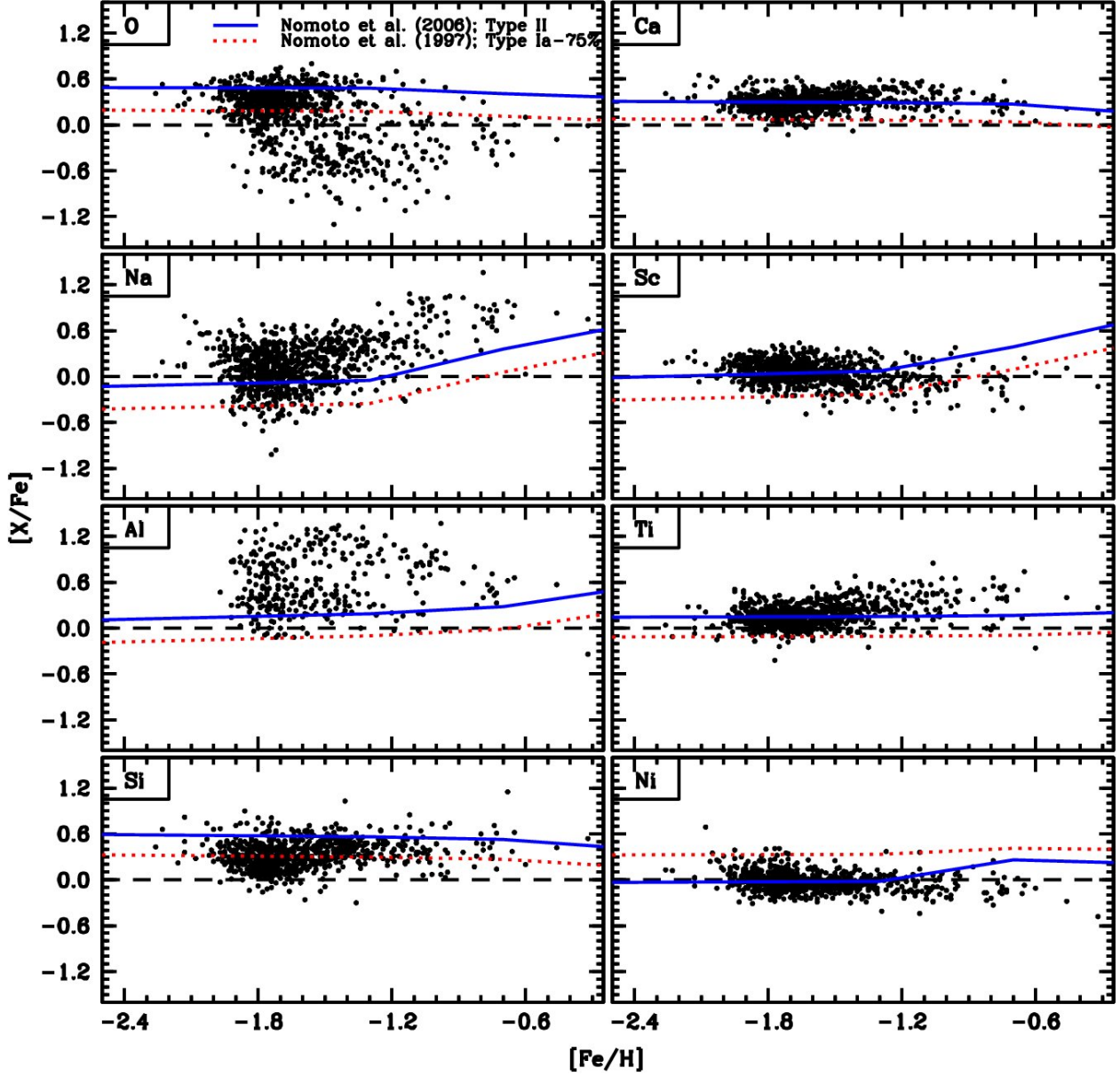


Fig. 13.— $[X/\text{Fe}]$ abundances for ω Cen stars plotted as a function of $[\text{Fe}/\text{H}]$. The solid blue lines indicate the combined Type II SNe yields of Nomoto et al. (2006) weighted by a standard IMF integrated from $0.07\text{--}50 M_{\odot}$, including contributions from hypernovae. The dotted red lines represent the expected abundance trends if the Type Ia SN yields from Nomoto et al. (1997) are mixed with the Type II yields with a 75% Type Ia and 25% Type II ratio. Note that the Type II yields have been systematically adjusted for $[\text{Sc}/\text{Fe}]$, $[\text{Ti}/\text{Fe}]$, and $[\text{Ni}/\text{Fe}]$ to match the average abundances of the RGB-MP stars.

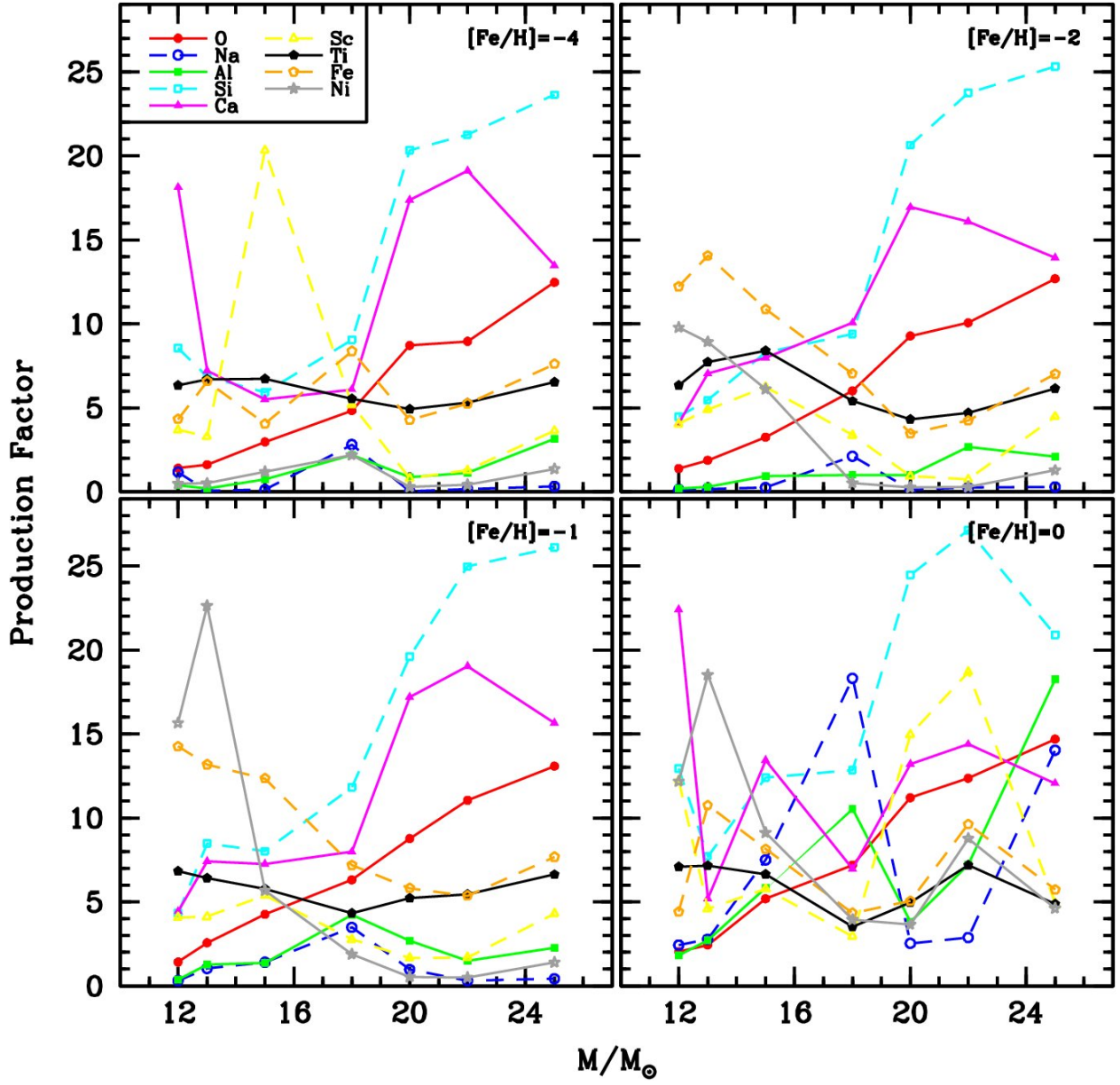


Fig. 14.— Production factors for $12-25 M_{\odot}$ Type II SNe from Woosley & Weaver (1995). The production factors are calculated as the ratio of an isotope's mass fraction in the ejecta compared to its mass fraction in the Sun. Note that the isotopes plotted here are ^{16}O , ^{23}Na , ^{27}Al , ^{28}Si , ^{40}Ca , ^{45}Sc , ^{48}Ti , ^{56}Fe , and ^{58}Ni .

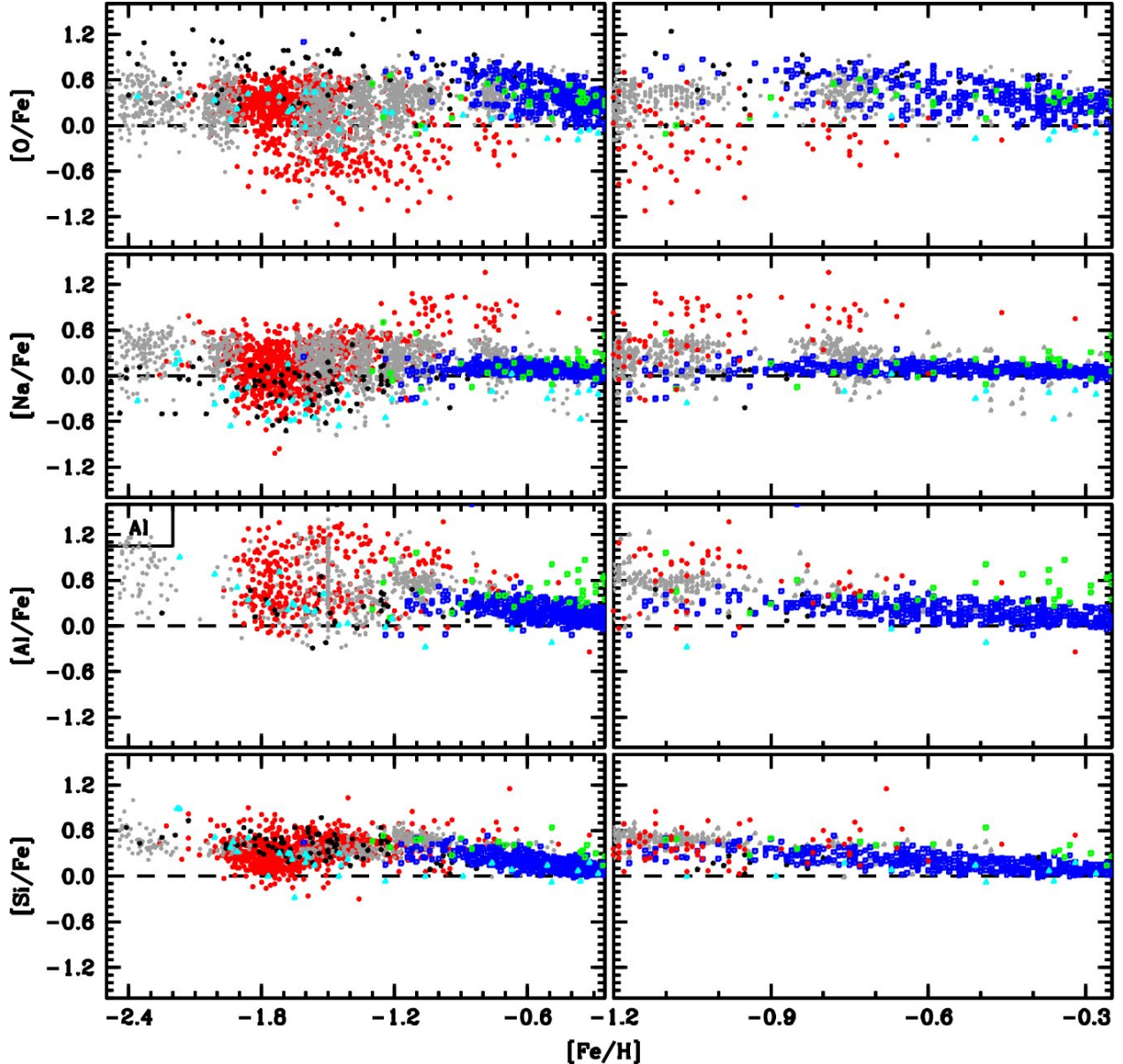


Fig. 15.— $[\text{O}/\text{Fe}]$, $[\text{Na}/\text{Fe}]$, $[\text{Al}/\text{Fe}]$, and $[\text{Si}/\text{Fe}]$ abundances for individual stars in ω Cen (filled red circles), other globular clusters (filled grey circles), Galactic halo (black stars), thin/thick disk (open blue boxes), bulge (open green boxes), and dwarf galaxies (open cyan triangles). The left panels show the $[\text{X}/\text{Fe}]$ abundances as a function of $[\text{Fe}/\text{H}]$ for ω Cen’s full metallicity range. The right panels show the same abundance trends for $[\text{Fe}/\text{H}] \geq -1.2$, but the ω Cen points are plotted on top. The literature references are listed in Table 8.

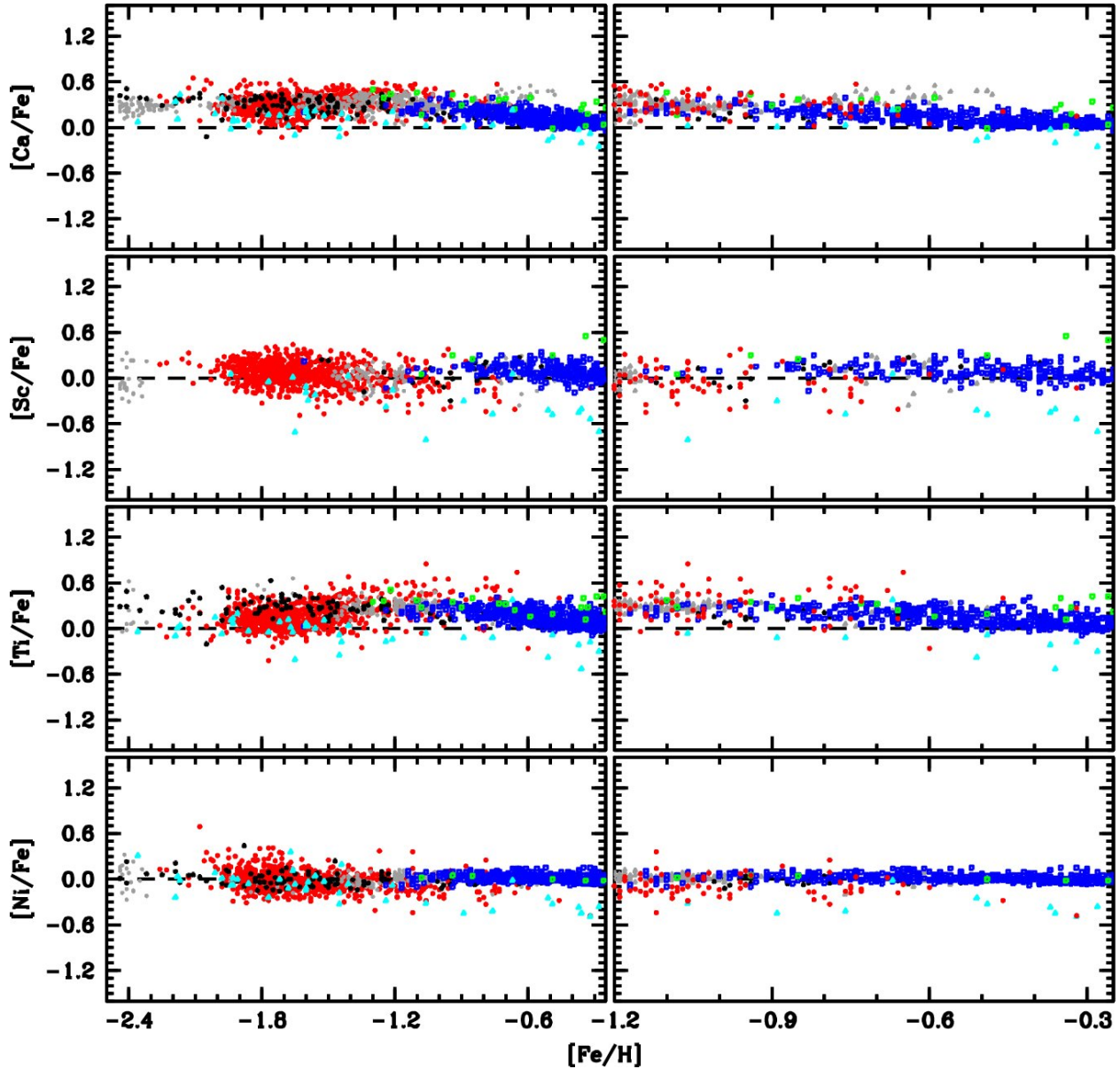


Fig. 16.— Similar plot to Figure 15 showing $[\text{Ca}/\text{Fe}]$, $[\text{Sc}/\text{Fe}]$, $[\text{Ti}/\text{Fe}]$, and $[\text{Ni}/\text{Fe}]$ abundances. The symbols are the same as those in Figure 15.

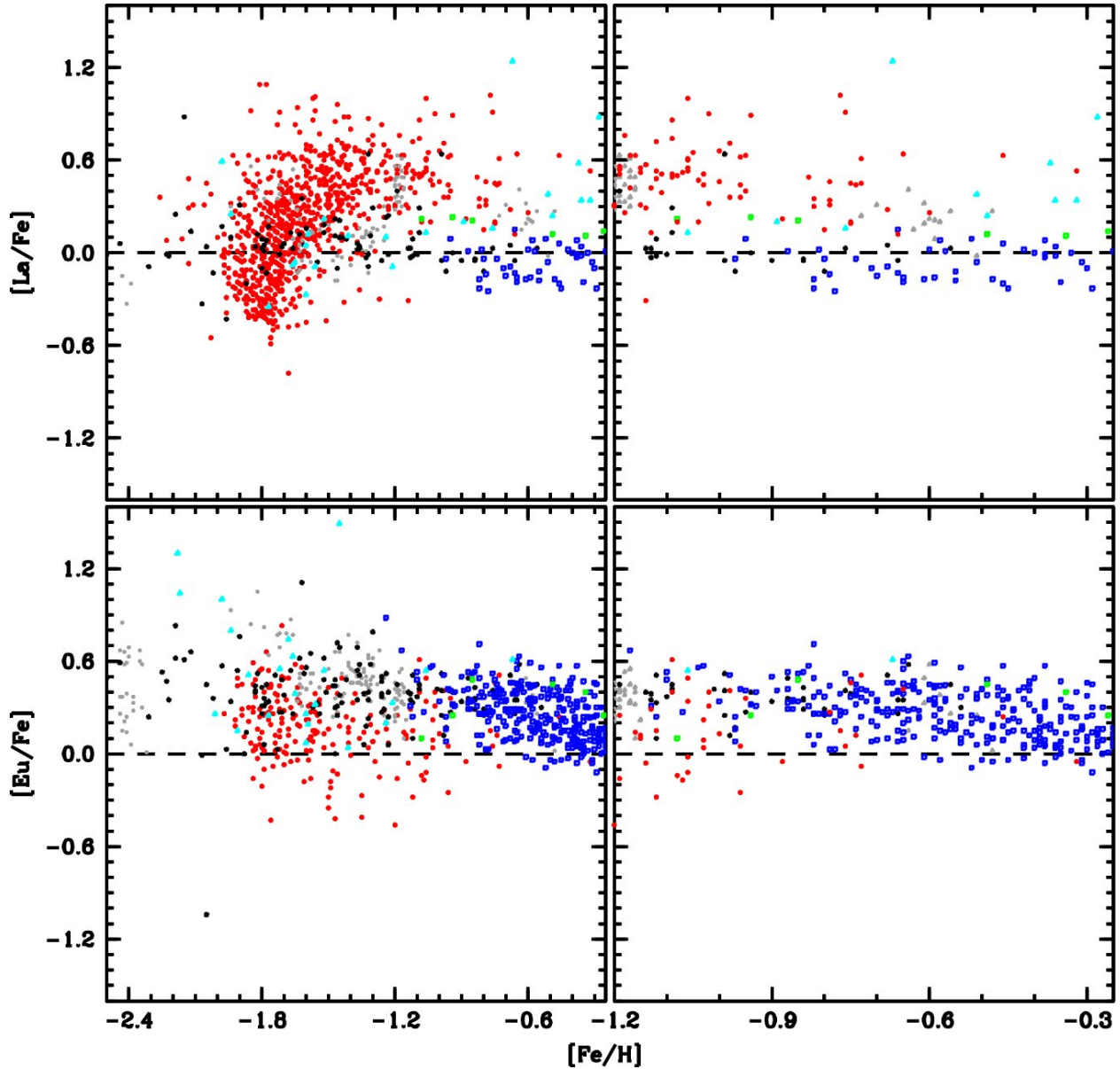


Fig. 17.— Similar plot to Figure 15 showing $[La/Fe]$ and $[Eu/Fe]$ abundances. The symbols are the same as those in Figure 15.

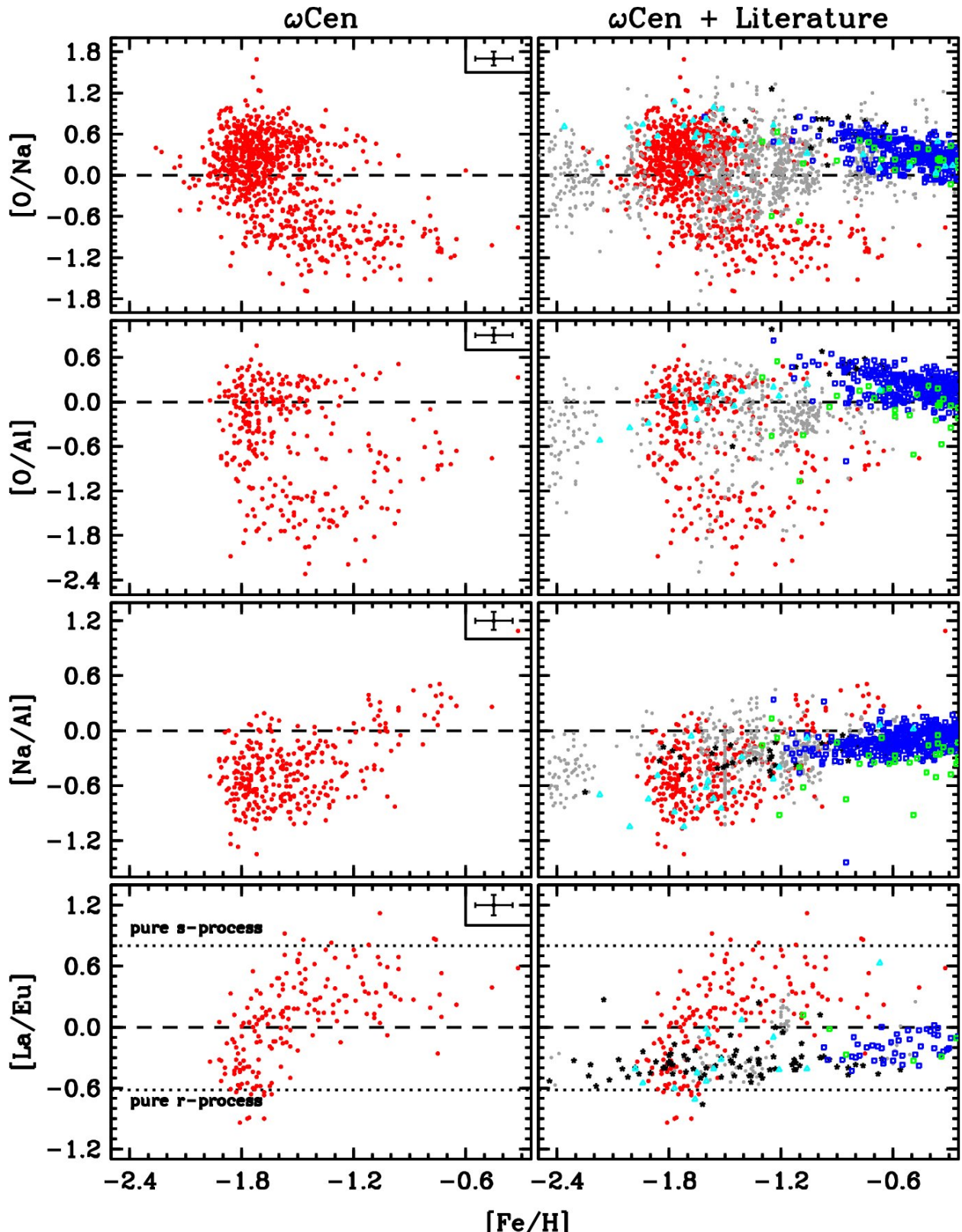


Fig. 18.— $[O/Na]$, $[O/Al]$, $[Na/Al]$, and $[La/Eu]$ abundances are plotted as a function of $[Fe/H]$ for ω Cen (left panels) and the literature (right panels). The symbols are the same as those in Figure 15. The dotted lines in the $[La/Eu]$ panels indicate the abundance ratios expected for pure r– and s–process enrichment given in McWilliam (1997).

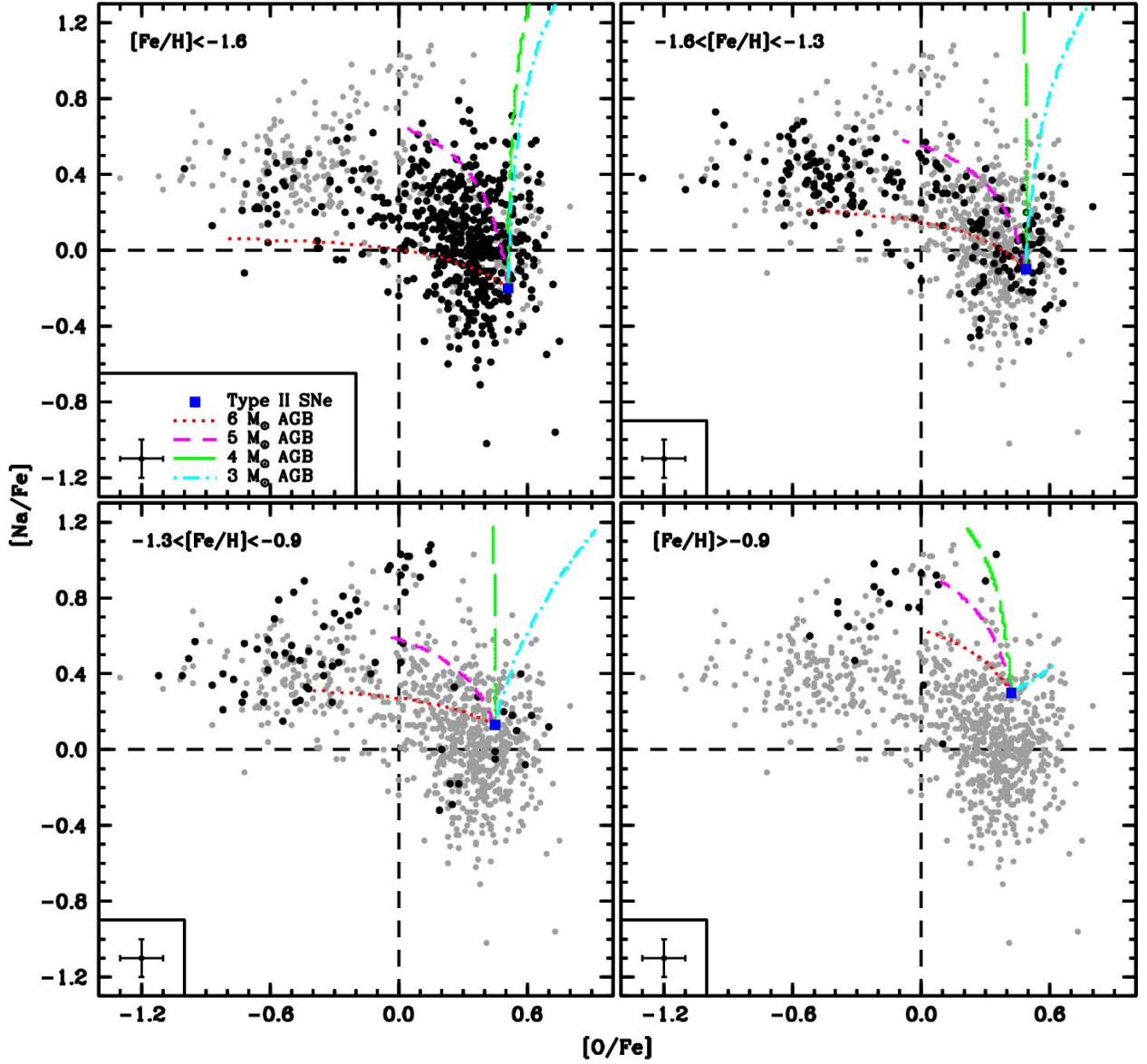


Fig. 19.— [Na/Fe] versus [O/Fe] abundances for the four primary ω Cen populations (see §4.1). The filled grey circles represent the full sample, and the filled black circles represent only the stars residing in the designated metallicity range. Individual yields from Ventura & D'Antona (2009) are shown for 3 (dot-dashed cyan lines), 4 (long dashed green lines), 5 (dashed magenta lines), and $6 M_{\odot}$ (dotted red lines) AGB stars of varying [Fe/H]. The filled blue squares indicate the approximate Type II SN+Hypernova yields from Nomoto et al. (2006) expected for the given metallicity regime.

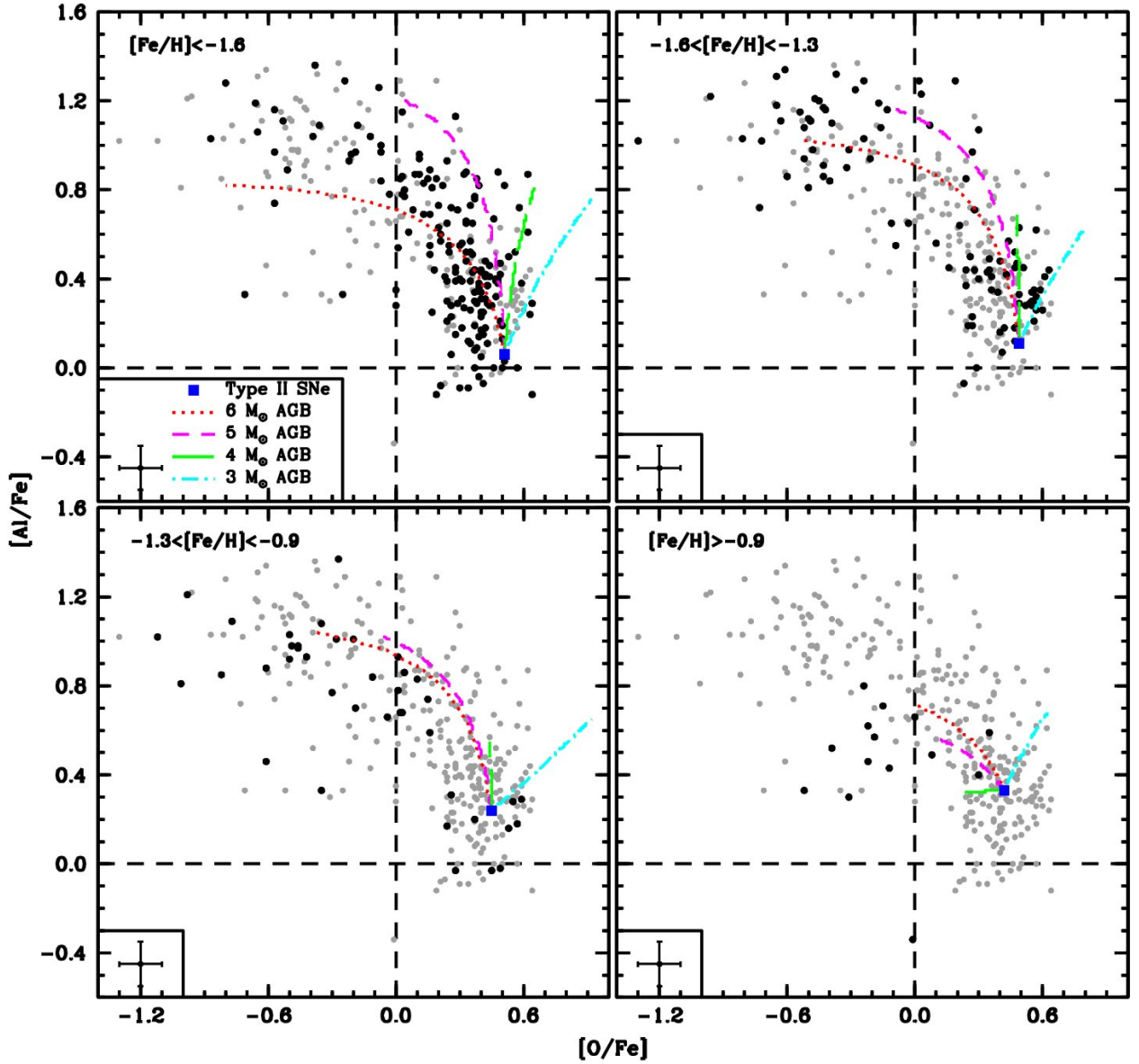


Fig. 20.— Similar plot to Figure 19 showing the run of $[Al/Fe]$ versus $[O/Fe]$ abundances for the different populations. The symbols are the same as those in Figure 19.

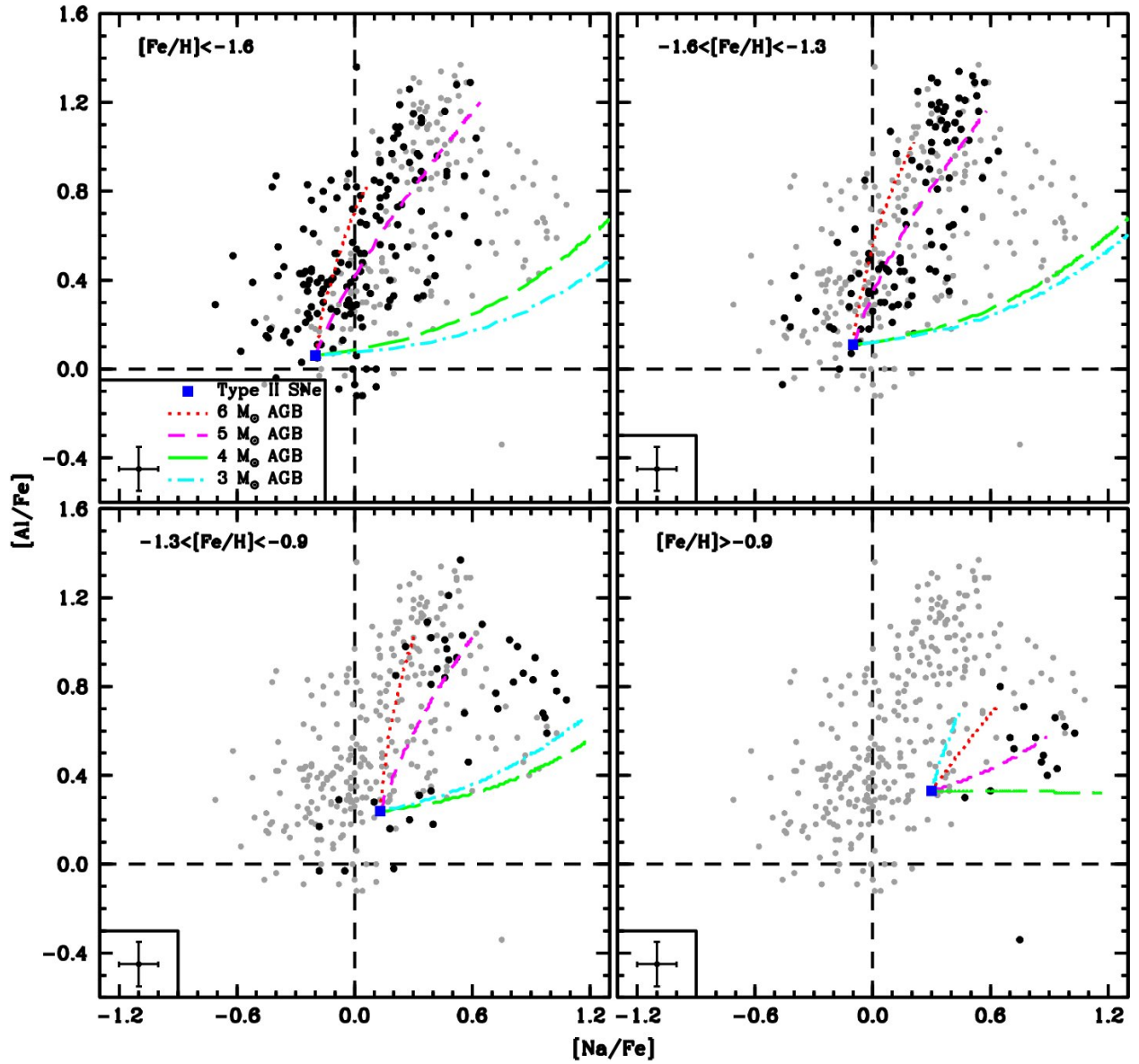


Fig. 21.— Similar plot to Figure 19 showing the run of $[Al/Fe]$ versus $[Na/Fe]$ abundances for the different populations. The symbols are the same as those in Figure 19.

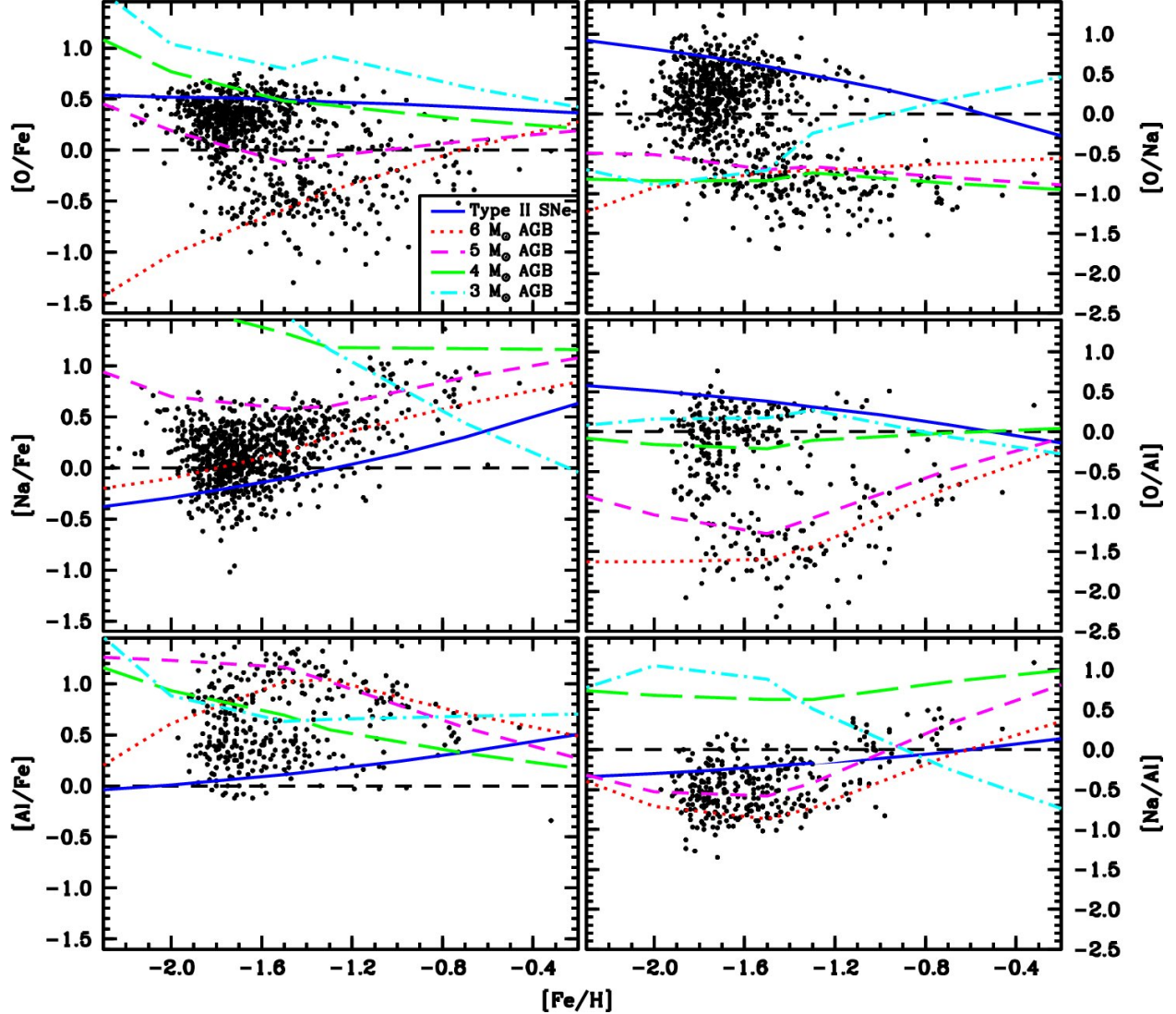


Fig. 22.— The abundances of O, Na, and Al are plotted as a function of [Fe/H] for the full sample that includes our new results and those from Johnson et al. (2008; 2009). The solid blue lines illustrate the Salpeter IMF-weighted Type II SN yields from Nomoto et al. (2006), and the other curves are the same as those in Figure 19.

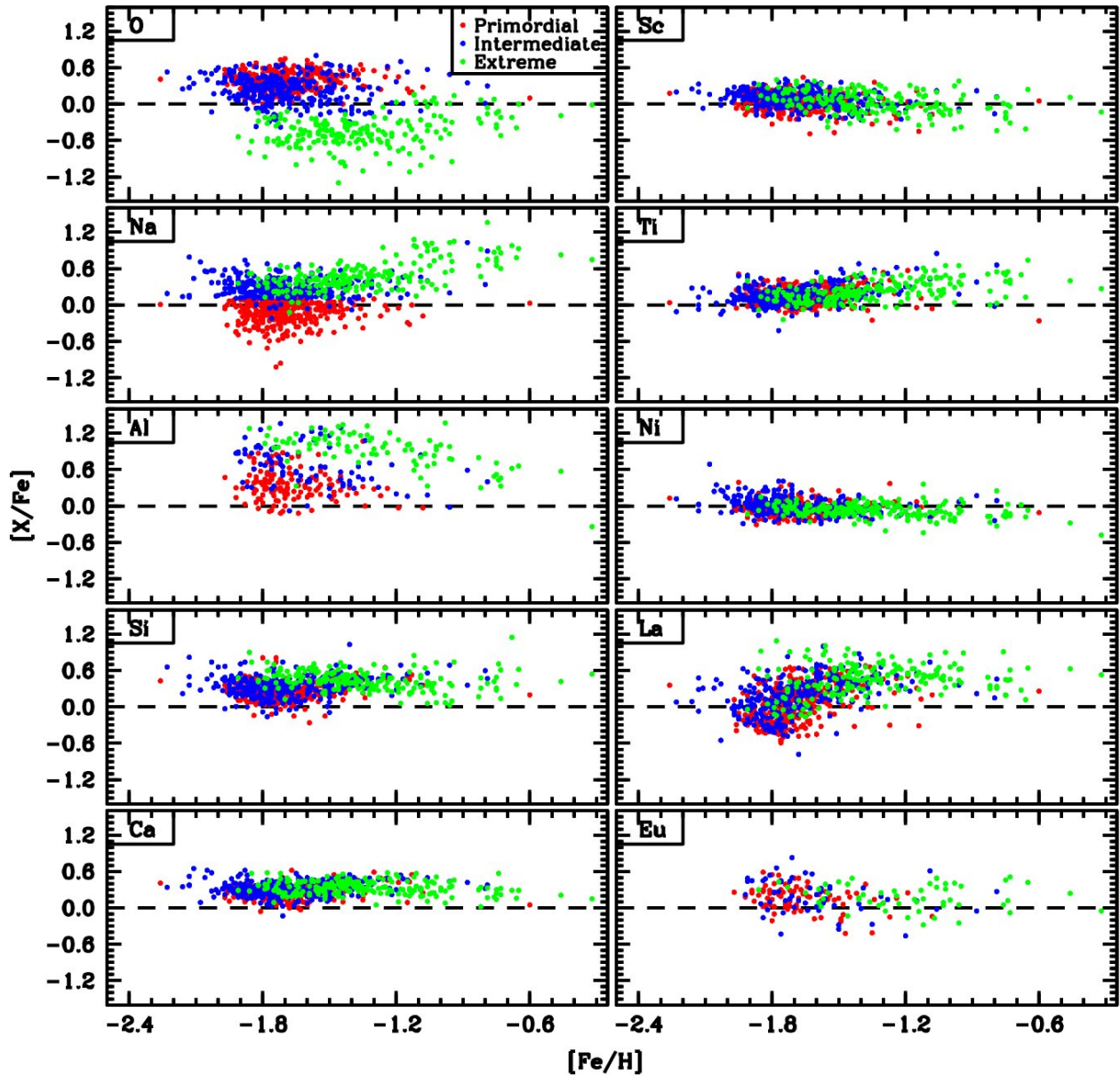


Fig. 23.— Similar plot to Figure 10 showing the abundance distribution of all elements as a function of $[\text{Fe}/\text{H}]$. The stars are broken down into the primordial (filled red circles), intermediate (filled blue circles), and extreme (filled green circles) components defined in §5.

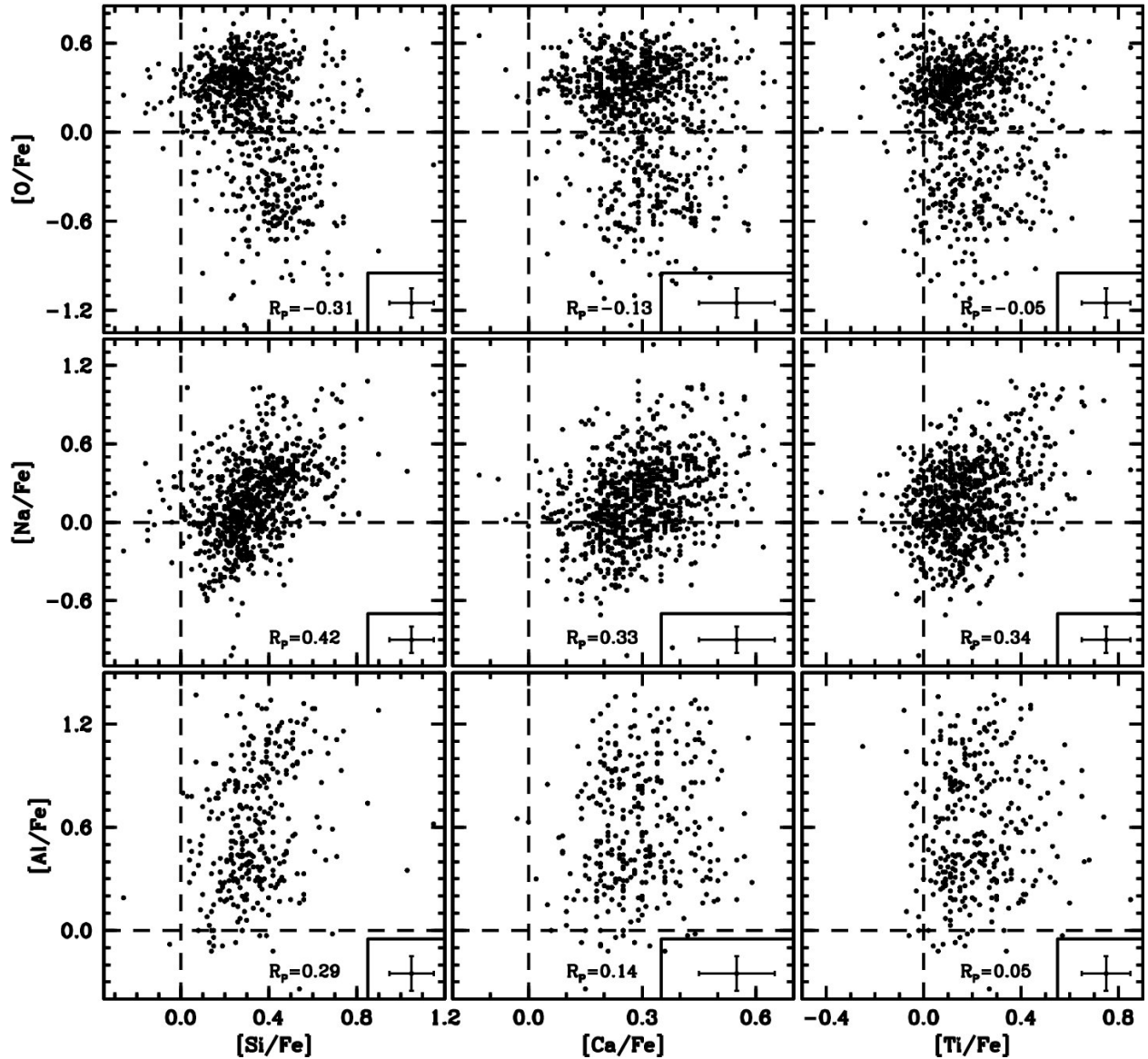


Fig. 24.— The light elements O, Na, and Al plotted as a function of the heavier α elements Si, Ca, and Ti for all ω Cen giants. The Pearson correlation coefficient (R_P) is also calculated and displayed for each panel.

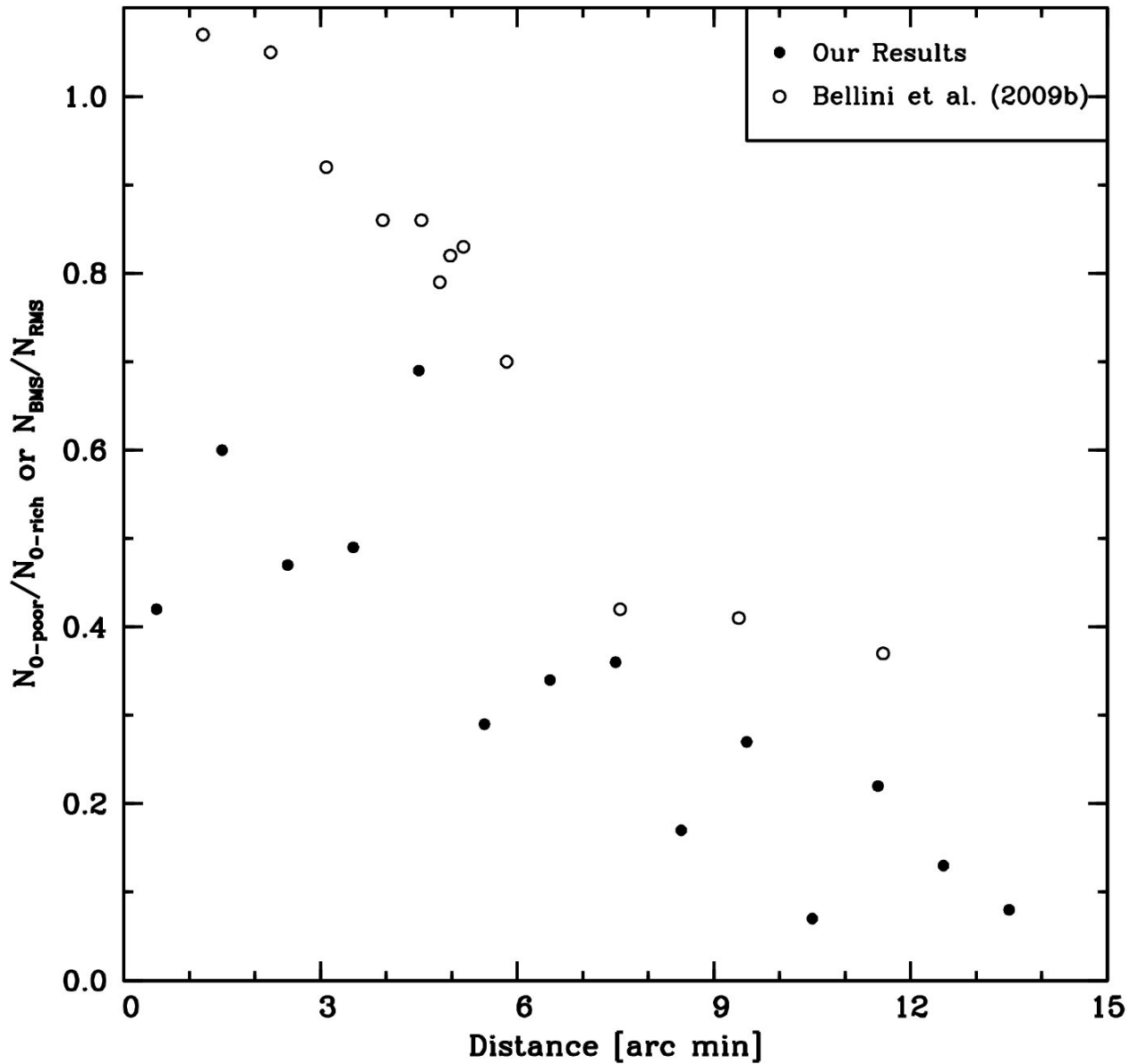


Fig. 25.— A plot illustrating the change in $N_{\text{O-poor}}/N_{\text{O-rich}}$ (our results) or $N_{\text{BMS}}/N_{\text{RMS}}$ (Bellini et al. 2009b) as a function of radial distance from the cluster center. Our results are shown as the filled circles, and the results from Bellini et al. (2009b) are shown as the open circles. Note that N_{BMS} refers to the number of blue main sequence stars and N_{RMS} the number of red main sequence stars in the Bellini et al. (2009b) sample.

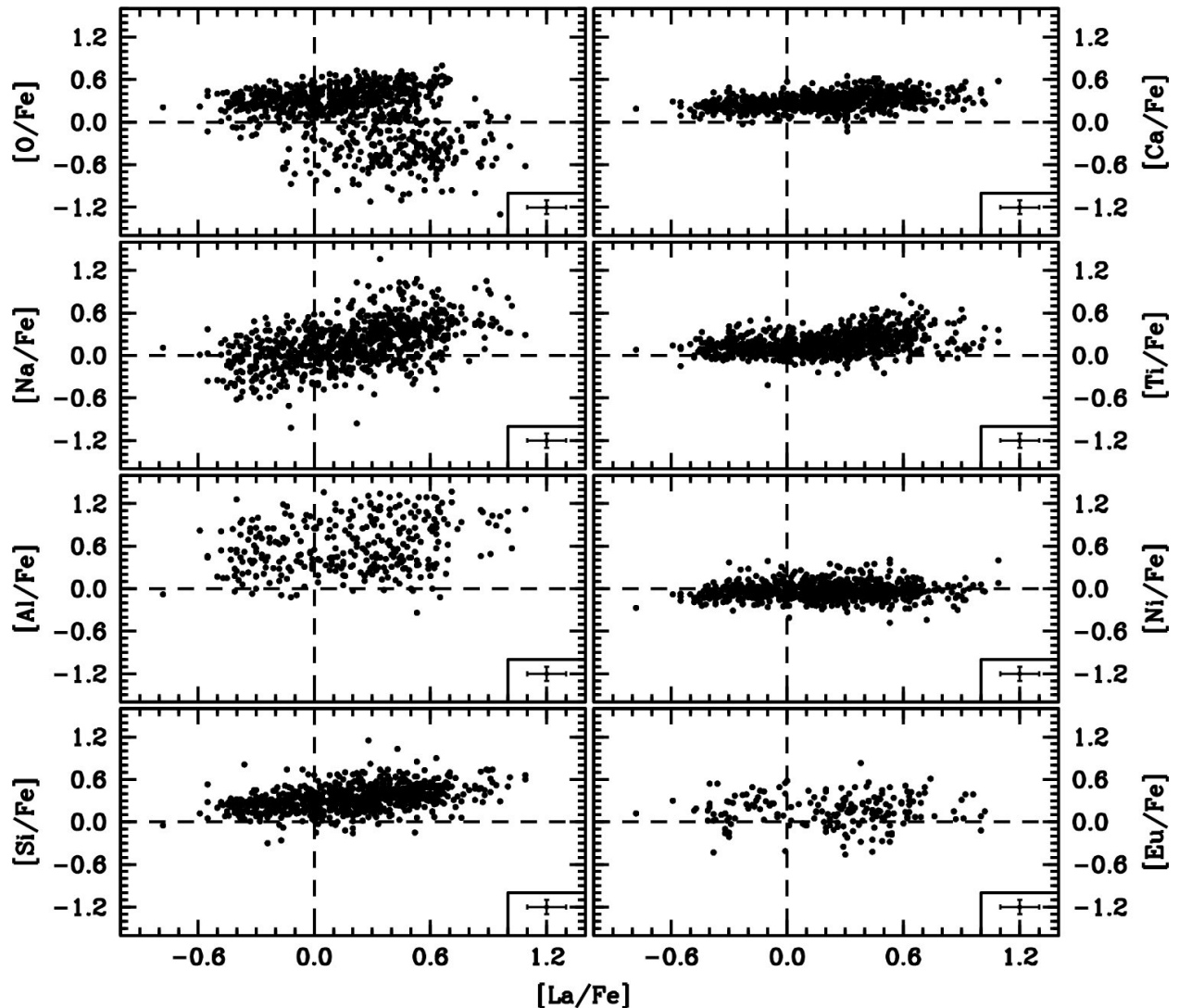


Fig. 26.— A plot of multiple elements as a function of [La/Fe]. The dashed lines indicate the solar-scaled abundance values.

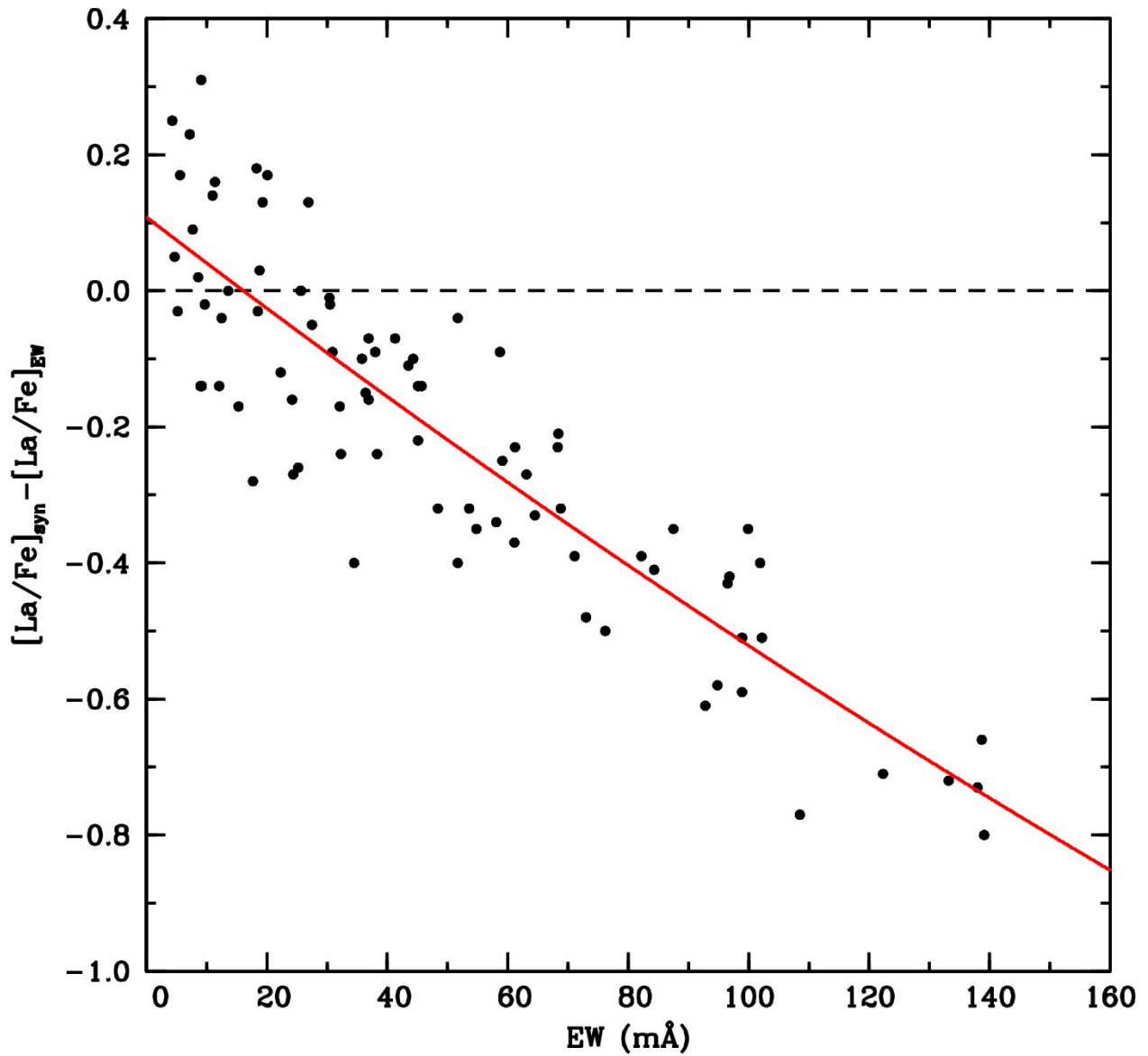


Fig. 27.— A plot of the difference between the $[\text{La}/\text{Fe}]$ abundances derived using an EW approach for the 6774 \AA La II line and a spectrum synthesis approach for the 6262 \AA La II line. The solid red line shows the least-squares fit to the data, and the horizontal dashed line indicates perfect agreement.

Table 1. Hydra Observation Log

Field	UT Date	Wavelength Center (Å)	Filter	Exposure (s)
1	2008 March 25	6250	E6257	3×3600
2	2008 March 25	6250	E6257	2×3600
...	2008 March 29	6250	E6257	1×2200
3	2008 March 26	6250	E6257	3×3600
4	2008 March 26	6250	E6257	3×3600
5	2008 March 26	6250	E6257	1×3600
...	2008 March 26	6250	E6257	1×1800
...	2008 March 27	6250	E6257	2×2700
6	2008 March 27	6250	E6257	3×3600
7	2008 March 28	6250	E6257	3×3600
8	2008 March 28	6250	E6257	3×3600
9	2008 March 28	6250	E6257	1×3600
...	2008 March 29	6250	E6257	1×3600
...	2008 March 29	6250	E6257	1×3000
10	2008 March 29	6250	E6257	3×3600
11	2009 March 06	6250	E6257	3×3600
12	2009 March 06	6250	E6257	1×3600
...	2009 March 06	6250	E6257	1×3000
13	2009 March 07	6250	E6257	3×3000
14	2009 March 08	6700	E6757	3×3000
15	2009 March 08	6700	E6757	2×3000
...	2009 March 08	6700	E6757	1×2700
...	2009 March 08	6700	E6757	1×1800

Table 2. Star Identifiers, Photometry, and Atmospheric Parameters

Star LEID ^a	Alt. ID ROA ^b	V	B-V	J	H	K _s	T _{eff} (K)	log g (cgs)	[Fe/H] Avg.	v _t (km s ⁻¹)	S/N 6250 Å	S/N 6650 Å
9	370	12.529	1.250	10.382	9.755	9.627	4500	1.20	-1.35	1.95	250	...
5009	548	12.912	1.080	10.752	10.185	10.040	4525	1.25	-1.86	1.75	200	...
6017	240	12.233	1.420	9.717	8.982	8.808	4145	0.85	-1.19	1.90	200	...
8014	6734	13.365	1.013	11.353	10.781	10.705	4700	1.75	-1.73	1.60	200	...
9013	6771	13.269	0.973	11.261	10.717	10.603	4700	1.50	-1.67	1.80	200	150
10009	...	12.573	1.234	10.331	9.664	9.520	4390	1.15	-1.43	1.70	150	...
10012	43	11.529	1.618	8.684	7.895	7.706	3930	0.25	-1.44	2.10	200	...
11019	537	12.841	1.223	10.595	9.952	9.823	4405	1.25	-1.54	1.65	225	...
11021	400	12.600	1.268	10.285	9.621	9.464	4330	1.10	-1.49	1.75	150	150
11024	91	11.738	1.333	9.294	8.639	8.410	4220	0.70	-1.76	1.90	300	...
12013	394	12.579	1.319	10.242	9.560	9.402	4300	1.10	-1.20	1.80	175	...
12014	6602	13.300	0.992	11.293	10.754	10.644	4710	1.60	-1.70	1.80	80	125
14010	435	12.807	0.993	10.803	10.255	10.131	4700	1.45	-1.89	1.80	200	100
15022	180	11.982	1.243	9.730	9.087	8.952	4405	0.95	-1.76	1.70	250	...
15023	234	12.182	1.166	9.964	9.352	9.231	4460	1.05	-1.80	1.95	200	...
15026	245	12.234	1.329	9.853	9.120	9.004	4260	0.95	-1.31	1.90	250	250
16009	252	12.232	1.201	9.915	9.286	9.117	4345	1.00	-1.76	1.80	275	...
16015	213	12.127	1.122	9.979	9.373	9.210	4510	1.05	-1.92	2.00	275	...
16019	6460	13.217	1.039	11.268	10.742	10.618	4775	1.65	-1.74	1.90	175	150
16027	6497	13.499	0.948	11.532	10.993	10.857	4740	1.70	-1.86	1.85	100	...
17014	212	12.120	1.363	9.747	9.077	8.936	4285	0.90	-1.60	1.75	150	200
17015	325	12.430	1.156	10.235	9.610	9.497	4470	1.15	-1.79	1.80	175	...
17027	6461	13.388	0.880	11.524	11.028	10.913	4900	1.75	-2.00	1.80	100	...
17029	6465	13.129	0.915	11.201	10.668	10.543	4795	1.60	-1.98	1.60	125	125
17032	605	12.989	1.150	10.841	10.226	10.106	4515	1.40	-1.54	1.75	150	...
17046	6545	13.266	0.873	11.364	10.858	10.738	4850	1.70	-1.84	1.35	90	100
18017	448	12.699	1.048	10.620	10.061	9.899	4600	1.35	-1.84	2.10	150	...
18020	146	11.917	1.360	9.529	8.838	8.681	4260	0.80	-1.71	2.05	>350	200
18035	581	12.922	1.061	10.855	10.227	10.123	4590	1.40	-1.66	1.70	125	...
18040	465	12.708	1.267	10.448	9.736	9.596	4355	1.20	-1.31	1.70	200	150
18047	408	12.570	1.104	10.450	9.844	9.698	4535	1.25	-1.85	1.85	175	...
19022	6442	13.075	0.929	11.212	10.689	10.576	4885	1.65	-1.80	1.80	150	...
19062	464	12.803	1.144	10.601	10.001	9.872	4470	1.30	-1.84	1.90	175	...
20018	6259	13.384	1.099	11.348	10.757	10.598	4615	1.60	-1.60	1.60	85	75
20037	6316	13.153	1.172	11.033	10.442	10.306	4545	1.50	-1.58	1.75	225	125
20042	6327	13.093	0.999	11.099	10.541	10.402	4695	1.55	-1.87	1.80	100	...
20049	6355	13.273	1.058	11.184	10.559	10.464	4570	1.55	-1.80	1.70	225	...
21032	172	11.947	1.394	9.550	8.782	8.620	4215	0.80	-1.50	1.80	>350	...
21035	362	12.457	1.151	10.343	9.716	9.547	4520	1.20	-1.87	1.95	200	...
21042	348	12.494	1.179	10.322	9.700	9.575	4485	1.20	-1.73	1.70	175	...
21063	6342	13.263	1.023	11.285	10.709	10.571	4700	1.60	-1.88	1.70	150	...
22023	6137	13.312	1.122	11.308	10.727	10.568	4660	1.60	-1.23	1.53	175	100
22037	307	12.339	1.186	10.178	9.559	9.402	4485	1.10	-1.76	1.80	215	...
22042	415	12.607	1.120	10.543	9.930	9.832	4605	1.30	-1.74	1.95	200	...
22049	6207	13.419	0.989	11.442	10.840	10.711	4685	1.65	-1.86	1.55	125	...

Table 2—Continued

Star LEID ^a	Alt. ID ROA ^b	V	B-V	J	H	K _s	T _{eff} (K)	log g (cgs)	[Fe/H] Avg.	v _t (km s ⁻¹)	S/N 6250 Å	S/N 6650 Å
22063	6234	13.358	1.006	11.312	10.799	10.623	4655	1.60	-1.81	1.75	175	...
23022	6119	13.396	0.983	11.450	10.875	10.799	4765	1.70	-1.93	1.75	150	...
23033	558	12.877	1.089	10.846	10.266	10.156	4655	1.45	-1.73	1.60	100	75
23042	570	12.906	1.053	10.891	10.278	10.179	4655	1.45	-1.84	1.80	150	150
23050	6179	13.106	1.020	11.132	10.539	10.459	4720	1.55	-1.84	1.80	225	...
23061	296	12.337	1.188	10.158	9.472	9.390	4460	1.10	-1.72	1.75	250	...
23068	96	11.658	1.459	9.084	8.344	8.191	4115	0.60	-1.64	2.10	300	250
24013	56	11.596	1.589	8.816	7.991	7.801	3950	0.40	-1.64	2.15	150	...
24027	5969	13.013	1.099	10.952	10.344	10.226	4600	1.45	-1.55	1.60	150	...
24040	5993	13.129	0.952	11.230	10.713	10.605	4850	1.65	-1.75	1.55	100	...
24046	74	11.657	1.367	9.263	8.574	8.406	4260	0.70	-1.76	1.95	300	...
24056	364	12.474	1.145	10.363	9.708	9.584	4525	1.20	-1.77	1.75	125	...
24062	352	12.628	1.307	10.304	9.691	9.469	4325	1.15	-1.41	1.60	150	...
25006	5941	13.444	0.835	11.620	11.106	11.016	4950	1.80	-1.78	1.60	150	75
25026	569	12.875	1.067	10.807	10.238	10.137	4630	1.40	-1.89	2.00	150	...
25043	89	11.734	1.500	9.239	8.449	8.257	4130	0.60	-1.50	2.05	250	...
25062	46	11.583	1.545	8.788	7.985	7.839	3965	0.40	-1.60	2.30	>350	...
25065	...	12.101	1.689	9.231	8.407	8.175	3900	0.55	-1.11	2.05	100	...
25068	58	11.542	1.434	9.052	8.354	8.176	4180	0.60	-1.71	2.00	175	...
26010	5759	12.972	0.998	11.088	10.571	10.442	4855	1.55	-1.68	1.25	125	125
26014	387	12.605	1.107	10.517	9.923	9.808	4585	1.30	-1.91	2.00	175	...
26022	5788	13.095	1.071	11.071	10.486	10.380	4660	1.50	-1.76	1.50	175	...
26025	61	11.411	1.591	8.671	7.877	7.757	4000	0.40	-1.63	2.45	275	...
26030	5809	13.403	0.960	11.527	10.975	10.887	4855	1.75	-1.87	1.65	100	...
26069	528	12.893	0.998	10.919	10.365	10.254	4735	1.45	-1.87	1.45	175	...
26072	303	12.415	1.163	10.258	9.632	9.503	4495	1.15	-1.73	1.75	200	150
26086	295	12.787	1.313	10.330	9.650	9.464	4205	1.10	-1.07	1.75	175	...
26088	161	11.895	1.379	9.484	8.791	8.616	4240	0.80	-1.59	1.85	175	...
27048	313	12.442	1.241	10.253	9.566	9.468	4445	1.15	-1.44	1.60	150	...
27050	5823	13.030	0.964	11.125	10.529	10.455	4795	1.55	-1.93	2.00	150	125
27073	566	12.959	1.109	10.848	10.207	10.064	4520	1.40	-1.68	1.60	175	...
27094	5880	13.381	1.019	11.393	10.824	10.708	4705	1.65	-1.80	1.90	90	100
27095	139	11.817	1.452	9.378	8.632	8.470	4195	0.70	-1.52	2.05	200	...
28016	5585	13.177	1.038	11.077	10.481	10.371	4575	1.50	-1.71	1.45	150	...
28020	424	12.690	1.008	10.638	10.062	9.972	4650	1.35	-1.84	1.55	150	...
28044	246	12.323	1.169	10.071	9.392	9.286	4395	1.05	-1.69	1.75	250	...
28069	185	12.084	1.296	9.799	9.156	8.995	4365	0.95	-1.76	1.85	250	150
28084	497	12.910	1.113	10.734	10.101	10.011	4490	1.35	-1.69	1.75	200	150
28092	380	12.521	1.207	10.301	9.649	9.522	4425	1.15	-1.69	1.85	225	...
29029	545	12.911	1.139	10.811	10.197	10.068	4555	1.40	-1.54	1.50	200	...
29031	375	12.584	1.047	10.568	9.983	9.863	4665	1.30	-1.80	1.75	175	...
29037	5640	13.213	0.982	11.303	10.795	10.684	4840	1.70	-1.74	1.80	125	...
29059	458	12.820	1.140	10.662	10.007	9.868	4475	1.30	-1.55	1.80	125	...
29067	84	11.793	1.663	8.879	8.092	7.826	3880	0.40	-1.25	1.90	150	...
29069	206	12.313	1.232	9.893	9.151	8.992	4215	0.95	-1.54	1.75	200	225

Table 2—Continued

Star LEID ^a	Alt. ID ROA ^b	V	B-V	J	H	K _s	T _{eff} (K)	log g (cgs)	[Fe/H] Avg.	v _t (km s ⁻¹)	S/N 6250 Å	S/N 6650 Å
29072	385	12.665	1.119	10.486	9.875	9.754	4490	1.25	-1.84	1.70	175	...
29085	450	12.839	1.039	10.802	10.228	10.074	4635	1.40	-1.68	1.55	200	...
29089	5686	13.439	1.008	11.446	10.874	10.732	4685	1.65	-1.76	1.50	90	...
29099	184	11.934	1.445	9.506	8.788	8.597	4210	0.75	-1.62	2.00	175	175
29106	209	11.951	1.317	9.657	9.007	8.827	4350	0.90	-1.92	1.90	175	...
30013	540	12.895	1.249	10.737	10.116	9.955	4485	1.35	-1.32	1.75	100	...
30019	5588	13.204	1.059	11.029	10.392	10.279	4480	1.45	-1.51	1.65	225	...
30022	496	12.793	0.998	10.775	10.214	10.096	4680	1.40	-1.80	1.75	150	200
30031	95	11.634	1.544	9.051	8.326	8.118	4100	0.55	-1.52	2.00	275	250
30069	5644	13.430	0.900	11.641	11.138	11.021	4985	1.80	-2.01	1.65	200	...
30094	512	12.934	1.145	10.722	10.070	9.935	4430	1.30	-1.54	1.60	100	...
30124	5707	13.299	1.077	11.167	10.583	10.423	4530	1.55	-1.54	1.50	175	...
31016	526	13.097	1.016	10.996	10.453	10.313	4595	1.50	-1.93	1.60	125	...
31041	361	12.596	1.091	10.378	9.762	9.637	4450	1.20	-1.69	1.65	175	...
31047	...	13.216	0.995	11.245	10.701	10.558	4725	1.60	-1.83	1.85	200	...
31048	504	12.770	1.020	10.840	10.302	10.166	4785	1.45	-1.60	1.45	150	...
31075	5413	13.487	0.992	11.588	11.006	10.876	4785	1.90	-1.74	1.60	50	...
31079	200	12.151	1.202	9.957	9.325	9.211	4470	1.05	-1.84	1.95	250	...
31094	292	12.405	1.130	10.288	9.690	9.570	4555	1.20	-1.74	1.80	250	150
31095	5434	13.103	1.059	11.100	10.524	10.372	4665	1.55	-1.77	1.65	75	125
31104	5446	13.160	0.953	11.284	10.739	10.619	4845	1.65	-1.83	1.60	125	...
31109	5451	13.482	1.056	11.446	10.829	10.719	4625	1.65	-1.48	1.65	150	...
31110	195	12.242	1.354	9.721	9.042	8.846	4160	0.85	-1.49	1.95	200	...
31119	327	12.586	1.234	10.159	9.484	9.308	4235	1.05	-1.53	1.75	175	...
31133	5489	13.311	0.922	11.445	10.949	10.827	4895	1.70	-1.87	1.55	100	...
31139	373	12.621	1.113	10.486	9.828	9.701	4500	1.25	-1.77	1.70	300	...
31141	261	12.368	1.159	10.077	9.434	9.284	4365	1.05	-1.66	1.65	200	...
31147	5511	13.298	0.997	11.286	10.747	10.634	4700	1.65	-1.56	1.75	100	...
31152	5522	13.195	1.046	11.170	10.576	10.442	4640	1.55	-1.75	2.15	75	...
32014	474	12.809	1.042	10.732	10.174	10.048	4620	1.40	-1.78	1.90	125	...
32026	544	12.978	1.083	10.858	10.241	10.126	4540	1.40	-1.44	1.55	125	...
32027	5367	13.054	1.030	10.994	10.407	10.300	4620	1.50	-1.81	1.85	85	...
32043	5394	13.269	0.985	11.370	10.860	10.746	4850	1.70	-1.71	1.70	75	...
32063	382	12.613	1.151	10.446	9.822	9.689	4485	1.20	-1.72	1.75	250	150
32069	5411	13.268	0.947	11.483	10.963	10.853	4980	1.75	-1.77	1.50	125	...
32100	5448	13.105	1.051	11.124	10.519	10.410	4690	1.55	-1.73	1.65	200	...
32101	502	12.940	1.117	10.761	10.150	10.026	4485	1.35	-1.65	1.85	150	150
32125	262	12.352	1.174	10.116	9.479	9.360	4425	1.10	-1.71	1.90	300	...
32130	5478	13.253	0.956	11.372	10.815	10.714	4840	1.65	-1.74	1.55	150	...
32138	48	11.402	1.579	8.750	8.035	7.844	4065	0.45	-1.76	2.40	200	...
32140	390	12.687	1.126	10.529	9.892	9.793	4500	1.25	-1.75	1.75	250	...
32144	5490	13.154	1.111	11.051	10.392	10.288	4535	1.45	-1.48	1.55	175	...
32165	5501	13.172	1.027	11.068	10.463	10.365	4570	1.50	-1.87	1.95	125	...
32169	5510	13.331	1.173	10.975	10.289	10.128	4285	1.35	-1.06	2.05	200	...
32171	251	12.189	1.383	9.897	9.176	9.051	4330	0.95	-1.46	1.80	175	...

Table 2—Continued

Star LEID ^a	Alt. ID ROA ^b	V	B–V	J	H	K _s	T _{eff} (K)	log g (cgs)	[Fe/H] Avg.	v _t (km s ^{−1})	S/N 6250 Å	S/N 6650 Å
33006	...	11.403	1.659	8.924	8.064	7.929	4125	0.50	−1.61	2.10	250	...
33011	159	11.879	1.337	9.537	8.844	8.715	4305	0.80	−1.75	2.05	300	...
33018	379	12.647	1.125	10.339	9.724	9.572	4365	1.15	−1.79	1.70	150	150
33030	5056	13.260	0.975	11.246	10.691	10.593	4695	1.60	−1.71	1.55	100	...
33051	...	11.979	1.213	9.778	9.150	8.993	4450	0.95	−1.65	1.75	300	...
33064	5108	13.197	1.051	11.220	10.587	10.503	4685	1.55	−1.76	1.55	175	...
33099	175	12.100	1.483	9.615	8.848	8.691	4155	0.80	−1.02	1.90	150	...
33114	71	11.645	1.531	9.092	8.344	8.125	4105	0.55	−1.58	2.05	200	325
33115	5198	13.417	1.051	11.400	10.812	10.658	4640	1.65	−1.24	1.35	100	...
33126	5216	13.447	1.073	11.362	10.775	10.572	4555	1.60	−1.50	1.70	125	...
33129	397	12.644	1.122	10.583	9.976	9.869	4605	1.30	−1.76	1.85	225	...
33138	560	13.032	1.057	10.966	10.375	10.234	4595	1.45	−1.74	1.85	100	...
33145	561	13.007	0.993	11.056	10.528	10.364	4750	1.55	−1.95	1.75	100	...
33154	5243	13.329	0.902	11.507	11.018	10.914	4965	1.75	−1.42	1.10	125	...
33167	5268	13.451	0.984	11.494	10.951	10.856	4765	1.70	−1.51	1.65	125	...
33177	5290	13.420	1.008	11.349	10.789	10.688	4630	1.65	−1.69	2.00	125	...
34008	434	12.629	1.174	10.510	9.897	9.749	4530	1.25	−1.71	1.80	175	100
34029	243	12.107	1.452	9.635	8.878	8.719	4170	0.80	−1.28	1.90	150	...
34040	503	12.748	1.098	10.662	10.061	9.949	4585	1.35	−1.70	1.75	150	...
34056	576	12.976	0.942	11.099	10.603	10.466	4875	1.60	−1.63	1.40	150	...
34069	254	12.357	1.192	10.131	9.500	9.340	4420	1.10	−1.63	1.80	250	...
34075	157	11.937	1.403	9.617	8.873	8.669	4270	0.80	−1.49	1.75	>350	150
34081	436	12.774	1.168	10.632	9.987	9.851	4495	1.30	−1.67	1.70	>350	...
34129	559	13.045	1.019	11.100	10.536	10.415	4750	1.55	−1.80	1.85	150	...
34130	5176	13.242	0.956	11.390	10.883	10.793	4920	1.70	−1.74	1.20	150	...
34134	45	11.483	1.497	9.009	8.301	8.139	4190	0.60	−1.69	1.75	300	...
34143	419	12.904	1.229	10.556	9.895	9.746	4310	1.25	−1.16	1.80	200	150
34163	494	12.928	1.007	11.008	10.434	10.321	4775	1.50	−1.73	1.50	100	...
34166	...	12.927	1.097	10.811	10.200	10.059	4535	1.35	−1.71	2.00	125	...
34169	467	12.760	1.179	10.482	9.861	9.737	4395	1.25	−1.56	1.80	175	...
34175	119	11.994	1.430	9.540	8.872	8.686	4215	0.80	−1.56	2.05	225	...
34180	517	13.030	1.503	10.336	9.593	9.329	4015	1.05	−0.79	1.95	200	150
34187	468	12.830	1.106	10.741	10.130	9.996	4565	1.35	−1.88	1.90	125	...
34193	111	12.048	1.207	9.662	8.958	8.787	4255	0.85	−1.78	1.80	>350	...
34207	229	12.221	1.266	9.844	9.181	9.011	4280	0.95	−1.48	1.70	175	150
34214	5256	13.210	0.946	11.313	10.794	10.672	4840	1.65	−1.74	1.30	100	...
34225	557	13.017	1.229	10.608	9.932	9.820	4265	1.25	−1.09	1.65	200	...
34229	402	12.616	1.067	10.521	9.936	9.815	4585	1.30	−1.86	2.05	225	...
35029	4676	13.264	1.015	11.212	10.635	10.514	4630	1.55	−1.65	1.55	200	...
35035	4686	13.234	0.993	11.194	10.607	10.488	4635	1.55	−1.89	1.70	250	...
35046	257	12.398	1.091	10.112	9.504	9.348	4390	1.10	−1.79	1.80	225	...
35053	275	12.303	1.084	10.107	9.485	9.370	4475	1.10	−1.86	1.95	200	...
35056	69	11.439	1.625	8.712	7.929	7.816	4015	0.40	−1.69	2.00	>350	...
35061	208	12.202	1.270	9.832	9.165	8.999	4285	0.95	−1.50	1.85	300	125
35066	67	11.444	1.486	8.891	8.194	8.000	4135	0.50	−1.76	1.90	300	...

Table 2—Continued

Star LEID ^a	Alt. ID ROA ^b	V	B–V	J	H	K _s	T _{eff} (K)	log g (cgs)	[Fe/H] Avg.	v _t (km s ^{−1})	S/N 6250 Å	S/N 6650 Å
35071	4735	13.459	0.990	11.576	11.035	10.965	4840	1.75	−1.39	1.34	75	...
35074	326	12.627	1.120	10.458	9.870	9.727	4505	1.25	−1.74	1.70	125	...
35087	5089	13.321	1.020	11.377	10.816	10.693	4755	1.65	−1.72	1.75	125	...
35090	174	11.977	1.451	9.496	8.737	8.613	4175	0.75	−1.38	1.95	300	...
35093	4775	13.158	0.839	11.501	10.999	10.874	5165	2.30	−1.36	0.85	75	...
35124	4817	13.395	1.054	11.309	10.737	10.606	4595	1.60	−1.32	1.35	200	...
35157	...	13.164	1.135	10.908	10.244	10.098	4380	1.40	−1.25	1.55	200	150
35165	...	12.259	1.097	10.146	9.502	9.371	4530	1.10	−1.78	1.70	200	...
35172	237	12.414	1.399	10.043	9.310	9.127	4245	1.00	−1.30	2.15	175	...
35190	452	12.862	1.129	10.755	10.154	9.997	4545	1.35	−1.78	1.65	125	...
35201	263	12.530	1.360	10.268	9.530	9.389	4335	1.10	−1.06	1.90	125	...
35204	420	12.932	1.025	10.922	10.338	10.202	4660	1.45	−2.00	1.85	75	...
35216	54	11.469	1.489	8.955	8.199	8.065	4150	0.55	−1.82	2.10	225	175
35228	518	12.951	1.077	10.852	10.263	10.130	4570	1.40	−1.77	1.55	150	...
35230	141	11.922	1.266	9.614	8.994	8.824	4360	0.85	−1.90	2.10	250	...
35235	125	11.693	1.393	9.250	8.553	8.367	4210	0.70	−1.73	1.75	>350	...
35240	115	11.671	1.356	9.197	8.450	8.328	4190	0.65	−1.80	2.00	200	...
35248	4937	13.165	1.027	11.160	10.609	10.465	4685	1.55	−1.70	1.85	150	...
35260	377	12.522	1.148	10.445	9.827	9.701	4575	1.25	−1.69	1.65	250	...
35261	4961	13.330	1.084	11.239	10.599	10.488	4555	1.55	−1.56	1.45	200	...
36028	535	12.871	1.001	10.872	10.349	10.239	4730	1.45	−1.65	1.30	175	115
36036	65	11.425	1.498	8.875	8.209	7.934	4130	0.50	−1.87	2.25	275	...
36048	4748	13.264	1.016	11.234	10.699	10.536	4660	1.60	−1.73	1.65	125	...
36059	4763	13.308	1.028	11.340	10.784	10.657	4730	1.65	−1.75	1.55	100	...
36061	592	13.064	1.140	10.967	10.363	10.228	4560	1.45	−1.37	1.65	175	...
36087	4797	13.186	1.028	11.218	10.603	10.539	4715	1.60	−1.81	1.65	125	...
36106	392	12.858	1.036	10.670	10.057	9.946	4485	1.30	−1.83	1.65	150	...
36110	...	13.272	0.980	11.255	10.691	10.524	4655	1.60	−1.97	2.05	75	...
36113	343	12.872	1.092	10.830	10.307	10.148	4660	1.45	−1.62	1.50	150	...
36134	...	12.567	1.220	10.436	9.783	9.635	4495	1.20	−0.96	1.70	150	175
36156	...	11.643	1.343	9.363	8.698	8.519	4355	0.75	−1.89	2.00	250	250
36179	148	12.108	1.554	9.568	8.781	8.645	4115	0.75	−1.13	2.00	150	200
36182	215	12.352	1.302	9.939	9.265	9.099	4250	0.95	−1.66	1.80	250	...
36191	336	12.808	1.369	10.518	9.816	9.619	4315	1.20	−0.75	1.65	150	...
36206	308	12.499	1.151	10.292	9.626	9.518	4435	1.15	−1.90	1.78	175	...
36228	49	11.365	1.661	8.742	8.042	7.829	4085	0.45	−1.77	2.25	275	...
36239	281	12.492	1.222	10.186	9.515	9.382	4340	1.10	−1.56	1.75	150	150
36259	355	12.568	1.112	10.365	9.725	9.600	4450	1.20	−1.84	1.85	275	...
36260	4912	13.491	1.006	11.472	10.884	10.792	4670	1.70	−1.40	1.35	75	...
36280	395	12.565	1.268	10.378	9.668	9.564	4430	1.15	−1.64	1.80	125	125
36282	290	12.351	1.155	10.179	9.575	9.449	4500	1.15	−1.88	1.95	225	...
37022	4437	13.395	0.930	11.477	10.935	10.821	4800	1.71	−1.60	1.70	100	...
37024	447	12.719	1.638	9.575	8.687	8.471	3800	0.60	−0.79	1.80	150	...
37051	349	12.795	1.030	10.752	10.232	10.062	4660	1.40	−1.94	1.95	175	...
37052	4738	13.195	1.070	11.145	10.601	10.467	4650	1.55	−1.58	1.75	100	...

Table 2—Continued

Star LEID ^a	Alt. ID ROA ^b	V	B-V	J	H	K _s	T _{eff} (K)	log g (cgs)	[Fe/H] Avg.	v _t (km s ⁻¹)	S/N 6250 Å	S/N 6650 Å
37055	562	13.036	1.092	10.954	10.358	10.221	4580	1.45	-1.46	1.60	175	...
37062	507	13.009	1.166	10.731	10.087	9.931	4370	1.30	-1.14	1.85	150	...
37071	391	12.621	1.054	10.571	9.995	9.897	4645	1.30	-1.78	1.55	100	...
37082	4770	13.231	1.020	11.233	10.666	10.513	4675	1.60	-1.86	1.80	100	...
37087	309	12.550	1.150	10.420	9.816	9.645	4520	1.20	-1.87	1.95	225	...
37094	443	12.988	1.089	10.879	10.292	10.222	4590	1.45	-1.90	1.75	175	...
37105	514	13.234	0.954	11.320	10.798	10.617	4790	1.65	-1.60	1.45	200	...
37110	...	12.077	1.574	9.345	8.577	8.359	3990	0.65	-0.79	2.35	125	...
37119	...	12.212	1.246	9.787	9.072	8.896	4220	0.90	-1.71	1.90	150	...
37136	...	12.631	1.118	10.624	10.065	9.895	4665	1.35	-1.88	1.75	125	...
37139	...	12.519	1.222	10.144	9.442	9.292	4265	1.05	-1.37	1.95	200	...
37143	...	12.794	1.143	10.684	10.093	9.943	4550	1.35	-1.76	1.50	200	...
37147	...	13.008	1.190	10.730	10.007	9.967	4370	1.30	-1.35	1.60	250	150
37157	...	12.396	1.132	10.207	9.573	9.385	4440	1.10	-1.85	1.65	150	...
37169	...	13.458	0.969	11.242	10.718	10.570	4525	1.60	-1.91	1.40	125	...
37179	...	12.793	1.040	10.759	10.206	10.075	4660	1.40	-1.92	1.60	150	150
37184	...	12.257	1.221	10.096	9.443	9.327	4480	1.10	-1.83	2.00	225	135
37196	...	12.752	1.113	10.625	10.019	9.864	4525	1.30	-1.95	1.95	125	...
37198	...	12.680	1.189	10.444	9.789	9.649	4405	1.20	-1.58	1.75	200	115
37215	...	12.868	1.038	10.830	10.292	10.169	4670	1.45	-1.97	1.65	125	...
37232	...	11.529	1.593	8.813	8.041	7.848	4005	0.45	-1.63	2.25	300	...
37247	238	12.430	1.163	10.191	9.506	9.363	4385	1.05	-1.88	1.75	200	...
37253	104	11.758	1.409	9.324	8.586	8.461	4215	0.70	-1.81	1.75	300	225
37271	169	12.080	1.294	9.655	8.978	8.802	4235	0.85	-1.74	1.90	200	175
37275	439	13.230	1.151	10.984	10.379	10.256	4430	1.45	-1.43	1.85	100	...
37318	324	12.510	1.538	9.716	8.919	8.704	3950	0.75	-0.88	1.75	100	250
37322	4938	13.450	0.887	11.583	11.078	10.989	4905	1.80	-1.93	1.70	150	...
37329	351	12.458	1.188	10.264	9.642	9.505	4465	1.15	-1.75	1.75	225	...
38011	253	12.217	1.365	9.940	9.250	9.092	4345	1.00	-1.31	1.75	175	...
38018	4429	13.139	1.032	11.062	10.456	10.371	4600	1.50	-1.60	1.65	175	...
38049	44	11.520	1.459	9.041	8.279	8.085	4155	0.55	-1.74	2.10	250	200
38052	77	11.635	1.434	9.179	8.471	8.274	4195	0.65	-1.71	1.90	>350	...
38056	515	12.905	1.107	10.821	10.199	10.138	4595	1.40	-1.79	1.85	175	...
38057	584	13.220	1.120	11.065	10.458	10.296	4495	1.45	-1.19	1.40	75	...
38059	151	11.964	1.555	9.443	8.604	8.476	4110	0.70	-1.15	1.95	100	250
38061	4495	13.299	0.941	11.461	10.928	10.870	4930	1.75	-1.72	1.30	100	...
38096	...	13.256	1.051	11.151	9.506	10.428	4565	1.55	-1.82	1.90	100	...
38097	...	12.271	1.383	9.568	8.748	8.599	4025	0.75	-1.14	1.65	200	...
38105	...	12.549	1.146	10.331	9.747	9.493	4420	1.15	-1.84	1.90	150	...
38112	...	12.942	1.161	10.712	10.039	9.888	4395	1.30	-1.51	1.70	150	...
38115	130	11.995	1.343	9.515	8.845	8.638	4190	0.80	-1.51	1.90	200	...
38129	...	12.284	1.187	9.897	9.195	9.000	4245	0.95	-1.68	1.50	275	...
38147	...	12.507	1.184	10.287	9.655	9.481	4420	1.15	-1.49	1.65	125	...
38149	...	11.762	1.579	9.197	8.460	8.213	4095	0.60	-1.27	1.95	275	...
38156	...	12.223	1.262	9.960	9.338	9.159	4390	1.00	-1.76	1.65	200	...

Table 2—Continued

Star LEID ^a	Alt. ID ROA ^b	V	B–V	J	H	K _s	T _{eff} (K)	log g (cgs)	[Fe/H] Avg.	v _t (km s ^{–1})	S/N 6250 Å	S/N 6650 Å
38166	...	12.242	1.206	9.949	8.688	8.489	4100	0.25	–2.03	1.60	225	...
38168	...	11.799	1.536	9.201	8.303	8.142	4030	0.55	–1.29	1.75	175	175
38169	...	12.561	1.361	10.199	9.506	9.365	4285	1.05	–1.53	1.70	200	...
38195	...	11.743	1.478	9.266	8.457	8.357	4160	0.65	–1.70	1.95	250	200
38198	...	12.474	1.374	10.122	9.425	9.242	4275	1.05	–1.44	1.95	175	...
38204	...	12.008	1.411	9.581	8.849	8.738	4225	0.80	–1.79	2.10	200	150
38206	...	13.159	1.066	11.160	9.292	10.495	4710	1.55	–1.61	1.60	150	...
38215	...	12.953	1.120	10.763	10.133	9.977	4455	1.35	–1.20	1.60	200	...
38223	...	12.520	1.169	10.290	9.625	9.462	4395	1.15	–1.74	1.75	175	...
38225	...	13.000	1.120	10.870	10.283	10.180	4555	1.40	–1.67	1.70	225	...
38226	...	13.007	1.100	10.867	10.285	10.163	4540	1.40	–1.64	1.55	100	...
38232	...	12.236	1.449	9.724	9.021	8.834	4160	0.85	–1.45	1.80	250	...
38255	...	12.561	1.240	10.359	9.671	9.524	4410	1.45	–1.22	1.70	175	...
38262	127	11.856	1.362	9.496	8.817	8.660	4290	0.80	–1.70	1.85	125	...
38276	168	12.283	1.342	10.014	9.277	9.141	4335	1.00	–1.61	1.90	275	...
38303	293	12.476	1.238	10.153	9.507	9.365	4340	1.10	–1.64	1.95	150	...
38319	416	12.764	1.182	10.583	9.985	9.832	4480	1.30	–1.50	1.70	175	...
38323	4578	13.340	1.118	11.163	10.530	10.376	4465	1.50	–1.11	1.45	225	...
38330	550	12.957	1.033	10.874	10.300	10.169	4595	1.45	–1.72	1.60	150	150
39026	287	12.333	1.373	9.943	9.208	9.059	4240	0.95	–1.48	1.65	200	...
39033	580	13.452	0.972	11.231	10.774	10.599	4525	1.20	–2.02	1.55	75	...
39034	334	12.513	1.087	10.278	9.640	9.535	4435	1.15	–1.67	1.60	150	...
39037	94	11.629	1.393	9.188	8.480	8.320	4215	0.65	–1.72	2.10	275	...
39043	604	13.139	1.002	11.109	10.574	10.475	4695	1.55	–1.58	1.75	150	...
39044	258	12.263	1.157	9.945	9.318	9.185	4360	1.00	–1.78	1.85	300	...
39048	451	12.887	1.420	10.106	9.335	9.114	3965	0.95	–0.65	1.75	150	...
39056	519	13.180	0.984	9.661	9.058	8.878	4800	1.85	–1.76	1.50	150	...
39063	4476	13.056	0.955	11.176	10.650	10.535	4860	1.60	–1.82	1.40	250	...
39067	86	11.545	1.480	9.306	8.531	8.383	4335	1.15	–1.34	1.70	300	...
39086	249	12.191	1.277	9.929	9.253	9.121	4375	1.00	–1.61	1.70	275	...
39088	304	12.324	1.214	10.127	9.506	9.346	4450	1.10	–1.79	1.85	150	...
39102	563	13.127	1.053	11.034	10.463	10.370	4605	1.50	–1.66	1.35	100	...
39119	...	12.651	1.128	10.473	9.883	9.728	4490	1.25	–1.79	1.70	200	...
39123	...	12.786	1.034	10.794	10.212	10.094	4690	1.40	–1.75	1.70	175	...
39129	...	12.843	1.361	10.639	9.982	9.833	4430	1.30	–1.34	1.75	200	...
39141	101	11.852	1.270	9.612	8.909	8.753	4375	0.85	–1.77	2.00	>350	325
39149	...	12.472	1.275	9.966	9.285	9.118	4180	0.95	–1.08	1.70	150	...
39165	80	11.620	1.422	9.207	8.570	8.414	4275	0.70	–1.97	2.15	200	225
39186	...	11.960	1.306	9.694	9.019	8.873	4370	0.90	–1.66	2.00	275	200
39187	...	12.546	0.724	9.737	9.053	8.907	4040	0.25	–2.13	1.80	250	...
39198	...	11.353	1.311	9.104	8.405	8.279	4385	1.00	–1.66	1.85	300	...
39204	...	12.673	1.108	10.452	9.856	9.712	4455	1.25	–1.85	1.95	125	...
39215	...	12.715	1.137	10.493	9.864	9.750	4445	1.25	–1.97	1.85	150	...
39216	...	12.916	1.048	10.790	10.171	10.069	4540	1.40	–1.78	1.55	125	...
39225	...	13.302	1.079	11.326	10.744	10.670	4725	1.65	–1.65	1.75	100	...

Table 2—Continued

Star LEID ^a	Alt. ID ROA ^b	V	B–V	J	H	K _s	T _{eff} (K)	log g (cgs)	[Fe/H] Avg.	v _t (km s ^{–1})	S/N 6250 Å	S/N 6650 Å
39235	...	12.400	1.225	9.972	9.267	9.147	4240	0.75	–1.59	1.70	250	...
39245	...	11.806	1.471	9.154	8.367	8.175	4035	0.60	–1.50	1.90	275	250
39257	...	11.934	1.582	9.234	8.472	8.242	4005	0.60	–1.47	1.95	275	...
39259	...	12.483	1.271	10.228	9.547	9.377	4365	1.10	–1.70	1.70	200	...
39284	...	11.598	1.486	9.041	8.350	8.169	4140	0.50	–1.76	2.05	>350	275
39289	...	12.714	1.174	10.533	9.966	9.782	4490	1.30	–1.84	1.45	250	...
39298	...	13.078	1.015	11.086	10.498	10.405	4695	1.55	–1.95	1.80	100	...
39301	...	12.863	1.128	10.747	10.125	10.013	4540	1.35	–1.90	1.65	175	...
39306	123	11.918	1.328	9.569	8.857	8.721	4290	0.80	–1.81	1.85	225	200
39325	117	11.906	1.592	9.370	8.530	8.404	4100	0.65	–1.40	2.05	200	...
39329	...	13.209	1.059	11.166	10.598	10.391	4605	1.55	–1.90	1.90	75	...
39345	356	12.734	1.076	10.677	10.116	9.944	4615	1.35	–1.77	1.65	175	...
39346	...	13.132	1.270	10.791	10.078	9.916	4285	1.30	–1.24	1.65	175	...
39352	97	11.740	1.380	9.401	8.680	8.502	4275	0.75	–1.79	1.85	150	...
39384	4570	13.296	1.069	11.231	10.673	10.565	4635	1.60	–1.36	1.75	150	...
39392	4579	13.413	1.194	11.108	10.440	10.265	4330	1.45	–0.75	1.90	150	...
39401	345	12.625	1.186	10.320	9.636	9.544	4350	1.15	–1.52	1.80	250	...
39921	...	12.700	1.199	10.400	9.692	9.586	4335	0.95	–1.56	1.60	150	...
40016	359	12.550	1.253	10.260	9.633	9.468	4365	1.15	–1.47	1.75	200	150
40031	501	12.850	1.037	10.730	10.150	10.041	4570	1.35	–1.80	1.85	250	...
40041	585	13.012	1.093	10.883	10.287	10.181	4550	1.40	–1.57	1.60	150	150
40108	...	13.081	1.038	11.050	10.444	10.326	4630	1.50	–1.86	1.60	100	...
40123	107	11.850	1.499	9.259	8.511	8.288	4080	0.65	–1.46	2.05	250	175
40135	78	11.773	1.353	9.341	8.552	8.421	4195	0.70	–1.92	2.20	250	...
40139	...	12.105	1.421	9.654	8.871	8.719	4175	0.75	–1.46	2.10	150	...
40162	...	12.878	1.008	10.842	10.203	10.068	4600	1.55	–1.59	1.55	300	...
40166	...	12.890	1.169	10.609	9.965	9.845	4380	1.10	–1.48	1.70	300	...
40168	...	12.860	1.096	10.726	10.128	9.997	4535	1.35	–1.71	1.65	150	...
40170	...	12.736	1.134	10.577	9.938	9.798	4480	1.25	–1.86	1.75	250	...
40207	...	12.444	1.226	9.952	9.239	9.095	4180	0.70	–1.54	1.90	150	...
40210	...	12.606	1.118	10.446	9.886	9.689	4510	1.25	–1.92	1.45	200	...
40216	...	11.943	1.398	9.457	8.653	8.564	4160	0.65	–1.63	1.75	275	250
40220	...	13.080	0.877	11.038	10.490	10.236	4565	1.45	–1.64	1.40	100	...
40232	...	12.130	1.649	9.520	8.678	8.495	4040	0.75	–1.04	1.90	225	...
40235	...	12.441	1.236	10.161	9.490	9.339	4355	0.90	–1.84	2.10	175	...
40237	...	12.607	1.202	10.196	9.540	9.366	4255	0.80	–1.65	1.80	150	...
40275	...	12.508	1.131	10.237	9.605	9.441	4385	0.95	–1.88	1.90	250	...
40291	...	12.098	1.331	9.751	9.059	8.917	4295	0.90	–1.64	1.75	200	...
40318	...	13.333	1.145	11.014	10.349	10.251	4345	1.40	–1.26	1.95	150	...
40339	...	12.261	1.583	9.597	8.681	8.572	4000	0.70	–1.25	2.15	200	...
40349	...	12.591	1.184	10.182	9.515	9.353	4255	0.80	–1.68	1.70	250	...
40358	...	12.808	1.323	10.140	9.351	9.171	4025	0.70	–1.03	1.90	150	200
40361	...	12.761	1.094	10.633	10.049	9.874	4530	1.30	–1.93	1.60	300	...
40371	...	12.324	1.324	9.765	9.033	8.820	4110	0.85	–1.45	1.85	300	...
40372	...	12.062	1.252	9.706	9.061	8.889	4305	0.90	–1.91	1.85	325	...

Table 2—Continued

Star LEID ^a	Alt. ID ROA ^b	V	B–V	J	H	K _s	T _{eff} (K)	log g (cgs)	[Fe/H] Avg.	v _t (km s ^{–1})	S/N 6250 Å	S/N 6650 Å
40373	...	12.584	1.187	10.431	9.803	9.628	4480	1.20	–1.78	1.60	150	...
40409	552	13.276	1.044	10.974	10.776	10.312	4480	1.15	–1.88	1.95	100	...
40420	374	12.996	1.260	11.031	10.825	10.330	4750	1.70	–2.05	1.25	100	75
40424	521	12.989	1.088	11.013	10.440	10.301	4700	1.85	–1.49	1.40	100	...
40472	73	11.463	1.608	8.698	7.877	7.748	3975	0.25	–1.69	2.10	250	...
40479	4369	13.063	1.105	10.848	10.250	10.114	4460	1.40	–1.61	1.60	250	...
41015	571	12.935	1.064	10.904	10.305	10.180	4635	1.45	–1.64	1.55	125	...
41025	4159	13.059	0.996	11.020	10.478	10.358	4670	1.50	–1.63	1.65	100	...
41033	463	12.900	1.258	10.257	9.503	9.330	4060	0.80	–1.03	2.00	150	...
41034	319	12.396	1.211	10.165	9.463	9.371	4400	1.10	–1.64	1.85	200	150
41035	233	12.141	1.219	9.854	9.204	9.055	4365	0.95	–1.82	2.00	175	...
41039	256	12.251	1.230	9.977	9.295	9.190	4375	1.00	–1.73	1.95	250	...
41060	178	11.906	1.474	9.418	8.671	8.517	4165	0.75	–1.50	1.95	>350	200
41061	235	12.159	1.304	9.810	9.123	8.997	4305	0.95	–1.59	1.60	275	200
41063	404	12.649	1.116	10.517	9.888	9.789	4530	1.25	–1.76	1.80	175	...
41164	...	13.034	1.101	10.851	10.246	10.017	4445	1.15	–1.63	1.80	200	...
41186	...	12.398	1.184	10.094	9.419	9.285	4345	0.85	–1.82	1.65	300	...
41201	...	13.320	0.946	11.333	10.772	10.550	4660	1.60	–2.08	1.45	75	...
41230	...	12.726	1.143	10.528	9.907	9.784	4465	1.25	–1.82	1.45	125	...
41232	...	12.946	0.987	10.970	10.426	10.309	4735	1.50	–2.06	1.75	75	...
41241	...	11.741	1.401	9.277	8.472	8.364	4170	0.65	–1.84	1.95	300	...
41243	...	12.519	1.121	10.307	9.676	9.521	4435	1.15	–1.80	1.65	300	...
41246	...	12.531	1.123	10.352	9.698	9.594	4470	1.20	–1.75	1.70	175	...
41258	...	12.711	1.018	10.602	10.006	9.844	4525	1.30	–2.16	1.80	125	...
41259	...	11.977	1.234	9.692	9.003	8.854	4350	0.90	–1.78	1.90	200	...
41262	...	13.112	0.863	11.373	10.949	10.790	5105	1.75	–1.17	1.40	100	...
41310	...	12.879	1.106	10.796	10.180	10.088	4585	1.40	–1.65	1.30	125	...
41312	...	12.977	1.072	10.790	10.182	10.092	4495	1.40	–2.13	0.90	100	...
41313	...	12.219	1.147	9.770	9.124	8.948	4240	0.65	–1.91	1.95	275	...
41321	...	12.378	1.115	9.972	9.340	9.209	4290	0.75	–1.89	2.25	175	...
41348	...	12.267	1.014	9.928	9.293	9.104	4330	0.95	–1.73	1.60	225	...
41366	...	12.987	1.092	10.838	10.184	10.086	4500	1.40	–1.74	1.70	100	...
41375	...	11.621	1.607	8.872	8.143	7.961	4005	0.25	–1.75	2.25	225	...
41380	...	11.810	1.661	9.054	8.315	8.061	3980	0.55	–1.23	1.95	150	...
41387	...	12.791	1.152	10.488	9.864	9.691	4355	1.00	–1.72	1.70	150	...
41389	...	12.799	1.114	10.663	9.999	9.899	4505	1.30	–1.89	1.50	150	...
41402	...	12.729	1.117	10.537	9.935	9.813	4485	1.15	–1.95	1.95	150	...
41435	202	12.331	1.240	9.857	9.132	9.001	4195	0.90	–1.59	1.75	200	...
41455	...	11.566	1.558	8.854	8.112	7.899	4015	0.45	–1.22	2.30	300	...
41476	179	12.031	1.651	9.020	8.188	7.960	3830	0.20	–1.41	1.90	175	...
41494	4339	13.328	1.080	11.140	10.563	10.453	4505	1.50	–1.54	1.45	275	...
42012	3875	13.379	1.089	11.299	10.705	10.613	4605	1.60	–1.58	1.65	125	...
42015	3881	13.057	1.138	10.879	10.249	10.105	4465	1.40	–1.59	1.75	200	100
42023	170	11.949	1.275	9.619	8.916	8.801	4315	0.85	–1.80	2.00	>350	...
42039	205	12.013	1.246	9.712	9.063	8.892	4350	0.90	–1.76	1.95	200	...

Table 2—Continued

Star LEID ^a	Alt. ID ROA ^b	V	B-V	J	H	K _s	T _{eff} (K)	log g (cgs)	[Fe/H] Avg.	v _t (km s ⁻¹)	S/N 6250 Å	S/N 6650 Å
42049	533	12.926	1.175	10.641	9.968	9.857	4365	1.30	-1.32	1.60	300	...
42054	72	11.484	1.436	8.989	8.297	8.097	4175	0.55	-1.83	2.05	275	200
42056	3957	13.140	0.941	11.235	10.717	10.625	4850	2.05	-1.86	1.65	150	...
42079	3976	13.204	1.067	11.094	10.487	10.361	4550	1.50	-1.42	1.40	125	...
42084	259	12.236	1.297	9.993	9.314	9.165	4385	1.00	-1.52	1.90	225	...
42106	346	13.209	1.075	10.831	10.373	10.149	4390	1.10	-1.72	1.55	100	...
42114	...	12.192	1.229	9.823	9.147	9.019	4295	0.95	-1.55	1.75	>350	...
42120	...	12.570	1.088	10.390	9.764	9.517	4430	1.20	-1.52	1.50	300	...
42134	...	13.208	0.999	11.211	10.618	10.519	4685	1.60	-1.74	1.65	125	...
42161	...	11.816	1.328	9.317	8.609	8.445	4175	0.55	-1.84	2.00	>350	150
42162	...	12.763	1.262	10.222	9.482	9.258	4110	1.00	-1.09	1.85	250	...
42169	...	12.640	1.213	10.481	9.810	9.655	4455	1.20	-1.34	1.60	200	...
42174	...	13.153	1.070	11.119	10.481	10.351	4600	1.50	-1.58	1.45	125	...
42175	...	12.402	1.226	10.129	9.468	9.289	4360	1.05	-1.66	1.60	275	...
42179	...	11.875	1.354	9.450	8.676	8.561	4210	0.60	-1.81	1.90	275	200
42182	...	12.992	1.037	10.932	10.363	10.264	4640	1.45	-1.77	1.25	125	...
42187	...	12.547	1.216	10.248	9.590	9.392	4330	0.95	-1.62	1.75	200	...
42196	...	12.950	1.046	10.824	10.184	9.950	4435	1.35	-2.13	1.65	125	...
42198	...	13.085	1.064	10.901	10.441	9.914	4330	0.80	-2.03	1.75	150	...
42205	...	11.996	1.567	9.310	8.592	8.283	4015	0.65	-1.35	2.30	275	...
42221	...	13.032	1.089	10.833	10.233	10.092	4470	1.15	-1.84	1.55	200	...
42260	...	12.986	1.165	10.769	10.145	10.016	4445	1.35	-1.78	1.80	125	...
42271	...	12.445	1.090	10.072	9.522	9.242	4310	0.70	-2.26	1.60	225	...
42302	...	11.584	1.513	8.992	8.363	8.076	4115	0.55	-1.81	2.05	300	250
42303	...	12.593	1.184	10.616	9.967	9.739	4610	1.70	-1.49	1.65	150	...
42309	...	13.123	1.034	11.164	10.689	10.412	4680	1.55	-0.80	1.45	125	...
42339	...	12.683	1.250	10.544	9.839	9.667	4445	1.45	-1.18	1.45	175	...
42345	...	12.891	1.026	10.905	10.333	10.209	4700	1.65	-2.00	1.80	225	...
42361	...	12.588	1.078	10.426	9.787	9.697	4500	1.20	-1.90	1.75	200	...
42384	...	12.316	1.313	9.569	8.847	8.656	4010	0.40	-1.51	1.95	200	...
42385	...	12.686	1.126	10.606	9.983	9.853	4565	1.30	-1.86	1.55	275	...
42407	...	13.358	1.048	11.378	10.790	10.699	4710	1.65	-1.48	1.20	75	...
42415	...	12.531	1.195	10.155	9.452	9.297	4265	0.85	-1.55	1.80	200	...
42438	538	13.067	1.159	10.811	10.149	10.020	4390	1.35	-1.32	1.60	200	...
42457	4047	13.314	1.072	11.183	10.629	10.482	4555	1.55	-1.66	1.65	75	...
42461	51	11.617	1.441	9.137	8.324	8.149	4135	0.55	-1.75	1.95	>350	150
42473	414	12.852	1.186	10.489	9.832	9.666	4295	1.05	-1.38	1.80	275	...
42497	398	12.619	1.147	10.407	9.766	9.636	4440	1.10	-1.84	1.90	250	150
42501	305	12.512	1.242	10.248	9.582	9.427	4370	1.10	-1.72	1.55	175	...
42503	4095	13.497	1.027	11.415	10.841	10.703	4595	1.65	-1.61	1.55	150	...
42508	600	13.041	1.137	10.783	10.144	9.990	4390	1.35	-1.72	1.90	225	...
43010	591	13.009	1.042	10.902	10.326	10.209	4580	1.45	-1.77	1.75	175	...
43024	3911	13.133	1.016	11.076	10.486	10.358	4615	1.50	-1.65	1.50	200	...
43036	440	12.716	1.133	10.489	9.842	9.729	4430	1.25	-1.40	1.55	100	...
43040	3937	13.226	1.009	11.207	10.630	10.520	4670	1.60	-1.62	1.70	150	...

Table 2—Continued

Star LEID ^a	Alt. ID ROA ^b	V	B-V	J	H	K _s	T _{eff} (K)	log g (cgs)	[Fe/H] Avg.	v _t (km s ⁻¹)	S/N 6250 Å	S/N 6650 Å
43060	3952	13.200	1.068	11.089	10.518	10.399	4575	1.50	-1.68	1.60	175	...
43061	357	12.602	1.431	9.744	8.973	8.780	3930	0.55	-1.12	2.15	150	...
43064	140	11.821	1.259	9.563	8.906	8.769	4395	0.85	-1.58	1.80	225	150
43068	405	12.756	1.167	10.509	9.858	9.758	4415	1.25	-1.43	1.60	175	...
43071	427	12.720	1.098	10.611	9.984	9.847	4535	1.30	-1.70	1.50	175	...
43079	3977	13.196	1.036	11.309	10.781	10.580	4800	1.65	-1.04	1.30	75	...
43087	360	12.675	1.173	10.448	9.813	9.671	4425	1.15	-1.64	1.80	250	...
43091	314	12.789	1.154	10.399	9.754	9.629	4295	1.00	-1.50	1.65	200	...
43095	116	11.997	1.232	9.618	8.972	8.794	4290	0.85	-1.83	1.90	150	...
43096	35	11.419	1.593	8.473	7.670	7.578	3900	0.20	-1.88	2.25	325	...
43099	39	11.600	1.625	8.565	7.683	7.549	3825	0.15	-1.47	1.90	275	...
43101	210	12.387	1.148	10.158	9.534	9.392	4430	1.10	-1.77	1.85	300	...
43104	...	12.855	1.166	10.707	10.059	9.952	4500	1.35	-1.51	1.65	200	...
43108	...	13.033	1.024	10.973	10.422	10.266	4625	1.45	-1.69	1.45	125	...
43111	...	12.918	1.065	10.836	10.256	10.146	4605	1.40	-1.59	1.75	125	...
43134	...	12.755	1.106	10.805	10.202	9.926	4645	1.40	-1.95	1.85	150	...
43139	...	12.565	1.050	10.687	10.051	9.923	4770	1.35	-1.72	1.30	125	...
43158	...	12.555	1.120	10.229	9.621	9.442	4345	0.90	-1.90	1.70	300	...
43189	...	12.085	1.486	9.521	8.829	8.582	4115	0.75	-1.43	2.15	200	...
43216	...	12.414	1.348	9.650	8.965	8.689	3990	0.40	-1.40	1.95	250	225
43233	...	12.817	1.093	10.610	10.009	9.837	4450	1.30	-1.92	1.45	200	...
43241	...	11.629	1.530	8.805	8.142	7.970	3995	0.25	-1.91	2.55	>350	...
43258	...	12.693	1.143	9.848	8.885	9.116	4070	0.20	-2.23	2.00	200	...
43261	...	11.612	1.411	8.931	8.231	8.068	4065	0.30	-1.80	2.00	250	...
43278	...	12.996	1.059	11.018	10.488	10.395	4790	1.55	-1.93	1.75	75	...
43326	...	12.103	1.528	9.321	8.413	8.258	3925	0.40	-1.24	1.85	150	200
43330	...	11.779	1.401	9.284	8.567	8.411	4175	0.60	-1.87	1.90	125	...
43351	...	11.686	1.574	9.206	8.391	8.224	4135	0.60	-0.98	2.40	200	...
43367	...	11.603	1.477	9.003	8.264	8.100	4095	0.40	-1.82	2.05	300	275
43389	...	12.856	1.301	10.387	9.686	9.500	4190	1.10	-1.38	1.75	200	...
43397	...	13.300	0.982	11.354	10.817	10.680	4760	1.65	-1.88	1.45	100	...
43399	...	12.785	1.140	10.757	10.149	10.024	4630	1.60	-1.77	1.60	150	...
43412	88	11.740	1.436	9.249	8.561	8.407	4190	0.60	-1.78	2.15	300	...
43433	...	12.461	1.224	10.075	9.413	9.238	4270	0.80	-1.80	1.65	200	...
43446	564	13.133	1.071	11.067	10.486	10.401	4630	1.50	-1.64	1.75	100	...
43458	522	12.941	0.967	10.994	10.389	10.280	4730	1.50	-1.28	1.55	175	...
43463	410	12.746	1.087	10.678	10.114	9.971	4615	1.35	-1.77	1.90	200	...
43475	593	13.376	1.044	11.181	10.676	10.457	4500	1.85	-0.60	1.60	300	...
43485	265	12.520	1.183	10.254	9.437	9.482	4360	0.95	-1.74	1.55	200	...
43539	4106	13.264	1.081	11.097	10.507	10.378	4510	1.40	-1.57	1.60	200	...
44026	341	12.607	1.185	10.192	9.536	9.368	4255	1.05	-1.33	1.75	250	...
44042	136	11.785	1.215	9.555	8.886	8.777	4420	0.85	-1.83	1.80	>350	225
44056	578	13.032	1.111	10.856	10.241	10.142	4495	1.40	-1.51	1.60	125	...
44065	350	12.434	1.132	10.279	9.651	9.505	4490	1.15	-1.78	1.80	200	...
44067	310	12.332	0.987	10.489	9.957	9.831	4900	2.25	-1.66	1.45	100	...

Table 2—Continued

Star LEID ^a	Alt. ID ROA ^b	V	B-V	J	H	K _s	T _{eff} (K)	log g (cgs)	[Fe/H] Avg.	v _t (km s ⁻¹)	S/N 6250 Å	S/N 6650 Å
44115	64	11.632	1.464	9.122	8.414	8.229	4160	0.60	-1.71	2.10	>350	...
44120	...	13.117	0.958	11.069	10.503	10.355	4630	1.50	-1.88	1.40	125	...
44143	...	11.876	1.197	9.674	9.008	8.858	4430	0.90	-1.79	1.85	300	200
44163	...	12.707	1.140	10.387	9.822	9.540	4335	0.95	-1.84	1.80	250	...
44188	...	13.299	1.151	11.056	10.414	10.294	4415	1.45	-1.60	1.70	150	...
44189	...	12.863	1.217	10.497	9.845	9.671	4290	1.20	-1.45	1.65	175	...
44198	...	12.179	1.258	9.933	9.302	9.132	4400	1.00	-1.79	2.10	225	...
44219	...	12.194	1.162	9.886	9.237	9.086	4350	1.00	-1.77	1.95	250	...
44231	...	12.691	1.140	10.616	9.986	9.834	4560	1.55	-1.46	1.35	250	...
44253	...	12.656	1.223	10.296	9.645	9.479	4300	0.90	-1.58	1.65	150	...
44271	...	13.069	0.989	10.995	10.464	10.288	4615	1.50	-1.80	1.90	100	...
44277	...	11.556	1.839	8.537	8.106	7.495	3900	0.25	-1.37	2.10	300	...
44304	...	12.864	1.140	10.465	9.807	9.686	4280	0.75	-1.85	1.65	200	...
44313	...	12.255	1.301	9.902	9.239	9.089	4305	0.95	-1.75	1.95	150	200
44327	...	11.823	1.276	9.491	8.742	8.628	4290	0.80	-1.87	1.75	275	215
44337	...	12.118	1.299	9.751	9.044	8.854	4260	0.75	-1.79	1.80	300	...
44343	...	12.446	1.230	10.130	9.473	9.248	4310	0.90	-1.79	1.60	275	...
44380	...	13.120	0.973	11.130	10.620	10.455	4725	1.55	-1.83	1.35	75	...
44424	...	12.737	1.049	10.646	10.073	9.910	4580	1.35	-1.83	1.70	150	...
44426	...	12.598	1.188	10.292	9.607	9.476	4335	1.05	-1.48	1.65	150	...
44435	433	12.938	1.179	10.667	10.026	9.879	4380	1.10	-1.49	1.65	200	...
44446	529	13.174	1.033	11.097	10.481	10.355	4575	1.50	-1.77	1.75	75	...
44449	100	11.789	1.584	9.207	8.471	8.267	4095	0.60	-1.37	2.35	200	...
44462	321	12.559	1.403	9.918	9.110	8.942	4040	0.90	-1.18	1.65	225	...
44488	3813	13.319	0.922	11.388	10.870	10.754	4805	1.70	-1.71	1.40	100	...
44493	499	12.863	1.073	10.762	10.171	10.001	4555	1.35	-1.72	1.45	200	...
45082	318	12.606	1.082	10.403	9.816	9.670	4475	1.20	-1.83	1.65	250	...
45089	197	12.288	1.074	10.107	9.531	9.408	4515	1.10	-1.85	2.00	175	...
45092	406	12.828	1.134	10.546	9.907	9.720	4360	1.25	-1.30	1.65	300	...
45093	573	13.149	1.040	11.186	10.579	10.519	4730	1.60	-1.61	1.45	100	...
45126	...	13.081	1.064	10.933	10.352	10.227	4530	1.45	-1.76	1.70	200	...
45177	...	11.736	1.418	9.207	8.501	8.307	4145	0.50	-1.83	2.00	300	...
45180	...	12.704	1.138	10.410	9.754	9.589	4350	1.00	-1.73	1.60	275	...
45206	...	12.390	1.114	10.313	9.740	9.582	4595	1.20	-1.74	1.60	150	...
45215	...	12.993	1.430	10.617	9.881	9.696	4240	1.20	-1.06	1.45	200	175
45232	...	11.409	1.384	8.600	7.957	7.710	4000	0.30	-1.91	2.45	300	...
45235	...	13.297	1.015	11.171	10.574	10.448	4540	1.55	-1.88	1.45	125	...
45238	...	12.485	1.188	10.089	9.405	9.276	4270	0.80	-1.73	1.75	250	...
45240	...	12.918	1.085	10.614	10.004	9.862	4375	1.30	-1.62	1.55	75	...
45246	...	12.488	1.244	9.904	9.227	9.050	4130	0.65	-1.55	1.80	200	...
45249	...	12.714	1.251	10.190	9.486	9.271	4140	0.60	-1.64	1.80	300	...
45272	...	12.207	1.336	9.567	8.849	8.659	4070	0.45	-1.76	1.90	250	200
45285	...	12.955	1.323	10.749	10.096	9.883	4405	1.30	-0.95	1.50	150	...
45292	...	12.901	1.155	10.605	9.952	9.821	4360	1.25	-1.59	1.55	150	...
45309	...	12.980	1.066	10.802	10.239	10.065	4500	1.15	-1.96	1.55	150	...

Table 2—Continued

Star LEID ^a	Alt. ID ROA ^b	V	B-V	J	H	K _s	T _{eff} (K)	log g (cgs)	[Fe/H] Avg.	v _t (km s ⁻¹)	S/N 6250 Å	S/N 6650 Å
45322	...	12.358	1.466	9.503	8.880	8.515	3945	0.25	-1.71	2.00	175	...
45326	...	13.043	1.108	10.794	10.139	10.025	4405	1.15	-1.53	1.50	175	...
45342	...	12.995	1.300	10.734	10.019	9.847	4340	1.30	-1.12	1.95	200	...
45343	...	12.493	1.187	10.184	9.545	9.395	4350	1.00	-1.63	1.65	250	...
45359	...	12.241	1.241	9.849	9.164	9.024	4270	0.80	-1.79	1.65	300	...
45373	...	12.434	1.247	9.929	9.231	9.056	4170	0.65	-1.68	1.75	225	...
45377	...	12.656	1.139	10.443	9.816	9.678	4445	1.20	-1.61	1.55	200	...
45389	...	12.181	1.219	9.810	9.124	8.958	4275	0.80	-1.72	1.65	>350	...
45410	...	13.056	1.048	10.991	10.347	10.278	4610	1.50	-1.80	1.60	100	...
45418	...	13.052	1.122	10.923	10.354	10.154	4525	1.40	-1.44	1.40	125	...
45453	144	12.252	1.310	9.599	8.830	8.710	4060	0.35	-1.86	1.95	>350	200
45454	42	11.644	1.495	8.945	8.226	8.046	4040	0.40	-1.78	2.25	200	...
45463	444	12.962	1.166	10.670	10.040	9.891	4370	1.15	-1.48	1.65	150	...
45482	586	13.071	1.084	10.883	10.283	10.147	4480	1.40	-1.49	1.45	125	...
46024	40	11.291	1.479	8.813	8.073	7.954	4190	0.50	-1.69	2.10	>350	...
46055	344	12.535	1.145	10.310	9.671	9.542	4430	1.15	-1.52	1.75	200	...
46062	62	11.494	1.595	8.680	7.918	7.696	3950	0.20	-1.81	2.20	>350	...
46073	267	12.544	1.242	10.038	9.368	9.182	4180	1.00	-1.09	1.75	175	200
46090	454	12.950	0.979	10.923	10.387	10.282	4695	1.50	-1.97	1.80	150	...
46092	92	11.830	1.571	9.113	8.297	8.128	3990	0.45	-1.45	2.10	>350	...
46121	...	12.891	1.400	10.101	9.400	9.175	3985	0.65	-0.96	2.00	>350	...
46140	...	12.478	1.129	10.254	9.583	9.482	4425	1.15	-1.67	1.80	250	...
46150	...	11.867	1.505	9.269	8.515	8.274	4065	0.65	-1.39	1.90	275	...
46166	...	12.605	1.160	10.345	9.910	9.661	4475	1.20	-1.69	1.55	150	...
46172	...	12.717	1.189	10.357	9.695	9.526	4290	0.90	-1.51	1.80	200	...
46194	...	12.267	1.173	9.675	9.022	8.840	4135	0.50	-1.80	1.80	>350	...
46196	...	13.103	0.952	11.173	10.658	10.553	4815	1.60	-1.79	1.50	75	...
46223	...	12.725	1.220	10.215	9.528	9.287	4150	0.60	-1.68	1.80	275	...
46248	...	11.354	1.393	8.805	8.121	7.980	4165	0.50	-1.87	1.75	>350	...
46279	...	13.146	0.868	11.171	10.628	10.519	4745	1.60	-1.78	1.40	125	...
46289	...	12.281	1.214	9.899	9.209	9.059	4270	0.75	-1.84	1.65	300	175
46301	...	12.283	1.175	10.050	9.377	9.235	4400	1.05	-1.76	1.80	250	...
46318	...	12.804	1.128	10.568	9.952	9.755	4405	0.95	-1.87	1.75	200	...
46323	...	12.341	1.227	9.930	9.294	9.104	4265	0.80	-1.75	1.70	300	...
46325	...	12.872	1.090	10.721	10.085	9.868	4460	1.10	-1.97	1.95	175	...
46348	...	12.914	1.094	10.701	10.059	9.938	4440	1.05	-1.91	1.90	200	...
46350	...	12.291	1.316	9.776	9.102	8.914	4170	0.70	-1.44	1.95	>350	...
46381	329	12.607	1.192	10.226	9.568	9.401	4280	0.90	-1.52	1.70	250	...
46388	574	13.034	1.050	10.938	10.316	10.227	4570	1.40	-1.81	1.95	250	...
46391	469	12.846	1.107	10.692	10.080	9.947	4505	1.35	-1.50	1.85	200	...
46398	3534	13.139	0.938	11.247	10.729	10.626	4860	1.65	-1.80	1.40	75	...
46405	3545	13.208	1.103	11.309	10.779	10.674	4835	1.65	-1.71	1.35	125	...
46438	3588	13.142	0.962	11.166	10.608	10.516	4740	1.60	-1.67	1.65	100	...
47012	155	11.890	1.415	9.480	8.791	8.588	4230	0.75	-1.63	1.75	>350	...
47039	489	12.807	1.063	10.723	10.122	10.014	4590	1.35	-1.67	1.60	275	...

Table 2—Continued

Star LEID ^a	Alt. ID ROA ^b	V	B-V	J	H	K _s	T _{eff} (K)	log g (cgs)	[Fe/H] Avg.	v _t (km s ⁻¹)	S/N 6250 Å	S/N 6650 Å
47055	3449	13.266	1.067	11.224	10.627	10.511	4665	1.60	-1.72	2.20	200	...
47074	459	13.009	1.041	10.660	10.436	10.323	4690	1.50	-1.62	1.55	125	...
47096	3489	13.259	1.086	11.101	10.483	10.350	4495	1.50	-1.22	1.50	125	...
47107	...	12.053	1.308	9.657	9.016	8.737	4240	0.75	-1.70	2.20	300	150
47110	...	12.444	1.148	10.101	9.474	9.355	4345	0.95	-1.81	1.75	275	...
47146	...	12.357	1.254	9.912	9.072	8.913	4150	0.65	-1.57	1.95	250	250
47150	...	12.731	1.203	10.199	9.469	9.322	4145	0.70	-1.48	2.05	250	...
47151	...	13.074	1.053	10.823	10.289	10.299	4620	1.50	-1.82	1.40	125	...
47153	...	11.945	1.620	9.129	8.330	8.141	3940	0.55	-1.14	2.20	300	...
47176	...	12.608	1.156	10.264	9.615	9.485	4325	1.00	-1.56	1.75	275	...
47186	...	11.868	1.609	9.091	8.235	8.041	3940	0.45	-1.23	2.05	>350	...
47187	...	12.641	1.319	10.316	9.628	9.475	4310	1.10	-1.17	1.65	275	...
47199	...	11.566	1.531	8.884	8.116	7.960	4035	0.35	-1.68	1.90	>350	250
47269	...	12.957	1.202	10.709	10.070	9.915	4400	1.20	-1.36	1.65	200	...
47299	...	13.412	1.053	11.362	10.761	10.670	4630	1.65	-1.73	1.65	100	...
47307	41	11.583	1.483	8.921	8.173	8.008	4055	0.50	-1.77	2.00	325	225
47331	...	13.187	0.991	11.245	10.716	10.592	4780	1.65	-1.76	1.40	100	...
47338	...	12.628	1.173	10.316	9.696	9.539	4355	0.95	-1.67	1.75	175	...
47339	...	13.024	0.943	11.047	10.463	10.317	4695	1.50	-1.47	1.40	150	...
47348	...	12.592	1.206	10.222	9.523	9.387	4275	0.90	-1.51	1.70	300	...
47354	...	13.147	1.282	10.911	10.247	10.065	4385	1.35	-0.95	1.70	175	175
47387	247	12.286	1.224	9.988	9.321	9.140	4335	1.00	-1.71	1.80	225	125
47399	85	11.701	1.588	8.943	8.173	7.957	3975	0.40	-1.44	2.00	300	...
47400	376	12.643	1.229	10.258	9.580	9.397	4260	0.95	-1.42	1.65	300	...
47405	75	11.668	1.338	9.226	8.500	8.377	4220	0.70	-1.89	2.10	300	...
47420	530	12.969	1.094	10.803	10.177	10.065	4495	1.35	-1.38	1.40	200	...
47443	597	13.052	1.005	11.000	10.432	10.306	4635	1.50	-1.83	1.55	250	...
47450	3606	13.504	0.979	11.471	10.893	10.791	4655	1.65	-1.67	1.60	175	...
48028	193	12.062	1.244	9.744	9.061	8.954	4340	0.90	-1.78	1.85	300	...
48036	3433	13.324	1.006	11.297	10.750	10.623	4675	1.60	-1.58	1.50	125	...
48049	76	11.525	1.511	8.825	8.098	7.912	4035	0.35	-1.76	2.10	>350	...
48060	52	11.316	1.622	8.635	7.952	7.763	4065	0.40	-1.88	2.50	>350	...
48067	498	12.931	1.151	10.720	10.114	9.958	4450	1.30	-1.52	1.80	225	...
48083	191	12.044	1.376	9.719	9.056	8.894	4320	1.10	-1.35	1.80	225	...
48099	300	12.443	1.684	9.503	8.691	8.444	3890	0.70	-0.68	1.65	>350	...
48116	...	12.847	1.474	10.129	9.342	9.109	3990	0.80	-0.74	1.95	175	200
48120	...	11.622	1.676	8.665	7.869	7.673	3875	0.15	-1.61	2.10	250	...
48150	...	11.727	1.740	8.599	7.886	7.582	3800	0.25	-1.15	2.15	250	...
48151	...	12.825	1.079	10.650	10.031	9.911	4490	1.20	-1.94	1.75	275	...
48186	...	12.968	1.068	10.777	10.221	10.053	4495	1.35	-1.97	1.85	150	...
48197	...	12.939	1.126	11.029	10.467	10.305	4770	2.00	-1.56	1.45	125	...
48221	...	13.022	1.143	10.721	10.050	9.926	4350	1.20	-1.28	1.55	250	...
48228	...	12.456	1.159	10.184	9.565	9.380	4380	0.95	-1.95	1.85	175	...
48235	...	12.020	1.468	9.474	8.650	8.529	4100	0.60	-1.41	1.85	300	150
48247	...	12.757	1.135	10.584	9.972	9.810	4475	1.25	-1.64	1.65	175	...

Table 2—Continued

Star LEID ^a	Alt. ID ROA ^b	V	B-V	J	H	K _s	T _{eff} (K)	log g (cgs)	[Fe/H] Avg.	v _t (km s ⁻¹)	S/N 6250 Å	S/N 6650 Å
48259	...	12.966	1.090	10.864	10.278	10.160	4575	1.40	-1.78	1.90	125	...
48281	106	11.797	1.357	9.431	8.719	8.592	4280	0.80	-1.78	1.65	150	...
48305	...	11.880	1.593	9.018	8.212	7.962	3900	0.40	-1.13	1.70	300	...
48323	500	13.081	1.461	10.286	9.458	9.273	3945	0.65	-0.73	2.00	250	250
48367	59	11.588	1.511	8.901	8.151	7.989	4040	0.40	-1.54	2.15	>350	175
48370	239	12.355	1.245	9.923	9.209	9.054	4220	0.85	-1.44	1.75	225	...
48392	120	11.802	1.391	9.367	8.645	8.483	4210	0.70	-1.71	1.90	300	...
48409	457	12.717	1.022	10.672	10.129	10.008	4665	1.35	-1.91	1.85	300	100
49013	312	12.325	1.299	10.046	9.399	9.231	4365	1.10	-1.56	1.70	>350	...
49022	430	12.726	1.076	10.560	9.941	9.821	4495	1.20	-1.83	1.60	225	...
49037	509	12.864	0.994	10.839	10.313	10.175	4690	1.45	-1.79	1.80	200	...
49056	231	12.305	1.511	9.382	8.613	8.404	3895	0.55	-0.66	2.10	300	...
49072	479	12.821	1.107	10.721	10.083	9.983	4550	1.35	-1.74	1.55	225	...
49088	3174	13.287	1.061	11.228	10.637	10.520	4615	1.55	-1.60	1.45	225	...
49111	3199	13.381	1.081	11.253	10.608	10.474	4505	1.55	-1.06	1.45	200	...
49123	...	11.292	1.599	8.776	8.113	7.911	4175	0.50	-1.96	2.35	>350	...
49134	...	12.627	1.226	10.236	9.542	9.425	4270	0.85	-1.61	1.75	325	125
49148	...	12.398	1.331	9.933	9.177	9.038	4180	0.80	-1.37	1.75	300	...
49177	...	12.851	1.173	10.517	9.883	9.736	4335	1.10	-1.43	1.65	225	...
49179	...	12.817	1.104	10.699	10.114	9.969	4550	1.35	-1.85	1.95	225	...
49188	...	13.170	0.980	11.174	10.703	10.574	4790	1.60	-1.81	1.10	100	...
49193	...	11.755	1.447	9.299	8.574	8.417	4195	0.70	-1.65	1.95	300	100
49205	...	12.983	1.100	10.806	10.234	10.104	4510	1.40	-1.80	1.70	175	...
49212	...	12.540	1.446	10.025	9.295	9.114	4145	0.90	-1.00	2.00	200	...
49238	...	12.421	1.194	10.179	9.536	9.334	4385	1.00	-1.82	1.85	125	...
49249	...	12.457	1.319	9.904	9.195	9.014	4130	0.60	-1.51	1.80	200	...
49252	...	12.615	1.145	10.424	9.818	9.638	4460	1.20	-1.77	1.45	100	...
49255	...	13.014	1.049	10.947	10.374	10.229	4605	1.45	-1.79	1.70	125	...
49293	244	12.305	1.255	9.900	9.226	9.041	4250	0.90	-1.54	1.70	250	...
49322	485	12.797	1.104	10.651	10.044	9.881	4505	1.20	-1.89	1.80	250	...
49333	3292	13.044	1.049	10.939	10.384	10.230	4580	1.45	-1.83	1.80	225	...
50022	3109	13.400	0.968	11.371	10.815	10.716	4680	1.65	-1.54	1.25	125	...
50037	568	13.013	1.050	10.820	10.216	10.055	4465	1.25	-1.53	1.70	250	...
50046	588	13.195	1.032	10.822	10.265	10.450	4650	1.70	-1.64	1.60	150	...
50066	428	12.900	1.179	10.592	9.942	9.786	4345	1.05	-1.38	1.70	250	...
50078	167	12.038	1.291	9.658	8.984	8.871	4295	0.85	-1.69	2.10	250	...
50108	330	12.591	1.117	10.407	9.712	9.593	4435	1.20	-1.35	1.65	200	...
50109	328	12.644	1.136	10.467	9.875	9.730	4495	1.25	-1.83	1.70	175	...
50133	...	11.601	1.449	9.035	8.296	8.157	4125	0.50	-1.76	1.90	>350	...
50163	...	13.427	1.038	11.358	10.876	10.493	4490	1.15	-2.11	1.60	100	...
50167	...	12.326	1.258	10.029	9.355	9.237	4355	1.00	-1.69	1.95	225	200
50172	...	12.999	1.101	10.765	10.158	9.998	4425	1.20	-1.61	1.60	200	...
50187	...	12.364	1.548	9.502	8.762	8.609	3945	0.50	-1.08	1.70	250	125
50191	...	12.293	1.247	10.314	9.729	9.494	4645	1.75	-1.41	1.50	200	...
50193	...	11.906	1.580	9.314	8.567	8.329	4075	0.65	-1.19	2.15	175	...

Table 2—Continued

Star LEID ^a	Alt. ID ROA ^b	V	B-V	J	H	K _s	T _{eff} (K)	log g (cgs)	[Fe/H] Avg.	v _t (km s ⁻¹)	S/N 6250 Å	S/N 6650 Å
50198	...	12.984	1.176	10.758	10.153	10.024	4445	1.30	-1.46	1.55	275	...
50218	188	12.290	1.304	9.819	9.103	8.945	4190	0.75	-1.41	1.80	200	150
50228	...	12.670	1.196	10.397	9.770	9.597	4380	1.05	-1.68	1.70	275	...
50245	203	12.297	1.194	10.037	9.356	9.212	4370	1.00	-1.72	1.80	150	200
50253	79	11.658	1.375	9.293	8.555	8.374	4250	0.70	-1.72	1.95	250	...
50259	108	11.714	1.668	8.865	8.043	7.859	3920	0.30	-1.45	2.10	300	...
50267	224	12.138	1.232	9.760	9.081	8.938	4280	0.85	-1.85	1.80	250	150
50291	221	12.380	1.188	10.083	9.479	9.304	4375	1.05	-1.76	1.65	125	150
50293	401	12.794	1.153	10.499	9.901	9.730	4380	1.10	-1.57	1.70	275	...
50294	589	12.974	1.069	10.918	10.320	10.223	4620	1.45	-1.62	1.70	200	...
50304	3311	13.332	1.026	11.242	10.672	10.514	4580	1.50	-1.63	1.75	150	...
51021	171	11.984	1.470	9.391	8.633	8.424	4075	0.60	-1.42	2.05	325	...
51024	516	12.895	1.123	10.562	9.932	9.762	4330	1.05	-1.48	1.60	275	...
51074	372	12.706	1.300	10.241	9.505	9.338	4180	1.05	-1.09	1.90	250	...
51079	301	12.504	1.229	10.157	9.500	9.338	4310	1.05	-1.39	1.70	325	200
51080	236	12.317	1.428	9.809	9.058	8.900	4150	0.75	-1.39	1.85	>350	...
51091	198	12.320	1.143	10.132	9.516	9.353	4465	1.10	-1.88	2.05	275	...
51121	285	12.473	1.115	10.352	9.741	9.636	4550	1.20	-1.74	1.95	250	...
51132	421	12.874	1.365	10.267	9.503	9.375	4090	1.05	-1.02	2.00	250	...
51136	2926	13.089	1.008	11.180	10.627	10.532	4815	1.60	-1.67	1.65	75	150
51156	122	11.855	1.395	9.561	8.902	8.732	4345	0.85	-1.59	1.85	>350	...
51254	...	12.402	1.316	10.110	9.407	9.289	4340	1.05	-1.33	1.70	>350	...
51257	602	12.955	1.022	10.925	10.338	10.231	4655	1.45	-1.90	1.85	250	...
51259	423	12.597	1.135	10.486	9.867	9.756	4550	1.25	-1.75	1.75	250	...
52017	66	11.435	1.616	8.639	7.880	7.730	3980	0.25	-1.72	2.15	>350	...
52035	...	11.498	1.574	9.026	8.330	8.128	4185	0.60	-1.46	2.35	>350	...
52039	2850	13.326	0.944	11.472	10.936	10.890	4920	1.75	-1.64	1.30	125	...
52103	286	12.551	1.378	9.937	9.192	9.007	4075	0.65	-1.41	1.90	300	150
52105	486	12.870	1.134	10.744	10.124	10.019	4535	1.40	-1.69	1.60	225	...
52106	2899	13.304	1.049	11.293	10.743	10.629	4695	1.60	-1.39	1.60	100	...
52109	121	12.009	1.149	9.580	8.993	8.790	4280	0.75	-1.98	1.95	250	...
52110	2903	13.260	1.038	11.286	10.680	10.619	4735	1.65	-1.66	1.30	100	...
52111	166	12.347	1.522	9.360	8.562	8.329	3850	0.60	-1.12	2.15	250	250
52133	411	12.984	1.082	10.901	10.317	10.172	4585	1.45	-1.77	1.70	175	...
52139	276	12.473	1.380	9.869	9.078	8.940	4075	0.60	-1.27	1.90	300	200
52151	311	12.485	1.178	10.495	9.885	9.733	4655	1.40	-1.67	1.80	300	...
52154	2944	13.278	0.960	11.447	10.929	10.811	4920	1.75	-1.64	1.45	125	...
52167	131	11.735	1.392	9.367	8.745	8.513	4290	0.75	-1.77	2.00	>350	...
52180	441	12.733	1.169	10.571	9.953	9.837	4500	1.35	-1.67	1.80	200	...
52192	554	12.930	1.100	10.861	10.282	10.157	4610	1.40	-1.34	1.90	100	...
52204	3000	13.305	0.911	11.483	10.956	10.833	4925	1.75	-1.81	1.55	125	...
52222	...	12.447	1.097	10.339	9.747	9.611	4560	1.20	-1.72	1.75	250	...
53012	483	12.742	1.063	10.657	10.063	9.977	4605	1.35	-1.83	1.90	300	...
53054	599	12.981	1.076	10.916	10.340	10.216	4615	1.45	-1.78	1.90	200	...
53058	422	12.678	1.126	10.579	9.982	9.836	4560	1.30	-1.74	1.85	200	...

Table 2—Continued

Star LEID ^a	Alt. ID ROA ^b	V	B–V	J	H	K _s	T _{eff} (K)	log g (cgs)	[Fe/H] Avg.	v _t (km s ^{−1})	S/N 6250 Å	S/N 6650 Å
53067	163	11.941	1.303	9.586	8.886	8.743	4290	0.80	−1.74	1.75	>350	...
53076	455	12.797	1.192	10.607	9.974	9.850	4465	1.30	−1.42	1.70	200	...
53114	138	12.037	1.390	9.378	8.631	8.495	4065	0.50	−1.45	1.90	225	...
53119	2928	13.385	0.984	11.477	10.930	10.810	4805	1.70	−1.57	1.65	75	...
53132	315	12.532	1.160	10.354	9.754	9.598	4485	1.20	−1.73	1.85	275	...
53178	337	12.407	1.154	10.219	9.575	9.455	4465	1.15	−1.77	1.65	>350	...
53185	124	11.776	1.380	9.284	8.569	8.395	4175	0.60	−1.64	1.90	>350	150
53203	2785	13.200	1.008	11.152	10.628	10.467	4650	1.55	−1.78	1.85	225	...
54018	2588	13.475	1.042	11.363	10.779	10.646	4560	1.60	−1.45	1.50	275	...
54022	2594	13.360	1.412	10.825	10.069	9.910	4135	1.15	−0.46	1.80	250	...
54031	332	12.560	1.507	9.970	9.235	9.023	4090	0.75	−1.15	1.85	>350	250
54064	2661	13.273	1.048	11.293	10.749	10.625	4725	1.60	−1.71	1.75	150	...
54073	456	12.756	1.072	10.755	10.185	10.140	4725	1.50	−1.65	1.65	175	...
54084	2674	13.201	1.044	11.226	10.656	10.557	4725	1.60	−1.50	1.55	100	...
54095	437	12.768	1.124	10.731	10.117	10.010	4625	1.50	−1.72	1.70	125	...
54105	386	12.771	1.293	10.194	9.473	9.277	4105	1.00	−1.00	1.90	250	...
54132	266	12.275	1.184	10.100	9.468	9.300	4465	1.10	−1.65	1.60	250	...
54148	105	11.593	1.547	9.087	8.309	8.171	4145	0.60	−1.54	2.00	>350	200
54154	2737	13.000	1.023	11.055	10.512	10.422	4785	1.55	−1.66	1.70	225	...
55028	270	12.247	1.520	9.738	8.981	8.821	4145	0.80	−1.19	1.80	300	200
55029	339	12.387	1.356	10.082	9.357	9.244	4320	1.05	−1.33	1.80	275	...
55056	2655	13.437	1.044	11.464	10.904	10.816	4740	1.70	−1.43	1.25	150	...
55063	177	11.955	1.414	9.603	8.875	8.724	4270	0.80	−1.48	1.80	>350	...
55071	248	12.150	1.695	9.239	8.410	8.185	3875	0.55	−0.75	2.00	>350	...
55089	277	12.268	1.203	10.110	9.501	9.333	4490	1.10	−1.70	2.00	300	...
55101	480	12.923	1.252	10.505	9.832	9.650	4240	1.15	−0.96	1.80	>350	...
55102	268	12.560	1.184	10.348	9.765	9.560	4445	1.20	−1.52	1.90	200	...
55111	182	11.969	1.476	9.502	8.804	8.591	4185	0.75	−1.49	1.90	325	...
55114	132	11.654	1.705	8.787	7.948	7.735	3895	0.20	−1.45	1.95	>350	...
55121	135	11.957	1.673	9.306	8.465	8.286	4015	0.60	−1.05	2.35	300	...
55122	220	12.315	1.296	9.923	9.201	9.081	4255	0.95	−1.36	1.80	200	175
55131	2732	13.414	1.086	11.453	10.885	10.707	4705	1.65	−1.52	1.50	125	...
55142	367	12.442	1.445	10.008	9.257	9.086	4195	1.20	−0.73	1.80	300	...
55149	505	12.894	1.321	10.581	9.883	9.708	4310	1.35	−0.83	1.75	275	...
55152	541	12.905	1.107	10.712	10.092	9.936	4455	1.30	−1.58	1.85	150	100
55165	418	12.649	1.118	10.529	9.897	9.775	4530	1.25	−1.65	1.65	150	...
56024	378	12.716	1.158	10.353	9.705	9.539	4300	1.00	−1.42	1.65	300	...
56028	473	12.825	1.042	10.617	9.983	9.921	4475	1.15	−1.86	1.95	275	125
56040	204	12.379	1.162	10.204	9.606	9.423	4475	1.15	−1.80	2.05	200	...
56056	2450	13.488	0.989	11.568	11.039	10.931	4810	1.75	−1.62	1.40	125	...
56070	445	12.957	1.116	10.773	10.154	10.026	4475	1.35	−1.44	1.60	275	...
56087	81	11.404	1.543	8.763	8.059	7.893	4085	0.45	−1.84	2.25	250	...
56106	534	12.860	1.118	10.809	10.197	10.062	4600	1.40	−1.64	1.90	200	100
56114	417	12.729	1.152	10.552	9.906	9.785	4470	1.25	−1.52	1.55	175	...
56118	532	12.890	1.084	10.838	10.279	10.108	4620	1.40	−1.64	1.70	125	...

Table 2—Continued

Star LEID ^a	Alt. ID ROA ^b	V	B-V	J	H	K _s	T _{eff} (K)	log g (cgs)	[Fe/H] Avg.	v _t (km s ⁻¹)	S/N 6250 Å	S/N 6650 Å
56128	2518	13.336	1.042	11.364	10.770	10.663	4705	1.85	-1.55	1.55	125	...
57010	207	12.154	1.412	9.744	9.001	8.864	4225	0.85	-1.52	1.85	>350	...
57029	2427	13.282	0.976	11.358	10.827	10.770	4835	1.70	-1.77	1.65	225	...
57054	110	11.589	1.595	8.972	8.190	7.989	4055	0.60	-1.32	2.05	275	...
57058	2462	13.230	1.064	11.235	10.673	10.542	4695	1.60	-1.71	1.70	150	125
57067	302	12.373	1.188	10.205	9.570	9.415	4470	1.10	-1.68	1.75	175	150
57073	368	12.470	1.151	10.355	9.746	9.608	4540	1.20	-1.76	1.75	225	...
57076	278	12.311	1.170	10.089	9.461	9.319	4435	1.10	-1.72	1.75	250	...
57083	2483	13.152	1.039	11.192	10.630	10.511	4735	1.60	-1.77	1.70	150	...
57085	2484	13.035	1.074	11.082	10.493	10.330	4705	1.50	-1.73	1.50	200	...
57091	2491	13.425	1.074	11.388	10.782	10.657	4620	1.65	-1.31	1.70	250	...
57114	2530	13.473	1.010	11.462	10.886	10.789	4685	1.70	-1.72	1.80	125	...
57127	2367	13.504	0.988	11.454	10.892	10.787	4650	1.65	-1.62	1.65	150	...
58043	531	12.923	1.079	10.863	10.294	10.165	4625	1.45	-1.77	1.85	250	...
58059	508	13.133	0.986	11.097	10.536	10.344	4625	1.45	-1.94	1.85	150	...
58077	2297	13.370	1.027	11.417	10.872	10.757	4760	1.70	-1.79	1.75	100	...
58087	133	11.760	1.337	9.438	8.724	8.609	4315	0.80	-1.69	1.75	>350	...
59016	2229	13.068	0.970	11.135	10.587	10.479	4785	1.60	-1.77	1.70	250	...
59024	...	11.855	1.629	9.113	8.322	8.143	3985	0.55	-0.82	2.55	250	...
59036	289	12.396	1.182	10.209	9.554	9.433	4455	1.15	-1.63	1.75	250	...
59047	192	11.975	1.413	9.653	9.001	8.794	4315	0.85	-1.44	1.80	300	...
59085	183	11.918	1.328	9.570	8.927	8.750	4310	0.85	-1.72	2.10	125	...
59089	363	12.694	1.212	10.468	9.827	9.670	4415	1.20	-1.45	1.65	175	...
59090	271	12.316	1.255	10.081	9.451	9.267	4405	1.05	-1.70	1.75	300	...
59094	164	12.174	1.157	10.091	9.527	9.386	4605	1.15	-1.91	1.75	175	125
60034	2059	13.394	1.018	11.451	10.891	10.792	4765	1.70	-1.76	1.70	125	...
60058	594	13.103	1.475	10.562	9.802	9.658	4130	1.15	-0.32	1.80	250	200
60059	2104	13.235	1.020	11.262	9.592	10.466	4655	1.55	-1.84	1.80	100	...
60064	2109	13.003	1.035	11.092	10.598	10.455	4830	1.60	-1.58	1.65	200	...
60065	288	12.335	1.226	10.156	9.538	9.393	4475	1.25	-1.75	1.75	150	...
60066	2118	13.086	1.253	11.067	10.470	10.330	4640	1.75	-0.98	1.55	200	...
60067	490	12.893	1.027	10.963	10.404	10.283	4775	1.80	-1.83	1.85	150	...
60069	556	13.022	1.171	11.041	10.448	10.352	4705	1.55	-1.41	1.80	100	...
60073	211	12.266	1.613	9.556	8.741	8.525	3985	0.75	-0.82	2.00	200	...
60088	2158	13.275	1.081	11.282	10.684	10.604	4695	1.60	-1.43	1.55	175	...
60101	446	12.680	1.092	10.579	9.962	9.830	4550	1.30	-1.76	1.85	200	...
61015	53	11.503	1.644	8.667	7.854	7.694	3935	0.35	-1.71	2.30	275	...
61026	2042	12.994	1.070	10.950	10.410	10.240	4640	1.45	-1.76	1.75	150	...
61042	260	12.209	1.306	9.927	9.220	9.096	4345	1.00	-1.56	1.70	>350	150
61046	543	12.878	1.062	10.841	10.252	10.134	4640	1.40	-1.73	1.70	175	100
61050	160	11.884	1.542	9.353	8.609	8.411	4125	0.70	-1.14	1.95	300	250
61067	371	12.528	1.605	9.875	9.096	8.899	4035	0.85	-0.94	1.90	300	...
61070	255	12.161	1.310	9.979	9.348	9.224	4470	1.05	-1.55	1.90	275	125
61075	2132	12.987	1.089	10.997	10.431	10.308	4700	1.50	-1.79	1.70	200	...
61085	158	11.846	1.699	9.088	8.287	8.081	3965	0.55	-1.26	2.30	>350	...

Table 2—Continued

Star LEID ^a	Alt. ID ROA ^b	V	B–V	J	H	K _s	T _{eff} (K)	log g (cgs)	[Fe/H] Avg.	v _t (km s ^{–1})	S/N 6250 Å	S/N 6650 Å
62018	1879	13.271	0.939	11.331	10.839	10.692	4800	1.65	–1.87	1.70	125	100
62058	407	12.564	1.280	10.416	9.786	9.626	4490	1.20	–1.37	1.70	250	...
63021	1878	13.169	1.181	11.031	10.389	10.293	4515	1.45	–1.46	1.65	275	...
63027	1898	13.024	1.058	10.993	10.417	10.310	4660	1.50	–1.64	1.85	150	...
63052	461	12.709	1.235	10.616	9.956	9.837	4535	1.30	–1.50	1.75	175	100
64023	1890	13.405	0.933	11.514	10.989	10.879	4850	1.75	–1.77	1.45	150	...
64049	181	12.015	1.346	9.769	9.130	8.952	4395	0.95	–1.68	1.75	250	...
64057	1957	13.469	1.027	11.579	11.025	10.906	4820	1.75	–1.66	1.50	150	...
64064	1978	13.348	1.005	11.370	10.817	10.720	4735	1.65	–1.74	1.75	100	...
64067	269	12.259	1.223	10.030	9.367	9.245	4415	1.05	–1.59	1.65	150	125
64074	1830	13.467	1.000	11.418	10.848	10.719	4635	1.65	–1.66	1.65	125	...
65042	579	12.882	1.076	10.983	10.440	10.332	4825	1.90	–1.83	1.30	150	125
65046	601	12.904	1.098	10.873	10.312	10.193	4665	1.45	–1.80	1.85	200	...
65057	1802	13.476	1.042	11.441	10.802	10.675	4600	1.65	–1.81	1.90	150	...
66015	1595	13.412	0.977	11.444	10.872	10.787	4735	1.70	–1.68	1.75	225	...
66026	438	12.672	1.130	10.585	9.986	9.873	4585	1.30	–1.68	1.80	250	...
66047	472	12.704	1.351	10.452	9.779	9.628	4375	1.30	–1.30	1.75	250	...
66054	232	12.111	1.290	9.908	9.226	9.123	4435	1.00	–1.59	1.80	>350	...
67049	1754	13.318	1.013	11.363	10.812	10.676	4740	1.65	–1.71	1.75	100	...
67063	199	12.084	1.348	9.756	9.056	8.873	4295	0.90	–1.50	1.90	175	...
68044	470	12.673	1.056	10.744	10.184	10.064	4775	1.65	–1.59	1.70	150	...
69007	1422	13.412	1.000	11.523	11.004	10.860	4835	1.75	–1.60	1.55	150	...
69012	109	11.666	1.390	9.268	8.555	8.414	4250	0.70	–1.78	1.95	>350	...
69027	1471	13.365	1.399	10.944	10.229	10.050	4225	1.35	–0.76	2.05	250	...
70032	449	12.690	1.124	10.571	9.937	9.832	4535	1.30	–1.70	1.55	>350	...
70035	595	12.969	1.229	10.850	10.177	10.035	4495	1.35	–1.45	1.95	150	...
70041	1493	13.221	1.102	11.237	10.636	10.550	4700	1.60	–1.54	1.70	175	...
70049	389	12.621	1.137	10.417	9.806	9.651	4455	1.20	–1.35	1.50	75	...
71013	1409	13.435	0.866	11.574	11.028	10.963	4895	1.75	–1.69	1.00	150	...
73025	150	11.864	1.685	9.194	8.360	8.166	4005	0.55	–1.42	2.35	>350	...
75021	442	12.630	1.164	10.473	9.863	9.718	4500	1.25	–1.74	1.80	275	...
76027	297	12.366	1.280	10.049	9.389	9.249	4335	1.05	–1.69	1.80	250	125
76038	316	12.535	1.411	10.009	9.238	9.049	4120	0.95	–1.24	1.85	>350	...
77025	194	12.197	1.339	9.861	9.171	9.008	4300	0.95	–1.58	1.85	300	...
77030	354	12.547	1.133	10.384	9.788	9.665	4515	1.20	–1.73	1.60	250	...
80026	481	12.803	1.106	10.702	10.084	9.950	4570	1.35	–1.86	1.95	125	...
80029	218	12.273	1.293	9.949	9.248	9.111	4310	1.00	–1.67	1.70	250	...
81018	217	12.282	1.174	10.015	9.377	9.244	4395	1.00	–1.81	1.95	275	...
81019	1209	13.401	1.097	11.336	10.747	10.618	4605	1.60	–1.49	1.65	150	...
81028	1241	13.332	0.899	11.312	10.712	10.580	4645	1.60	–1.74	1.60	200	...
82015	1026	13.277	0.980	11.383	10.818	10.702	4810	1.70	–1.70	1.65	200	...
82029	1107	13.469	0.813	11.608	11.070	10.973	4885	1.80	–1.76	1.05	150	...
85027	264	12.370	1.260	10.035	9.358	9.217	4315	1.00	–1.56	1.75	200	...
85031	369	12.634	1.045	10.389	9.771	9.615	4420	1.20	–1.77	1.80	175	...
89009	403	12.650	1.126	10.497	9.890	9.753	4510	1.25	–1.76	1.90	150	...

Table 2—Continued

Star LEID ^a	Alt. ID ROA ^b	V	B-V	J	H	K _s	T _{eff} (K)	log g (cgs)	[Fe/H] Avg.	v _t (km s ⁻¹)	S/N 6250 Å	S/N 6650 Å

Note. — The possible carbon stars shown in Figures 1 and 3 are: LEID 32059, 33062, 35250, 37199, 39105, 41071, 42044, 43199, 43368, 44126, 44262, 44361, 44484, and 52030. Coordinates and photometry for these stars can be found in van Leeuwen et al. (2000).

^aIdentifier from van Leeuwen et al. (2000).

^bIdentifier from Woolley (1966).

Table 3a. Fe Atomic Parameters, Equivalent Widths, and Solar Abundances

Wavelength (Å)	Ion	E.P. (eV)	Log gf	Log ϵ_{\odot}	Star (LEID)	Equivalent Widths (mÅ)													
						6151.62	6157.73	6165.36	6173.34	6180.20	6187.99	6200.32	6219.28	6226.74	6229.23	6232.64	6246.32	6252.56	6265.14
9	Fe I	Fe I	Fe I	Fe I	5009	73	55	35	107	68	...	99	136	14	37	81	110	162	137
5009	Fe I	Fe I	Fe I	Fe I	6017	36	22	16	59	30	10	58	90	...	23	45	77	116	95
6017	Fe I	Fe I	Fe I	Fe I	8014	103	...	46	133	100	46	123	158	...	69	113	130
8014	Fe I	Fe I	Fe I	Fe I	9013	30	27	11	51	28	17	58	87	...	18	45	67	113	85
9013	Fe I	Fe I	Fe I	Fe I	10009	29	26	12	48	27	8	56	88	40	74	110	88
10009	Fe I	Fe I	Fe I	Fe I	10012	66	...	31	103	61	31	95	123	15	40	78	107	147	...
10012	Fe I	Fe I	Fe I	Fe I	11019	119	80	42	148	105	48	140	183	26	81	106	142	192	165
11019	Fe I	Fe I	Fe I	Fe I	11021	64	55	26	92	59	28	91	119	19	39	73	100	147	123
11021	Fe I	Fe I	Fe I	Fe I	11024	72	66	28	99	75	33	96	128	20	44	81	103	151	134
11024	Fe I	Fe I	Fe I	Fe I	12013	69	39	21	100	59	24	90	135	11	36	68	96	162	139
12013	Fe I	Fe I	Fe I	Fe I	12014	91	78	46	121	93	45	114	148	32	59	100	126	170	163
12014	Fe I	Fe I	Fe I	Fe I	14010	35	26	7	48	19	...	52	90	...	14	47	71	98	76
14010	Fe I	Fe I	Fe I	Fe I	15022	22	10	...	42	18	6	42	72	60
15022	Fe I	Fe I	Fe I	Fe I	15023	50	24	14	69	38	12	62	109	7	23	49	77	128	...
15023	Fe I	Fe I	Fe I	Fe I	15026	44	23	17	69	37	11	67	105	8	24	49	84	136	109
15026	Fe I	Fe I	Fe I	Fe I	16009	88	82	41	121	84	44	109	137	...	57	105	135	...	157
16009	Fe I	Fe I	Fe I	Fe I	16015	45	28	15	86	46	18	72	112	10	27	53	89	132	111
16015	Fe I	Fe I	Fe I	Fe I	16019	32	19	8	58	29	11	57	93	5	15	40	75	122	95
16019	Fe I	Fe I	Fe I	Fe I	16027	21	22	10	46	28	15	51	80	4	13	42	70
16027	Fe I	Fe I	Fe I	Fe I	17014	21	32	20	...	44	71	...	7	...	51	99	75
17014	Fe I	Fe I	Fe I	Fe I	17015	69	60	38	105	71	23	92	132	19	36	78	109	148	144
17015	Fe I	Fe I	Fe I	Fe I	17027	43	27	13	69	41	16	68	99	6	20	49	81	129	100
17027	Fe I	Fe I	Fe I	Fe I	17029	15	10	18	...	33	44	13	32	68	112
17029	Fe I	Fe I	Fe I	Fe I	17032	53	51	27	89	62	17	79	104	...	28	68	94	139	124
17032	Fe I	Fe I	Fe I	Fe I	17046	11	13	15	...	37	54	41	90	52	...
17046	Fe I	Fe I	Fe I	Fe I	18017	21	50	19	7	49	81	...	13	32	68	112	84
18017	Fe I	Fe I	Fe I	Fe I	18020	67	49	24	99	63	24	94	141	10	36	74	106	173	135
18020	Fe I	Fe I	Fe I	Fe I	18035	32	25	11	73	27	14	61	89	46	74	114	100
18035	Fe I	Fe I	Fe I	Fe I	18040	76	75	38	107	78	37	103	133	20	51	83	110	148	151

Table 3a—Continued

Star (LEID)	Wavelength (Å)	Equivalent Widths (mÅ)											
		Fe I	Fe I	Fe I	Fe I	Fe I	Fe I	Fe I	Fe I	Fe I	Fe I	Fe I	Fe I
18047	6151.62	6157.73	6165.36	6173.34	6180.20	6187.99	6200.32	6219.28	6226.74	6229.23	6232.64	6246.32	6252.56
19022	2.18	4.07	4.14	2.22	2.73	3.94	2.61	2.20	3.88	2.84	3.65	3.60	2.40
19062	-3.33	-1.22	-1.51	-2.89	-2.66	-1.69	-2.41	-2.42	-2.19	-3.00	-1.23	-0.85	-1.71
20018	48	32	...	76	55	...	69	97	51	90	113
20037	56	50	...	83	55	18	81	102	...	30	67	98	135
20042	17	19	...	52	40	72	35	62	100
20049	27	25	10	57	28	...	57	81	...	17	43	73	108
21032	84	64	34	111	77	37	110	138	20	54	87	115	168
21035	40	21	..	64	37	14	64	97	...	17	47	75	124
21042	44	30	18	75	48	21	67	101	...	25	56	87	124
21063	24	23	..	51	17	10	47	74	...	6	37	60	100
22023	63	60	31	93	59	28	88	106	13	37	83	95	123
22037	43	27	16	66	39	14	64	112	...	21	47	74	115
22042	30	29	14	64	37	14	64	96	...	17	45	75	124
22049	..	21	..	43	31	..	42	81	...	12	37	71	98
22063	28	23	10	49	21	..	51	80	...	13	39	68	109
23022	14	34	16	7	37	69	...	9	31	51	95
23033	31	24	..	66	37	..	61	80	41	63	107
23042	25	50	21	8	51	84	..	16	38	66	108
23050	18	16	..	48	20	7	45	80	5	8	31	61	..
23061	46	26	14	76	45	15	70	104	13	25	53	80	139
23068	87	52	29	120	80	31	117	162	17	52	84	114	181
24013	110	68	40	137	97	36	122	159	21	68	85	126	203
24027	45	45	15	73	43	18	68	100	..	25	57	91	116
24040	18	34	18	..	35	65	47	..
24046	68	38	17	94	58	19	87	127	12	33	70	97	154
24056	36	21	..	62	34	13	62	89	9	21	48	78	125
24062	69	61	35	102	75	35	103	123	21	48	87	104	151
25006	..	11	..	26	11	7	25	62	..	7	..	42	..
25026	26	53	25	..	49	80	38	67	108

Table 3a—Continued

Star (LEID)	Wavelength (Å)	Equivalent Widths (mÅ)											
		Fe I	Fe I	Fe I	Fe I	Fe I	Fe I	Fe I	Fe I	Fe I	Fe I	Fe I	Fe I
25043	6157.73	6165.36	6173.34	6180.20	6187.99	6200.32	6219.28	6226.74	6229.23	6232.64	6246.32	6252.56	6265.14
25062	104	54	32	130	90	40	114	160	21	60	93	126	200
25065	136	...	156	120	36	130	165	21	60	93	127	204	...
25068	78	42	22	109	68	23	106	137	16	44	74	100	161
26010	27	...	27	10	...	52	...	62
26014	28	13	9	57	28	7	57	82	...	14	37	72	107
26022	31	...	48	53	80	6	13	...	65	107	...
26025	99	52	25	130	83	30	124	170	15	52	...	195	163
26030	...	20	10	42	...	10	30	64	26	59	95
26069	22	...	37	18	...	42	70	...	9	30	53	94	...
26072	48	23	...	72	33	...	72	103	...	23	50	72	125
26086	105	...	53	136	95	50	116	80	117	145	...
26088	74	50	29	108	70	29	97	136	11	34	68	103	163
27048	63	52	27	96	62	26	91	116	...	33	76	104	138
27050	38	15	...	34	68	24	58	95	66
27073	44	30	15	70	39	15	63	99	8	25	50	85	119
27094	43	23	...	53	82	81	115	86
27095	82	...	35	124	78	34	117	146	...	48	100	126	174
28016	39	31	...	67	39	...	73	98	...	25	51	83	119
28020	27	16	...	52	25	...	46	87	35	59	112
28044	52	36	18	80	51	17	80	113	12	32	63	87	144
28069	57	33	15	86	55	18	80	109	...	30	64	93	142
28084	42	27	...	73	45	21	77	98	...	32	51	87	127
28092	50	37	...	84	46	18	74	114	...	28	62	91	133
29029	48	34	16	75	49	20	71	98	...	30	63	86	120
29031	25	17	...	46	...	11	44	79	37	67	...
29037	19	...	10	45	20	...	45	76	37	61	...
29059	57	41	20	89	51	19	78	114	...	35	59	95	140
29067	132	89	...	158	129	78	...	167	...	102	101	129	187
29069	75	60	32	107	68	25	99	131	...	40	84	103	157

Table 3a—Continued

Star (LEID)	Wavelength (Å)	Equivalent Widths (mÅ)											
		Fe I	Fe I	Fe I	Fe I	Fe I	Fe I	Fe I	Fe I	Fe I	Fe I	Fe I	Fe I
29072	6157.73	6165.36	6173.34	6180.20	6187.99	6200.32	6219.28	6226.74	6229.23	6232.64	6246.32	6252.56	6265.14
29085	2.18	4.07	4.14	2.22	2.73	3.94	2.61	2.20	3.88	2.84	3.65	3.60	2.40
29089	-3.33	-1.22	-1.51	-2.89	-2.66	-1.69	-2.41	-2.42	-2.19	-3.00	-1.23	-0.85	-1.71
29099	7.52	7.52	7.52	7.52	7.52	7.52	7.52	7.52	7.52	7.52	7.52	7.52	7.52
29106
30013	69	33	99	76	35	93	119	...	51	94	114
30019	60	53	29	89	57	25	83	109	...	33	70	97	145
30022	27	45	26	10	43	78	39	66	104
30031	98	73	34	133	90	36	120	156	24	60	99	128	180
30069	9	8	...	21	47	40	69
30094	71	45	26	83	44	15	80	111	15	33	72	88	125
30124	43	42	...	73	47	15	76	95	12	24	61	84	121
31016	28	15	6	42	19	...	42	74	...	11	...	54	90
31041	47	37	...	70	45	17	65	99	...	23	52	85	125
31047	16	...	8	47	22	81	32	65	98
31048	23	46	23	...	47	14	37	64	...
31075	...	15	...	37	...	16	47	79	29	60	97
31079	40	22	10	68	38	...	64	101	...	20	51	76	132
31094	34	22	16	66	35	14	63	14	48	74	...
31095	29	55	23	...	52	80	...	13	47	72	106
31104	18	...	7	33	14	...	31	65	21
31109	45	31	...	69	43	19	76	98	...	32	65	83	121
31110	91	77	36	121	84	39	112	143	17	50	96	119	157
31119	78	...	43	108	76	36	106	142	22	49	92	112	162
31133	14	28	14	...	33	56	...	8	...	50	...
31139	37	24	12	65	34	11	63	100	...	24	50	75	126
31141	52	37	18	79	45	18	74	110	...	27	58	90	128
31147	...	40	11	64	...	19	71	102	50	92	125
31152	66	41	12	57	104	77	132	87
32014	29	14	8	52	32	9	51	85	36	70	116

Table 3a—Continued

Star (LEID)	Wavelength (Å)	Equivalent Widths (mÅ)											
		Fe I	Fe I	Fe I	Fe I	Fe I	Fe I	Fe I	Fe I	Fe I	Fe I	Fe I	Fe I
32026	6151.62	6157.73	6165.36	6173.34	6180.20	6187.99	6200.32	6219.28	6226.74	6229.23	6232.64	6246.32	6252.56
Ion	Fe I	Fe I	Fe I	Fe I	Fe I	Fe I	Fe I	Fe I	Fe I	Fe I	Fe I	Fe I	Fe I
E.P. (eV)	2.18	4.07	4.14	2.22	2.73	3.94	2.61	2.20	3.88	2.84	3.65	3.60	2.40
Log gf	-3.33	-1.22	-1.51	-2.89	-2.66	-1.69	-2.41	-2.42	-2.19	-3.00	-1.23	-0.85	-1.71
Log ϵ_{\odot}	7.52	7.52	7.52	7.52	7.52	7.52	7.52	7.52	7.52	7.52	7.52	7.52	7.52
32100	26	21	...	53	30	9	54	79	36	70	103
32101	52	43	19	76	45	18	78	103	...	21	61	93	135
32125	53	34	13	79	48	16	77	119	9	27	62	...	134
32130	...	11	9	35	...	8	39	65	52	90	...
32138	94	48	25	127	82	28	118	160	14	50	...	120	194
32140	41	31	...	71	45	11	62	97	...	19	44	77	126
32144	47	31	19	74	45	18	78	107	15	34	63	93	124
32165	26	15	9	58	27	...	50	89	...	19	38	77	113
32169	110	...	62	143	103	49	131	150	30	67	125	135	...
32171	74	...	26	108	67	28	99	46	97	108	152
33006	96	58	31	127	91	37	126	173	23	55	88	116	178
33011	66	35	17	88	61	20	84	124	9	33	63	96	158
33018	59	29	22	73	50	16	87	108	...	29	54	82	...
33030	15	47	56	77	64	66	98
33051	53	40	18	83	49	21	76	112	...	26	63	85	135
33064	32	22	...	50	32	...	50	81	...	15	39	76	105
33099	106	109	60	150	105	52	...	156	...	82	...	148	...
33114	88	62	34	122	85	34	114	170	21	52	83	119	178
33115	54	65	37	...	58	25	87	101	...	31	79	96	129
33126	43	45	23	73	46	19	77	102	10	25	79	96	122
33129	34	20	10	59	31	12	60	85	8	13	38	70	118
33138	39	33	...	62	38	92	52	82	118
33145	16	9	...	37	19	5	...	70	6	...	35
33154	...	23	67	74
33167	39	30	16	48	33	14	54	96	...	21	67	80	114

Table 3a—Continued

	Wavelength (Å)	6151.62	6157.73	6165.36	6173.34	6180.20	6187.99	6200.32	6219.28	6226.74	6229.23	6232.64	6246.32	6252.56	6265.14
Ion	Fe I	Fe I	Fe I	Fe I	Fe I	Fe I	Fe I	Fe I	Fe I	Fe I	Fe I	Fe I	Fe I	Fe I	Fe I
E.P. (eV)	2.18	4.07	4.14	2.22	2.73	3.94	2.61	2.20	3.88	2.84	3.65	3.60	2.40	2.18	2.18
Log gf	-3.33	-1.22	-1.51	-2.89	-2.66	-1.69	-2.41	-2.42	-2.19	-3.00	-1.23	-0.85	-1.71	-2.56	-2.56
Log ϵ_{\odot}	7.52	7.52	7.52	7.52	7.52	7.52	7.52	7.52	7.52	7.52	7.52	7.52	7.52	7.52	7.52
Star (LEID)															
33177	40	22	19	61	100	45	86	115	93	93
34008	...	38	...	78	48	14	75	106	16	...	61	86	135	109	109
34029	98	87	52	134	97	54	122	168	33	75	105	138	187
34040	36	27	...	67	36	13	61	91	52	83	121	97	97
34056	...	17	17	43	71	33	55	...	65	65
34069	55	28	21	92	51	19	82	108	...	31	59	91	132	109	109
34075	81	59	34	113	85	34	109	144	19	49	85	112
34081	49	35	17	77	44	22	73	98	10	25	54	86	131	109	109
34129	21	11	7	42	30	...	40	72	28	63	97	73	73
34130	7	...	17	...	37	28	44
34134	77	41	25	109	71	23	102	124	13	41	74	110	...	112	112
34143	47	119	88	50	106	147	...	60	103	136	188
34163	24	18	...	49	48	81	...	13	24	62
34166	42	37	...	81	...	14	74	60	83	123
34169	61	...	24	88	53	22	83	111	8	38	84	100	132	127	127
34175	87	62	24	127	84	30	113	152	...	50	91	110	173
34180	121	156	123	85	77	...	140	144
34187	...	22	...	51	28	10	59	79	5	13	35	76	112	88	88
34193	52	33	19	84	54	18	82	124	15	31	58	88	...	115	115
34207	65	55	27	97	73	29	96	135	15	44	72	106	154	124	124
34214	13	29	27	65	57	...	64	64
34225	55	134	93	51	126	145	...	66	119	131	164
34229	23	21	11	51	25	...	50	85	...	11	32	71	117	86	86
35029	32	24	15	53	34	12	...	84	...	22	39	72	105	82	82
35035	24	18	...	47	27	...	47	80	4	10	37	63	102	81	81
35046	46	35	15	79	45	15	72	112	12	24	54	79	132
35053	34	24	7	57	29	11	63	97	...	20	38	76	117	95	95
35056	96	61	42	129	81	32	122	154	...	61	79	121	186	150	150
35061	74	65	34	110	79	30	103	...	18	44	85	114	166
35066	76	43	21	107	71	25	104	133	15	40	66	107	155	128	128

Equivalent Widths (mÅ)

Table 3a—Continued

	Wavelength (Å)	6151.62	6157.73	6165.36	6173.34	6180.20	6187.99	6200.32	6219.28	6226.74	6229.23	6232.64	6246.32	6252.56	6265.14
Ion	Fe I	Fe I	Fe I	Fe I	Fe I	Fe I	Fe I	Fe I	Fe I	Fe I	Fe I	Fe I	Fe I	Fe I	Fe I
E.P. (eV)	2.18	4.07	4.14	2.22	2.73	3.94	2.61	2.20	3.88	2.84	3.65	3.60	2.40	2.18	
Log gf	-3.33	-1.22	-1.51	-2.89	-2.66	-1.69	-2.41	-2.42	-2.19	-3.00	-1.23	-0.85	-1.71	-2.56	
Log ϵ_{\odot}	7.52	7.52	7.52	7.52	7.52	7.52	7.52	7.52	7.52	7.52	7.52	7.52	7.52	7.52	
Star (LEID)															
35071	34	49	79	11	19	...	55	92
35074	39	33	...	66	36	12	59	96	...	20	47	82	115	99	
35087	19	11	39	27	7	40	79	...	12	36	68	98	
35090	94	...	39	123	92	43	123	159	20	63	108	127	
35093	16	...	23	13	31	46	51	80	...	
35124	50	51	26	79	54	21	83	94	15	33	66	96	127	...	
35157	73	...	36	116	78	34	96	121	...	49	97	113	
35165	41	22	11	65	39	13	62	88	7	18	45	72	122	101	
35172	47	136	107	51	127	66	113	141	
35190	37	...	13	63	33	19	57	98	7	24	49	70	118	85	
35201	58	135	102	52	120	67	112	125	
35204	15	20	...	35	...	12	37	65	...	8	27	64	90	73	
35216	66	42	25	108	61	20	102	146	15	41	69	104	156	140	
35228	30	25	...	60	24	15	55	87	48	77	112	92	
35230	52	29	...	78	44	11	75	112	...	24	53	93	147	116	
35235	67	41	20	93	59	24	101	115	...	35	67	113	143	116	
35240	72	45	21	104	63	14	91	140	...	28	69	104	144	...	
35248	...	28	10	59	28	10	57	87	7	20	41	83	115	...	
35260	36	25	11	71	36	14	62	98	...	16	47	87	
35261	49	41	20	69	43	15	72	97	...	23	55	85	118	100	
36028	22	...	9	58	43	77	...	18	39	69	
36036	82	40	18	118	69	25	109	137	13	37	66	115	182	...	
36048	27	23	...	65	24	20	56	84	37	71	104	82	
36059	23	52	32	16	53	76	...	14	42	62	105	74	
36061	53	51	21	85	61	24	87	108	9	34	74	97	132	...	
36087	...	18	...	44	25	9	44	69	...	15	29	65	102	78	
36106	39	30	11	65	...	14	66	89	8	20	40	80	109	101	
36110	...	12	24	...	45	85	60	98	70	
36113	32	27	...	55	28	12	56	82	10	70	110	86	
36134	89	93	50	121	88	55	25	63	90	127	159	...	

Equivalent Widths (mÅ)

Table 3a—Continued

	Wavelength (Å)	6151.62	6157.73	6165.36	6173.34	6180.20	6187.99	6200.32	6219.28	6226.74	6229.23	6232.64	6246.32	6252.56	6265.14
Ion	Fe I	Fe I	Fe I	Fe I	Fe I	Fe I	Fe I	Fe I	Fe I	Fe I	Fe I	Fe I	Fe I	Fe I	Fe I
E.P. (eV)	2.18	4.07	4.14	2.22	2.73	3.94	2.61	2.20	3.88	2.84	3.65	3.60	2.40	2.18	
Log gf	-3.33	-1.22	-1.51	-2.89	-2.66	-1.69	-2.41	-2.42	-2.19	-3.00	-1.23	-0.85	-1.71	-2.56	
Log ϵ_{\odot}	7.52	7.52	7.52	7.52	7.52	7.52	7.52	7.52	7.52	7.52	7.52	7.52	7.52	7.52	7.52
Star (LEID)															
36156	55	27	19	92	53	16	82	110	7	26	59	84	140	140	122
36179	64	148	110	56	137	178	...	80	...	146
36182	69	52	26	103	64	27	93	120	...	37	75	103	149	149	131
36191	99	...	63	145	117	60	123	151	...	78	119	139
36206	35	23	...	71	37	16	67	97	...	23	48	84	124	98	
36228	88	46	24	115	75	30	115	145	16	46	77	121	191	156	
36239	61	96	60	24	90	113	...	31	80	106	142	142	
36259	35	...	11	68	36	11	60	99	...	21	47	80	123	101	
36260	...	52	...	71	...	17	66	87	...	30	61	80	113	84	
36280	61	52	23	93	56	...	87	118	9	38	70	94
36282	36	20	...	61	32	...	59	95	6	15	40	73	119	93	
37022	12	57	31	...	54	86	...	15	40	70	114	114	
37024	148	163	...	101	...	179	134
37051	22	14	10	37	25	...	46	79	35	69	107	107	...
37052	46	28	16	66	27	15	62	93	...	22	42	86	117	83	
37055	49	42	...	79	47	...	77	97	...	31	65	90	122	107	
37062	78	...	41	122	84	42	112	53	92	128
37071	51	45	102	78	
37082	21	41	38	75	32	62	98	72	
37087	34	26	10	70	37	...	67	93	47	76	120	...	
37094	27	18	10	53	25	13	48	74	...	13	42	63	109	82	
37105	27	23	...	51	22	11	44	73	8	...	42	64	99	72	
37110	144	...	90	194	148	74	170	244	48	111	164	172	231	...	
37119	72	41	23	101	65	27	99	133	13	37	70	104	153	125	
37136	22	18	...	46	...	12	37	75	5	13	35	61	105	79	
37139	83	59	33	122	80	35	115	144	20	55	89	127	
37143	45	28	...	66	39	14	69	90	11	25	53	81	118	101	
37147	71	68	30	102	78	34	98	121	19	46	79	106	150	...	
37157	42	32	10	73	44	...	68	99	7	20	49	78	118	95	
37169	...	30	...	45	33	80	...	24	43	71	

Equivalent Widths (mÅ)

Table 3a—Continued

Star (LEID)	Wavelength (Å)	Equivalent Widths (mÅ)											
		Fe I	Fe I	Fe I	Fe I	Fe I	Fe I	Fe I	Fe I	Fe I	Fe I	Fe I	Fe I
37179	6157.73	6165.36	6173.34	6180.20	6187.99	6200.32	6219.28	6226.74	6229.23	6232.64	6246.32	6252.56	6265.14
37184	40	24	12	65	37	12	62	96	10	16	48	78	133
37196	35	21	12	56	28	12	58	87	...	14	46	75	127
37198	64	49	25	94	61	32	84	112	9	29	75	98	150
37215	29	...	41	38	66	24	58	100	...
37232	100	65	31	133	87	34	128	170	...	56	92	119	192
37247	57	28	10	69	39	...	74	102	10	22	52	82	127
37253	66	35	20	95	61	18	88	122	12	36	65	93	137
37271	71	44	...	100	68	29	92	128	14	40	73	105	151
37275	66	68	...	94	65	28	92	...	10	54	86	112	141
37318	125	...	65	156	118	79	138	178	126	142	...
37322	...	10	...	25	...	4	...	57	6	8	19	44	80
37329	44	30	10	61	41	17	70	105	...	19	56	75	124
38011	87	...	48	117	88	40	113	57	103	116	...
38018	43	37	...	71	35	13	61	96	...	21	51	81	120
38049	82	44	22	113	71	23	109	129	11	48	69	112	185
38052	74	47	22	103	73	27	105	135	15	42	75	107	158
38056	30	24	...	58	27	...	55	84	...	9	45	70	108
38057	73	64	27	85	56	111	22	...	75	108	137
38059	113	...	60	150	117	58	136	174	...	82	...	146	200
38061	13	16	9	27	34	66	...	6	...	40	76
38096	37	33	...	59	47	12	58	107	77	127
38097	105	78	57	123	96	59	117	165	36	77	107	127	181
38105	39	...	18	67	37	12	62	99	6	18	48	81	126
38112	63	...	27	100	51	32	93	...	13	45	79	102	136
38115	83	55	30	106	69	29	108	146	...	52	94	101	163
38129	59	40	19	83	56	18	79	104	...	32	64	92	132
38147	61	...	29	91	56	25	81	110	14	36	71	98	119
38149	105	...	43	138	100	49	132	165	30	69	116	138	...
38156	46	35	...	76	46	18	74	107	...	30	58	88	128

Table 3a—Continued

Star (LEID)	Wavelength (Å)	Equivalent Widths (mÅ)											
		Fe I	Fe I	Fe I	Fe I	Fe I	Fe I	Fe I	Fe I	Fe I	Fe I	Fe I	Fe I
38166	6151.62	6157.73	6165.36	6173.34	6180.20	6187.99	6200.32	6219.28	6226.74	6229.23	6232.64	6246.32	6252.56
38168	2.18	4.07	4.14	2.22	2.73	3.94	2.61	2.20	3.88	2.84	3.65	3.60	2.40
38169	-3.33	-1.22	-1.51	-2.89	-2.66	-1.69	-2.41	-2.42	-2.19	-3.00	-1.23	-0.85	-1.71
38195	7.52	7.52	7.52	7.52	7.52	7.52	7.52	7.52	7.52	7.52	7.52	7.52	7.52
38198	85	...	28	110	77	39	106	...	49	98	112	...	146
38204	66	46	...	101	63	18	90	130	...	41	67	101	156
38206	27	24	...	53	26	12	54	80	8	...	41	73	106
38215	70	...	49	109	77	48	92	120	18	53	94	112	...
38223	45	28	17	78	45	19	77	104	10	25	49	85	130
38225	38	23	19	62	35	12	61	94	...	23	49	85	121
38226	50	38	...	70	41	...	61	97	...	25	52	81	122
38232	92	69	38	120	82	41	117	149	25	62	91	...	161
38255	79	85	39	126	83	42	106	124	...	58	97	125	155
38262	62	28	...	93	56	...	91	123	11	35	70	92	...
38276	73	43	24	99	67	23	96	125	18	40	74	102	164
38303	64	98	58	22	91	34	76	97	153
38319	53	45	...	80	47	21	89	110	...	33	67	88	126
38323	63	72	30	98	77	40	92	116	...	41	91	110	138
38330	37	54	33	15	56	89	...	17	40	72	110
39026	84	...	36	120	82	36	111	133	23	55	88	104	157
39033	18	40	39	69	...	15	30	56	96
39034	47	24	...	76	44	...	71	100	14	33	51	87	130
39037	75	40	19	100	65	24	98	125	...	42	71	105	171
39043	30	24	13	57	29	18	57	92	...	18	41	75	...
39044	52	31	15	76	48	17	68	104	...	27	60	93	131
39048	127	158	141	81	142
39056	28	...	10	36	26	...	50	76	...	13	...	60	94
39063	19	...	6	34	14	...	31	51	...	9	23	...	57
39067	87	71	36	113	83	37	112	140	...	49	92	111	165
39086	56	45	19	90	56	22	81	115	...	32	67	96	141

Table 3a—Continued

Star (LEID)	Wavelength (Å)	Equivalent Widths (mÅ)											
		Fe I	Fe I	Fe I	Fe I	Fe I	Fe I	Fe I	Fe I	Fe I	Fe I	Fe I	Fe I
39088	6151.62	6157.73	6165.36	6173.34	6180.20	6187.99	6200.32	6219.28	6226.74	6229.23	6232.64	6246.32	6252.56
39102	2.18	4.07	4.14	2.22	2.73	3.94	2.61	2.20	3.88	2.84	3.65	3.60	2.40
39119	-3.33	-1.22	-1.51	-2.89	-2.66	-1.69	-2.41	-2.42	-2.19	-3.00	-1.23	-0.85	-1.71
39123	7.52	7.52	7.52	7.52	7.52	7.52	7.52	7.52	7.52	7.52	7.52	7.52	7.52
39129	73	...	109	69	38	93	132	...	45	93	116
39141	64	34	17	88	54	18	88	117	11	28	65	96	152
39149	94	...	129	97	50	127	152	...	70	114	137
39165	56	24	...	88	49	...	78	126	...	27	53	85	141
39186	62	39	15	88	57	20	94	123	...	30	62	99	...
39187	55	...	17	87	52	19	82	115	8	27	63	96	142
39198	63	38	22	95	56	21	89	112	14	35	61	95	139
39204	40	24	...	60	42	...	58	95	42	74	123
39215	35	22	12	63	31	10	60	93	...	17	45	75	117
39216	36	...	15	63	37	13	54	83	...	20	52	71	113
39225	27	33	14	60	38	12	54	87	40	82	109
39235	68	64	26	100	72	31	91	126	13	45	72	108	145
39245	95	74	40	123	90	47	118	...	25	66	92	115	177
39257	103	...	46	136	101	51	130	155	...	76	106	129	188
39259	56	38	15	83	50	23	79	112	12	29	66	93	130
39284	79	45	18	108	65	27	100	141	14	42	72	102	173
39289	35	24	13	62	36	14	58	84	...	21	43	71	110
39298	8	48	12	...	39	71	41	63	96
39301	29	...	13	64	32	12	57	76	...	10	42	66	...
39306	57	34	...	87	57	19	88	113	...	28	60	95	140
39325	108	...	54	142	105	52	141	69	125	127	...
39329	25	24	...	47	28	11	59	90	...	12	52	74	116
39345	28	21	20	60	34	8	56	80	41	69	111
39346	77	79	51	112	92	42	110	129	28	61	94	114	148
39352	61	37	23	95	57	24	93	121	14	33	65	94	145
39384	49	56	25	88	52	20	79	104	...	26	60	96	127

Table 3a—Continued

Star (LEID)	Wavelength (Å)	Equivalent Widths (mÅ)											
		Fe I	Fe I	Fe I	Fe I	Fe I	Fe I	Fe I	Fe I	Fe I	Fe I	Fe I	Fe I
39392	6151.62	6157.73	6165.36	6173.34	6180.20	6187.99	6200.32	6219.28	6226.74	6229.23	6232.64	6246.32	6252.56
39401	2.18	4.07	4.14	2.22	2.73	3.94	2.61	2.20	3.88	2.84	3.65	3.60	2.40
39921	-3.33	-1.22	-1.51	-2.89	-2.66	-1.69	-2.41	-2.42	-2.19	-3.00	-1.23	-0.85	-1.71
40016	7.52	7.52	7.52	7.52	7.52	7.52	7.52	7.52	7.52	7.52	7.52	7.52	7.52
40031
40041	45	74	48	23	...	103	64	91	121
40108	31	16	15	41	28	...	49	88	...	16	28	67	100
40123	107	...	36	134	93	44	133	...	29	63	101
40135	71	29	...	94	61	18	90	127	7	31	71	99	155
40139	92	...	38	125	93	44	112	162	...	65	102	129	182
40162	45	46	...	75	44	15	67	92	...	27	60	83	118
40166	66	56	23	95	61	29	86	38	82	103	142
40168	39	...	13	71	41	...	62	87	...	13	50	81	115
40170	41	28	8	62	33	11	62	92	...	16	46	77	116
40207	73	...	30	104	74	33	109	137	...	47	97	122	...
40210	30	21	10	58	27	...	52	79	7	17	40	61	104
40216	78	55	29	104	68	27	101	145	15	46	81	101	154
40220	48	...	16	62	45	14	64	84	...	22	46	70	100
40232	118	...	71	152	118	72	139	...	42	94	128	139	212
40235	54	36	10	79	48	...	78	110	5	22	57	87	130
40237	57	94	58	27	87	115	...	36	85	108	...
40275	40	30	10	65	41	11	64	94	5	19	50	79	124
40291	62	44	...	96	54	22	89	119	...	26	74	97	...
40318	85	135	91	51	109	...	18	64	92	139	...
40339	113	...	64	144	119	63	139	85	131	143	...
40349	61	51	27	97	65	25	88	114	10	37	73	103	155
40358	74	154	105	67	139	91	135	149	203
40361	34	18	8	55	33	12	58	84	6	17	39	74	104
40371	91	...	41	122	87	41	116	146	...	60	98	121	...
40372	51	26	...	77	43	19	78	111	6	26	48	82	129

Table 3a—Continued

Star (LEID)	Wavelength (Å)	Equivalent Widths (mÅ)											
		Fe I	Fe I	Fe I	Fe I	Fe I	Fe I	Fe I	Fe I	Fe I	Fe I	Fe I	Fe I
40373	6151.62	6157.73	6165.36	6173.34	6180.20	6187.99	6200.32	6219.28	6226.74	6229.23	6232.64	6246.32	6252.56
40409	2.18	4.07	4.14	2.22	2.73	3.94	2.61	2.20	3.88	2.84	3.65	3.60	2.40
40420	-3.33	-1.22	-1.51	-2.89	-2.66	-1.69	-2.41	-2.42	-2.19	-3.00	-1.23	-0.85	-1.71
40424	7.52	7.52	7.52	7.52	7.52	7.52	7.52	7.52	7.52	7.52	7.52	7.52	7.52
40472	92	55	27	122	82	38	118	159	11	54	80	113	183
40479	50	44	...	84	44	24	73	94	...	21	59	80	122
41015	33	65	...	14	57	91	10	24	49	78	122
41025	...	20	...	46	38	15	60	95	42	64	111
41033	74	156	120	71	139	...	49	97	125	144	...
41034	60	38	16	86	49	22	89	113	10	32	59	93	142
41035	54	31	52	18	80	123	8	25	52	93	148
41039	55	40	18	81	55	18	78	119	8	32	63	97	144
41060	89	...	42	130	93	44	113	149	19	63	92	120	...
41061	73	57	29	95	64	28	100	128	14	45	71	99	143
41063	35	31	15	66	31	...	59	98	7	...	52	75	117
41164	46	...	18	77	51	18	74	100	...	25	66	97	128
41186	45	29	13	74	45	15	73	99	11	24	50	84	123
41201	17	...	10	30	18	...	21	64	48	80	55
41230	36	32	16	61	42	...	63	88	46	84	109
41232	16	60	80	...
41241	62	36	18	100	60	22	93	117	15	36	66	98	156
41243	39	23	...	66	35	14	64	93	8	...	45	73	118
41246	29	24	...	65	38	12	56	93	...	20	44	79	110
41258	15	12	...	40	19	...	35	65	...	11	31	51	96
41259	60	31	...	88	52	15	82	111	...	31	59	89	142
41262	24	...	21	59	...	16	...	79	...	14	...	80	...
41310	46	39	16	...	30	...	67	88	9	22	38	71	113
41312	19	14	17	9	50	49	29	47	71
41313	56	38	...	84	47	16	79	118	...	25	62	88	136
41321	45	23	...	80	41	16	74	112	...	22	55	88	142

Table 3a—Continued

Star (LEID)	Wavelength (Å)	Equivalent Widths (mÅ)											
		Fe I	Fe I	Fe I	Fe I	Fe I	Fe I	Fe I	Fe I	Fe I	Fe I	Fe I	Fe I
41348	6157.73	6165.36	6173.34	6180.20	6187.99	6200.32	6219.28	6226.74	6229.23	6232.64	6246.32	6252.56	6265.14
41366	2.18	4.07	4.14	2.22	2.73	3.94	2.61	2.20	3.88	2.84	3.65	3.60	2.40
41375	-3.33	-1.22	-1.51	-2.89	-2.66	-1.69	-2.41	-2.42	-2.19	-3.00	-1.23	-0.85	-1.71
41380	7.52	7.52	7.52	7.52	7.52	7.52	7.52	7.52	7.52	7.52	7.52	7.52	7.52
41387	39	24	16	62	25	12	53	83	... 16	... 16	70	121	85
41389	42	17	... 58	37	12	67	91	5	... 18	39	79	117	121
41402	84	63	34	110	77	35	103	139	18	39	79	117	90
41435	132	104	60	170	117	61	158	200	... 94	94	121	156	146
41455	113	... 46	129	101	... 51	25	68	94	12	27	62	92	127
41476	56	36	... 45	21	69	44	20	69	96	... 27	57	84	122
41494	69	... 73	21	70	44	111	69	37	112	... 32	64	96	133
42012	60	50	18	88	56	19	87	112	... 119	47	81	108	164
42015	55	31	17	85	51	17	82	116	9	30	60	95	119
42023	56	36	... 45	90	54	16	82	120	... 119	26	... 44	106	138
42039	69	... 73	42	25	106	71	24	100	... 100	44	68	106	112
42049	15	... 51	7	36	... 83	9	36	67	... 102	... 124	25	54	58
42054	47	51	... 22	99	59	30	91	71	... 124	39	77	112	143
42056	45	46	24	78	51	23	71	95	... 81	... 129	20	71	102
42079	64	... 20	... 55	... 15	99	... 13	55	19	93	12	36	66	109
42084	58	... 67	26	97	62	26	90	120	... 136	35	79	98	126
42106	62	57	26	97	62	26	90	120	... 136	27	67	95	127
42114	62	57	26	97	62	26	90	120	... 136	... 117	47	85	104
42120	45	46	24	78	51	23	71	95	... 81	... 129	41	64	102
42134	... 67	37	15	99	62	19	93	129	12	36	66	96	130
42161	103	... 74	74	151	114	63	136	... 136	... 117	86	127	147	185
42162	74	... 46	38	99	72	35	95	117	... 117	47	85	104	138
42169	34	46	21	69	42	10	65	85	... 112	21	56	97	111
42174	58	43	24	88	55	24	86	112	14	31	65	96	137
42175	62	35	19	93	54	17	80	128	... 128	34	61	91	148

Table 3a—Continued

Star (LEID)	Wavelength (Å)	Equivalent Widths (mÅ)											
		Fe I	Fe I	Fe I	Fe I	Fe I	Fe I	Fe I	Fe I	Fe I	Fe I	Fe I	Fe I
42182	6151.62	6157.73	6165.36	6173.34	6180.20	6187.99	6200.32	6219.28	6226.74	6229.23	6232.64	6246.32	6252.56
42187	59	49	...	89	56	24	81	113	31	71	101
42196	...	22	...	63	23	7	57	71	...	9	36	68	97
42198	38	...	11	69	34	16	54	96	...	17	53	77	125
42205	119	...	60	151	114	57	143	193	...	87	124	152	217
42221	37	23	11	58	30	15	58	85	...	21	44	76	106
42260	41	...	84	41	16	73	14	75	98	118	...
42271	25	14	...	50	21	12	...	74	38	62	...
42302	90	45	28	115	75	30	112	145	15	50	79	107	171
42303	63	...	89	51	25	77	108	15	34	...	87	130	...
42309	74	76	58	116	84	47	98	131	...	51	98	121	149
42339	70	...	46	105	74	45	99	...	21	53	...	111	...
42345	16	32	17	7	37	64	26	55	92
42361	32	20	8	54	33	12	59	81	40	69	112
42384	96	...	40	123	94	44	109	...	25	58	100	117	159
42385	38	27	11	61	31	...	52	80	...	14	40	66	107
42407	45	...	23	58	41	16	...	77	59	85	97
42415	71	...	28	97	68	31	94	124	...	44	80	111	153
42438	77	...	38	102	68	36	96	124	...	47	94	113	...
42457	13	70	...	18	71	86	...	17	66	95	115
42461	76	42	23	111	67	26	106	135	12	43	69	103	158
42473	79	...	34	114	83	42	103	139	...	54	99	119	131
42497	45	27	...	70	40	13	63	101	...	19	52	82	121
42501	54	42	23	92	44	18	74	106	12	25	69	90	129
42503	46	32	15	65	52	24	62	90	...	24	41	88	118
42508	58	45	17	88	50	21	80	113	...	24	63	88	136
43010	35	...	12	56	33	10	53	88	6	14	38	69	112
43024	31	32	15	64	35	17	62	88	...	20	46	75	113
43036	71	...	22	82	56	...	89	116	20	47	71	98	126
43040	36	38	14	77	36	15	59	88	...	12	74	105	92

Table 3a—Continued

Star (LEID)	Wavelength (Å)	Equivalent Widths (mÅ)											
		Ion	Fe I										
43060	6151.62	6157.73	6165.36	6173.34	6180.20	6187.99	6200.32	6219.28	6226.74	6229.23	6232.64	6246.32	6252.56
43061	2.18	4.07	4.14	2.22	2.73	3.94	2.61	2.20	3.88	2.84	3.65	3.60	2.40
43064	-3.33	-1.22	-1.51	-2.89	-2.66	-1.69	-2.41	-2.42	-2.19	-3.00	-1.23	-0.85	-1.71
43068	7.52	7.52	7.52	7.52	7.52	7.52	7.52	7.52	7.52	7.52	7.52	7.52	7.52
43071
43079
43087
43091
43095	63	31	20	84	57	20	83	120	12	22	65	90	144
43096	95	51	28	133	86	35	117	55	88	129	193
43099	115	...	52	131	102	56	132	121	130	...
43101	43	25	10	72	40	...	71	104	9	22	51	79	134
43104	52	83	56	22	86	104	...	31	69	97	139
43108	37	...	24	50	36	11	...	91	10	...	46	84	102
43111	36	31	...	66	40	18	65	97	...	18	45	84	121
43134	20	...	8	40	...	9	...	73	...	9	31	...	97
43139	18	18	9	44	...	15	...	73	8	...	32	57	...
43158	41	25	...	68	32	13	60	98	8	20	46	71	125
43189	100	...	50	141	100	48	...	178	...	73	111	148	193
43216	95	...	50	135	96	46	126	...	36	69	104	134	189
43233	29	31	17	55	27	9	56	91	7	21	37	81	104
43241	95	52	...	143	80	28	120	161	...	46	84	124	206
43258	39	27	...	79	41	15	70	58	84	142
43261	69	44	23	106	67	23	99	146	...	42	76	104	161
43278	19	44	17	70	...	7	...	57	90
43326	106	...	55	151	113	57	131	162	...	79	118	156	192
43330	65	49	...	102	62	22	95	127	...	37	66	104	159
43351	127	123	...	178	128	60	164	189	...	79	144	166	215
43367	77	41	21	110	70	24	104	133	11	41	75	103	168
43389	86	...	38	115	86	44	111	148	28	58	99	119	...

Table 3a—Continued

	Wavelength (Å)	6151.62	6157.73	6165.36	6173.34	6180.20	6187.99	6200.32	6219.28	6226.74	6229.23	6232.64	6246.32	6252.56	6265.14
Ion	Fe I	Fe I	Fe I	Fe I	Fe I	Fe I	Fe I	Fe I	Fe I	Fe I	Fe I	Fe I	Fe I	Fe I	Fe I
E.P. (eV)	2.18	4.07	4.14	2.22	2.73	3.94	2.61	2.20	3.88	2.84	3.65	3.60	2.40	2.18	2.18
Log gf	-3.33	-1.22	-1.51	-2.89	-2.66	-1.69	-2.41	-2.42	-2.19	-3.00	-1.23	-0.85	-1.71	-2.56	-2.56
Log ϵ_{\odot}	7.52	7.52	7.52	7.52	7.52	7.52	7.52	7.52	7.52	7.52	7.52	7.52	7.52	7.52	7.52
Star (LEID)															
43397	32	18	63	...	13	29	52	90	58
43399	32	21	...	61	30	...	60	88	14	49	70	104	89
43412	74	44	20	101	64	24	97	134	...	38	70	115	162	140	140
43433	58	43	15	84	54	23	86	110	11	29	66	90	139	115	115
43446	...	36	16	62	98	10	75	124	97	97
43458	48	...	30	87	56	24	74	97	...	28	...	103	117	106	106
43463	28	12	11	53	23	7	47	84	35	71	117	83	83
43475	58	130	...	71	133	147	...	60	110	141	174
43485	52	31	18	80	41	28	75	100	14	28	63	88	127	101	101
43539	48	48	24	86	54	22	77	114	...	25	61	85	129	98	98
44026	80	...	40	120	90	48	110	136	...	58	108	126
44042	48	27	15	77	43	...	66	108	9	22	51	82	130	106	106
44056	50	49	23	87	52	17	84	98	...	39	63	86	145	109	109
44065	38	34	10	71	36	17	62	102	...	23	48	88	126	99	99
44067	22	43	20	...	46	70	...	8	27	53	99	72	72
44115	83	48	25	111	73	29	115	144	...	45	75	116	153
44120	22	23	...	42	...	8	48	76	...	15	...	55	98
44143	48	27	11	67	46	15	68	105	7	28	57	84	134	108	108
44163	51	35	18	84	46	19	79	100	...	30	61	93	133	119	119
44188	62	72	44	28	86	116	...	27	...	85	126	108	108
44189	73	...	40	109	72	29	94	123	...	49	100	101
44198	46	28	9	73	42	19	69	109	47	88	142	109	109
44219	59	38	15	82	47	17	84	111	...	25	56	96	145	117	117
44231	51	46	21	79	52	29	82	98	14	36	68	86	117
44253	63	51	...	84	61	25	90	113	19	31	71	99	137	124	124
44271	...	11	45	34	8	...	75	65	102	76	76
44277	134	76	66	...	120	...	133	168	...	109	108	...	212
44304	45	...	13	81	53	33	75	105	...	25	64	88	121	112	112
44313	64	46	...	82	55	22	85	122	8	...	65	103	149	126	126
44327	58	27	16	82	52	21	75	115	...	31	59	89	138	113	113

Equivalent Widths (nmÅ)

Table 3a—Continued

Star (LEID)	Wavelength (Å)	Equivalent Widths (mÅ)											
		Fe I	Fe I	Fe I	Fe I	Fe I	Fe I	Fe I	Fe I	Fe I	Fe I	Fe I	Fe I
44337	6151.62	6157.73	6165.36	6173.34	6180.20	6187.99	6200.32	6219.28	6226.74	6229.23	6232.64	6246.32	6252.56
44343	2.18	4.07	4.14	2.22	2.73	3.94	2.61	2.20	3.88	2.84	3.65	3.60	2.40
44380	-3.33	-1.22	-1.51	-2.89	-2.66	-1.69	-2.41	-2.42	-2.19	-3.00	-1.23	-0.85	-1.71
44424	7.52	7.52	7.52	7.52	7.52	7.52	7.52	7.52	7.52	7.52	7.52	7.52	7.52
44426													
44435	64	56	25	97	63	29	88	117	35	72	106	139	125
44446	35	73	33	14	60	95	...	43	82	102	87
44449	122	...	60	153	118	44	153	184	...	68	...	155	212
44462	107	89	52	129	101	54	125	...	40	84	113	127	...
44488	20	19	...	43	29	10	32	66	5	14	69
44493	34	21	...	59	35	15	57	88	...	25	40	81	111
45082	40	25	...	63	32	11	59	92	...	23	44	77	114
45089	32	20	...	63	31	12	63	104	40	80	130
45092	81	...	41	110	73	45	97	129	...	54	93	109	161
45093	37	22	...	55	28	...	59	78	...	15	38	...	98
45126	39	25	21	66	38	15	64	91	6	...	50	81	126
45177	73	41	20	100	60	21	87	123	...	39	65	108	167
45180	57	40	17	79	47	21	76	109	...	26	60	86	122
45206	33	...	10	47	58	88	...	24	39	67	107
45215	93	...	59	110	91	55	114	140	42	82	102	...	155
45232	98	40	26	124	79	31	120	174	...	62	77	114	192
45235	28	29	...	53	...	15	39	84	40	66	107
45238	58	46	23	88	56	21	85	118	...	37	66	100	145
45240	82	53	25	70	...	16	35	62	87	134	119
45246	84	...	40	118	80	41	108	138	...	51	96	121	...
45249	77	64	33	117	77	37	107	133	21	46	90	113	164
45272	79	66	36	115	77	31	102	132	...	48	94	111	154
45285	83	86	...	126	91	128	...	64	104	121	...
45292	58	56	21	99	64	31	82	107	15	37	73	88	...
45309	23	...	12	45	22	7	44	74	...	13	33	66	106

Table 3a—Continued

	Wavelength (Å)	6151.62	6157.73	6165.36	6173.34	6180.20	6187.99	6200.32	6219.28	6226.74	6229.23	6232.64	6246.32	6252.56	6265.14
Ion	Fe I	Fe I	Fe I	Fe I	Fe I	Fe I	Fe I	Fe I	Fe I	Fe I	Fe I	Fe I	Fe I	Fe I	Fe I
E.P. (eV)	2.18	4.07	4.14	2.22	2.73	3.94	2.61	2.20	3.88	2.84	3.65	3.60	2.40	2.18	
Log gf	-3.33	-1.22	-1.51	-2.89	-2.66	-1.69	-2.41	-2.42	-2.19	-3.00	-1.23	-0.85	-1.71	-2.56	
Log ϵ_{\odot}	7.52	7.52	7.52	7.52	7.52	7.52	7.52	7.52	7.52	7.52	7.52	7.52	7.52	7.52	7.52
Star (LEID)															
45322	93	...	48	130	76	38	115	157	...	62	101	126	177	167	
45326	58	48	22	83	53	...	80	29	63	90	126	109	
45342	90	86	56	137	109	60	110	...	20	70	120	134	
45343	59	34	19	84	50	22	77	110	...	25	60	95	145	96	
45359	53	36	23	84	50	20	80	116	7	31	62	94	133	112	
45373	76	...	28	101	76	37	97	128	...	47	89	107	162	...	
45377	47	37	22	78	54	27	76	105	...	30	58	88	125	104	
45389	...	41	21	88	53	17	84	106	10	34	63	95	142	113	
45410	33	18	...	61	...	10	58	72	...	18	50	70	104	93	
45418	58	55	...	81	49	28	76	110	18	27	60	94	118	112	
45453	67	...	17	98	62	30	91	130	...	37	85	101	152	144	
45454	97	55	30	135	84	...	122	166	...	50	78	131	178	...	
45463	66	62	25	98	67	...	96	126	19	46	84	102	151	...	
45482	25	84	...	20	72	96	...	30	69	97	122	...	
46024	84	55	25	113	76	30	100	46	87	121	178	...	
46055	58	54	18	84	56	19	81	107	...	27	68	95	129	120	
46062	99	67	30	131	90	34	120	164	...	54	91	123	183	...	
46073	98	...	54	141	106	57	127	160	...	79	...	148	
46090	23	...	6	34	...	6	43	61	50	99	...	
46092	114	...	49	148	112	52	145	164	32	74	110	136	
46121	129	147	127	81	61	108	137	
46140	46	35	22	82	47	19	73	109	8	28	56	87	140	116	
46150	102	86	44	129	97	50	129	164	33	67	98	121	197	...	
46166	42	...	23	75	43	25	67	99	...	17	55	82	119	101	
46172	76	107	67	24	104	120	20	43	89	111	...	124	
46194	65	43	22	94	62	24	87	121	10	35	71	98	...	128	
46196	...	8	9	...	16	...	69	53	75	65	
46223	70	64	35	105	74	37	98	125	...	41	89	109	
46248	67	43	18	97	63	22	87	114	...	40	64	102	143	123	
46279	...	17	...	48	26	...	43	72	63	91	67	

Equivalent Widths (mÅ)

Table 3a—Continued

Star (LEID)	Wavelength (Å)	Equivalent Widths (mÅ)											
		Fe I	Fe I	Fe I	Fe I	Fe I	Fe I	Fe I	Fe I	Fe I	Fe I	Fe I	Fe I
46289	6157.73	6165.36	6173.34	6180.20	6187.99	6200.32	6219.28	6226.74	6229.23	6232.64	6246.32	6252.56	6265.14
46301	2.18	4.07	4.14	2.22	2.73	3.94	2.61	2.20	3.88	2.84	3.65	3.60	2.40
46318	-3.33	-1.22	-1.51	-2.89	-2.66	-1.69	-2.41	-2.42	-2.19	-3.00	-1.23	-0.85	-1.71
46323	7.52	7.52	7.52	7.52	7.52	7.52	7.52	7.52	7.52	7.52	7.52	7.52	7.52
46325
46348	33	11	61	37	11	62	96	...	17	46	83	123	94
46350	81	70	31	121	80	36	110	149	...	43	88	118	161
46381	66	56	32	99	66	34	90	127	...	31	81	102	...
46388	32	19	8	57	28	...	55	84	40	74	113
46391	51	44	...	84	52	28	79	119	...	31	63	91	140
46398	12	28	...	8	...	59	28	...	85
46405	32	15	10	45	65	41	70	84
46438	22	...	14	58	44	73	37	60	106
47012	76	51	30	109	70	26	100	139	23	42	81	105	145
47039	38	...	9	58	33	11	58	87	10	16	45	78	113
47055	26	59	...	15	51	70	107	93
47074	...	21	15	53	60	82	...	18	36	79	106
47096	65	68	33	92	62	34	...	109	11	40	85	111	141
47107	73	53	22	112	70	27	94	152	15	40	73	114	175
47110	46	37	22	80	45	15	76	108	9	27	56	89	130
47146	83	...	44	114	91	39	117	163	20	54	106	115	167
47150	84	...	40	117	86	42	115	57	98	131	...
47151	51	31	9	51	70	43	65	99
47153	138	...	65	170	131	58	144	189	...	95	134	168	232
47176	62	49	27	95	67	22	91	120	...	35	76	105	142
47186	112	102	54	146	116	58	139	...	38	86	118	150	199
47187	92	...	52	125	96	45	119	136	...	61	117	122	...
47199	84	47	24	116	70	27	92	150	15	46	76	116	157
47269	67	...	33	95	69	31	97	121	12	41	85	111	140
47299	...	19	9	55	98	...	21	45	...	120

Table 3a—Continued

Star (LEID)	Wavelength (Å)	Equivalent Widths (mÅ)											
		Fe I	Fe I	Fe I	Fe I	Fe I	Fe I	Fe I	Fe I	Fe I	Fe I	Fe I	Fe I
47307	6151.62	6157.73	6165.36	6173.34	6180.20	6187.99	6200.32	6219.28	6226.74	6229.23	6232.64	6246.32	6252.56
47331	2.18	4.07	4.14	2.22	2.73	3.94	2.61	2.20	3.88	2.84	3.65	3.60	2.40
47338	-3.33	-1.22	-1.51	-2.89	-2.66	-1.69	-2.41	-2.42	-2.19	-3.00	-1.23	-0.85	-1.71
47339	7.52	7.52	7.52	7.52	7.52	7.52	7.52	7.52	7.52	7.52	7.52	7.52	7.52
47348	73	53	32	102	69	30	90	123	...	42	82	102	150
47354	87	...	57	132	103	56	120	140	...	80	124	131	...
47387	61	41	21	86	52	21	85	115	14	31	63	100	143
47399	108	82	42	141	99	51	125	169	31	78	99	120	187
47400	75	69	27	107	75	36	102	128	17	51	93	119	144
47405	66	30	20	95	60	21	93	133	...	38	62	97	171
47420	64	51	...	84	54	26	76	109	16	37	70	92	134
47443	28	24	8	44	24	...	44	76	...	21	34	49	108
47450	37	69	35	15	56	80	11	11	45	70	110
48028	56	35	16	85	48	17	82	117	...	27	58	92	144
48036	38	31	14	65	78	58	82	111
48049	90	52	32	122	78	34	122	166	22	56	84	107	190
48060	89	49	20	126	76	31	113	165	...	48	90	117	203
48067	56	...	22	90	58	27	92	108	...	35	73	102	137
48083	73	82	33	113	70	33	96	132	...	47	95	120	158
48099	141	150	127	92	...	172	129
48116	165	127	84	76	...	147
48120	115	73	43	140	101	55	140	161	107	135	198
48150	130	...	77	164	115	70	...	194	53	...	120	147	227
48151	36	18	12	54	35	11	58	86	...	19	51	69	120
48186	32	20	...	57	21	...	62	92	...	15	51	75	115
48197	11	56	...	13	65	82	16	17	44	74	111
48221	73	75	33	111	74	41	108	119	...	50	84	114	...
48228	40	28	...	69	36	16	66	102	...	49	86	125	106
48235	96	81	36	124	87	40	118	141	...	82	96	123	163
48247	44	41	19	76	45	16	68	100	...	27	58	86	129

Table 3a—Continued

Star (LEID)	Wavelength (Å)	Equivalent Widths (mÅ)											
		Fe I	Fe I	Fe I	Fe I	Fe I	Fe I	Fe I	Fe I	Fe I	Fe I	Fe I	Fe I
48259	6151.62	6157.73	6165.36	6173.34	6180.20	6187.99	6200.32	6219.28	6226.74	6229.23	6232.64	6246.32	6252.56
48281	2.18	4.07	4.14	2.22	2.73	3.94	2.61	2.20	3.88	2.84	3.65	3.60	2.40
48303	-3.33	-1.22	-1.51	-2.89	-2.66	-1.69	-2.41	-2.42	-2.19	-3.00	-1.23	-0.85	-1.71
48323	7.52	7.52	7.52	7.52	7.52	7.52	7.52	7.52	7.52	7.52	7.52	7.52	7.52
48367	98	61	27	134	88	34	132	171	25	57	89	131	186
48370	77	71	38	115	80	34	106	142	...	43	87	119	...
48392	69	51	20	104	67	28	95	125	...	39	73	109	164
48409	31	14	...	46	23	7	45	78	6	...	31	63	106
49013	68	52	25	100	56	28	93	119	16	37	76	105	153
49022	38	20	...	68	34	...	65	93	5	19	38	68	109
49037	32	18	10	48	...	6	57	82	...	15	39	71	...
49056	143	...	90	178	146	81	173	207	56	123	152	174	...
49072	44	23	15	60	42	...	65	87	47	78	124
49088	36	22	12	59	36	18	66	88	...	24	45	78	112
49111	72	...	55	111	85	45	102	...	25	58	97	114	...
49123	69	24	16	105	62	20	97	148	...	35	60	97	169
49134	70	53	24	101	65	29	96	124	18	36	80	108	142
49148	91	77	46	118	91	48	116	147	26	64	89	115	171
49177	66	65	34	100	68	34	94	121	...	37	86	115	152
49179	28	...	10	62	37	...	60	84	6	9	44	73	109
49188	21	20	...	35	55	51	79
49193	74	56	23	115	79	31	102	132	...	39	83	110	167
49205	41	27	13	77	44	10	68	94	...	26	55	79	115
49212	118	...	69	161	120	70	140	178	...	80	140	147	...
49238	45	31	21	76	43	14	76	99	...	23	52	92	132
49249	87	70	38	114	80	38	110	135	21	48	88	113	155
49252	39	38	...	49	48	23	59	92	12	24	...	73	108
49255	26	14	8	41	...	14	53	82	...	12	33	64	99
49293	76	72	...	113	80	39	101	127	...	48	83	109	140
49322	34	25	14	58	37	11	57	93	...	14	40	69	117

Table 3a—Continued

	Wavelength (Å)	6151.62	6157.73	6165.36	6173.34	6180.20	6187.99	6200.32	6219.28	6226.74	6229.23	6232.64	6246.32	6252.56	6265.14
Ion	Fe I	Fe I	Fe I	Fe I	Fe I	Fe I	Fe I	Fe I	Fe I	Fe I	Fe I	Fe I	Fe I	Fe I	Fe I
E.P. (eV)	2.18	4.07	4.14	2.22	2.73	3.94	2.61	2.20	3.88	2.84	3.65	3.60	2.40	2.18	2.18
Log gf	-3.33	-1.22	-1.51	-2.89	-2.66	-1.69	-2.41	-2.42	-2.19	-3.00	-1.23	-0.85	-1.71	-2.56	-2.56
Log ϵ_{\odot}	7.52	7.52	7.52	7.52	7.52	7.52	7.52	7.52	7.52	7.52	7.52	7.52	7.52	7.52	7.52
Star (LEID)															
49333	34	20	7	60	29	22	55	79	6	11	39	74	115	98	98
50022	...	29	...	64	35	...	67	98	14	27	40	69	111	80	80
50037	49	47	19	79	47	24	76	104	...	29	67	96	140	116	116
50046	32	34	19	57	60	77	49	92	113	87	87
50066	60	64	34	93	81	35	90	128	...	44	89	113	153
50078	63	44	...	96	62	25	93	125	...	31	70	96	160	129	129
50108	67	59	23	100	63	28	83	111	16	40	79	102	137	130	130
50109	47	23	...	65	41	...	67	97	...	23	41	81	123	93	93
50133	76	44	...	103	64	23	99	142	...	39	73	104	155
50163	23	16	...	48	23	...	30	67	96
50167	57	45	14	87	51	21	83	116	...	34	64	99	147	118	118
50172	59	53	20	87	54	21	77	104	...	25	72	104	134
50187	105	...	52	137	107	59	134	...	43	88	113	146
50191	45	51	22	78	48	23	72	98	...	25	62	92	121
50193	111	...	59	154	115	57	138	175	...	90	134	154
50198	55	61	...	90	...	22	92	100	15	31	79	99	145	119	119
50218	84	...	35	115	86	40	105	136	21	56	98	118	161
50228	58	35	...	85	59	23	83	110	16	24	68	95	138	121	121
50245	44	33	...	80	49	19	79	104	...	31	47	90	135	111	111
50253	67	45	...	104	70	26	102	126	...	37	74	103	...	132	132
50259	119	...	49	154	113	55	142	169	40	80	113	143
50267	60	35	20	85	60	25	85	120	9	26	...	91	135	121	121
50291	60	30	12	72	56	...	80	94	8	36	59	88	136
50293	49	46	28	83	56	28	87	111	11	35	64	96	138	117	117
50294	28	25	18	58	40	...	63	81	9	15	44	84	112	89	89
50304	37	37	14	70	42	16	55	98	12	17	51	88	131	102	102
51021	102	77	49	135	101	48	147	169	29	70	100	...	214
51024	61	57	34	94	61	27	92	127	14	51	89	102	139	124	124
51074	106	...	55	149	118	56	134	161	...	82	132	142
51079	74	68	37	106	69	33	96	128	...	46	90	110	151	146	146

Equivalent Widths (mÅ)

Table 3a—Continued

Star (LEID)	Wavelength (Å)	Equivalent Widths (mÅ)											
		Fe I	Fe I	Fe I	Fe I	Fe I	Fe I	Fe I	Fe I	Fe I	Fe I	Fe I	Fe I
51080	94	...	46	124	95	50	119	154	30	63	101	127	175
51091	46	22	8	74	36	15	64	111	48	81	135
51121	32	29	...	64	36	...	63	105	...	19	46	74	120
51132	117	...	70	150	121	65	151	179	50	89	...	151	181
51136	10	...	78	...	12	39	65	...
51156	62	51	22	98	60	26	95	123	...	34	72	100	153
51254	81	...	34	98	75	34	101	129	...	54	95	127	153
51257	26	19	8	48	26	9	51	79	...	11	30	66	102
51259	44	32	13	73	37	12	63	96	...	23	51	87	122
52017	91	52	28	122	78	34	119	158	16	54	85	117	174
52035	101	70	30	149	93	36	135	177	...	56	96	141	207
52039	...	12	18	57	7	...	27	58	...
52103	103	...	55	129	101	61	137	157	33	72	109	128	181
52105	39	39	...	69	...	67	103	...	16	57	86	117	176
52106	...	34	18	75	56	27	32	61	92	122	174
52109	51	29	11	81	45	...	78	111	13	22	55	90	144
52110	38	...	13	50	26	...	51	76	35	69	90
52111	140	159	133	87	132	159	...
52133	...	36	12	46	91	...	18	46	78	...	94
52139	105	85	63	131	111	59	139	158	44	89	105	123	177
52151	37	21	...	66	34	16	64	96	45	81	110
52154	14	...	6	29	13	...	42	67	6	53	92
52167	71	35	18	86	58	20	92	134	11	35	68	94	143
52180	51	78	46	20	74	107	...	31	60	98	129
52192	59	46	...	82	61	23	93	120	...	32	75	97	151
52204	9	32	52	55	...	60
52222	41	61	32	14	52	101	8	22	42	73	118
53012	28	16	...	57	32	15	53	90	...	14	44	75	114
53054	31	24	7	61	32	10	62	97	...	19	39	80	116
53058	40	27	9	65	40	14	66	95	7	...	47	75	121

Table 3a—Continued

Star (LEID)	Wavelength (Å)	Equivalent Widths (mÅ)											
		Fe I	Fe I	Fe I	Fe I	Fe I	Fe I	Fe I	Fe I	Fe I	Fe I	Fe I	Fe I
53067	6151.62	6157.73	6165.36	6173.34	6180.20	6187.99	6200.32	6219.28	6226.74	6229.23	6232.64	6246.32	6252.56
53076	62	...	23	92	68	37	96	117	...	38	82	103	140
53114	96	82	43	129	95	45	121	145	...	68	104	115	190
53119	23	18	...	52	31	16	44	81	...	41	...	105	164
53132	43	38	...	76	42	16	68	102	6	27	54	87	128
53178	41	22	11	67	39	12	64	99	9	16	46	83	112
53185	80	45	22	110	68	28	102	138	18	47	74	110	166
53203	29	26	13	57	32	12	56	88	...	14	38	77	110
54018	53	50	19	78	54	23	73	100	...	28	63	95	120
54022	127	...	88	164	141	81	157	183	...	115	133	157	...
54031	107	...	67	136	112	61	125	161	45	89	119	130	...
54064	...	20	26	12	46	...	6	...	41	66	104
54073	24	51	50	90	8	20	38	76	...
54084	30	31	14	60	...	12	51	91	7	16	...	70	...
54095	33	23	16	64	24	10	63	91	74	111	...
54105	78	147	113	60	140	178	...	88	138	155	...
54132	52	34	23	77	41	17	77	101	16	30	63	89	131
54148	90	64	29	123	86	31	110	151	22	58	89	110	182
54154	25	23	9	47	24	9	49	73	36	71	105
55028	98	...	49	128	103	54	125	...	40	77	110	124	172
55029	83	...	35	113	80	39	107	137	17	56	108	118	158
55056	35	35	...	62	39	...	51	89	10	...	61	77	106
55063	80	72	32	114	77	35	105	138	20	50	89	112	160
55071	150	...	99	182	142	75	156	195	...	120	140	160	...
55089	46	28	13	74	44	13	78	112	...	21	53	95	145
55101	105	...	66	143	111	58	137	85	120	142	...
55102	58	52	15	86	54	24	85	118	...	30	73	105	144
55111	95	70	38	121	87	42	124	147	24	57	96	119	172
55114	114	...	47	146	111	59	135	169	38	87	109	129	...
55121	137	...	80	178	142	72	163	205	...	111	167	167	...

Table 3a—Continued

	Wavelength (Å)	6151.62	6157.73	6165.36	6173.34	6180.20	6187.99	6200.32	6219.28	6226.74	6229.23	6232.64	6246.32	6252.56	6265.14
Ion	Fe I	Fe I	Fe I	Fe I	Fe I	Fe I	Fe I	Fe I	Fe I	Fe I	Fe I	Fe I	Fe I	Fe I	Fe I
E.P. (eV)	2.18	4.07	4.14	2.22	2.73	3.94	2.61	2.20	3.88	2.84	3.65	3.60	2.40	2.18	2.18
Log gf	-3.33	-1.22	-1.51	-2.89	-2.66	-1.69	-2.41	-2.42	-2.19	-3.00	-1.23	-0.85	-1.71	-2.56	-2.56
Log ϵ_{\odot}	7.52	7.52	7.52	7.52	7.52	7.52	7.52	7.52	7.52	7.52	7.52	7.52	7.52	7.52	7.52
Star (LEID)															
55122	90	...	45	119	82	48	108	135	...	63	101	117	...	156	...
55131	50	...	12	57	52	84	11	...	47	80	104	89	...
55142	116	...	79	157	121	66	141	176	...	85	137	148
55149	110	...	62	139	114	61	135	83	124	138
55152	...	49	15	91	65	21	80	128	80	95	...	115	...
55165	44	29	14	74	42	...	67	95	...	29	49	78	128	104	104
56024	76	...	98	74	33	96	119	17	...	35	91	106	150
56028	36	24	...	63	35	...	59	92	...	16	46	73	119	95	95
56040	42	26	...	76	44	...	68	101	7	...	54	90	128	105	105
56056	27	...	14	51	22	8	52	81	...	17	34	69	88	61	...
56070	67	...	30	91	64	29	81	111	14	36	80	101	...	118	...
56087	92	48	28	119	82	27	109	153	...	47	81	113	182	155	155
56106	43	27	11	67	38	17	67	96	...	20	55	80	125	94	94
56114	52	47	20	87	56	21	81	107	18	33	58	90	133	108	...
56118	35	27	...	70	38	19	63	96	8	17	44	81	116	94	94
56128	42	28	...	62	40	...	60	89	...	25	...	79	117
57010	84	67	29	112	80	32	107	143	...	69	93	110	170	143	143
57029	...	17	...	36	32	68	...	14	26	58	97
57054	119	94	53	150	109	48	132	172	35	85	105	139	200
57058	26	24	12	63	37	9	58	86	51	71	...	84	...
57067	53	...	13	75	39	23	72	107	...	23	...	40	62	110	79
57073	35	32	12	68	42	15	62	93	...	19	49	78	122	92	...
57076	49	78	55	19	70	111	...	22	57	90	127	110	...
57083	30	...	9	49	26	11	49	79	40	62	110	79	...
57085	31	19	...	56	28	8	54	78	8	16	33	63	106	79	...
57091	53	59	30	79	52	30	85	116	...	32	76	103	126
57114	39	21	12	58	38	...	56	76	...	9	43	67	107	91	...
57127	40	27	14	63	55	91	...	11	48	77	112
58043	27	19	11	54	28	12	55	89	...	16	...	71	109	83	83
58059	18	...	10	51	24	...	52	73	35	66	108	80	80

Equivalent Widths (mÅ)

Table 3a—Continued

Star (LEID)	Wavelength (Å)	Equivalent Widths (mÅ)											
		Fe I	Fe I	Fe I	Fe I	Fe I	Fe I	Fe I	Fe I	Fe I	Fe I	Fe I	Fe I
58077	6151.62	6157.73	6165.36	6173.34	6180.20	6187.99	6200.32	6219.28	6226.74	6229.23	6232.64	6246.32	6252.56
58087	61	33	22	90	57	19	84	116	9	31	...	89	127
59016	...	13	9	37	...	39	73	...	12	34	55	98	70
59024	153	...	91	201	157	...	182	260	...	125	177	182	...
59036	52	41	20	82	46	16	76	111	54	96	127
59047	83	...	39	119	93	35	100	126	13	51	78	119	156
59085	66	37	18	86	60	...	92	128	74	92	162
59089	62	55	30	97	61	27	92	125	19	43	74	95	138
59090	54	39	13	87	54	20	83	116	13	34	65	95	139
59094	26	...	6	50	29	11	...	78	34	61	105
60034	24	40	28	...	55	74	...	7	41	...	109
60058	130	167	137	95	156	131	163	154	...
60059	36	...	9	48	44	75	68	110
60064	30	23	11	47	21	10	45	82	...	21	43	65	109
60065	53	...	13	79	43	19	71	100	12	26	55	95	136
60066	68	...	31	107	69	39	94	121	...	52	100	114	141
60067	14	...	12	55	15	...	40	72	...	14	31	61	105
60069	44	53	28	74	42	23	66	98	57	101	132
60073	128	...	86	169	135	79	146	117	156
60088	42	69	32	17	66	95	...	31	56	81	117
60101	40	23	8	67	40	13	62	95	...	21	53	77	119
61015	114	71	36	140	98	37	127	189	22	69	97	123	191
61026	34	...	11	65	38	...	46	86	...	17	36	66	117
61042	71	52	26	102	67	27	89	124	...	39	68	100	149
61046	32	16	...	61	31	17	55	88	39	69	115
61050	108	...	51	146	109	51	128	158	...	73	113	137	170
61067	125	...	66	153	123	79	144	182	56	110	...	154	...
61070	65	40	21	98	56	27	96	...	11	29	73	102	148
61075	30	...	6	47	21	...	51	74	63	105	...
61085	127	...	63	169	130	63	148	194	...	93	146	158	...

Table 3a—Continued

Star (LEID)	Wavelength (Å)	Equivalent Widths (mÅ)											
		Ion	Fe I										
6151.62	6157.73	6165.36	6173.34	6180.20	6187.99	6200.32	6219.28	6226.74	6229.23	6232.64	6246.32	6252.56	6265.14
2.18	4.07	4.14	2.22	2.73	3.94	2.61	2.20	3.88	2.84	3.65	3.60	2.40	2.18
-3.33	-1.22	-1.51	-2.89	-2.66	-1.69	-2.41	-2.42	-2.19	-3.00	-1.23	-0.85	-1.71	-2.56
Log ϵ_{\odot}	7.52	7.52	7.52	7.52	7.52	7.52	7.52	7.52	7.52	7.52	7.52	7.52	7.52
<hr/>													
62018	17	17	64	...	28	54	93	...
62058	75	108	70	36	90	122	...	38	77	109	144
63021	60	52	26	90	59	...	82	113	...	38	72	98	133
63027	38	22	15	62	...	11	51	90	...	20	52	75	113
63052	53	50	18	88	55	23	80	118	...	25	71	95	136
64023	14	...	13	...	15	...	56	55	92
64049	63	42	26	85	52	24	84	121	...	33	71	89	139
64057	...	18	...	44	50	66	...	13	36	66	90
64064	27	38	18	14	...	76	32	60	101
64067	18	81	51	29	85	110	...	36	59	91	132
64074	32	30	18	62	39	12	54	85	49	77	112
65042	18	16	...	34	38	31	56	...
65046	29	16	7	55	29	...	50	80	6	67	108
65057	...	45	11	58	73	82	...	15	47	73	105
66015	21	...	49	24	10	53	82	15	48	68	102
66026	39	31	...	68	34	14	65	96	9	21	49	80	125
66047	87	81	45	124	89	42	106	143	27	58	97	117	165
66054	54	39	...	88	50	22	81	115	...	31	65	98	139
67049	32	22	...	48	60	87	78	105	80
67063	70	52	33	111	80	40	110	137	...	49	87	130	160
68044	...	28	10	56	28	18	54	11	52	70	107
69007	21	...	47	29	12	50	72	...	15	39	67
69012	67	36	19	97	58	24	90	130	15	35	63	96	150
69027	116	...	77	155	120	74	138	...	44	109	141	150	...
70032	41	32	15	71	38	15	66	95	12	27	54	80	114
70035	71	45	...	97	69	27	98	137	...	44	76	103	157
70041	42	34	19	62	44	11	57	88	...	13	51	81	114
70049	67	...	79	...	39	79	108	25	...	78	99	144	...
71013	17	...	10	25	13	...	26	57	5	9	24	50	56
73025	122	...	53	159	118	56	155	186	...	87	140	146	218

Table 3a—Continued

Star (LEID)	Equivalent Widths (mÅ)													
	Wavelength (Å)	6151.62	6157.73	6165.36	6173.34	6180.20	6187.99	6200.32	6219.28	6226.74	6232.64	6246.32	6252.56	6265.14
Ion	Fe I	Fe I	Fe I	Fe I	Fe I	Fe I	Fe I	Fe I	Fe I	Fe I	Fe I	Fe I	Fe I	Fe I
E.P. (eV)	2.18	4.07	4.14	2.22	2.73	3.94	2.61	2.20	3.88	2.84	3.65	3.60	2.40	2.18
Log gf	-3.33	-1.22	-1.51	-2.89	-2.66	-1.69	-2.41	-2.42	-2.19	-3.00	-1.23	-0.85	-1.71	-2.56
Log ϵ_{\odot}	7.52	7.52	7.52	7.52	7.52	7.52	7.52	7.52	7.52	7.52	7.52	7.52	7.52	7.52
75021	44	31	14	74	39	13	68	98	8	25	50	83	120	101
76027	61	47	19	91	62	25	90	116	11	33	71	97	139	122
76038	100	...	48	129	104	59	127	162	32	81	109	169
77025	75	52	27	104	70	30	99	130	16	43	76	106	157	...
77030	36	25	12	60	37	19	64	91	9	22	48	77	122	94
80026	29	61	57	102	...	16	39	68	120	91
80029	66	44	...	92	62	20	86	119	...	37	76	98	143	124
81018	51	31	13	74	42	11	71	105	...	22	54	89	127	106
81019	49	43	18	71	46	15	73	106	...	22	66	89	115	107
81028	28	26	...	49	20	...	48	75	5	10	37	73	101	77
82015	28	...	7	42	21	12	48	81	...	10	39	69	100	72
82029	...	14	9	28	52	39	77	55	...
85027	72	56	29	102	65	26	102	120	...	41	77	97	153	...
85031	58	36	...	73	45	17	75	104	...	28	62	84	135	113
89009	42	18	...	57	51	16	72	98	9	...	54	79	133	99

Table 3b. Fe Atomic Parameters, Equivalent Widths, and Solar Abundances

Wavelength (Å)	Ion	E.P. (eV)	Log g _f	Log ε _⊙	Star (LEID)	Equivalent Widths (mÅ)													
						6270.23	6271.28	6290.97	6297.79	6301.50	6302.49	6311.50	6315.81	6322.69	6335.33	6336.83	6344.15	6149.24	6247.56
9	Fe I	2.86	3.33	4.73	6017	Fe I	Fe I	Fe I	Fe I	Fe I	Fe I	Fe I	Fe I	Fe I	Fe I	Fe I	Fe II	Fe II	
5009	Fe I	-2.62	-2.74	-0.72	8014	Fe I	2.22	3.65	3.69	2.83	4.07	2.59	2.20	3.69	2.43	3.89	3.89	3.89	3.89
34	Fe I	7.52	7.52	7.52	9013	Fe I	-2.74	-0.68	-1.11	-3.17	-1.69	-2.41	-2.22	-0.78	-2.92	-2.78	-2.78	-2.78	-2.78
101	44	10009	Fe I	23	...	111	106	...	34	24	87	134	102	91	24	41
...	10012	Fe I	40	...	132	115	71	42	137	185	129	35	40
...	11019	Fe I	...	108	102	71	39	23	90	131	94	85	17	34	29
...	11021	Fe I	...	127	126	75	38	31	98	147	102	101	18	37	18
...	11024	Fe I	19	...	109	97	67	34	23	93	141	88	77	17	35
...	12013	Fe I	49	149	133	100	68	40	115	164	115	115	26	46	40
...	12014	Fe I	19	...	68	92	60	15	...	45	103	54	37	20	32
...	14010	Fe I	...	55	54	41	83	43	27	15	31	24
...	15022	Fe I	35	...	85	55	...	18	82	...	71	55	22	37	29
...	15023	Fe I	12	...	94	92	46	20	11	70	120	69	50	16	39
...	15026	Fe I	...	142	135	92	64	32	117	162	124	...	33	41	40
...	16009	Fe I	41	12	93	90	51	20	10	85	118	78	61	...	34
...	16015	Fe I	26	...	79	77	39	...	10	60	102	59	42	18	30
...	16019	Fe I	26	9	64	70	43	61	95	58	38	16	32
...	16027	Fe I	...	55	41	78	51	20	17	23	23
...	17014	Fe I	67	...	119	114	69	...	34	90	148	95	97	18	36
...	17015	Fe I	31	9	...	84	81	51	...	16	67	112	70	50	15
...	17027	Fe I	40	45	9	26	...	39	...	37
...	17029	Fe I	14	...	6	38	47	8	35	74	57	29	37
...	17032	Fe I	58	106	99	68	34	14	81	121	96	79	17
...	17046	Fe I	40	9	26	...	39	...	37
...	18017	Fe I	27	66	71	39	9	...	50	98	57	29	18
...	18020	Fe I	59	...	16	106	33	19	94	142	94	87	22
...	18035	Fe I	33	14	...	80	88	46	13	13	58	97	69	41	...
...	18040	Fe I	82	...	134	120	91	...	31	105	139	107	105	24	39

Table 3b—Continued

	Wavelength (Å)	6270.23	6271.28	6290.97	6297.79	6301.50	6302.49	6311.50	6315.81	6322.69	6335.33	6336.83	6344.15	6149.24	6247.56
Ion	Fe I	Fe I	Fe I	Fe I	Fe I	Fe I	Fe I	Fe I	Fe I	Fe I	Fe I	Fe I	Fe I	Fe II	Fe II
E.P. (eV)	2.86	3.33	4.73	2.22	3.65	3.69	2.83	4.07	2.59	2.20	3.69	2.43	3.89	3.89	
Log gf	-2.62	-2.74	-0.72	-2.74	-0.68	-1.11	-3.17	-1.69	-2.41	-2.22	-0.78	-2.92	-2.78	-2.43	
Log ϵ_{\odot}	7.52	7.52	7.52	7.52	7.52	7.52	7.52	7.52	7.52	7.52	7.52	7.52	7.52	7.52	7.52
Star (LEID)															
18047	33	78	76	51	11	15	73	99	62	40	15	31	
19022	13	48	59	...	5	9	32	77	49	18	15	33	
19062	37	8	...	87	90	47	...	8	73	112	78	58	13	32	
20018	49	88	87	66	109	87	49	11	35	
20037	51	...	23	101	95	64	...	21	83	128	87	79	13	35	
20042	14	57	56	6	38	82	50	27	15	...	
20049	30	72	83	40	13	9	58	98	66	43	13	29	
21032	64	132	114	82	47	32	112	148	103	100	24	36	
21035	37	85	83	50	...	10	65	110	67	42	15	29	
21042	41	94	94	53	20	13	75	113	75	59	14	36	
21063	20	63	64	28	50	87	56	37	...	24	
22023	63	107	103	69	...	28	84	117	100	...	27	41	
22037	30	5	...	92	85	50	21	15	67	115	73	46	23	33	
22042	34	80	76	62	114	66	48	15	39	
22049	22	60	76	36	...	13	54	89	59	40	9	24	
22063	28	...	9	57	64	40	...	9	51	92	58	35	17	26	
23022	22	55	57	30	10	...	39	81	12	19	
23033	40	77	80	52	64	101	72	45	13	30	
23042	26	62	65	48	97	54	41	17	26	
23050	25	58	68	32	8	...	46	92	56	35	15	29	
23061	38	90	93	...	20	14	68	115	73	54	18	36	
23068	74	23	28	139	126	85	43	27	114	161	106	98	18	35	
24013	85	153	125	...	65	32	136	188	117	...	16	26	
24027	43	13	...	82	68	107	81	60	20	36	
24040	26	...	33	72	47	24	24	29	
24046	53	98	27	17	91	136	88	73	21	38	
24056	35	81	82	50	13	...	66	106	68	44	14	40	
24062	68	120	113	83	48	31	100	143	101	100	18	39	
25006	15	40	44	...	16	33	
25026	23	69	68	43	...	7	49	97	58	33	16	27	

Equivalent Widths (nmÅ)

Table 3b—Continued

Star (LEID)	Wavelength (Å)	Equivalent Widths (mÅ)											
		Fe I	Fe I	Fe I	Fe I	Fe I	Fe I	Fe I	Fe I	Fe I	Fe I	Fe II	Fe II
25043	6270.23	6271.28	6290.97	6297.79	6301.50	6302.49	6311.50	6315.81	6322.69	6335.33	6336.83	6344.15	6149.24
25062	85	28	...	132	120	89	62	38	122	175	122	126	36
25065	111	66	...	136	...	53	35	130	190	...	114	22	35
25068	63	16	24	123	116	132	51	157	202	157	30
26010	23	42	...	33	...	105	159	94	79	...	36
26014	23	5	...	69	73	31	...	7	34	81	41	...	30
26022	29	69	53	99	57	40	...
26025	80	25	...	158	139	...	44	27	125	191	...	112	24
26030	17	41	52	42	83	60	26	12
26069	22	57	58	...	10	...	43	77	49	22	14
26072	35	69	75	49	73	116	...	56	22
26086	102	138	121	71	129	171	150	...
26088	62	23	...	107	104	78	33	...	99	144	94	87	26
27048	67	113	102	78	41	26	88	125	97	78	24
27050	49	57	32	36	81	46
27073	39	89	85	17	63	110	73	60	18
27094	55	64	36	54	...	63	35	...
27095	84	137	121	98	...	28	112	...	117	...	24
28016	38	15	...	73	83	47	...	15	62	106	67	53	12
28020	21	67	72	38	...	12	45	94	58	...	31
28044	49	93	87	...	22	16	80	119	82	67	17
28069	49	12	...	99	91	62	29	17	80	130	81	60	20
28084	38	75	79	62	11	...	67	112	...	57	16
28092	45	100	97	62	19	19	80	124	82	67	17
29029	47	92	88	...	21	22	74	113	85	65	20
29031	56	63	7	44	93	54	...	19
29037	21	60	71	48	...	56	...	14
29059	49	96	94	71	117	87	68	...
29067	100	55	...	155	35	134	198	132	140	...
29069	69	128	112	82	43	28	101	145	108	97	20

Table 3b—Continued

	Star (LEID)	Equivalent Widths (mÅ)	Wavelength (Å)	Ion	Fe I	Fe II	Fe II	Fe II	6247.56										
			6270.23	6271.28	6290.97	6297.79	6301.50	6302.49	6311.50	6315.81	6322.69	6335.33	6336.83	6344.15	6419.24				
E.P. (eV)	2.86	3.33	4.73	2.22	3.65	3.69	2.83	4.07	2.59	2.20	3.69	2.43	3.89	3.89					
Log gf	-2.62	-2.74	-0.72	-2.74	-0.68	-1.11	-3.17	-1.69	-2.41	-2.22	-0.78	-2.92	-2.78	-2.43					
Log ϵ_{\odot}	7.52	7.52	7.52	7.52	7.52	7.52	7.52	7.52	7.52	7.52	7.52	7.52	7.52	7.52	7.52	7.52	7.52	7.52	7.52
29072	30	...	66	61	101	38	19	29		
29085	34	9	...	77	84	44	56	95	67	44	21	34				
29089	59	70	46	91	53		
29099	75	126	86	33	109	151	110	112	17	31				
29106	45	15	...	83	81	58	16	72	126	76	55	8	35				
30013	81	120	93	96	132	115	22	47				
30019	56	...	26	93	32	16	87	119	90	71	20	35					
30022	20	50	71	...	11	...	42	88	57	...	18	36					
30031	86	22	34	135	123	95	60	30	126	178	116	124	22	35					
30069	35	...	18	22	57	32	15	7	25					
30094	55	19	21	87	96	66	89	128	90	82	...	35					
30124	45	86	85	...	24	16	76	107	76	52	18	37					
31016	22	58	...	36	47	93	50	26					
31041	40	85	65	106	74	53	21	34					
31047	18	...	48	40	81	57	31					
31048	17	...	49	61	48	85	54	31	...	43					
31075	29	58	66	86	62		
31079	30	11	15	87	86	12	71	115	...	46	16	36				
31094	33	...	78	81	47	...	11	60	108	67	45	20	39						
31095	31	...	70	13	12	51	96	...	41	10	33						
31104	19	...	51	51	34	69	40	17	14	34					
31109	51	82	104	61	69	106	77	...	22		
31110	86	29	26	124	...	96	57	34	121	164	118	119	21	33					
31119	75	...	34	120	...	81	47	25	108	153	104	106	...	30					
31133	37	25	71	44	25					
31139	34	70	75	12	65	105	65	43	20	35					
31141	45	96	95	58	...	22	75	115	81	65	22	37					
31147	83	86	65	62	94	64		
31152	57	72		
32014	16	10	...	61	...	43	10	67	102	65	42	21					

Table 3b—Continued

Star (LEID)	Wavelength (Å)	Equivalent Widths (mÅ)											
		Fe I	Fe I	Fe I	Fe I	Fe I	Fe I	Fe I	Fe I	Fe I	Fe I	Fe II	Fe II
32026	6270.23	6271.28	6290.97	6297.79	6301.50	6302.49	6311.50	6315.81	6322.69	6335.33	6336.83	6344.15	6149.24
Ion	Fe I	Fe I	Fe I	Fe I	Fe I	Fe I	Fe I	Fe I	Fe I	Fe I	Fe I	Fe I	Fe II
E.P. (eV)	2.86	3.33	4.73	2.22	3.65	3.69	2.83	4.07	2.59	2.20	3.69	2.43	3.89
Log gf	-2.62	-2.74	-0.72	-2.74	-0.68	-1.11	-3.17	-1.69	-2.41	-2.22	-0.78	-2.92	-2.78
Log ϵ_{\odot}	7.52	7.52	7.52	7.52	7.52	7.52	7.52	7.52	7.52	7.52	7.52	7.52	7.52
32027
32043	20	62	58	34	88	47
32063	43	11	...	89	...	61	22	14	79	116	81	63	16
32069	12	29	47	38	73	30
32100	25	...	12	66	75	11	53	...	61	42	17
32101	40	99	94	19	73	119	93	64	20
32125	52	97	93	57	24	14	73	125	77	74	15
32130	20	53	28	33
32138	77	22	...	136	...	41	20	118	176	...	95	...	32
32140	38	86	83	...	10	18	62	105	...	52	...
32144	50	96	100	56	...	31	80	120	84	61	21
32165	25	73	9	44	94	27
32169	100	158	143	129	...	51	138	181	136	...	43
32171	80	...	30	...	120	88	...	35	101	150	109	...	32
33006	81	27	25	132	119	...	50	28	127	166	...	111	18
33011	52	12	...	113	99	...	24	17	88	132	...	65	21
33018	45	85	98	57	23	...	72	128	81	...	27
33030	18	66	84	50	54	...	68	...	31
33051	41	91	...	59	24	...	83	116	80	61	26
33064	22	65	77	45	83	62	40	...
33099	107	182	130	115	...	39	144	170	137	...	38
33114	73	24	89	44	29	120	159	106	111	24
33115	93	92	64	78	117	87	...	39
33126	55	102	87	88	118	90	64	...
33129	27	70	75	41	15	...	53	106	61	44	16
33138	30	72	77	50	...	12	57	112	82
33145	49	...	30	37	83	39
33154	29	60	37
33167	68	84	51	18	...	59	92	74	...	21	40

Table 3b—Continued

Star (LEID)	Wavelength (Å)	Equivalent Widths (mÅ)											
		Fe I	Fe I	Fe I	Fe I	Fe I	Fe I	Fe I	Fe I	Fe I	Fe I	Fe II	Fe II
33177	31	78	92	51	31
34008	38	12	...	90	95	...	26	17	78	119	77	59	28
34029	93	37	...	140	70	42	130	177	124	...	26
34040	36	73	15	14	65	103	74	56	36
34056	52	62	43	79	21	32
34069	46	12	17	87	86	61	22	...	84	127	79	63	44
34075	75	85	45	23	...	99	142	104	96	38
34081	50	98	91	58	79	113	80	57	33
34129	57	64	44	87	55	29	19
34130	43	62	30	...	42	...	38
34134	63	17	...	119	100	76	38	21	101	149	94	85	36
34143	93	134	...	106	...	48	118	151	133	...	46
34163	47	46	31	48	95	46	...	23
34166	31	82	95	53	73	120	89	...	17
34169	64	110	104	65	...	23	85	126	95	...	37
34175	78	25	...	114	111	83	40	23	107	165	105	109	46
34180	115	85	...	154	124	...	64	165	232	177	...
34187	31	62	75	40	52	97	...	41	40
34193	50	12	...	104	94	62	26	24	90	129	82	67	36
34207	59	21	...	112	106	72	33	32	91	138	96	...	43
34214	17	48	57	...	9	10	...	75	41	...	17
34225	99	127	131	110	127	25	...
34229	26	78	76	52	98	64	42	39
35029	30	75	78	...	12	10	59	102	70	47	34
35035	27	62	67	35	...	11	47	87	54	28	28
35046	44	90	88	52	19	13	74	118	76	59	18
35053	32	79	74	42	...	9	64	110	69	44	34
35056	73	152	47	...	118	168	108	105	...
35061	83	131	116	79	...	26	104	142	110	105	23
35066	58	19	18	105	...	74	32	17	102	149	90	83	22

Table 3b—Continued

Star (LEID)	Wavelength (Å)	Equivalent Widths (mÅ)											
		Fe I	Fe I	Fe I	Fe I	Fe I	Fe I	Fe I	Fe I	Fe I	Fe I	Fe II	Fe II
35071	6270.23	6271.28	6290.97	6297.79	6301.50	6302.49	6311.50	6315.81	6322.69	6335.33	6336.83	6344.15	6149.24
35074	2.86	3.33	4.73	2.22	3.65	3.69	2.83	4.07	2.59	2.20	3.69	2.43	3.89
35087	-2.62	-2.74	-0.72	-2.74	-0.68	-1.11	-3.17	-1.69	-2.41	-2.22	-0.78	-2.92	-2.78
35090	7.52	7.52	7.52	7.52	7.52	7.52	7.52	7.52	7.52	7.52	7.52	7.52	7.52
35093
35124	60	93	80	66	116	77	39
35157	83	116	93	...	47	100	134	123
35165	39	10	22	78	85	45	...	14	66	107	69	47	16
35172	112	161	...	119	...	39	136	...	149	...	40
35190	36	79	76	47	16	14	68	108	67	52	16
35201	99	142	...	104	...	45	121	...	138	...	51
35204	12	61	71	33	84	49
35216	63	...	13	117	...	74	28	21	85	152	88	87	17
35228	42	67	75	17	57	96	64	42	...
35230	42	106	90	...	19	...	71	133	73	58	...
35235	57	122	118	76	36	19	90	142	87	78	16
35240	61	121	104	63	108	136	88	...	34
35248	34	...	11	73	78	...	10	...	58	107	70	51	18
35260	33	70	75	45	...	13	62	115	70	43	21
35261	48	75	81	66	24	19	70	115	79	62	13
36028	21	8	...	58	61	44	...	56	...	39
36036	64	21	...	126	115	...	31	22	103	171	94	93	...
36048	31	65	72	43	57	97	68	47	14
36059	63	54	...	64	...	28
36061	61	...	29	102	92	66	...	27	87	126	99	...	42
36087	22	55	59	34	...	8	45	87	55	28	...
36106	37	...	14	77	56	106	76	59	...
36110	65	76	35	50	85	56
36113	75	17	64	...	71	19	38
36134	99	142	49	123	158	133	...

Table 3b—Continued

Star (LEID)	Wavelength (Å)	Equivalent Widths (mÅ)											
		Fe I	Fe I	Fe I	Fe I	Fe I	Fe I	Fe I	Fe I	Fe I	Fe I	Fe II	Fe II
36156	6270.23	6271.28	6290.97	6297.79	6301.50	6302.49	6311.50	6315.81	6322.69	6335.33	6336.83	6344.15	6149.24
36179	2.86	3.33	4.73	2.22	3.65	3.69	2.83	4.07	2.59	2.20	3.69	2.43	3.89
36182	-2.62	-2.74	-0.72	-2.74	-0.68	-1.11	-3.17	-1.69	-2.41	-2.22	-0.78	-2.92	-2.78
36191	7.52	7.52	7.52	7.52	7.52	7.52	7.52	7.52	7.52	7.52	7.52	7.52	7.52
36206	35
36228	69	18	129	82	41	22	114	168	103	102	17
36239	67	103	104	84	34	15	88	130	97	38
36259	35	69	73	51	10	68	108	70	49	15
36260	39	83	78	15	67
36280	56	13	94	94	75	26	17	86	133	91	76	...
36282	26	72	75	40	11	62	110	66	43	16	33
37022	39	53	97	68
37024	101	54	157	226	163	...
37051	58	60	36	53	93	60
37052	30	17	82	90	52	10	24	64	85	37
37055	55	22	91	93	77	18	79	119	87	21
37062	84	87	43	106	37	50
37071	24	58	68	10	40	91	51	35	...
37082	46	60	48	81	33	...
37087	71	77	8	64	110	69	47
37094	69	73	43	47	87	47	11
37105	32	57	64	44	6	42	81	59	21
37110	130	185	151	183	240	184	47
37119	62	20	112	103	76	31	16	97	140	92	85	15
37136	15	55	48	51	36	...
37139	75	30	31	122	40	33	115	157	112	103
37143	39	71	75	45	14	60	101	69	45	13
37147	66	23	34	119	112	77	44	32	102	130	98	97	24
37157	41	72	75	49	13	69	110	72	49	15	29
37169	29	55	80	50	93	59	7	23

Table 3b—Continued

Star (LEID)	Wavelength (Å)	Equivalent Widths (mÅ)											
		Fe I	Fe I	Fe I	Fe I	Fe I	Fe I	Fe I	Fe I	Fe I	Fe I	Fe II	Fe II
37179	6270.23	6271.28	6290.97	6297.79	6301.50	6302.49	6311.50	6315.81	6322.69	6335.33	6336.83	6344.15	6149.24
37184	2.86	3.33	4.73	2.22	3.65	3.69	2.83	4.07	2.59	2.20	3.69	2.43	3.89
37196	-2.62	-2.74	-0.72	-2.74	-0.68	-1.11	-3.17	-1.69	-2.41	-2.22	-0.78	-2.92	-2.43
37198	7.52	7.52	7.52	7.52	7.52	7.52	7.52	7.52	7.52	7.52	7.52	7.52	7.52
37215	20	40	59	25	...	9	36	83	48
37232	79	25	...	129	41	39	120	189	112	120	20
37247	35	8	...	82	86	56	...	19	71	105	73
37253	48	112	106	67	30	19	90	133	86	79	12
37271	62	15	16	98	101	75	34	16	96	138	94	87	18
37275	82	95	...	88	...	23	115	152	111	98	...
37318	108	...	68	...	154	119	...	67	152	200	151	...	32
37322	10	32	73	39
37329	41	85	74	53	23	...	67	119	74	57	18
38011	84	33	...	135	118	92	...	44	112	153	122	...	20
38018	44	72	79	55	59	104	75	60	22
38049	61	...	25	97	...	76	34	16	96	153	97	83	20
38052	65	102	...	30	16	102	142	94	84	18
38056	31	70	52	100	71	39	19
38057	69	...	48	108	95	108	99	...	45
38059	114	142	118	...	57	143	199	149
38061	39	48	32	64	36	...	31
38096	27	59	74	48	14	...	54	110	74
38097	90	44	55	138	126	97	63	44	128	173	115	126	25
38105	36	78	92	49	65	111	71	47	16
38112	61	...	22	110	104	73	35	26	85	...	96	...	32
38115	72	24	...	130	114	81	116	157	112	104	26
38129	52	91	84	68	...	19	83	127	83	71	22
38147	56	107	100	25	88	130	96	...	40
38149	99	...	46	156	131	109	65	42	118	172	136	...	31
38156	40	87	93	68	...	16	75	114	75	60	13

Table 3b—Continued

Star (LEID)	Wavelength (Å)	Equivalent Widths (mÅ)												
		Fe I	Fe I	Fe I	Fe I	Fe I	Fe I	Fe I	Fe I	Fe I	Fe I	Fe I	Fe I	
38166	6270.23	6271.28	6290.97	6297.79	6301.50	6302.49	6311.50	6315.81	6322.69	6335.33	6336.83	6344.15	6149.24	6247.56
38168	92	143	136	93	64	46	122	175	121	128	...	42
38169	61	...	30	120	110	82	39	30	98	141	101	...	16	35
38195	68	43	35	112	158	106	107	13	30
38198	76	135	124	81	53	33	105	...	106	...	27	40
38204	61	117	106	70	...	13	92	144	94	85	...	33
38206	50	10	52	95	57	...	25	41
38215	78	...	49	119	113	97	111	144	112	...	24	46
38223	34	89	82	11	72	113	82	52	21	34
38225	38	8	...	68	82	51	60	100	65	43	25	35
38226	47	84	84	51	70	107	81	...	15	38
38232	81	36	40	135	122	93	63	37	119	169	113	116	17	34
38255	83	137	123	89	...	42	111	158	127	...	21	36
38262	59	20	...	94	92	65	32	18	89	142	84	74	...	39
38276	66	116	127	81	36	24	96	143	95	92	19	36
38303	66	118	110	69	...	19	91	133	103	35
38319	44	104	99	65	81	117	80	65	...	43
38323	71	...	52	114	...	85	...	47	99	137	111	...	31	...
38330	33	70	77	...	13	...	57	96	77	50	...	31
39026	79	34	...	120	111	...	55	33	107	152	115	...	17	35
39033	66	45	85	50	28	...	25
39034	33	91	88	53	68	103	72	63	...	37
39037	62	17	...	112	104	68	...	14	99	142	90	85	26	41
39043	38	83	80	60	107	72	41	21	46
39044	46	16	...	99	95	64	82	127	...	62	18	33
39048	117	169	138	...	74	156	204	171
39056	53	60	...	9	...	41	84	61	...	15	19	
39063	37	53	25	...	7	29	75	45	...	17	29	
39067	78	34	...	134	119	85	59	30	113	147	108	...	25	31
39086	57	...	104	99	...	29	21	85	120	89	71	24	24	

Table 3b—Continued

Star (L-EID)	Equivalent Widths (mÅ)											
	Wavelength (Å)	6270.23	6271.28	6290.97	6297.79	6301.50	6302.49	6311.50	6315.81	6322.69	6335.33	6336.83
Ion	Fe I	Fe I	Fe I	Fe I	Fe I	Fe I	Fe I	Fe I	Fe I	Fe I	Fe I	Fe I
E.P. (eV)	2.86	3.33	4.73	2.22	3.65	3.69	2.83	4.07	2.59	2.20	3.69	2.43
Log gf	-2.62	-2.74	-0.72	-2.74	-0.68	-1.11	-3.17	-1.69	-2.41	-2.22	-0.78	-2.92
Log ϵ_{\odot}	7.52	7.52	7.52	7.52	7.52	7.52	7.52	7.52	7.52	7.52	7.52	7.52
39088	38	...	12	72	83	13	75	113	75	52
39102	29	...	16	69	80	50	...	18	60	92	68	...
39119	27	8	...	70	81	43	...	10	58	97	62	...
39123	20	63	68	11	38	95	54	28
39129	80	117	83	...	28	101	135	116	102
39141	51	103	...	62	25	12	89	126	84	68
39149	98	134	...	103	...	49	111	156	142	...
39165	42	103	82	136	...	63
39186	51	102	...	24	...	83	133	...	77
39187	43	92	94	62	...	10	80	124	84	75
39198	51	...	15	92	...	59	23	...	94	136	87	73
39204	26	11	...	83	76	...	10	...	64	119	89	...
39215	32	72	75	56	60	107	71	...
39216	29	...	24	66	82	41	60	111	75	...
39225	27	70	54	100	68	...
39235	71	...	24	116	107	79	95	133	99	...
39245	82	37	...	151	129	97	...	44	125	169	110	125
39257	97	142	32	131	178	121	...
39259	51	...	17	99	87	68	21	...	77	119	84	74
39284	68	129	109	72	33	21	96	151	95	89
39289	32	74	74	50	...	11	60	98	63	38
39298	19	52	67	40	38	77	44	...
39301	41	72	74	44	61	97	66	...
39306	49	10	...	88	90	67	86	125	81	65
39325	173	133	111	...	44	143	181	129	...
39329	65	57	110	72	...
39345	63	65	58	10	14	14	58	103	71	44
39346	73	35	49	129	128	92	65	41	125	148	122	...
39352	51	10	...	112	101	...	31	15	84	139	84	71
39384	49	...	97	...	106	64	7.52	7.52	7.52	7.52

Table 3b—Continued

Star (LEID)	Wavelength (Å)	Equivalent Widths (mÅ)											
		Fe I	Fe I	Fe I	Fe I	Fe I	Fe I	Fe I	Fe I	Fe I	Fe I	Fe II	Fe II
39392	6270.23	6271.28	6290.97	6297.79	6301.50	6302.49	6311.50	6315.81	6322.69	6336.83	6344.15	6149.24	6247.56
39401	2.86	3.33	4.73	2.22	3.65	3.69	2.83	4.07	2.59	2.20	3.69	2.43	3.89
39921	-2.62	-2.74	-0.72	-2.74	-0.68	-1.11	-3.17	-1.69	-2.41	-2.22	-0.78	-2.92	-2.43
40016	64	20	28	104	100	79	...	22	99	137	93	92	27
40031	27	...	15	67	41	36
40041	55	98	65	114	96	...	17	36
40108	11	56	67	40	...	9	51	93	60	...	24
40123	94	44	...	155	144	174	121	123	...
40135	59	...	19	109	99	62	17	...	94	150	98	...	16
40139	86	28	27	129	30	117	161	126	...	27	43
40162	89	86	...	25	12	70	111	82	59	14	32
40166	67	...	29	109	106	75	...	23	92	...	101	87	42
40168	37	67	79	69	105	64	45	...
40170	36	9	...	79	76	14	67	108	74	55	11
40207	84	129	...	84	...	31	105	154	116	...	26
40210	27	65	81	38	...	7	50	86	53	37	9
40216	64	24	...	117	105	79	...	27	103	144	98	98	18
40220	45	82	86	50	69	21	29
40232	103	...	54	154	74	...	200	163
40235	53	7	15	97	...	55	...	10	77	119	80	63	34
40237	72	110	100	78	...	13	87	...	106	...	25
40275	34	78	85	44	73	107	68	50	17
40291	63	19	...	105	98	71	...	22	91	139	92	83	22
40318	...	37	...	140	126	99	...	49	109	153	138
40339	120	...	48	173	146	125	...	57	138	218	154
40349	66	19	...	102	101	77	25	24	90	...	94	79	22
40358	106	66	146	201	161	...
40361	27	68	66	42	54	91	57	36	9
40371	83	129	121	92	...	39	114	164	120	...	20
40372	36	85	83	10	72	117	75	57	16

Table 3b—Continued

Star (LEID)	Wavelength (Å)	Equivalent Widths (mÅ)											
		Fe I	Fe I	Fe I	Fe I	Fe I	Fe I	Fe I	Fe I	Fe I	Fe I	Fe II	Fe II
40373	6270.23	6271.28	6290.97	6297.79	6301.50	6302.49	6311.50	6315.81	6322.69	6335.33	6336.83	6344.15	6149.24
40409	2.86	3.33	4.73	2.22	3.65	3.69	2.83	4.07	2.59	2.20	3.69	2.43	3.89
40420	-2.62	-2.74	-0.72	-2.74	-0.68	-1.11	-3.17	-1.69	-2.41	-2.22	-0.78	-2.92	-2.78
40424	36
40472	80	24	...	131	...	81	41	...	116	165	101	104	20
40479	47	...	30	96	...	63	...	20	79	111	88	67	...
41015	39	77	71	13	62	102	66	38	15
41025	86	57	19	...	68	104	63	...	20
41033	113	...	50	181	160	119	...	68	158	197	162
41034	48	98	102	66	24	20	84	127	89	68	23
41035	39	12	12	84	...	59	23	...	76	117	74	55	14
41039	52	101	105	57	...	16	85	125	85	66	20
41060	79	...	31	131	...	89	111	172	111	109	23
41061	65	...	27	110	98	75	36	19	84	130	92	87	20
41063	35	79	90	56	64	...	68	45	20
41164	99	96	14	76	...	81	...	23
41186	42	81	89	56	...	11	75	112	71	60	23
41201	35	74	42
41230	75	79	48	...	13	66	94	71
41232	67	21	30
41241	55	13	25	17	95	149	88	73	12
41243	32	...	17	75	...	49	...	10	66	104	67	50	18
41246	38	81	14	70	107	69	49	...
41258	22	44	42	88	50	21	5
41259	44	10	...	76	85	64	16	16	74	118	87	58	16
41262	34	48	83	60	56	72
41310	26	72	66	87	57	...	31
41312	36	73
41313	44	10	12	93	86	12	77	127	79	62	18
41321	96	...	62	81	127	79	...	20

Table 3b—Continued

	Wavelength (Å)	6270.23	6271.28	6290.97	6297.79	6301.50	6302.49	6311.50	6315.81	6322.69	6335.33	6336.83	6344.15	6149.24	6247.56
Ion	Fe I	Fe I	Fe I	Fe I	Fe I	Fe I	Fe I	Fe I	Fe I	Fe I	Fe I	Fe I	Fe I	Fe II	Fe II
E.P. (eV)	2.86	3.33	4.73	2.22	3.65	3.69	2.83	4.07	2.59	2.20	3.69	2.43	3.89	3.89	3.89
Log gf	-2.62	-2.74	-0.72	-2.74	-0.68	-1.11	-3.17	-1.69	-2.41	-2.22	-0.78	-2.92	-2.78	-2.43	-2.43
Log ϵ_{\odot}	7.52	7.52	7.52	7.52	7.52	7.52	7.52	7.52	7.52	7.52	7.52	7.52	7.52	7.52	7.52
Star (LEID)															
41348	91	60	78	115	75	...	24
41366	32	7	...	87	...	53	...	10	66	98	19	...	32
41375	77	136	115	84	115	166	109	109	21	39	...
41380	126	148	142	118	198	138
41387	54	101	105	69	19	...	77	...	90	...	12	41	...
41389	32	67	76	46	...	15	56	93	64	...	12
41402	30	79	55	106	64	40	8	37	...
41435	70	123	105	75	45	37	105	152	99
41455	105	188	163	120	98	59	161	216	156	40	...
41476	93	70	41	169	133	107	...	41	140	195	126
41494	52	...	92	94	65	21	78	114	90	62	20	31	...
42012	45	91	96	18	73	114	84	58	12	36	...
42015	55	105	66	27	...	84	125	89	77	16	36	...
42023	43	102	94	60	...	12	88	131	84	66	17	39	...
42039	45	98	93	...	18	11	86	119	82	59	21	34	...
42049	72	114	104	83	...	31	98	140	106	97	...	42	...
42054	59	14	...	113	...	74	29	...	103	155	97	85	14	33	...
42056	11	64	10	37	71
42079	48	18	...	95	90	62	...	16	78	106	78	...	20	40	...
42084	73	116	96	134	108	...	26	43	...
42106	46	19	...	75	81	67	...	22	74	...	74	15	35
42114	66	117	110	74	40	19	91	136	97	92	22	42	...
42120	52	13	...	85	...	60	...	23	82	115	87	70	25	43	...
42134	71	94	56	...	15	35	...
42161	58	...	19	108	103	66	27	13	90	143	92	71	21	31	...
42162	103	...	51	152	67	132	177	149	35	...
42169	77	108	81	26	95	134	108	...	26	44	...
42174	82	75	50	20	...	64	34	...
42175	52	92	93	...	29	...	85	122	92	74	15	35	...
42179	54	12	...	92	69	...	17	92	134	81	70	19	19	19	...

Equivalent Widths (nmÅ)

Table 3b—Continued

Star (LEID)	Wavelength (Å)	Equivalent Widths (mÅ)											
		Fe I	Fe I	Fe I	Fe I	Fe I	Fe I	Fe I	Fe I	Fe I	Fe I	Fe I	Fe I
42182	6270.23	6271.28	6290.97	6297.79	6301.50	6302.49	6311.50	6315.81	6322.69	6335.33	6336.83	6344.15	6149.24
42187	2.86	3.33	4.73	2.22	3.65	3.69	2.83	4.07	2.59	2.20	3.69	2.43	3.89
42196	-2.62	-2.74	-0.72	-2.74	-0.68	-1.11	-3.17	-1.69	-2.41	-2.22	-0.78	-2.92	-2.43
42198	7.52	7.52	7.52	7.52	7.52	7.52	7.52	7.52	7.52	7.52	7.52	7.52	7.52
42205	120	38	...	173	45	137	198	154
42221	28	...	68	71	55	102	67	45	22	25
42260	49	...	20	100	86	66	75	111	83
42271	55	65	53	37	...
42302	65	...	20	115	104	79	33	23	101	161	105
42303	83	...	72	...	16	82	119	88	...	28
42309	82	109	121	102	98	141	114
42339	82	...	51	116	110	83	...	31	96	27	...
42345	22	49	59	30	39	21	7
42361	31	62	67	39	50	102	59	38	36
42384	92	34	40	140	...	102	...	41	118	170	118	...	29
42385	34	60	64	50	9	...	49	98	62	41	11
42407	36	61	75	56
42415	65	21	21	106	...	79	33	26	96	137	104	...	28
42438	70	120	117	89	52	29	99	135	112	...	34
42457	21	80	84	64	74	96
42461	61	18	...	116	...	77	33	24	106	151	95	95	33
42473	87	133	123	42	110	...	124
42497	36	82	79	48	69	114	75	53	...
42501	59	91	...	59	23	...	78	120	81	71	30
42503	75	86	48	72	104	82
42508	62	...	16	90	...	70	22	...	86	126	92	74	26
43010	69	78	53	93	65	36	33
43024	37	74	84	49	16	61	97	64	36
43036	62	113	115	70	94	121	...	23	43
43040	34	75	79	...	13	...	75	106

Table 3b—Continued

Star (LEID)	Wavelength (Å)	Equivalent Widths (mÅ)											
		Fe I	Fe I	Fe I	Fe I	Fe I	Fe I	Fe I	Fe I	Fe I	Fe I	Fe II	Fe II
43060	6270.23	6271.28	6290.97	6297.79	6301.50	6302.49	6311.50	6315.81	6322.69	6335.33	6336.83	6344.15	6149.24
43061	2.86	3.33	4.73	2.22	3.65	3.69	2.83	4.07	2.59	2.20	3.69	2.43	3.89
43064	-2.62	-2.74	-0.72	-2.74	-0.68	-1.11	-3.17	-1.69	-2.41	-2.22	-0.78	-2.92	-2.43
43068	7.52	7.52	7.52	7.52	7.52	7.52	7.52	7.52	7.52	7.52	7.52	7.52	7.52
43071	53	53	63	108	105	66	24	21	88	134	89	72	25
43079	46	23	87	117	113	89	...	36	103	138	100	... 31	31
43087	64	... 102	95	70	90	... 117	113	11	85	123	78	59	... 36
43091	51	23	153	153	153	153	153	42	20	122	180	106	... 31
43095	82	13	67	97	90	47	76	7	61	96	70	123	... 36
43096	91	47	... 104	104	97	76	... 104	42	20	122	192	115	55
43099	39	16	... 104	104	97	76	... 104	42	20	122	192	115	55
43101	62	... 14	... 14	... 14	82	... 13	77	50	14	... 60	69	102	41
43104	... 43108	... 43111	... 43134	... 43139	... 43158	... 43189	... 43216	... 43233	... 43241	... 43258	... 43261	... 43278	... 43326
43108	42	... 13	67	77	50	145	113	... 66	88	... 14	... 117	... 117	... 54
43111	... 43134	... 17	... 17	60	61	145	101	... 79	134	88	128	186	144
43139	35	... 33	59	170	142	101	... 101	... 79	15	... 51	82	... 66	51
43158	106	41	54	155	142	101	... 101	... 79	15	... 44	44	129	132
43216	90	... 32	... 17	51	61	142	101	... 79	134	88	128	186	144
43233	78	... 44	... 44	69	76	113	113	... 79	15	... 43	43	129	132
43241	... 62	... 14	85	88	54	101	101	... 60	134	88	128	186	144
43258	116	... 117	... 117	90	91	113	101	... 39	117	117	117	127	56
43261	59	... 207	... 43	91	58	101	101	... 60	134	88	127	56	... 20
43278	127	... 126	... 126	207	180	136	136	... 71	126	112	112	108	50
43326	64	26	38	133	122	98	98	... 122	134	117	117	108	57
43330	85	33	38	133	122	98	98	... 122	134	117	117	108	57
43351	127	... 26	... 26	207	180	136	136	... 71	126	112	112	108	57
43367	64	26	38	133	122	98	98	... 122	134	117	117	108	57
43389	85	33	38	133	122	98	98	... 122	134	117	117	108	57

Table 3b—Continued

	Wavelength (Å)	6270.23	6271.28	6290.97	6297.79	6301.50	6302.49	6311.50	6315.81	6322.69	6335.33	6336.83	6344.15	6149.24	6247.56
Ion	Fe I	Fe I	Fe I	Fe I	Fe I	Fe I	Fe I	Fe I	Fe I	Fe I	Fe I	Fe I	Fe I	Fe II	Fe II
E.P. (eV)	2.86	3.33	4.73	2.22	3.65	3.69	2.83	4.07	2.59	2.20	3.69	2.43	3.89	3.89	3.89
Log gf	-2.62	-2.74	-0.72	-2.74	-0.68	-1.11	-3.17	-1.69	-2.41	-2.22	-0.78	-2.92	-2.78	-2.43	-2.43
Log ϵ_{\odot}	7.52	7.52	7.52	7.52	7.52	7.52	7.52	7.52	7.52	7.52	7.52	7.52	7.52	7.52	7.52
Star (LEID)															
43397	31	41	72	54
43399	69	17	64	100	69	53	...	23
43412	61	15	...	113	107	69	29	11	93	157	89	82	21	37	...
43433	48	16	...	86	87	64	...	23	92	123	86	76	11	41	...
43446	37	76	90	66	113	78	...	18
43458	50	95	20	76	111	90	46	...
43463	27	...	13	62	74	40	45	100	56	39	...
43475	104	141	139	111	129	168	138	124	38
43485	41	10	...	83	85	62	25	...	71	114	78	55	19	34	...
43539	38	10	...	91	73	104	75	55	23	33	...
44026	89	...	37	143	118	96	...	42	117	153	129
44042	38	...	9	71	81	46	17	...	71	116	64	50	20	32	...
44056	55	...	23	...	91	62	30	...	82	123	87	...	24	37	...
44065	34	82	79	22	70	121	78	60	20	30	...
44067	16	55	58	30	15	...	46	78	51
44115	66	18	127	86	37	12	90	155	...	86	19	40	...
44120	65	...	43	48	73	55	35
44143	42	...	17	94	92	53	21	...	68	111	72	50	...	36	...
44163	47	14	...	92	94	59	21	9	86	119	79	67	15
44188	59	93	99	69	...	13	88	119	84	...	20	32	...
44189	66	...	34	112	100	86	134	104	35
44198	40	96	90	49	76	118	73	55	...	39	...
44219	44	94	91	...	27	...	90	136	88	74	18
44231	48	90	85	63	...	25	75	107	82	69	17	37	...
44253	56	28	...	112	99	70	22	28	92	119	86	83	26	37	...
44271	20	64	79	48	48	107	57	...	18	34	...
44277	99	49	...	142	88	...	151	230	136	128
44304	63	77	87	63	...	14	73	111	83	84	17
44313	51	111	112	66	...	25	90	126	87	69	18
44327	43	95	95	57	...	16	78	117	84	61	13	34	...

Equivalent Widths (nmÅ)

Table 3b—Continued

Star (LEID)	Equivalent Widths (mÅ)									
	Wavelength (Å)	Fe I								
44337	45	...	95	93	...	22	...	85	124	82
44343	47	16	100	98	56	26	20	77	122	81
44380	61	39	70
44424	26	...	15	60	51	102	64
44426	68	...	121	108	78	...	32	96	137	104
44435	62	19	23	103	96	74	40	23	93	129
44446	31	55
44449	113	144	112	...	165
44462	94	57	58	155	...	103	...	127	182	124
44488	20	...	61	74	56	...
44493	31	70	...	44	15	14	62	...
45082	28	69	16	14	63	...
45089	86	19	65	108	68
45092	76	113	121	89	...	37	100	...
45093	25	62	67	50	...	63
45126	29	69	83	45	...	19	67	108
45177	57	20	13	111	95	74	25	...	96	141
45180	42	20	...	89	89	65	26	...	78	115
45206	32	75	79	38	59	98
45215	88	51	61	137	133	107	121	...
45232	75	21	16	152	...	83	51	19	118	184
45235	72	64	51	12	...	61	91
45238	59	15	23	96	94	71	25	13	90	131
45240	59	102	89	68	95	...
45246	84	...	31	126	...	86	...	41	102	...
45249	71	...	20	110	...	86	...	34	116	150
45272	78	121	116	80	43	19	111	148
45285	91	139	121	102	...	56	110	150
45292	56	96	92	68	81	128
45309	19	63	61	12	42	88

Table 3b—Continued

Star (LEID)	Wavelength (Å)	Equivalent Widths (mÅ)											
		Fe I	Fe I	Fe I	Fe I	Fe I	Fe I	Fe I	Fe I	Fe I	Fe I	Fe II	Fe II
45322	6270.23	6271.28	6290.97	6297.79	6301.50	6302.49	6311.50	6315.81	6322.69	6335.33	6336.83	6344.15	6149.24
Ion	Fe I	Fe I	Fe I	Fe I	Fe I	Fe I	Fe I	Fe I	Fe I	Fe I	Fe I	Fe I	Fe II
E.P. (eV)	2.86	3.33	4.73	2.22	3.65	3.69	2.83	4.07	2.59	2.20	3.69	2.43	3.89
Log gf	-2.62	-2.74	-0.72	-2.74	-0.68	-1.11	-3.17	-1.69	-2.41	-2.22	-0.78	-2.92	-2.78
Log ϵ_{\odot}	7.52	7.52	7.52	7.52	7.52	7.52	7.52	7.52	7.52	7.52	7.52	7.52	7.52
45326	82	...	34	135	126	97	51	28	116	...	111	113	...
45342	49	95	59	79	124	83	76	26
45343	101	147	129	123	...	37	127	158	148	...
45359	49	95	98	63	23	80	111	81	65	27
45373	49	26	97	98	62	23	...	84	125	84	15
45377	72	111	108	75	...	26	107	138	105	...
45389	50	93	19	79	121	76	69
45410	18	107	103	66	...	21	83	122	82	72
45418	48	64	78	...	15	...	48	90	62	...
45453	69	110	111	74	...	21	94	...	101	99
45454	80	139	121	123	178	116	...
45463	68	18	109	100	87	89	136	98	76
45482	55	99	95	79	109	88	74
46024	72	21	115	121	...	38	26	110	171	104	102
46055	52	109	106	62	29	...	86	122	90	76
46062	89	27	23	133	127	...	41	23	119	181	109	121	...
46073	110	137	112	...	60	123	...	146
46090	17	48	50	31	88	46	...	10
46092	109	44	42	164	156	109	72	44	140	192	137
46121	122	167	133	...	73	140	236	157	...	38
46140	49	105	95	56	...	21	75	118	82	66	...
46150	92	36	60	158	135	99	65	47	130	172	114	130	21
46166	48	...	17	84	89	49	...	15	68	108	77	62	...
46172	59	16	26	115	121	77	...	32	95	132	99	...	42
46194	59	20	21	106	70	33	25	96	131	87	84	14	38
46196	14	...	16	35	51	22	69	...	18	...
46223	79	123	104	85	...	26	101	144	115	98	...
46248	58	100	93	72	...	20	91	135	80	78	...
46279	21	53	59	37	6	...	44	71	44	27	29

Table 3b—Continued

	Wavelength (Å)	6270.23	6271.28	6290.97	6297.79	6301.50	6302.49	6311.50	6315.81	6322.69	6335.33	6336.83	6344.15	6149.24	6247.56
Ion	Fe I	Fe I	Fe I	Fe I	Fe I	Fe I	Fe I	Fe I	Fe I	Fe I	Fe I	Fe I	Fe I	Fe II	Fe II
E.P. (eV)	2.86	3.33	4.73	2.22	3.65	3.69	2.83	4.07	2.59	2.20	3.69	2.43	3.89	3.89	3.89
Log gf	-2.62	-2.74	-0.72	-2.74	-0.68	-1.11	-3.17	-1.69	-2.41	-2.22	-0.78	-2.92	-2.78	-2.43	-2.43
Log ϵ_{\odot}	7.52	7.52	7.52	7.52	7.52	7.52	7.52	7.52	7.52	7.52	7.52	7.52	7.52	7.52	7.52
Star (LEID)															
46289	41	13	..	93	95	58	20	..	74	114	..	54	18	34	34
46301	38	10	14	89	87	..	14	..	68	114	72	48	37
46318	29	84	86	42	..	13	60	103	64	50	34
46323	43	20	..	96	96	63	..	16	80	126	83	68	19	36	36
46325	30	..	9	59	75	45	..	10	60	102	62	27	27
46325	32	73	77	51	..	10	58	98	64	40	17
46348	32	149	120	94	49	41	120	170	111	114	32	41	41
46350	73	108	..	83	41	30	97	140	97	86	..	40	40
46381	68	19	26
46388	25	62	75	40	35	35
46391	53	110	109	62	29
46398	34	26
46405	16	51	67	50	15	27
46438	30	34
47012	66	22	32	124	115	72	38	30	104	148	97	93	16	37	37
47039	30	63	70	42	18	37
47055	9	77	99	48	34
47074	22	13	81
47096	75	110	78	46
47107	64	121	35	26
47110	44	98	96	58	20	13	77	120	73	60	12	36	36
47146	84	127	124	85	45	28	109	..	111	33
47150	95	153	130	99	37
47151	32	61	60
47153	136	187	155	142	65	164	220	162
47176	69	106	105	75	35	16	92	128	101	76	..	40	40
47186	108	52	..	190	158	106	90	48	146	201	130	36	36
47187	91	119	124	103	33	112	..	125
47199	63	22	31	144	123	88	41	21	105	155	89	90	21	38	38
47269	69	108	102	80	28	95	135	110	..	29	..
47299	33	12	19	71	80	45	55	85	66

Equivalent Widths (mÅ)

Table 3b—Continued

Star (LEID)	Wavelength (Å)	Equivalent Widths (mÅ)											
		Fe I	Fe I	Fe I	Fe I	Fe I	Fe I	Fe I	Fe I	Fe I	Fe I	Fe II	Fe II
47307	6270.23	6271.28	6290.97	6297.79	6301.50	6302.49	6311.50	6315.81	6322.69	6335.33	6336.83	6344.15	6149.24
Ion	Fe I	Fe I	Fe I	Fe I	Fe I	Fe I	Fe I	Fe I	Fe I	Fe I	Fe I	Fe I	Fe II
E.P. (eV)	2.86	3.33	4.73	2.22	3.65	3.69	2.83	4.07	2.59	2.20	3.69	2.43	3.89
Log gf	-2.62	-2.74	-0.72	-2.74	-0.68	-1.11	-3.17	-1.69	-2.41	-2.22	-0.78	-2.92	-2.43
Log ϵ_{\odot}	7.52	7.52	7.52	7.52	7.52	7.52	7.52	7.52	7.52	7.52	7.52	7.52	7.52
47331	33
47338	48	20	...	103	94	53	86	125	83	62	...
47339	51	70	76	49	67	91	73	...	40
47348	64	...	27	116	104	31	100	137	104	78	...
47354	97	31	...	153	...	113	83	47	113	162
47387	48	95	99	65	...	12	79	126	81	65	18
47399	92	42	...	156	131	...	70	47	140	185	121	130	27
47400	75	25	...	110	109	89	50	42	105	146	106	109	...
47405	115	103	71	31	19	93	144	85	73	...
47420	54	100	96	65	30	...	83	111	83	...	28
47443	24	65	78	40	15	97	57	...	25
47450	27	58	67	49	15	...	59	107	79	54	...
48028	45	14	...	104	94	58	27	...	83	122	83	62	18
48036	41	73	73	45	...	12	57	92	66	...	35
48049	72	24	...	136	44	27	111	174	105	105	...
48060	67	25	...	146	119	81	44	...	117	193	104	101	...
48067	61	112	106	74	...	17	96	132	97	80	...
48083	82	144	121	94	...	31	120	153	116	119	...
48099	...	55	82	179	58	141	210	154
48116	111	...	81	...	168	135	...	83	157	206	173	...	37
48120	94	31	124	...	59	33	140	200	122
48150	107	57	...	189	154	...	87	44	161	227	158	...	27
48151	33	8	...	68	69	53	57	108	56	32	...
48186	28	81	69	49	48	98	66
48197	29	9	...	72	72	...	17	...	62	91	66	38	...
48221	76	131	122	89	50	28	96	141	121	...	38
48228	89	81	46	21	...	73	115	73	56	7
48235	87	33	29	128	117	98	60	45	117	161	115	126	26
48247	42	93	94	52	...	22	76	111	82	60	35

Table 3b—Continued

Star (LEID)	Wavelength (Å)	Equivalent Widths (mÅ)											
		Fe I	Fe I	Fe I	Fe I	Fe I	Fe I	Fe I	Fe I	Fe I	Fe I	Fe II	Fe II
48259	21	74	89	20	54	111	91
48281	48	18	...	106	99	...	23	...	85	119	95	...	13
48305	95	58	53	...	143	115	86	40	135	185	117	...	32
48323	127	...	67	...	160	131	...	73	157	204	171	...	29
48367	87	30	...	138	134	...	52	35	132	182	115	117	41
48370	78	...	29	118	...	89	...	38	107	143	118	107	25
48392	66	19	...	106	...	77	37	15	96	142	97	90	20
48409	22	51	56	34	42	91	54	31	...
49013	63	...	34	107	100	74	35	22	96	135	90	79	18
49022	28	76	76	44	14	...	57	97	58	32	20
49037	...	7	...	54	64	49	97	59	...	17
49056	131	85	85	...	168	142	69	181	240	175	...
49072	39	17	...	87	82	49	66	108	59	...	42
49088	34	16	27	78	86	48	26	...	63	110	76	48	...
49111	78	40	45	116	118	96	...	52	105	133	131	...	40
49123	50	124	94	154	...	79	...
49134	63	19	...	103	...	76	37	24	99	144	92	...	21
49148	84	39	36	120	115	85	62	45	120	160	115	121	38
49177	76	...	49	125	113	79	...	26	92	133	105	...	20
49179	28	76	...	36	...	7	62	103	67	39	14
49188	40	15	34
49193	68	115	41	...	107	147	105	90	21
49205	34	67	85	67	100	76
49212	123	...	54	176	148	139	...	61	141	189	162	...	46
49238	51	80	...	55	20	...	76	122	101	69	13
49249	80	33	38	129	117	90	50	31	113	151	108	121	36
49252	44	91	86	54
49255	66	75	34	...	18	64	96	61	...	32
49293	78	29	33	115	106	90	47	23	103	143	105	100	17
49322	28	82	72	39	...	8	56	102	59	44	...

Table 3b—Continued

Star (LEID)	Wavelength (Å)	Equivalent Widths (mÅ)											
		Fe I	Fe I	Fe I	Fe I	Fe I	Fe I	Fe I	Fe I	Fe I	Fe I	Fe II	Fe II
49333	6270.23	6271.28	6290.97	6297.79	6301.50	6302.49	6311.50	6315.81	6322.69	6335.33	6336.83	6344.15	6149.24
50022	19	65	66	51	72	109	69	44
50037	55	15	...	107	94	70	...	13	...	59	83	59	...
50046	33	84	90	20	77	114	84	...	24
50066	65	130	122	89	59	102	62	51	10
50078	59	117	105	66	...	26	95	137	99	...	27
50108	63	20	29	111	...	94	41	23	89	128	105	91	...
50109	33	13	...	75	85	45	...	11	62	106	70	45	...
50133	65	21	17	111	105	71	28	22	102	146	95	82	19
50163	65	62	80	10
50167	47	107	95	73	88	130	91	71	24
50172	60	85	...	68	85	117	87
50187	101	54	48	...	138	106	82	55	134	182	120	...	29
50191	45	13	...	90	87	56	...	18	70	105	79	...	38
50193	118	171	60	147	209	156
50198	61	91	91	80	...	23	82	121	101	88	17
50218	84	36	27	130	...	96	47	37	106	157	117	...	29
50228	49	10	...	89	...	64	27	23	82	121	82	68	15
50245	56	17	...	89	...	56	...	14	77	139	84	...	14
50253	63	...	20	119	104	82	93	20
50259	106	48	31	170	134	109	77	47	149	203	134
50267	51	20	...	93	93	11	88	125	85	69	...
50291	51	90	77	110	74	62	...
50293	53	18	...	100	101	70	28	13	84	122	89	79	...
50294	33	...	15	77	77	43	63	105	74	47	...
50304	14	78	71	48	...	9	74	96	69	...	37
51021	90	...	51	142	139	111	65	40	122	180	119	127	...
51024	64	111	108	77	34	23	98	129	91	82	...
51074	108	158	...	116	...	53	134	174	148
51079	73	...	20	115	109	76	49	49	108	152	111	105	...

Table 3b—Continued

Star (LEID)	Wavelength (Å)	Equivalent Widths (mÅ)											
		Fe I	Fe I	Fe I	Fe I	Fe I	Fe I	Fe I	Fe I	Fe I	Fe I	Fe I	Fe I
51080	6270.23	6271.28	6290.97	6297.79	6301.50	6302.49	6311.50	6315.81	6322.69	6335.33	6336.83	6344.15	6149.24
51091	2.86	3.33	4.73	2.22	3.65	3.69	2.83	4.07	2.59	2.20	3.69	2.43	3.89
51121	-2.62	-2.74	-0.72	-2.74	-0.68	-1.11	-3.17	-1.69	-2.41	-2.22	-0.78	-2.92	-2.78
51132	7.52	7.52	7.52	7.52	7.52	7.52	7.52	7.52	7.52	7.52	7.52	7.52	7.52
51136
51156	62	118	107	76	39	...	96	142	94	84	26
51254	77	...	26	123	109	88	...	44	107	142	116	...	29
51257	16	46	64	32	13	...	48	99	60	35	13
51259	41	...	14	81	79	46	67	101	76	46	14
52017	71	20	...	133	112	76	41	31	118	180	101	100	21
52035	93	138	...	60	29	137	202	124	132	26
52039	34	55	42	76	43	...	18
52103	93	47	47	144	...	113	...	41	133	173	121
52105	38	77	94	58	...	22	71	111	74	59	11
52106	44	87	57	68	110	86	...	41
52109	43	81	88	45	17	...	78	126	76	59	...
52110	71	52	83
52111	125	211	171	141	...	77	157	207	156
52133	20	76	94	70
52139	89	48	...	158	140	96	82	52	124	173	117	124	26
52151	83	74	54	70	102	67	55	15
52154	22	9	...	42	60	34	80	43	...	21
52167	59	...	24	111	113	69	27	15	94	135	84	70	20
52180	54	13	27	102	97	58	...	13	80	124	82	68	...
52192	53	23	...	103	112	21	100	...	27
52204	29	28	74	47
52222	30	72	75	51	59	110	65	46	20
53012	71	81	...	14	7	58	98	62	44	...
53054	...	10	...	80	87	54	104	...	45	12
53058	34	13	89	65	113	72	50	17

Table 3b—Continued

Star (LEID)	Wavelength (Å)	Equivalent Widths (mÅ)											
		Fe I	Fe I	Fe I	Fe I	Fe I	Fe I	Fe I	Fe I	Fe I	Fe I	Fe II	Fe II
53067	6270.23	6271.28	6290.97	6297.79	6301.50	6302.49	6311.50	6315.81	6322.69	6335.33	6336.83	6344.15	6149.24
53076	61	19	...	109	113	90	...	32	91	137	93	...	35
53114	86	...	42	141	123	91	65	37	125	174	122	131	40
53119	40
53132	44	92	93	52	...	14	72	113	75	57	36
53178	39	11	...	85	74	51	23	15	70	112	75	52	36
53185	64	19	29	115	...	81	38	24	104	152	100	96	42
53203	29	66	73	43	...	7	56	100	60	39	41
54018	53	87	92	63	...	19	75	110	90	71	22
54022	140	...	74	198	160	138	...	83	164	205	182	...	50
54031	101	172	145	64	135	185	130	...	35
54064	84	45	50	98	55	...	33
54073	33	69	74	10	51	97	60	34	16
54084	61	...	43	...	24	61	100	72	...	44
54095	70	66	56	...	22	65	109	74	48	...
54105	111	...	57	...	152	65	144	188	151
54132	45	15	17	99	92	58	20	...	71	116	78	60	18
54148	79	29	31	135	123	83	48	30	116	168	105	108	38
54154	26	...	53	44	91	54	32	43
55028	95	45	60	159	143	109	76	48	132	174	119	...	32
55029	83	130	124	95	59	33	109	151	112	111	42
55056	36	69	75	...	18	...	51	96	71	60	...
55063	76	131	116	87	52	27	106	150	111	...	39
55071	135	175	65	169	242	178	...	35
55089	14	91	89	50	...	12	75	124	81	...	41
55101	116	138	109	...	65	133	178	156
55102	62	112	107	71	...	26	91	139	101	87	46
55111	82	...	28	132	121	...	56	27	118	165	113	115	39
55114	94	47	35	158	...	99	75	42	134	...	120
55121	137	...	68	...	185	145	...	65	169	233	177

Table 3b—Continued

Star (LEID)	Wavelength (Å)	Equivalent Widths (mÅ)											
		Fe I	Fe I	Fe I	Fe I	Fe I	Fe I	Fe I	Fe I	Fe I	Fe I	Fe II	Fe II
55122	6270.23	6271.28	6290.97	6297.79	6301.50	6302.49	6311.50	6315.81	6322.69	6335.33	6336.83	6344.15	6149.24
55131	44	62	...	54	12	19	64	109	85	52
55142	130	166	...	131	...	81	156	192	168	...
55149	108	167	153	124	...	70	127	170	153	...
55152	58	98	95	62	...	21	91	122	93	...
55165	35	15	80	93	49	62	106	66	55
56024	75	115	...	74	50	38	98	142	105	...
56028	40	84	91	43	...	8	64	107	69	44
56040	40	92	95	49	11	...	71	110	79	56
56056	23	10	45	69	45	92	62	31
56070	61	100	99	81	88	122	100	...
56087	70	20	140	116	81	117	168	101	98
56106	44	88	18	...	62	120	76	51
56114	50	105	61	36	80	127	93	67
56118	35	10	80	80	47	20	...	63	109	78	56
56128	94	20	72	...	76	...
57010	71	25	133	123	86	48	27	106	150	107	114
57029	54	68	32	80	44	...
57054	103	41	176	150	106	79	45	144	199	130	139
57058	39	68	70	40	44	95	62	...
57067	34	80	58	17	...	73	116	75	60
57073	...	15	79	80	53	67	114	71	49
57076	39	9	16	89	97	55	26	...	78	117	77	61	18
57083	23	69	68	...	15	...	55	92	51	...	39
57085	25	7	...	60	69	38	...	16	57	93	63	40	15
57091	53	...	36	109	110	21	83	122	107	...	23
57114	29	73	76	53	73	102	75	40	...
57127	73	83	15	59	92	68	45	17
58043	26	61	73	53	104	71	44	17
58059	52	62	38	54	91	57

Table 3b—Continued

	Star (LEID)	Equivalent Widths (mÅ)													
Wavelength (Å)		6270.23	6271.28	6290.97	6297.79	6301.50	6302.49	6311.50	6315.81	6322.69	6335.33	6336.83	6344.15	6149.24	6247.56
Ion	Fe I	Fe I	Fe I	Fe I	Fe I	Fe I	Fe I	Fe I	Fe I	Fe I	Fe I	Fe I	Fe I	Fe II	Fe II
E.P. (eV)	2.86	3.33	4.73	2.22	3.65	3.69	2.83	4.07	2.59	2.20	3.69	2.43	3.89	3.89	
Log gf	-2.62	-2.74	-0.72	-2.74	-0.68	-1.11	-3.17	-1.69	-2.41	-2.22	-0.78	-2.92	-2.78	-2.43	
Log ϵ_{\odot}	7.52	7.52	7.52	7.52	7.52	7.52	7.52	7.52	7.52	7.52	7.52	7.52	7.52	7.52	
58077	25	75	55	85	64	...	10	34	
58087	53	...	18	96	98	73	...	17	86	133	81	69	...	37	
59016	17	67	43	...	53	...	17	...	
59024	146	239	202	156	190	282	191	
59036	51	18	...	98	85	61	21	9	78	126	84	62	25	36	
59047	79	...	37	119	123	84	...	23	105	146	110	...	26	43	
59085	63	111	124	68	...	25	94	150	102	83	21	...	
59089	61	22	...	116	109	69	...	22	94	134	93	78	22	39	
59090	48	92	92	63	25	...	83	122	83	72	16	35	
59094	22	56	...	13	...	46	93	58	...	13	31	...	
60034	51	60	39	...	8	...	96	65	
60058	133	196	200	165	...	87	156	209	185	49	
60059	62	69	
60064	22	...	11	62	65	54	...	56	42	
60065	44	80	87	55	73	114	78	69	10	37	
60066	129	61	38	96	138	117	...	48	
60067	18	52	40	82	47	...	9	34	
60069	36	17	...	86	105	...	12	...	73	117	94	
60073	136	...	61	199	164	136	...	69	157	212	155	
60088	40	75	79	14	61	94	74	47	...	43	
60101	34	72	81	56	64	102	73	43	17	36	
61015	87	29	29	160	132	93	52	38	133	197	122	
61026	60	84	40	58	99	61	54	
61042	64	111	107	72	35	...	93	137	93	83	19	38	
61046	34	72	70	39	...	15	62	100	74	46	...	31	
61050	107	171	142	108	84	46	137	...	135	...	32	47	
61067	118	...	62	...	160	124	...	67	143	197	161	
61070	48	98	98	66	30	...	94	141	87	77	...	43	
61075	23	54	57	38	14	...	44	94	56	29	...	31	
61085	117	51	...	178	...	127	...	52	152	219	151	

Table 3b—Continued

	Wavelength (Å)	6270.23	6271.28	6290.97	6297.79	6301.50	6302.49	6311.50	6315.81	6322.69	6335.33	6336.83	6344.15	6149.24	6247.56
Ion	Fe I	Fe I	Fe I	Fe I	Fe I	Fe I	Fe I	Fe I	Fe I	Fe I	Fe I	Fe I	Fe I	Fe II	Fe II
E.P. (eV)	2.86	3.33	4.73	2.22	3.65	3.69	2.83	4.07	2.59	2.20	3.69	2.43	3.89	3.89	
Log gf	-2.62	-2.74	-0.72	-2.74	-0.68	-1.11	-3.17	-1.69	-2.41	-2.22	-0.78	-2.92	-2.78	-2.43	
Log ϵ_{\odot}	7.52	7.52	7.52	7.52	7.52	7.52	7.52	7.52	7.52	7.52	7.52	7.52	7.52	7.52	7.52
Star (LEID)															
62018	11	55	58	9	...	73	48	27
62058	74	...	28	110	106	83	...	28	88	144	98	86	43
63021	53	...	32	92	101	20	84	131	97	...	21	38	
63027	68	76	8	60	100	79	39	
63052	57	25	...	108	102	62	83	121	93	80	22	33	
64023	...	8	37	53	37	78	40	...	15	31		
64049	90	19	12	86	124	81	68	19	39		
64057	57	66	36	...	10	51	92	59	...	15	37		
64064	21	...	65	48	91	73	32		
64067	55	...	106	103	64	93	...	95	83	21	37		
64074	36	69	102	75	47	...	29		
65042	17	...	42	40	...	48	
65046	24	...	63	67	43	11	50	96	58	34	...	31	
65057	77	92	56	...	8	54	117	21	
66015	31	...	11	72	71	...	7	49	94	60	39	33	
66026	38	10	...	85	82	53	...	15	71	112	72	54	17	39	
66047	75	26	37	124	117	91	55	41	111	155	111	107	...	34	
66054	49	17	...	111	102	62	32	...	85	124	92	68	26	40	
67049	22	...	66	67	37	44	31	
67063	...	34	129	130	87	100	160	102	103	
68044	32	...	76	83	50	53	100	74	45	...	35		
69007	21	...	56	61	52	91	63	30	...	35		
69012	52	12	...	99	101	68	26	18	89	140	85	71	...	35	
69027	123	...	182	79	157	...	175	
70032	88	93	46	15	64	106	70	48	...	31	
70035	55	101	96	138	97	87	...	40	
70041	31	...	85	81	49	19	14	63	107	73	56	...	38		
70049	62	126	99	...	28	...	138	109	...	25	...	
71013	45	52	23	...	9	22	69	42	32		
73025	120	41	47	187	155	119	...	55	150	210	147	30	

Equivalent Widths (mÅ)

Table 3b—Continued

Star (LEID)	Wavelength (Å)	Equivalent Widths (mÅ)											
		Fe I	Fe I	Fe I	Fe I	Fe I	Fe I	Fe I	Fe I	Fe I	Fe I	Fe II	Fe II
75021	6270.23	6271.28	6290.97	6297.79	6301.50	6302.49	6311.50	6315.81	6322.69	6335.33	6336.83	6344.15	6149.24
76027	61	92	88	46	76	114	68	55
76038	94	51	3.33	4.73	2.22	3.65	3.69	2.83	4.07	2.59	2.20	3.69	3.89
77025	69	21	-2.74	-0.72	-2.74	-0.68	-1.11	-3.17	-1.69	-2.41	-2.22	-0.78	-2.78
77030	7.52	7.52	7.52	7.52	7.52	7.52	7.52	7.52	7.52	7.52	-2.43
80026	58	17	70	65	97	72	...
80029	45	11	110	99	69	34	24	91	135	88	78
81018	84	88	47	14	14	81	122	75	55
81019	24	88	85	56	...	18	74	106	80	...
81028	68	68	...	14	...	49	90	62	34
82015	52	66	42	92	61	35
82029	39	48	34	62	42	...
85027	61	119	115	74	37	...	94	140	96	97
85031	44	95	94	76	117	81	61
89009	43	78	91	53	60	111	78	...

Table 4a. O–Eu Atomic Parameters, Equivalent Widths, and Solar Abundances

Wavelength (Å)	Ion	E.P. (eV)	Log gf	Log ϵ_{\odot}	Star (LEID)	Equivalent Widths (mÅ)													
						6300.31	6154.23	6160.75	6696.03	6698.67	6155.13	6237.32	6161.29	6162.18	6166.44	6169.04	6169.56	6210.67	6305.66
5009	syn	9	5	14	37	36	59	202	63	88	110
52	syn	52	80	...	5017	3	22	9	35	150	33	48	78	3	...
8014	syn	...	14	...	9013	51	...	109	248	101	129	144
9013	syn	...	7	syn	10009	20	18	28	148	35	56	68
10009	syn	24	34	...	10012	26	20	28	...	33	57	68
10012	syn	31	51	...	11019	38	40	74	197	70	93	116	16
11019	syn	9	16	...	11021	30	33	100	254	107	140	144	62	121	...
11021	syn	13	21	syn	11024	34	28	69	189	69	92	110	10
11024	syn	7	18	...	12013	38	27	73	197	75	95	117	19
12013	syn	36	63	...	12014	23	16	45	183	53	74	102
12014	syn	...	9	syn	14010	44	43	88	225	95	119	139
14010	syn	2	4	...	15022	15	12	27	139	25	50	63
15022	syn	...	5	...	15023	23	9	24	...	18	30	57
15023	syn	4	5	...	15026	22	8	26	...	37	58	75	...	7	...
15026	syn	42	56	syn	16009	20	14	25	163	30	53	68
16009	syn	4	10	...	16015	18	11	39	155	35	66	75
16015	syn	2	3	...	16019	19	12	31	151	35	56	70
16019	syn	...	7	syn	16027	23	19	25	...	29	60	61
16027	syn	2	17014	18	12	26	130	23	42	58
17014	syn	13	...	syn	17015	27	26	67	190	61	91	96	14
17015	syn	...	4	...	17027	15	15	33	162	38	65	73	5
17027	syn	17029	10	7	...	122	9	32	35
17029	syn	6	17032	13	9	12	132	...	28	51
17032	syn	13	37	...	17046	34	33	52	186	67	92	90	...	25	...
17046	syn	2	12	...	18017	15	11
18017	syn	7	7	...	18020	10	...	17	146	26	44	60
18020	syn	12	25	syn	18035	28	18	57	195	61	87	104	9	21	...
18035	syn	4	11	...	18040	12	8	31	147	30	48	94	8	6	...
18040	syn	33	46	syn	46	41	94	205	91	106	129	18

Table 4a—Continued

Star (LEID)	Wavelength (Å)	Equivalent Widths (mÅ)											
		[O I]	6154.23	6160.75	6696.03	6698.67	6155.13	6237.32	6162.18	6166.44	6169.04	6169.56	6210.67
18047	Na I	syn	...	12	24	10	32	157	37	62	72
19022	Na I	syn	6	10	3	14	...	21	40	53	...
19062	Al I	syn	2	9	23	13	39	164	40	67	84
20018	Si I	syn	8	20	22	20	...	175	...	80	86
20037	Si I	syn	12	29	34	24	50	177	53	79	106
20042	Ca I	syn	4	6	13	7	34	134	26	44	57
20049	Ca I	syn	5	5	23	12	34	151	40	56	72
21032	Ca I	syn	12	23	33	20	67	212	86	98	130
21035	Ca I	syn	3	11	20	12	32	158	35	57	77
21042	Ca I	syn	4	6	24	19	45	168	43	64	81
21063	Ca I	syn	...	4	15	12	26	141	...	55	59
22023	Sc I	syn	37	46	syn	syn	51	48	74	191	69	83	123
22037	Sc I	syn	...	11	20	12	38	165	40	65	76
22042	Sc I	syn	...	11	21	17	31	178	...	57	74
22049	Sc I	syn	...	15	20	11	28	140	28	43	72
22063	Sc I	syn	...	4	14	13	24	149	23	45	65
23022	Sc I	syn	6	8	16	10	17	129	19	37	52
23033	Sc I	syn	...	13	syn	syn	24	16	38	148	33	64	78
23042	Sc I	syn	...	8	syn	syn	...	16	20	133	24	45	60
23050	Sc I	syn	...	10	16	9	20	144	25	44	61
23061	Sc I	syn	...	8	18	15	36	161	40	65	80
23068	Sc I	syn	7	12	syn	syn	26	20	76	225	78	101	124
24013	Sc I	syn	54	79	28	24	102	248	102	121	153
24027	Sc I	syn	17	29	35	27	51	174	53	80	93
24040	Sc I	syn	5	5	22	11	8	132	16	27	51
24046	Sc I	syn	11	16	26	18	49	187	50	76	93
24056	Sc I	syn	5	12	15	11	34	153	33	56	73
24062	Sc I	syn	17	31	40	34	81	208	86	114	116
25006	Sc I	syn	...	12	12	15	13	...	31	42	...
25026	Sc I	syn	...	14	28	13	34	146	27	41	72

Table 4a—Continued

Wavelength (Å)	Star (LEID)	Equivalent Widths (mÅ)											
		Na I	Al I	Si I	Ca I	Si I	Ca I	Al I	Si I	Ca I	Si I	Ca I	Sc I
6300.31	6154.23	6160.75	6696.03	6698.67	6155.13	6237.32	6161.29	6166.44	6169.04	6169.56	6210.67	6305.66	
[O I]	Na I	Na I	Al I	Al I	Si I	Si I	Ca I	Ca I	Ca I	Ca I	Sc I	Sc I	
0.00	2.10	2.10	3.14	3.14	5.62	5.61	2.52	2.52	2.52	2.52	0.00	0.02	
E.P. (eV)	-9.75	-1.57	-1.27	-1.57	-1.89	-0.78	-1.07	-1.28	-0.07	-1.11	-0.42	-1.53	-1.30
Log gf	8.93	6.33	6.33	6.47	7.55	7.55	6.36	6.36	6.36	6.36	3.10	3.10	
Log ϵ_{\odot}													
25043	syn	31	55	38	38	89	243	93	115	140	38
25062	syn	6	17	27	15	73	238	84	116	127	43
25065	syn	134	142	51	...	172	383	180	167	194	...
25068	syn	18	19	35	18	61	...	62	83	110	...
26010	syn	...	4	syn	...	33	14	16	...	13	40	48	...
26014	syn	...	3	13	...	21	143	23	50	66	...
26022	syn	...	10	19	14	25	144	23	47	59	...
26025	syn	17	37	23	17	60	258	74	100	123	37
26030	syn	...	8	17	...	29	140	27	43	53	...
26069	syn	9	16	10	15	128	21	38	63	...
26072	syn	...	3	syn	...	21	...	30	154	39	69	69	...
26086	syn	105	128	74	...	124	281	125	135	162	70
26088	syn	5	9	31	18	61	190	66	76	111	...
27048	syn	26	48	47	43	59	198	65	87	109	12
27050	syn	12	...	19	133	23	36	49	...
27073	syn	10	23	18	12	39	162	43	69	76	...
27094	syn	3	...	syn	...	22	136	30
27095	syn	29	51	36	...	69	225	77	102	120	29
28016	syn	...	10	29	...	50	162	50	60	89	...
28020	syn	...	5	26	14	21	...	27	38	67	...
28044	syn	14	22	27	19	43	170	48	72	89	...
28069	syn	5	17	syn	...	24	17	41	173	48	65	93	...
28084	syn	...	12	syn	...	24	21	46	170	47	72	90	9
28092	syn	...	9	23	16	45	180	50	74	95	...
29029	syn	...	11	29	21	48	169	56	76	97	...
29031	syn	...	11	7	16	152	26	44	55	...
29037	syn	...	6	25	22	27	...	29	48	55	...
29059	syn	...	16	21	27	67	174	46	83	87	7
29067	syn	48	55	48	51	146	306	165	149	167	109
29069	syn	25	41	syn	syn	38	36	69	198	74	119	94	...

Table 4a—Continued

Star (LEID)	Wavelength (Å)	Equivalent Widths (mÅ)												
		[O I]	6154.23	6160.75	6696.03	6698.67	6155.13	6237.32	6162.18	6166.44	6169.04	6169.56	6210.67	6305.66
29072	syn	...	6	17	9	25	144	30	52	66	...
29085	syn	4	10	29	23	39	150	39	54	78	...
29089	syn	...	14	25	21	26	136	29	59	57	...
29099	syn	21	34	syn	syn	35	30	89	221	81	109	131	29	...
29106	syn	...	4	14	12	42	164	43	66	81
30013	syn	36	49	47	...	88	208	74	110	109	27	...
30019	syn	9	30	26	33	52	177	61	87	97	8	...
30022	syn	syn	...	16	144	22	45	59
30031	syn	31	58	syn	syn	30	34	89	244	92	124	135	41	87
30069	syn	...	4	15	...	11	...	15	29	45
30094	syn	17	30	37	17	73	180	63	87	101
30124	syn	8	19	25	18	49	169	55	72	106
31016	syn	...	6	14	129	19	45	58
31041	syn	...	20	32	26	36	162	41	65	78	7	...
31047	syn	5	4	11	8	23	134	27	46	61
31048	syn	5	9	6	31	...	28	40	51
31075	syn	...	14	32	149	28
31079	syn	5	18	16	31	159	28	54	70
31094	syn	3	9	20	13	24	...	28	55	72
31095	syn	14	...	syn	...	51	17	...	160	44	70	65
31104	12	16	...	23	45	49
31109	syn	7	14	28	31	50	161	49	...	95	...	15
31110	syn	14	29	32	37	89	220	84	105	130	27	...
31119	syn	17	33	39	37	87	206	89	100	125	22	...
31133	syn	...	19	14	9	29	144	...	48	48
31139	syn	...	8	15	14	28	160	32	56	66
31141	syn	16	17	32	25	47	178	50	67	93
31147	syn	12	17	31	...	31	66	77
31152	syn	14	17	44	...	48	166	27	66	71
32014	syn	4	15	10	...	153	33	53	61

Table 4a—Continued

Star (LEID)	Wavelength (Å)	Equivalent Widths (mÅ)												
		[O I]	6154.23	6160.75	6696.03	6698.67	6155.13	6237.32	6162.18	6166.44	6169.04	6169.56	6210.67	6305.66
32026	syn	17	22	40	26	73	189	66	86	110	12	...
32027	syn	9	19	15	16	155	43	42	88
32043	syn	2	17	...	19	...	18	45	65
32063	syn	19	33	syn	syn	27	23	39	171	45	62	84	...	12
32069	syn	...	7	21	...	28	...	28	39
32100	syn	4	12	16	10	31	148	30	51	69
32101	syn	29	36	syn	...	29	27	44	169	56	65	105	6	...
32125	syn	...	9	22	18	38	180	48	68	89
32130	syn	...	12	16	5	15	136	19	36
32138	syn	12	16	21	11	65	226	65	81	128	34	60
32140	syn	7	10	18	15	33	159	48	71	78
32144	syn	12	17	33	20	57	169	60	76	110	7	...
32165	syn	...	16	14	5	19	140	...	54	60
32169	syn	103	131	66	...	122	270	123	134	166	45	...
32171	syn	23	50	40	...	69	209	72	95	106	20	...
33006	syn	9	19	29	21	76	220	83	106	128	36	60
33011	syn	5	6	24	15	46	177	51	75	97
33018	syn	...	11	syn	9	51	156	50	73	88
33030	syn	12	17	...	28	143	26	38	64
33051	syn	11	23	33	26	45	170	48	71	92	9	...
33064	syn	...	8	14	4	30	148	...	45	74
33099	syn	69	74	47	...	121	254	107	141	158
33114	syn	10	18	syn	syn	33	24	86	216	84	102	126	27	46
33115	syn	35	54	45	...	82	187	79	81	120
33126	syn	10	17	33	31	69	174	56	72	109	11	...
33129	syn	17	13	23	155	31	47	75
33138	syn	...	10	34	38	164	37	50	82	...	11
33145	syn	8	10	13	...	20	...	23	35	67
33154	20	27	...	14	...	47	50
33167	syn	14	29	30	38	156	37	60	82

Table 4a—Continued

Star (LEID)	Wavelength (Å)	Equivalent Widths (mÅ)												
		[O I]	6154.23	6160.75	6696.03	6698.67	6155.13	6237.32	6162.18	6166.44	6169.04	6169.56	6210.67	6305.66
33177	syn	9	6	150	38	59	66	...
34008	syn	10	...	syn	23	21	58	177	53	70	99	...
34029	syn	44	65	49	47	...	247	115	134	154	51	91
34040	syn	7	12	19	9	38	158	38	50	79
34056	syn	...	10	14	13	24	135	23	38	62
34069	syn	3	20	19	40	167	44	69	85
34075	syn	28	38	syn	syn	48	46	75	213	84	113	111	24	...
34081	syn	8	16	21	20	47	170	53	68	93
34129	syn	...	8	16	...	21	136	23	40	62
34130	syn	8	14	13	...	14	34	45
34134	syn	10	15	25	24	54	197	58	89	98	15	25
34143	syn	60	72	syn	syn	60	226	97	117	136	40	...
34163	syn	...	10	22	...	22	34	63
34166	syn	...	12	27	161	50	61	76
34169	syn	19	33	46	47	66	189	55	82	102	16	...
34175	syn	10	10	39	33	72	212	69	95	120
34180	syn	139	159	syn	syn	67	364	170	...	202	145	...
34187	syn	3	...	12	16	13	20	149	38	44	74	3
34193	syn	...	7	23	16	43	181	47	72	86
34207	syn	7	8	syn	...	27	27	58	186	64	84	104
34214	syn	...	12	8	8	...	123	16
34225	syn	68	74	56	242	103	134	140	45	...
34229	syn	5	11	18	12	32	157	35	50	64
35029	syn	...	10	22	13	36	147	38	53	79	5	...
35035	syn	...	3	11	15	20	139	22	44	64
35046	syn	5	14	26	18	40	165	46	66	83	5	...
35053	syn	...	7	16	15	23	158	31	55	66
35056	syn	21	41	29	22	...	220	77	112	114	33	61
35061	syn	33	53	syn	syn	45	62	67	215	77	100	122	23	...
35066	syn	10	27	17	53	191	64	84	99	19	26

Table 4a—Continued

Star (LEID)	Equivalent Widths (mÅ)											
	Wavelength (Å)	[O I]	Na I	Al I	Si I	Ca I	Ca II	Ca I	Ca II	Sc I	Sc II	
35071	6300.31	6154.23	6160.75	6696.03	6698.67	6155.13	6237.32	6161.29	6162.18	6169.04	6169.56	
35074	0.00	2.10	3.14	5.62	5.61	2.52	1.90	2.52	2.52	0.00	0.02	
35087	-9.75	-1.57	-1.27	-1.89	-0.78	-1.07	-1.28	-0.07	-1.11	-0.69	-0.42	
35090	8.93	6.33	6.47	7.55	7.55	6.36	6.36	6.36	6.36	6.36	3.10	
35093	18	24	36	
35124	syn	9	17	27	24	35	165	45	63	
35157	syn	...	15	18	11	30	147	24	71	
35165	syn	31	47	44	46	98	226	97	106	
35172	syn	...	16	11	...	18	...	25	34	
35190	syn	28	42	48	45	59	190	68	79	
35201	syn	58	72	syn	syn	48	...	89	210	82	98	
35204	syn	4	12	24	14	33	154	36	60	
35216	syn	61	81	49	...	239	102	127	154	
35228	syn	7	12	21	10	41	153	36	...	
35230	syn	18	20	47	228	91	112	
35235	syn	12	24	30	...	26	...	18	32	
35240	syn	7	21	11	53	194	58	91	
35248	syn	...	4	22	16	27	151	22	51	
35260	syn	...	5	24	17	...	185	33	65	
35261	syn	3	10	25	16	39	183	58	76	
36028	syn	8	15	syn	syn	15	15	...	197	52	82	
36036	syn	3	10	30	27	37	172	34	68	
36048	syn	...	25	23	18	35	...	36	66	
36059	syn	10	31	19	49	171	52	75	
36061	syn	...	57	15	15	22	44	
36087	syn	...	10	26	14	50	214	52	83	
36106	syn	9	6	22	19	30	147	34	...	
36110	syn	6	13	29	37	59	70	
36113	syn	6	9	47	39	58	194	73	96	
36134	syn	95	116	syn	syn	14	14	...	137	26	40	

Table 4a—Continued

Table 4a—Continued

Star (LEID)	Wavelength (Å)	Equivalent Widths (mÅ)									
		Ca I	Ca II	Ca I	Ca II	Ca I	Ca II	Ca I	Ca II	Ca I	Ca II
37179	syn	...	17	syn	...	15	145	26	30
37184	syn	...	9	syn	syn	16	16	31	169	34	51
37196	syn	8	10	17	...	35	151	30	51
37198	syn	25	43	syn	syn	47	38	72	189	71	81
37215	syn	...	4	12	11	...	22	43
37232	syn	9	19	33	20	76	230	84	108
37247	syn	12	16	23	22	45	165	38	55
37253	syn	...	9	syn	...	24	16	48	178	52	73
37271	syn	6	16	syn	...	38	18	51	192	65	95
37275	syn	41	41	49	...	88	194	76	95
37318	syn	128	168	syn	syn	54	351	167	172
37322	syn	6	5	19	14	19	...	14	30
37329	syn	4	4	19	15	32	165	39	62
38011	syn	49	65	53	...	94	219	88	106
38018	syn	...	22	35	26	44	165	38	64
38049	syn	18	30	syn	syn	31	25	52	208	60	91
38052	syn	4	20	15	54	192	62	86
38056	syn	9	17	16	10	29	152	38	56
38057	syn	36	39	48	...	86	210	83	106
38059	syn	69	89	syn	syn	56	...	130	278	128	149
38061	syn	...	11	16	12	13
38096	syn	...	16	26	16	...	159	41	...
38097	syn	18	47	58	36	127	277	126	148
38105	syn	6	10	22	14	36	161	35	68
38112	syn	26	46	38	...	68	194	73	89
38115	syn	...	11	36	...	61	199	41	...
38129	syn	14	24	26	20	41	177	49	76
38147	syn	23	34	41	34	67	185	65	89
38149	syn	43	62	49	49	102	252	102	131
38156	syn	...	9	20	15	33	162	42	72

Table 4a—Continued

Star (LEID)	Wavelength (Å)	Equivalent Widths (mÅ)											
		[O I]	6154.23	6160.75	6696.03	6698.67	6155.13	6237.32	6162.18	6166.44	6169.04	6169.56	6210.67
Ion	Na I	Al I	Al I	Si I	Si I	Ca I	Ca I	Ca I	Ca I	Sc I	Sc I	Sc I	Sc I
E.P. (eV)	2.10	3.14	5.62	5.61	2.52	1.90	2.52	2.52	2.52	0.00	0.00	0.02	0.02
Log gf	-1.57	-1.57	-1.57	-1.89	-0.78	-1.07	-1.28	-0.07	-1.11	-0.69	-0.42	-1.53	-1.30
Log ϵ_{\odot}	8.93	6.33	6.33	6.47	6.47	7.55	7.55	6.36	6.36	6.36	6.36	3.10	3.10
38166	syn	9	19	25	16	40	160	34	64	75	...
38168	syn	48	56	syn	syn	48	...	88	230	84	126	123	...
38169	syn	13	37	39	31	78	209	82	101	123	20
38195	syn	9	16	syn	...	27	23	72	206	75	94	118	26
38198	syn	36	51	42	50	46	214	85	96	124	23
38204	syn	6	11	syn	...	28	28	56	178	57	78	95	13
38206	syn	...	13	24	26	23	...	31	44	76	...
38215	syn	73	81	55	...	92	225	90	112	146	18
38223	syn	5	14	18	13	37	161	47	69	83	10
38225	syn	12	10	23	14	44	162	36	55	82	9
38226	syn	27	29	46	33	56	168	47	60	96	...
38232	syn	20	30	36	34	95	225	97	123	129	38
38255	syn	48	67	47	...	95	227	90	115	129	38
38262	syn	6	10	24	20	59	192	52	77	92	7
38276	syn	6	12	34	21	68	200	72	100	108	12
38303	syn	21	40	40	33	70	194	67	86	100	11
38319	syn	...	17	28	...	51	179	55	84	83	6
38323	syn	30	45	49	57	89	203	82	107	120	23
38330	syn	7	11	syn	...	21	11	35	147	35	54	79	7
39026	syn	11	33	44	39	83	222	93	115	135	23
39033	syn	9	17	14	11	15	...	14	41	63	...
39034	syn	...	9	19	...	42	169	42	59	77	...
39037	syn	7	22	22	58	196	52	76	104	10
39043	syn	...	6	30	23	33	164	37	52	79	...
39044	syn	...	13	21	12	35	164	42	72	80	6
39048	syn	150	164	77	367	171	176	205	156
39056	syn	7	15	10	18	137	28	49	61	...
39063	syn	...	10	15	9	14	54
39067	syn	36	51	35	39	...	209	86	114	116	35
39086	syn	12	23	23	18	55	178	52	75	99	8

Table 4a—Continued

Star (LEID)	Wavelength (Å)	Equivalent Widths (mÅ)											
		[O I]	6154.23	6160.75	6696.03	6698.67	6155.13	6237.32	6162.18	6166.44	6169.04	6169.56	6210.67
Ion	Na I	Al I	Al I	Si I	Si I	Ca I	Ca I	Ca I	Ca I	Sc I	Sc I	Sc I	Sc I
E.P. (eV)	2.10	3.14	5.62	5.61	2.52	1.90	2.52	2.52	2.52	0.00	0.00	0.02	0.02
Log gf	-1.57	-1.57	-1.89	-0.78	-1.07	-1.28	-0.07	-1.11	-0.69	-0.42	-1.53	-1.30	-1.30
Log ϵ_{\odot}	8.93	6.33	6.47	7.55	7.55	6.36	6.36	6.36	6.36	3.10	3.10	3.10	3.10
39088	syn	6	16	26	30	40	162	40	...	99	7
39102	syn	5	5	18	24	...	30	48	63
39119	syn	5	15	14	32	153	31	57	69	...
39123	syn	6	17	17	133	17	44	56
39129	syn	20	37	...	197	76	96	109	26	...
39141	syn	3	7	syn	...	22	12	45	178	51	75	95	7
39149	syn	59	69	53	...	108	241	107	115	140	48
39165	syn	8	4	syn	...	22	...	31	179	41	50	81	6
39186	syn	...	10	syn	...	27	15	38	183	43	77	76	...
39187	syn	5	10	21	13	43	180	42	68	85	...
39198	syn	...	5	26	17	45	179	50	75	96	7
39204	syn	8	11	21	19	27	155	36	49	72	...
39215	syn	5	12	33	23	36	163	36	58	74	...
39216	syn	15	18	10	...	29	144	38	55	76	...
39225	syn	8	12	26	26	...	138	41	66	70	...
39235	syn	24	40	43	50	71	201	68	87	123	19
39245	syn	25	49	syn	syn	32	23	...	236	96	121	134	60
39257	syn	38	63	38	46	109	250	109	132	148	66
39259	syn	6	10	25	17	50	175	46	75	85	8
39284	syn	15	16	syn	syn	24	22	60	208	55	81	106	...
39289	syn	...	10	14	12	30	154	30	56	72	...
39298	syn	4	8	23	12	25	141	13	33	69	...
39301	syn	8	9	29	19	49	71	84	...
39306	syn	...	12	syn	syn	26	14	46	184	51	71	89	10
39325	syn	57	81	47	...	117	249	105	132	159	61
39329	syn	...	12	25	24	146	...	83
39345	syn	3	10	23	26	46	146	32	59	77	5
39346	syn	29	55	53	48	...	245	107	123	145	40
39352	syn	9	17	25	18	48	181	58	73	94	13
39384	syn	9	17	46	39	60	195	60	76	108	...

Table 4a—Continued

Star (LEID)	Wavelength (Å)	Equivalent Widths (mÅ)												
		[O I]	6154.23	6160.75	6696.03	6698.67	6155.13	6237.32	6162.18	6166.44	6169.04	6169.56	6210.67	6305.66
39392	syn	112	126	72	281	115	150	159	60	...
39401	syn	21	44	42	38	69	200	70	...	117	26	...
39921	syn	7	10	34	24	56	185	60	83	93	12	...
40016	syn	10	20	syn	...	34	29	72	203	68	102	123
40031	syn	...	11	19	18	28	144	32	50	70
40041	syn	14	25	syn	syn	37	37	66	177	56	63	103
40108	syn	4	14	...	19	147	32	35	66
40123	syn	40	47	syn	syn	45	237	91	122	138	40	...
40135	syn	7	8	24	16	42	180	56	74	91	...	17
40139	syn	50	83	47	...	80	224	91	120	131	38	59
40162	syn	12	21	24	31	54	156	43	65	81
40166	syn	33	51	46	47	67	193	71	87	118	14	...
40168	syn	12	17	28	25	36	159	43	56	80	...	11
40170	syn	...	9	17	14	38	152	37	...	84
40207	syn	27	39	42	...	90	211	85	89	123	25	...
40210	syn	4	9	12	...	46	141	28	58	59
40216	syn	9	13	syn	syn	28	15	67	194	68	92	109	20	32
40220	syn	...	26	39	33	57	161	40	66	89
40232	syn	118	148	54	...	148	320	141	154	178	108	...
40235	syn	10	13	25	20	46	165	47	70	84	8	...
40237	syn	23	37	45	...	79	195	75	83	101	22	...
40275	syn	...	6	18	17	36	160	40	58	73
40291	syn	13	15	41	38	60	189	54	74	96
40318	syn	86	100	58	242	101	138	148	45	...
40339	syn	90	111	62	...	137	284	138	149	171	88	...
40349	syn	16	23	36	30	63	184	59	87	104	9	...
40358	syn	107	120	syn	syn	49	294	132	145	185	92	...
40361	syn	5	7	19	...	30	141	28	52	75
40371	syn	32	55	41	43	94	222	94	115	137	34	...
40372	syn	3	6	20	15	32	165	33	57	79

Table 4a—Continued

	Wavelength (Å)	[O I]	6154.23	6160.75	6696.03	6698.67	6155.13	6237.32	6162.18	6166.44	6169.04	6169.56	6210.67	6305.66
Ion	Na I	Na I	Al I	Al I	Si I	Si I	Ca I	Sc I	Sc I					
E.P. (eV)	0.00	2.10	3.14	5.62	5.61	2.52	1.90	2.52	2.52	2.52	2.52	0.00	0.02	
Log gf	-9.75	-1.57	-1.27	-1.89	-0.78	-1.07	-1.28	-0.07	-1.11	-0.69	-0.42	-1.53	-1.30	
Log ϵ_{\odot}	8.93	6.33	6.33	6.47	6.47	7.55	7.55	6.36	6.36	6.36	6.36	3.10	3.10	
Star (LEID)														
40373	syn	9	23	35	20	41	74	86	5	...
40409	syn	4	4	25	20	29	157	29	50	82
40420	syn	7	18	124	23
40424	syn	24	36	41	141	...	60	72
40472	syn	8	8	27	17	77	216	73	102	118	30	48
40479	syn	...	18	31	18	58	182	60	74	97	7	...
41015	syn	20	23	25	...	157	38	73	79
41025	syn	...	23	20	...	34	153	99
41033	syn	117	138	60	...	153	298	144	148	195	99	...
41034	syn	...	10	syn	...	26	16	52	183	50	83	90
41035	syn	...	6	21	8	35	173	43	...	96	9	7
41039	syn	10	15	21	16	51	178	53	65	95
41060	syn	25	39	syn	syn	33	34	92	224	88	127	125	44	79
41061	syn	...	26	syn	syn	27	25	58	190	73	89	105	11	28
41063	syn	3	30	17	37	165	40	62	73	9	...
41164	syn	20	36	35	38	63	181	60	76	103
41186	syn	8	24	17	39	163	41	61	84
41201	syn	9	13	13
41230	syn	11	16	22	23	39	155	35	65	79	7	...
41232	syn	7	30	149	23	24	56
41241	syn	...	7	17	...	45	189	57	80	94	10	...
41243	syn	7	13	22	16	30	150	37	57	73
41246	syn	9	7	29	19	34	152	44	67	77
41258	syn	3	5	10	...	17	139	15	31	61
41259	syn	3	37	175	44	74	75	8	10
41262	syn	...	34	63	30	54	...	49
41310	syn	10	14	47	160	49	78
41312	syn	3	15	25	37	60
41313	syn	4	6	25	16	...	182	44	68	85
41321	syn	10	16	30	...	35	188	39	64	78

Table 4a—Continued

Star (LEID)	Wavelength (Å)	Equivalent Widths (mÅ)												
		[O I]	6154.23	6160.75	6696.03	6698.67	6155.13	6237.32	6162.18	6166.44	6169.04	6169.56	6210.67	6305.66
41348	Na I
41366	syn	13	18	43	28	42	166	47	76	85	7
41375	syn	...	12	38	38	152	36	63	90	...
41380	syn	68	109	38	43	65	217	62	84	123	...
41387	syn	17	28	54	...	106	279	134	148	166	90
41389	syn	6	38	35	69	182	64	73	104	15
41402	syn	9	10	15	11	29	148	25	44	75	...
41435	syn	...	32	21	10	...	151	38	50	72	...
41455	syn	80	103	34	30	75	212	75	99	115	20
41476	syn	58	82	45	...	126	297	128	144	172	84
41494	syn	...	15	60	59	...	333	...	150	175	122
42012	syn	7	17	34	34	62	171	60	82	99	...
42015	syn	7	12	syn	32	34	53	164	54	74	98	...
42023	syn	3	6	32	27	62	181	63	85	102	14
42039	syn	7	19	21	17	35	173	45	69	81	...
42049	syn	32	61	48	46	83	215	86	102	134	...
42054	syn	4	8	syn	22	20	55	195	60	83	104	14
42056	syn	5	21	13	39	173	40	64	82	...
42079	syn	21	40	42	39	62	179	61	79	101	9
42084	syn	22	45	42	44	56	190	67	86	95	20
42106	syn	23	42	44	...	61	178	78	79	95	...
42114	syn	17	31	40	34	59	197	60	85	105	19
42120	syn	9	29	35	42	55	175	52	69	92	16
42134	syn	5	9	24	...	22	49	53	...
42161	syn	7	11	syn	27	13	43	191	49	80	93	11
42162	syn	106	113	64	288	121	148	169	77
42169	syn	45	56	49	52	...	198	88	97	125	19
42174	syn	27	36	49	37	...	169	51	74	87	7
42175	syn	12	20	24	25	53	178	55	75	97	7
42179	syn	8	18	syn	syn	24	9	44	179	50	75	...

Table 4a—Continued

	Wavelength (Å)	[O I]	6154.23	6160.75	6696.03	6698.67	6155.13	6237.32	6162.18	6166.44	6169.04	6169.56	6210.67	6305.66
Ion	Na I	Al I	Al I	Al I	Si I	Si I	Ca I	Sc I	Sc I					
E.P. (eV)	0.00	2.10	3.14	5.62	5.61	2.52	1.90	2.52	2.52	2.52	2.52	0.00	0.02	
Log gf	-9.75	-1.57	-1.57	-1.89	-0.78	-1.07	-1.28	-0.07	-1.11	-0.69	-0.42	-1.53	-1.30	
Log ϵ_{\odot}	8.93	6.33	6.33	6.47	6.47	7.55	7.55	6.36	6.36	6.36	6.36	3.10	3.10	
Star (LEID)														
42182	syn	5	9	15	14	...	144	21	
42187	syn	19	34	45	45	36	192	63	92	97	14	
42196	syn	13	33	150	39	52	73	...	
42198	syn	19	12	33	26	55	171	39	80	71	...	
42205	syn	74	102	55	...	129	287	125	147	170	...	
42221	syn	9	17	19	16	28	155	37	58	65	9	
42260	syn	10	40	201	74	75	99	16	
42271	syn	2	7	15	...	25	134	21	41	69	6	
42302	syn	7	8	syn	...	26	15	67	225	65	89	103	21	
42303	syn	10	28	24	30	53	166	65	82	89	17	
42309	syn	40	77	86	75	68	236	84	100	142	12	
42339	syn	60	75	38	194	78	103	124	36	
42345	syn	...	6	12	13	...	131	16	37	55	...	
42361	syn	7	8	16	13	27	155	25	47	66	...	
42384	syn	25	30	34	...	99	223	96	122	128	41	
42385	syn	...	5	16	13	33	151	40	61	70	...	
42407	syn	...	27	165	50	76	80	...	
42415	syn	...	31	41	32	62	202	72	93	114	13	
42438	syn	42	56	39	...	84	210	80	102	116	29	
42457	syn	...	15	39	150	40	63	79	...	
42461	syn	...	11	syn	...	24	19	60	195	61	89	101	16	
42473	syn	45	69	54	...	84	214	84	111	125	36	
42497	syn	...	7	syn	syn	...	14	37	160	40	58	79	4	
42501	syn	5	29	18	...	163	48	77	79	15	
42503	syn	...	12	32	10	51	180	38	64	86	...	
42508	syn	7	16	29	26	61	177	55	82	97	22	
43010	syn	...	8	20	11	25	145	30	46	70	3	
43024	syn	10	19	23	10	34	...	40	59	75	5	
43036	syn	14	44	195	56	92	111	12	
43040	syn	9	21	31	34	42	156	37	57	81	...	

Table 4a—Continued

Star (LEID)	Wavelength (Å)	Ion	E.P. (eV)	Log gf	Log ϵ_{\odot}	Na I	Al I	Si I	Si II	Ca I	Ca II	Ca III	Ca IV	Sc I	Sc II	Sc III
43060	6300.31	6154.23	6160.75	6169.03	6169.67	6155.13	6155.13	6166.44	6166.44	6169.04	6169.56	6210.67	6305.66
43061	[O I]	0.00	2.10	2.10	3.14	3.14	5.62	5.61	2.52	1.90	2.52	2.52	0.00	0.02	0.02	0.02
43064	...	-9.75	-1.57	-1.27	-1.57	-1.89	-0.78	-1.07	-1.28	-0.07	-1.11	-0.69	-0.42	-1.53	-1.30	3.10
43068	...	8.93	6.33	6.33	6.47	6.47	7.55	7.55	6.36	6.36	6.36	6.36	3.10	107	230	35
Equivalent Widths (mÅ)																
43071	syn	11	29	42	67	75	75	...
43074	syn	129	151	69	368	174	174	207	146	...
43077	syn	7	syn	26	18	45	174	47	71	88	9	13
43081	syn	28	28	41	30	83	190	73	78	127	7	...
43084	syn	...	27	23	11	33	...	43	63	77	11	...
43087	syn	25	51	47	47	56	180	61	75	95
43091	syn	17	23	26	...	49	179	50	75	89	11	...
43095	syn	30	35	39	45	86	212	85	110	106	20	...
43101	syn	...	11	13	16	44	180	48	70	94
43104	syn	11	13	25	19	66	243	73	97	126	34	60
43108	syn	57	79	44	40	121	286	118	139	160	104	...
43111	syn	6	11	21	13	33	156	38	55	80
43134	syn	24	35	48	40	60	195	71	95	110	13	...
43139	syn	19	29	40	...	163	...	77	71
43158	syn	5	14	22	41	169	...	55	84
43189	syn	3	20	10	...	108	16	51	51
43216	syn	...	7	8	28	39	55
43233	syn	...	8	19	8	29	147	39	60	73
43241	syn	60	77	53	...	114	247	108	128	155	60	...
43258	syn	45	69	syn	43	46	113	244	108	126	153	49	...
43261	syn	13	16	150	33	50	70
43278	syn	17	31	29	...	65	247	70	98	133	45	...
43326	syn	67	92	syn	19	19	52	185	46	85	105	13	...
43330	syn	...	25	62	...	124	301	125	147	174	67	...
43351	syn	76	91	19	10	54	195	59	83	102	14	...
43367	syn	12	29	syn	20	...	26	129	20
43389	syn	24	44	47	...	120	270	118	136	163	84	...

Table 4a—Continued

	Wavelength (Å)	[O I]	6154.23	6160.75	6696.03	6698.67	6155.13	6237.32	6162.18	6166.44	6169.04	6169.56	6210.67	6305.66
Ion	Na I	Na I	Al I	Al I	Si I	Si I	Ca I	Sc I	Sc I					
E.P. (eV)	0.00	2.10	3.14	5.62	5.61	2.52	1.90	2.52	2.52	2.52	2.52	0.00	0.02	
Log gf	-9.75	-1.57	-1.27	-1.89	-0.78	-1.07	-1.28	-0.07	-1.11	-0.69	-0.42	-1.53	-1.30	
Log ϵ_{\odot}	8.93	6.33	6.33	6.47	6.47	7.55	7.55	6.36	6.36	6.36	6.36	3.10	3.10	
Star (LEID)														
43397	syn	...	6	17	...	19	46	42	...	
43399	syn	...	7	20	10	...	156	39	56	78	4	
43412	syn	4	5	28	18	56	196	57	78	104	...	
43433	syn	6	22	26	24	54	178	55	86	87	9	
43446	syn	16	14	30	44	80	...	15	
43458	syn	27	46	47	44	64	188	66	92	102	...	
43463	syn	...	16	19	11	17	153	...	52	48	...	
43475	syn	51	75	72	240	98	130	148	...	
43485	syn	6	18	26	23	38	164	47	70	84	...	
43539	syn	15	22	24	20	45	171	61	84	85	9	
44026	syn	41	59	51	...	90	219	86	108	130	33	
44042	syn	5	9	syn	...	21	16	32	163	42	57	80	5	
44056	syn	...	11	61	181	59	85	103	...	
44065	syn	...	2	20	17	29	157	34	53	81	...	
44067	syn	5	10	19	16	22	37	57	5	
44115	syn	10	17	24	25	56	204	66	100	97	16	
44120	syn	...	9	15	16	34	133	29	54	58	...	
44143	syn	5	7	syn	...	22	16	36	167	41	62	72	8	
44163	syn	8	11	29	21	46	171	50	56	103	8	
44188	syn	23	28	48	26	...	197	77	101	102	23	
44189	syn	51	64	223	79	101	115	26	
44198	syn	...	9	21	14	38	166	40	54	77	...	
44219	syn	...	7	21	19	35	171	44	68	79	6	
44231	syn	11	26	38	31	56	170	64	79	97	13	
44253	syn	...	24	35	36	...	174	69	76	96	12	
44271	syn	7	14	144	...	90	
44277	syn	37	62	46	...	133	298	115	126	140	121	
44304	syn	17	28	38	37	57	167	69	...	105	15	
44313	syn	11	19	syn	...	36	33	54	183	56	73	98	13	
44327	syn	4	9	18	15	46	167	46	60	91	...	

Table 4a—Continued

Star (LEID)	Wavelength (Å)	Ion	E.P. (eV)	Log gf	Log ϵ_{\odot}	Equivalent Widths (mÅ)
4300.31	6154.23	Na I	6.00	-1.57	8.93	6160.75
[O I]	2.10	Al I	3.14	-1.27	6.33	6696.03
		Si I	5.62	-1.89	6.47	6698.67
		Ca I	2.52	-0.78	7.55	6155.13
		Ca I	1.90	-1.07	7.55	6237.32
		Ca I	2.52	-1.28	6.36	6161.29
		Ca I	2.52	-0.07	6.36	6162.18
		Ca I	2.52	-1.11	6.36	6169.04
		Sc I	0.00	-0.42	3.10	6210.67
		Sc I	0.02	-1.53	3.10	6305.66
4337	syn	6	11	syn	syn	21
4343	syn	9	36	...	25	18
4380	syn	...	5	41
4424	syn	6	24	174
4426	syn	24	47	...	46	46
4426	syn	...	27	...	40	30
4435	syn	10	30	...	16	65
4446	syn	47	84	...	45	189
4449	syn	45	65	...	100	164
4462	syn	8	15	...	67	201
4468	syn	8	8	...	45	66
4493	syn	4	6	...	11	40
45082	syn	9	20	...	35	100
45089	syn	41	62	...	22	111
45092	syn	8	10	...	27	111
45093	syn	6	27	111
45126	syn	...	7	...	27	111
45177	syn	8	12	...	30	111
45180	syn	6	15	111
45206	syn	57	81	syn	syn	191
45215	syn	14	29	...	24	191
45232	syn	25	22	...	24	191
45235	syn	22	28	...	27	191
45238	syn	...	29	...	27	191
45240	syn	45	56	...	24	191
45246	syn	19	30	...	27	191
45249	syn	15	43	syn	syn	191
45272	syn	72	84	...	38	191
45285	syn	23	36	...	38	191
45292	syn	3	3	...	16	191
45309	syn	3	3	...	26	191

Table 4a—Continued

Star (LEID)	Wavelength (Å)	Equivalent Widths (mÅ)											
		[O I]	6154.23	6160.75	6696.03	6698.67	6155.13	6237.32	6162.18	6166.44	6169.04	6169.56	6210.67
Ion	Na I	Al I	Al I	Si I	Si I	Ca I	Ca I	Ca I	Ca I	Sc I	Sc I	Sc I	Sc I
E.P. (eV)	2.10	3.14	5.62	5.61	2.52	1.90	2.52	2.52	2.52	0.00	0.00	0.02	0.02
Log gf	-1.57	-1.57	-1.89	-0.78	-1.07	-1.28	-0.07	-1.11	-0.69	-0.42	-1.53	-1.30	-1.30
Log ϵ_{\odot}	8.93	6.33	6.47	7.55	7.55	6.36	6.36	6.36	6.36	3.10	3.10	3.10	3.10
45322	syn	24	46	40	39	...	228	101	124	142	...
45326	syn	19	24	30	23	58	173	58	73	94	...
45342	syn	76	94	56	245	105	121	154	45
45343	syn	13	25	33	33	47	174	50	80	83	7
45359	syn	11	18	26	17	45	178	50	75	92	...
45373	syn	32	32	33	199	70	90	113	21
45377	syn	5	6	18	...	44	166	48	62	87	...
45389	syn	...	17	28	19	53	175	51	77	91	...
45410	syn	29	147	33	43	75	4
45418	syn	9	13	31	...	68	173	56	92
45453	syn	17	49	syn	syn	44	46	58	199	57	86	113	...
45454	syn	25	45	45	37	...	258	72	91	142	...
45463	syn	22	51	37	...	62	192	80	96	114	17
45482	syn	...	42	43	43	67	184	62	75	101	...
46024	syn	9	12	27	23	62	226	64	89	114	19
46055	syn	19	25	42	32	29	180	56	69	106	...
46062	syn	18	43	31	23	65	225	80	109	116	...
46073	syn	63	82	syn	syn	57	248	106	125	150	60
46090	syn	...	9	8	...	23	134	...	48	52	...
46092	syn	53	72	49	...	123	268	118	142	156	61
46121	syn	79	89	76	65	...	331	165	...	204	100
46140	syn	14	15	25	23	47	175	50	72	85	...
46150	syn	23	41	42	32	...	253	109	139	143	66
46166	syn	11	13	38	23	44	170	59	75	85	...
46172	syn	20	48	44	36	69	202	84	100	124	18
46194	syn	16	19	25	22	53	183	58	76	107	...
46196	syn	6	22	15	...	127	...	43	53	...
46223	syn	23	37	30	...	72	198	71	92	114	21
46248	syn	...	29	23	21	53	178	57	81	96	11
46279	syn	...	26	139	28

Table 4a—Continued

Star (LEID)	Wavelength (Å)	Equivalent Widths (mÅ)											
		[O I]	6154.23	6160.75	6696.03	6698.67	6155.13	6237.32	6162.18	6166.44	6169.04	6169.56	6210.67
Ion	Na I	Al I	Al I	Si I	Si I	Ca I	Ca I	Ca I	Ca I	Sc I	Sc I	Sc I	Sc I
E.P. (eV)	2.10	3.14	5.62	5.61	2.52	1.90	2.52	2.52	2.52	0.00	2.52	0.00	0.02
Log gf	-1.57	-1.57	-1.89	-0.78	-1.07	-1.28	-0.07	-1.11	-0.69	-0.42	-1.53	-1.30	-1.30
Log ϵ_{\odot}	8.93	6.33	6.47	7.55	7.55	6.36	6.36	6.36	6.36	3.10	3.10	3.10	3.10
46289	syn	10	40	syn	...	21	15	39	163	39	60	88	...
46301	syn	...	6	26	12	45	165	38	61	87	...
46318	syn	5	3	11	30	159	31	56	77
46323	syn	13	20	20	...	54	174	50	78	82	...
46325	syn	...	14	24	147	27	47	69	...
46348	syn	11	15	21	154	44	62	66	...
46350	syn	13	21	44	38	71	223	76	100	110	...
46381	syn	21	33	34	...	77	190	67	93	114	...
46388	syn	...	17	18	17	...	145	31	57	70	5
46391	syn	13	33	32	52	179	45	77	85	8
46398	syn	...	7	28	21	...	23	29	63	...
46405	syn	...	9	21	...	23	...	25	44	66	...
46438	syn	...	11	13	18	21	...	24	57	54	...
47012	syn	7	11	27	23	63	198	67	87	115	...
47039	syn	5	17	26	20	29	152	33	54	70	...
47055	syn	...	1	18	18	38	169	44	68	88	...
47074	syn	...	10	25	...	36	...	23	46	67	...
47096	syn	30	42	50	57	78	190	68	86	118	19
47107	syn	...	18	syn	...	35	26	55	205	61	79	112	...
47110	syn	5	10	30	22	41	167	50	72	89	...
47146	syn	31	49	syn	syn	52	50	99	231	90	98	141	36
47150	syn	43	57	48	...	89	219	90	108	132	34
47151	syn	...	18	24	20	30	147	33	53	69	...
47153	syn	81	109	65	...	134	331	130	173
47176	syn	27	39	48	40	58	197	70	93	107	12
47186	syn	65	95	48	50	131	292	137	146	174	83
47187	syn	44	51	54	219	97	113	136	41
47199	syn	...	23	syn	syn	27	21	61	205	63	91	103	39
47269	syn	34	53	43	45	73	201	69	95	119	21
47299	syn	13	25	...	28	161	26	53	88	...

Table 4a—Continued

	Wavelength (Å)	[O I]	6154.23	6160.75	6696.03	6698.67	6155.13	6237.32	6162.18	6166.44	6169.04	6169.56	6210.67	6305.66
Ion	Na I	Na I	Al I	Al I	Si I	Si I	Ca I	Sc I	Sc I					
E.P. (eV)	0.00	2.10	3.14	5.62	5.61	2.52	1.90	2.52	2.52	2.52	2.52	0.00	0.02	
Log gf	-9.75	-1.57	-1.27	-1.57	-1.89	-0.78	-1.07	-1.28	-0.07	-1.11	-0.69	-1.53	-1.30	
Log ϵ_\odot	8.93	6.33	6.33	6.47	6.47	7.55	7.55	6.36	6.36	6.36	6.36	3.10	3.10	
Star (LEID)														
47307	syn	14	...	syn	syn	17	195	64	78	113	...	
47331	syn	...	11	136	22	
47338	syn	8	8	19	21	45	168	48	70	86	...	
47339	syn	24	28	42	33	50	151	59	...	91	...	
47348	syn	24	31	25	...	68	194	67	86	112	16	
47354	syn	87	97	syn	syn	66	246	109	126	157	54	
47387	syn	6	...	syn	...	25	15	37	167	52	68	95	8	
47399	syn	21	36	36	37	113	252	106	106	133	133	
47400	syn	29	45	38	40	78	204	78	110	112	18	
47405	syn	8	25	20	43	194	51	69	89	...	
47420	syn	24	34	40	39	59	185	77	74	121	...	
47443	syn	...	11	24	...	26	144	30	...	67	...	
47450	syn	8	9	16	14	35	149	43	65	78	...	
48028	syn	9	18	23	17	38	172	44	66	91	11	
48036	syn	18	32	27	...	156	30	59	77	11	
48049	syn	10	17	28	21	74	228	79	104	121	37	
48060	syn	15	25	28	22	46	241	65	92	113	32	
48067	syn	...	35	32	34	63	186	64	84	105	12	
48083	syn	35	39	47	...	78	214	75	94	118	30	
48099	syn	159	154	102	392	177	169	187	...	
48116	syn	147	164	syn	syn	85	403	188	...	230	152	
48120	syn	20	30	33	33	107	268	108	133	144	89	
48150	syn	40	52	50	...	148	309	148	156	160	...	
48151	syn	10	12	22	21	26	141	36	49	71	...	
48186	syn	10	24	32	156	35	62	68	10	
48197	syn	...	10	25	18	43	155	40	69	69	...	
48221	syn	34	54	45	...	81	208	82	100	114	22	
48228	syn	...	18	20	15	29	159	41	64	77	...	
48235	syn	38	50	syn	syn	41	39	97	225	95	113	134	29	
48247	syn	12	36	35	26	47	167	53	70	93	...	

Equivalent Widths (mÅ)

Table 4a—Continued

Star (LEID)	Wavelength (Å)	[O I]	Na I	Al I	Si I	Si I	Ca I	Sc I	Sc I				
	E.P. (eV)	0.00	2.10	3.14	5.62	5.61	2.52	1.90	2.52	2.52	2.52	0.00	0.02
	Log ϵ_{\odot}	-9.75	-1.57	-1.57	-1.89	-0.78	-1.07	-1.28	-0.07	-1.11	-0.69	-0.42	-1.53
	Star (LEID)	8.93	6.33	6.47	7.55	7.55	6.36	6.36	6.36	6.36	6.36	3.10	3.10
48259	syn	...	10	30	142	34	52	81
48281	syn	...	10	23	19	35	176	37	...	78	...
48305	syn	37	81	48	49	128	297	151	175	...	101
48323	syn	148	162	syn	syn	79	394	174	191	206	153
48367	syn	25	40	syn	syn	29	25	72	247	80	108	131	36
48370	syn	...	50	51	58	81	214	84	113	114	29
48392	syn	14	27	36	31	52	190	58	81	106	17
48409	syn	7	9	syn	...	17	15	23	42	56	4
49013	syn	14	15	34	25	65	195	63	93	102	14
49022	syn	4	16	...	23	152	33	40	79	...
49037	syn	...	9	23	15	25	163	...	42	77	...
49056	syn	146	175	68	...	170	364	175	188	212	142
49072	syn	...	2	25	13	...	157	32	61	72	10
49088	syn	...	11	24	17	...	148	41	66	77	...
49111	syn	80	92	59	219	92	105	135	34
49123	syn	5	9	21	13	44	200	47	69	91	...
49134	syn	...	19	syn	...	26	27	69	190	71	93	110	...
49148	syn	28	43	45	34	104	231	98	119	139	34
49177	syn	25	50	53	56	88	190	75	94	120	19
49179	syn	...	15	16	147	33	51	75	7
49188	syn	...	6	16	6	41	38	...
49193	syn	20	38	syn	syn	43	33	46	208	67	91	112	17
49205	syn	7	9	19	...	33	158	41	73	82	7
49212	syn	103	126	70	300	135	145	182	87
49238	syn	...	4	36	156	...	77	95	...
49249	syn	15	27	40	39	81	212	88	111	120	27
49252	syn	...	16	23	24	...	153	37	...	9	...
49255	syn	7	9	141	29	52	69	...
49293	syn	32	51	33	35	80	205	84	105	123	20
49322	syn	20	14	32	154	26	45	57	5

Table 4a—Continued

Star (LEID)	Wavelength (Å)	Equivalent Widths (mÅ)												
		[O I]	6154.23	6160.75	6696.03	6698.67	6155.13	6237.32	6162.18	6166.44	6169.04	6169.56	6210.67	6305.66
49333	syn	...	6	15	12	28	147	37	46	69
50022	syn	...	11	34	14	26	140	32	57	66	6	...
50037	syn	21	32	41	36	55	187	54	86	96
50046	syn	8	6	28	15	37	148	35	51	67
50066	syn	33	52	40	46	59	201	85	126	...	23	...
50078	syn	8	18	27	23	36	187	39	66	100	14	...
50108	syn	28	38	43	...	67	192	65	98	102	11	...
50109	syn	...	10	19	18	29	154	40	55	80
50133	syn	...	17	23	19	56	198	58	81	105	22	25
50163	syn	...	12	144	...	74
50167	syn	...	13	syn	...	32	22	53	177	49	72	95	7	17
50172	syn	16	44	48	32	58	178	63	82	105
50187	syn	37	56	syn	syn	48	44	125	275	126	140	164	77	149
50191	syn	24	36	48	38	58	180	58	...	108	16	...
50193	syn	70	88	55	265	110	138	161	80	...
50198	syn	18	36	53	44	65	192	73	107
50218	syn	36	56	syn	syn	42	...	86	221	84	106	125	33	...
50228	syn	9	21	21	25	51	181	61	74	104
50245	syn	8	10	syn	...	27	14	...	168	42	6	...
50253	syn	6	22	22	25	52	182	59	88	100	14	...
50259	syn	47	67	40	45	121	270	114	143	163	83	146
50267	syn	9	16	syn	...	25	17	39	174	46	63	99
50291	syn	9	10	syn	...	25	176	57	65	76	12	18
50293	syn	6	14	25	22	57	181	55	74	99	5	...
50294	syn	9	19	38	31	...	166	42	66	91
50304	syn	...	8	26	...	158	47	64	88	11	...
51021	syn	17	41	33	33	95	249	104	145	131	46	91
51024	syn	...	21	37	...	73	194	75	99	114	15	...
51074	syn	85	93	66	265	118	140	162	58	...
51079	syn	38	53	syn	syn	51	47	79	210	76	104	122	17	...

Table 4a—Continued

	Wavelength (Å)	[O I]	6154.23	6160.75	6696.03	6698.67	6155.13	6237.32	6162.18	6166.44	6169.04	6169.56	6210.67	6305.66
Ion	Na I	Al I	Al I	Al I	Si I	Si I	Ca I	Sc I	Sc I					
E.P. (eV)	0.00	2.10	3.14	5.62	5.61	2.52	1.90	2.52	2.52	2.52	2.52	0.00	0.02	
Log gf	-9.75	-1.57	-1.27	-1.57	-1.89	-0.78	-1.07	-1.28	-0.07	-1.11	-0.69	-1.53	-1.30	
Log ϵ_{\odot}	8.93	6.33	6.33	6.47	6.47	7.55	7.55	6.36	6.36	6.36	6.36	3.10	3.10	
Star (LEID)														
51080	syn	25	45	46	40	111	242	109	131	140	45	
51091	syn	9	16	16	20	33	172	30	55	73	6	
51121	syn	...	10	18	...	27	159	25	51	66	...	
51132	syn	124	134	69	75	...	328	157	...	193	97	
51136	syn	...	5	15	17	...	146	
51156	syn	13	29	syn	syn	35	34	50	195	49	77	100	15	
51254	syn	40	63	52	56	83	221	88	109	125	22	
51257	syn	8	6	21	17	23	141	33	49	62	...	
51259	syn	...	21	32	28	30	160	41	59	76	5	
52017	syn	6	16	27	18	64	228	74	94	122	30	
52035	syn	29	49	48	...	76	...	88	108	151	48	
52039	syn	4	6	22	8	13	...	18	36	50	...	
52103	syn	39	69	syn	syn	55	47	123	261	123	141	151	70	
52105	syn	5	18	20	22	44	170	48	69	86	...	
52106	syn	38	33	49	29	53	175	56	81	105	...	
52109	syn	5	17	22	20	34	184	37	57	81	...	
52110	syn	4	20	33	49	66	...	
52111	syn	147	161	syn	syn	71	345	168	164	200	145	
52133	syn	...	16	164	30	62	76	...	
52139	syn	21	36	syn	...	52	42	127	281	122	140	159	50	
52151	syn	8	11	25	...	42	151	44	61	72	...	
52154	syn	17	49	55	...	
52167	syn	6	10	26	15	46	189	53	73	91	11	
52180	syn	9	23	26	21	44	170	55	75	96	13	
52192	syn	38	28	53	...	50	66	100	...	
52204	syn	...	10	12	...	15	24	44	...	
52222	syn	5	19	12	25	...	32	49	68	...	
53012	syn	5	4	22	14	26	152	29	51	66	...	
53054	syn	...	8	18	15	32	151	37	54	67	8	
53058	syn	6	6	26	21	36	164	41	72	72	...	

Equivalent Widths (mÅ)

Table 4a—Continued

Star (LEID)	Wavelength (Å)	Equivalent Widths (mÅ)												
		[O I]	6154.23	6160.75	6696.03	6698.67	6155.13	6237.32	6162.18	6166.44	6169.04	6169.56	6210.67	6305.66
53067	Na I	2.10	Na I	Al I	Al I	Si I	Si I	Ca I	Ca I	Ca I	Ca I	Sc I	Sc I	...
53076	syn	20	50	49	40	68	190	78	...	102
53114	syn	18	36	36	38	95	234	97	117	144	38	...
53119	...	15	19	...	139	...	54	61
53132	syn	...	23	38	27	39	168	43	66	84
53178	syn	...	8	19	11	29	159	32	53	75	...	7
53185	syn	9	24	syn	...	23	19	64	198	66	84	111	16	32
53203	syn	4	6	19	16	30	143	35	55	66
54018	syn	29	45	39	31	46	182	55	82	100	7	...
54022	syn	144	167	85	357	163	178	198	141	...
54031	syn	45	72	syn	syn	53	57	...	282	140	146	173	87	...
54064	syn	8	9	25	...	32	156	...	49	75
54073	syn	12	16	16	159	20
54084	syn	10	23	19	...	21	154	...	62	77
54095	syn	24	14	...	147	31	67
54105	syn	102	132	66	...	131	285	125	154	170	86	...
54132	syn	...	6	24	16	42	173	43	75	76	13	...
54148	syn	5	16	syn	...	32	23	76	220	83	110	121	33	57
54154	syn	...	10	19	12	24	39	63
55028	syn	27	49	syn	...	48	47	118	255	119	136	154	63	...
55029	syn	31	53	46	48	85	216	89	105	128	20	...
55056	syn	16	20	43	27	41	157	46	56	86	7	...
55063	syn	28	39	41	...	82	195	77	91	130	25	...
55071	syn	134	163	69	...	174	366	175	43	60	77	148
55089	syn	...	6	30	18	38	175	43	67
55101	syn	99	123	65	...	127	265	113	138	167	66	...
55102	syn	7	15	37	21	54	178	52	74	98	5	...
55111	syn	16	30	36	33	89	226	91	112	132	38	67
55114	syn	31	50	38	34	110	238	115	122	147	82	134
55121	syn	105	131	64	323	150	168	194	116	...

Table 4a—Continued

Star (LEID)	Wavelength (Å)	Equivalent Widths (mÅ)												
		[O I]	6154.23	6160.75	6696.03	6698.67	6155.13	6237.32	6162.18	6166.44	6169.04	6169.56	6210.67	6305.66
55122	syn	51	64	syn	syn	57	55	96	221	93	122	119	38	57
55131	syn	...	10	15	...	39	158	34	55	89
55142	syn	98	129	56	...	142	285	126	147	178	79	...
55149	syn	87	118	58	...	119	260	122	137	164	71	...
55152	syn	21	46	syn	syn	46	37	58	187	65	103	87
55165	syn	12	10	21	19	...	156	41	58	81	7	...
56024	syn	23	40	49	41	71	201	75	99	110	20	...
56028	syn	...	3	syn	...	23	13	...	154	30	52	74
56040	syn	...	6	19	18	...	172	41	61	86
56056	syn	5	9	26	140	31	42	66
56070	syn	29	47	45	45	82	198	78	97	111	24	...
56087	syn	4	13	22	16	72	223	72	94	120	39	73
56106	syn	5	6	34	156	36	57	82	3	...
56114	syn	11	11	37	20	50	176	62	82	93
56118	syn	6	16	16	20	29	158	42	69	63	...	6
56128	syn	4	4	23	152	43	55	80	10	12
57010	syn	14	24	35	26	82	210	88	104	129	22	...
57029	syn	4	6	17	14	...	143	27	38	54
57054	syn	48	44	37	39	108	289	124	144	165	78	146
57058	syn	...	11	syn	...	22	22	...	159	48	58	83
57067	syn	8	...	syn	...	17	163	43	64	78
57073	syn	8	11	26	9	43	163	40	59	80
57076	syn	13	22	38	175	45	66	79	7	...
57083	syn	6	16	13	23	134	27	50	57
57085	syn	3	23	12	25	142	26	49	63
57091	syn	22	47	48	48	67	190	60	...	116	9	...
57114	syn	3	24	...	42	157	35	57	74	7	...
57127	syn	9	13	158	48
58043	syn	3	19	15	25	140	30	55	65	...	7
58059	syn	6	15	...	30	145	35	...	71

Table 4a—Continued

Star (LEID)	Wavelength (Å)	Equivalent Widths (mÅ)												
		[O I]	6154.23	6160.75	6696.03	6698.67	6155.13	6237.32	6162.18	6166.44	6169.04	6169.56	6210.67	6305.66
58077	syn	...	10	27	14	...	141	19
58087	syn	2	6	20	15	41	179	50	72	88
59016	syn	4	7	17	20	141	17	47	44
59024	syn	108	154	70	...	150	360	157	172	216
59036	syn	12	19	34	30	48	170	40	63	91	7	...
59047	syn	31	51	48	...	81	212	88	108	120	26	...
59085	syn	...	7	35	186	49	94	102	15	...
59089	syn	10	13	36	28	70	189	68	99	104	16	...
59090	syn	9	16	29	24	45	175	49	69	94	9	...
59094	syn	...	15	syn	...	17	...	19	...	25	46	61
60034	syn	3	17	13	19	131	21	49	69
60058	syn	164	156	syn	...	97	370	175	172	214	136	...
60059	syn	...	15	15	142	...	43	62
60064	syn	...	14	31	19	29	...	27	45	68
60065	syn	...	11	14	29	157	42	55	99
60066	syn	53	70	47	...	79	209	75	102	117	28	...
60067	syn	...	7	18	...	134	22
60069	syn	10	37	45	56	177	50	70	96
60073	syn	137	164	69	...	161	356	163	172	201	139	...
60088	syn	...	7	31	25	41	170	42	73	82
60101	syn	...	10	21	12	37	154	37	60	69
61015	syn	12	17	29	22	90	243	91	117	135	51	95
61026	syn	...	18	26	36	153	...	69	78
61042	syn	15	23	syn	...	33	25	58	192	64	81	117	12	...
61046	syn	...	5	syn	syn	...	15	33	144	31	46	71
61050	syn	60	87	syn	syn	50	...	105	258	111	139	148	51	...
61067	syn	124	163	72	73	...	340	158	167	200	124	...
61070	syn	11	15	syn	...	33	22	42	193	49	80	94	8	...
61075	syn	6	7	16	...	136	26	44	65
61085	syn	71	101	58	...	140	302	140	163	179	104	...

Table 4a—Continued

	Star (LEID)	Wavelength (Å)	[O I]	6154.23	6160.75	6696.03	6698.67	6155.13	6237.32	6162.18	6166.44	6169.04	6169.56	6210.67	6305.66
Ion		Na I	Na I	Al I	Al I	Si I	Si I	Ca I	Sc I	Sc I					
E.P. (eV)	0.00	2.10	3.14	5.62	5.61	2.52	1.90	2.52	2.52	2.52	2.52	2.52	0.00	0.02	
Log gf	-9.75	-1.57	-1.27	-1.57	-1.89	-0.78	-1.07	-1.28	-0.07	-1.11	-0.69	-0.42	-1.53	-1.30	
Log ϵ_{\odot}	8.93	6.33	6.33	6.47	6.47	7.55	7.55	6.36	6.36	6.36	6.36	6.36	3.10	3.10	
	62018	syn	5	10	syn	...	23	18	35	57
	62058	syn	...	45	50	46	70	197	72	91	117	14	...
	63021	syn	...	15	44	32	74	188	62	95	117
	63027	syn	...	13	26	14	26	150	30	53	74
	63052	syn	17	14	syn	...	32	22	57	183	55	84	100
	64023	syn	8	8	15	...	134	...	49	46
	64049	syn	19	20	38	31	51	186	50	95	...	9	...
	64057	syn	5	9	11	12	...	140	22	49	73
	64064	syn	14	26	16	23	142	27	45	64
	64067	syn	...	11	syn	...	19	5	36	164	51	66	81	11	...
	64074	syn	...	7	19	11	34	154	45	71	82
	65042	syn	5	16	16	12	...	25	39	52
	65046	syn	...	6	17	12	...	139	30	51	61
	65057	37	28	...	183	...	86	83
	66015	syn	4	12	28	16	31	144	30	54	69
	66026	syn	9	12	17	16	35	162	39	63	77
	66047	syn	17	44	94	233	108	112	148	30	51
	66054	syn	15	27	38	34	45	180	51	77	91	10	...
	67049	syn	...	17	6	...	12	...	30
	67063	syn	19	26	25	27	60	180	71	97	108	...	26
	68044	syn	4	9	22	20	...	146	37	64
	69007	syn	4	22	...	31	53	67
	69012	syn	...	11	24	17	40	187	51	78	89	...	18
	69027	syn	134	140	76	321	126	167	183	114	...
	70032	syn	...	25	24	17	37	160	40	63	79
	70035	syn	20	18	41	21	57	193	59	84	110	12	...
	70041	syn	24	33	28	14	41	159	42	60	84
	70049	syn	17	30	37	...	167	53	89	101	...	20
	71013	syn	...	9	13	18	34	67
	73025	syn	67	100	53	...	139	296	137	155	180	95	...

Table 4a—Continued

Star (LEID)	Wavelength (Å)	Equivalent Widths (mÅ)											
		[O I]	6154.23	6160.75	6696.03	6698.67	6155.13	6237.32	6162.18	6166.44	6169.04	6169.56	6210.67
75021	Na I	syn	4	18	18	45	162	33	66	81
76027	Na I	syn	8	20	syn	...	36	20	54	188	59	78	107
76038	Al I	syn	24	46	54	41	122	265	122	139	157
77025	Al I	syn	10	24	33	24	66	198	69	93	109
77030	Si I	syn	6	19	21	32	151	34	54	75
80026	Si I	syn	...	9	30	...	151	38
80029	Si I	syn	5	10	27	22	55	189	58	80	102
81018	Si I	syn	9	21	22	16	36	159	35	59	84
81019	Si I	syn	7	13	41	25	48	180	56	87	90
81028	Si I	syn	...	10	17	8	18	...	23	50	58
82015	Si I	syn	4	6	21	...	17	...	30	50	57
82029	Si I	syn	6	15	10	18	31	40
85027	Ca I	syn	...	17	29	24	66	190	73	95	102
85031	Ca I	syn	19	21	24	18	...	172	44	70	83
89009	Ca I	syn	11	14	34	163	43	64	94

^alines displaying the “syn” designation indicate those that were determined via spectrum synthesis instead of equivalent width measurements.

Table 4b. O–Eu Atomic Parameters, Equivalent Widths, and Solar Abundances

Wavelength (Å)	Ion	E.P. (eV)	Log g _f	Log ε _∞	Star (LEID)	Equivalent Widths (mÅ)												
						6245.62	6309.88	6146.23	6258.11	6261.10	6303.76	6312.24	6336.11	Ti I	Ni I	6175.37	6176.81	Ni I
5009	Sc II	1.51	−1.07	3.10	6017	45	18	...	83	72	...	16	...	27	35	21	9	71
	Sc II	1.50	−1.58	3.10	8014	38	40	35	...	4	...	19	5	...	26	syn
					9013	36	151	135	61	49	50	35	52	38	10	99
					10009	64	16	6	38	29	...	7	...	14	13	...	25	syn
					10012	36	36	25	12	16	...	29	syn	9
					11019	54	96	86	25	12	12	36	13	...	65	syn
					11021	57	29	...	88	81	29	21	13	23	36	16	16	115
					11024	67	27	...	94	87	37	20	22	27	49	...	60	syn
					12013	83	79	19	13	11	22	25	12	68	syn
					12014	36	134	127	61	41	36	40	53	35	14	90
					14010	31	8	...	37	17	29	syn
					15022	26	21	6	13	syn
					15023	51	24	...	52	41	8	...	10	14	40	syn
					15026	88	48	40	7	...	5	9	15	15	...	33
					16009	52	17	...	132	121	49	38	42	26	55	26	...	76
					16015	46	15	...	57	52	...	10	...	12	20	...	7	41
					16019	37	12	...	39	36	9	14	28	syn
					16027	28	8	...	32	26	...	6	...	7	33	syn
					17014	64	13	15	...	21	...
					17015	46	21	...	91	87	20	23	36	22	...	61
					17027	24	48	41	...	6	8	21	23	15	...	40
					17029	31	8	23	13	7
					17032	59	78	70	27	...	15	16	35	12	7	51
					17046	34	14	10	19	8
					18017	40	9	25	6	12
					18020	59	17	...	87	78	28	19	15	22	29	19	6	64
					18035	55	41	39	14	...	5	13	11	9	7	26
					18040	68	115	106	42	...	24	25	44	25	8	77

Table 4b—Continued

	Wavelength (Å)	6245.62	6309.88	6146.23	6258.11	6261.10	6303.76	6312.24	6336.11	6375.37	6176.81	6177.25	6186.71	6327.60	6262.29	6645.06
Ion	Sc II	Sc II	Ti I	Ni I	La II	Eu II										
E.P. (eV)	1.51	1.50	1.87	1.44	1.43	1.44	1.46	1.44	4.09	4.09	1.83	4.11	1.68	0.40	1.38	
Log gf	-1.07	-1.58	-1.51	-0.38	-0.49	-1.56	-1.55	-1.69	-0.55	-0.42	-3.53	-0.96	-3.14	-1.22	+0.12	
Log ϵ_{\odot}	3.10	3.10	4.99	4.99	4.99	4.99	4.99	4.99	6.25	6.25	6.25	6.25	6.25	1.22	0.51	
Star (LEID)																
18047	45	13	...	42	34	14	37	syn	...
19022	27	13	...	26	15	9	4	14
19062	49	18	...	51	46	16	...	8	11	19	11	35	syn	...
20018	55	60	46	19	36	syn	8
20037	50	...	9	66	65	17	32	12	4	47	syn	10	
20042	24	11	...	22	21	5	3	10	syn	...
20049	40	41	34	11	11	16	7	27	syn	...
21032	64	28	...	118	107	37	31	23	31	45	39	18	72	syn	...	
21035	50	20	...	42	39	...	8	...	13	19	6	...	29	syn	...	
21042	44	55	48	9	12	16	12	...	43	syn	...	
21063	40	...	2	29	24	...	4	4
22023	61	84	67	31	syn	10	
22037	47	22	...	45	41	9	18	20	9	3	39	syn	...	
22042	45	35	35	11	7	30	syn	...	
22049	39	30	29	7	30	syn	...	
22063	34	7	...	42	25	5	25	syn	...	
23022	28	22	14	...	3	
23033	53	18	...	42	32	29	syn	9	
23042	33	35	29	21	...	13	
23050	30	14	...	26	27	11	7	
23061	48	25	5	51	45	...	8	19	8	38	syn	...
23068	73	32	...	129	122	41	34	26	22	36	27	8	80	syn	15	
24013	76	28	82	65	56	28	33	38	99	syn	...	
24027	53	...	52	46	7	15	26	8	...	41	syn	...	
24040	30	8	6	9	
24046	63	20	...	81	75	20	12	...	15	22	16	6	54	syn	...	
24056	48	...	52	39	7	10	30	syn	...	
24062	62	...	12	110	102	36	30	24	39	29	9	72	syn	
25006	25	9	16	...	12	
25026	36	...	37	27	6	12	16	...	11	

Table 4b—Continued

	Wavelength (Å)	6245.62	6309.88	6146.23	6258.11	6261.10	6303.76	6312.24	6336.11	Ti I	6175.37	6176.81	Ni I	6186.71	6327.60	6262.29	6645.06
Ion	Sc II	Sc II	Ti I	Ni I	Ni I	Ni I	Ni I	Ni I	La II	Eu II							
E.P. (eV)	1.51	1.50	1.87	1.44	1.43	1.44	1.46	1.44	4.09	4.09	4.09	4.11	4.11	0.40	0.40	1.38	
Log gf	-1.07	-1.58	-1.51	-0.38	-0.49	-1.56	-1.55	-1.69	-0.55	-0.42	-3.53	-0.96	-3.14	-1.22	+0.12		
Log ϵ_{\odot}	3.10	3.10	4.99	4.99	4.99	4.99	4.99	4.99	4.99	6.25	6.25	6.25	6.25	6.25	1.22	0.51	
Star (LEID)																	
25043	85	31	..	148	137	58	44	35	24	46	30	..	89	syn	..		
25062	79	42	14	169	149	54	44	31	22	33	37	10	90	syn	..		
25065	..	42	152	122	134	69	50	70	..	132	syn	..			
25068	71	34	..	99	88	..	23	..	21	33	23	..	72	syn	..		
26010	36	19	12	
26014	37	31	29	3	12	
26022	43	15	..	45	20	
26025	78	32	..	159	43	35	29	22	30	32	32	11	85	syn	..		
26030	17	16	10	10	syn	..		
26069	28	26	22	
26072	50	16	..	43	42	11	12	15	31	syn	
26086	172	173	84	89	69	33	50	51	97	syn	..	
26088	60	..	6	88	90	27	19	13	21	10	58	syn	..	
27048	81	74	..	14	12	23	40	15	8	
27050	31	16	..	22	19	4	7	15	syn	
27073	42	45	41	15	23	37	syn	
27094	43	11	..	33	15	..	5	..	6	7	7	22	syn	..	
27095	132	113	21	79	syn	..	
28016	43	47	47	16	34	syn	
28020	41	27	28	14	13	8	17	syn	
28044	56	20	3	67	58	..	9	7	17	22	12	9	48	syn	
28069	49	24	..	57	53	..	6	9	16	20	12	6	49	syn	
28084	44	59	48	13	13	27	14	7	36	syn	
28092	54	66	59	12	50	syn	
29029	55	22	3	65	62	..	10	46	syn	
29031	44	21	24	
29037	44	25	21	13	
29059	63	..	8	68	59	19	14	49	syn	
29067	73	36	90	100	108	syn	
29069	70	31	..	99	94	31	74	syn	

Equivalent Widths (mÅ)

Table 4b—Continued

	Wavelength (Å)	6245.62	6309.88	6146.23	6258.11	6261.10	6303.76	6312.24	6336.11	6175.37	6176.81	6186.71	6177.25	6327.60	6262.29	6645.06
Ion	Sc II	Sc II	Ti I	Ni I	La II	Eu II										
E.P. (eV)	1.51	1.50	1.87	1.44	1.43	1.44	1.46	1.44	4.09	4.09	4.11	4.11	4.18	0.40	1.38	
Log gf	-1.07	-1.58	-1.51	-0.38	-0.49	-1.56	-1.55	-1.69	-0.55	-0.42	-3.53	-0.96	-3.14	-1.22	+0.12	
Log ϵ_{\odot}	3.10	3.10	4.99	4.99	4.99	4.99	4.99	4.99	6.25	6.25	6.25	6.25	6.25	1.22	0.51	
Star (LEID)																
29072	39	37	32	7	14	6	...	29	syn	...	
29085	44	34	8	14	27	syn	...	
29089	40	36	28	syn	...	
29099	79	119	112	47	33	28	26	36	32	11	86	syn	29
29106	58	64	50	12	19	15	...	35	syn	...	
30013	79	111	88	...	18	...	22	44	20	9	66	syn	...
30019	55	22	...	71	64	25	14	...	20	30	30	14	...	46	syn	...
30022	36	12	...	25	24	15	...	5
30031	84	34	...	171	156	61	45	33	24	54	22	...	87	syn	14	
30069	20	9	6	...	4	
30094	54	72	63	7	14	58	syn	...
30124	45	62	49	28	33	syn	...
31016	28	10	...	33	24	syn	...	
31041	60	54	41	...	7	...	19	40	syn	...
31047	44	25	16	
31048	40	18	15	10	
31075	44	27	
31079	55	44	36	...	4	...	10	21	7	5	34	syn	...	
31094	50	16	...	37	38	29	syn	13
31095	48	37	17	syn	10	
31104	syn	...	
31109	50	50	49	36	syn	...
31110	75	133	127	52	42	33	31	43	35	...	93	syn	...	
31119	65	31	...	115	103	...	29	24	29	51	22	12	...	syn	...	
31133	26	10	...	22	16	11	7	...	9	
31139	46	18	...	44	36	10	21	...	7	35	syn	...	
31141	65	29	...	60	56	...	7	...	18	25	...	4	45	syn	...	
31147	34	19	25	13	...	38	syn	...	
31152	58	55	33	24	23	12	...	syn	...	
32014	33	27	27	13	17	...	5	25	syn	...	

Table 4b—Continued

Star (LEID)	Wavelength (Å)	Equivalent Widths (mÅ)											
		Sc II	Ti I	Ti I	Ti I	Ti I	Ni I	Ni I	Ni I	La II	Eu II		
32026	6245.62	6309.88	6146.23	6258.11	6261.10	6303.76	6312.24	6336.11	6175.37	6186.71	6327.60	6262.29	6645.06
Ion	Sc II	Sc II	Ti I	Ni I	Ni I	Ni I	Ni I	La II	Eu II				
E.P. (eV)	1.51	1.50	1.87	1.44	1.43	1.44	1.46	1.44	4.09	1.83	4.11	0.40	1.38
Log gf	-1.07	-1.58	-1.51	-0.38	-0.49	-1.56	-1.55	-1.69	-0.42	-3.53	-0.96	-3.14	+0.12
Log ϵ_{\odot}	3.10	3.10	4.99	4.99	4.99	4.99	4.99	4.99	6.25	6.25	6.25	1.22	0.51
32027	51	79	69	17	23	39	15	9	54
	42	36	9	25	...	5	17
32043	43	15	19	syn
	52	27	...	55	50	17	19	19	12	...	44
32063	52	19	9	15
	26	25	26	10	22	6	8	syn
32069	37	6	63	54	15	...	13	20	22	10	51
	51	4	64	61	...	11	9	17	20	12	40
32100	53	24	18	9
	29	31	...	144	137	45	44	...	19	...	17
32101	75	44	10	...	51	48	11	88
	57	73	74	21	25	11	...	7
32125	32130	36	31	33	14	30
	75	31	...	144	163	147	89	...	70	41	67	36	43
32138	32140	44	10	...	99	92	18
	57	149	134	51	40	35	24	39	30	10	...
32144	32165	59	25	...	76	67	19	11	...	17	27	16	7
	32169	51	...	50	57	53	10	21	10	...	39
	32171	43	...	34	39	22	16	...	71
33006	80	69	57	...	7	...	20	23	16	...
	33011	59	25	...	76	67	19	11	...	15	...	8	43
33018	51	189	175	76
	33030	43	129	125	48	36	30	26	40	35	...
33051	66	28	55	55	24	9	...
	33064	42	12	64	61	8	...
33099	14	...	36	31	8	...	12	12	...	113
	33114	67	48	42	13
33115	55	34	34	61	...
	33126	53
33129	41	14	15	19	9	12	...
	33138	44	33	...
33145
33154	32
	33167	36	41	32

Table 4b—Continued

	Wavelength (Å)	6245.62	6309.88	6146.23	6258.11	6261.10	6303.76	6312.24	6336.11	6175.37	6176.81	6186.71	6177.25	6327.60	6262.29	6645.06
Ion	Sc II	Sc II	Ti I	Ni I	La II	Eu II										
E.P. (eV)	1.51	1.50	1.87	1.44	1.43	1.44	1.46	1.44	4.09	4.09	4.11	4.11	4.11	0.40	1.38	
Log gf	-1.07	-1.58	-1.51	-0.38	-0.49	-1.56	-1.55	-1.69	-0.55	-0.42	-3.53	-0.96	-3.14	-1.22	+0.12	
Log ϵ_{\odot}	3.10	3.10	4.99	4.99	4.99	4.99	4.99	4.99	6.25	6.25	6.25	6.25	6.25	1.22	0.51	
Star (LEID)																
33177	38	21	17
34008	54	25	...	51	48	21	44	syn	...
34029	87	29	...	179	170	77	62	53	40	45	48	106	syn	...
34040	45	47	39	10	14	15	30	syn	...
34056	35	27	20	13
34069	56	16	...	59	52	19	30	10	9	46	syn	
34075	84	31	...	110	99	38	29	21	24	56	21	...	74	syn	...	
34081	51	24	...	57	59	6	16	24	9	5	38	syn	...	
34129	34	17	6	20	10	...	18	syn	...	
34130	33	12	
34134	66	32	5	85	101	28	19	13	20	31	24	7	68	syn	...	
34143	...	39	...	140	121	50	29	61	28	...	84	syn	17	
34163	32	syn	...	
34166	59	43	38	19	12	...	syn	...	
34169	70	83	69	...	15	19	21	31	18	60	syn	...
34175	60	109	102	36	18	76	syn	...
34180	84	...	169	138	55	137	syn	34
34187	50	19	...	38	32	19	27	syn	...
34193	55	27	4	67	62	...	11	...	16	25	12	5	44	syn	...	
34207	56	16	...	81	84	18	14	15	21	42	20	9	64	syn	9	
34214	50	22	6	18	
34225	...	27	...	152	141	81	52	...	36	9	97	syn	...	
34229	46	16	...	35	26	31	syn	...
35029	43	40	34	8	12	10	13	...	31	syn	...
35035	41	18	...	33	27	18	20	syn	...
35046	55	22	9	56	52	14	15	27	...	7	41	syn	...	
35053	49	37	31	7	11	7	3	30	syn	...	
35056	72	32	...	137	142	53	32	30	20	85	syn	...	
35061	83	32	...	106	97	...	20	44	18	8	77	syn	24	
35066	65	27	...	93	89	28	18	14	16	23	25	6	67	syn	...	

Equivalent Widths (mÅ)

Table 4b—Continued

	Wavelength (Å)	6245.62	6309.88	6146.23	6258.11	6261.10	6303.76	6312.24	6336.11	6175.37	6176.81	6186.71	6177.25	6327.60	6262.29	6645.06
Ion	Sc II	Sc II	Ti I	Ni I	La II	Eu II										
E.P. (eV)	1.51	1.50	1.87	1.44	1.43	1.44	1.46	1.44	4.09	4.09	4.11	4.11	4.11	0.40	1.38	
Log gf	-1.07	-1.58	-1.51	-0.38	-0.49	-1.56	-1.55	-1.69	-0.55	-0.42	-3.53	-0.96	-3.14	-1.22	+0.12	
Log ϵ_{\odot}	3.10	3.10	4.99	4.99	4.99	4.99	4.99	4.99	4.99	6.25	6.25	6.25	6.25	1.22	0.51	
Star (LEID)																
35071
35074	57	48	40	8	16	20	7	...	35	syn	...
35087	42	22
35090	82	34	...	146	121	60	48	34	30	56	28	...	97	syn
35093	syn
35124	63	69	39	11	45	syn	...
35157	...	34	...	111	91	30	33	31	79	syn	17
35165	47	25	45	4	13	19	11	7	35	syn	...
35172	163	155	...	51	69	37	63	102	syn	...
35190	49	16	...	38	42	12	19	6	...	syn	...
35201	124	...	39	...	28	58	29	11	87	syn
35204	35	26
35216	63	22	...	95	86	27	17	10	9	63	syn	12
35228	47	11	18	33	syn	...
35230	55	25	...	49	49	...	7	...	15	18	12	40	syn	...
35235	61	30	5	84	75	16	7	64	syn	...
35240	67	87	82	11	...	37	13	63	syn	...
35248	46	12	...	45	41	...	5	20	28	syn	...
35260	48	41	37	4	30	...
35261	44	67	60	18	25	9	10	...	39	syn	...
36028	48	30	20	...	9	6	8	18
36036	100	98	...	18	14	21	8	68	syn	...
36048	41	40	29	10	7	16	syn
36059	41	34	26	16	12	15
36061	52	82	72	...	20	13	56	syn	...
36087	37	27	28	7	14	19	syn	...
36106	52	21	...	35	33
36110	9	10	...	20	...
36113	42	30	33	13	31	syn	...
36134	102	136	56	35	54	27	...	98	syn	11

Table 4b—Continued

Star (LEID)	Wavelength (Å)	Equivalent Widths (mÅ)														
		Sc II	Ti I	Ni I	Ni I											
36156	6245.62	6309.88	6146.23	6258.11	6261.10	6303.76	6312.24	6336.11	6175.37	6176.81	6177.25	6186.71	6327.60	6262.29	6645.06	
Ion	Sc II	Sc II	Ti I	Ni I	Ni I	Lα II	Eu II									
E.P. (eV)	1.50	1.87	1.44	1.43	1.44	1.44	1.44	1.44	1.44	1.44	1.44	4.09	4.11	1.68	0.40	1.38
Log gf	-1.07	-1.58	-1.51	-0.38	-0.49	-1.56	-1.55	-1.69	-0.55	-0.42	-3.53	-0.96	-3.14	-1.22	+0.12	0.51
Log ϵ_{\odot}	3.10	3.10	4.99	4.99	4.99	4.99	4.99	4.99	6.25	6.25	6.25	6.25	6.25	1.22	0.51	syn

Table 4b—Continued

	Wavelength (Å)	6245.62	6309.88	6146.23	6258.11	6261.10	6303.76	6312.24	6336.11	Ti I	6175.37	6176.81	6186.71	6327.60	6262.29	6645.06
Ion	Sc II	Sc II	Ti I	Ni I	Ni I	Ni I	Ni I	Ni I	La II	Eu II						
E.P. (eV)	1.51	1.50	1.87	1.44	1.43	1.44	1.44	1.44	4.09	4.09	4.11	4.11	4.11	0.40	1.38	
Log gf	-1.07	-1.58	-1.51	-0.38	-0.49	-1.56	-1.55	-1.69	-0.55	-0.42	-3.53	-0.96	-3.14	-1.22	+0.12	
Log ϵ_{\odot}	3.10	3.10	4.99	4.99	4.99	4.99	4.99	4.99	4.99	6.25	6.25	6.25	6.25	1.22	0.51	
Star (LEID)																
37179	41	16	27	10	14	14	12	10	...	syn	5
37184	52	40	31	6	14	30	...	13
37196	45	37	31	5	26	syn	...
37198	66	72	32	20	30	24	51	syn	7
37215	35	20	12	syn
37232	139	137	44	35	29	24	44	33	89	syn	...
37247	53	52	46	12	5	37	syn	...
37253	62	28	...	71	85	12	14	17	17	25	8	54	syn	13
37271	58	...	8	85	81	16	15	17	36	14	7	59	syn	9
37275	74	29	...	91	89	19	...	15	28	45	28	69	syn	...
37318	104	...	74	...	128	123	116	51	55	...	126	syn	21
37322	33	3
37329	51	22	...	47	41	11	16	14	33	syn	...
38011	95	128	118	...	28	41	...	53	84	syn	...
38018	56	50	40	12	28	6	33	syn	...
38049	76	33	3	99	91	...	14	13	18	27	26	66	syn	13
38052	64	20	...	98	96	26	17	16	21	22	33	69	syn	...
38056	43	13	...	35	32	36	syn	...
38057	85	78	29	...	23	56	syn	...
38059	121	184	...	72	75	41	53	50	syn	21	
38061	26	18	9	6	
38096	40	42	29	7	34	syn	...	
38097	61	21	168	82	70	57	37	48	43	24	...	93	syn	...
38105	46	19	...	42	47	7	35	syn	...	
38112	62	89	78	26	17	21	25	47	10	11	60	syn	...	
38115	72	113	85	...	27	20	22	67	syn	...
38129	55	20	...	72	63	12	15	32	12	...	48	syn	...	
38147	61	70	71	...	20	26	...	34	23	syn	...	
38149	93	165	...	58	56	33	54	47	18	105	syn	
38156	54	57	50	...	8	...	18	28	11	5	39	syn	...	

Equivalent Widths (mÅ)

Table 4b—Continued

	Wavelength (Å)	6245.62	6309.88	6146.23	6258.11	6261.10	6303.76	6312.24	6336.11	6175.37	6176.81	6177.25	6186.71	6327.60	6262.29	6645.06	
Ion	Sc II	Sc II	Ti I	Ni I	La II	Eu II											
E.P. (eV)	1.51	1.50	1.87	1.44	1.43	1.44	1.46	1.44	4.09	4.09	4.11	4.11	4.18	0.40	1.38		
Log gf	-1.07	-1.58	-1.51	-0.38	-0.49	-1.56	-1.55	-1.69	-0.55	-0.42	-3.53	-0.96	-3.14	-1.22	+0.12		
Log ϵ_{\odot}	3.10	3.10	4.99	4.99	4.99	4.99	4.99	4.99	6.25	6.25	6.25	6.25	6.25	1.22	0.51		
Star (LEID)																	
38166	54	17	...	53	49	20	14	...	40	
38168	89	148	128	...	43	45	27	72	syn	17	...	
38169	60	28	...	99	103	38	...	24	29	38	26	...	69	syn	
38175	69	25	9	121	117	39	34	24	21	35	30	...	77	syn	24	...	
38198	69	104	100	...	40	...	30	56	21	13	78	syn	
38204	66	85	78	14	29	18	5	58	syn	13	...	
38204	42	30	25	6	28	syn
38206	95	96	50	43	25	30	47	27	12	81	syn	
38215	53	52	24	...	18	18	22	11	6	42	syn	
38223	56	51	41	13	31	syn	
38225	44	60	45	14	25	9	syn	
38226	55	149	151	68	53	38	28	44	32	13	84	syn	
38232	77	35	17	131	109	26	47	26	...	87	syn	
38255	...	28	...	65	63	...	13	...	15	14	33	syn	
38262	68	28	...	85	69	11	17	57	syn	
38276	50	22	...	93	85	27	25	...	26	36	18	...	55	syn	
38303	70	83	68	19	32	64	syn	
38319	61	125	118	...	38	28	30	42	30	...	79	syn	
38323	77	...	17	102	96	...	37	29	50	25	30	
38330	40	...	40	35	10	6	...	16	22	syn	6	...	
39026	68	15	20	17	10	30	
39033	53	39	12	39	syn	
39034	51	23	...	87	83	20	15	...	15	26	16	8	66	syn	
39037	65	19	...	36	33	14	19	26	syn	
39043	41	61	58	7	46	syn	
39044	55	27	164	...	143	63	70	70	34	126	syn	
39048	21	22	14	6	...	18	
39056	31	12	12	...	4	...	syn	
39063	28	132	136	55	42	41	27	44	30	...	84	syn	
39067	78	69	69	19	...	11	19	26	14	9	58	syn	
39086	58	

Equivalent Widths (mÅ)

Table 4b—Continued

	Wavelength (Å)	6245.62	6309.88	6146.23	6258.11	6261.10	6303.76	6312.24	6336.11	6175.37	6176.81	6186.71	6177.25	6327.60	6262.29	6645.06
Ion	Sc II	Sc II	Ti I	Ni I	La II	Eu II										
E.P. (eV)	1.51	1.50	1.87	1.44	1.43	1.44	1.46	1.44	4.09	4.09	1.83	4.11	1.68	0.40	1.38	
Log gf	-1.07	-1.58	-1.51	-0.38	-0.49	-1.56	-1.55	-1.69	-0.55	-0.42	-3.53	-0.96	-3.14	-1.22	+0.12	
Log ϵ_{\odot}	3.10	3.10	4.99	4.99	4.99	4.99	4.99	4.99	6.25	6.25	6.25	6.25	6.25	1.22	0.51	
Star (LEID)																
39088	59	28	56	44	9	12	8	40	...	
39102	47	20	46	40	7	
39119	48	15	43	36	28	...	
39123	39	16	23	9	
39129	89	105	96	28	30	36	...	65	syn	...	
39141	59	23	65	66	...	8	...	17	23	16	5	54	syn	12
39149	142	130	71	43	60	38	...	104	syn	...
39165	58	23	41	43	7	11	31	7	...	44	syn	11
39186	54	20	53	8	40	syn	14
39187	53	69	60	...	6	...	13	55	syn	...
39198	65	22	74	69	19	10	...	19	27	11	6	57	syn	...
39204	49	42	44	11	18	9	8	33	syn	...
39215	48	14	42	33	32	syn	...
39216	48	41	36	22	33	syn	...
39225	43	42	41	11	17	9	syn	...
39235	79	99	88	...	15	...	22	73	syn	...
39245	74	42	155	78	65	52	32	48	47	21	101	syn	6	
39257	...	37	177	83	66	59	34	41	53	11	104	syn	...	
39259	55	15	68	62	...	9	...	21	19	21	...	38	syn	...
39284	70	27	91	90	32	16	15	18	33	19	...	66	syn	4
39289	40	44	41	13	13	13	...	29	syn	...
39298	35	23	17	24	syn	...
39301	41	52	36	13	18	12	...	30	syn	...
39306	58	23	66	63	19	24	18	...	48	syn	...
39325	168	96	67	71	35	66	39	11	99	syn	...	
39329	38	38	10	12	10	6	...	syn	...
39345	48	36	34	...	6	24	23	syn	...
39346	61	28	153	146	73	57	50	47	45	40	14	85	syn	...
39352	61	5	74	68	15	...	18	34	20	...	58	syn	...
39384	42	60	49	19	21	...	26	syn	...

Equivalent Widths (mÅ)

Table 4b—Continued

	Wavelength (Å)	6245.62	6309.88	6146.23	6258.11	6261.10	6303.76	6312.24	6336.11	6175.37	6176.81	6186.71	6177.25	6327.60	6262.29	6645.06
Ion	Sc II	Sc II	Ti I	Ni I	La II	Eu II										
E.P. (eV)	1.51	1.50	1.87	1.44	1.43	1.44	1.46	1.44	4.09	4.09	1.83	4.11	1.68	0.40	1.38	
Log gf	-1.07	-1.58	-1.51	-0.38	-0.49	-1.56	-1.55	-1.69	-0.55	-0.42	-3.53	-0.96	-3.14	-1.22	+0.12	
Log ϵ_{\odot}	3.10	3.10	4.99	4.99	4.99	4.99	4.99	4.99	6.25	6.25	6.25	6.25	6.25	1.22	0.51	
Star (LEID)																
39392	178	165	...	74	79	54	58	57	25	103	sym	...
39401	63	79	73	...	16	...	26	42	69	syn	...
39921	56	74	67	...	16	...	20	27	40	syn	...	
40016	58	88	84	...	16	10	25	37	21	10	63	syn	4	
40031	51	13	...	31	31	17	27	
40041	52	17	...	54	41	12	syn	8	
40108	32	13	13	...	7	23	syn	...	
40123	87	35	...	146	132	66	34	38	26	45	42	...	98	syn	10	
40135	74	68	...	16	...	17	23	14	9	56	syn	...	
40139	...	35	...	133	117	50	36	35	31	48	36	11	87	syn	...	
40162	53	59	58	...	9	...	15	21	11	...	37	syn	...	
40166	67	23	...	83	84	22	11	...	22	7	59	syn	...	
40168	51	22	...	34	36	11	23	11	...	38	syn	...	
40170	45	14	...	48	37	11	20	36	syn	...	
40207	79	35	...	105	94	...	34	31	26	47	26	...	89	syn	...	
40210	38	35	31	10	...	8	28	syn	...	
40216	63	23	...	100	98	34	24	...	25	27	26	...	67	syn	15	
40220	61	24	...	58	47	13	45	syn	...	
40232	...	35	122	105	99	45	82	45	16	...	121	syn	...	
40235	53	61	60	15	7	...	16	42	syn	...	
40237	81	83	74	17	33	17	61	syn	...
40275	46	45	42	20	23	11	5	37	syn	...	
40291	69	76	66	34	13	...	58	syn	...	
40318	...	22	...	131	129	...	35	64	34	53	87	syn	...	
40339	...	40	197	105	88	86	44	58	53	17	120	syn	...	
40349	67	26	...	90	84	...	19	34	19	...	54	syn	...	
40358	...	46	91	93	...	51	66	21	...	syn	24	
40361	38	19	...	31	33	8	23	syn	...	
40371	...	33	...	142	134	...	36	41	28	48	32	11	87	syn	...	
40372	49	20	...	59	50	7	16	18	13	...	41	syn	...	

Table 4b—Continued

	Wavelength (Å)	6245.62	6309.88	6146.23	6258.11	6261.10	6303.76	6312.24	6336.11	Ti I	6175.37	6176.81	Ni I	6186.71	6327.60	6262.29	6645.06
Ion	Sc II	Sc II	Ti I	Ni I	Ni I	Ni I	Ni I	Ni I	La II	Eu II							
E.P. (eV)	1.51	1.50	1.87	1.44	1.43	1.44	1.44	1.46	1.44	4.09	4.09	4.11	4.11	4.11	0.40	1.38	
Log gf	-1.07	-1.58	-1.51	-0.38	-0.49	-1.56	-1.55	-1.69	-0.55	-0.42	-3.53	-0.96	-3.14	-1.22	+0.12		
Log ϵ_{\odot}	3.10	3.10	4.99	4.99	4.99	4.99	4.99	4.99	4.99	6.25	6.25	6.25	6.25	6.25	1.22	0.51	
Star (LEID)																	
40373	57	17	...	49	39	...	8	...	13	36	syn	...	
40409	42	11	
40420	12	11	syn	7	
40424	43	24	...	33	41	16	32	syn	...	
40472	69	29	14	137	128	46	38	25	19	35	27	7	7	76	syn	...	
40479	51	16	...	59	59	16	49	syn	...	
41015	58	42	30	syn	...	
41025	42	30	31	16	24	syn	...	
41033	...	56	86	100	52	79	49	...	129	syn	...
41034	53	66	57	...	12	syn	...	
41035	57	14	...	66	53	14	6	6	...	21	14	5	5	42	syn	...	
41039	57	24	4	69	59	...	10	...	10	29	11	49	syn	...	
41060	78	36	15	...	137	57	44	41	29	45	38	10	98	syn	6	syn	
41061	66	21	...	83	90	...	13	58	syn	8	
41063	54	...	42	43	5	...	5	10	17	syn	...	
41164	62	24	...	62	54	...	6	...	40	13	44	syn	...	
41186	58	23	...	57	51	4	14	21	8	38	syn	...	
41201	33	9	...	23	13	12	
41230	49	38	18	15	33	syn	...	
41232	19	10	syn	...	
41241	62	16	...	79	78	24	16	15	63	syn	...	
41243	50	23	...	44	40	10	6	35	syn	
41246	45	16	...	48	43	17	20	11	34	syn	...	
41258	35	25	
41259	59	19	...	67	47	...	9	28	11	44	syn	...	
41262	syn	...	
41310	43	34	35	...	12	10	23	16	
41312	20	5	7	20	syn	...	
41313	54	14	...	62	59	...	6	5	10	25	8	40	syn	...	
41321	61	57	48	19	16	...	44	syn	...	

Equivalent Widths (mÅ)

Table 4b—Continued

	Wavelength (Å)	6245.62	6309.88	6146.23	6258.11	6261.10	6303.76	6312.24	6336.11	6175.37	6176.81	6186.71	6327.60	6262.29	6645.06
Ion	Sc II	Sc II	Ti I	Ni I	Ni I	Ni I	Ni I	La II	Eu II						
E.P. (eV)	1.51	1.50	1.87	1.44	1.43	1.44	1.46	1.44	4.09	4.09	4.11	4.11	0.40	1.38	
Log gf	-1.07	-1.58	-1.51	-0.38	-0.49	-1.56	-1.55	-1.69	-0.55	-0.42	-3.53	-0.96	-3.14	-1.22	+0.12
Log ϵ_{\odot}	3.10	3.10	4.99	4.99	4.99	4.99	4.99	4.99	6.25	6.25	6.25	6.25	1.22	0.51	
Star (LEID)															
41348	61	60	54	44
41366	52	17	48	15	19	9
41375	86	26	...	101	95	77	syn	...
41380	...	38	110	85	90	39	132	syn	...
41387	65	66	61	16	52	syn	...
41389	36	33	37	...	9	...	9	32	syn	...
41402	45	45	41	11	20	15	syn	...
41435	67	97	96	35	21	18	19	7	71	syn	...
41455	...	37	197	...	79	80	37	53	52	...	126	syn	...
41476	...	47	124	114	101	...	69	66	...	107	syn	...
41494	54	72	56	...	11	...	20	45	syn	...
42012	43	57	57	13	16	31	10	...	47	syn	...
42015	48	19	...	82	75	...	13	...	15	29	18	12	56	syn	...
42023	55	19	...	59	56	17	8	...	17	24	10	...	45	syn	...
42039	52	62	56	...	7	48	syn	...
42049	111	100	...	23	...	32	48	28	16	68	syn	...
42054	...	25	...	97	89	24	18	...	20	23	32	11	69	syn	9
42056	9	6	syn	...
42079	56	71	64	...	9	6	25	35	18	6	54	syn	...
42084	74	38	...	80	78	28	18	32	23	7	66	syn	...
42106	57	83	59	24	44	syn	...
42114	84	73	...	14	...	24	40	17	11	62	syn	...
42120	65	66	55	...	15	...	21	34	...	6	50	syn	...
42134	30	32	8	11	6	syn	...
42161	61	29	...	82	76	...	13	10	20	33	58	syn	...
42162	...	43	173	...	72	81	39	55	54	19	107	syn	9
42169	77	94	36	31	44	23	81	syn	...
42174	65	74	50	...	16	syn	...
42175	...	21	...	68	68	24	12	...	23	29	16	...	51	syn	...
42179	63	23	...	80	74	15	22	21	9	50	syn	11

Table 4b—Continued

Star (LEID)	Wavelength (Å)	Equivalent Widths (mÅ)													
		6245.62 Sc II	6309.88 Sc II	6146.23 Ti I	6258.11 Ti I	6261.10 Ti I	6303.76 Ti I	6312.24 Ti I	6336.11 Ni I	6175.37 Ni I	6176.81 Ni I	6327.60 La II	6262.29 Eu II	6645.06 Eu II	
42182	25	26	10	7	12	25	...	
42187	65	77	66	22	33	14	...	61	syn	...	
42196	41	29	30	9	8	syn	...	
42198	42	20	26	...	6	...	syn	...	
42205	...	33	210	67	87	34	47	60	...	115	
42221	45	37	33	10	10	15	...	26	syn	...	
42260	60	66	48	17	33	11	...	48	syn	...
42271	36	29	22	12	24	syn	...
42302	...	23	...	109	96	33	25	...	25	68	syn	15
42303	52	...	9	82	77	...	22	...	22	30	25	11	54	syn	...
42309	67	81	74	27	39	58	syn	...
42339	77	117	96	49	24	...	73	syn	...
42345	33	19	16	7	12	...	5	...	syn	...
42361	50	16	...	36	30	18	...	8	21	syn	...	
42384	...	30	...	144	145	68	55	45	29	44	33	16	93	syn	...
42385	46	44	36	7	...	18	8	syn	...
42407	40	61	31	19	...	33	syn	...
42415	86	81	19	25	36	22	10	66	syn	...
42438	...	34	...	102	92	27	41	24	...	79	syn	11
42457	54	51	54	11	syn	...
42461	67	26	...	100	91	25	23	...	19	28	27	5	63	syn	17
42473	87	35	...	111	101	38	40	...	37	53	34	11	88	syn	...
42497	47	16	...	45	43	6	37	syn	...
42501	55	23	...	66	64	18	19	23	13	...	41	syn	...
42503	43	46	40	10	26	11	syn	...
42508	49	16	...	75	68	19	...	26	11	...	46	syn	...
43010	45	39	32	14	13	...	26	syn	...
43024	39	38	12	14	12	5	26	syn	...
43036	82	74	22	...	23	syn	...
43040	57	47	40	25	10	syn	...

Table 4b—Continued

	Wavelength (Å)	6245.62	6309.88	6146.23	6258.11	6261.10	6303.76	6312.24	6336.11	6175.37	6176.81	6177.25	6186.71	6327.60	6262.29	6645.06	
Ion	Sc II	Sc II	Ti I	Ni I	La II	Eu II											
E.P. (eV)	1.51	1.50	1.87	1.44	1.43	1.44	1.44	1.44	4.09	4.09	4.11	4.11	4.11	0.40	1.38		
Log gf	-1.07	-1.58	-1.51	-0.38	-0.49	-1.56	-1.55	-1.69	-0.55	-0.42	-3.53	-0.96	-3.14	-1.22	+0.12		
Log ϵ_{\odot}	3.10	3.10	4.99	4.99	4.99	4.99	4.99	4.99	6.25	6.25	6.25	6.25	6.25	1.22	0.51		
Star (LEID)																	
43060	57	26	...	46	48	12	30	syn	...	
43061	144	118	121	62	72	74	48	48	126	syn	...	
43064	...	27	...	79	66	...	12	...	20	21	20	55	syn	7	
43068	63	80	78	18	38	23	11	59	syn	
43071	48	47	36	21	13	...	35	syn	
43079	59	17	...	68	59	syn	
43087	57	71	57	20	45	syn	...	
43091	102	86	34	35	17	28	28	39	8	66	syn	
43095	55	26	6	63	59	...	5	...	16	26	52	syn	...	
43096	77	28	...	151	121	41	34	30	28	27	39	80	syn	...	
43099	...	28	104	82	83	38	49	50	35	35	107	syn	...	
43101	55	55	46	15	18	22	8	37	syn	...	
43104	67	67	67	...	9	...	23	33	15	52	syn	...	
43108	...	29	...	36	10	...	17	18	syn	
43111	38	8	
43134	...	11	5	22	syn	
43139	43	11	24	...	6	5	syn	...	
43158	46	18	...	49	32	...	9	...	12	15	8	6	32	syn	
43189	169	83	63	68	38	54	42	15	110	syn	
43216	78	39	...	172	76	64	54	34	51	41	100	syn	...	17	
43233	49	16	...	40	36	syn	
43241	163	50	27	...	18	19	28	syn	
43258	50	45	45	19	18	...	6	36	syn	
43261	...	27	7	99	92	21	19	...	20	23	25	9	70	syn	
43278	32	16	syn	
43326	190	103	80	92	34	59	46	38	38	121	syn	27	...	
43330	56	22	...	88	73	20	54	syn
43351	180	...	61	75	42	59	57	130	syn	
43367	...	28	...	97	97	27	24	18	22	29	11	71	syn	9	
43389	64	133	134	67	47	...	35	45	34	18	74	syn	

Equivalent Widths (mÅ)

Table 4b—Continued

	Wavelength (Å)	6245.62	6309.88	6146.23	6258.11	6261.10	6303.76	6312.24	6336.11	6175.37	6176.81	6177.25	6186.71	6327.60	6262.29	6645.06	
Ion	Sc II	Sc II	Ti I	Ni I	La II	Eu II											
E.P. (eV)	1.51	1.50	1.87	1.44	1.43	1.44	1.44	1.44	4.09	4.09	4.11	4.11	4.11	0.40	1.38		
Log gf	-1.07	-1.58	-1.51	-0.38	-0.49	-1.56	-1.55	-1.69	-0.55	-0.42	-3.53	-0.96	-3.14	-1.22	+0.12		
Log ϵ_{\odot}	3.10	3.10	4.99	4.99	4.99	4.99	4.99	4.99	6.25	6.25	6.25	6.25	6.25	1.22	0.51		
Star (LEID)																	
43397	29	16	
43399	37	45	37	13	
43412	65	93	76	...	11	...	12	34	18	62	syn	...	
43433	...	21	...	68	63	36	11	9	47	syn	
43446	57	9	23	18	syn	
43458	58	20	...	62	65	31	35	19	...	47	syn	
43463	44	32	24	5	11	23	syn	
43475	74	100	48	32	97	syn	...	
43485	51	26	...	60	56	16	24	16	...	44	syn	
43539	51	67	59	18	10	39	syn	
44026	116	107	...	25	...	25	44	48	...	95	syn	
44042	52	23	...	51	45	15	21	8	5	38	syn	7	...	
44056	59	12	...	70	67	43	syn	
44065	48	47	46	17	17	4	41	syn	
44067	37	14	...	24	20	16	syn	...	
44115	71	30	6	97	100	...	27	11	69	syn	...	
44120	45	25	13	syn	
44143	47	26	...	60	44	...	7	5	14	20	14	...	40	syn	6	...	
44163	54	68	60	7	...	29	19	9	46	syn	
44188	56	94	65	19	20	10	65	syn	
44189	85	79	27	20	43	24	...	81	syn	...	
44198	54	21	...	52	45	14	16	23	17	6	57	syn	...	
44219	54	15	...	56	53	...	16	13	11	5	38	syn	
44231	59	27	...	68	67	17	7	57	syn	
44253	...	22	...	78	72	14	16	syn	
44271	39	
44277	81	37	99	92	82	113	syn	...	
44304	57	67	57	10	58	syn	
44313	66	67	58	15	16	15	33	...	60	syn	6	...	
44327	52	23	...	63	55	21	24	21	21	21	47	syn

Table 4b—Continued

	Wavelength (Å)	6245.62	6309.88	6146.23	6258.11	6261.10	6303.76	6312.24	6336.11	Ti I	6175.37	6176.81	Ni I	6186.71	6327.60	6262.29	6645.06	
Ion	Sc II	Sc II	Ti I	Ni I	Ni I	Ni I	Ni I	Ni I	Ni I	La II	Eu II							
E.P. (eV)	1.51	1.50	1.87	1.44	1.43	1.44	1.44	1.44	4.09	4.09	4.09	4.11	4.11	4.18	0.40	1.38		
Log gf	-1.07	-1.58	-1.51	-0.38	-0.49	-1.56	-1.55	-1.69	-0.55	-0.42	-3.53	-0.96	-3.14	-1.22	+0.12			
Log ϵ_\odot	3.10	3.10	4.99	4.99	4.99	4.99	4.99	4.99	4.99	6.25	6.25	6.25	6.25	6.25	1.22	0.51		
Star (LEID)																		
44337	55	66	57	20	15	12	17	49	syn	9	
44343	50	67	55	22	8	50	syn	...	
44380	29	13	13	syn	...	
44424	39	27	22	8	syn	
44426	...	31	79	73	26	35	19	61	syn	...	
44435	57	79	78	11	27	38	10	59	syn	...	
44446	35	31	19	22	13	39	syn	...	
44449	111	syn	...	
44462	66	37	93	84	63	42	49	53	28	...	106	syn	
44488	13	11	7	...	syn	...	
44493	45	19	44	...	9	...	11	7	27	syn	...	
45082	46	12	39	33	...	7	19	29	syn	...	
45089	57	37	30	12	17	10	7	7	34	syn	...	
45092	97	94	45	28	...	37	76	syn	...	
45093	...	16	29	23	10	12	syn	...	
45126	38	19	53	35	...	11	...	15	syn	...	
45177	60	25	87	89	17	12	10	19	30	20	8	58	syn	
45180	50	21	64	60	13	27	18	7	7	50	syn	
45206	42	27	25	syn	...	
45215	77	177	101	77	72	39	55	41	21	21	82	syn	13	...	
45232	81	38	155	55	44	37	21	34	35	...	88	syn	
45235	39	41	23	
45238	64	23	5	75	68	...	16	16	21	25	25	54	syn	
45240	53	22	syn	...	
45246	111	110	34	34	...	31	41	34	...	78	syn	
45249	74	29	110	114	50	44	32	27	43	27	13	78	syn	
45272	73	30	106	104	39	26	23	42	42	7	7	71	syn	24	...	
45285	130	116	88	syn	
45292	66	78	71	29	63	syn	
45309	35	12	21	17	15	syn

Equivalent Widths (mÅ)

Table 4b—Continued

	Wavelength (Å)	6245.62	6309.88	6146.23	6258.11	6261.10	6303.76	6312.24	6336.11	Ti I	Ti I	Ti I	6175.37	6176.81	6177.25	6186.71	6327.60	6262.29	6645.06
Ion	Sc II	Sc II	Ti I	Ni I	Ni I	Ni I	Ni I	Ni I	Ni I	Ni I	La II	Eu II							
E.P. (eV)	1.51	1.50	1.87	1.44	1.43	1.44	1.44	1.46	4.09	4.09	4.09	4.11	4.11	4.11	4.11	0.40	1.38		
Log gf	-1.07	-1.58	-1.51	-0.38	-0.49	-1.56	-1.55	-1.69	-0.55	-0.42	-3.53	-0.96	-3.14	-3.14	-3.14	-1.22	+0.12		
Log ϵ_{\odot}	3.10	3.10	4.99	4.99	4.99	4.99	4.99	4.99	4.99	4.99	4.99	4.99	4.99	4.99	4.99	6.25	6.25	6.25	6.25
Star (LEID)																			
45322	69	...	12	143	140	45	60	49	29	91	syn
45326	53	67	62	20	28	15	15	12	12	42	syn
45342	168	149	58	11	11
45343	69	30	...	64	56	11	18	5	44	44	44	syn
45359	58	65	61	15	47	47	47	syn
45373	73	103	94	...	23	24	26	36	26	26	10	75	75	syn
45377	58	19	...	57	48	20	29	16	16	6	46	46	syn
45389	55	28	...	70	58	...	13	...	21	21	21	20	7	45	45	syn
45410	36	17	...	30	27	syn
45418	62	63	62	25	16	30	13	13	...	41	41	syn
45453	74	87	84	20	36	17	17	7	66	66	syn	17
45454	117	120	7	90	90	syn
45463	69	101	89	30	27	26	...	31	29	66	66	syn
45482	60	52	58	10	22	35	17	46	46	syn
46024	77	22	...	106	105	...	20	20	23	42	19	...	79	79	syn
46055	67	66	61	21	27	15	15	syn
46062	80	29	...	143	136	46	34	35	21	88	88	syn
46073	142	39	40	47	47	syn	34
46090	30	16	16	5	5	...	20	20	syn
46092	162	76	64	54	37	58	45	45	110	110	syn
46121	105	105	104	72	67	88	88	124	124	syn
46140	56	61	53	21	12	13	16	24	16	16	7	53	53	syn
46150	82	...	18	...	171	85	65	58	37	60	35	35	20	94	94	syn
46166	65	44	41	...	8	46	46	syn
46172	17	100	86	43	23	23	...	69	69	syn
46194	59	30	...	77	68	21	18	11	27	30	15	15	...	57	57	syn
46196	41	12
46223	90	94	22	47	19	19	...	70	70	syn
46248	57	23	...	82	84	27	19	27	21	32	26	26	6	67	67	syn
46279	28	26	25	14	syn

Equivalent Widths (mÅ)

Table 4b—Continued

Table 4b—Continued

	Wavelength (Å)	6245.62	6309.88	6146.23	6258.11	6261.10	6303.76	6312.24	6336.11	6375.37	6176.81	6177.25	6186.71	6327.60	6262.29	6645.06
Ion	Sc II	Sc II	Ti I	Ni I	La II	Eu II										
E.P. (eV)	1.51	1.50	1.87	1.44	1.43	1.44	1.46	1.44	4.09	4.09	4.11	4.11	4.11	0.40	1.38	
Log gf	-1.07	-1.58	-1.51	-0.38	-0.49	-1.56	-1.55	-1.69	-0.55	-0.42	-3.53	-0.96	-3.14	-1.22	+0.12	
Log ϵ_\odot	3.10	3.10	4.99	4.99	4.99	4.99	4.99	4.99	6.25	6.25	6.25	6.25	6.25	1.22	0.51	
Star (LEID)																
47307	72	104	100	23	19	...	19	46	...	69	syn
47331	8	19
47338	51	61	59	...	10	...	28	18	...	45	syn	...	
47339	...	18	55	46	6	36	syn	...	
47348	64	101	81	...	27	...	28	30	28	...	73	syn	...
47354	149	134	40	93	syn	30
47387	60	24	...	66	61	13	7	...	16	9	46	syn	12
47399	74	41	...	204	186	84	75	58	34	41	55	26	26	110	syn	...
47400	70	109	102	38	33	...	24	43	24	15	15	73	syn	...
47405	64	28	...	70	69	10	16	...	15	8	50	syn	...	
47420	63	67	63	13	15	9	49	syn	...	
47443	36	13	...	25	22	9	...	syn	...	
47450	39	9	...	37	39	23	25	27	syn	...	
48028	57	...	5	63	57	10	10	7	19	10	47	syn	...	
48036	51	37	44	31	syn	...
48049	75	27	...	152	143	42	36	26	26	10	83	syn	...	
48060	87	34	125	46	30	...	15	21	33	...	73	syn	...	
48067	60	...	9	85	75	15	9	66	syn	...	
48083	...	39	...	105	97	21	81	syn	...	
48099	142	136	145	...	73	73	...	125	syn	...	
48116	...	52	151	140	150	66	63	92	...	144	syn	33	
48120	77	24	84	73	61	110	syn	...	
48150	101	122	93	94	55	131	syn	...
48151	46	40	36	
48186	41	17	...	38	25	11	
48197	6	36	37	11	24	syn	...	
48221	78	44	...	114	98	...	30	...	31	44	79	syn	...	
48228	48	20	...	50	45	12	14	40	syn	...	
48235	77	30	...	135	138	60	54	40	27	47	31	10	84	syn	20	
48247	53	55	46	22	18	5	43	syn	...

Equivalent Widths (mÅ)

Table 4b—Continued

	Wavelength (Å)	6245.62	6309.88	6146.23	6258.11	6261.10	6303.76	6312.24	6336.11	6175.37	6176.81	6186.71	6327.60	6262.29	6645.06	
Ion	Sc II	Sc II	Ti I	Ni I	Ni I	Ni I	Ni I	La II	Eu II							
E.P. (eV)	1.51	1.50	1.87	1.44	1.43	1.44	1.46	1.44	4.09	4.09	1.83	4.11	0.40	1.38		
Log gf	-1.07	-1.58	-1.51	-0.38	-0.49	-1.56	-1.55	-1.69	-0.55	-0.42	-3.53	-0.96	-3.14	-1.22	+0.12	
Log ϵ_{\odot}	3.10	3.10	4.99	4.99	4.99	4.99	4.99	4.99	6.25	6.25	6.25	6.25	1.22	0.51		
Star (LEID)																
48259	43	37	31	13	28	syn	...	
48281	59	28	...	67	58	21	...	15	15	12	48	syn	...	
48305	...	49	102	92	79	39	116	syn	...	
48323	147	140	147	61	60	85	34	135	syn	26	
48367	...	35	...	143	137	49	42	30	22	38	32	...	88	syn	31	
48370	...	27	...	102	98	...	20	...	21	51	31	...	71	syn	...	
48392	74	29	...	88	81	33	20	...	23	36	19	...	67	syn	...	
48409	42	15	...	26	21	13	4	syn	9	...	
49013	66	32	8	86	79	24	...	14	22	35	15	8	56	syn	...	
49022	43	19	...	40	30	30	syn	...	
49037	40	35	24	...	6	...	15	syn	...	
49056	153	125	138	57	77	71	...	37	148	syn	
49072	48	37	35	15	10	...	syn	...	
49088	42	46	34	14	13	31	syn	...	
49111	102	110	56	36	42	37	10	...	syn	...	
49123	60	31	...	79	76	23	14	55	syn	...	
49134	58	92	87	...	15	...	20	29	24	9	66	syn	7	
49148	69	25	21	134	135	62	52	44	34	51	33	13	92	syn	...	
49177	...	6	91	98	...	21	...	18	67	syn	...	
49179	44	44	8	7	36	syn	...	
49188	32	19	syn	...	
49193	...	32	...	96	87	30	15	...	24	32	29	...	65	syn	17	
49205	54	19	...	51	50	12	16	...	5	...	syn	...	
49212	...	45	176	...	84	94	34	17	120	syn	...	
49238	52	61	49	16	16	18	17	13	16	...	42	syn	...	
49249	63	30	...	134	123	54	39	33	31	48	24	12	81	syn	...	
49252	57	20	15	52	syn	...	
49255	35	30	7	syn	...	
49293	69	106	106	49	34	...	29	10	78	syn	...	
49322	42	19	...	40	36	12	18	28	syn	...	

Table 4b—Continued

	Wavelength (Å)	6245.62	6309.88	6146.23	6258.11	6261.10	6303.76	6312.24	6336.11	6175.37	6176.81	6177.25	6186.71	6327.60	6262.29	6645.06
Ion	Sc II	Sc II	Ti I	Ni I	La II	Eu II										
E.P. (eV)	1.51	1.50	1.87	1.44	1.43	1.44	1.46	1.44	4.09	4.09	4.11	4.11	4.18	0.40	1.38	
Log gf	-1.07	-1.58	-1.51	-0.38	-0.49	-1.56	-1.55	-1.69	-0.55	-0.42	-3.53	-0.96	-3.14	-1.22	+0.12	
Log ϵ_{\odot}	3.10	3.10	4.99	4.99	4.99	4.99	4.99	4.99	6.25	6.25	6.25	6.25	6.25	1.22	0.51	
Star (LEID)																
49333	49	13	...	36	33	28
50022	41	...	33	32	32	15	20	syn
50037	59	...	75	58	20	31	11	49	syn	...
50046	45	...	43	34	12	syn	...
50066	74	...	91	86	31	26	57	syn	...
50078	66	...	70	65	20	14	56	syn	...
50108	72	...	84	82	24	36	24	12	12	66	syn	...
50109	47	...	42	42	13	34	syn	...
50133	71	...	8	96	85	31	23	28	24	9	69	syn
50163	26	31	syn	...
50167	52	25	...	69	58	17	30	10	56	syn	9
50172	68	...	71	61	19	13	27	29	10	46	syn	...
50187	74	38	78	69	40	51	54	32	108	syn	18	...
50191	54	...	63	52	17	50	syn	...
50193	...	48	...	183	...	73	86	33	62	43	10	129	syn	...
50198	56	...	82	78	25	8	51	syn	...
50218	127	113	50	44	...	34	56	30	10	20	syn	...
50228	50	...	68	64	24	11	51	syn
50245	52	...	56	56	11	19	47	syn	8
50253	72	75	17	62	syn	...
50259	199	98	84	73	33	55	52	24	110	syn	...
50267	60	...	70	69	...	8	25	23	20	48	syn	7
50291	50	57	9	...	23	14	52	52	...	16
50293	57	...	4	83	66	...	14	17	14	23	22	50	syn	...
50294	56	37	...	11	...	20	25	syn	...
50304	52	14	...	52	51	17	30	syn	...
51021	74	43	...	153	66	62	52	36	50	41	20	97	syn	...
51024	61	...	10	88	84	33	22	...	30	32	33	68	syn	...
51074	181	160	66	44	...	39	16	syn
51079	101	90	51	...	18	26	39	26	10	81	...	81	syn	18

Equivalent Widths (mÅ)

Table 4b—Continued

	Wavelength (Å)	6245.62	6309.88	6146.23	6258.11	6261.10	6303.76	6312.24	6336.11	6175.37	6176.81	6177.25	6186.71	6327.60	6262.29	6645.06
Ion	Sc II	Sc II	Ti I	Ni I	La II	Eu II										
E.P. (eV)	1.51	1.50	1.87	1.44	1.43	1.44	1.46	1.44	4.09	4.09	1.83	4.11	1.68	0.40	1.38	
Log gf	-1.07	-1.58	-1.51	-0.38	-0.49	-1.56	-1.55	-1.69	-0.55	-0.42	-3.53	-0.96	-3.14	-1.22	+0.12	
Log ϵ_{\odot}	3.10	3.10	4.99	4.99	4.99	4.99	4.99	4.99	6.25	6.25	6.25	6.25	6.25	1.22	0.51	
Star (LEID)																
51080	76	44	...	153	152	67	57	48	35	47	41	12	96	syn	...	
51091	59	...	40	39	11	16	9	...	38	syn	...	
51121	51	...	42	32	...	7	28	syn	...	
51132	216	200	97	49	52	...	104	syn	...	
51136	52	22	syn	...	
51156	78	...	83	69	32	14	22	24	24	...	62	syn	19	
51254	79	30	11	101	97	48	...	32	28	49	26	8	87	syn	...	
51257	40	...	25	39	10	8	23	syn	...	
51259	54	...	50	45	14	36	syn	...	
52017	72	28	8	139	134	42	39	24	23	26	38	...	78	syn	...	
52035	...	29	...	187	166	55	43	27	29	90	syn	...	
52039	38	16	9	7	5	...	12	
52103	74	42	...	186	186	95	83	68	41	55	52	30	101	syn	15	
52105	47	13	...	58	55	12	...	13	17	5	40	syn	...	
52106	57	50	36	25	17	
52109	55	50	49	13	25	6	46	syn	
52110	43	29	36	syn	
52111	115	133	131	127	65	90	...	47	140	syn	10	
52133	56	...	44	54	...	7	...	26	...	23	51	syn	
52139	62	19	...	175	...	87	82	66	62	88	67	44	129	syn	13	
52151	52	18	...	46	44	...	9	...	12	20	15	syn	...	
52154	18	syn	...	
52167	70	79	75	...	17	...	17	30	14	51	syn	
52180	51	22	...	71	57	38	49	syn	
52192	52	57	64	26	39	15	syn	...	
52204	22	7	syn	...	
52222	49	16	...	32	29	7	28	syn	...	
53012	47	32	29	5	...	syn	...	
53054	45	...	2	42	32	...	8	...	10	12	11	...	30	syn	...	
53058	55	44	43	8	10	...	40	

Table 4b—Continued

	Wavelength (Å)	6245.62	6309.88	6146.23	6258.11	6261.10	6303.76	6312.24	6336.11	Ti I	Ti I	Ti I	6175.37	6176.81	6177.25	6186.71	6327.60	6262.29	6645.06
Ion	Sc II	Sc II	Ti I	Ni I	Ni I	Ni I	Ni I	Ni I	Ni I	Ni I	La II	Eu II							
E.P. (eV)	1.51	1.50	1.87	1.44	1.43	1.44	1.44	1.44	4.09	4.09	4.09	4.09	4.11	4.11	4.11	0.40	1.38		
Log gf	-1.07	-1.58	-1.51	-0.38	-0.49	-1.56	-1.55	-1.69	-0.55	-0.42	-3.53	-0.96	-3.14	-3.14	-3.14	-1.22	+0.12		
Log ϵ_\odot	3.10	3.10	4.99	4.99	4.99	4.99	4.99	4.99	4.99	6.25	6.25	6.25	6.25	6.25	6.25	6.25	0.51		
Star (LEID)																			
53067	61	27	...	65	70	18	...	9	19	33	16	53	syn		
53076	67	25	...	82	72	17	31	42	24	17	69	syn		
53114	79	155	153	71	54	38	36	43	44	20	101	syn		
53119	36	16	syn		
53132	58	57	46	17	25	11	...	36	syn		
53178	47	20	...	44	42	...	10	12	7	14	11	4	41	syn		
53185	70	23	4	101	95	...	25	18	25	40	22	9	68	syn	27		
53203	32	37	35	7	5	27	syn		
54018	56	25	...	62	62	...	16	45	syn		
54022	145	111	136	66	69	74	29	...	syn		
54031	89	46	...	197	112	90	82	50	61	56	...	107	syn	22		
54064	36	29	26	8	23		
54073	39	31	34	10	16	25	syn		
54084	43	23	...	34	31	21	syn		
54095	38	48	45	24	8	...	42	syn		
54105	200	110	72	93	42	72	46	16	116	syn		
54132	59	56	49	15	18	13	8	39	syn	...	26		
54148	75	34	...	142	128	46	34	29	22	35	34	9	89	syn	19		
54154	38	9	20	6	8	5	20	syn		
55028	86	194	181	90	70	57	35	54	44	16	96	syn		
55029	109	103	47	33	...	26	51	25	...	86	syn		
55056	47	35	26	7	12	syn		
55063	84	31	...	100	96	...	19	22	30	42	25	...	77	syn		
55071	147	120	128	63	87	76	27	...	syn		
55089	51	48	40	...	6	...	13	40	syn		
55101	157	164	75	63	94	46	41	68	...	114	syn		
55102	7	75	67	28	18	35	...	10	58	syn		
55111	73	37	...	127	133	54	42	37	32	40	34	12	87	syn		
55114	81	33	92	79	70	42	49	65	...	117	syn		
55121	...	49	97	111	46	77	64	152	syn		

Equivalent Widths (mÅ)

Table 4b—Continued

	Wavelength (Å)	6245.62	6309.88	6146.23	6258.11	6261.10	6303.76	6312.24	6336.11	Ti I	6175.37	6176.81	6186.71	6327.60	6262.29	6645.06
Ion	Sc II	Sc II	Ti I	Ni I	Ni I	Ni I	Ni I	Ni I	La II	Eu II						
E.P. (eV)	1.51	1.50	1.87	1.44	1.43	1.44	1.44	1.44	4.09	4.09	4.11	4.11	4.11	0.40	1.38	
Log gf	-1.07	-1.58	-1.51	-0.38	-0.49	-1.56	-1.55	-1.69	-0.55	-0.42	-3.53	-0.96	-3.14	-1.22	+0.12	
Log ϵ_{\odot}	3.10	3.10	4.99	4.99	4.99	4.99	4.99	4.99	4.99	6.25	6.25	6.25	6.25	1.22	0.51	
Star (LEID)																
55122	88	115	117	50	35	32	12	91	16
55131	42	46	42	...	8	...	14	12	22	syn
55142	193	76	101	46	70	61
55149	...	37	173	159	76	34	56	44	...	108	syn	...
55152	59	68	26	...	24	23	22	17	65	syn	13
55165	48	45	39	6	37	syn
55166	...	26	96	82	19	32	41	28	...	73	syn	...
56024	40	43	37	8	8	7	...	13	6	5	29	syn	8
56028	48	4	44	48	13	...	7	35	syn	...
56040	48	13	13	syn	...
56056	44	85	81	...	20	...	32	51	19	7	62	syn
56070	75	35	...	128	135	...	34	30	20	86	syn	...
56087	73	55	45	11	32	syn	12
56106	48	10	69	64	23	23	syn	...
56114	51	44	33	10	24	11	32	syn	...
56118	46	41	37
56128	38	112	107	40	38	31	25	47	30	10	82	syn
57010	66	31	9	...	23	9	8	4	8	47	...
57029	39	51	50	...	8	15	25	22	6	42	syn
57054	83	36	...	42	37	16	...	15	17
57058	49	3	49	47	10	30	syn	9
57067	51	43	40	11	6	...	16	33	syn	...
57073	46	22	19	32	14	...	56	syn
57076	57	31	22	14	17	27	syn	...
57083	37	28	8
57085	42	14
57091	65	70	61
57114	44	20	42
57127	50	29	47	15	23	9
58043	41	39	26	8	9	31	syn
58059	44	25	15	14	6

Equivalent Widths (mÅ)

Table 4b—Continued

	Wavelength (Å)	6245.62	6309.88	6146.23	6258.11	6261.10	6303.76	6312.24	6336.11	6175.37	6176.81	6186.71	6177.25	6327.60	6262.29	6645.06	
Ion	Sc II	Sc II	Ti I	Ni I	La II	Eu II											
E.P. (eV)	1.51	1.50	1.87	1.44	1.43	1.44	1.46	1.44	4.09	4.09	1.83	4.11	1.68	0.40	1.38		
Log gf	-1.07	-1.58	-1.51	-0.38	-0.49	-1.56	-1.55	-1.69	-0.55	-0.42	-3.53	-0.96	-3.14	-1.22	+0.12		
Log ϵ_{\odot}	3.10	3.10	4.99	4.99	4.99	4.99	4.99	4.99	6.25	6.25	6.25	6.25	6.25	1.22	0.51		
Star (LEID)																	
58077	35	29	32	11	39	syn	...	
58087	60	26	...	65	64	12	...	24	16	49	syn	...	
59016	35	23	22	6	
59024	132	103	113	51	57	73	151	syn	...	
59036	...	23	9	57	67	18	15	21	17	52	syn	...	
59047	79	...	18	106	107	...	24	...	28	40	32	...	79	syn	...		
59085	68	78	81	20	10	53	syn	...	
59089	64	...	5	83	79	...	21	18	10	56	syn	...	
59090	53	65	59	15	22	7	47	syn	...	
59094	40	34	21	13	10	24	syn	13	
60034	15	9	15	syn	...	
60058	119	140	63	27	...	31	
60059	49	41	42	syn	...	
60064	41	32	29	17	12	syn	...	
60065	55	60	50	44	syn	...
60066	76	99	88	28	35	26	11	72	syn	...
60067	43	21	12	8	15	syn	...
60069	58	12	...	50	50	20	27	10	syn	...
60073	105	133	52	79	119	syn	...
60088	56	42	42	26	29	16	30	syn	...
60101	50	21	...	42	16	27	syn	...
61015	...	33	...	166	71	52	42	30	33	45	21	100	
61026	39	28	34	
61042	62	26	...	87	84	26	15	12	19	7	57	syn	12	
61046	46	35	40	28	syn	5	
61050	...	33	...	167	153	77	61	59	...	55	40	96	syn	18	
61067	98	140	109	108	52	75	65	129	syn	...	
61070	62	...	6	68	63	24	37	14	11	50	syn	12	
61075	34	25	29	syn	...	
61085	...	44	111	86	88	39	53	65	128	syn	...	

Table 4b—Continued

	Wavelength (Å)	6245.62	6309.88	6146.23	6258.11	6261.10	6303.76	6312.24	6336.11	6175.37	6176.81	6177.25	6186.71	6327.60	6262.29	6645.06
Ion	Sc II	Sc II	Ti I	Ni I	La II	Eu II										
E.P. (eV)	1.51	1.50	1.87	1.44	1.43	1.44	1.46	1.44	4.09	4.09	1.83	4.11	1.68	0.40	1.38	
Log gf	-1.07	-1.58	-1.51	-0.38	-0.49	-1.56	-1.55	-1.69	-0.55	-0.42	-3.53	-0.96	-3.14	-1.22	+0.12	
Log ϵ_{\odot}	3.10	3.10	4.99	4.99	4.99	4.99	4.99	4.99	6.25	6.25	6.25	6.25	6.25	1.22	0.51	
Star (LEID)																
62018	26
62058	74	98	88	88	18	19	20	...	31	26	...	67	syn	...
63021	52	83	65	20	18	13	30	41	18	...	62	syn	...	
63027	43	17	...	40	31	...	9	...	22	14	...	9	...	syn	...	
63052	50	69	69	20	25	19	...	48	syn	9	
64023	27	18	...	6	17	11	syn	...	
64049	...	27	...	62	58	12	26	13	8	51	syn	...	
64057	36	33	29	12	16	5	...	24	syn	...	
64064	36	27	10	syn	
64067	51	68	16	54	syn	13	
64074	47	41	16	syn	...	
65042	16	10	syn	7	
65046	38	20	23	14	9	...	23	syn	...	
65057	47	56	47	18	34	24	...	49	syn	...	
66015	44	35	26	...	7	...	19	
66026	49	20	...	46	42	15	28	7	...	41	syn	...	
66047	59	130	128	50	42	34	36	54	25	16	81	syn	...	
66054	65	...	6	68	63	...	14	...	16	32	12	...	55	syn	...	
67049	26	12	11	14	syn	...	
67063	...	20	...	102	114	36	20	22	19	17	67	syn	...	
68044	44	16	...	37	32	33	syn	...	
69007	35	8	...	26	15	17	16	...	5	...	syn	...	
69012	62	28	4	78	79	16	22	23	8	56	syn	...	
69027	...	39	123	97	124	55	...	48	...	127	syn	...	
70032	49	49	44	...	9	...	11	20	8	...	33	syn	...	
70035	53	89	77	15	25	15	9	57	syn	...	
70041	49	40	38	11	32	syn	...	
70049	67	69	44	35	syn	...	
71013	29	14	syn	...	
73025	...	51	108	87	83	37	...	50	16	120	

Table 4b—Continued

	Wavelength (Å)	6245.62	6309.88	6146.23	6258.11	6261.10	6303.76	6312.24	6336.11	6175.37	6176.81	6177.25	6186.71	6327.60	6262.29	6645.06
Ion	Sc II	Sc II	Ti I	Ni I	La II	Eu II										
E.P. (eV)	1.51	1.50	1.87	1.44	1.43	1.44	1.44	1.44	4.09	4.09	4.11	4.11	4.11	0.40	1.38	
Log gf	-1.07	-1.58	-1.51	-0.38	-0.49	-1.56	-1.55	-1.69	-0.55	-0.42	-3.53	-0.96	-3.14	-1.22	+0.12	
Log ϵ_{\odot}	3.10	3.10	4.99	4.99	4.99	4.99	4.99	4.99	4.99	6.25	6.25	6.25	6.25	6.25	0.51	
Star (LEID)																
75021	46	22	...	52	45	12	11	6	38	syn	...
76027	54	70	69	...	9	...	20	31	20	9	58	syn	15	
76038	39	81	72	56	43	63	48	25	107	syn	...	
77025	67	93	93	32	28	28	38	38	28	9	73	syn	...	
77030	47	43	44	11	23	syn	...	
80026	46	39	32	syn	...	
80029	58	87	78	24	14	12	20	36	14	6	59	syn	...	
81018	54	18	...	57	46	...	6	6	14	42	syn	...	
81019	46	...	5	62	53	9	18	37	syn	...	
81028	40	37	34	14	9	...	syn	...	
82015	34	21	21	5	15	syn	...	
82029	27	18	syn	...	
85027	6	84	86	...	19	...	29	36	22	11	69	syn	...	
85031	53	56	54	14	48	syn	...	
89009	48	13	...	53	54	16	10	syn	...	

Equivalent Widths (mA)

Table 5. Chemical Abundance Ratios

Star LEID	Alt. ID ROA	[FeI/H] Avg.	[FeII/H] Avg.	[O/Fe] Avg.	[Na/Fe]	[Al/Fe]	[Si/Fe]	[Ca/Fe]	[Sc/Fe]	[ScI/Fe]	[ScII/Fe]	[Ti/Fe]	[Ni/Fe]	[LaII/Fe]	[EuII/Fe]	Code ^a				
9	370	-1.34	-1.35	+0.57	-0.38	... +0.23	+0.19	... +0.12	-0.33	+0.11	-0.12	-0.01	... +0.16	... +0.16				
5099	548	-1.87	-1.84	-1.86	+0.51	-0.42 ... +0.20	+0.30 +0.23 +0.11	-0.06 +0.03 +0.14	-0.33	+0.11	-0.08	-0.08	+0.16 ... +0.54	+0.54 ... +0.54				
6017	240	-1.32	-1.05	-1.19	-0.77	+0.37 ... +0.31	+0.23 ... +0.23	... +0.11	-0.24	+0.15	+0.23	-0.02	+0.18 ... +0.23	+0.18 ... +0.23	...	1				
8014	6734	-1.65	-1.80	-1.73	+0.61	+0.23 ... +0.30	+0.32 ... +0.30	... +0.15	+0.15	+0.14	+0.23	-0.02	+0.04 ... +0.04	+0.04 ... +0.04				
9013	6771	-1.74	-1.60	-1.67	+0.56	-0.10 ... +0.34	+0.52 ... +0.18	... +0.18	-0.06	-0.06	-0.06	+0.04	+0.01 ... +0.01	+0.01 ... +0.42	+0.30	...				
10009	...	-1.48	-1.38	-1.43	-0.32	+0.26 ... +0.40	+0.26 ... +0.37	... +0.37	-0.09	-0.09	-0.09	+0.16	-0.14 ... +0.45	-0.14 ... +0.45				
10012	43	-1.53	-1.35	-1.44	+0.24	+0.11 ... +0.33	+0.24 ... +0.19	... +0.19	-0.29	-0.11	-0.20	+0.10	-0.10 ... +0.09	-0.10 ... +0.09				
11019	537	-1.50	-1.57	-1.54	+0.49	-0.09 ... +0.35	+0.49 ... +0.44	... +0.44	-0.19	+0.13 ... +0.13	-0.03	+0.36	-0.04 ... +0.46	+0.46 ... +0.46				
11021	400	-1.47	-1.50	-1.49	+0.39	-0.02 ... +0.34	+0.39 ... +0.31	... +0.36	-0.08	+0.03 ... +0.03	-0.02	+0.27	+0.03 ... +0.27	+0.03 ... +0.54	+0.30	...				
11024	91	-1.82	-1.70	-1.76	+0.26	+0.03 ... +0.22	+0.03 ... +0.18	... +0.18	+0.22	+0.13 ... +0.13	+0.11	-0.05	-0.34 ... -0.34	-0.34 ... -0.34				
12013	394	-1.22	-1.17	-1.20	+0.37	+0.28 ... +0.28	+0.30 ... +0.28	... +0.28	+0.30	... +0.03	+0.03	-0.02	+0.12 ... +0.12	+0.12 ... +0.12	+0.30 ... +0.28			
12014	6602	-1.74	-1.66	-1.70	+0.50	-0.01 ... +0.00	+0.50 ... +0.08	... +0.08	+0.15 ... +0.15	+0.17 ... +0.17	+0.17 ... +0.17	-0.10	+0.13 ... +0.13	+0.13 ... +0.13	-0.30 ... +0.29	+0.28 ... +0.29	3,4 1,4			
14010	435	-1.96	-1.82	-1.89	+0.29	-0.19 ... +0.33	+0.29 ... +0.33	... +0.33	+0.17 ... +0.17	-0.10	-0.10	-0.11	-0.11 ... -0.11	-0.11 ... -0.11	+0.11 ... +0.29	+0.29 ... +0.29		
15022	180	-1.87	-1.64	-1.76	+0.44	-0.36 ... +0.05	+0.44 ... +0.05	... +0.05	+0.09 ... +0.09	-0.24 ... -0.24	... -0.24	-0.24	+0.09 ... +0.09	-0.07 ... -0.07	-0.55 ... -0.55			
15023	234	-1.83	-1.77	-1.80	+0.42	-0.29 ... +0.21	+0.42 ... +0.21	... +0.21	+0.12 ... +0.12	...	+0.11 ... +0.11	+0.13 ... +0.13	-0.09 ... -0.09	-0.30 ... -0.30	-0.30 ... -0.30	+0.28 ... +0.28	3,4 1,4			
15026	245	-1.36	-1.25	-1.31	-0.50	+0.35 ... +0.35	+1.12 ... +0.33	... +0.33	+0.29 ... +0.29	-0.11 ... -0.11	+0.33 ... +0.33	+0.29 ... +0.29	-0.18 ... -0.18	+0.39 ... +0.39	+0.39 ... +0.39	+0.25 ... +0.25		
16009	252	-1.88	-1.64	-1.76	+0.28	-0.22 ... +0.09	+0.28 ... +0.09	... +0.09	+0.17 ... +0.17	+0.02 ... +0.02	+0.02 ... +0.02	+0.04 ... +0.04	-0.14 ... -0.14	-0.24 ... -0.24	-0.24 ... -0.24			
16015	213	-1.95	-1.88	-1.92	+0.39	-0.44 ... +0.31	+0.39 ... +0.31	... +0.31	+0.26 ... +0.26	+0.26 ... +0.26	+0.31 ... +0.31	-0.03 ... -0.03	-0.03 ... -0.03	-0.14 ... -0.14	-0.14 ... -0.14	-0.14 ... -0.14		
16019	6460	-1.74	-1.74	-1.74	+0.64	+0.01 ... +0.29	+0.64 ... +0.29	... +0.29	+0.37 ... +0.25	+0.25 ... +0.25	+0.12 ... +0.12	+0.11 ... +0.11	+0.13 ... +0.13	-0.09 ... -0.09	-0.30 ... -0.30	-0.30 ... -0.30	+0.07 ... +0.07	3 1		
16027	6497	-1.94	-1.78	-1.86	+0.46	-0.16 ... +0.24	+0.46 ... +0.24	... +0.24	+0.27 ... +0.27	+0.24 ... +0.24	+0.22 ... +0.22	-0.07 ... -0.07	-0.07 ... -0.07	+0.16 ... +0.16	+0.16 ... +0.16	+0.16 ... +0.16	+0.25 ... +0.25	
17014	212	-1.57	-1.62	-1.60	+0.37	+0.11 ... +0.00	+0.37 ... +0.00	... +0.00	+0.28 ... +0.28	+0.25 ... +0.25	-0.21 ... -0.21	+0.17 ... +0.17	-0.02 ... -0.02	+0.20 ... +0.20	-0.06 ... -0.06	+0.50 ... +0.50	+0.02 ... +0.02	
17015	325	-1.84	-1.74	-1.79	+0.28	-0.52 ... +0.15	+0.28 ... +0.15	... +0.15	+0.26 ... +0.26	+0.26 ... +0.26	+0.00 ... +0.00	+0.08 ... +0.08	+0.04 ... +0.04	+0.18 ... +0.18	+0.10 ... +0.10	-0.31 ... -0.31
17027	6461	-2.09	-1.90	-2.00	+0.24 ... +0.21	...	+0.24 ... +0.21	...	+0.11 ... +0.11	+0.11 ... +0.11	
17029	6465	-1.96	-1.99	-1.98	+0.35	+0.49 ... +0.27	+0.35 ... +0.27	... +0.27	+0.32 ... +0.32	+0.32 ... +0.32	+0.38 ... +0.38	+0.36 ... +0.36	+0.21 ... +0.21	+0.28 ... +0.28	+0.44 ... +0.44	-0.08 ... -0.08	+0.54 ... +0.54	
17032	605	-1.51	-1.57	-1.54	+0.19	+0.33 ... +0.39	+0.19 ... +0.39	... +0.39	+0.38 ... +0.38	+0.38 ... +0.38	+0.36 ... +0.36	+0.36 ... +0.36	+0.17 ... +0.17	+0.17 ... +0.17	+0.25 ... +0.25	+0.25 ... +0.25	+0.45 ... +0.45	1 1	...	
17046	6545	-1.91	-1.76	-1.84	+0.14	+0.16 ... +0.16	+0.14 ... +0.16	... +0.16	+0.26 ... +0.26	+0.26 ... +0.26	...	+0.17 ... +0.17	+0.17 ... +0.17	-0.05 ... -0.05	+0.19 ... +0.19	-0.13 ... -0.13
18017	448	-2.01	-1.67	-1.84	+0.37	+0.08 ... -0.14	+0.37 ... -0.14	... -0.14	+0.09 ... -0.14	+0.09 ... -0.14	...	-0.05 ... -0.05	-0.05 ... -0.05	-0.05 ... -0.05	-0.05 ... -0.05	-0.05 ... -0.05	-0.13 ... -0.13
18020	146	-1.78	-1.63	-1.71	+0.16	+0.21 ... +0.51	+0.16 ... +0.51	... +0.51	+0.25 ... +0.25	+0.25 ... +0.25	-0.28 ... -0.28	-0.07 ... -0.07	-0.17 ... -0.17	+0.21 ... +0.21	-0.10 ... -0.10	-0.10 ... -0.10	+0.27 ... +0.27	+0.20 ... +0.20
18035	581	-1.75	-1.57	-1.66	+0.19	-0.06 ... +0.19	+0.19 ... +0.19	... +0.19	+0.14 ... +0.14	+0.14 ... +0.14	+0.14 ... +0.14	+0.25 ... +0.25	+0.20 ... +0.20	+0.21 ... +0.21	-0.14 ... -0.14	-0.14 ... -0.14	+0.01 ... +0.01	+0.01 ... +0.01
18040	465	-1.33	-1.29	-1.31	+0.16	+0.29 ... +0.45	+0.16 ... +0.45	... +0.45	+0.38 ... +0.43	+0.38 ... +0.43	-0.23 ... -0.23	+0.17 ... +0.17	-0.03 ... -0.03	+0.33 ... +0.33	-0.16 ... -0.16	-0.16 ... -0.16	+0.41 ... +0.41	+0.19 ... +0.19
18047	408	-1.86	-1.83	-1.85	+0.09	+0.18 ... +0.25	+0.09 ... +0.25	... +0.25	+0.34 ... +0.34	+0.34 ... +0.34	...	-0.02 ... -0.02	-0.02 ... -0.02	+0.13 ... +0.13	+0.10 ... +0.10	+0.10 ... +0.10	-0.11 ... -0.11	-0.11 ... -0.11
19022	6442	-1.83	-1.77	-1.80	+0.47	+0.34 ... +0.17	+0.47 ... +0.17	... +0.17	+0.17 ... +0.17	+0.17 ... +0.17	...	+0.01 ... +0.01	+0.01 ... +0.01	+0.15 ... +0.15	+0.02 ... +0.02	+0.02 ... +0.02
19062	464	-1.88	-1.79	-1.84	+0.62	-0.21 ... +0.34	+0.62 ... +0.34	... +0.34	+0.26 ... +0.26	+0.26 ... +0.26	...	+0.15 ... +0.15	+0.15 ... +0.15	+0.34 ... +0.34	-0.03 ... -0.03	-0.03 ... -0.03	+0.39 ... +0.39	+0.39 ... +0.39
20018	6259	-1.52	-1.67	-1.60	+0.30	+0.18 ... +0.40	+0.30 ... +0.40	... +0.40	+0.21 ... +0.21	+0.21 ... +0.21	...	+0.31 ... +0.31	+0.31 ... +0.31	+0.04 ... +0.04	+0.04 ... +0.04	+0.04 ... +0.04	+0.53 ... +0.53	+0.53 ... +0.53	1,3 1,3	...

Table 5—Continued

Star LEID	Alt. ID ROA	[FeI/H]	[FeII/H]	[FeIII/H] Avg.	[O/Fe]	[Na/Fe]	[Al/Fe]	[Si/Fe]	[Ca/Fe]	[ScI/Fe]	[ScII/Fe]	[Sc Avg.]	[Ti/Fe]	[Ni/Fe]	[LaII/Fe]	[EuII/Fe]	Code ^a
20037	6316	-1.50	-1.65	-1.58	+0.57	+0.29	+0.62	+0.36	+0.39	+0.18	+0.16	+0.17	+0.42	-0.06	+0.69	+0.27	
20042	6327	-1.95	-1.79	-1.87	+0.39	-0.02	...	+0.08	+0.31	...	-0.06	-0.06	+0.03	-0.31	-0.28	...	
20049	6355	-1.86	-1.73	-1.80	+0.59	-0.14	...	+0.28	+0.31	...	+0.15	+0.25	-0.07	+0.15	...	4	
21032	172	-1.54	-1.45	-1.50	+0.55	-0.11	...	+0.18	+0.31	-0.21	-0.01	-0.11	+0.21	+0.01	+0.15	...	
21035	362	-1.87	-1.87	-1.87	+0.35	+0.02	...	+0.27	+0.31	...	+0.19	+0.19	+0.25	-0.02	-0.23	...	
21042	348	-1.72	-1.73	-1.73	+0.48	-0.26	...	+0.30	+0.32	...	+0.03	+0.03	+0.17	-0.08	-0.18	...	
21063	6342	-1.87	-1.88	-1.88	+0.43	-0.29	...	+0.25	+0.39	...	+0.25	+0.25	+0.34	
22023	6137	-1.20	-1.25	-1.23	-0.98	+0.48	+1.21	+0.46	+0.48	...	+0.17	+0.17	+0.29	+0.02	+0.66	+0.07	
22037	307	-1.83	-1.69	-1.76	+0.22	+0.01	...	+0.12	+0.29	...	+0.05	+0.05	+0.14	-0.08	-0.59	...	
22042	415	-1.76	-1.71	-1.74	+0.60	+0.06	...	+0.26	+0.33	...	+0.08	+0.08	+0.04	-0.01	+0.24	...	
22049	6207	-1.77	-1.94	-1.86	+0.66	+0.40	...	+0.31	+0.37	...	+0.26	+0.26	+0.18	+0.07	+0.11	...	
22063	6234	-1.87	-1.75	-1.81	+0.41	-0.25	...	+0.20	+0.23	...	-0.08	-0.08	+0.16	-0.18	-0.09	...	
23022	6119	-1.90	-1.95	-1.93	+0.13	+0.26	...	+0.30	+0.25	...	+0.07	+0.07	+0.16	1	
23033	558	-1.66	-1.80	-1.73	-0.57	+0.19	+0.97	+0.31	+0.41	...	+0.19	+0.19	+0.17	+0.09	+0.30	+0.34	
23042	570	-1.85	-1.82	-1.84	+0.03	+0.03	+0.78	+0.41	+0.17	...	+0.02	+0.02	+0.18	-0.01	...	+0.59	
23050	6179	-1.87	-1.80	-1.84	+0.20	+0.20	...	+0.17	+0.26	...	+0.02	+0.02	+0.14	+0.13	
23061	296	-1.77	-1.67	-1.72	+0.37	-0.22	...	+0.13	+0.21	...	+0.09	+0.09	+0.15	-0.08	-0.38	...	
23068	96	-1.72	-1.55	-1.64	+0.41	-0.36	+0.15	+0.24	+0.24	-0.24	+0.13	-0.06	+0.23	-0.13	-0.47	+0.19	
24013	56	-1.67	-1.60	-1.64	+0.33	+0.67	...	+0.37	+0.32	+0.08	+0.07	+0.08	+0.35	-0.06	+0.19	...	
24027	5969	-1.55	-1.54	-1.55	-0.49	+0.42	...	+0.39	+0.45	-0.02	+0.16	+0.07	+0.11	-0.10	+0.33	...	
24040	5993	-1.87	-1.63	-1.75	+0.57	+0.06	...	+0.28	+0.06	...	+0.02	-0.22	...	1	
24046	74	-1.85	-1.66	-1.76	+0.20	+0.13	...	+0.27	+0.19	...	-0.01	-0.01	+0.13	-0.16	-0.30	...	
24056	364	-1.82	-1.71	-1.77	+0.25	+0.05	...	+0.04	+0.21	...	+0.13	+0.13	+0.17	-0.12	-0.36	...	
24062	352	-1.39	-1.43	-1.41	+0.56	+0.06	...	+0.36	+0.48	-0.10	+0.14	+0.02	+0.36	-0.10	+0.36	...	
25006	5941	-1.85	-1.70	-1.78	+0.38	+0.40	...	+0.24	+0.06	...	-0.01	-0.01	...	+0.09	...	+0.66	
25026	569	-1.93	-1.85	-1.89	+0.47	+0.37	...	+0.45	+0.32	...	+0.09	+0.09	+0.29	+0.24	
25043	89	-1.53	-1.46	-1.50	-0.13	+0.36	...	+0.44	+0.34	-0.09	+0.11	+0.01	+0.30	-0.11	+0.34	...	
25062	46	-1.75	-1.45	-1.60	+0.28	-0.45	...	+0.15	+0.05	-0.37	+0.12	-0.13	+0.09	-0.19	-0.45	...	
25065	...	-1.15	-1.07	-1.11	+0.03	+0.96	...	+0.40	+0.57	...	-0.10	-0.10	+0.56	+0.06	+0.39	...	
25068	58	-1.79	-1.62	-1.71	+0.16	+0.19	...	+0.45	+0.32	...	+0.14	+0.14	+0.14	-0.05	-0.40	...	
26010	5759	-1.72	-1.63	-1.68	+0.20	-0.26	+0.63	+0.38	+0.00	...	+0.06	+0.06	+0.06	-0.18	+0.49	...	
26014	387	-1.95	-1.87	-1.91	+0.45	-0.49	...	+0.11	+0.24	...	+0.08	+0.08	+0.12	+0.07	
26022	5788	-1.76	-1.75	-1.76	+0.11	+0.13	...	+0.23	+0.23	...	+0.09	+0.09	+0.12	+0.14	
26025	61	-1.81	-1.44	-1.63	+0.24	+0.06	...	+0.13	-0.03	-0.34	+0.04	-0.15	+0.08	-0.21	-0.23	...	

Table 5—Continued

Star LEID	Alt. ID ROA	[Fe/H] [FeII/H]	[FeI/H] Avg.	[O/Fe] Avg.	[Na/Fe]	[Al/Fe]	[Si/Fe]	[Ca/Fe]	[Sc/Fe] Avg.	[ScI/Fe]	[ScII/Fe]	[Ti/Fe]	[Ni/Fe]	[LaII/Fe]	[EuII/Fe]	Code ^a
26030	5809	-1.76	-1.97	-1.87	+0.40	+0.19	...	+0.30	+0.46	...	-0.18	+0.13	+0.06	+0.47	...	4
26069	528	-1.84	-1.89	-1.87	+0.37	+0.55	...	+0.22	+0.27	...	-0.04	-0.04	-0.15	-0.15
26072	303	-1.83	-1.62	-1.73	+0.37	-0.58	+0.08	+0.12	+0.18	...	-0.01	-0.01	-0.02	-0.23	+0.38	...
26086	295	-1.06	-1.08	-1.07	+0.04	+1.02	...	+0.64	+0.46	-0.04	-0.04	-0.04	+0.57	-0.13	+0.52	...
26088	161	-1.71	-1.47	-1.59	+0.43	-0.40	...	+0.18	+0.16	...	+0.05	+0.05	+0.07	-0.16	-0.01	...
27048	313	-1.43	-1.45	-1.44	-0.53	+0.49	...	+0.52	+0.38	-0.05	...	-0.05	+0.16	-0.11	+0.32	...
27050	5823	-1.93	...	-1.93	+0.53	+0.12	+0.30	...	+0.15	+0.15	+0.20	-0.13	+0.23	...
27073	566	-1.71	-1.65	-1.68	+0.23	+0.26	...	+0.07	+0.28	...	+0.04	+0.04	+0.01	-0.01	+0.28	...
27094	5880	-1.80	...	-1.80	+0.00	-0.24	+0.35	+0.31	+0.28	...	+0.07	+0.07	+0.07	+0.13	-0.11	+0.55
27095	139	-1.60	-1.44	-1.52	-0.43	+0.39	...	+0.26	+0.20	-0.18	...	-0.18	+0.24	-0.15	+0.63	...
28016	5585	-1.60	-1.82	-1.71	+0.48	-0.03	...	+0.37	+0.50	...	+0.11	+0.11	+0.22	+0.04	+0.61	...
28020	424	-1.86	-1.81	-1.84	+0.14	-0.22	...	+0.38	+0.17	...	+0.09	+0.09	+0.10	+0.04	+0.03	...
28044	246	-1.74	-1.63	-1.69	+0.15	+0.31	...	+0.26	+0.24	...	+0.05	+0.05	+0.11	-0.09	+0.00	...
28069	185	-1.78	-1.73	-1.76	+0.33	+0.03	+0.66	+0.26	+0.25	...	+0.05	+0.05	+0.05	-0.12	-0.20	+0.19
28084	497	-1.77	-1.61	-1.69	+0.42	-0.03	+0.31	+0.28	+0.33	+0.13	+0.02	+0.07	+0.22	-0.04	+0.19	+0.00
28092	380	-1.74	-1.64	-1.69	+0.45	-0.22	...	+0.20	+0.30	...	+0.14	+0.14	+0.12	-0.15	+0.29	...
29029	545	-1.53	-1.54	-1.54	+0.44	-0.18	...	+0.23	+0.40	...	+0.10	+0.10	+0.10	+0.24	+0.09	+0.11
29031	375	-1.89	-1.70	-1.80	-0.11	+0.17	...	-0.08	+0.20	...	+0.11	+0.11	-0.04	...	-0.16	...
29037	5640	-1.73	-1.74	-1.74	+0.48	-0.12	...	+0.45	+0.24	...	+0.26	+0.26	+0.11	+0.11	+0.08	...
29059	458	-1.64	-1.45	-1.55	+0.24	-0.04	...	+0.20	+0.24	-0.21	+0.23	+0.01	+0.27	-0.14	+0.25	...
29067	84	-1.22	-1.27	-1.25	+0.45	-0.01	...	+0.65	+0.48	-0.25	-0.09	-0.17	+0.19	+0.07	+0.23	...
29069	206	-1.62	-1.45	-1.54	-0.17	+0.30	+1.19	+0.45	+0.23	...	+0.15	+0.15	+0.11	-0.08	+0.29	+0.32
29072	385	-1.92	-1.75	-1.84	+0.39	-0.24	...	+0.08	+0.15	...	+0.03	+0.03	-0.05	-0.22	-0.37	...
29085	450	-1.73	-1.63	-1.68	-0.72	-0.12	...	+0.41	+0.35	+0.14	-0.15	+0.41	...
29089	5686	-1.76	...	-1.76	+0.33	+0.27	...	+0.42	+0.28	...	+0.20	+0.20	+0.13	...	+0.31	...
29099	184	-1.58	-1.66	-1.62	+0.03	+0.30	+1.15	+0.41	+0.45	-0.04	+0.35	+0.15	+0.37	+0.01	+0.42	+0.56
29106	209	-1.89	-1.95	-1.92	+0.44	-0.45	...	+0.16	+0.35	...	+0.27	+0.27	+0.02	+0.02	-0.23	...
30013	540	-1.31	-1.32	-1.32	-0.52	+0.45	...	+0.28	+0.42	+0.28	+0.36	+0.32	+0.32	-0.13	+0.87	...
30019	5588	-1.50	-1.51	-1.51	+0.50	+0.11	...	+0.30	+0.31	-0.10	+0.07	-0.01	+0.25	-0.11	+0.46	...
30022	496	-1.87	-1.72	-1.80	+0.46	...	+0.00	+0.14	+0.19	...	-0.06	-0.06	+0.02	-0.16	+0.42	...
30031	95	-1.57	-1.47	-1.52	+0.21	+0.39	+0.64	+0.34	+0.37	-0.04	+0.14	+0.05	+0.41	-0.12	+0.22	+0.04
30069	5644	-2.00	-2.02	-2.01	+0.56	+0.15	...	+0.39	+0.30	...	+0.10	+0.10	+0.10	+0.16
30094	512	-1.58	-1.49	-1.54	+0.05	+0.28	...	+0.24	+0.41	...	+0.11	+0.11	+0.05	-0.13	+0.47	...
30124	5707	-1.61	-1.46	-1.54	+0.49	+0.03	...	+0.14	+0.37	...	+0.08	+0.08	+0.08	-0.01	+0.34	...

Table 5—Continued

Star LEID	Alt. ID ROA	[Fe/H] [FeII/H]	[FeIII/H] Avg.	[O/Fe] [O/Fe] Avg.	[Na/Fe] [Al/Fe]	[Si/Fe] [Ca/Fe]	[ScI/Fe] [ScII/Fe] Avg.	[ScII/Fe] [Sc/Fe]	[Ti/Fe] [Ni/Fe]	[EuII/Fe] [LaII/Fe]	[EuII/Fe] Code ^a
31016	526	-2.00	-1.85	-1.93	+0.48	... +0.02	... +0.18	... -0.11	-0.07	+0.15	... +0.23
31041	361	-1.79	-1.58	-1.69	-0.57	+0.24	... +0.43	+0.18	+0.09	-0.03	+0.33
31047	...	-1.90	-1.75	-1.83	+0.42	-0.11	... +0.04	+0.25	+0.26	+0.00
31048	504	-1.73	-1.47	-1.60	-0.07	-0.06	... +0.30	+0.08	-0.01	-0.16	+0.04
31075	5413	-1.74	...	-1.74	+0.46	+0.30	... +0.43	+0.43	+0.33	+0.17
31079	200	-1.88	-1.80	-1.84	+0.39	+0.07	... +0.24	+0.18	+0.20	+0.04	-0.10
31094	292	-1.83	-1.65	-1.74	+0.39	-0.20	... +0.16	+0.10	+0.03	+0.03	-0.07
31095	5434	-1.74	-1.79	-1.77	-0.24	+0.59	+1.29	+0.61	+0.45	+0.28	+0.26
31104	5446	-1.90	-1.76	-1.83 +0.32	+0.23	+0.43
31109	5451	-1.53	-1.43	-1.48	+0.45	-0.10	... +0.28	+0.32	+0.26	+0.18	+0.06
31110	195	-1.53	-1.44	-1.49	+0.47	-0.07	... +0.37	+0.25	-0.31	+0.22	-0.04
31119	327	-1.50	-1.56	-1.53	+0.52	+0.14	... +0.49	+0.42	-0.17	+0.16	-0.01
31133	5489	-1.87	-1.86	-1.87	+0.11	+0.67	... +0.20	+0.54	...	+0.06	+0.20
31139	373	-1.86	-1.67	-1.77	+0.28	-0.15	... +0.11	+0.17	...	+0.06	+0.13
31141	261	-1.79	-1.53	-1.66	-0.39	+0.20	... +0.39	+0.24	...	+0.03	+0.23
31147	5511	-1.56	...	-1.56	+0.80	+0.23	... +0.28	+0.19	...	+0.03	+0.11
31152	5522	-1.75	...	-1.75	+0.31	+0.44	... +0.64	+0.31	...	+0.43	+0.53
32014	474	-1.87	-1.68	-1.78	+0.58	-0.01	... +0.10	+0.22	...	-0.08	-0.04
32026	544	-1.46	-1.42	-1.44	+0.49	+0.20	... +0.30	+0.52	+0.16	+0.03	+0.33
32027	5367	-1.80	-1.81	-1.81	+0.14	+0.34	... +0.28	+0.29	...	+0.18	+0.19
32043	5394	-1.71	-1.70	-1.71	+0.69	-0.55	... +0.11	+0.14	...	+0.22	+0.22
32063	382	-1.72	-1.71	-1.72	+0.13	+0.56	+0.69	+0.05	+0.27	+0.17	+0.13
32069	5411	-1.80	-1.74	-1.77	+0.27	+0.09	... +0.37	+0.19	...	+0.01	+0.19
32100	5448	-1.77	-1.68	-1.73	+0.12	+0.00	... +0.06	+0.28	...	+0.07	+0.07
32101	502	-1.69	-1.61	-1.65	+0.35	+0.63	+0.57	+0.37	+0.30	-0.16	+0.13
32125	262	-1.77	-1.64	-1.71	+0.53	-0.15	... +0.21	+0.23	...	+0.12	+0.27
32130	5478	-1.84	-1.64	-1.74	+0.39	+0.27	... -0.02	+0.22	...	-0.02	+0.03
32138	48	-1.83	-1.68	-1.76	+0.34	-0.04	... +0.09	+0.13	-0.11	+0.12	+0.08
32140	390	-1.81	-1.68	-1.75	+0.11	+0.00	... +0.15	+0.30	...	-0.16	+0.15
32144	5490	-1.52	-1.43	-1.48	+0.45	+0.05	... +0.19	+0.40	-0.07	+0.19	+0.06
32165	5501	-1.92	-1.82	-1.87	+0.42	+0.38	... +0.00	+0.16	...	+0.09	+0.08
32169	5510	-1.12	-0.99	-1.06	-0.04	+0.97	... +0.42	+0.35	-0.20	+0.23	+0.02
32171	251	-1.50	-1.41	-1.46	-1.30	+0.38	... +0.29	+0.27	-0.09	+0.04	+0.17
33006	...	-1.63	-1.59	-1.61	+0.52	-0.13	... +0.23	+0.27	-0.06	+0.21	+0.07
									+0.07	+0.39	-0.09

Table 5—Continued

Star LEID	Alt. ID ROA	[FeI/H]	[FeII/H]	[FeIII/H] Avg.	[O/Fe]	[Na/Fe]	[Al/Fe]	[Si/Fe]	[Ca/Fe]	[Sc/Fe]	[ScII/Fe]	[ScIII/Fe] Avg.	[Ti/Fe]	[Ni/Fe]	[LaII/Fe]	[EuII/Fe]	Code ^a
33011	159	-1.84	-1.66	-1.75	+0.40	-0.35	+0.20	+0.18	...	+0.09	+0.16	-0.08	-0.50	
33018	379	-1.81	-1.76	-1.79	+0.44	-0.01	+0.28	+0.04	+0.31	...	+0.20	+0.20	-0.18	-0.01	+0.40	...	
33030	5056	-1.69	-1.73	-1.71	+0.07	+0.44	...	+0.06	+0.19	...	+0.18	+0.18	+0.27	-0.24	
33051	...	-1.69	-1.60	-1.65	-0.66	+0.23	...	+0.40	+0.28	+0.01	+0.16	+0.08	+0.13	-0.05	-0.16	1	
33064	5108	-1.73	-1.79	-1.76	+0.16	-0.02	...	-0.12	+0.36	...	+0.07	+0.07	+0.04	+0.16	+0.16	...	
33099	175	-1.14	-0.90	-1.02	-0.46	+0.26	...	+0.07	+0.19	+0.49	+0.08	+0.32	...	
33114	71	-1.67	-1.49	-1.58	+0.42	-0.20	+0.18	+0.30	+0.22	-0.32	+0.07	-0.13	+0.21	-0.07	+0.26	+0.11	
33115	5198	-1.23	-1.25	-1.24	-0.66	+0.53	...	+0.28	+0.58	...	+0.13	+0.13	-0.04	-0.18	+0.63	...	
33126	5216	-1.52	-1.47	-1.50	+0.25	+0.02	...	+0.35	+0.39	+0.15	+0.18	+0.16	+0.17	+0.25	+0.53	...	
33129	397	-1.82	-1.69	-1.76	+0.48	+0.15	+0.22	...	-0.04	-0.04	+0.32	+0.02	+0.29	...	
33138	560	-1.74	...	-1.74	+0.54	+0.06	...	+0.74	+0.32	+0.30	+0.13	+0.21	+0.35	...	-0.06	...	
33145	561	-1.95	...	-1.95	+0.50	+0.45	...	+0.20	+0.33	+0.48	
33154	5243	-1.38	-1.46	-1.42	...	+0.33	...	+0.17	-0.08	...	-0.12	-0.12	
33167	5268	-1.52	-1.49	-1.51	+0.67	+0.35	...	+0.35	+0.27	...	-0.08	-0.08	+0.04	+0.03	+0.51	...	
33177	5290	-1.73	-1.64	-1.69	+0.24	-0.05	...	+0.12	-0.12	-0.05	+0.30	...	
34008	434	-1.62	-1.79	-1.71	+0.36	+0.22	+0.65	+0.31	+0.48	...	+0.18	+0.18	+0.13	+0.13	+0.38	+0.83	
34029	243	-1.28	-1.27	-1.28	+0.26	+0.33	...	+0.46	+0.47	-0.05	+0.06	+0.01	+0.52	-0.01	+0.40	...	
34040	503	-1.71	-1.68	-1.70	+0.37	+0.08	...	+0.02	+0.26	...	+0.06	+0.06	+0.06	+0.13	-0.07	+0.00	
34056	576	-1.62	-1.63	-1.63	+0.27	+0.13	...	+0.06	+0.25	...	+0.01	+0.01	+0.08	-0.09	
34069	254	-1.74	-1.51	-1.63	+0.23	-0.60	...	+0.12	+0.14	...	-0.08	-0.08	-0.03	-0.10	-0.28	...	
34075	157	-1.50	-1.47	-1.49	-0.45	+0.34	+1.20	+0.56	+0.42	-0.10	+0.17	+0.03	+0.27	-0.03	+0.11	...	
34081	436	-1.68	-1.66	-1.67	+0.41	+0.11	...	+0.21	+0.35	...	+0.13	+0.13	+0.15	-0.10	+0.22	...	
34129	559	-1.87	-1.73	-1.80	+0.44	+0.12	...	+0.15	+0.22	...	+0.07	+0.07	+0.10	+0.25	...	4	
34130	5176	-1.79	-1.68	-1.74	+0.57	+0.07	+0.04	...	+0.13	+0.13	+0.01	
34134	45	-1.76	-1.61	-1.69	+0.19	-0.07	...	+0.29	+0.23	-0.29	+0.11	-0.09	+0.13	-0.10	-0.37	...	
34143	419	-1.19	-1.12	-1.16	-0.50	+0.48	+0.92	+0.44	+0.22	-0.08	+0.06	-0.01	+0.30	-0.13	+0.63	+0.14	
34163	494	-1.79	-1.67	-1.73	+0.24	+0.13	...	+0.15	...	-0.05	-0.05	...	-0.05	...	-0.07	...	
34166	...	-1.76	-1.65	-1.71	+0.37	+0.02	...	+0.25	+0.19	...	+0.24	+0.24	-0.01	+0.15	+0.16	...	
34169	467	-1.64	-1.48	-1.56	-0.34	+0.32	...	+0.63	+0.29	+0.07	+0.34	+0.21	+0.22	-0.03	+1.01	...	
34175	119	-1.64	-1.48	-1.56	+0.60	-0.29	...	+0.41	+0.20	...	+0.01	+0.01	+0.17	-0.16	+0.49	...	
34180	517	-0.79	...	-0.79	+0.30	+0.89	+0.40	+0.47	+0.38	+0.12	...	+0.12	+0.66	+0.09	+0.46	+0.27	
34187	468	-1.93	-1.83	-1.88	+0.50	-0.06	...	+0.23	+0.26	-0.11	+0.23	+0.06	+0.14	+0.07	-0.12	...	
34193	111	-1.87	-1.69	-1.78	+0.33	-0.37	...	+0.24	+0.19	...	+0.08	+0.08	+0.00	-0.20	-0.37	...	
34207	229	-1.62	-1.34	-1.48	+0.27	-0.45	+0.23	+0.18	+0.13	...	-0.24	-0.24	-0.03	-0.17	+0.24	-0.11	

Table 5—Continued

Star LEID	Alt. ID ROA	[Fe/H] [FeII/H]	[FeI/H] Avg.	[O/Fe] Avg.	[Na/Fe]	[Al/Fe]	[Si/Fe]	[Ca/Fe]	[Sc/Fe] Avg.	[ScII/Fe]	[Ti/Fe]	[Ni/Fe]	[LaII/Fe]	[EuII/Fe]	Code ^a
34214	5256	-1.79	-1.69	-1.74	+0.46	+0.31	...	-0.10	+0.26	...	+0.41	+0.15	+0.16	...	1
34225	557	-1.07	-1.10	-1.09	-0.11	+0.46	...	+0.36	+0.30	-0.19	-0.18	-0.19	-0.19	+0.74	...
34229	402	-1.92	-1.80	-1.86	+0.23	+0.15	...	+0.22	+0.30	...	+0.11	+0.07	+0.16	+0.17	...
35029	4676	-1.72	-1.57	-1.65	+0.37	-0.02	...	+0.15	+0.27	+0.04	+0.14	+0.09	+0.16	-0.09	+0.37
35035	4686	-1.91	-1.87	-1.89	+0.64	-0.31	...	+0.25	+0.25	...	+0.25	+0.25	+0.17	+0.09	-0.06
35046	257	-1.86	-1.71	-1.79	+0.43	-0.04	...	+0.35	+0.25	-0.21	+0.18	-0.02	+0.29	+0.00	-0.07
35053	275	-1.95	-1.76	-1.86	+0.35	-0.12	...	+0.25	+0.19	...	+0.11	+0.11	-0.02	-0.22	-0.42
35056	69	-1.69	...	-1.69	+0.18	+0.28	...	+0.35	+0.19	-0.31	+0.11	-0.10	+0.22	-0.09	+0.09
35061	208	-1.52	-1.47	-1.50	-0.81	+0.49	+1.03	+0.67	+0.34	-0.06	+0.22	+0.08	+0.17	-0.12	+0.20
35066	67	-1.85	-1.66	-1.76	+0.37	+0.03	...	+0.28	+0.22	-0.29	+0.03	-0.13	+0.12	-0.17	-0.55
35071	4735	-1.41	-1.37	-1.39	...	+0.14	...	+0.32	+0.35	+0.39	...
35074	326	-1.80	-1.68	-1.74	-0.36	+0.23	...	+0.40	+0.34	...	+0.24	+0.16	-0.07	+0.14	4
35087	5089	-1.78	-1.66	-1.72	+0.22	+0.34	...	+0.13	+0.33	+0.40	+0.13	+0.26	+0.01	...	+0.19
35090	174	-1.44	-1.32	-1.38	-0.32	+0.23	...	+0.45	+0.32	-0.37	+0.07	-0.15	+0.27	-0.07	+0.47
35093	4775	-1.34	-1.38	-1.36	...	+0.22	...	-0.30	+0.08	-0.24	...
35124	4817	-1.37	-1.26	-1.32	-0.14	+0.41	...	+0.48	+0.42	+0.19	...	+0.19	+0.17	-0.10	+0.54
35157	...	-1.25	...	-1.25	-0.50	+0.55	+1.03	+0.33	+0.35	-0.06	...	-0.06	+0.23	-0.07	+0.28
35165	...	-1.78	-1.78	-1.78	+0.08	+0.20	...	+0.26	+0.30	...	+0.12	+0.12	+0.21	+0.04	-0.27
35172	237	-1.26	-1.33	-1.30	-0.21	+0.59	...	+0.29	+0.26	+0.00	...	+0.00	+0.50	+0.07	+0.76
35190	452	-1.76	-1.79	-1.78	+0.30	+0.18	...	+0.13	+0.40	...	+0.12	+0.12	+0.10	-0.05	+0.18
35201	263	-1.14	-0.98	-1.06	-0.35	+0.39	...	+0.06	+0.11	-0.03	...	-0.03	+0.11	-0.29	+0.53
35204	420	-2.00	...	-2.00	+0.60	+0.37	...	+0.66	+0.26	...	+0.16	+0.16	...	+0.31	...
35216	54	-1.89	-1.74	-1.82	+0.39	-0.40	-0.04	+0.15	+0.23	-0.26	-0.01	-0.13	+0.15	-0.03	+0.16
35228	518	-1.77	...	-1.77	+0.07	+0.13	...	+0.27	+0.21	+0.18	+0.22	+0.20	...	+0.01	+0.07
35230	141	-1.90	...	-1.90	+0.14	+0.53	...	+0.38	+0.24	...	+0.16	+0.16	+0.11	-0.01	-0.25
35235	125	-1.79	-1.66	-1.73	+0.17	...	+0.25	+0.14	...	+0.16	+0.16	+0.00	-0.13	-0.48	...
35240	115	-1.89	-1.71	-1.80	+0.27	-0.01	...	+0.30	+0.27	...	+0.21	+0.21	+0.11	-0.04	-0.40
35248	4937	-1.69	-1.70	-1.75	-0.48	...	+0.47	+0.43	+0.20	+0.00	+0.10	+0.26	+0.07	+0.63	...
35260	377	-1.75	-1.62	-1.69	+0.56	-0.43	...	+0.25	+0.23	...	+0.08	+0.08	+0.04	-0.20	+0.11
35261	4961	-1.56	-1.56	-1.58	-0.31	...	+0.25	+0.44	+0.01	+0.10	+0.05	+0.30	-0.04	+0.08	...
36028	535	-1.71	-1.58	-1.65	+0.30	+0.27	+0.55	+0.10	+0.09	...	+0.19	+0.19	+0.21	-0.24	+0.00
36036	65	-1.87	...	-1.87	+0.47	-0.23	...	+0.32	+0.25	-0.16	...	-0.16	+0.19	+0.01	-0.33
36048	4748	-1.74	-1.72	-1.73	+0.26	+0.56	...	+0.31	+0.35	...	+0.14	+0.14	+0.13	-0.06	+0.33
36059	4763	-1.70	-1.79	-1.75	+0.36	+0.45	...	+0.44	+0.45	...	+0.20	+0.20	+0.14	+0.16	...

Table 5—Continued

Star LEID	Alt. ID ROA	[Fe/H] [FeI/H]	[Fe/H] Avg.	[O/Fe] [O/Fe]	[Na/Fe] [Al/Fe]	[Si/Fe] [Ca/Fe]	[Sc/Fe] [ScII/Fe]	[ScII/Fe] Avg.	[Ti/Fe] [Ni/Fe]	[La/Fe] [EuII/Fe]	[EuII/Fe] Code ^a
36061	592	-1.43	-1.31	-1.37	-0.58	+0.66	+0.44	+0.43	-0.03	+0.00	+0.49
36087	4797	-1.84	-1.78	-1.81	+0.11	+0.21	...	+0.23	+0.15	+0.15	-0.06
36106	392	-1.83	...	-1.83	-0.37	+0.01	...	+0.54	+0.37	+0.21	-0.04
36110	...	-1.97	...	-1.97	+0.37	+0.39	...	+0.49	+0.35
36113	343	-1.65	-1.59	-1.62	+0.56	-0.03	...	+0.31	+0.38
36134	...	-0.96	...	-0.96	+0.01	+1.03	+0.03	+0.43	+0.26	+0.38	-0.25
36156	...	-1.87	-1.91	-1.89	+0.43	-0.04	+0.29	+0.22	+0.36	+0.11	+0.44
36179	148	-1.13	...	-1.13	-0.42	+0.52	+0.93	+0.24	+0.25
36182	215	-1.74	-1.58	-1.66	+0.63	-0.05	...	+0.37	+0.25	-0.13	-0.04
36191	336	-0.83	-0.67	-0.75	-0.34	+0.65	...	+0.31	+0.24	-0.14	-0.09
36206	308	-1.90	...	-1.90	+0.57	-0.11	...	+0.29	+0.32	+0.12	+0.45
36228	49	-1.83	-1.71	-1.77	+0.43	-0.59	...	+0.23	+0.10	-0.41	-0.20
36239	281	-1.65	-1.47	-1.56	-0.24	+0.42	+1.03	+0.56	+0.31	-0.12	-0.38
36259	355	-1.93	-1.75	-1.84	+0.26	-0.36	...	+0.31	+0.21
36260	4912	-1.40	...	-1.40	-0.05	-0.08	...	+0.45	+0.21
36280	395	-1.62	-1.66	-1.64	+0.49	+0.41	+0.42	+0.43	+0.46	+0.13	-0.04
36282	290	-1.95	-1.81	-1.88	+0.51	-0.27	...	+0.13	+0.10	-0.23	-0.16
37022	4437	-1.55	-1.64	-1.60	+0.60	+0.44	+0.19	+0.18	-0.06
37024	447	-0.79	...	-0.79	-0.16	+1.36	+0.33	+0.17	-0.03
37051	349	-1.94	...	-1.94	+0.54	+0.27	...	+0.51	+0.32	+0.19	-0.02
37052	4738	-1.64	-1.52	-1.58	+0.59	+0.23	+0.24	+0.20	-0.09
37055	562	-1.47	-1.45	-1.46	-0.54	+0.35	...	+0.38	+0.39	+0.08	-0.05
37062	507	-1.30	-0.97	-1.14	-0.82	+0.40	...	+0.21	+0.32	-0.10	+0.04
37071	391	-1.83	-1.72	-1.78	-0.13	+0.15	...	+0.51	+0.05
37082	4770	-1.95	-1.76	-1.86	+0.48	-0.01	...	+0.27	+0.17
37087	309	-1.89	-1.85	-1.87	-0.08	+0.17	...	+0.28	+0.31
37094	443	-1.91	-1.88	-1.90	+0.48	+0.09	...	+0.24	+0.21
37105	514	-1.67	-1.53	-1.60	+0.65	+0.02	...	+0.39	+0.20
37110	...	-0.88	-0.69	-0.79	-0.06	+0.75	...	+0.39	+0.17	-0.44	...
37119	...	-1.79	-1.62	-1.71	+0.53	+0.19	...	+0.34	+0.30
37136	...	-1.88	...	-1.88	+0.29	+0.21	...	+0.27	+0.24
37139	...	-1.49	-1.25	-1.37	+0.50	-0.22	...	+0.39	+0.19
37143	...	-1.73	-1.79	-1.76	+0.42	+0.29	...	+0.30	+0.36
37147	...	-1.39	-1.30	-1.35	+0.24	+0.32	+0.44	+0.47	-0.15	+0.25	-0.27

Table 5—Continued

Star LEID	Alt. ID ROA	[FeI/H]	[FeII/H]	[FeIII/H] Avg.	[O/Fe]	[Na/Fe]	[Al/Fe]	[Si/Fe]	[Ca/Fe]	[ScI/Fe]	[ScII/Fe]	[ScIII/Fe] Avg.	[Ti/Fe]	[Ni/Fe]	[LaII/Fe]	[EuII/Fe]	Code ^a
37157	...	-1.85	-1.84	-1.85	+0.37	+0.21	...	+0.31	+0.44	+0.16	+0.14	+0.15	+0.17	-0.02	-0.23	...	
37169	...	-1.88	-1.94	-1.91	+0.36	+0.37	...	+0.49	+0.52	+0.16	+0.16	+0.16	+0.46	+0.14	+0.58	...	
37179	...	-1.86	-1.98	-1.92	+0.62	+0.56	+0.87	+0.22	+0.31	+0.26	+0.26	+0.29	+0.29	+0.30	+0.27	+0.22	
37184	...	-1.89	-1.77	-1.83	+0.42	+0.04	+0.48	+0.23	+0.24	-0.14	+0.14	+0.00	+0.08	-0.01	-0.27	+0.37	
37196	...	-1.95	...	-1.95	+0.57	+0.28	...	+0.23	+0.36	...	+0.21	+0.21	+0.13	+0.04	+0.00	...	
37198	...	-1.57	-1.59	-1.58	-0.24	+0.52	+1.29	+0.60	+0.47	-0.25	+0.31	+0.03	+0.40	-0.01	+0.39	+0.02	
37215	...	-1.97	...	-1.97	+0.57	-0.06	...	+0.44	+0.17	...	+0.15	+0.15	+0.13	+0.12	+0.12	...	
37232	...	-1.75	-1.51	-1.63	+0.38	-0.25	...	+0.29	+0.14	-0.49	...	-0.49	+0.07	-0.10	+0.09	...	
37247	238	-1.88	...	-1.88	+0.03	+0.35	...	+0.45	+0.35	+0.14	+0.23	+0.19	+0.13	-0.05	-0.30	...	
37253	104	-1.84	-1.77	-1.81	+0.43	-0.19	+0.11	+0.29	+0.21	...	+0.17	+0.17	+0.11	-0.07	-0.18	+0.24	
37271	169	-1.79	-1.68	-1.74	+0.38	-0.11	+0.09	+0.40	+0.30	-0.12	+0.11	+0.00	+0.19	-0.10	+0.02	+0.02	
37275	439	-1.43	...	-1.43	-0.17	+0.49	...	+0.45	+0.41	...	+0.26	+0.26	+0.23	+0.08	+0.63	...	
37318	324	-0.90	-0.85	-0.88	+0.35	+1.03	+0.59	+0.36	+0.42	+0.08	+0.36	+0.22	+0.38	+0.17	+0.22	-0.05	
37322	4938	-1.93	...	-1.93	+0.53	+0.22	...	+0.47	+0.25	...	+0.29	+0.29	+0.29	-0.29	
37329	351	-1.82	-1.68	-1.75	+0.43	-0.42	...	+0.19	+0.20	...	+0.09	+0.09	+0.01	-0.12	-0.18	...	
38011	253	-1.27	-1.34	-1.31	-0.60	+0.56	...	+0.38	+0.44	+0.04	+0.55	+0.30	+0.40	+0.13	+0.46	...	
38018	4429	-1.66	-1.53	-1.60	-0.11	+0.28	...	+0.40	+0.29	+0.41	+0.24	+0.33	+0.07	-0.11	+0.67	...	
38049	44	-1.85	-1.62	-1.74	-0.19	+0.32	+0.97	+0.41	+0.20	-0.25	+0.14	-0.05	+0.01	-0.12	-0.32	+0.12	
38052	77	-1.76	-1.65	-1.71	+0.36	-0.50	...	+0.13	+0.23	-0.27	-0.06	-0.16	+0.19	-0.06	-0.20	...	
38056	515	-1.86	-1.71	-1.79	+0.24	+0.36	...	+0.08	+0.30	...	+0.01	+0.01	+0.06	+0.20	+0.03	...	
38057	584	-1.27	-1.11	-1.19	-0.31	+0.25	...	+0.24	+0.51	-0.23	...	-0.23	+0.19	-0.23	+0.54	...	
38059	151	-1.15	...	-1.15	-0.28	+0.46	+1.01	+0.39	+0.44	-0.18	+0.70	+0.26	+0.39	-0.16	+0.52	+0.10	
38061	4495	-1.79	-1.65	-1.72	+0.42	+0.26	...	+0.22	+0.10	...	-0.05	-0.05	-0.05	-0.15	
38096	...	-1.82	...	-1.82	+0.43	+0.31	...	+0.40	+0.36	...	+0.14	+0.14	+0.22	+0.25	+0.60	...	
38097	...	-1.23	-1.04	-1.14	+0.19	-0.32	...	+0.45	+0.43	-0.59	-0.32	-0.45	+0.18	-0.18	-0.31	...	
38105	...	-1.94	-1.74	-1.84	+0.19	+0.02	...	+0.27	+0.23	...	+0.08	+0.08	+0.05	+0.03	+0.04	4	
38112	...	-1.53	-1.49	-1.51	+0.02	+0.47	...	+0.34	+0.42	+0.15	+0.25	+0.20	+0.30	-0.06	+0.63	...	
38115	130	-1.64	-1.38	-1.51	+0.28	+0.14	...	+0.24	+0.11	-0.31	+0.14	-0.09	+0.04	-0.24	-0.44	...	
38129	...	-1.83	-1.53	-1.68	-0.07	+0.17	...	+0.26	+0.17	...	+0.00	+0.00	+0.00	-0.20	-0.13	...	
38147	...	-1.54	-1.43	-1.49	-0.42	+0.36	...	+0.43	+0.34	...	+0.12	+0.12	+0.26	-0.02	+0.64	...	
38149	...	-1.39	-1.15	-1.27	-0.63	+0.25	...	+0.43	+0.24	-0.36	+0.22	-0.07	+0.27	-0.13	+0.30	...	
38156	...	-1.77	-1.75	-1.76	+0.36	-0.15	...	+0.18	+0.27	...	+0.17	+0.17	+0.10	-0.06	-0.04	4	
38166	...	-2.18	-1.87	-2.03	-0.13	+0.37	...	+0.53	+0.28	...	-0.02	-0.02	-0.11	-0.55	
38168	...	-1.42	-1.15	-1.29	-0.82	+0.21	+0.85	+0.05	+0.35	+0.25	+0.25	+0.25	-0.03	-0.41	+0.01	-0.05	...

Table 5—Continued

Star LEID	Alt. ID ROA	[FeI/H]	[FeII/H]	[FeIII/H] Avg.	[O/Fe]	[Na/Fe]	[Al/Fe]	[Si/Fe]	[Ca/Fe]	[Sc/Fe]	[ScII/Fe]	[ScIII/Fe] Avg.	[Ti/Fe]	[Ni/Fe]	[LaII/Fe]	[EuII/Fe]	Code ^a
38169	...	-1.52	-1.54	-1.53	+0.51	+0.16	...	+0.42	+0.47	+0.00	+0.10	+0.05	+0.35	+0.01	+0.56	...	
38195	...	-1.64	-1.76	-1.70	+0.50	-0.06	+0.13	+0.33	+0.34	-0.11	+0.10	-0.01	+0.35	+0.00	+0.35	+0.49	...
38198	...	-1.52	-1.36	-1.44	-0.96	+0.44	...	+0.50	+0.17	-0.14	+0.12	-0.01	+0.21	-0.04	+0.71
38204	...	-1.87	-1.71	-1.79	+0.32	-0.12	+0.27	+0.44	+0.18	-0.21	+0.21	+0.00	+0.09	-0.14	+0.29	+0.25	...
38206	...	-1.72	-1.49	-1.61	+0.51	+0.09	...	+0.33	+0.09	...	+0.03	+0.03	-0.07	-0.03	+0.56
38215	...	-1.19	-1.20	-1.20	+0.03	+0.83	...	+0.36	+0.55	-0.14	...	-0.14	+0.36	-0.09	+0.31
38223	...	-1.84	-1.63	-1.74	+0.21	-0.08	...	+0.09	+0.22	+0.04	+0.21	+0.13	+0.33	-0.10	-0.44
38225	...	-1.78	-1.55	-1.67	+0.12	+0.13	...	+0.15	+0.26	+0.32	+0.01	+0.16	+0.09	-0.12	+0.02
38226	...	-1.65	-1.63	-1.64	-0.29	+0.58	...	+0.63	+0.42	...	+0.24	+0.24	+0.17	-0.09	+0.34
38232	...	-1.44	-1.45	-1.45	+0.57	+0.00	...	+0.36	+0.40	-0.03	+0.17	+0.07	+0.45	-0.09	+0.32
38255	...	-1.16	-1.28	-1.22	-0.53	+0.51	...	+0.25	+0.43	+0.21	-0.01	+0.10	+0.49	-0.04	+0.62
38262	127	-1.80	-1.59	-1.70	+0.32	-0.23	...	+0.23	+0.28	-0.32	+0.12	-0.10	+0.12	-0.10	-0.12
38276	168	-1.60	-1.61	-1.61	+0.40	-0.25	...	+0.28	+0.40	-0.17	-0.07	-0.12	+0.34	-0.05	+0.19
38303	293	-1.70	-1.58	-1.64	-0.51	+0.47	...	+0.52	+0.34	-0.12	+0.30	+0.09	+0.09	+0.00	+0.94
38319	416	-1.61	-1.38	-1.50	-0.14	-0.02	...	+0.08	+0.21	-0.24	+0.17	-0.04	+0.11	-0.18	+0.15
38323	4578	-1.19	-1.03	-1.11	-0.54	+0.15	...	+0.40	+0.36	-0.05	+0.34	+0.14	+0.34	-0.15	+0.51
38330	550	-1.75	-1.68	-1.72	+0.04	+0.13	+0.77	+0.16	+0.28	+0.25	+0.07	+0.16	+0.21	-0.07	+0.18	+0.15	...
39026	287	-1.43	-1.53	-1.48	+0.47	-0.02	...	+0.50	+0.55	-0.19	+0.20	+0.00	+0.40	+0.02	+0.49
39033	580	-2.09	-1.95	-2.02	+0.17	+0.57	...	+0.32	+0.18	-0.10	+0.24
39034	334	-1.77	-1.57	-1.67	+0.04	-0.16	...	+0.01	+0.20	...	+0.06	+0.06	-0.07	-0.19	-0.33	...	4
39037	94	-1.86	-1.57	-1.72	+0.24	-0.16	...	+0.24	+0.16	-0.41	-0.09	-0.25	+0.09	-0.16	-0.25
39043	604	-1.65	-1.50	-1.58	+0.66	-0.28	...	+0.31	+0.25	...	-0.02	-0.02	-0.01	-0.06	+0.48
39044	258	-1.82	-1.73	-1.78	+0.38	+0.03	...	+0.13	+0.19	-0.25	+0.13	-0.13	-0.06	+0.10	-0.05	-0.08	...
39048	451	-0.65	...	-0.65	+0.00	+0.93	...	+0.62	+0.29	+0.24	...	+0.24	+0.74	-0.07	+0.64
39056	519	-1.71	-1.80	-1.76	+0.36	+0.35	...	+0.19	+0.30	...	+0.09	+0.09	+0.04	+0.08
39063	4476	-1.87	-1.76	-1.82	+0.25	+0.32	...	+0.18	+0.22	...	-0.02	-0.02	-0.04	+0.05	+0.11
39067	86	-1.31	-1.37	-1.34	-0.16	+0.37	...	+0.31	+0.34	+0.09	+0.38	+0.23	+0.58	-0.01	+0.58
39086	249	-1.65	-1.57	-1.61	-0.04	+0.18	...	+0.11	+0.29	-0.19	+0.11	-0.04	+0.19	-0.08	+0.22
39088	304	-1.86	-1.71	-1.79	-0.87	+0.13	...	+0.48	+0.39	+0.04	+0.23	+0.14	+0.21	-0.01	-0.12	...	4
39102	563	-1.68	-1.63	-1.66	+0.36	-0.29	...	+0.30	+0.05	...	+0.17	+0.17	+0.17	-0.02	-0.30
39119	...	-1.90	-1.68	-1.79	+0.29	-0.07	...	+0.13	+0.21	...	-0.01	-0.01	+0.04	-0.10	-0.41
39123	...	-1.86	-1.64	-1.75	+0.35	-0.09	...	+0.12	+0.09	...	+0.02	+0.02	+0.03	-0.11	-0.30
39129	...	-1.34	...	-1.34	+0.29	-0.17	...	+0.15	+0.25	+0.17	+0.55	+0.36	+0.33	-0.05	+0.61
39141	101	-1.76	-1.77	-1.77	+0.34	-0.26	-0.09	+0.15	+0.32	-0.17	+0.06	-0.05	+0.17	-0.04	-0.17	+0.22	...

Table 5—Continued

Star LEID	Alt. ID ROA	[FeII/H]	[FeIII/H]	[O/Fe] Avg.	[Fe/H] Avg.	[Na/Fe]	[Al/Fe]	[Si/Fe]	[Ca/Fe]	[ScI/Fe]	[ScII/Fe]	[Sc/Fe] Avg.	[Ti/Fe]	[Ni/Fe]	[LaII/Fe]	[EuII/Fe]	Code ^a
39149	...	-1.21	-0.95	-1.08	-0.72	+0.29	+0.24	+0.20	-0.34	-0.34	+0.18	-0.11	+0.50	
39165	80	-1.97	...	-1.97	+0.49	-0.03	+0.47	+0.36	+0.22	-0.09	+0.02	-0.05	-0.08	+0.26	+0.26	4	
39186	...	-1.74	-1.57	-1.66	+0.35	-0.17	+0.11	+0.14	+0.10	...	-0.09	-0.07	-0.23	+0.26	+0.23	...	
39187	...	-2.13	...	-2.13	+0.27	+0.13	...	+0.50	+0.37	...	+0.20	+0.20	-0.07	+0.02	-0.07	...	
39198	...	-1.70	-1.61	-1.66	+0.36	-0.49	...	+0.19	+0.23	-0.20	+0.08	-0.06	+0.20	-0.12	-0.30	...	
39204	...	-1.93	-1.76	-1.85	+0.31	+0.18	...	+0.34	+0.16	...	+0.16	+0.16	+0.07	-0.04	+0.19	...	
39215	...	-1.97	...	-1.97	+0.22	+0.19	...	+0.67	+0.41	...	+0.14	+0.14	+0.11	+0.07	-0.03	...	
39216	...	-1.78	...	-1.78	+0.13	+0.45	...	-0.16	+0.27	...	+0.22	+0.22	+0.08	+0.10	+0.20	...	
39225	...	-1.65	...	-1.65	+0.40	+0.19	...	+0.38	+0.26	...	+0.13	+0.13	+0.25	-0.03	+0.60	...	
39235	...	-1.67	-1.50	-1.59	-0.47	+0.40	...	+0.64	+0.36	-0.19	+0.38	+0.09	+0.09	-0.04	+0.34	...	
39245	...	-1.54	-1.46	-1.50	+0.54	+0.18	+0.29	+0.24	+0.26	+0.09	+0.16	+0.12	+0.41	+0.05	+0.29	-0.35	
39257	...	-1.50	-1.43	-1.47	+0.48	+0.33	...	+0.54	+0.36	-0.20	+0.01	-0.09	+0.42	-0.04	+0.39	...	
39259	...	-1.75	-1.65	-1.70	+0.40	-0.17	...	+0.23	+0.27	-0.12	-0.02	-0.07	+0.11	-0.08	+0.18	...	
39284	...	-1.84	-1.67	-1.76	-0.22	+0.13	+0.93	+0.32	+0.23	...	+0.04	+0.04	+0.13	-0.11	-0.38	-0.43	
39289	...	-1.85	-1.83	-1.84	+0.25	+0.11	...	+0.13	+0.32	...	+0.08	+0.08	+0.18	-0.01	-0.16	...	
39298	...	-1.95	...	-1.95	+0.53	+0.20	...	+0.44	+0.31	...	+0.18	+0.18	+0.09	+0.28	-0.20	...	
39301	...	-1.88	-1.92	-1.90	+0.50	+0.24	...	+0.55	+0.56	...	+0.18	+0.18	+0.30	+0.14	+0.35	...	
39306	123	-1.87	-1.74	-1.81	-0.21	-0.01	+0.57	+0.27	+0.31	-0.13	+0.05	-0.04	+0.10	-0.02	-0.30	+0.06	
39325	117	-1.35	-1.44	-1.40	-0.54	+0.58	...	+0.40	+0.40	-0.11	...	-0.11	+0.52	-0.04	+0.57	...	
39329	...	-1.83	-1.96	-1.90	+0.45	+0.27	...	+0.71	+0.40	...	+0.17	+0.17	+0.30	+0.09	+0.25	...	
39345	356	-1.78	-1.75	-1.77	-0.29	-0.05	...	+0.44	+0.40	+0.11	+0.20	+0.15	+0.17	+0.07	+0.17	...	
39346	...	-1.24	...	-1.24	+0.62	+0.18	...	+0.52	+0.49	-0.04	+0.01	-0.02	+0.62	-0.01	+0.52	...	
39352	97	-1.79	-1.78	-1.79	-0.07	+0.13	...	+0.30	+0.29	-0.09	+0.15	+0.03	+0.18	+0.03	-0.42	...	
39384	4570	-1.42	-1.29	-1.36	+0.65	-0.06	...	+0.42	+0.36	...	-0.15	-0.15	+0.25	+0.00	+0.66	...	
39392	4579	-0.85	-0.65	-0.75	-0.15	+0.77	...	+0.28	+0.14	-0.21	...	-0.21	+0.39	-0.18	+0.20	...	
39401	345	-1.59	-1.44	-1.52	-0.39	+0.38	...	+0.48	+0.20	+0.17	+0.18	+0.04	+0.05	+0.64	
39921	...	-1.69	-1.43	-1.56	+0.18	-0.23	...	+0.27	+0.28	-0.15	+0.01	-0.07	+0.07	-0.20	+0.11	...	
40016	359	-1.53	-1.40	-1.47	+0.41	-0.11	+0.07	+0.27	+0.41	...	+0.05	+0.05	+0.09	-0.09	+0.44	-0.42	
40031	501	-1.87	-1.73	-1.80	+0.22	+0.16	...	+0.31	+0.21	...	+0.04	+0.04	+0.00	+0.02	
40041	585	-1.55	-1.59	-1.57	+0.07	+0.32	+1.09	+0.50	+0.46	...	+0.03	+0.03	+0.13	...	+1.00	+0.08	
40108	...	-1.86	-1.86	-1.86	+0.11	+0.09	...	+0.08	+0.27	+0.22	+0.10	+0.39	
40123	107	-1.46	...	-1.46	-0.49	+0.29	+1.11	+0.40	+0.19	-0.34	+0.15	-0.10	+0.16	-0.07	+0.34	-0.13	
40135	78	-1.97	-1.87	-1.92	+0.37	-0.03	...	+0.38	+0.23	-0.17	...	-0.17	+0.16	-0.01	-0.13	...	
40139	...	-1.55	-1.36	-1.46	-0.55	+0.68	...	+0.38	+0.25	-0.12	-0.07	-0.07	+0.21	-0.11	+0.37	...	

Table 5—Continued

Star LEID	Alt. ID ROA	[FeI/H]	[FeII/H]	[FeIII/H] Avg.	[O/Fe]	[Na/Fe]	[Al/Fe]	[Si/Fe]	[Ca/Fe]	[Sc/Fe]	[ScII/Fe]	[ScIII/Fe] Avg.	[Ti/Fe]	[Ni/Fe]	[LaII/Fe]	[EuII/Fe]	Code ^a
40162	...	-1.54	-1.64	-1.59	+0.35	+0.28	...	+0.35	+0.33	+0.27	+0.31	-0.06	+0.52	
40166	...	-1.53	-1.42	-1.48	-0.88	+0.57	...	+0.56	+0.37	-0.12	+0.04	-0.04	+0.23	
40168	...	-1.79	-1.62	-1.71	+0.00	+0.27	...	+0.40	+0.28	+0.20	+0.12	+0.16	-0.06	+0.32	
40170	...	-1.87	-1.84	-1.86	+0.27	+0.05	...	+0.23	+0.37	...	+0.02	+0.02	+0.23	+0.07	+0.21	...	
40207	...	-1.63	-1.44	-1.54	-0.42	+0.32	...	+0.39	+0.30	-0.25	+0.15	-0.05	+0.13	-0.02	+0.77	...	
40210	...	-1.94	-1.90	-1.92	+0.34	+0.11	...	+0.01	+0.40	...	+0.10	+0.10	+0.33	+0.05	-0.28	...	
40216	...	-1.70	-1.55	-1.63	+0.40	-0.23	+0.23	+0.17	+0.25	-0.31	-0.03	-0.17	+0.15	-0.13	+0.28	+0.18	
40220	...	-1.66	-1.62	-1.64	-0.61	+0.41	...	+0.56	+0.44	...	+0.31	+0.31	+0.24	+0.03	+0.49	...	
40232	...	-1.04	...	-1.04	+0.05	+1.02	...	+0.33	+0.43	-0.06	-0.22	-0.14	+0.45	-0.09	+0.47	...	
40235	...	-1.93	-1.74	-1.84	+0.28	+0.21	...	+0.40	+0.26	-0.04	+0.08	+0.02	+0.21	-0.04	-0.02	...	
40237	...	-1.76	-1.54	-1.65	-1.00	+0.43	...	+0.51	+0.38	-0.01	+0.41	+0.20	+0.03	-0.14	+0.83	...	
40275	...	-1.97	-1.78	-1.88	+0.07	-0.15	...	+0.30	+0.27	...	+0.03	+0.03	+0.04	+0.01	-0.13	...	
40291	...	-1.72	-1.56	-1.64	-0.61	+0.04	...	+0.58	+0.23	...	+0.27	+0.27	+0.00	-0.12	+0.02	...	
40318	...	-1.26	...	-1.26	-0.05	+0.95	...	+0.47	+0.47	+0.17	-0.14	+0.01	+0.46	+0.05	+0.83	...	
40339	...	-1.25	...	-1.25	-0.23	+0.71	...	+0.64	+0.34	-0.24	-0.01	-0.13	+0.38	-0.04	+0.70	...	
40349	...	-1.73	-1.62	-1.68	+0.25	+0.21	...	+0.47	+0.32	-0.42	+0.12	-0.15	+0.18	-0.08	+0.24	...	
40358	...	-1.03	...	-1.03	-0.19	+0.73	+0.70	+0.23	+0.25	-0.30	-0.05	-0.18	+0.20	-0.19	+0.51	+0.09	
40361	...	-1.92	-1.94	-1.93	+0.33	+0.08	...	+0.28	+0.37	...	+0.15	+0.15	+0.12	-0.07	-0.22	...	
40371	...	-1.53	-1.37	-1.45	+0.10	+0.30	...	+0.52	+0.30	-0.33	+0.01	-0.16	+0.22	-0.10	+0.43	...	
40372	...	-1.98	-1.83	-1.91	+0.36	-0.33	...	+0.32	+0.18	...	+0.08	+0.08	+0.12	-0.03	-0.30	...	
40373	...	-1.80	-1.76	-1.78	-0.32	+0.36	...	+0.47	+0.38	+0.00	+0.12	+0.06	+0.15	-0.05	+0.08	...	
40409	552	-2.00	-1.76	-1.88	+0.58	-0.40	...	+0.45	+0.27	+0.11	-0.04	+0.51	
40420	374	-2.05	...	-2.05	+0.40	+0.55	...	+0.46	+0.62	+0.03	+0.35	+0.45	...	4	
40424	521	-1.49	...	-1.49	+0.19	+0.32	...	+0.60	+0.20	...	+0.15	+0.15	-0.03	-0.05	+0.47	...	
40472	73	-1.85	-1.52	-1.69	+0.34	-0.44	...	+0.26	+0.11	-0.50	+0.00	-0.25	+0.09	-0.23	-0.17	...	
40479	4369	-1.66	-1.56	-1.61	+0.37	+0.08	...	+0.24	+0.40	-0.09	+0.00	-0.05	+0.09	-0.04	+0.43	...	
41015	571	-1.63	-1.64	-1.64	+0.09	+0.61	...	+0.32	+0.37	...	+0.32	+0.32	+0.09	+0.00	+0.24	...	
41025	4159	-1.65	-1.60	-1.63	+0.53	+0.39	...	+0.09	+0.48	...	+0.04	+0.04	-0.05	-0.06	-0.02	...	
41033	463	-1.03	...	-1.03	+0.10	+0.91	...	+0.39	+0.41	-0.15	+0.14	-0.01	+0.26	+0.03	+0.44	...	
41034	319	-1.71	-1.57	-1.64	+0.40	-0.17	+0.34	+0.18	+0.28	...	+0.04	+0.04	+0.08	...	+0.09	...	
41035	233	-1.87	-1.76	-1.82	+0.34	-0.33	...	+0.09	+0.29	-0.12	-0.02	-0.07	+0.15	-0.05	-0.39	...	
41039	256	-1.78	-1.67	-1.73	+0.18	+0.11	...	+0.16	+0.28	...	+0.07	+0.07	+0.13	+0.03	+0.03	...	
41060	178	-1.54	-1.46	-1.50	+0.40	+0.21	+0.16	+0.35	+0.37	+0.07	+0.17	+0.12	+0.39	-0.01	+0.38	-0.28	
41061	235	-1.59	-1.58	-1.59	+0.28	+0.16	+0.44	+0.26	+0.36	-0.15	+0.07	-0.04	+0.14	+0.09	+0.09	-0.04	

Table 5—Continued

Star LEID	Alt. ID ROA	[FeI/H]	[FeII/H]	[FeIII/H] Avg.	[O/Fe]	[Na/Fe]	[Al/Fe]	[Si/Fe]	[Ca/Fe]	[Sc/Fe]	[ScI/Fe]	[ScII/Fe]	[ScIII/Fe] Avg.	[Ti/Fe]	[Ni/Fe]	[LaII/Fe]	[EuII/Fe]	Code ^a
41063	404	-1.81	-1.70	-1.76	-0.05	-0.22	...	+0.37	+0.30	+0.21	+0.26	+0.13	-0.16	+0.16	
41164	...	-1.74	-1.52	-1.63	-0.42	+0.51	...	+0.51	+0.42	...	+0.10	+0.03	+0.01	+0.78	
41186	...	-1.89	-1.75	-1.82	+0.05	+0.13	...	+0.32	+0.28	...	+0.14	+0.14	-0.01	-0.13	-0.18	
41201	...	-2.08	...	-2.08	+0.53	+0.71	...	+0.28	+0.09	...	+0.16	+0.16	+0.21	+0.69:	
41230	...	-1.82	...	-1.82	-0.28	+0.32	...	+0.42	+0.37	+0.09	...	+0.09	+0.10	+0.03	+0.05
41232	...	-2.06	...	-2.06	+0.51	+0.56	...	+0.50	+0.24	+0.31
41241	...	-1.91	-1.76	-1.84	+0.35	-0.37	...	+0.11	+0.23	-0.38	-0.01	-0.19	+0.16	+0.02	-0.27
41243	...	-1.90	-1.70	-1.80	+0.20	+0.16	...	+0.28	+0.20	...	+0.14	+0.14	+0.01	-0.10	-0.35
41246	...	-1.87	-1.63	-1.75	-0.17	-0.02	...	+0.36	+0.27	...	-0.06	-0.06	+0.07	-0.05	-0.30
41258	...	-2.14	-2.18	-2.16	+0.25	+0.14	...	+0.22	+0.35	...	+0.25	+0.25	+0.28	...	+0.09	...	4	...
41259	...	-1.86	-1.70	-1.78	+0.12	-0.48	...	+0.22	-0.14	+0.05	-0.05	-0.08	-0.05	-0.05	-0.07
41262	...	-1.17	...	-1.17	+0.01	+0.46	...	+0.46	+0.48	+0.42
41310	...	-1.66	-1.64	-1.65	-0.10	+0.18	...	+0.66	+0.57	...	+0.10	+0.10	+0.24	+0.02	+0.00
41312	...	-2.13	...	-2.13	+0.43	+0.16	...	+0.36	+0.38	+0.00	-0.08	+0.48	...	2,4	...
41313	...	-2.00	-1.81	-1.91	+0.45	-0.27	...	+0.39	+0.25	...	-0.12	-0.12	-0.02	-0.19	+0.19
41321	...	-2.05	-1.72	-1.89	+0.14	+0.30	...	+0.44	+0.19	...	+0.15	+0.15	-0.02	-0.04	-0.01	...	4	...
41348	...	-1.84	-1.62	-1.73	-0.67	+0.22	...	+0.57	+0.26	-0.30	+0.25	-0.03	-0.01	-0.11	+0.25
41366	...	-1.82	-1.66	-1.74	+0.25	+0.07	...	+0.81	+0.27	...	+0.11	+0.11	+0.16	-0.09	-0.36
41375	...	-1.90	-1.59	-1.75	-0.61	+0.22	...	+0.70	+0.09	...	+0.06	+0.06	+0.06	-0.24	-0.16
41380	...	-1.23	...	-1.23	-0.72	+0.56	...	+0.48	+0.30	-0.24	-0.09	-0.17	+0.34	+0.11	+0.28	...	1	...
41387	...	-1.72	-1.71	-1.72	-0.17	+0.43	...	+0.61	+0.48	+0.17	+0.31	+0.24	+0.09	-0.03	+0.91
41389	...	-1.86	-1.92	-1.89	+0.42	+0.21	...	+0.18	+0.28	...	+0.07	+0.07	+0.21	-0.04	+0.14
41402	...	-1.95	-1.94	-1.95	+0.19	+0.32	...	+0.31	+0.30	...	+0.14	+0.14	+0.23	+0.18	-0.16
41435	202	-1.59	...	-1.59	+0.30	+0.20	...	+0.40	+0.35	-0.28	+0.24	-0.02	+0.12	-0.19	+0.27
41455	...	-1.24	-1.20	-1.22	+0.02	+0.56	...	+0.19	+0.22	-0.30	-0.20	-0.25	+0.24	-0.14	+0.35
41476	179	-1.41	...	-1.41	+0.56	+0.39	...	+1.03	+0.48	-0.04	+0.13	+0.04	+0.48	+0.18	+0.43
41494	4339	-1.55	-1.53	-1.54	+0.59	-0.02	...	+0.42	+0.44	...	+0.22	+0.22	+0.20	-0.03	+0.63
42012	3875	-1.62	-1.58	-1.58	+0.52	+0.03	...	+0.47	+0.43	...	+0.08	+0.08	+0.36	+0.05	+0.66
42015	3881	-1.58	-1.59	-1.59	+0.52	-0.12	+0.28	+0.36	+0.39	+0.21	+0.01	+0.11	+0.30	+0.00	+0.59
42023	170	-1.88	-1.71	-1.80	+0.31	-0.43	...	+0.18	+0.15	...	-0.04	-0.04	+0.12	-0.12	-0.41
42039	205	-1.84	-1.68	-1.76	+0.08	+0.12	...	+0.20	+0.16	...	+0.05	+0.05	+0.03	-0.02	-0.19
42049	533	-1.37	-1.27	-1.32	+0.07	+0.46	...	+0.46	+0.49	+0.29	-0.04	+0.41
42054	72	-1.83	-1.83	-1.83	+0.36	-0.26	+0.43	+0.33	+0.31	-0.16	-0.02	-0.09	+0.25	+0.04	-0.27
42056	3957	-1.86	...	-1.86	+0.66	+0.21	...	+0.40	+0.30	-0.17	-0.16	+0.46

Table 5—Continued

Star LEID	Alt. ID ROA	[FeI/H]	[FeII/H]	[FeIII/H] Avg.	[O/Fe]	[Na/Fe]	[Al/Fe]	[Si/Fe]	[Ca/Fe]	[ScI/Fe]	[ScII/Fe]	[ScIII/Fe] Avg.	[Ti/Fe]	[Ni/Fe]	[LaII/Fe]	[EuII/Fe]	Code ^a
42079	3976	-1.44	-1.40	-1.42	-0.33	+0.40	...	+0.45	+0.42	+0.02	+0.09	+0.12	-0.02	+0.55	
42084	259	-1.56	-1.47	-1.52	-0.54	+0.44	...	+0.51	+0.21	+0.16	+0.18	+0.23	-0.13	+0.64	
42106	346	-1.72	...	-1.72	-0.23	+0.65	...	+0.64	+0.57	...	+0.25	+0.25	+0.31	+0.06	+0.42	...	
42114	...	-1.63	-1.46	-1.55	-0.46	+0.21	...	+0.44	+0.23	-0.10	...	-0.10	-0.02	-0.11	+0.37	...	
42120	...	-1.63	-1.40	-1.52	-0.64	+0.13	...	+0.48	+0.25	+0.13	+0.26	+0.19	+0.08	-0.10	+0.60	...	
42134	...	-1.79	-1.69	-1.74	+0.39	+0.01	...	+0.08	...	-0.05	-0.05	+0.08	-0.18	+0.30	
42161	...	-1.92	-1.76	-1.84	+0.26	-0.02	+0.28	+0.26	+0.23	-0.29	+0.08	-0.11	+0.08	+0.04	-0.41	+0.02	
42162	...	-1.07	-1.11	-1.09	-0.26	+0.81	...	+0.52	+0.33	-0.17	+0.05	-0.06	+0.34	-0.10	+0.51	...	
42169	...	-1.34	-1.34	-1.34	-0.66	+0.60	...	+0.51	+0.49	+0.05	+0.35	+0.20	+0.54	+0.06	+0.65	...	
42174	...	-1.60	-1.56	-1.58	-0.92	+0.66	...	+0.65	+0.44	+0.19	+0.46	+0.33	+0.46	-0.05	+0.38	...	
42175	...	-1.64	-1.67	-1.66	+0.26	+0.19	...	+0.29	+0.34	-0.25	-0.09	-0.17	+0.23	-0.02	+0.19	...	
42179	...	-1.92	-1.70	-1.81	+0.16	+0.11	+0.69	+0.14	+0.20	...	+0.02	+0.02	+0.12	-0.09	-0.34	+0.10	
42182	...	-1.83	-1.71	-1.77	+0.42	+0.05	...	+0.20	+0.35	...	-0.21	-0.21	+0.41	-0.10	+0.22	...	
42187	...	-1.68	-1.55	-1.62	-0.49	+0.38	...	+0.64	+0.27	-0.05	+0.20	+0.07	+0.04	-0.08	+0.13	...	
42196	...	-2.14	-2.11	-2.13	+0.28	+0.79	...	+0.82	+0.52	...	+0.33	+0.13	+0.03	+0.29	
42198	...	-2.03	...	-2.03	+0.50	+0.57	...	+0.74	+0.58	...	+0.08	+0.08	...	+0.26	+0.38	...	
42205	...	-1.35	...	-1.35	-0.60	+0.64	...	+0.54	+0.33	-0.19	-0.07	-0.13	+0.42	-0.03	+0.61	...	
42221	...	-1.91	-1.77	-1.84	+0.14	+0.34	...	+0.30	+0.29	+0.11	+0.20	-0.01	-0.10	-0.16	
42260	...	-1.78	...	-1.78	-0.62	+0.29	...	+0.60	+0.58	+0.43	+0.38	+0.40	+0.19	+0.08	+1.09	...	
42271	...	-2.26	...	-2.26	+0.41	+0.01	...	+0.43	+0.41	+0.19	+0.16	+0.18	+0.04	+0.13	+0.36	4	
42302	...	-1.81	...	-1.81	+0.31	-0.19	+0.39	+0.30	+0.32	-0.20	-0.04	-0.12	+0.24	+0.02	-0.31	+0.29	
42303	...	-1.42	-1.55	-1.49	+0.64	+0.21	...	+0.26	+0.34	+0.49	+0.23	+0.36	+0.59	+0.15	+0.67	...	
42309	...	-0.80	...	-0.80	+0.01	+0.34	...	+0.60	+0.32	-0.28	-0.04	-0.16	-0.02	-0.24	+0.15	...	
42339	...	-1.18	-1.18	-1.18	-0.27	+0.68	...	+0.06	+0.31	+0.24	+0.38	+0.31	+0.45	-0.02	+0.76	...	
42345	...	-2.02	-1.97	-2.00	+0.35	+0.16	...	+0.34	+0.25	...	+0.23	+0.23	+0.06	+0.13	+0.10	...	
42361	...	-1.98	-1.81	-1.90	+0.37	+0.12	...	+0.22	+0.24	...	+0.08	+0.08	+0.06	-0.05	-0.05	...	
42384	...	-1.62	-1.40	-1.51	+0.49	+0.02	...	+0.24	+0.23	-0.45	-0.14	-0.30	+0.20	-0.11	+0.44	...	
42385	...	-1.84	-1.87	-1.86	+0.27	-0.16	...	+0.23	+0.44	...	+0.21	+0.21	+0.32	+0.02	-0.30	4	
42407	...	-1.48	...	-1.48	+0.33	+0.37	...	+0.49	...	+0.01	+0.01	+0.53	+0.16	+0.65	
42415	...	-1.67	-1.43	-1.55	-0.35	+0.19	...	+0.42	+0.29	-0.38	...	-0.38	+0.06	-0.11	+0.54	...	
42438	538	-1.31	-1.33	-1.32	-0.53	+0.49	...	+0.21	+0.39	+0.10	+0.14	+0.12	+0.24	-0.11	+0.73	...	
42457	4047	-1.66	...	-1.66	+0.41	+0.11	...	+0.24	...	+0.30	+0.30	+0.32	...	+0.36	...	4	
42461	51	-1.83	-1.67	-1.75	+0.40	-0.24	+0.25	+0.27	+0.22	-0.31	+0.06	-0.13	+0.15	-0.14	-0.40	...	
42473	414	-1.38	...	-1.38	-0.62	+0.60	...	+0.48	+0.35	+0.06	+0.25	+0.16	+0.27	+0.02	+0.66	...	

Table 5—Continued

Star LEID	Alt. ID ROA	[FeI/H]	[FeII/H]	[FeIII/H] Avg.	[O/Fe]	[Na/Fe]	[Al/Fe]	[Si/Fe]	[Ca/Fe]	[ScI/Fe]	[ScII/Fe]	[ScIII/Fe] Avg.	[Ti/Fe]	[Ni/Fe]	[LaII/Fe]	[EuII/Fe]	Code ^a
42497	398	-1.90	-1.78	-1.84	+0.26	-0.16	+0.72	+0.27	+0.29	-0.09	+0.02	-0.04	+0.10	+0.02	-0.16	+0.30	...
42501	305	-1.70	-1.73	-1.72	+0.37	-0.25	...	+0.32	+0.24	-0.20	+0.15	-0.02	+0.26	-0.07	+0.50
42503	4095	-1.61	...	-1.61	+0.34	-0.04	...	+0.13	+0.38	...	+0.12	+0.05	-0.10	+0.31
42508	600	-1.74	-1.70	-1.72	+0.64	+0.04	...	+0.42	+0.36	+0.19	+0.06	+0.12	+0.34	-0.07	+0.65
43010	591	-1.86	-1.67	-1.77	+0.37	-0.09	...	+0.17	+0.16	-0.03	+0.14	+0.05	+0.05	+0.00	-0.09	...	4
43024	3911	-1.66	-1.63	-1.65	+0.09	+0.26	...	+0.09	+0.23	+0.14	...	+0.14	+0.07	-0.12	+0.04
43036	440	-1.45	-1.34	-1.40	-0.16	+0.04	...	+0.35	+0.30	-0.20	...	-0.20	+0.13	-0.15	-0.04
43040	3937	-1.62	...	-1.62	+0.22	+0.27	...	+0.49	+0.30	...	+0.32	+0.16	+0.15	+0.62
43060	3952	-1.68	...	-1.68	+0.25	+0.33	...	+0.31	+0.25	...	+0.29	+0.16	-0.09	+0.64
43061	357	-1.12	...	-1.12	+0.16	+0.98	...	+0.69	+0.51	+0.12	...	+0.12	+0.47	+0.14	+0.48
43064	140	-1.62	-1.54	-1.58	+0.23	-0.46	-0.07	+0.13	+0.14	-0.18	-0.06	-0.12	+0.13	-0.11	-0.32	-0.16	...
43068	405	-1.43	...	-1.43	-0.12	+0.28	...	+0.34	+0.45	-0.47	+0.19	-0.14	+0.12	-0.08	+0.38
43071	427	-1.69	-1.70	-1.70	-0.26	+0.46	...	+0.13	+0.25	+0.33	+0.13	+0.23	+0.04	-0.01	+0.00
43079	3977	-1.00	-1.07	-1.04	-0.87	+0.34	...	+0.28	+0.25	...	-0.14	-0.14	+0.16	...	+0.20	...	1
43087	360	-1.72	-1.55	-1.64	+0.26	+0.32	...	+0.18	+0.26	+0.03	+0.13	+0.08	+0.12	-0.06	+0.29
43091	314	-1.51	-1.49	-1.50	+0.07	+0.35	...	+0.51	+0.49	-0.08	...	-0.08	+0.28	-0.07	+0.36
43095	1116	-1.87	-1.79	-1.83	-0.07	+0.00	...	+0.15	+0.30	...	+0.11	+0.11	+0.05	+0.03	-0.37	...	4
43096	35	-1.88	...	-1.88	+0.34	-0.10	...	+0.51	+0.23	-0.41	+0.19	-0.11	+0.11	+0.03	-0.15
43099	39	-1.47	...	-1.47	+0.07	+0.45	...	+0.69	+0.38	-0.21	-0.25	-0.23	+0.24	+0.08	+0.22
43101	210	-1.85	-1.68	-1.77	+0.35	-0.01	...	+0.18	+0.16	...	+0.16	+0.16	+0.21	-0.08	-0.39
43104	...	-1.51	-1.50	-1.51	-0.44	+0.44	...	+0.56	+0.52	+0.14	+0.31	+0.22	+0.12	-0.03	+0.46
43108	...	-1.65	-1.72	-1.69	-0.12	+0.62	...	+0.59	+0.49	...	+0.33	+0.33	+0.26	+0.05	+0.39
43111	...	-1.72	-1.46	-1.59	+0.29	-0.06	...	+0.35	+0.28	+0.01	+0.03	+0.19
43134	...	-1.95	-1.95	-1.95	+0.20	+0.07	...	+0.34	+0.11	...	-0.01	-0.01	+0.51	+0.39	-0.10	...	4
43139	...	-1.71	-1.73	-1.72	+0.12	+0.00	...	-0.04	+0.15	...	-0.05	-0.05	+0.34	+0.08	-0.18
43158	...	-2.00	-1.80	-1.90	+0.25	-0.01	...	+0.11	+0.24	...	+0.02	+0.02	+0.06	-0.10	-0.15
43189	...	-1.37	-1.48	-1.43	-0.38	+0.59	...	+0.53	+0.36	-0.07	...	-0.07	+0.50	+0.03	+0.68
43216	...	-1.48	-1.32	-1.40	-0.09	+0.36	+0.55	+0.51	+0.30	-0.50	-0.02	-0.26	+0.25	-0.12	+0.26	-0.01	...
43233	...	-1.92	...	-1.92	+0.07	+0.54	...	+0.17	+0.30	...	+0.22	+0.22	+0.09	...	-0.03
43241	...	-1.91	...	-1.91	-0.54	+0.36	...	+0.48	+0.29	-0.06	...	-0.06	+0.40	-0.13	-0.04
43258	...	-2.23	...	-2.23	+0.53	+0.19	...	+0.66	+0.34	...	+0.20	+0.20	-0.11	+0.12	+0.08
43261	...	-1.90	-1.70	-1.80	+0.17	-0.23	...	+0.11	+0.17	-0.58	-0.08	-0.33	+0.03	-0.10	-0.25
43278	...	-1.93	...	-1.93	+0.55	+0.60	...	+0.41	+0.41	...	+0.12	+0.12	+0.09	...	+0.63	...	1
43326	...	-1.24	...	-1.24	-0.61	+0.42	+0.40	+0.24	-0.42	...	-0.42	+0.32	+0.00	+0.35	+0.20

Table 5—Continued

Star LEID	Alt. ID ROA	[FeII/H]	[FeI/H]	[O/Fe] Avg.	[Fe/H] Avg.	[Na/Fe]	[Al/Fe]	[Si/Fe]	[Ca/Fe]	[Sc/Fe]	[ScII/Fe]	[ScIII/Fe] Avg.	[Ti/Fe]	[Ni/Fe]	[LaII/Fe]	[EuII/Fe]	Code ^a
43330	...	-1.89	-1.84	-1.87	+0.17	+0.37	...	+0.32	+0.31	-0.25	+0.02	-0.11	+0.13	-0.02	-0.18	...	
43351	...	-1.12	-0.85	-0.98	-0.42	+0.32	...	+0.19	+0.08	-0.41	+0.04	-0.41	+0.17	-0.25	+0.36	...	
43367	...	-1.89	-1.74	-1.82	-0.07	+0.25	+1.00	+0.33	+0.23	-0.32	-0.02	-0.17	+0.17	+0.00	-0.29	-0.03	
43389	...	-1.39	-1.36	-1.38	+0.56	+0.10	...	+0.56	+0.47	-0.11	+0.11	+0.00	+0.42	-0.07	+0.68	...	
43397	...	-1.88	...	-1.88	+0.58	+0.08	...	+0.25	+0.19	...	+0.14	+0.14	
43399	...	-1.70	-1.84	-1.77	+0.35	-0.06	...	+0.17	+0.39	+0.17	+0.12	+0.14	+0.22	+0.04	+0.27	...	
43412	88	-1.88	-1.67	-1.78	+0.25	-0.39	...	+0.33	+0.21	...	+0.12	+0.12	+0.01	-0.13	-0.43	...	
43433	...	-1.82	-1.77	-1.80	+0.12	+0.12	...	+0.40	+0.38	-0.29	-0.06	-0.17	+0.06	-0.04	+0.10	4	
43446	564	-1.60	-1.67	-1.64	+0.61	+0.30	...	+0.11	+0.46	+0.29	+0.37	+0.35	-0.06	+0.44	
43458	522	-1.25	-1.30	-1.28	-0.58	+0.50	...	+0.42	+0.50	...	-0.07	-0.07	+0.24	+0.06	+0.52	1	
43463	410	-1.91	-1.63	-1.77	+0.27	+0.35	...	+0.17	+0.11	...	+0.08	+0.08	-0.02	-0.22	-0.23	...	
43475	593	-0.66	-0.54	-0.60	+0.10	+0.03	...	+0.20	+0.05	...	+0.05	+0.05	-0.26	-0.11	+0.26	...	
43485	265	-1.77	-1.70	-1.74	+0.29	+0.04	...	+0.36	+0.30	...	+0.05	+0.05	+0.10	-0.03	-0.27	4	
43539	4106	-1.61	-1.53	-1.57	+0.37	+0.27	...	+0.18	+0.34	+0.04	+0.12	+0.08	+0.20	-0.07	+0.17	...	
44026	341	-1.33	...	-1.33	-0.47	+0.39	...	+0.38	+0.29	-0.15	...	-0.15	+0.07	+0.00	+0.54	...	
44042	136	-1.86	-1.80	-1.83	+0.26	+0.01	+0.06	+0.30	+0.29	-0.14	+0.07	-0.04	+0.11	-0.04	-0.37	+0.03	
44056	578	-1.55	-1.46	-1.51	+0.52	-0.22	...	+0.40	...	-0.07	-0.07	-0.07	+0.19	-0.09	+0.55	...	
44065	350	-1.79	-1.76	-1.78	+0.38	-0.71	...	+0.26	+0.19	...	+0.09	+0.09	+0.09	-0.01	-0.13	...	
44067	310	-1.66	...	-1.66	+0.36	+0.07	...	+0.27	+0.07	+0.59	+0.30	+0.44	+0.07	+0.01	+0.26	...	
44115	64	-1.80	-1.61	-1.71	+0.24	-0.02	...	+0.31	+0.18	-0.37	+0.09	-0.14	+0.13	-0.06	-0.25	...	
44120	...	-1.88	...	-1.88	+0.48	+0.13	...	+0.30	+0.39	...	+0.34	+0.13	-0.24	+0.23	...	4	
44143	...	-1.83	-1.74	-1.79	+0.39	-0.16	+0.36	+0.27	+0.25	+0.07	+0.05	+0.06	+0.12	-0.01	-0.32	-0.10	
44163	...	-1.85	-1.82	-1.84	+0.21	+0.10	...	+0.46	+0.34	-0.12	+0.19	+0.04	+0.15	+0.10	+0.14	...	
44188	...	-1.69	-1.50	-1.60	+0.49	+0.38	...	+0.52	+0.50	+0.16	+0.21	+0.18	+0.33	+0.06	+0.60	...	
44189	...	-1.53	-1.36	-1.45	-0.96	+0.73	...	+0.73	+0.35	-0.03	...	-0.03	+0.06	-0.05	+0.57	1	
44198	...	-1.92	-1.65	-1.79	+0.44	-0.11	...	+0.20	+0.16	...	+0.02	+0.02	+0.02	-0.12	-0.10	4	
44219	...	-1.81	-1.72	-1.62	-0.25	...	+0.26	+0.15	-0.22	-0.04	-0.13	+0.25	+0.30	-0.05	+0.51	...	
44231	...	-1.42	-1.49	-1.46	-0.50	+0.13	...	+0.39	+0.43	+0.25	+0.24	+0.25	+0.30	-0.05	+0.60	...	
44253	...	-1.67	-1.48	-1.58	+0.10	+0.13	...	+0.45	+0.20	-0.29	-0.18	-0.23	+0.06	-0.25	+0.10	...	
44271	...	-1.91	-1.69	-1.80	+0.31	+0.28	...	+0.05	+0.42	...	+0.08	+0.08	...	-0.38	
44277	...	-1.37	...	-1.37	+0.27	+0.11	...	+0.44	+0.20	-0.03	-0.05	-0.04	+0.25	+0.01	+0.16	...	
44304	...	-1.87	-1.82	-1.85	-0.61	+0.52	...	+0.74	+0.57	+0.12	+0.16	+0.14	+0.14	+0.15	+0.92	...	
44313	...	-1.79	-1.71	-1.75	-0.25	+0.20	+0.99	+0.56	+0.28	+0.01	+0.26	+0.14	+0.16	+0.01	+0.20	-0.08	...
44327	...	-1.87	-1.87	-1.87	+0.21	-0.07	...	+0.26	+0.32	...	+0.07	+0.07	+0.09	+0.09	-0.38	...	

Table 5—Continued

Star LEID	Alt. ID ROA	[FeI/H]	[FeII/H]	[FeIII/H] Avg.	[O/Fe]	[Na/Fe]	[Al/Fe]	[Si/Fe]	[Ca/Fe]	[ScI/Fe]	[ScII/Fe]	[ScIII/Fe] Avg.	[Ti/Fe]	[Ni/Fe]	[LaII/Fe]	[EuII/Fe]	Code ^a	
44337	...	-1.92	-1.66	-1.79	+0.18	-0.09	+0.44	+0.23	+0.19	...	+0.05	+0.15	-0.08	-0.38	+0.02	...		
44343	...	-1.79	-1.78	-1.79	-0.22	+0.37	...	+0.31	+0.31	...	+0.09	+0.07	+0.02	-0.01		
44380	...	-1.83	...	-1.83	+0.63	-0.08	...	+0.19	...	+0.01	+0.01	+0.01	+0.24	+0.43		
44424	...	-1.91	-1.75	-1.83	+0.30	+0.14	...	+0.36	+0.18	...	+0.06	+0.06	-0.09	-0.23	+0.13	
44426	...	-1.48	...	-1.48	-0.62	+0.40	...	+0.58	+0.33	-0.03	+0.05	+0.05	+0.01	-0.10	+0.21	
44435	433	-1.54	-1.43	-1.49	+0.23	+0.15	...	+0.37	+0.36	...	+0.05	+0.05	+0.08	-0.03	+0.37	
44446	529	-1.80	-1.74	-1.77	+0.27	+0.48	...	+0.08	+0.43	...	-0.01	-0.01	+0.01	+0.18	+0.20	
44449	100	-1.37	-1.37	-1.37	-0.73	+0.47	...	+0.30	+0.28	-0.04	...	-0.04	...	+0.07	+0.07	
44462	321	-1.13	-1.23	-1.18	+0.70	+0.12	...	+0.69	+0.54	+0.07	+0.02	+0.04	+0.30	+0.03	+0.26	
44488	3813	-1.71	...	-1.71	+0.65	+0.36	...	+0.43	-0.13	-0.18	+0.14	+0.31	
44493	499	-1.76	-1.68	-1.72	+0.07	+0.03	...	+0.15	+0.17	...	+0.08	+0.08	+0.28	-0.09	-0.08	...	4	
45082	318	-1.86	-1.79	-1.83	+0.23	-0.17	...	+0.21	+0.28	...	-0.05	-0.05	+0.09	-0.03	-0.43	
45089	197	-1.85	...	-1.85	+0.25	+0.40	...	+0.47	+0.19	...	+0.24	+0.24	+0.02	+0.03	+0.20	
45092	406	-1.30	...	-1.30	-0.35	+0.48	...	+0.70	+0.41	-0.11	...	-0.11	+0.22	+0.04	+0.70	
45093	573	-1.68	-1.54	-1.61	+0.29	+0.06	...	+0.41	+0.23	...	-0.01	-0.01	-0.06	-0.24	+0.01	
45126	...	-1.78	-1.74	-1.76	+0.51	+0.01	...	+0.20	+0.32	...	+0.06	+0.06	+0.06	+0.23	+0.03	+0.26	...	
45177	...	-1.92	-1.74	-1.83	+0.23	-0.28	...	+0.33	+0.29	-0.40	+0.00	+0.00	-0.20	+0.08	-0.06	-0.27	...	
45180	...	-1.78	-1.68	-1.73	+0.32	+0.01	...	+0.27	+0.40	...	+0.02	+0.02	+0.02	+0.10	-0.04	+0.28	...	
45206	...	-1.77	-1.70	-1.74	+0.39	+0.05	...	+0.02	+0.16	+0.20	+0.01	+0.11	-0.13	...	+0.04	
45215	...	-0.97	-1.14	-1.06	+0.57	+0.40	+0.18	+0.56	+0.50	+0.17	+0.27	+0.22	+0.85	-0.09	+0.60	-0.02	...	
45232	...	-1.91	...	-1.91	+0.38	+0.29	...	+0.49	+0.22	+0.20	+0.28	+0.24	+0.49	+0.08	-0.19	
45235	...	-1.88	...	-1.88	+0.33	+0.33	+0.74	...	+0.74	+0.62	...	+0.22	+0.22	+0.07	
45238	...	-1.79	-1.66	-1.73	+0.24	+0.41	...	+0.41	+0.34	-0.06	+0.08	+0.01	+0.15	-0.02	+0.13	
45240	...	-1.62	...	-1.62	-0.58	+0.32	...	+0.50	+0.44	-0.07	+0.19	+0.06	+0.39	...	+0.61	...	1	
45246	...	-1.55	...	-1.55	-0.60	+0.57	...	+0.58	+0.33	-0.28	...	-0.28	+0.11	-0.02	+0.36	
45249	...	-1.64	...	-1.64	+0.36	+0.20	...	+0.53	+0.51	-0.17	+0.14	-0.02	+0.35	+0.00	+0.29	
45272	...	-1.76	...	-1.76	+0.08	+0.34	+0.71	+0.41	+0.39	...	+0.17	+0.17	+0.16	-0.04	+0.49	+0.45	...	
45285	...	-0.95	...	-0.95	-0.95	+0.57	...	+0.10	+0.17	-0.38	...	-0.38	+0.34	+0.11	+0.40	
45292	...	-1.59	...	-1.59	+0.09	+0.43	...	+0.63	+0.42	-0.28	+0.37	+0.04	+0.15	+0.14	+0.42	
45309	...	-2.06	-1.86	-1.96	+0.32	-0.33	...	+0.24	+0.29	...	-0.07	-0.07	-0.05	-0.07	-0.39	
45322	...	-1.71	...	-1.71	+0.19	+0.32	...	+0.74	+0.38	...	+0.16	+0.16	+0.19	+0.04	+0.34	
45326	...	-1.62	-1.43	-1.53	-0.33	+0.24	...	+0.23	+0.28	...	+0.06	+0.06	+0.02	-0.15	+0.18	
45342	...	-1.12	...	-1.12	-0.58	+0.69	...	+0.31	+0.29	+0.00	...	+0.00	+0.61	-0.44	+0.72	
45343	...	-1.76	-1.49	-1.63	-0.73	+0.21	...	+0.43	+0.21	-0.29	+0.18	+0.18	-0.05	+0.02	-0.26	-0.10

Table 5—Continued

Star LEID	Alt. ID ROA	[FeI/H]	[FeII/H]	[FeIII/H] Avg.	[O/Fe]	[Na/Fe]	[Al/Fe]	[Si/Fe]	[Ca/Fe]	[Sc/Fe]	[ScII/Fe]	[ScIII/Fe] Avg.	[Ti/Fe]	[Ni/Fe]	[LaII/Fe]	[EuII/Fe]	Code ^a
45359	...	-1.84	-1.73	-1.79	-0.03	+0.17	...	+0.32	+0.30	+0.18	+0.00	-0.12	-0.03	
45373	...	-1.68	...	-1.68	+0.08	+0.44	...	+0.37	+0.32	-0.23	+0.03	+0.20	+0.00	+0.33	
45377	...	-1.63	-1.59	-1.61	+0.23	-0.31	...	-0.04	+0.22	...	+0.06	-0.01	-0.06	+0.11	
45389	...	-1.79	-1.64	-1.72	+0.04	+0.05	...	+0.29	+0.25	...	+0.04	+0.04	+0.00	-0.15	+0.07	...	
45410	...	-1.80	...	-1.80	+0.40	+0.31	+0.19	+0.08	+0.14	+0.00	...	+0.00	
45418	...	-1.44	...	-1.44	+0.00	-0.16	...	+0.12	+0.46	...	+0.28	+0.25	-0.17	+0.39	
45453	144	-1.93	-1.78	-1.86	-0.80	+0.52	+1.28	+0.90	+0.28	...	+0.32	-0.08	-0.07	+0.63	+0.30	...	
45454	42	-1.78	...	-1.78	-0.57	+0.46	...	+0.74	+0.33	+0.07	-0.08	-0.14	
45463	444	-1.48	-1.47	-1.48	+0.30	+0.43	...	+0.26	+0.40	-0.02	+0.28	+0.14	+0.40	+0.01	+0.43	...	
45482	586	-1.52	-1.46	-1.49	-0.51	+0.51	...	+0.54	+0.41	...	+0.25	+0.25	+0.02	-0.03	+0.69	...	
46024	40	-1.70	-1.67	-1.69	+0.37	-0.12	...	+0.29	+0.29	-0.18	-0.01	-0.09	+0.20	-0.04	+0.15	...	
46055	344	-1.63	-1.41	-1.52	-0.63	+0.25	...	+0.42	+0.15	...	+0.23	-0.01	-0.15	+0.48	
46062	62	-1.81	...	-1.81	+0.11	+0.33	...	+0.51	+0.20	...	+0.15	+0.15	+0.18	-0.02	+0.03	...	
46073	267	-1.09	...	-1.09	-1.01	+0.39	+0.81	+0.33	+0.19	-0.19	...	-0.19	-0.24	-0.25	+0.49	+0.40	
46090	454	-2.00	-1.93	-1.97	+0.42	+0.27	...	-0.03	+0.37	...	+0.08	+0.02	+0.16	+0.02	...	4	
46092	92	-1.45	...	-1.45	-0.50	+0.47	...	+0.49	+0.43	-0.32	-0.32	+0.22	+0.00	+0.49	
46121	...	-0.97	-0.94	-0.96	+0.49	+0.20	...	+0.69	+0.44	-0.41	+0.25	-0.08	+0.18	+0.07	+0.36	...	
46140	...	-1.73	-1.61	-1.67	+0.32	+0.17	...	+0.29	+0.26	...	+0.15	+0.15	+0.27	-0.04	+0.16	...	
46150	...	-1.39	-1.38	-1.39	+0.44	+0.00	...	+0.36	+0.36	+0.11	+0.26	+0.18	+0.37	-0.02	+0.35	...	
46166	...	-1.72	-1.66	-1.69	-0.61	+0.14	...	+0.45	+0.43	...	+0.38	+0.01	+0.11	+0.39	
46172	...	-1.61	-1.40	-1.51	-0.33	+0.34	...	+0.46	+0.39	-0.19	...	-0.19	+0.27	-0.04	+0.31	...	
46194	...	-1.88	-1.72	-1.80	-0.05	+0.25	...	+0.39	+0.26	...	+0.08	+0.08	-0.07	-0.04	
46196	...	-1.88	-1.70	-1.79	+0.34	+0.32	...	+0.37	+0.31	...	+0.21	...	+0.17	
46223	...	-1.68	...	-1.68	+0.05	+0.40	...	+0.30	+0.33	-0.25	...	-0.25	+0.03	-0.05	+0.32	...	
46248	...	-1.88	-1.85	-1.87	+0.27	+0.48	...	+0.40	+0.34	-0.16	+0.03	-0.06	+0.34	+0.06	-0.11	...	
46279	...	-1.81	-1.75	-1.78	+0.30	+0.68	...	+0.46	...	-0.07	-0.07	+0.11	+0.01	+0.18	
46289	...	-1.93	-1.75	-1.84	+0.06	+0.48	+0.61	+0.25	+0.21	...	-0.04	-0.04	-0.05	-0.15	-0.31	-0.16	
46301	...	-1.86	-1.65	-1.76	+0.25	-0.36	...	+0.21	+0.25	...	-0.03	-0.03	+0.03	-0.03	-0.15	4	
46318	...	-1.97	-1.76	-1.87	+0.22	-0.18	...	+0.22	+0.27	...	-0.04	-0.04	-0.03	+0.02	-0.19	...	
46323	...	-1.85	-1.64	-1.75	+0.15	+0.22	...	+0.08	+0.22	...	+0.15	+0.05	-0.12	-0.46	
46325	...	-2.01	-1.92	-1.97	+0.37	+0.36	...	+0.43	+0.22	...	+0.18	+0.14	+0.01	-0.08	...	4	
46348	...	-1.96	-1.86	-1.91	+0.06	+0.41	...	+0.32	+0.31	...	-0.05	-0.05	+0.12	+0.00	+0.01	...	
46350	...	-1.56	-1.32	-1.44	+0.52	-0.17	...	+0.41	+0.10	...	-0.05	-0.05	-0.14	+0.27	
46381	329	-1.60	-1.44	-1.52	-0.28	+0.23	...	+0.21	+0.32	...	+0.19	+0.19	+0.14	-0.17	+0.21	...	

Table 5—Continued

Star LEID	Alt. ID ROA	[FeI/H]	[FeII/H]	[FeIII/H] Avg.	[O/Fe]	[Na/Fe]	[Al/Fe]	[Si/Fe]	[Ca/Fe]	[ScI/Fe]	[ScII/Fe]	[ScIII/Fe] Avg.	[Ti/Fe]	[Ni/Fe]	[LaII/Fe]	[EuII/Fe]	Code ^a	
46388	574	-1.92	-1.69	-1.81	+0.18	+0.39	...	+0.29	+0.20	+0.15	+0.12	+0.13	+0.29	...	+0.11	
46391	469	-1.55	-1.44	-1.50	+0.65	+0.17	...	+0.31	+0.14	-0.12	-0.07	-0.09	-0.04	-0.02	+0.23	
46398	3534	-1.80	-1.80	-1.80	+0.35	+0.06	...	+0.81	+0.25	...	+0.07	+0.07	
46405	3545	-1.64	-1.77	-1.71	+0.31	+0.13	...	+0.23	+0.25	...	-0.01	-0.01	+0.24	...	+0.21	
46438	3588	-1.71	-1.63	-1.67	+0.57	+0.08	...	+0.14	+0.08	...	-0.07	-0.07	-0.01	
47012	155	-1.61	-1.65	-1.63	+0.40	-0.27	...	+0.27	+0.31	...	+0.08	+0.08	+0.20	-0.03	+0.08	
47039	489	-1.76	-1.58	-1.67	-0.38	+0.05	...	+0.32	+0.19	...	-0.06	-0.06	+0.03	-0.13	-0.13	...	4	
47055	3449	-1.79	-1.64	-1.72	+0.73	-0.96	...	+0.24	+0.38	...	+0.18	+0.18	+0.20	+0.35	+0.22	
47074	459	-1.64	-1.60	-1.62	+0.20	-0.04	...	+0.21	+0.10	...	+0.19	+0.19	-0.08	+0.14	-0.02	
47096	3489	-1.32	-1.12	-1.22	-0.48	+0.25	...	+0.48	+0.28	+0.04	...	+0.04	+0.05	-0.13	+0.48
47107	...	-1.74	-1.65	-1.70	+0.50	+0.04	+0.19	+0.40	+0.18	...	+0.02	+0.02	+0.11	+0.01	+0.26	-0.07	...	
47110	...	-1.84	-1.78	-1.81	+0.40	-0.11	...	+0.44	+0.32	...	+0.20	+0.20	+0.11	-0.09	-0.21	
47146	...	-1.59	-1.55	-1.57	-0.63	+0.42	+1.11	+0.71	+0.44	-0.11	+0.12	+0.00	+0.19	+0.03	+0.86	+0.15	...	
47150	...	-1.54	-1.42	-1.48	-0.62	+0.46	...	+0.44	+0.23	-0.26	+0.11	-0.08	+0.18	-0.05	+0.49	
47151	...	-1.84	-1.79	-1.82	-0.14	+0.43	...	+0.44	+0.38	...	+0.27	+0.27	+0.23	...	+0.51	
47153	...	-1.14	...	-1.14	-0.36	+0.45	...	+0.58	+0.29	...	+0.01	+0.01	+0.16	-0.06	+0.57	
47176	...	-1.64	-1.48	-1.56	-0.29	+0.45	...	+0.58	+0.35	-0.23	+0.27	+0.02	-0.01	-0.07	+0.22	...	1	
47186	...	-1.30	-1.16	-1.23	-0.13	+0.40	...	+0.51	+0.32	-0.42	+0.12	-0.15	+0.18	-0.16	+0.30	
47187	...	-1.17	...	-1.17	-0.73	+0.25	...	+0.31	+0.30	-0.05	...	-0.05	+0.26	-0.15	+0.63	
47199	...	-1.83	-1.52	-1.68	+0.01	+0.54	+0.28	+0.08	-0.54	+0.19	-0.17	-0.03	-0.19	-0.48	+0.16	
47269	...	-1.45	-1.27	-1.36	-0.49	+0.46	...	+0.42	+0.34	+0.03	+0.16	+0.09	+0.07	-0.29	+0.39	
47299	...	-1.73	...	-1.73	+0.33	+0.45	...	+0.31	+0.30	...	+0.38	+0.38	+0.18	...	+0.83	
47307	41	-1.86	-1.68	-1.77	-0.03	+0.16	+0.78	+0.05	+0.13	...	+0.19	+0.19	+0.05	-0.08	-0.28	+0.27	...	
47331	...	-1.79	-1.72	-1.76	+0.48	+0.25	...	+0.34	-0.10	-0.35	
47338	...	-1.79	-1.55	-1.67	+0.27	-0.14	...	+0.16	+0.21	...	-0.02	-0.02	+0.05	-0.06	-0.06	
47339	...	-1.48	-1.46	-1.47	-0.58	+0.49	...	+0.46	+0.49	...	-0.09	-0.09	+0.23	-0.05	+0.85	
47348	...	-1.59	-1.42	-1.51	+0.00	+0.25	...	+0.01	+0.24	-0.26	+0.07	-0.09	+0.16	-0.05	+0.20	
47354	...	-0.95	...	-0.95	-0.30	+0.72	+0.77	+0.35	+0.36	+0.07	...	+0.07	+0.48	-0.08	+0.63	+0.36	...	
47387	247	-1.77	-1.65	-1.71	+0.30	-0.08	-0.09	+0.19	+0.19	-0.24	+0.09	-0.08	+0.04	-0.08	-0.09	+0.23	...	
47399	85	-1.49	-1.38	-1.44	+0.46	-0.08	...	+0.41	+0.31	-0.04	+0.00	-0.02	+0.46	-0.01	+0.08	
47400	376	-1.46	-1.38	-1.42	+0.12	+0.30	...	+0.37	+0.31	-0.33	+0.17	-0.08	+0.25	-0.11	+0.35	
47405	75	-1.89	...	-1.89	+0.49	+0.09	...	+0.42	+0.23	...	+0.21	+0.21	+0.10	-0.03	-0.01	
47420	530	-1.43	-1.32	-1.38	-0.48	+0.30	...	+0.37	+0.43	...	+0.21	+0.21	+0.11	-0.25	+0.18	
47443	597	-1.82	-1.83	-1.83	+0.31	+0.23	...	+0.36	...	+0.05	+0.05	+0.05	-0.04	+0.31	-0.03	

Table 5—Continued

Star LEID	Alt. ID ROA	[Fe/H] [FeII/H]	[FeIII/H] Avg.	[O/Fe] [O/Fe]	[Na/Fe] [Na/Fe]	[Al/Fe] [Al/Fe]	[Si/Fe] [Si/Fe]	[Ca/Fe] [Ca/Fe]	[ScI/Fe] [ScII/Fe]	[ScII/Fe] Avg.	[Sc/Fe] [Sc/Fe]	[Ti/Fe] [Ti/Fe]	[Ni/Fe] [Ni/Fe]	[LaII/Fe] [LaII/Fe]	[EuII/Fe] [EuII/Fe]	Code ^a
47450	3606	-1.67	...	-1.67	+0.52	+0.07	...	+0.10	+0.36	...	-0.07	-0.07	+0.14	+0.17
48028	193	-1.81	-1.74	-1.78	+0.02	+0.21	...	+0.26	+0.24	+0.01	+0.13	+0.07	+0.13	+0.02	-0.33	...
48036	3433	-1.60	-1.55	-1.58	-0.01	+0.51	...	+0.41	+0.25	+0.48	+0.22	+0.35	+0.11	+0.00	+0.56	4
48049	76	-1.76	...	-1.76	+0.33	-0.07	...	+0.37	+0.32	-0.16	+0.10	-0.03	+0.32	+0.00	-0.07	...
48060	52	-1.88	...	-1.88	+0.24	+0.28	...	+0.48	+0.22	+0.02	+0.30	+0.16	+0.38	-0.07	+0.03	...
48067	498	-1.55	-1.48	-1.52	+0.12	+0.38	...	+0.36	+0.33	+0.03	+0.17	+0.10	+0.32	-0.10	+0.47	...
48083	191	-1.37	-1.33	-1.35	-0.40	+0.27	...	+0.33	+0.22	+0.00	+0.14	+0.07	+0.12	-0.14	+0.60	...
48099	300	-0.68	...	-0.68	-0.22	+0.98	...	+1.15	+0.29	+0.50	+0.02	+0.28	...
48116	...	-0.75	-0.72	-0.74	-0.12	+0.94	+0.43	+0.71	+0.57	+0.09	-0.11	-0.01	+0.55	+0.03	+0.44	+0.12
48120	...	-1.61	...	-1.61	+0.46	-0.03	...	+0.54	+0.34	-0.05	-0.03	-0.04	+0.25	+0.16	+0.18	...
48150	...	-1.21	-1.09	-1.15	+0.25	-0.29	...	+0.50	+0.09	...	+0.22	+0.22	-0.04	+0.07	+0.31	...
48151	...	-1.94	...	-1.94	+0.44	+0.37	...	+0.50	+0.29	...	+0.23	+0.23	+0.16	...	+0.04	4
48186	...	-1.97	...	-1.97	+0.44	+0.58	+0.40	+0.37	+0.18	+0.28	+0.07	+0.01	+0.00	...
48197	...	-1.52	-1.59	-1.56	+0.56	-0.08	...	+0.24	+0.36	+0.38	-0.02	+0.31	...
48221	...	-1.28	-1.27	-1.28	-0.43	+0.33	...	+0.27	+0.32	-0.20	+0.32	+0.06	+0.25	+0.00	+0.53	...
48228	...	-1.92	-1.98	-1.95	+0.10	+0.42	...	+0.37	+0.36	...	+0.14	+0.14	+0.28	+0.08	+0.00	...
48235	...	-1.50	-1.31	-1.41	-0.32	+0.29	+0.90	+0.39	+0.28	-0.34	-0.04	-0.19	+0.23	-0.22	+0.31	+0.14
48247	...	-1.69	-1.58	-1.64	+0.29	+0.39	...	+0.42	+0.32	...	+0.11	+0.11	+0.00	-0.07	+0.35	...
48259	...	-1.78	...	-1.78	+0.55	+0.04	+0.22	...	+0.12	+0.12	+0.01	-0.03	+0.23	...
48281	106	-1.77	-1.78	-1.78	+0.38	-0.17	...	+0.29	+0.15	...	+0.16	+0.16	+0.20	-0.03	+0.39	...
48305	...	-1.21	-1.05	-1.13	+0.20	+0.00	...	+0.53	+0.55	-0.06	+0.00	-0.03	+0.11	-0.02	+0.13	...
48323	500	-0.83	-0.64	-0.73	-0.22	+0.86	+0.46	+0.61	+0.32	-0.04	...	-0.04	+0.41	-0.13	+0.45	-0.08
48367	59	-1.66	-1.41	-1.54	-0.03	+0.17	+0.65	+0.24	+0.14	-0.32	-0.11	-0.21	+0.10	-0.22	-0.15	+0.35
48370	239	-1.50	-1.38	-1.44	-0.96	+0.35	...	+0.67	+0.32	-0.16	-0.15	-0.16	-0.02	-0.10	+0.12	4
48392	120	-1.77	-1.64	-1.71	-0.65	+0.22	...	+0.51	+0.19	-0.19	+0.17	-0.01	+0.17	-0.04	-0.15	...
48409	457	-1.91	...	-1.91	+0.16	+0.34	+0.89	+0.36	+0.18	+0.42	+0.15	+0.28	+0.11	-0.02	+0.11	+0.44
49013	312	-1.55	-1.56	-1.56	+0.51	+0.03	...	+0.31	+0.37	-0.02	+0.21	+0.09	+0.29	-0.11	+0.12	...
49022	430	-1.89	-1.76	-1.83	+0.35	-0.16	...	+0.11	+0.23	...	+0.05	+0.05	+0.01	-0.02	-0.13	...
49037	509	-1.82	-1.75	-1.79	+0.46	+0.13	...	+0.34	+0.37	...	+0.08	+0.08	+0.25	+0.17	-0.07	...
49056	231	-0.76	-0.56	-0.66	-0.39	+0.78	...	+0.37	+0.16	-0.41	...	-0.41	+0.13	-0.18	+0.12	...
49072	479	-1.71	-1.76	-1.74	+0.41	-1.02	...	+0.23	+0.26	+0.37	+0.19	+0.28	-0.02	+0.10	-0.12	...
49088	3174	-1.60	...	-1.60	+0.33	-0.02	...	+0.20	+0.27	...	+0.06	+0.06	+0.03	+0.10
49111	3199	-0.99	-1.13	-1.06	-0.44	+0.89	...	+0.35	+0.42	+0.20	...	+0.20	+0.46	-0.28	+0.61	...
49123	...	-1.96	...	-1.96	+0.46	+0.00	...	+0.30	+0.25	...	+0.16	+0.16	+0.25	-0.01	-0.29	...

Table 5—Continued

Star LEID	Alt. ID ROA	[Fe/H] [FeII/H]	[FeI/H] Avg.	[O/Fe] [O/H] Avg.	[Na/Fe]	[Al/Fe]	[Si/Fe]	[Ca/Fe]	[Sc/Fe]	[ScII/Fe]	[ScIII/Fe]	[Ti/Fe]	[Ni/Fe]	[LaII/Fe]	[EuII/Fe]	Code ^a
49134	...	-1.66	-1.55	-1.61	+0.31	-0.03	+0.31	+0.28	+0.36	...	+0.02	+0.11	-0.10	+0.30	-0.18	...
49148	...	-1.39	-1.35	-1.37	+0.40	+0.14	...	+0.37	+0.45	-0.10	-0.07	-0.09	+0.35	-0.06	+0.40	...
49177	...	-1.46	-1.40	-1.43	-1.02	+0.37	...	+0.67	+0.39	-0.13	-0.13	-0.13	+0.16	-0.16	+0.46	...
49179	...	-1.93	-1.77	-1.85	+0.40	+0.35	...	+0.14	+0.23	+0.39	+0.13	+0.26	+0.44	+0.14	-0.25	...
49188	...	-1.81	-1.81	-1.81	+0.42	+0.02	...	+0.48	-0.06	...	+0.11	+0.11	+0.09	...	+0.31	...
49193	...	-1.71	-1.58	-1.65	-0.71	+0.35	+0.99	+0.53	+0.20	-0.33	+0.04	-0.14	+0.06	-0.08	+0.06	+0.25
49205	...	-1.80	...	-1.80	+0.40	+0.04	...	+0.15	+0.36	+0.23	+0.23	+0.23	+0.24	-0.05	+0.16	...
49212	...	-1.03	-0.96	-1.00	-0.56	+0.79	...	+0.47	+0.33	-0.12	-0.08	-0.10	+0.35	-0.23	+0.66	...
49238	...	-1.82	-1.82	-1.82	+0.32	-0.40	...	+0.35	...	+0.13	+0.13	+0.13	+0.40	-0.04	+0.01	...
49249	...	-1.58	-1.43	-1.43	+0.41	-0.03	...	+0.47	+0.30	-0.38	-0.08	-0.23	+0.29	-0.11	+0.38	...
49252	...	-1.77	...	-1.77	+0.02	+0.23	...	+0.40	+0.31	+0.16	+0.35	+0.25	-0.42	+0.06	-0.10	1
49255	...	-1.88	-1.69	-1.79	+0.09	+0.19	+0.23	+0.08	-0.26	+0.19
49293	244	-1.53	-1.54	-1.54	+0.00	+0.49	...	+0.39	+0.44	-0.21	+0.20	+0.00	+0.39	-0.03	+0.44	...
49322	485	-1.92	-1.86	-1.89	+0.19	+0.12	...	+0.31	+0.28	+0.21	+0.10	+0.16	+0.13	+0.03	+0.05	...
49333	3292	-1.83	...	-1.83	+0.35	-0.09	...	+0.19	+0.25	...	+0.13	+0.13	+0.09	+0.04	+0.08	...
50022	3109	-1.55	-1.53	-1.54	+0.14	-0.04	...	+0.20	+0.20	+0.14	+0.12	+0.08	+0.10	-0.06	-0.11	...
50037	568	-1.61	-1.44	-1.53	-0.53	+0.37	...	+0.46	+0.32	...	+0.13	+0.13	+0.11	-0.13	+0.23	...
50046	588	-1.63	-1.65	-1.64	+0.39	-0.04	...	+0.25	+0.19	...	+0.22	+0.22	+0.06	-0.11	+0.44	...
50066	428	-1.46	-1.30	-1.38	+0.08	+0.44	...	+0.42	+0.42	-0.05	+0.24	+0.09	+0.16	-0.20	+0.44	...
50078	167	-1.79	-1.59	-1.69	+0.41	+0.02	...	+0.28	+0.28	+0.06	+0.16	+0.05	+0.09	-0.08	+0.31	...
50108	330	-1.43	-1.27	-1.35	-1.10	+0.32	...	+0.24	+0.28	-0.22	+0.22	+0.00	+0.13	-0.10	+0.45	1
50109	328	-1.83	...	-1.83	+0.33	+0.09	...	+0.32	+0.30	...	+0.15	+0.15	+0.11	+0.00	-0.22	...
50133	...	-1.87	-1.65	-1.76	+0.06	+0.04	...	+0.28	+0.22	-0.27	+0.22	-0.03	+0.18	-0.07	-0.44	4
50163	...	-2.10	-2.11	-2.11	+0.34	+0.44	+0.65	...	-0.07	-0.07	+0.28	...	+0.31	...
50167	...	-1.77	-1.61	-1.69	+0.29	-0.02	+0.29	+0.34	+0.23	-0.14	+0.01	-0.07	+0.03	-0.10	+0.14	+0.05
50172	...	-1.61	...	-1.61	-0.44	+0.47	...	+0.59	+0.44	...	+0.38	+0.38	+0.26	-0.06	+0.36	...
50187	...	-1.22	-0.94	-1.08	+0.28	-0.18	-0.03	+0.36	+0.25	-0.17	-0.17	-0.17	-0.06	-0.16	+0.20	-0.14
50191	...	-1.44	-1.37	-1.41	-0.35	+0.44	...	+0.51	+0.48	+0.42	+0.20	+0.31	+0.15	-0.01	+0.54	...
50193	...	-1.19	...	-1.19	-0.31	+0.44	...	+0.40	+0.10	-0.19	+0.09	-0.05	+0.31	-0.16	+0.56	...
50198	...	-1.47	-1.44	-1.46	-0.50	+0.29	...	+0.62	+0.52	...	+0.13	+0.13	+0.24	-0.13	+0.73	...
50218	188	-1.52	-1.29	-1.41	-0.65	+0.37	+1.18	+0.29	+0.27	-0.23	...	-0.23	+0.25	-0.09	+0.44	+0.17
50228	...	-1.70	-1.66	-1.68	+0.38	+0.15	...	+0.26	+0.40	...	+0.04	+0.04	+0.28	+0.05	+0.13	...
50245	203	-1.79	-1.65	-1.72	+0.17	-0.02	+0.25	+0.19	+0.22	-0.19	+0.05	-0.07	+0.08	-0.03	-0.12	+0.03
50253	79	-1.76	-1.68	-1.72	-0.38	+0.01	...	+0.28	+0.23	-0.17	+0.26	+0.04	+0.06	-0.11	+0.05	...

Table 5—Continued

Star LEID	Alt. ID ROA	[Fe/H] [FeII/H]	[FeIII/H] Avg.	[O/Fe] [O/Fe] Avg.	[Na/Fe] [Al/Fe]	[Si/Fe] [Ca/Fe]	[Sc/Fe] [ScI/Fe]	[ScII/Fe] Avg.	[Ti/Fe] [Sc/Fe]	[Ni/Fe]	[La/Fe] [EuII/Fe]	[EuII/Fe]	Code ^a
50259	108	-1.45	...	-1.45	-0.10	+0.33	...	+0.57	-0.05	-0.05	+0.41	+0.00	+0.32
50267	224	-1.85	...	-1.85	+0.40	+0.18	+0.31	+0.35	+0.27	+0.26	+0.13	+0.06	-0.05
50291	221	-1.79	-1.72	-1.76	+0.41	+0.00	-0.07	+0.25	+0.28	+0.15	+0.11	+0.13	+0.17
50293	401	-1.66	-1.48	-1.57	+0.27	-0.19	...	+0.17	+0.26	-0.45	+0.08	-0.19	+0.18
50294	589	-1.71	-1.53	-1.62	+0.02	+0.23	...	+0.51	+0.37	...	+0.24	+0.24	+0.25
50304	3311	-1.71	-1.54	-1.63	+0.58	-0.18	...	+0.46	+0.27	+0.40	+0.00	+0.20	+0.17
51021	171	-1.44	-1.39	-1.42	+0.47	-0.06	...	+0.29	+0.30	-0.18	+0.06	-0.06	+0.30
51024	516	-1.53	-1.43	-1.48	+0.38	-0.05	...	+0.27	+0.42	-0.16	+0.13	-0.02	+0.27
51074	372	-1.09	...	-1.09	-0.61	+0.58	...	+0.48	+0.29	-0.24	...	-0.24	+0.45
51079	301	-1.43	-1.34	-1.39	-0.47	+0.47	+1.21	+0.53	+0.35	-0.27	...	-0.27	+0.21
51080	236	-1.39	-1.39	-1.39	+0.49	+0.13	...	+0.45	+0.50	-0.16	+0.15	-0.01	+0.46
51091	198	-1.88	...	-1.88	+0.28	+0.34	...	+0.32	+0.32	+0.27	+0.10	+0.19	+0.07
51121	285	-1.83	-1.64	-1.74	+0.36	-0.02	...	+0.06	+0.11	...	+0.09	+0.09	+0.10
51132	421	-1.03	-1.01	-1.02	+0.01	+0.92	...	+0.73	+0.51	-0.08	...	-0.08	+0.65
51136	2926	-1.68	-1.66	-1.67	+0.17	-0.19	...	+0.16	+0.62	...	+0.26	+0.26	...
51156	122	-1.62	-1.55	-1.59	-0.52	+0.20	+0.94	+0.42	+0.21	-0.05	+0.32	+0.13	+0.21
51254	...	-1.39	-1.27	-1.33	-0.37	+0.51	...	+0.56	+0.43	-0.15	+0.10	-0.03	+0.30
51257	602	-1.90	-1.90	-1.90	+0.35	+0.22	...	+0.46	+0.34	...	+0.19	+0.19	+0.25
51259	423	-1.75	-1.74	-1.75	-0.21	+0.42	...	+0.51	+0.29	+0.12	+0.24	+0.18	+0.21
52017	66	-1.86	-1.58	-1.72	+0.28	-0.28	...	+0.28	+0.15	-0.43	-0.01	-0.22	+0.10
52035	...	-1.50	-1.41	-1.46	-0.65	+0.30	...	+0.35	+0.21	+0.00	-0.19	-0.09	+0.44
52039	2850	-1.74	-1.53	-1.64	+0.21	-0.03	...	+0.08	+0.00	...	+0.11	+0.11	-0.10
52103	286	-1.35	-1.46	-1.41	+0.61	+0.38	+0.41	+0.66	+0.55	+0.17	+0.15	+0.16	+0.68
52105	486	-1.65	-1.73	-1.69	+0.49	+0.08	...	+0.26	+0.40	...	+0.01	+0.01	+0.38
52106	2899	-1.40	-1.37	-1.39	-0.32	+0.57	...	+0.40	+0.42	+0.37	+0.17	+0.27	-0.05
52109	121	-1.98	...	-1.98	+0.18	+0.18	...	+0.46	+0.31	...	+0.19	+0.19	+0.04
52110	2903	-1.66	...	-1.66	+0.26	-0.06	...	+0.12	+0.20	...	+0.18	+0.12	...
52111	166	-1.00	-1.23	-1.12	+0.15	+1.08	+0.74	+0.85	+0.29	-0.04	+0.51	+0.24	+0.36
52133	411	-1.77	...	-1.77	+0.32	+0.32	...	+0.33	...	+0.33	+0.36	+0.33	+0.41
52139	276	-1.33	-1.21	-1.27	+0.24	-0.18	+0.17	+0.45	+0.49	-0.27	-0.35	-0.31	+0.41
52151	311	-1.67	-1.67	-1.67	+0.37	+0.10	...	+0.22	+0.33	...	+0.09	+0.09	+0.32
52154	2944	-1.70	-1.58	-1.64	+0.29	+0.04	...	+0.10	-0.04	...	-0.28
52167	131	-1.81	-1.73	-1.77	+0.42	-0.14	...	+0.25	+0.24	-0.11	+0.28	+0.08	-0.07
52180	441	-1.64	-1.69	-1.67	+0.35	+0.21	...	+0.28	+0.34	+0.31	+0.09	+0.20	+0.22

Table 5—Continued

Star LEID	Alt. ID ROA	[FeI/H]	[FeII/H]	[FeIII/H] Avg.	[O/Fe]	[Na/Fe]	[Al/Fe]	[Si/Fe]	[Ca/Fe]	[Sc/Fe]	[ScII/Fe]	[ScIII/Fe] Avg.	[Ti/Fe]	[Ni/Fe]	[LaII/Fe]	[EuII/Fe]	Code ^a
52192	554	-1.36	-1.31	-1.34	+0.57	+0.20	+0.08	...	-0.08	+0.01	-0.06	+0.25	
52204	3000	-1.81	...	-1.81	+0.31	+0.29	...	+0.05	+0.08	...	-0.08	-0.08	+0.00	+0.00	+0.01	...	
52222	...	-1.79	-1.65	-1.72	+0.34	-0.09	...	+0.09	+0.08	...	+0.00	+0.00	-0.09	+0.00	+0.02	...	
53012	483	-1.83	...	-1.83	+0.48	-0.12	...	+0.31	+0.25	...	+0.22	+0.22	+0.05	+0.06	+0.03	4	
53054	599	-1.78	-1.77	-1.78	+0.44	+0.00	...	+0.23	+0.27	+0.31	+0.17	+0.24	+0.25	-0.02	+0.02	...	
53058	422	-1.77	-1.71	-1.74	-0.26	-0.05	...	+0.37	+0.33	...	+0.23	+0.23	+0.23	-0.04	+0.04	...	
53067	163	-1.79	-1.69	-1.74	+0.19	-0.12	...	+0.25	+0.25	-0.13	+0.11	-0.01	+0.12	-0.03	-0.21	...	
53076	455	-1.42	-1.42	-1.42	-0.38	+0.39	...	+0.49	+0.38	...	+0.09	+0.09	+0.21	+0.09	+0.57	...	
53114	138	-1.50	-1.39	-1.45	+0.35	-0.02	...	+0.37	+0.32	-0.39	+0.15	-0.12	+0.32	-0.02	+0.32	...	
53119	2928	-1.64	-1.49	-1.57	...	+0.48	...	+0.28	+0.16	+0.11	+0.07	+0.26	...	
53132	315	-1.76	-1.70	-1.73	-0.32	+0.37	...	+0.53	+0.29	...	+0.22	+0.22	+0.13	-0.02	+0.30	...	
53178	337	-1.82	-1.71	-1.77	+0.32	-0.16	...	+0.11	+0.19	-0.16	+0.04	-0.06	+0.25	-0.19	-0.14	...	
53185	124	-1.73	-1.54	-1.64	+0.19	+0.01	-0.12	+0.14	+0.21	-0.31	-0.03	-0.17	+0.06	-0.10	-0.12	+0.43	
53203	2785	-1.80	-1.75	-1.78	+0.43	-0.12	...	+0.28	+0.26	...	-0.03	-0.03	+0.25	+0.01	+0.33	...	
54018	2588	-1.48	-1.41	-1.45	+0.02	+0.57	...	+0.37	+0.34	-0.06	+0.15	+0.05	+0.23	-0.02	+0.58	...	
54022	2594	-0.52	-0.41	-0.46	-0.19	+0.83	...	+0.42	+0.21	...	+0.11	+0.11	+0.40	-0.28	+0.63	...	
54031	332	-1.14	-1.15	-1.15	+0.53	+0.18	+0.16	+0.54	+0.46	-0.08	+0.15	+0.03	+0.60	+0.00	+0.55	+0.12	
54064	2661	-1.76	-1.65	-1.71	+0.31	+0.16	...	+0.28	+0.34	...	+0.00	+0.00	+0.03	+0.09	
54073	456	-1.66	-1.63	-1.65	+0.30	+0.35	...	-0.03	+0.29	...	-0.02	-0.02	+0.09	-0.07	+0.33	...	
54084	2674	-1.60	-1.39	-1.50	+0.20	+0.25	...	-0.09	+0.19	...	+0.02	+0.02	+0.07	+0.09	+0.20	1	
54095	437	-1.72	-1.72	-1.72	+0.64	+0.26	+0.30	...	+0.05	+0.05	+0.27	+0.14	+0.17	...	
54105	386	-1.00	...	-1.00	-0.20	+0.79	...	+0.47	+0.29	-0.17	...	-0.17	+0.44	-0.14	+0.46	...	
54132	266	-1.65	-1.64	-1.65	+0.33	-0.36	...	+0.16	+0.27	+0.22	+0.19	+0.21	+0.15	-0.11	-0.16	...	
54148	105	-1.62	-1.46	-1.54	+0.27	-0.42	+0.19	+0.23	+0.25	-0.14	+0.06	-0.04	+0.28	-0.14	+0.02	+0.21	
54154	2737	-1.72	-1.59	-1.66	+0.36	+0.11	...	+0.13	+0.04	...	-0.13	-0.13	+0.27	-0.12	+0.21	...	
55028	270	-1.21	-1.16	-1.19	+0.45	-0.05	-0.03	+0.39	+0.42	-0.18	+0.25	+0.04	+0.57	-0.15	+0.51	+0.25	
55029	339	-1.35	-1.30	-1.33	-0.43	+0.33	...	+0.44	+0.34	-0.27	...	-0.27	+0.25	-0.06	+0.52	...	
55056	2655	-1.44	-1.42	-1.43	-0.27	+0.25	...	+0.38	+0.35	+0.25	+0.12	+0.19	-0.04	-0.30	+0.88	...	
55063	177	-1.49	-1.47	-1.48	-0.50	+0.33	...	+0.29	+0.33	-0.10	+0.15	+0.02	+0.12	-0.04	+0.61	...	
55071	248	-0.76	-0.73	-0.75	-0.39	+0.72	...	+0.49	+0.30	-0.24	...	-0.24	+0.13	-0.12	+0.19	...	
55089	277	-1.78	-1.61	-1.70	+0.42	-0.29	...	+0.28	+0.21	...	+0.01	+0.01	-0.01	-0.05	-0.05	...	
55101	480	-0.96	...	-0.96	-0.49	+0.83	...	+0.39	+0.34	-0.12	...	-0.12	+0.38	-0.04	+0.62	...	
55102	268	-1.58	-1.46	-1.52	+0.66	-0.11	...	+0.23	+0.16	-0.47	...	-0.47	+0.29	-0.05	+0.44	...	
55111	182	-1.48	-1.49	-1.49	+0.36	+0.01	...	+0.36	+0.38	+0.00	+0.11	+0.06	+0.36	-0.06	+0.31	...	

Table 5—Continued

Star LEID	Alt. ID ROA	[FeII/H]	[FeIII/H]	[Fe/H] Avg.	[O/Fe]	[Na/Fe]	[Al/Fe]	[Si/Fe]	[Ca/Fe]	[ScI/Fe]	[ScII/Fe]	[Sc/Fe] Avg.	[Ti/Fe]	[Ni/Fe]	[LaII/Fe]	[EuII/Fe]	Code ^a
55114	132	-1.45	...	-1.45	+0.47	+0.07	...	+0.48	+0.21	-0.14	+0.01	-0.07	+0.23	+0.10	+0.30	...	
55121	135	-1.05	...	-1.05	-0.35	+0.65	...	+0.39	+0.23	-0.16	-0.06	-0.11	+0.24	-0.01	+0.65	...	
55122	220	-1.42	-1.30	-1.36	-0.42	+0.54	+1.16	+0.61	+0.37	+0.01	+0.40	+0.21	+0.26	-0.05	+0.24	+0.10	
55131	2732	-1.52	...	-1.52	+0.42	-0.14	...	-0.15	+0.28	...	+0.03	+0.03	+0.22	-0.04	+0.52	...	
55142	367	-0.69	-0.78	-0.73	-0.52	+0.60	...	+0.14	+0.22	-0.31	...	-0.31	+0.36	-0.16	+0.61	...	
55149	505	-0.80	-0.86	-0.83	-0.24	+0.65	...	+0.17	+0.30	-0.04	-0.10	-0.07	+0.51	-0.17	+0.49	...	
55152	541	-1.61	-1.55	-1.58	+0.03	+0.53	+1.23	+0.57	+0.37	...	+0.21	+0.21	+0.10	+0.48	+0.32	1	
55165	418	-1.71	-1.58	-1.65	+0.25	+0.06	...	+0.18	+0.19	+0.12	+0.05	+0.08	-0.03	-0.11	-0.35	...	
56024	378	-1.51	-1.33	-1.42	-0.43	+0.24	...	+0.48	+0.29	-0.15	-0.14	-0.15	+0.09	-0.03	+0.69	...	
56028	473	-1.93	-1.78	-1.86	+0.36	-0.62	+0.51	+0.28	+0.19	...	-0.02	-0.02	+0.23	-0.11	-0.40	+0.21	
56040	204	-1.86	-1.74	-1.80	+0.40	-0.19	...	+0.26	+0.27	...	+0.09	+0.09	+0.28	-0.03	+0.15	...	
56056	2450	-1.62	...	-1.62	+0.22	-0.04	...	+0.29	+0.25	...	+0.07	+0.07	+0.07	+0.26	+0.07	...	
56070	445	-1.44	...	-1.44	-0.26	+0.51	...	+0.52	+0.56	+0.33	+0.32	+0.32	+0.32	+0.04	+0.62	...	
56087	81	-1.84	...	-1.84	+0.49	-0.25	...	+0.30	+0.36	+0.16	+0.24	+0.20	+0.41	+0.06	-0.26	...	
56106	534	-1.67	-1.61	-1.64	+0.39	-0.21	...	+0.19	-0.14	+0.10	-0.02	-0.02	+0.18	-0.15	+0.14	+0.35	
56114	417	-1.53	-1.50	-1.52	+0.39	-0.09	...	+0.25	+0.32	...	+0.05	+0.05	+0.36	-0.10	-0.12	...	
56118	532	-1.65	-1.62	-1.64	+0.13	+0.06	...	+0.15	+0.22	-0.09	+0.08	+0.00	+0.16	+0.02	+0.14	...	
56128	2518	-1.49	-1.61	-1.55	+0.50	-0.48	...	+0.09	+0.23	+0.38	+0.08	+0.23	+0.06	...	+0.05	...	
57010	207	-1.52	-1.52	-1.47	-0.02	...	+0.30	+0.39	-0.22	+0.08	-0.07	+0.28	-0.04	+0.52	...		
57029	2427	-1.79	-1.74	-1.77	+0.57	+0.05	...	+0.27	+0.28	...	+0.18	+0.18	-0.09	-0.28	+0.18	...	
57054	110	-1.31	-1.33	-1.32	+0.28	+0.16	...	+0.32	+0.42	+0.16	+0.03	+0.09	+0.35	+0.01	+0.22	...	
57058	2462	-1.73	-1.68	-1.71	+0.31	+0.13	+0.56	+0.34	+0.44	...	+0.25	+0.25	+0.23	+0.34	+0.41	+0.50	
57067	302	-1.76	-1.59	-1.68	+0.21	+0.11	-0.08	-0.05	+0.19	...	+0.04	+0.04	+0.08	-0.27	-0.78	4	
57073	368	-1.76	-1.75	-1.76	+0.00	+0.17	...	+0.18	+0.36	...	+0.08	+0.08	+0.20	+0.01	-0.18	...	
57076	278	-1.75	-1.68	-1.72	-0.64	+0.33	+0.26	-0.08	+0.20	+0.06	+0.09	+0.00	-0.16	...	
57083	2483	-1.73	-1.80	-1.77	+0.37	+0.23	...	+0.19	+0.23	+0.11	+0.27	+0.32	4	
57085	2484	-1.71	-1.75	-1.73	+0.30	-0.31	...	+0.22	+0.26	...	+0.10	+0.10	+0.15	-0.05	-0.21	...	
57091	2491	-1.32	-1.29	-1.31	-0.15	+0.39	...	+0.48	+0.39	+0.00	+0.27	+0.14	+0.24	-0.11	+0.66	...	
57114	2530	-1.72	...	-1.72	+0.52	-0.34	...	+0.26	+0.35	+0.40	+0.21	+0.31	+0.22	+0.17	+0.52	...	
57127	2367	-1.69	-1.55	-1.62	+0.40	+0.16	+0.42	...	+0.22	+0.22	+0.03	+0.00	+0.29	...	
58043	531	-1.82	-1.71	-1.77	+0.35	-0.14	...	+0.24	+0.19	+0.16	+0.09	+0.13	+0.05	+0.04	-0.09	...	
58059	508	-1.94	...	-1.94	+0.39	+0.36	...	+0.23	+0.48	...	+0.27	+0.17	+0.16	+0.09	1	...	
58077	2297	-1.77	-1.81	-1.79	+0.59	+0.16	...	+0.39	+0.27	...	+0.10	+0.10	+0.23	+0.26	-0.01	...	
58087	133	-1.78	-1.60	-1.69	+0.24	-0.51	...	+0.10	+0.20	...	+0.07	+0.07	+0.04	-0.14	-0.37	...	

Table 5—Continued

Star LEID	Alt. ID ROA	[Fe/H] [FeII/H]	[Fe/H] Avg.	[O/Fe] [O/Fe]	[Na/Fe] [Na/Fe]	[Al/Fe] [Al/Fe]	[Si/Fe] [Si/Fe]	[Ca/Fe] [Ca/Fe]	[Sc/Fe] [ScI/Fe]	[ScII/Fe] [ScII/Fe]	[Ti/Fe] [Ti/Fe]	[Ni/Fe] [Ni/Fe]	[LaII/Fe] [LaII/Fe]	[EuII/Fe] [EuII/Fe]	Code ^a	
59016	2229	-1.80	-1.73	-1.77	+0.42	+0.06	...	+0.42	+0.17	...	+0.07	+0.06	-0.23	+0.16	...	
59024	...	-0.82	...	-0.82	-0.31	+0.47	...	+0.31	+0.02	+0.00	-0.27	+0.30	...	
59036	289	-1.70	-1.55	-1.63	-0.18	+0.21	...	+0.43	+0.21	-0.14	+0.00	-0.07	+0.34	-0.06	+0.19	
59047	192	-1.47	-1.41	-1.44	-0.61	+0.44	...	+0.41	+0.44	-0.01	+0.29	+0.14	+0.33	-0.01	+0.34	
59085	183	-1.76	-1.68	-1.72	+0.42	-0.39	...	+0.39	+0.24	+0.04	+0.21	+0.13	+0.16	-0.04	+0.02	
59089	363	-1.47	-1.43	-1.45	+0.47	-0.21	...	+0.28	+0.37	-0.01	+0.19	+0.09	+0.20	-0.09	+0.01	
59090	271	-1.69	-1.71	-1.70	+0.30	+0.12	...	+0.36	+0.31	+0.02	+0.10	+0.06	+0.14	-0.06	+0.34	
59094	164	-1.90	-1.92	-1.91	+0.11	+0.47	+0.87	...	+0.22	+0.22	+0.09	+0.09	+0.11	+0.11	-0.04	+0.49
60034	2059	-1.76	...	-1.76	+0.36	-0.07	...	+0.21	+0.22	+0.32	+0.26	...	
60058	594	-0.33	-0.30	-0.32	-0.01	+0.75	-0.34	+0.54	+0.15	-0.13	...	-0.13	+0.27	-0.48	+0.53	
60059	2104	-1.84	...	-1.84	+0.29	+0.37	...	+0.19	...	+0.32	+0.35	...	+0.44	
60064	2109	-1.63	-1.52	-1.58	+0.38	+0.21	...	+0.32	+0.13	...	-0.01	-0.01	+0.13	+0.13	+0.18	
60065	288	-1.72	-1.78	-1.75	+0.35	+0.03	...	+0.23	+0.25	...	+0.26	+0.26	+0.18	+0.11	-0.02	
60066	2118	-0.98	-0.99	-0.98	-0.27	+0.54	...	+0.07	+0.28	+0.28	+0.32	+0.30	+0.29	-0.20	+0.71	
60067	490	-1.83	-1.82	-1.83	+0.68	+0.08	...	+0.51	+0.31	...	+0.31	+0.31	+0.03	+0.11	+0.08	
60069	556	-1.41	...	-1.41	-0.29	+0.09	...	+0.45	+0.32	...	-0.08	-0.08	+0.09	-0.09	+0.88	
60073	211	-0.82	...	-0.82	+0.07	+0.92	...	+0.48	+0.34	-0.06	...	-0.06	+0.23	-0.17	+0.35	
60088	2158	-1.51	-1.35	-1.43	+0.28	-0.36	...	+0.23	+0.28	...	+0.17	+0.17	-0.01	+0.03	-0.32	
60101	446	-1.82	-1.70	-1.76	+0.33	+0.06	...	+0.17	+0.25	...	+0.12	+0.12	+0.07	-0.01	-0.19	
61015	53	-1.71	...	-1.71	+0.41	-0.19	...	+0.43	+0.21	-0.23	+0.07	-0.08	+0.27	+0.06	+0.11	
61026	2042	-1.76	...	-1.76	+0.21	+0.41	...	+0.63	+0.45	...	+0.07	+0.07	+0.05	
61042	260	-1.57	-1.55	-1.56	+0.26	+0.14	+0.50	+0.28	+0.35	-0.14	+0.06	-0.04	+0.22	-0.18	+0.15	
61046	543	-1.73	-1.72	-1.73	+0.13	-0.24	+0.83	+0.26	+0.24	...	+0.16	+0.15	+0.03	+0.08	-0.02	
61050	160	-1.24	-1.03	-1.14	-1.12	+0.39	+1.02	+0.23	+0.20	-0.43	-0.28	-0.35	+0.19	-0.21	+0.29	
61067	371	-0.94	...	-0.94	+0.14	+1.05	...	+0.74	+0.46	+0.04	+0.26	+0.15	+0.49	+0.05	+0.89	
61070	255	-1.57	-1.53	-1.55	+0.55	+0.04	+0.30	+0.25	+0.24	-0.05	+0.10	+0.02	+0.29	-0.01	+0.33	
61075	2132	-1.84	-1.73	-1.79	+0.29	+0.09	...	+0.38	+0.23	...	+0.00	+0.00	+0.08	...	+0.09	
61085	158	-1.26	...	-1.26	-0.46	+0.47	...	+0.53	+0.34	-0.17	-0.01	-0.09	+0.25	-0.07	+0.57	
62018	1879	-1.90	-1.83	-1.87	+0.47	+0.32	+0.32	+0.42	+0.15	...	-0.01	-0.01	...	+0.12	...	
62058	407	-1.36	-1.37	-1.37	-0.11	+0.41	...	+0.49	+0.38	+0.01	+0.26	+0.14	+0.32	-0.02	+0.31	
63021	1878	-1.45	-1.46	-1.46	+0.36	-0.11	...	+0.40	+0.50	...	+0.07	+0.07	+0.30	+0.11	+0.59	
63027	1898	-1.72	-1.56	-1.64	+0.38	+0.10	...	+0.20	+0.15	...	+0.01	+0.01	+0.16	+0.06	-0.24	
63052	461	-1.48	-1.51	-1.50	+0.35	+0.08	+0.44	+0.23	+0.33	...	+0.08	+0.08	+0.21	-0.04	+0.34	
64023	1890	-1.81	-1.72	-1.77	+0.42	+0.30	...	+0.14	+0.32	...	-0.02	-0.02	+0.32	+0.01	+0.12	

Table 5—Continued

Star LEID	Alt. ID ROA	[FeI/H]	[FeII/H]	[O/Fe] Avg.	[Fe/H] Avg.	[Na/Fe]	[Al/Fe]	[Si/Fe]	[Ca/Fe]	[Sc/Fe] Avg.	[ScI/Fe]	[ScII/Fe]	[Ti/Fe]	[Ni/Fe]	[LaII/Fe]	[EuII/Fe]	Code ^a
64049	181	-1.69	-1.66	-1.68	-1.66	+0.34	+0.51	+0.45	-0.08	+0.04	-0.02	+0.07	-0.12	+0.11	
64057	1957	-1.68	-1.63	-1.66	-1.66	+0.26	+0.02	+0.29	...	+0.09	+0.19	+0.02	+0.25	+0.25	
64064	1978	-1.80	-1.67	-1.74	-1.64	+0.64	+0.58	+0.34	+0.21	...	+0.06	+0.14	+0.24	+0.04	...	2	
64067	269	-1.59	-1.58	-1.59	-1.59	+0.25	-0.22	+0.19	-0.26	+0.10	-0.04	-0.02	+0.17	-0.10	-0.17	+0.22	
64074	1830	-1.67	-1.65	-1.66	-1.66	+0.51	-0.24	...	+0.07	+0.35	...	+0.22	+0.18	+0.04	+0.62	...	
65042	579	-1.83	...	-1.83	-1.83	+0.61	+0.27	...	+0.36	+0.20	+0.07	+0.12	+0.28	+0.48	
65046	601	-1.83	-1.77	-1.80	-1.80	+0.50	-0.06	...	+0.21	+0.23	...	+0.12	+0.12	+0.04	-0.12	...	
65057	1802	-1.76	-1.85	-1.81	+0.66	+0.58	...	+0.31	+0.31	+0.36	+0.40	+1.09	...	
66015	1595	-1.74	-1.62	-1.68	-1.68	+0.03	+0.00	...	+0.32	+0.25	...	+0.18	+0.18	+0.20	+0.19	+0.18	...
66026	438	-1.69	-1.67	-1.68	-1.68	+0.00	+0.12	...	+0.11	+0.28	...	+0.08	+0.08	+0.13	+0.02	-0.01	...
66047	472	-1.22	-1.37	-1.30	-1.30	+0.55	+0.10	...	+0.59	+0.11	+0.06	+0.09	+0.54	+0.01	+0.46	...	
66054	232	-1.62	-1.55	-1.59	-1.59	-0.72	+0.30	...	+0.44	+0.24	+0.02	+0.09	+0.21	-0.09	-0.02	...	
67049	1754	-1.72	-1.69	-1.71	-1.71	+0.28	+0.38	+0.03	+0.08	+0.20	-0.04	...	
67063	199	-1.50	...	-1.50	-1.50	+0.27	+0.12	...	+0.16	+0.16	-0.20	-0.23	-0.22	+0.28	-0.07	+0.08	
68044	470	-1.59	-1.58	-1.59	-1.59	+0.29	-0.14	...	+0.23	+0.32	...	+0.02	+0.02	+0.13	+0.17	-0.02	...
69007	1422	-1.64	-1.56	-1.60	-1.60	+0.72	-0.18	+0.19	...	-0.13	-0.12	+0.02	+0.45	...	
69012	109	-1.85	-1.70	-1.78	-1.78	+0.33	-0.09	...	+0.24	+0.19	-0.19	+0.08	-0.05	+0.13	-0.09	-0.30	...
69027	1471	-0.76	...	-0.76	-0.76	+0.08	+0.87	...	+0.42	+0.18	+0.14	-0.12	+0.01	+0.53	-0.16	+0.91	...
70032	449	-1.69	-1.70	-1.70	-1.70	+0.09	+0.44	...	+0.25	+0.30	...	+0.14	+0.14	+0.19	-0.13	-0.01	...
70035	595	-1.46	-1.44	-1.45	-1.45	+0.63	+0.14	...	+0.23	+0.25	+0.01	+0.01	+0.01	+0.24	-0.17	+0.34	...
70041	1493	-1.57	-1.51	-1.54	-1.54	+0.14	+0.60	...	+0.13	+0.29	...	+0.14	+0.14	+0.06	-0.13	+0.12	...
70049	389	-1.32	-1.37	-1.35	-1.35	+0.30	+0.09	...	+0.45	+0.13	-0.15	+0.23	+0.04	-0.25	+0.05	+0.50	...
71013	1409	-1.77	-1.60	-1.69	-1.69	+0.19	+0.15	...	+0.25	+0.21	...	+0.01	+0.01	-0.05	+0.14	...	
73025	150	-1.37	-1.46	-1.42	-1.42	-0.31	+0.64	...	+0.53	+0.48	-0.02	+0.21	+0.10	+0.46	-0.04	+0.67	...
75021	442	-1.79	-1.69	-1.74	-1.74	+0.17	-0.13	...	+0.20	+0.28	...	+0.08	+0.08	+0.24	-0.08	+0.09	...
76027	297	-1.70	-1.68	-1.69	-1.69	+0.43	+0.06	+0.37	+0.35	...	+0.10	+0.10	+0.07	+0.01	+0.45	+0.35	
76038	316	-1.25	-1.22	-1.24	-1.24	+0.59	-0.08	...	+0.47	+0.46	-0.24	...	-0.24	+0.34	+0.06	+0.47	
77025	194	-1.60	-1.56	-1.58	-1.58	+0.48	+0.05	...	+0.28	+0.31	...	+0.20	+0.20	+0.32	+0.01	+0.21	...
77030	354	-1.81	-1.64	-1.73	-1.73	+0.23	+0.06	...	+0.27	+0.20	-0.03	+0.07	+0.02	+0.19	-0.25	-0.02	...
80026	481	-1.86	...	-1.86	-1.86	+0.46	+0.07	...	+0.50	+0.38	...	+0.21	+0.21	+0.13	+0.21	+0.24	...
80029	218	-1.67	...	-1.67	-1.67	+0.40	-0.22	...	+0.30	+0.32	...	+0.15	+0.15	+0.25	-0.09	+0.10	...
81018	217	-1.89	-1.72	-1.81	-1.81	-0.08	+0.28	...	+0.27	+0.19	...	+0.01	+0.01	+0.07	-0.04	-0.40	...
81019	1209	-1.55	-1.42	-1.49	-1.49	-0.06	...	+0.37	+0.38	-0.08	+0.02	+0.02	+0.24	-0.07	+0.41	...	
81028	1241	-1.82	-1.66	-1.74	-1.74	+0.29	+0.04	...	+0.01	+0.04	...	+0.14	+0.14	+0.15	+0.12	-0.06	...

Table 5—Continued

Star LEID	Alt. ID ROA	[FeI]/H]	[FeII]/H]	[FeIII]/H) Avg.	[O/Fe]	[Na/Fe]	[Al/Fe]	[Si/Fe]	[Ca/Fe]	[ScI/Fe]	[ScII/Fe]	[Sc/Fe] Avg.	[Ti/Fe]	[Ni/Fe]	[LaII/Fe]	[EuII/Fe]	Code ^a
82015	1026	-1.70	...	-1.70	+0.60	-0.03	...	+0.23	+0.16	...	+0.06	+0.01	-0.23	+0.31	
82029	1107	-1.80	-1.72	-1.76	+0.26	+0.24	...	+0.17	+0.03	...	+0.05	+0.05	...	+0.39	
85027	264	-1.58	-1.53	-1.56	+0.34	-0.07	...	+0.23	+0.32	-0.09	...	-0.09	+0.13	+0.00	+0.32	...	
85031	369	-1.77	...	-1.77	+0.12	+0.46	...	+0.31	+0.28	...	+0.22	+0.22	+0.11	+0.00	+0.08	...	
89009	403	-1.81	-1.70	-1.76	+0.31	+0.27	...	+0.31	...	-0.07	-0.07	-0.07	+0.22	-0.09	+0.11	...	

^a 1 = [O/Fe] upper limit; 2 = [Na/Fe] upper limit; 3 = [Al/Fe] upper limit; 4 = [La/Fe] upper limit.

Table 6a. Chemical Abundance Measurement Uncertainties

Star	N-FeI	σ/\sqrt{N}	N-FeII	σ/\sqrt{N}	N-Na	σ/\sqrt{N}	N-Al	σ/\sqrt{N}	N-Si	σ/\sqrt{N}
9	21	0.02	2	0.02	2	0.07	2	0.12
5009	22	0.02	2	0.06	1	2	0.12
6017	19	0.02	2	0.11	2	0.04	1	...
8014	22	0.03	2	0.14	1	2	0.09
9013	22	0.03	2	0.13	1	...	1	...	2	0.06
10009	22	0.02	2	0.02	2	0.05	2	0.16
10012	24	0.02	1	...	2	0.00	2	0.17
11019	24	0.02	2	0.06	2	0.01	2	0.06
11021	24	0.03	2	0.07	2	0.01	1	...	2	0.01
11024	25	0.02	2	0.08	2	0.08	2	0.02
12013	25	0.03	2	0.06	2	0.06	2	0.12
12014	21	0.03	2	0.03	1	...	1	...	2	0.10
14010	14	0.03	2	0.04	2	0.06	2	0.10
15022	20	0.02	2	0.02	1	2	0.11
15023	25	0.03	2	0.11	2	0.08	2	0.06
15026	21	0.03	2	0.08	2	0.05	2	0.03	1	...
16009	25	0.02	1	...	2	0.13	2	0.01
16015	23	0.02	2	0.01	2	0.09	2	0.01
16019	21	0.02	2	0.03	1	...	1	...	2	0.07
16027	14	0.03	2	0.09	1	2	0.03
17014	23	0.03	2	0.07	1	...	1	...	2	0.13
17015	24	0.02	2	0.13	1	2	0.12
17027	12	0.04	2	0.09	2	0.06
17029	20	0.03	2	0.04	1	2	0.02
17032	23	0.03	2	0.07	2	0.16	2	0.12
17046	13	0.05	2	0.21	2	0.26	2	0.08
18017	20	0.02	2	0.04	2	0.15	1	...
18020	23	0.02	2	0.03	2	0.04	2	0.00	2	0.00
18035	23	0.03	1	...	2	0.08	2	0.06
18040	23	0.03	2	0.01	2	0.04	2	0.09	2	0.09
18047	23	0.02	2	0.03	1	2	0.08
19022	21	0.02	2	0.07	2	0.03
19062	22	0.02	2	0.10	2	0.16	2	0.02
20018	17	0.03	2	0.16	2	0.06	1	...	2	0.10
20037	22	0.03	2	0.15	2	0.09	1	...	2	0.04
20042	17	0.03	1	...	2	0.04	2	0.01
20049	22	0.02	2	0.06	2	0.10	2	0.04
21032	24	0.02	2	0.04	2	0.02	2	0.01
21035	21	0.02	2	0.02	2	0.13	2	0.01
21042	23	0.02	2	0.11	2	0.10	2	0.07
21063	20	0.03	1	...	1	2	0.06
22023	21	0.03	2	0.01	2	0.08	2	0.10	2	0.11
22037	24	0.03	2	0.04	1	2	0.00
22042	20	0.02	2	0.13	1	2	0.06
22049	19	0.03	2	0.11	1	2	0.01
22063	21	0.02	2	0.05	1	2	0.12

Table 6a—Continued

Star	N-FeI	σ/\sqrt{N}	N-FeII	σ/\sqrt{N}	N-Na	σ/\sqrt{N}	N-Al	σ/\sqrt{N}	N-Si	σ/\sqrt{N}
23022	18	0.03	2	0.07	2	0.07	2	0.04
23033	18	0.03	2	0.09	1	...	2	0.02	2	0.03
23042	18	0.03	2	0.05	1	...	2	0.15	1	...
23050	20	0.02	2	0.00	1	2	0.01
23061	23	0.02	2	0.05	1	2	0.07
23068	26	0.02	2	0.05	2	0.01	2	0.12	2	0.06
24013	22	0.03	2	0.01	2	0.01	2	0.08
24027	19	0.02	2	0.02	2	0.01	2	0.06
24040	12	0.03	2	0.11	2	0.15	2	0.04
24046	22	0.01	2	0.04	2	0.06	2	0.02
24056	22	0.02	2	0.16	2	0.04	2	0.06
24062	24	0.02	2	0.11	2	0.02	2	0.07
25006	12	0.03	2	0.06	1	2	0.22
25026	18	0.02	2	0.02	1	2	0.06
25043	25	0.03	2	0.01	2	0.04	2	0.13
25062	21	0.01	2	0.01	2	0.13	2	0.02
25065	14	0.02	1	...	2	0.10	1	...
25068	23	0.02	1	...	2	0.13	2	0.07
26010	11	0.05	2	0.08	1	...	1	...	2	0.12
26014	22	0.03	1	...	1	1	...
26022	13	0.02	1	...	1	2	0.10
26025	21	0.01	2	0.01	2	0.06	2	0.07
26030	17	0.03	2	0.10	1	1	...
26069	17	0.03	2	0.01	1	2	0.01
26072	17	0.03	2	0.01	1	...	1	...	1	...
26086	16	0.04	1	...	2	0.01	1	...
26088	24	0.02	2	0.03	2	0.01	2	0.04
27048	22	0.02	2	0.01	2	0.05	2	0.14
27050	14	0.03	1	...
27073	22	0.02	2	0.02	2	0.07	2	0.05
27094	13	0.04	1	...	1	...	1	...
27095	18	0.02	2	0.05	2	0.02	1	...
28016	21	0.03	2	0.06	1	1	...
28020	18	0.03	1	...	1	2	0.01
28044	23	0.02	2	0.09	2	0.04	2	0.05
28069	24	0.02	2	0.03	2	0.13	1	...	2	0.04
28084	20	0.03	2	0.11	1	...	1	...	2	0.12
28092	22	0.02	2	0.09	1	2	0.06
29029	21	0.02	2	0.04	1	2	0.04
29031	14	0.02	2	0.06	1	1	...
29037	14	0.02	2	0.08	1	2	0.08
29059	20	0.02	1	...	1	2	0.30
29067	18	0.05	1	...	2	0.11	2	0.24
29069	22	0.02	2	0.04	2	0.07	2	0.03	2	0.17
29072	17	0.02	2	0.04	1	2	0.05
29085	20	0.03	2	0.01	2	0.10	2	0.11

Table 6a—Continued

Star	N-FeI	σ/\sqrt{N}	N-FeII	σ/\sqrt{N}	N-Na	σ/\sqrt{N}	N-Al	σ/\sqrt{N}	N-Si	σ/\sqrt{N}
29089	14	0.03	1	2	0.12
29099	21	0.03	2	0.02	2	0.01	2	0.02	2	0.14
29106	23	0.02	2	0.23	1	2	0.13
30013	16	0.03	2	0.11	2	0.04	1	...
30019	22	0.02	2	0.02	2	0.18	2	0.30
30022	16	0.02	2	0.05	1	...	1	...
30031	25	0.02	2	0.01	2	0.05	2	0.04	2	0.25
30069	12	0.03	2	0.14	1	1	...
30094	24	0.03	1	...	2	0.01	2	0.12
30124	22	0.02	2	0.08	2	0.05	2	0.04
31016	17	0.03	1	...	1
31041	18	0.02	2	0.01	1	2	0.09
31047	14	0.02	1	...	2	0.21	2	0.09
31048	14	0.03	1	...	2	0.01
31075	13	0.04	1	1	...
31079	21	0.02	2	0.08	1	2	0.15
31094	19	0.02	2	0.04	2	0.19	2	0.01
31095	16	0.02	2	0.17	1	...	1	...	2	0.31
31104	14	0.04	2	0.10	1	...
31109	19	0.02	1	...	2	0.04	2	0.17
31110	24	0.02	2	0.01	2	0.05	2	0.28
31119	22	0.02	1	...	2	0.02	2	0.17
31133	12	0.03	1	...	1	2	0.03
31139	20	0.02	2	0.01	1	2	0.14
31141	22	0.02	2	0.03	2	0.12	2	0.10
31147	16	0.04	2	0.06	1	...
31152	10	0.04	2	0.08	1	...
32014	20	0.03	2	0.06	1	2	0.05
32026	19	0.03	2	0.04	2	0.08	2	0.01
32027	16	0.03	2	0.16	1	2	0.13
32043	13	0.04	1	...	1	1	...
32063	23	0.02	2	0.06	2	0.01	2	0.02	2	0.13
32069	11	0.05	1	...	1	1	...
32100	18	0.02	2	0.01	2	0.15	2	0.01
32101	21	0.02	2	0.04	2	0.09	1	...	2	0.18
32125	23	0.02	2	0.18	1	2	0.11
32130	11	0.04	1	...	1	2	0.18
32138	21	0.01	1	...	2	0.08	2	0.08
32140	20	0.02	1	...	2	0.06	2	0.12
32144	22	0.03	2	0.10	2	0.08	2	0.04
32165	17	0.03	1	...	1	2	0.15
32169	19	0.03	1	...	2	0.03	1	...
32171	18	0.03	2	0.16	2	0.09	1	...
33006	24	0.02	2	0.13	2	0.03	2	0.07
33011	23	0.02	2	0.01	2	0.10	2	0.01
33018	20	0.03	1	...	1	...	1	...	1	...

Table 6a—Continued

Star	N-FeI	σ/\sqrt{N}	N-FeII	σ/\sqrt{N}	N-Na	σ/\sqrt{N}	N-Al	σ/\sqrt{N}	N-Si	σ/\sqrt{N}
33030	14	0.04	2	0.07	1	1	...
33051	21	0.02	2	0.04	2	0.06	2	0.09
33064	18	0.02	1	...	1	2	0.23
33099	17	0.06	2	0.07	2	0.12	1	...
33114	23	0.02	2	0.06	2	0.01	2	0.05	2	0.04
33115	17	0.04	1	...	2	0.01	1	...
33126	21	0.03	1	...	2	0.01	2	0.18
33129	23	0.02	2	0.11	2	0.07
33138	17	0.02	1	1	...
33145	13	0.04	2	0.06	1	...
33154	5	0.08	1	...	1	1	...
33167	20	0.02	2	0.06	1	2	0.23
33177	14	0.03	1	...	2	0.26
34008	21	0.03	2	0.01	1	...	1	...	2	0.16
34029	21	0.02	2	0.04	2	0.00	2	0.16
34040	19	0.02	1	...	2	0.01	2	0.11
34056	11	0.04	2	0.05	1	2	0.17
34069	24	0.02	2	0.05	1	2	0.19
34075	20	0.02	2	0.01	2	0.06	2	0.05	2	0.17
34081	22	0.02	1	...	2	0.00	2	0.16
34129	17	0.02	1	...	1	1	...
34130	9	0.04	2	0.20	2	0.44
34134	24	0.02	1	...	2	0.04	2	0.16
34143	17	0.03	2	0.10	2	0.06	2	0.08	1	...
34163	14	0.06	2	0.09	1
34166	15	0.03	2	0.01	1	1	...
34169	21	0.03	1	...	2	0.01	2	0.21
34175	23	0.03	2	0.16	2	0.18	2	0.11
34180	15	0.05	2	0.01	2	0.10	1	...
34187	19	0.02	2	0.25	1	2	0.12
34193	24	0.02	2	0.06	1	2	0.07
34207	24	0.02	2	0.00	2	0.15	1	...	2	0.19
34214	13	0.05	1	...	1	2	0.24
34225	15	0.04	1	...	2	0.11	1	...
34229	19	0.02	2	0.17	2	0.08	2	0.04
35029	21	0.02	2	0.01	1	2	0.02
35035	21	0.02	2	0.10	1	2	0.30
35046	23	0.02	1	...	2	0.12	2	0.06
35053	22	0.02	1	...	1	2	0.17
35056	20	0.03	2	0.04	2	0.05
35061	21	0.03	1	...	2	0.01	2	0.10	2	0.40
35066	25	0.02	2	0.05	1	2	0.02
35071	12	0.05	1	...	1	1	...
35074	21	0.03	2	0.10	2	0.04	2	0.13
35087	17	0.02	1	...	1	2	0.01
35090	21	0.02	4	0.02	2	0.02	2	0.23

Table 6a—Continued

Star	N-FeI	σ/\sqrt{N}	N-FeII	σ/\sqrt{N}	N-Na	σ/\sqrt{N}	N-Al	σ/\sqrt{N}	N-Si	σ/\sqrt{N}
35093	12	0.04	1	...	1	1	...
35124	19	0.03	1	...	2	0.01	2	0.10
35157	17	0.04	2	0.06	2	0.13	1	...
35165	25	0.02	2	0.10	2	0.00	2	0.04
35172	14	0.03	1	...	2	0.03	1	...
35190	23	0.02	2	0.04	2	0.02	2	0.09
35201	14	0.03	2	0.01	2	0.06	1	...
35204	17	0.03	2	0.11	1	...
35216	24	0.02	2	0.07	2	0.01	2	0.05	2	0.03
35228	19	0.03	1	2	0.07
35230	20	0.02	2	0.12	2	0.06
35235	23	0.03	2	0.06	2	0.03	2	0.02
35240	19	0.03	1	...	1	1	...
35248	21	0.02	1	...	1	2	0.15
35260	20	0.03	2	0.03	1	2	0.12
35261	23	0.02	2	0.21	2	0.10	2	0.03
36028	14	0.04	2	0.01	2	0.00	1	...	2	0.22
36036	23	0.02	2	0.12	2	0.03
36048	19	0.03	2	0.08	1	2	0.14
36059	14	0.02	2	0.06	1	1	...
36061	22	0.02	1	...	1	2	0.10
36087	20	0.03	1	...	1	2	0.20
36106	20	0.03	2	0.26	2	0.01
36110	13	0.03	2	0.07	1	...
36113	15	0.03	2	0.05	2	0.08	2	0.11
36134	17	0.04	2	0.01	2	0.09	1	...
36156	24	0.02	2	0.07	2	0.01	1	...	2	0.12
36179	15	0.03	2	0.01	2	0.05	1	...
36182	23	0.02	2	0.04	2	0.05	2	0.16
36191	17	0.03	1	...	2	0.11	1	...
36206	21	0.02	1	2	0.01
36228	24	0.02	2	0.08	2	0.10	2	0.03
36239	19	0.02	1	...	2	0.11	2	0.02	2	0.24
36259	21	0.02	2	0.07	1	2	0.11
36260	15	0.04	2	0.10	1	...
36280	22	0.02	1	...	1	...	1	...	2	0.08
36282	21	0.02	2	0.04	1	2	0.08
37022	13	0.03	1	...	1
37024	10	0.08	1
37051	16	0.03	1	1	...
37052	22	0.03	1	...	2	0.16
37055	20	0.02	2	0.09	2	0.04	2	0.22
37062	13	0.03	2	0.04	2	0.11	1	...
37071	12	0.04	1	...	1	2	0.03
37082	13	0.02	1	...	1	2	0.30
37087	17	0.02	2	0.04	2	0.14	2	0.01

Table 6a—Continued

Star	N-FeI	σ/\sqrt{N}	N-FeII	σ/\sqrt{N}	N-Na	σ/\sqrt{N}	N-Al	σ/\sqrt{N}	N-Si	σ/\sqrt{N}
37094	19	0.02	2	0.06	1	1	...
37105	20	0.03	2	0.06	2	0.23	2	0.13
37110	18	0.04	1	...	2	0.09	1	...
37119	25	0.01	2	0.11	1	2	0.14
37136	17	0.03	2	0.18	2	0.26
37139	22	0.01	2	0.07	2	0.02	2	0.08
37143	22	0.03	2	0.06	2	0.18	2	0.05
37147	25	0.02	2	0.02	2	0.04	1	...	2	0.21
37157	22	0.02	2	0.03	1	2	0.08
37169	15	0.03	2	0.13	2	0.13	1	...
37179	18	0.03	1	...	1	...	1	...	1	...
37184	22	0.02	2	0.05	1	...	2	0.05	2	0.19
37196	20	0.02	2	0.09	1	...
37198	21	0.03	2	0.15	2	0.01	2	0.01	2	0.08
37215	15	0.04	1	1	...
37232	22	0.02	2	0.03	2	0.06	2	0.04
37247	22	0.02	2	0.08	2	0.11
37253	23	0.02	2	0.16	1	...	1	...	2	0.05
37271	25	0.02	2	0.04	2	0.13	1	...	2	0.13
37275	19	0.04	2	0.15	1	...
37318	17	0.02	1	...	2	0.13	2	0.02	1	...
37322	14	0.05	2	0.20	2	0.08
37329	22	0.03	2	0.06	2	0.15	2	0.11
38011	18	0.02	2	0.20	2	0.04	1	...
38018	19	0.03	1	...	1	2	0.06
38049	24	0.03	2	0.06	2	0.01	2	0.01	2	0.08
38052	22	0.02	2	0.07	1	2	0.08
38056	16	0.02	2	0.04	2	0.01	2	0.02
38057	17	0.04	1	...	2	0.12	1	...
38059	17	0.02	2	0.01	2	0.11	1	...
38061	15	0.04	1	...	1	2	0.09
38096	18	0.03	1	2	0.01
38097	26	0.02	2	0.02	2	0.13	2	0.11
38105	21	0.02	2	0.07	2	0.01	2	0.00
38112	21	0.03	2	0.01	2	0.03	1	...
38115	21	0.02	2	0.01	5	0.01	1	...
38129	22	0.02	2	0.01	2	0.00	2	0.10
38147	19	0.02	1	...	2	0.05	2	0.10
38149	21	0.02	2	0.00	2	0.01	2	0.21
38156	21	0.02	2	0.15	1	2	0.06
38166	22	0.02	2	0.01	2	0.02	2	0.02
38168	21	0.03	1	...	2	0.09	2	0.01	1	...
38169	24	0.02	2	0.09	2	0.13	2	0.08
38195	21	0.02	2	0.11	2	0.01	1	...	2	0.14
38198	18	0.03	2	0.04	2	0.04	2	0.30
38204	21	0.02	1	...	2	0.04	1	...	2	0.19

Table 6a—Continued

Star	N-FeI	σ/\sqrt{N}	N-FeII	σ/\sqrt{N}	N-Na	σ/\sqrt{N}	N-Al	σ/\sqrt{N}	N-Si	σ/\sqrt{N}
38206	17	0.03	2	0.01	1	2	0.25
38215	20	0.03	2	0.09	2	0.10	1	...
38223	22	0.02	2	0.01	2	0.12	2	0.07
38225	22	0.02	2	0.05	2	0.22	2	0.02
38226	18	0.03	2	0.13	2	0.13	1	...
38232	25	0.02	2	0.07	2	0.05	2	0.18
38255	20	0.04	2	0.04	2	0.02	1	...
38262	21	0.03	1	...	2	0.01	2	0.10
38276	24	0.02	2	0.03	2	0.04	2	0.02
38303	17	0.02	1	...	2	0.04	2	0.10
38319	20	0.03	1	...	1	1	...
38323	20	0.03	1	...	2	0.03	2	0.30
38330	19	0.02	1	...	2	0.04	1	...	2	0.04
39026	21	0.02	2	0.10	2	0.16	2	0.13
39033	13	0.03	1	...	2	0.01	2	0.11
39034	20	0.03	1	...	1	1	...
39037	23	0.02	2	0.01	1	2	0.18
39043	18	0.03	2	0.10	1	2	0.08
39044	21	0.02	2	0.01	1	2	0.02
39048	12	0.04	2	0.06	1	...
39056	16	0.03	2	0.13	2	0.01	1	...
39063	16	0.03	2	0.02	1	2	0.03
39067	22	0.03	2	0.08	2	0.03	2	0.25
39086	22	0.02	2	0.06	2	0.00	2	0.09
39088	20	0.02	2	0.14	2	0.13	2	0.26
39102	19	0.03	1	...	2	0.15	1	...
39119	21	0.02	2	0.06	1	2	0.14
39123	20	0.03	1	...	1	1	...
39129	17	0.03	1	1	...
39141	23	0.02	2	0.06	2	0.04	1	...	2	0.01
39149	16	0.04	2	0.00	2	0.08	1	...
39165	15	0.02	2	0.28	1	...	1	...
39186	17	0.02	1	...	1	...	1	...	2	0.04
39187	22	0.02	2	0.01	2	0.01
39198	23	0.03	2	0.03	1	2	0.01
39204	18	0.03	2	0.06	2	0.04	2	0.11
39215	20	0.02	2	0.11	2	0.04
39216	20	0.03	2	0.12	1	...
39225	17	0.02	2	0.06	2	0.13
39235	21	0.02	2	0.08	2	0.00	2	0.28
39245	23	0.03	2	0.07	2	0.06	2	0.06	2	0.04
39257	17	0.02	2	0.11	2	0.03	2	0.30
39259	24	0.02	2	0.15	2	0.01	2	0.06
39284	24	0.02	2	0.06	2	0.13	2	0.03	2	0.16
39289	22	0.02	2	0.05	1	2	0.17
39298	16	0.03	2	0.02	2	0.02

Table 6a—Continued

Star	N-FeI	σ/\sqrt{N}	N-FeII	σ/\sqrt{N}	N-Na	σ/\sqrt{N}	N-Al	σ/\sqrt{N}	N-Si	σ/\sqrt{N}
39301	18	0.03	2	0.04	2	0.09	2	0.02
39306	21	0.02	2	0.11	1	...	2	0.04	2	0.03
39325	16	0.04	1	...	2	0.01	1	...
39329	16	0.02	1	...	1	1	...
39345	21	0.03	2	0.01	2	0.10	2	0.25
39346	25	0.03	2	0.06	2	0.09
39352	24	0.02	2	0.06	2	0.01	2	0.08
39384	20	0.03	2	0.01	2	0.01	2	0.08
39392	22	0.04	1	...	2	0.05	1	...
39401	19	0.02	2	0.08	2	0.08	2	0.15
39921	23	0.02	2	0.01	2	0.06	2	0.03
40016	25	0.03	2	0.07	2	0.04	1	...	2	0.11
40031	15	0.02	1	...	1	2	0.17
40041	13	0.03	2	0.07	2	0.00	2	0.12	2	0.18
40108	20	0.03	1	...	1	1	...
40123	16	0.03	2	0.11	2	0.00	1	...
40135	22	0.02	1	...	2	0.08	2	0.04
40139	20	0.02	2	0.01	2	0.08	1	...
40162	19	0.03	2	0.08	2	0.02	2	0.29
40166	20	0.02	2	0.05	2	0.00	2	0.19
40168	17	0.02	1	...	2	0.06	2	0.15
40170	22	0.02	2	0.14	1	2	0.10
40207	17	0.03	2	0.04	2	0.04	1	...
40210	22	0.03	2	0.20	2	0.04	1	...
40216	24	0.02	2	0.08	2	0.06	2	0.10	2	0.06
40220	17	0.04	2	0.06	1	2	0.08
40232	17	0.03	2	0.05	1	...
40235	23	0.03	1	...	2	0.06	2	0.11
40237	16	0.04	2	0.00	2	0.02	1	...
40275	22	0.02	2	0.05	1	2	0.15
40291	20	0.02	2	0.02	2	0.13	2	0.15
40318	17	0.04	2	0.06	1	...
40339	18	0.03	2	0.01	1	...
40349	23	0.02	2	0.02	2	0.07	2	0.09
40358	14	0.03	2	0.06	2	0.11	1	...
40361	22	0.02	2	0.21	2	0.02	1	...
40371	18	0.01	2	0.01	2	0.03	2	0.21
40372	21	0.02	2	0.01	2	0.06	2	0.11
40373	20	0.02	1	...	2	0.08	2	0.03
40409	16	0.03	2	0.04	1	2	0.12
40420	13	0.03	1	1	...
40424	11	0.04	1	1	...
40472	22	0.02	2	0.00	2	0.12	2	0.02
40479	21	0.03	1	...	1	2	0.04
41015	19	0.03	2	0.16	1	2	0.21
41025	16	0.04	2	0.04	1	1	...

Table 6a—Continued

Star	N-FeI	σ/\sqrt{N}	N-FeII	σ/\sqrt{N}	N-Na	σ/\sqrt{N}	N-Al	σ/\sqrt{N}	N-Si	σ/\sqrt{N}
41033	18	0.03	2	0.00	1	...
41034	24	0.02	2	0.01	1	...	1	...	2	0.00
41035	22	0.03	2	0.13	1	2	0.13
41039	23	0.02	2	0.02	2	0.04	2	0.09
41060	19	0.02	2	0.02	2	0.01	2	0.15	2	0.20
41061	24	0.02	2	0.01	1	...	2	0.00	2	0.18
41063	19	0.02	1	...	1	2	0.03
41164	16	0.02	2	0.04	2	0.01	2	0.22
41186	23	0.02	2	0.11	1	2	0.03
41201	12	0.04	1	1	...
41230	18	0.03	2	0.04	2	0.19
41232	6	0.06	1
41241	22	0.02	2	0.18	1	1	...
41243	21	0.02	2	0.02	1	2	0.05
41246	19	0.03	1	...	2	0.22	2	0.00
41258	17	0.02	2	0.23	2	0.08	1	...
41259	23	0.02	2	0.12	1
41262	14	0.04	1	2	0.18
41310	17	0.04	1	...	2	0.04	1	...
41312	12	0.04	1	1	...
41313	22	0.02	2	0.05	2	0.04	2	0.02
41321	17	0.01	2	0.08	2	0.04	1	...
41348	16	0.02	2	0.07	2	0.08	2	0.02
41366	20	0.02	1	...	1	1	...
41375	20	0.02	2	0.04	1	2	0.25
41380	17	0.04	2	0.13	1	...
41387	16	0.03	2	0.25	2	0.01	2	0.15
41389	20	0.02	1	...	1	2	0.04
41402	18	0.02	2	0.25	2	0.15	2	0.07
41435	23	0.03	1	2	0.09
41455	20	0.03	1	...	2	0.01	1	...
41476	15	0.04	2	0.01	2	0.16
41494	22	0.02	2	0.03	1	2	0.18
42012	20	0.02	2	0.16	2	0.08	2	0.22
42015	21	0.02	2	0.11	2	0.04	1	...	2	0.13
42023	22	0.01	2	0.09	2	0.06	2	0.03
42039	20	0.02	2	0.02	2	0.13	2	0.11
42049	20	0.03	1	...	2	0.08	2	0.17
42054	20	0.02	2	0.08	2	0.02	1	...	2	0.14
42056	14	0.03	1	1	...
42079	20	0.03	2	0.08	2	0.06	2	0.12
42084	15	0.03	2	0.02	2	0.08	2	0.23
42106	18	0.04	2	0.03	1	...
42114	22	0.03	2	0.06	2	0.03	2	0.13
42120	21	0.02	2	0.03	2	0.16	2	0.29
42134	11	0.03	2	0.09	2	0.01

Table 6a—Continued

Star	N-FeI	σ/\sqrt{N}	N-FeII	σ/\sqrt{N}	N-Na	σ/\sqrt{N}	N-Al	σ/\sqrt{N}	N-Si	σ/\sqrt{N}
42161	25	0.01	2	0.04	2	0.07	1	...	2	0.10
42162	17	0.04	1	...	2	0.09	1	...
42169	18	0.02	2	0.05	2	0.06	2	0.23
42174	17	0.04	1	...	2	0.06	2	0.01
42175	22	0.02	2	0.11	2	0.02	2	0.19
42179	22	0.02	2	0.07	2	0.08	2	0.08	2	0.17
42182	11	0.03	1	...	2	0.04	2	0.17
42187	22	0.03	2	0.07	2	0.03	2	0.19
42196	17	0.03	1	...	1	1	...
42198	18	0.02	2	0.27	2	0.00
42205	18	0.02	2	0.01	1	...
42221	20	0.02	2	0.12	2	0.01	2	0.13
42260	17	0.04	1	1	...
42271	12	0.02	2	0.28	1	...
42302	24	0.02	2	0.12	1	...	2	0.01
42303	16	0.02	1	...	2	0.11	2	0.28
42309	19	0.03	2	0.14	2	0.05
42339	16	0.03	1	...	2	0.04	1	...
42345	16	0.02	2	0.26	1	2	0.25
42361	20	0.02	2	0.11	2	0.11	2	0.11
42384	20	0.02	2	0.15	2	0.09	1	...
42385	21	0.02	2	0.11	1	2	0.14
42407	13	0.03	1
42415	22	0.02	2	0.04	1	2	0.07
42438	19	0.02	1	...	2	0.04	1	...
42457	16	0.03	1
42461	24	0.02	1	...	1	...	1	...	2	0.08
42473	16	0.03	2	0.02	1	...
42497	20	0.02	1	...	1	...	2	0.14	1	...
42501	21	0.03	2	0.08	1	2	0.02
42503	19	0.03	1	2	0.20
42508	22	0.02	1	...	2	0.03	2	0.15
43010	19	0.02	2	0.01	1	2	0.00
43024	22	0.02	2	0.08	2	0.02	2	0.10
43036	18	0.04	2	0.06	1	1	...
43040	18	0.03	1	2	0.17
43060	17	0.03	1	1	...
43061	17	0.03	2	0.01	1	...
43064	23	0.02	2	0.04	1	...	1	...	2	0.06
43068	22	0.03	2	0.16	2	0.03
43071	18	0.02	1	...	1	2	0.06
43079	15	0.04	1	...	2	0.08	2	0.13
43087	17	0.01	1	...	2	0.06	1	...
43091	21	0.02	1	...	2	0.11	2	0.26
43095	23	0.02	1	...	1	2	0.27
43096	20	0.01	2	0.11	2	0.07

Table 6a—Continued

Star	N-FeI	σ/\sqrt{N}	N-FeII	σ/\sqrt{N}	N-Na	σ/\sqrt{N}	N-Al	σ/\sqrt{N}	N-Si	σ/\sqrt{N}
43099	15	0.03	2	0.00	2	0.14
43101	22	0.03	2	0.08	2	0.04	2	0.04
43104	17	0.03	1	...	2	0.03	2	0.11
43108	16	0.04	2	0.22	1	2	0.25
43111	21	0.02	2	0.08	2	0.14	1	...
43134	12	0.03	1	...	1	2	0.03
43139	14	0.04	1	...	1	1	...
43158	22	0.02	2	0.01	1	2	0.14
43189	20	0.03	1	...	2	0.04	1	...
43216	21	0.03	2	0.08	2	0.01	2	0.00	2	0.23
43233	20	0.03	1	1	...
43241	17	0.02	2	0.02	1	...
43258	19	0.02	1	2	0.01
43261	21	0.02	1	...	1	2	0.05
43278	14	0.02	1	1	...
43326	18	0.04	2	0.01	2	0.12	1	...
43330	21	0.03	2	0.17	1	2	0.21
43351	19	0.04	2	0.10	2	0.06	1	...
43367	25	0.02	2	0.11	2	0.08	2	0.00	2	0.00
43389	21	0.02	2	0.01	2	0.04	2	0.12
43397	12	0.03	1	1	...
43399	17	0.03	1	...	1	2	0.04
43412	24	0.02	2	0.00	2	0.10	2	0.02
43433	24	0.02	2	0.28	2	0.16	2	0.16
43446	14	0.02	1	...	2	0.18
43458	17	0.03	1	...	2	0.04	2	0.11
43463	20	0.03	1	...	1	2	0.00
43475	17	0.03	1	...	2	0.02	1	...
43485	24	0.02	2	0.04	2	0.14	2	0.16
43539	20	0.03	2	0.06	2	0.05	2	0.12
44026	19	0.03	2	0.01	1	...
44042	23	0.03	2	0.04	2	0.04	1	...	2	0.09
44056	21	0.03	2	0.01	1
44065	21	0.03	2	0.05	1	2	0.13
44067	18	0.04	2	0.04	2	0.15
44115	21	0.03	2	0.09	2	0.00	2	0.19
44120	14	0.03	1	2	0.22
44143	24	0.02	1	...	2	0.06	1	...	2	0.07
44163	24	0.02	1	...	2	0.08	2	0.07
44188	18	0.03	2	0.02	2	0.09	2	0.07
44189	17	0.03	1	...	1	1	...
44198	20	0.02	1	...	1	2	0.02
44219	21	0.02	1	...	1	2	0.14
44231	22	0.02	2	0.11	2	0.08	2	0.11
44253	24	0.03	2	0.04	1	2	0.21
44271	15	0.03	2	0.04	1	1	...

Table 6a—Continued

Star	N-FeI	σ/\sqrt{N}	N-FeII	σ/\sqrt{N}	N-Na	σ/\sqrt{N}	N-Al	σ/\sqrt{N}	N-Si	σ/\sqrt{N}
44277	17	0.05	2	0.03	1	...
44304	21	0.04	1	...	2	0.03	2	0.18
44313	21	0.02	1	...	2	0.01	2	0.00	2	0.17
44327	22	0.02	2	0.13	2	0.04	2	0.12
44337	21	0.02	1	...	2	0.04	2	0.05	2	0.13
44343	24	0.02	2	0.20	2	0.21	2	0.06
44380	11	0.05	1
44424	17	0.03	1	...	1	1	...
44426	22	0.03	2	0.05	2	0.21
44435	25	0.02	2	0.01	1	2	0.04
44446	12	0.03	1	...	2	0.15	1	...
44449	14	0.04	1	...	2	0.08	1	...
44462	19	0.03	2	0.02	2	0.01	2	0.10
44488	14	0.03	1	2	0.04
44493	19	0.03	2	0.18	2	0.18	1	...
45082	20	0.02	2	0.04	2	0.01	2	0.09
45089	17	0.03	2	0.06	2	0.09
45092	19	0.02	2	0.00	2	0.20
45093	14	0.03	1	...	2	0.09	2	0.01
45126	22	0.03	2	0.08	1	2	0.04
45177	23	0.02	1	...	1	1	...
45180	23	0.02	1	...	2	0.07	2	0.10
45206	18	0.03	2	0.13	1	1	...
45215	19	0.03	1	...	2	0.03	2	0.08	2	0.15
45232	24	0.02	2	0.05	2	0.19
45235	17	0.03	2	0.18	1	...
45238	25	0.02	1	...	2	0.08	2	0.11
45240	16	0.04	1	1	...
45246	19	0.03	2	0.07	1	...
45249	22	0.03	2	0.02	2	0.18
45272	22	0.03	2	0.13	2	0.10	1	...
45285	16	0.04	2	0.06	1	...
45292	20	0.03	2	0.01	2	0.04
45309	19	0.03	2	0.00	2	0.15	1	...
45322	22	0.03	2	0.04	2	0.16
45326	18	0.03	2	0.02	2	0.08	2	0.06
45342	19	0.04	2	0.03	1	...
45343	23	0.02	2	0.06	2	0.03	2	0.19
45359	24	0.02	2	0.13	2	0.01	2	0.02
45373	20	0.02	2	0.16	1	...
45377	19	0.02	1	...	2	0.11	1	...
45389	22	0.02	2	0.08	1	2	0.05
45410	18	0.03
45418	20	0.03	2	0.06	1	...
45453	20	0.03	1	...	2	0.17	2	0.01	2	0.23
45454	17	0.02	2	0.04	2	0.10

Table 6a—Continued

Star	N-FeI	σ/\sqrt{N}	N-FeII	σ/\sqrt{N}	N-Na	σ/\sqrt{N}	N-Al	σ/\sqrt{N}	N-Si	σ/\sqrt{N}
45463	21	0.02	2	0.21	2	0.11	1	...
45482	16	0.03	2	0.11	1	2	0.20
46024	21	0.02	2	0.01	2	0.11	2	0.13
46055	22	0.03	2	0.01	2	0.08	2	0.07
46062	22	0.02	2	0.10	2	0.05
46073	15	0.04	2	0.02	2	0.08	1	...
46090	14	0.03	2	0.16	1	1	...
46092	22	0.02	2	0.04	1	...
46121	14	0.04	1	...	2	0.08	2	0.06
46140	23	0.03	1	...	2	0.13	2	0.14
46150	25	0.03	2	0.01	2	0.02	2	0.05
46166	22	0.03	1	...	2	0.13	2	0.04
46172	21	0.03	1	...	2	0.13	2	0.06
46194	25	0.02	2	0.16	2	0.11	2	0.14
46196	13	0.06	1	...	1	2	0.01
46223	20	0.03	2	0.01	1	...
46248	22	0.02	1	...	1	2	0.14
46279	17	0.03	1	...	1
46289	21	0.02	2	0.06	2	0.22	1	...	2	0.08
46301	23	0.02	1	...	1	2	0.08
46318	22	0.03	1	...	2	0.27	1	...
46323	24	0.02	2	0.04	2	0.04	1	...
46325	21	0.02	1	...	1	1	...
46348	21	0.02	1	...	2	0.05	1	...
46350	23	0.03	2	0.07	2	0.03	2	0.13
46381	23	0.02	1	...	2	0.02	1	...
46388	19	0.02	1	...	1	2	0.17
46391	21	0.03	1	...	1	2	0.18
46398	10	0.04	1	...	1	1	...
46405	13	0.03	2	0.02	1	1	...
46438	12	0.04	1	...	1	2	0.31
47012	26	0.02	2	0.12	2	0.01	2	0.13
47039	22	0.03	1	...	2	0.18	2	0.09
47055	14	0.03	1	...	1	2	0.00
47074	16	0.04	1	...	1	1	...
47096	19	0.03	1	...	2	0.04	2	0.27
47107	22	0.02	1	...	1	...	1	...	2	0.05
47110	24	0.02	2	0.16	2	0.04	2	0.06
47146	21	0.03	1	...	2	0.01	2	0.06	2	0.17
47150	16	0.04	1	...	2	0.05	1	...
47151	13	0.03	1	...	1	2	0.10
47153	19	0.03	2	0.02	1	...
47176	23	0.02	1	...	2	0.03	2	0.09
47186	22	0.04	1	...	2	0.04	2	0.22
47187	17	0.03	2	0.09	1	...
47199	25	0.03	2	0.06	1	...	2	0.02	2	0.08

Table 6a—Continued

Star	N-FeI	σ/\sqrt{N}	N-FeII	σ/\sqrt{N}	N-Na	σ/\sqrt{N}	N-Al	σ/\sqrt{N}	N-Si	σ/\sqrt{N}
47269	20	0.02	1	...	2	0.01	2	0.23
47299	17	0.04	1	1	...
47307	23	0.02	1	...	1	...	2	0.01	1	...
47331	14	0.05	1	...	1
47338	22	0.03	1	...	2	0.12	2	0.21
47339	17	0.03	1	...	2	0.11	2	0.04
47348	22	0.02	1	...	2	0.08	1	...
47354	18	0.05	2	0.07	2	0.01	1	...
47387	23	0.02	2	0.08	1	...	1	...	2	0.01
47399	24	0.03	2	0.16	2	0.00	2	0.21
47400	25	0.03	1	...	2	0.00	2	0.22
47405	22	0.02	1	2	0.09
47420	21	0.02	2	0.04	2	0.05	2	0.20
47443	19	0.04	1	...	1	1	...
47450	21	0.03	2	0.15	2	0.17
48028	23	0.02	2	0.01	2	0.02	2	0.05
48036	17	0.03	1	...	1	2	0.12
48049	23	0.02	2	0.01	2	0.07
48060	22	0.02	2	0.01	2	0.08
48067	20	0.02	1	...	1	2	0.22
48083	21	0.04	1	...	2	0.11	1	...
48099	13	0.05	2	0.19	0	0.00
48116	13	0.04	1	...	2	0.03	2	0.05	1	...
48120	19	0.03	2	0.04	2	0.19
48150	19	0.03	1	...	2	0.06	1	...
48151	22	0.03	2	0.08	2	0.16
48186	18	0.03	2	0.10
48197	20	0.03	1	...	1	2	0.07
48221	20	0.04	1	...	2	0.02	1	...
48228	19	0.03	2	0.35	1	2	0.11
48235	25	0.03	2	0.01	2	0.05	2	0.00	2	0.17
48247	22	0.02	1	...	2	0.14	2	0.06
48259	20	0.03	1
48281	17	0.02	2	0.18	1	2	0.10
48305	20	0.03	1	...	2	0.18	2	0.21
48323	16	0.05	1	...	2	0.06	2	0.10	1	...
48367	24	0.02	1	...	2	0.00	2	0.02	2	0.13
48370	20	0.03	1	...	1	2	0.27
48392	23	0.02	1	...	2	0.01	2	0.11
48409	20	0.03	2	0.09	1	...	2	0.13
49013	24	0.02	2	0.08	2	0.13	2	0.04
49022	21	0.03	2	0.04	1	1	...
49037	16	0.03	1	...	1	2	0.05
49056	20	0.02	1	...	2	0.04	1	...
49072	19	0.03	1	...	1	2	0.08
49088	24	0.03	1	2	0.06

Table 6a—Continued

Star	N-FeI	σ/\sqrt{N}	N-FeII	σ/\sqrt{N}	N-Na	σ/\sqrt{N}	N-Al	σ/\sqrt{N}	N-Si	σ/\sqrt{N}
49111	20	0.03	1	...	2	0.06	1	...
49123	18	0.02	2	0.01	2	0.01
49134	23	0.02	2	0.04	1	...	1	...	2	0.21
49148	26	0.03	2	0.00	2	0.01	2	0.03
49177	21	0.03	2	0.12	2	0.08	2	0.23
49179	20	0.03	2	0.08	1	1	...
49188	8	0.02	1	...	1	1	...
49193	19	0.02	1	...	2	0.03	2	0.05	2	0.06
49205	19	0.03	2	0.08	1	...
49212	19	0.03	1	...	2	0.01	1	...
49238	21	0.03	2	0.14	1
49249	26	0.03	2	0.01	2	0.01	2	0.17
49252	15	0.05	1	2	0.21
49255	19	0.04	1	...	1
49293	24	0.03	2	0.15	2	0.01	2	0.22
49322	22	0.03	1	...	1	2	0.04
49333	22	0.03	1	2	0.12
50022	18	0.05	1	...	1	2	0.19
50037	22	0.03	2	0.04	2	0.04	2	0.12
50046	17	0.04	2	0.21	2	0.22	2	0.08
50066	20	0.03	2	0.06	2	0.01	2	0.27
50078	20	0.02	1	...	2	0.08	2	0.13
50108	25	0.03	1	...	2	0.06	1	...
50109	21	0.02	1	2	0.17
50133	23	0.02	2	0.04	1	2	0.12
50163	10	0.05	1	...	1
50167	21	0.02	2	0.07	1	...	1	...	2	0.03
50172	18	0.03	2	0.14	2	0.02
50187	20	0.02	2	0.03	2	0.01	2	0.06	2	0.14
50191	21	0.02	1	...	2	0.01	2	0.06
50193	16	0.03	2	0.04	1	...
50198	21	0.03	5	0.10	2	0.05	2	0.09
50218	22	0.02	1	...	2	0.01	2	0.08	1	...
50228	23	0.03	2	0.12	2	0.05	2	0.27
50245	20	0.03	2	0.22	2	0.12	1	...	2	0.07
50253	17	0.03	2	0.02	2	0.15	2	0.23
50259	22	0.03	2	0.01	2	0.25
50267	22	0.02	2	0.03	1	...	2	0.06
50291	18	0.03	1	...	2	0.12	1	...	1	...
50293	25	0.02	1	...	2	0.09	2	0.14
50294	22	0.03	1	...	2	0.02	2	0.09
50304	22	0.03	1	...	1	1	...
51021	23	0.03	1	...	2	0.10	2	0.19
51024	24	0.02	1	...	1	1	...
51074	17	0.03	2	0.10	1	...
51079	24	0.04	1	...	2	0.04	2	0.02	2	0.14

Table 6a—Continued

Star	N-FeI	σ/\sqrt{N}	N-FeII	σ/\sqrt{N}	N-Na	σ/\sqrt{N}	N-Al	σ/\sqrt{N}	N-Si	σ/\sqrt{N}
51080	22	0.02	2	0.06	2	0.03	2	0.10
51091	20	0.03	2	0.01	2	0.26
51121	19	0.03	1	...	1	1	...
51132	19	0.03	1	...	2	0.08	2	0.18
51136	9	0.04	2	0.15	1	2	0.17
51156	21	0.02	2	0.03	2	0.07	2	0.01	2	0.19
51254	20	0.03	2	0.01	2	0.04	2	0.23
51257	22	0.03	2	0.04	2	0.18	2	0.12
51259	21	0.02	2	0.11	1	2	0.14
52017	25	0.02	2	0.01	2	0.12	2	0.02
52035	20	0.03	2	0.06	2	0.01	1	...
52039	11	0.05	2	0.14	2	0.06	2	0.20
52103	22	0.02	1	...	2	0.06	2	0.05	2	0.09
52105	19	0.03	2	0.16	2	0.14	2	0.21
52106	16	0.03	1	...	2	0.19	2	0.06
52109	22	0.03	2	0.18	2	0.15
52110	12	0.03	1	1	...
52111	14	0.04	2	0.06	2	0.06	2	0.08	1	...
52133	12	0.04	1
52139	25	0.03	2	0.02	2	0.01	1	...	2	0.06
52151	17	0.03	2	0.13	2	0.06	1	...
52154	16	0.05	1	...	1
52167	24	0.02	2	0.01	2	0.01	2	0.02
52180	22	0.03	1	...	2	0.11	2	0.09
52192	18	0.02	2	0.10	2	0.05
52204	9	0.04	1	1	...
52222	20	0.03	2	0.04	1	2	0.02
53012	20	0.02	2	0.27	2	0.00
53054	19	0.03	2	0.17	1	2	0.10
53058	19	0.02	2	0.03	2	0.15	2	0.13
53067	25	0.02	2	0.05	2	0.14	2	0.00
53076	21	0.02	2	0.04	2	0.14	2	0.08
53114	24	0.03	2	0.04	2	0.03	2	0.21
53119	10	0.03	1	...	1	1	...
53132	22	0.02	2	0.05	1	2	0.04
53178	25	0.03	2	0.08	1	2	0.04
53185	25	0.02	2	0.07	2	0.09	1	...	2	0.11
53203	22	0.02	2	0.25	2	0.01	2	0.15
54018	21	0.02	2	0.01	2	0.01	2	0.08
54022	19	0.04	1	...	2	0.01	1	...
54031	19	0.03	1	...	2	0.04	2	0.02	2	0.23
54064	14	0.03	1	...	2	0.09	1	...
54073	17	0.03	2	0.17	2	0.09	1	...
54084	16	0.04	1	...	2	0.05	1	...
54095	18	0.04	1	2	0.01
54105	16	0.03	2	0.06	1	...

Table 6a—Continued

Star	N-FeI	σ/\sqrt{N}	N-FeII	σ/\sqrt{N}	N-Na	σ/\sqrt{N}	N-Al	σ/\sqrt{N}	N-Si	σ/\sqrt{N}
54132	25	0.02	2	0.11	1	2	0.05
54148	26	0.02	1	...	2	0.17	1	...	2	0.03
54154	18	0.02	2	0.11	1	2	0.05
55028	23	0.03	2	0.16	2	0.04	1	...	2	0.18
55029	23	0.03	2	0.01	2	0.02	2	0.23
55056	18	0.03	1	...	2	0.08	2	0.04
55063	22	0.02	2	0.02	2	0.05	1	...
55071	16	0.04	1	...	2	0.06	1	...
55089	21	0.03	1	...	1	2	0.01
55101	16	0.04	2	0.02	1	...
55102	21	0.03	2	0.12	2	0.03	2	0.05
55111	24	0.02	2	0.11	2	0.03	2	0.15
55114	21	0.03	2	0.01	2	0.15
55121	17	0.02	2	0.01	1	...
55122	21	0.03	2	0.06	2	0.06	2	0.05	2	0.17
55131	19	0.03	1	1	...
55142	17	0.04	1	...	2	0.07	1	...
55149	17	0.03	2	0.01	2	0.06	1	...
55152	18	0.03	1	...	2	0.08	2	0.04	2	0.08
55165	21	0.03	1	...	2	0.20	2	0.17
56024	19	0.03	1	...	2	0.03	2	0.10
56028	20	0.02	1	...	1	...	1	...	2	0.03
56040	20	0.02	2	0.04	1	2	0.15
56056	20	0.03	2	0.01	1	...
56070	19	0.02	2	0.00	2	0.18
56087	22	0.02	2	0.18	2	0.07
56106	20	0.02	1	...	2	0.15
56114	22	0.03	2	0.09	2	0.13	2	0.10
56118	23	0.02	2	0.08	2	0.11	2	0.26
56128	13	0.02	1	...	2	0.15	1	...
57010	24	0.03	2	0.05	2	0.01	2	0.06
57029	13	0.04	2	0.14	2	0.06	2	0.10
57054	24	0.03	1	...	2	0.18	2	0.24
57058	18	0.03	1	...	1	...	1	...	2	0.13
57067	19	0.02	1	...	1	...	1	...	1	...
57073	21	0.02	1	...	2	0.08	2	0.20
57076	22	0.02	2	0.06	2	0.01
57083	18	0.03	2	0.14	1	2	0.14
57085	23	0.03	2	0.01	1	2	0.08
57091	20	0.03	2	0.08	2	0.08	2	0.21
57114	20	0.03	1	1	...
57127	17	0.02	2	0.08	2	0.06
58043	19	0.02	2	0.01	1	2	0.08
58059	16	0.03	1	1	...
58077	12	0.03	2	0.20	1	2	0.04
58087	23	0.02	1	...	2	0.10	2	0.06

Table 6a—Continued

Star	N-FeI	σ/\sqrt{N}	N-FeII	σ/\sqrt{N}	N-Na	σ/\sqrt{N}	N-Al	σ/\sqrt{N}	N-Si	σ/\sqrt{N}
59016	14	0.03	1	...	2	0.02	1	...
59024	16	0.04	2	0.11	1	...
59036	22	0.03	2	0.05	2	0.04	2	0.12
59047	22	0.03	2	0.04	2	0.01	1	...
59085	19	0.03	1	...	1	1	...
59089	24	0.03	2	0.05	2	0.08	2	0.06
59090	23	0.02	2	0.09	2	0.03	2	0.11
59094	16	0.03	2	0.06	1	...	1	...	1	...
60034	15	0.04	1	2	0.12
60058	16	0.05	1	...	2	0.21	1	...	1	...
60059	10	0.03	1
60064	18	0.04	1	...	1	2	0.01
60065	21	0.03	2	0.21	1	1	...
60066	17	0.04	1	...	2	0.02	1	...
60067	16	0.04	2	0.22	1	1	...
60069	20	0.03	1	2	0.21
60073	17	0.04	2	0.04	1	...
60088	19	0.03	1	...	1	2	0.12
60101	21	0.02	2	0.05	1	2	0.04
61015	25	0.02	2	0.04	2	0.05
61026	18	0.04	1	1	...
61042	21	0.02	2	0.07	2	0.02	1	...	2	0.07
61046	20	0.03	1	...	1	...	2	0.03	1	...
61050	20	0.04	2	0.01	2	0.03	2	0.02	1	...
61067	18	0.02	2	0.11	2	0.20
61070	21	0.02	1	...	2	0.09	1	...	2	0.03
61075	17	0.03	1	...	2	0.15	1	...
61085	18	0.02	2	0.04	1	...
62018	12	0.03	1	...	2	0.01	1	...	1	...
62058	20	0.02	1	...	1	2	0.15
63021	20	0.02	2	0.05	1	2	0.03
63027	18	0.02	1	...	1	2	0.02
63052	22	0.03	2	0.04	2	0.21	1	...	2	0.05
64023	13	0.05	2	0.05	2	0.15	1	...
64049	19	0.02	2	0.07	2	0.12	2	0.11
64057	15	0.03	2	0.12	2	0.04	2	0.23
64064	14	0.03	1	...	1	2	0.00
64067	18	0.03	2	0.01	1	...	1	...	2	0.25
64074	17	0.02	1	...	1	2	0.04
65042	10	0.02	1	2	0.22
65046	20	0.02	1	...	1	2	0.07
65057	16	0.05	1	2	0.06
66015	20	0.02	1	...	2	0.17	2	0.01
66026	23	0.02	2	0.10	2	0.08	2	0.17
66047	26	0.03	1	...	2	0.12
66054	22	0.02	2	0.01	2	0.02	2	0.14

Table 6a—Continued

Star	N–FeI	σ/\sqrt{N}	N–FeII	σ/\sqrt{N}	N–Na	σ/\sqrt{N}	N–Al	σ/\sqrt{N}	N–Si	σ/\sqrt{N}
67049	13	0.04	1	...	1
67063	20	0.03	2	0.06	2	0.24
68044	19	0.02	1	...	2	0.10	2	0.14
69007	16	0.03	1	...	1
69012	25	0.02	1	...	1	2	0.05
69027	15	0.04	2	0.11	1	...
70032	22	0.03	1	...	1	2	0.08
70035	18	0.03	1	...	2	0.18	2	0.09
70041	23	0.03	1	...	2	0.04	2	0.10
70049	15	0.05	1	...	2	0.02	1	...
71013	18	0.04	1	...	1	1	...
73025	21	0.02	1	...	2	0.04	1	...
75021	21	0.03	2	0.04	1	2	0.22
76027	24	0.02	2	0.11	2	0.11	1	...	2	0.06
76038	22	0.02	1	...	2	0.04	2	0.04
77025	23	0.01	2	0.06	2	0.07	2	0.05
77030	22	0.02	1	...	1	2	0.23
80026	13	0.03	1	1	...
80029	23	0.02	2	0.01	2	0.11
81018	24	0.02	2	0.05	2	0.07	2	0.05
81019	20	0.03	2	0.05	2	0.00	2	0.03
81028	20	0.02	1	...	1	2	0.09
82015	18	0.02	2	0.06	1	...
82029	12	0.04	2	0.05	1	2	0.08
85027	21	0.03	2	0.00	1	2	0.11
85031	19	0.02	2	0.13	2	0.10
89009	19	0.03	2	0.06	2	0.09

Table 6b. Chemical Abundance Measurement Uncertainties

Star	N-Ca	σ/\sqrt{N}	N-ScI	σ/\sqrt{N}	N-ScII	σ/\sqrt{N}	N-Ti	σ/\sqrt{N}	N-Ni	σ/\sqrt{N}
9	5	0.04	1	...	3	0.04	5	0.06
5009	5	0.07	1	...	2	0.04	3	0.05	3	0.10
6017	5	0.05	5	0.04	5	0.09
8014	5	0.05	1	...	3	0.09	3	0.06
9013	4	0.03	1	...	2	0.05	3	0.05
10009	5	0.05	1	...	2	0.25	6	0.05	3	0.14
10012	5	0.04	2	0.19	1	...	3	0.02	3	0.12
11019	5	0.03	1	...	1	...	5	0.04	5	0.06
11021	5	0.04	1	...	2	0.01	5	0.06	4	0.08
11024	5	0.03	2	0.10	5	0.03	5	0.01
12013	5	0.02	5	0.05	5	0.06
12014	5	0.05	1	...	2	0.17	1	...
14010	4	0.09	2	0.11	2	0.01	2	0.04
15022	4	0.02	1	4	0.09	2	0.02
15023	5	0.06	2	0.01	4	0.05	4	0.07
15026	5	0.07	1	...	1	...	5	0.04	4	0.10
16009	5	0.07	2	0.10	3	0.06	4	0.03
16015	5	0.04	2	0.08	2	0.02	3	0.03
16019	4	0.06	2	0.08	3	0.13	2	0.25
16027	5	0.05	2	0.09	3	0.03
17014	5	0.07	1	...	1	...	3	0.05	4	0.04
17015	5	0.05	1	...	2	0.01	4	0.08	4	0.02
17027	4	0.14	1
17029	4	0.15	1	...	2	0.09	2	0.04
17032	5	0.06	1	...	1	...	4	0.09	5	0.08
17046	2	0.01	2	0.11
18017	5	0.04	2	0.15	2	0.19	1	...
18020	5	0.03	2	0.10	2	0.15	5	0.06	5	0.04
18035	5	0.09	2	0.17	1	...	4	0.12	5	0.05
18040	5	0.08	1	...	1	...	4	0.05	5	0.08
18047	5	0.05	2	0.12	2	0.02	2	0.06
19022	4	0.01	2	0.04	2	0.11	3	0.06
19062	5	0.03	2	0.05	4	0.12	4	0.04
20018	3	0.09	1	...	2	0.08	2	0.01
20037	5	0.04	1	...	1	...	3	0.14	5	0.08
20042	5	0.08	2	0.06	2	0.04	3	0.05
20049	5	0.05	1	...	3	0.16	4	0.03
21032	5	0.04	1	...	2	0.08	5	0.03	5	0.04
21035	5	0.04	2	0.04	3	0.10	4	0.08
21042	5	0.07	1	...	3	0.03	4	0.06
21063	4	0.08	1	...	5	0.08
22023	5	0.09	1	...	2	0.10	1	...
22037	5	0.05	2	0.01	3	0.09	5	0.07
22042	4	0.13	1	...	2	0.05	3	0.08
22049	5	0.07	1	...	2	0.05	2	0.21
22063	5	0.08	2	0.16	2	0.11	2	0.28

Table 6b—Continued

Star	N-Ca	σ/\sqrt{N}	N-ScI	σ/\sqrt{N}	N-ScII	σ/\sqrt{N}	N-Ti	σ/\sqrt{N}	N-Ni	σ/\sqrt{N}
23022	5	0.06	1	...	3	0.12
23033	5	0.05	2	0.11	2	0.06	1	...
23042	5	0.04	1	...	2	0.01	1	...
23050	5	0.07	1	...	2	0.06	2	0.09
23061	5	0.04	2	0.02	4	0.08	4	0.08
23068	5	0.04	2	0.10	2	0.07	5	0.02	5	0.04
24013	5	0.05	2	0.17	2	0.13	3	0.06	4	0.06
24027	5	0.04	1	...	1	...	3	0.02	4	0.09
24040	5	0.14	1	3	0.06
24046	5	0.04	2	0.15	4	0.06	5	0.03
24056	5	0.05	1	...	3	0.03	2	0.06
24062	5	0.04	1	...	1	...	6	0.01	5	0.06
25006	3	0.03	1	2	0.13
25026	5	0.08	1	...	3	0.12	3	0.11
25043	5	0.04	2	0.12	2	0.18	5	0.04	4	0.08
25062	5	0.03	2	0.10	2	0.02	6	0.04	5	0.02
25065	5	0.13	1	...	3	0.12	4	0.11
25068	4	0.06	2	0.05	3	0.05	4	0.05
26010	4	0.08	1	...	1
26014	5	0.04	1	...	3	0.02	3	0.05
26022	5	0.09	2	0.09	2	0.21	2	0.12
26025	5	0.06	2	0.11	2	0.09	5	0.05	5	0.02
26030	5	0.10	1	...	1	...	2	0.06
26069	5	0.08	1	...	2	0.01	1	...
26072	5	0.05	2	0.11	2	0.04	4	0.08
26086	5	0.07	1	5	0.07	4	0.08
26088	5	0.06	1	...	6	0.04	2	0.03
27048	5	0.04	1	4	0.02	5	0.07
27050	5	0.07	2	0.08	2	0.01	3	0.15
27073	5	0.05	1	...	2	0.01	3	0.02
27094	2	0.03	2	0.12	3	0.18	4	0.12
27095	5	0.04	1	2	0.08	2	0.11
28016	5	0.08	1	...	2	0.04	2	0.02
28020	4	0.05	1	...	2	0.06	4	0.06
28044	5	0.03	2	0.10	5	0.01	5	0.04
28069	5	0.04	2	0.01	4	0.06	5	0.04
28084	5	0.04	1	...	1	...	3	0.10	5	0.04
28092	5	0.04	1	...	2	0.00	3	0.10
29029	5	0.04	2	0.08	4	0.03	1	...
29031	5	0.11	1	...	2	0.08
29037	4	0.07	1	...	2	0.01	1	...
29059	5	0.10	1	...	1	...	4	0.12	2	0.13
29067	5	0.13	1	...	2	0.06	2	0.11	3	0.04
29069	5	0.04	2	0.09	3	0.06	2	0.10
29072	5	0.04	1	...	2	0.00	4	0.08
29085	5	0.06	2	0.06	3	0.07

Table 6b—Continued

Star	N-Ca	σ/\sqrt{N}	N-ScI	σ/\sqrt{N}	N-ScII	σ/\sqrt{N}	N-Ti	σ/\sqrt{N}	N-Ni	σ/\sqrt{N}
29089	5	0.07	1	...	2	0.04
29099	5	0.05	1	...	1	...	5	0.05	5	0.04
29106	5	0.04	1	...	3	0.08	3	0.04
30013	5	0.09	1	...	1	...	3	0.11	5	0.07
30019	5	0.02	1	...	2	0.08	4	0.10	4	0.04
30022	4	0.11	2	0.07	2	0.03	1	...
30031	5	0.03	2	0.15	2	0.15	5	0.09	4	0.14
30069	4	0.02	2	0.04	2	0.12
30094	5	0.07	1	...	3	0.04	2	0.21
30124	5	0.06	1	...	2	0.07	2	0.18
31016	5	0.06	2	0.04	2	0.06
31041	5	0.04	1	...	1	...	3	0.04	2	0.03
31047	5	0.04	1	...	2	0.07
31048	4	0.10	1	...	1	...	2	0.09
31075	2	0.20	1	...	1
31079	5	0.06	1	...	3	0.01	5	0.07
31094	4	0.02	2	0.11	2	0.06	1	...
31095	4	0.12	1	...	1	...	1	...
31104	4	0.05
31109	4	0.04	1	...	1	...	2	0.04	1	...
31110	5	0.06	1	...	1	...	5	0.03	4	0.06
31119	5	0.06	1	...	2	0.04	4	0.03	4	0.11
31133	4	0.17	2	0.01	2	0.04	3	0.11
31139	5	0.07	2	0.05	2	0.02	4	0.06
31141	5	0.06	2	0.07	3	0.04	4	0.08
31147	3	0.03	1	...	4	0.03
31152	5	0.10	2	0.03	4	0.08
32014	4	0.09	1	...	2	0.05	4	0.02
32026	5	0.06	1	...	1	...	3	0.02	5	0.06
32027	5	0.11	1	...	1	...	4	0.11
32043	4	0.05	1	...	1	...	1	...
32063	5	0.06	1	...	2	0.01	3	0.15	4	0.05
32069	3	0.20	1	...	1	...	1	...
32100	5	0.07	1	...	2	0.05	5	0.08
32101	5	0.06	1	...	1	...	5	0.08	5	0.06
32125	5	0.05	2	0.03	5	0.04	5	0.02
32130	4	0.14	1	...	1	...	2	0.04
32138	5	0.07	2	0.06	2	0.08	4	0.02	2	0.11
32140	5	0.04	2	0.19	2	0.04	3	0.04
32144	5	0.06	1	...	1	...	2	0.06	4	0.04
32165	4	0.05	1	...	2	0.06	1	...
32169	5	0.07	1	...	1	...	4	0.07	3	0.12
32171	5	0.05	1	...	1	...	3	0.01	2	0.02
33006	5	0.03	2	0.05	1	...	5	0.04	5	0.05
33011	5	0.03	1	...	4	0.07	5	0.03
33018	5	0.05	1	...	2	0.01	4	0.07

Table 6b—Continued

Star	N-Ca	σ/\sqrt{N}	N-ScI	σ/\sqrt{N}	N-ScII	σ/\sqrt{N}	N-Ti	σ/\sqrt{N}	N-Ni	σ/\sqrt{N}
33030	5	0.09	1	...	1	...	2	0.08
33051	5	0.04	1	...	2	0.08	3	0.05	5	0.01
33064	4	0.11	2	0.12	1	...	3	0.06
33099	5	0.07	3	0.10	1	...
33114	5	0.06	2	0.05	1	...	5	0.03	5	0.04
33115	5	0.10	1	...	2	0.05	2	0.04
33126	5	0.09	1	...	1	...	2	0.02	1	...
33129	5	0.08	1	...	4	0.16	4	0.03
33138	5	0.08	1	...	1	...	3	0.14
33145	4	0.06	2	0.04
33154	3	0.08	1
33167	5	0.06	1	...	2	0.04	5	0.05
33177	4	0.06	2	0.13	1	...
34008	5	0.07	2	0.04	2	0.04	2	0.01
34029	4	0.03	2	0.12	2	0.23	5	0.09	4	0.07
34040	5	0.08	1	...	2	0.03	4	0.09
34056	5	0.11	1	...	2	0.05	1	...
34069	5	0.04	2	0.15	2	0.01	5	0.07
34075	5	0.06	1	...	2	0.21	5	0.04	4	0.13
34081	5	0.05	2	0.01	3	0.05	5	0.04
34129	5	0.05	2	0.04	4	0.12
34130	4	0.03	1	1	...
34134	5	0.04	2	0.02	2	0.05	6	0.06	5	0.04
34143	4	0.03	1	...	1	...	3	0.06	4	0.12
34163	4	0.07	1
34166	4	0.07	1	...	2	0.01	2	0.09
34169	5	0.07	1	...	1	...	4	0.07	4	0.04
34175	5	0.05	1	...	3	0.08	2	0.13
34180	3	0.09	1	3	0.17	2	0.21
34187	5	0.07	1	...	2	0.06	2	0.01	1	...
34193	5	0.04	2	0.01	4	0.02	5	0.07
34207	5	0.03	2	0.17	5	0.03	5	0.07
34214	2	0.27	1	...	1	...	2	0.07
34225	4	0.04	1	...	1	...	4	0.09	3	0.21
34229	5	0.07	2	0.06	2	0.05	1	...
35029	5	0.06	1	...	1	...	3	0.13	4	0.11
35035	5	0.06	2	0.01	2	0.00	2	0.09
35046	5	0.04	1	...	2	0.06	4	0.15	4	0.05
35053	5	0.06	1	...	2	0.01	5	0.07
35056	4	0.05	2	0.08	2	0.08	5	0.06	2	0.11
35061	5	0.03	1	...	2	0.17	3	0.03	4	0.12
35066	5	0.04	2	0.02	2	0.10	5	0.04	5	0.05
35071	2	0.01
35074	5	0.05	1	...	3	0.09	4	0.06
35087	5	0.11	1	...	1	...	1
35090	5	0.08	1	...	2	0.15	5	0.06	4	0.12

Table 6b—Continued

Star	N-Ca	σ/\sqrt{N}	N-ScI	σ/\sqrt{N}	N-ScII	σ/\sqrt{N}	N-Ti	σ/\sqrt{N}	N-Ni	σ/\sqrt{N}
35093	4	0.07
35124	5	0.06	1	2	0.12	3	0.13
35157	5	0.07	1	2	0.13	4	0.08
35165	5	0.05	2	0.03	2	0.03	5	0.02
35172	4	0.04	1	4	0.07	3	0.09
35190	4	0.06	2	0.11	2	0.08	3	0.03
35201	4	0.07	1	2	0.04	5	0.10
35204	4	0.10	1	1	...
35216	5	0.04	1	...	2	0.11	5	0.06	2	0.04
35228	5	0.09	1	...	1	3	0.05
35230	4	0.11	2	0.01	3	0.05	4	0.01
35235	5	0.04	3	0.02	3	0.01	3	0.07
35240	5	0.04	1	...	3	0.01	3	0.16
35248	5	0.08	1	...	2	0.16	3	0.02	2	0.01
35260	4	0.05	1	...	2	0.01	2	0.15
35261	5	0.05	1	...	1	...	2	0.01	5	0.05
36028	3	0.09	1	...	4	0.16	1	...
36036	5	0.04	2	0.02	4	0.02	3	0.01
36048	3	0.06	1	...	2	0.06	3	0.11
36059	3	0.02	1	...	2	0.04	3	0.14
36061	5	0.03	1	...	1	...	3	0.05	2	0.01
36087	4	0.09	1	...	2	0.06	3	0.08
36106	3	0.09	2	0.06	2	0.06	2	0.02
36110	5	0.06	3	0.10
36113	2	0.20	1	...	2	0.09	2	0.08
36134	5	0.07	1	...	1	...	2	0.01	4	0.13
36156	5	0.06	2	0.01	3	0.02	2	0.08
36179	4	0.02	2	0.03	5	0.11
36182	5	0.04	1	...	1	...	4	0.04	4	0.08
36191	4	0.06	1	2	0.02	3	0.13
36206	5	0.03	1	...	4	0.14	3	0.05
36228	5	0.05	2	0.01	2	0.06	6	0.05	4	0.03
36239	5	0.04	1	...	1	...	2	0.05	4	0.06
36259	4	0.05	2	0.14	2	0.01	2	0.04
36260	3	0.06	1	...	1	...	1	...
36280	5	0.05	1	...	1	...	3	0.05	1	...
36282	4	0.03	1	...	2	0.03	3	0.12	4	0.02
37022	3	0.10	2	0.02	1	...	2	0.06
37024	2	0.08	1	...	1	...	3	0.14	1	...
37051	5	0.06	1	...	1	...	1	...
37052	4	0.08	1	...	1	...	2	0.01	4	0.08
37055	5	0.08	1	...	1	...	2	0.01	2	0.05
37062	3	0.12	1	...	1	...	2	0.14	2	0.21
37071	3	0.06	1	...	2	0.06
37082	4	0.08	1	...	1	...	2	0.17
37087	2	0.06	2	0.19	2	0.01	4	0.03

Table 6b—Continued

Star	N-Ca	σ/\sqrt{N}	N-ScI	σ/\sqrt{N}	N-ScII	σ/\sqrt{N}	N-Ti	σ/\sqrt{N}	N-Ni	σ/\sqrt{N}
37094	5	0.02	1	...	2	0.04	2	0.02
37105	5	0.09	1	...	2	0.07	3	0.04
37110	5	0.07	1	2	0.13	5	0.08
37119	5	0.02	2	0.13	5	0.05	5	0.04
37136	4	0.05	1	...	2	0.14	1	...
37139	5	0.04	2	0.13	4	0.04	5	0.07
37143	5	0.05	1	...	2	0.06	3	0.03
37147	5	0.07	1	...	1	...	4	0.03	3	0.12
37157	2	0.14	1	...	1	...	3	0.09	2	0.18
37169	3	0.08	1	...	1	...	4	0.06
37179	4	0.16	1	...	3	0.28	4	0.08
37184	5	0.08	1	...	1	...	3	0.10	2	0.04
37196	5	0.06	1	...	2	0.01	2	0.02
37198	5	0.08	1	...	1	...	2	0.22	4	0.04
37215	4	0.06	1	...	1	...	1	...
37232	5	0.04	2	0.04	5	0.03	4	0.07
37247	5	0.08	1	...	1	...	2	0.00	3	0.03
37253	5	0.04	2	0.07	4	0.07	5	0.04
37271	5	0.03	1	...	1	...	5	0.05	5	0.08
37275	5	0.08	1	...	4	0.02	4	0.04
37318	4	0.10	1	...	1	...	4	0.03	3	0.15
37322	4	0.07	1	1	...
37329	5	0.07	2	0.04	2	0.01	4	0.06
38011	5	0.06	1	...	1	...	4	0.08	2	0.00
38018	5	0.07	1	...	1	...	2	0.04	4	0.10
38049	5	0.03	1	...	2	0.09	5	0.04	4	0.02
38052	5	0.01	2	0.03	2	0.16	5	0.03	4	0.06
38056	5	0.04	2	0.08	2	0.03	1	...
38057	4	0.06	1	3	0.06	2	0.08
38059	5	0.06	1	...	1	...	3	0.13	3	0.03
38061	1	1	...	1	...	2	0.13
38096	3	0.06	1	...	1	...	3	0.10
38097	5	0.07	2	0.15	2	0.13	4	0.12	5	0.04
38105	5	0.07	2	0.02	2	0.08	2	0.06
38112	5	0.04	1	...	1	...	5	0.06	5	0.13
38115	5	0.01	1	...	1	...	4	0.07	2	0.04
38129	5	0.04	2	0.11	3	0.05	4	0.10
38147	5	0.04	1	...	4	0.13	2	0.03
38149	5	0.04	1	...	1	...	3	0.10	5	0.06
38156	5	0.04	1	...	3	0.02	5	0.06
38166	5	0.05	2	0.16	2	0.01	3	0.08
38168	5	0.06	1	...	4	0.07	2	0.04
38169	5	0.04	2	0.11	2	0.04	4	0.05	4	0.03
38195	5	0.04	1	...	2	0.14	6	0.02	4	0.05
38198	5	0.08	1	...	1	...	3	0.10	5	0.09
38204	5	0.06	1	...	1	...	2	0.01	5	0.07

Table 6b—Continued

Star	N-Ca	σ/\sqrt{N}	N-ScI	σ/\sqrt{N}	N-ScII	σ/\sqrt{N}	N-Ti	σ/\sqrt{N}	N-Ni	σ/\sqrt{N}
38206	4	0.06	1	...	2	0.01	2	0.06
38215	5	0.06	1	5	0.08	5	0.08
38223	5	0.02	1	...	1	...	4	0.18	5	0.04
38225	5	0.08	1	...	1	...	2	0.04	2	0.04
38226	5	0.09	1	...	2	0.08	3	0.08
38232	5	0.05	2	0.16	2	0.10	6	0.07	5	0.05
38255	5	0.05	1	...	1	...	2	0.14	4	0.11
38262	5	0.07	2	0.14	2	0.11	3	0.03	2	0.06
38276	5	0.04	1	...	2	0.01	4	0.06	4	0.06
38303	5	0.07	1	...	1	...	2	0.05	3	0.07
38319	5	0.07	1	...	1	...	3	0.05	3	0.14
38323	5	0.06	1	...	1	...	4	0.05	3	0.09
38330	5	0.05	1	...	1	...	4	0.09	2	0.10
39026	5	0.01	1	...	1	...	4	0.05	4	0.05
39033	4	0.08	2	0.13	3	0.02
39034	5	0.08	2	0.04	2	0.07	2	0.10
39037	5	0.06	1	...	2	0.17	4	0.04	5	0.05
39043	5	0.08	1	...	2	0.02	3	0.00
39044	5	0.03	1	...	2	0.01	2	0.03	2	0.04
39048	4	0.09	1	2	0.12	1	...
39056	5	0.07	1	...	2	0.08	3	0.01
39063	2	0.04	1	...	1	...	2	0.05
39067	4	0.05	1	...	1	...	5	0.06	4	0.08
39086	5	0.05	1	...	1	...	4	0.06	5	0.04
39088	4	0.06	1	...	2	0.01	3	0.09	3	0.08
39102	4	0.02	2	0.04	2	0.01	1	...
39119	5	0.05	2	0.12	2	0.01	1	...
39123	5	0.08	2	0.01	1	...	1	...
39129	4	0.03	1	...	1	...	2	0.02	4	0.07
39141	5	0.02	1	...	2	0.07	3	0.03	5	0.04
39149	5	0.08	1	3	0.06	4	0.11
39165	5	0.06	2	0.09	2	0.05	3	0.12	4	0.15
39186	5	0.07	2	0.07	2	0.00	1	...
39187	5	0.04	1	...	3	0.05	2	0.03
39198	5	0.03	1	...	2	0.14	4	0.08	5	0.07
39204	5	0.05	1	...	2	0.07	5	0.05
39215	5	0.06	2	0.14	2	0.03	1	...
39216	5	0.03	1	...	2	0.01	2	0.04
39225	4	0.05	1	...	2	0.04	3	0.06
39235	5	0.06	1	...	1	...	3	0.08	2	0.10
39245	4	0.02	2	0.25	2	0.01	4	0.05	5	0.04
39257	5	0.05	1	...	1	...	4	0.10	5	0.07
39259	5	0.05	1	...	2	0.16	3	0.01	4	0.07
39284	5	0.05	2	0.11	5	0.07	4	0.07
39289	5	0.07	1	...	2	0.02	3	0.06
39298	5	0.13	1	...	2	0.04	1	...

Table 6b—Continued

Star	N-Ca	σ/\sqrt{N}	N-ScI	σ/\sqrt{N}	N-ScII	σ/\sqrt{N}	N-Ti	σ/\sqrt{N}	N-Ni	σ/\sqrt{N}
39301	3	0.01	1	...	2	0.08	4	0.04
39306	5	0.04	1	...	2	0.07	2	0.03	4	0.02
39325	5	0.07	1	4	0.07	5	0.10
39329	3	0.05	1	...	1	...	4	0.08
39345	5	0.08	2	0.06	1	...	3	0.05	2	0.16
39346	4	0.04	1	...	2	0.06	5	0.07	5	0.07
39352	5	0.04	1	...	1	...	4	0.05	4	0.06
39384	5	0.08	1	...	4	0.14	1	...
39392	4	0.04	1	4	0.07	5	0.04
39401	4	0.03	1	...	1	...	3	0.04	3	0.06
39921	5	0.04	1	...	1	...	3	0.03	3	0.10
40016	5	0.05	1	...	4	0.05	5	0.03
40031	5	0.04	2	0.17	2	0.05	2	0.01
40041	5	0.11	2	0.12	3	0.12
40108	5	0.11	1	...	4	0.07
40123	4	0.01	1	...	2	0.15	5	0.07	4	0.07
40135	5	0.04	1	3	0.09	5	0.04
40139	5	0.03	2	0.03	1	...	5	0.04	5	0.05
40162	5	0.08	1	...	3	0.02	4	0.03
40166	5	0.05	1	...	2	0.16	4	0.08	3	0.08
40168	5	0.06	1	...	2	0.03	2	0.06	4	0.06
40170	4	0.04	2	0.11	3	0.12	2	0.00
40207	5	0.10	1	...	2	0.11	4	0.08	4	0.10
40210	2	0.18	1	...	4	0.14	1	...
40216	5	0.04	2	0.03	2	0.12	4	0.05	4	0.02
40220	5	0.09	2	0.12	2	0.04	2	0.16
40232	5	0.09	1	...	1	...	3	0.06	5	0.15
40235	5	0.05	1	...	1	...	4	0.08	2	0.01
40237	5	0.10	1	...	1	...	2	0.02	4	0.07
40275	5	0.05	1	...	2	0.01	5	0.06
40291	5	0.07	1	...	2	0.02	3	0.13
40318	4	0.05	1	...	1	...	4	0.11	3	0.08
40339	5	0.08	1	...	1	...	4	0.07	5	0.07
40349	5	0.04	1	...	2	0.13	3	0.01	3	0.09
40358	4	0.07	1	...	1	...	2	0.06	3	0.06
40361	2	0.08	2	0.02	2	0.08	2	0.04
40371	5	0.05	1	...	1	...	4	0.06	4	0.08
40372	5	0.04	2	0.04	3	0.05	4	0.03
40373	3	0.05	1	...	2	0.17	3	0.08	2	0.06
40409	5	0.06	1	...	1	...
40420	2	0.17	1	...	1	...
40424	4	0.07	2	0.04	2	0.13	2	0.05
40472	5	0.05	2	0.03	2	0.08	6	0.03	5	0.05
40479	5	0.06	1	...	2	0.13	2	0.04	2	0.09
41015	4	0.08	1	...	1	...	1	...
41025	3	0.10	1	...	2	0.07	2	0.06

Table 6b—Continued

Star	N-Ca	σ/\sqrt{N}	N-ScI	σ/\sqrt{N}	N-ScII	σ/\sqrt{N}	N-Ti	σ/\sqrt{N}	N-Ni	σ/\sqrt{N}
41033	5	0.11	1	...	1	...	2	0.14	4	0.13
41034	5	0.05	1	...	3	0.04
41035	4	0.04	2	0.13	2	0.18	5	0.07	4	0.03
41039	5	0.06	2	0.05	4	0.01	4	0.10
41060	5	0.06	2	0.10	2	0.08	5	0.04	5	0.08
41061	5	0.03	2	0.12	2	0.18	3	0.10	1	...
41063	5	0.07	1	...	1	...	4	0.05	2	0.08
41164	5	0.06	2	0.11	3	0.04	3	0.13
41186	5	0.05	2	0.08	3	0.09	4	0.09
41201	1	2	0.13	1	...	2	0.05
41230	5	0.05	1	2	0.04	3	0.05
41232	5	0.16	2	0.23
41241	5	0.03	1	...	2	0.20	5	0.06	1	...
41243	5	0.04	2	0.01	2	0.02	3	0.08
41246	5	0.02	2	0.08	2	0.01	4	0.03
41258	5	0.09	1	...	1
41259	5	0.06	2	0.08	2	0.13	3	0.07	3	0.10
41262	2	0.14
41310	3	0.08	1	...	4	0.16	2	0.17
41312	3	0.07	1	...	2	0.11
41313	4	0.05	2	0.18	4	0.05	4	0.12
41321	5	0.06	1	...	2	0.01	3	0.02
41348	5	0.03	1	...	1	...	2	0.00	1	...
41366	5	0.04	2	0.12	1	...	3	0.05
41375	5	0.06	2	0.23	2	0.01	1	...
41380	5	0.04	1	...	1	...	3	0.08	2	0.29
41387	5	0.08	1	...	1	...	2	0.01	2	0.08
41389	5	0.09	1	...	3	0.13	2	0.13
41402	4	0.06	1	...	2	0.01	3	0.08
41435	5	0.04	1	...	1	...	5	0.05	3	0.11
41455	5	0.06	1	...	1	...	3	0.09	4	0.08
41476	3	0.09	1	...	1	...	3	0.05	3	0.12
41494	5	0.04	1	...	3	0.05	2	0.04
42012	5	0.04	1	...	3	0.12	4	0.08
42015	5	0.04	1	...	2	0.04	3	0.03	5	0.05
42023	5	0.04	2	0.10	4	0.09	4	0.08
42039	5	0.04	1	...	3	0.01	1	...
42049	5	0.05	3	0.08	5	0.04
42054	5	0.03	2	0.06	1	...	4	0.04	5	0.04
42056	3	0.14	1	...	1	...
42079	5	0.05	1	...	1	...	4	0.07	5	0.08
42084	5	0.05	1	...	2	0.05	3	0.12	5	0.07
42106	5	0.07	1	...	2	0.16	2	0.07
42114	5	0.04	1	3	0.02	5	0.06
42120	5	0.07	1	...	1	...	3	0.07	4	0.08
42134	4	0.06	1	...	1	...	3	0.02

Table 6b—Continued

Star	N-Ca	σ/\sqrt{N}	N-ScI	σ/\sqrt{N}	N-ScII	σ/\sqrt{N}	N-Ti	σ/\sqrt{N}	N-Ni	σ/\sqrt{N}
42161	5	0.03	1	...	2	0.01	4	0.01	3	0.06
42162	4	0.01	1	...	1	...	3	0.11	5	0.06
42169	4	0.07	1	...	1	...	2	0.12	4	0.10
42174	4	0.07	1	...	1	...	3	0.12	1	...
42175	5	0.04	1	...	1	...	4	0.09	4	0.04
42179	5	0.04	2	0.11	2	0.01	5	0.02
42182	2	0.35	1	...	2	0.35	3	0.09
42187	5	0.07	1	...	1	...	2	0.04	4	0.09
42196	4	0.06	1	...	2	0.07	2	0.08
42198	5	0.11	1	3	0.05
42205	5	0.06	1	...	1	...	3	0.18	4	0.06
42221	5	0.08	1	...	1	...	2	0.01	4	0.09
42260	4	0.11	1	...	1	...	2	0.10	4	0.09
42271	5	0.06	1	...	1	...	2	0.03	2	0.11
42302	5	0.08	2	0.02	1	...	4	0.06	2	0.04
42303	5	0.04	1	...	1	...	4	0.04	5	0.04
42309	5	0.11	1	...	1	...	3	0.09	2	0.01
42339	4	0.05	1	...	1	...	2	0.13	3	0.12
42345	4	0.08	1	...	2	0.01	3	0.10
42361	5	0.08	2	0.11	2	0.02	3	0.10
42384	5	0.08	1	...	1	...	5	0.04	5	0.06
42385	5	0.06	1	...	3	0.08	2	0.07
42407	4	0.08	1	...	1	...	3	0.07
42415	5	0.02	1	3	0.08	5	0.03
42438	5	0.05	1	...	1	...	2	0.04	4	0.09
42457	5	0.04	1	...	3	0.12
42461	5	0.04	2	0.06	2	0.11	4	0.04	5	0.05
42473	5	0.04	1	...	2	0.18	4	0.05	5	0.08
42497	5	0.04	1	...	2	0.08	3	0.04	1	...
42501	4	0.06	2	0.13	2	0.06	3	0.08	4	0.04
42503	5	0.10	1	...	2	0.01	3	0.12
42508	5	0.06	1	...	2	0.09	3	0.13	3	0.09
43010	5	0.05	1	...	1	...	2	0.01	3	0.08
43024	4	0.02	1	2	0.04	5	0.04
43036	4	0.08	2	0.01	2	0.01	2	0.04
43040	5	0.07	1	...	2	0.01	2	0.12
43060	3	0.05	2	0.04	2	0.06	2	0.04
43061	4	0.09	1	3	0.09	5	0.05
43064	5	0.04	2	0.04	1	...	3	0.03	4	0.05
43068	5	0.12	1	...	1	...	2	0.03	5	0.06
43071	4	0.02	1	...	1	...	2	0.05	3	0.01
43079	5	0.07	2	0.21	2	0.05
43087	5	0.05	1	...	1	...	2	0.05	2	0.01
43091	5	0.08	1	5	0.06	5	0.08
43095	5	0.04	2	0.02	4	0.13	3	0.04
43096	5	0.04	2	0.06	2	0.13	5	0.04	4	0.04

Table 6b—Continued

Star	N-Ca	σ/\sqrt{N}	N-ScI	σ/\sqrt{N}	N-ScII	σ/\sqrt{N}	N-Ti	σ/\sqrt{N}	N-Ni	σ/\sqrt{N}
43099	5	0.06	1	...	1	...	3	0.08	5	0.08
43101	5	0.04	1	...	3	0.14	4	0.07
43104	2	0.03	1	...	1	...	3	0.06	4	0.05
43108	3	0.16	1	...	2	0.25	2	0.05
43111	4	0.11	1	...	1	...
43134	4	0.09	1	...	1	...	1	...
43139	3	0.06	2	0.18	2	0.19	1	...
43158	5	0.02	2	0.04	3	0.11	5	0.03
43189	5	0.07	1	4	0.05	5	0.07
43216	5	0.07	1	...	2	0.06	4	0.08	4	0.07
43233	4	0.08	2	0.11	2	0.01
43241	5	0.04	1	3	0.12	3	0.03
43258	5	0.04	1	...	2	0.04	4	0.09
43261	5	0.03	1	...	1	...	5	0.02	5	0.02
43278	3	0.09	1	...	1
43326	5	0.06	1	4	0.12	5	0.12
43330	5	0.04	1	...	2	0.08	2	0.04	2	0.06
43351	5	0.06	1	3	0.08	4	0.08
43367	5	0.03	1	...	1	...	5	0.04	5	0.02
43389	5	0.08	2	0.11	1	...	4	0.06	5	0.03
43397	3	0.12	2	0.09
43399	4	0.08	1	...	1	...	2	0.02	1	...
43412	5	0.04	1	...	3	0.05	4	0.09
43433	5	0.05	1	...	1	...	2	0.00	4	0.12
43446	3	0.12	1	...	1	...	1	...	2	0.27
43458	5	0.04	2	0.13	2	0.08	4	0.01
43463	4	0.14	1	...	2	0.02	3	0.10
43475	4	0.04	1	...	1	...	3	0.10
43485	5	0.03	2	0.01	2	0.01	4	0.02
43539	5	0.05	1	...	1	...	2	0.03	3	0.03
44026	5	0.05	1	3	0.06	4	0.12
44042	5	0.05	1	...	2	0.02	2	0.00	5	0.05
44056	5	0.04	2	0.25	2	0.04	1	...
44065	5	0.05	1	...	2	0.04	4	0.08
44067	3	0.04	1	...	2	0.03	2	0.01	1	...
44115	5	0.05	1	...	2	0.08	4	0.05	2	0.01
44120	5	0.07	1	...	1	...	1	...
44143	5	0.07	1	...	2	0.05	4	0.04	4	0.02
44163	5	0.09	1	...	1	...	3	0.02	4	0.04
44188	4	0.06	2	0.01	1	...	3	0.11	3	0.08
44189	4	0.05	1	3	0.12	4	0.12
44198	5	0.06	2	0.06	2	0.01	4	0.04
44219	5	0.04	1	...	2	0.13	4	0.12	2	0.16
44231	5	0.03	1	...	2	0.07	2	0.04	3	0.15
44253	4	0.07	1	...	1	...	3	0.03	5	0.04
44271	2	0.08	1

Table 6b—Continued

Star	N-Ca	σ/\sqrt{N}	N-ScI	σ/\sqrt{N}	N-ScII	σ/\sqrt{N}	N-Ti	σ/\sqrt{N}	N-Ni	σ/\sqrt{N}
44277	5	0.14	1	...	2	0.10	3	0.02	1	...
44304	4	0.06	1	...	1	...	3	0.02	1	...
44313	5	0.05	1	...	1	...	4	0.10	3	0.10
44327	5	0.06	2	0.04	2	0.01	4	0.03
44337	5	0.05	1	...	5	0.08	2	0.01
44343	5	0.05	1	...	2	0.04	3	0.03
44380	2	0.08	1	2	0.23
44424	4	0.11	1	...	2	0.01	1	...
44426	5	0.06	1	...	1	...	2	0.01	4	0.06
44435	5	0.04	1	...	3	0.03	4	0.05
44446	5	0.05	1	...	1	...	4	0.01
44449	2	0.02	1	1	...
44462	4	0.07	2	0.30	2	0.01	3	0.09	5	0.05
44488	2	0.19	1	...	2	0.11
44493	4	0.08	2	0.03	2	0.07	3	0.05
45082	5	0.06	2	0.17	3	0.09	2	0.04
45089	4	0.05	1	...	2	0.01	5	0.03
45092	5	0.06	1	4	0.09	2	0.02
45093	5	0.10	1	...	2	0.02	2	0.01
45126	5	0.07	2	0.03	3	0.13	1	...
45177	5	0.04	1	...	2	0.06	5	0.04	5	0.04
45180	5	0.06	2	0.05	2	0.01	5	0.05
45206	4	0.05	1	...	1	...	2	0.03
45215	4	0.03	1	...	1	...	5	0.13	5	0.04
45232	5	0.06	2	0.08	2	0.06	4	0.03	4	0.03
45235	2	0.12	1	...	2	0.14
45238	5	0.03	1	...	2	0.13	5	0.05	4	0.02
45240	2	0.18	1	...	1	...	1
45246	5	0.07	1	4	0.03	4	0.04
45249	5	0.09	2	0.05	2	0.15	5	0.06	5	0.05
45272	5	0.05	2	0.11	5	0.05	5	0.08
45285	5	0.05	1	2	0.07	1	...
45292	5	0.01	1	...	1	...	2	0.01	2	0.00
45309	5	0.05	2	0.06	1	...	2	0.20
45322	4	0.05	1	...	6	0.05	2	0.03
45326	5	0.05	1	...	2	0.00	5	0.04
45342	4	0.05	1	3	0.08	1	...
45343	5	0.05	1	...	2	0.09	3	0.06	3	0.09
45359	5	0.04	1	...	2	0.01	2	0.02
45373	4	0.03	1	...	1	...	4	0.04	5	0.04
45377	5	0.06	2	0.14	2	0.03	5	0.04
45389	5	0.04	2	0.01	3	0.05	5	0.03
45410	5	0.08	1	...	2	0.02	2	0.01
45418	4	0.09	1	...	3	0.14	4	0.06
45453	5	0.04	1	...	2	0.02	5	0.08
45454	4	0.13	2	0.06	2	0.18

Table 6b—Continued

Star	N-Ca	σ/\sqrt{N}	N-ScI	σ/\sqrt{N}	N-ScII	σ/\sqrt{N}	N-Ti	σ/\sqrt{N}	N-Ni	σ/\sqrt{N}
45463	5	0.03	1	...	1	...	5	0.03	3	0.04
45482	5	0.08	1	...	3	0.08	4	0.05
46024	5	0.06	2	0.04	2	0.22	4	0.03	4	0.10
46055	5	0.09	1	...	2	0.01	3	0.03
46062	5	0.04	2	0.16	5	0.03	2	0.06
46073	4	0.03	1	1	...	3	0.05
46090	4	0.09	1	...	1	...	3	0.08
46092	5	0.07	1	4	0.03	4	0.08
46121	3	0.08	1	...	1	...	2	0.05	4	0.05
46140	5	0.05	1	...	5	0.09	5	0.03
46150	4	0.05	2	0.23	1	...	5	0.10	5	0.08
46166	5	0.05	1	...	3	0.06	1	...
46172	5	0.03	1	3	0.14	3	0.08
46194	5	0.04	2	0.01	5	0.06	4	0.10
46196	3	0.12	1	1	...
46223	5	0.04	1	2	0.06	4	0.13
46248	5	0.03	2	0.15	2	0.08	5	0.08	5	0.05
46279	2	0.21	1	...	2	0.04	1	...
46289	5	0.04	2	0.10	5	0.11	2	0.08
46301	5	0.06	1	...	2	0.01	1	...
46318	5	0.06	1	...	2	0.02	3	0.05
46323	5	0.06	1	...	4	0.06	1	...
46325	4	0.05	1	...	1	...	3	0.09
46348	4	0.07	2	0.01	2	0.03	1	...
46350	5	0.06	1	...	4	0.03	5	0.08
46381	5	0.06	1	...	4	0.06	4	0.11
46388	4	0.03	1	...	1	...	4	0.10
46391	5	0.07	1	...	1	...	3	0.04	5	0.04
46398	4	0.09	1
46405	4	0.05	2	0.09	2	0.15
46438	4	0.07	1	...	1
47012	5	0.04	2	0.05	5	0.05	5	0.01
47039	5	0.07	2	0.09	1	...	2	0.14
47055	5	0.03	1	...	2	0.06	2	0.12
47074	4	0.11	1	...	2	0.12	2	0.03
47096	5	0.08	1	1	...	5	0.08
47107	5	0.04	1	...	3	0.02	5	0.03
47110	5	0.02	1	...	3	0.03	4	0.08
47146	5	0.10	1	...	2	0.09	4	0.03	5	0.04
47150	5	0.06	1	...	2	0.23	3	0.09	4	0.04
47151	5	0.07	2	0.05	1
47153	4	0.06	1	...	4	0.16	4	0.11
47176	5	0.02	1	...	2	0.08	2	0.05	3	0.03
47186	5	0.07	1	...	1	...	3	0.08	4	0.07
47187	4	0.04	1	3	0.09	4	0.05
47199	5	0.04	2	0.08	2	0.03	5	0.04	3	0.03

Table 6b—Continued

Star	N-Ca	σ/\sqrt{N}	N-ScI	σ/\sqrt{N}	N-ScII	σ/\sqrt{N}	N-Ti	σ/\sqrt{N}	N-Ni	σ/\sqrt{N}
47269	5	0.04	1	...	2	0.16	2	0.06	3	0.05
47299	5	0.10	1	...	2	0.00
47307	4	0.06	1	...	4	0.02	3	0.14
47331	2	0.23	1	...
47338	5	0.04	1	...	3	0.03	3	0.04
47339	4	0.02	1	...	2	0.04	2	0.09
47348	5	0.04	1	...	1	...	3	0.08	4	0.04
47354	4	0.05	1	2	0.06	2	0.15
47387	5	0.03	1	...	2	0.08	4	0.07	3	0.05
47399	5	0.06	2	0.23	2	0.02	5	0.13	5	0.05
47400	5	0.05	1	...	1	...	4	0.03	5	0.06
47405	5	0.05	2	0.04	4	0.06	3	0.05
47420	5	0.11	1	...	3	0.06	3	0.08
47443	4	0.08	2	0.04	2	0.01	1	...
47450	5	0.02	2	0.15	2	0.06	3	0.09
48028	5	0.04	1	...	1	...	6	0.04	3	0.03
48036	4	0.10	1	...	1	...	2	0.13	1	...
48049	5	0.04	2	0.05	2	0.16	5	0.06	3	0.02
48060	5	0.05	2	0.11	2	0.12	3	0.08	4	0.06
48067	5	0.04	1	...	1	...	3	0.07	3	0.14
48083	5	0.06	1	...	1	...	2	0.01	2	0.21
48099	4	0.14	3	0.08	3	0.10
48116	3	0.10	1	...	1	...	3	0.07	4	0.10
48120	5	0.06	2	0.12	2	0.20	3	0.05	1	...
48150	5	0.12	1	...	3	0.10	2	0.01
48151	5	0.04	1	...	2	0.01
48186	5	0.05	1	...	2	0.01	2	0.07	1	...
48197	5	0.08	4	0.15	1	...
48221	5	0.04	1	...	2	0.07	3	0.07	3	0.08
48228	5	0.03	2	0.03	3	0.10	2	0.04
48235	5	0.06	2	0.18	2	0.16	5	0.04	5	0.07
48247	5	0.04	1	...	2	0.03	4	0.07
48259	5	0.04	1	...	2	0.01	2	0.01
48281	4	0.09	2	0.04	4	0.11	3	0.09
48305	4	0.09	2	0.28	1	...	3	0.06	2	0.18
48323	4	0.06	1	3	0.06	5	0.05
48367	5	0.04	2	0.10	1	...	5	0.02	4	0.06
48370	5	0.05	1	...	1	...	3	0.04	4	0.10
48392	5	0.03	1	...	2	0.14	4	0.10	4	0.07
48409	3	0.02	1	...	2	0.05	2	0.01	2	0.07
49013	5	0.04	2	0.06	2	0.06	5	0.04	5	0.06
49022	5	0.10	2	0.01	2	0.05	1	...
49037	4	0.15	1	...	3	0.12	1	...
49056	5	0.07	1	3	0.11	5	0.08
49072	4	0.09	1	...	1	...	2	0.03	2	0.11
49088	4	0.05	1	...	2	0.07	3	0.12

Table 6b—Continued

Star	N-Ca	σ/\sqrt{N}	N-ScI	σ/\sqrt{N}	N-ScII	σ/\sqrt{N}	N-Ti	σ/\sqrt{N}	N-Ni	σ/\sqrt{N}
49111	4	0.05	1	5	0.07	2	0.18
49123	5	0.05	2	0.03	4	0.09	1	...
49134	5	0.04	1	...	3	0.05	5	0.03
49148	5	0.06	2	0.16	2	0.14	6	0.02	5	0.07
49177	5	0.09	1	4	0.06	2	0.16
49179	4	0.04	1	...	1	...	2	0.16	2	0.02
49188	3	0.15	1	...	1
49193	5	0.04	1	...	1	...	4	0.08	4	0.02
49205	5	0.03	1	...	2	0.11	2	0.04	3	0.01
49212	4	0.07	1	...	1	...	3	0.07	3	0.18
49238	4	0.04	1	...	5	0.11	4	0.06
49249	5	0.04	1	...	2	0.05	5	0.04	5	0.08
49252	2	0.13	1	...	1	...	1	...	2	0.23
49255	4	0.06	2	0.01	1	...
49293	5	0.03	1	...	1	...	4	0.08	3	0.08
49322	5	0.08	1	...	2	0.01	2	0.01	2	0.05
49333	5	0.06	1	...	2	0.02	1	...
50022	5	0.06	1	...	1	...	2	0.03	2	0.04
50037	5	0.04	1	...	2	0.09	4	0.08
50046	5	0.08	1	...	2	0.04	1	...
50066	4	0.12	1	...	1	...	3	0.08	2	0.01
50078	5	0.05	1	...	1	...	4	0.09	2	0.01
50108	5	0.05	1	...	1	...	2	0.03	5	0.04
50109	5	0.04	1	...	2	0.04	2	0.05
50133	5	0.04	2	0.07	1	...	5	0.06	4	0.03
50163	2	0.06	1	...	1
50167	5	0.05	2	0.14	2	0.00	2	0.02	4	0.09
50172	5	0.03	1	...	4	0.07	4	0.10
50187	5	0.05	2	0.40	2	0.07	2	0.01	5	0.06
50191	4	0.05	1	...	1	...	2	0.05	2	0.16
50193	4	0.02	1	...	1	...	3	0.09	2	0.22
50198	4	0.05	1	...	2	0.00	3	0.07
50218	5	0.04	1	4	0.05	5	0.09
50228	5	0.04	1	...	3	0.13	2	0.02
50245	2	0.09	1	...	1	...	3	0.05	1	...
50253	5	0.03	1	...	1	...	1	...	2	0.08
50259	5	0.05	2	0.23	4	0.11	5	0.06
50267	5	0.06	1	...	3	0.03	4	0.05
50291	4	0.11	2	0.01	1	...	2	0.02	3	0.05
50293	5	0.05	1	...	1	...	5	0.05	4	0.07
50294	4	0.08	1	...	2	0.19	2	0.13
50304	4	0.09	1	...	2	0.16	2	0.05	2	0.06
51021	5	0.08	2	0.15	2	0.00	4	0.02	5	0.04
51024	5	0.03	1	...	1	...	5	0.05	4	0.04
51074	4	0.02	1	3	0.09	3	0.06
51079	5	0.04	1	4	0.12	5	0.07

Table 6b—Continued

Star	N-Ca	σ/\sqrt{N}	N-ScI	σ/\sqrt{N}	N-ScII	σ/\sqrt{N}	N-Ti	σ/\sqrt{N}	N-Ni	σ/\sqrt{N}
51080	5	0.07	1	...	2	0.01	5	0.04	5	0.06
51091	5	0.08	1	...	1	...	2	0.04	4	0.04
51121	5	0.08	1	...	3	0.10	1	...
51132	3	0.07	1	3	0.12	3	0.04
51136	1	2	0.06
51156	5	0.07	1	...	1	...	4	0.12	4	0.04
51254	5	0.03	1	...	2	0.19	5	0.07	5	0.12
51257	5	0.05	1	...	2	0.18	3	0.10
51259	5	0.05	1	...	1	...	2	0.01	2	0.06
52017	5	0.04	2	0.08	2	0.11	6	0.04	4	0.02
52035	4	0.06	1	...	1	...	5	0.11	2	0.06
52039	4	0.02	1	...	1	...	4	0.08
52103	5	0.08	2	0.16	2	0.01	5	0.08	5	0.04
52105	5	0.05	2	0.13	4	0.08	3	0.06
52106	5	0.04	1	...	1	...	2	0.08	2	0.11
52109	5	0.08	1	...	2	0.04	4	0.06
52110	3	0.02	1	...	1
52111	4	0.10	1	...	1	...	3	0.01	4	0.06
52133	4	0.11	1	...	3	0.08	2	0.05
52139	5	0.07	2	0.15	2	0.15	4	0.05	5	0.08
52151	5	0.07	2	0.11	3	0.09	4	0.09
52154	3	0.09	1
52167	5	0.05	1	...	1	...	3	0.06	4	0.07
52180	5	0.02	1	...	2	0.03	2	0.06	2	0.09
52192	4	0.08	1	...	2	0.10	3	0.08
52204	3	0.10	1	1	...
52222	4	0.03	2	0.10	2	0.02	2	0.07
53012	5	0.06	1	...	2	0.02	1	...
53054	5	0.06	2	0.17	1	...	4	0.08	4	0.08
53058	5	0.06	1	...	3	0.10	2	0.19
53067	5	0.06	1	...	2	0.06	4	0.08	4	0.07
53076	4	0.07	2	0.13	2	0.07	5	0.04
53114	5	0.04	1	...	1	...	5	0.07	5	0.04
53119	3	0.10	1	...	1	...
53132	5	0.04	1	...	2	0.04	4	0.05
53178	5	0.07	1	...	2	0.02	4	0.13	5	0.08
53185	5	0.04	2	0.06	2	0.16	5	0.05	5	0.06
53203	5	0.04	1	...	3	0.07	2	0.06
54018	5	0.05	1	...	2	0.07	3	0.08	1	...
54022	4	0.06	1	...	3	0.16	4	0.06
54031	4	0.07	1	...	2	0.10	4	0.13	4	0.04
54064	4	0.10	1	...	2	0.01	2	0.08
54073	2	0.37	1	...	2	0.07	3	0.04
54084	4	0.11	2	0.03	2	0.01	1	...
54095	3	0.07	1	...	2	0.01	3	0.09
54105	5	0.05	1	4	0.16	5	0.11

Table 6b—Continued

Star	N-Ca	σ/\sqrt{N}	N-ScI	σ/\sqrt{N}	N-ScII	σ/\sqrt{N}	N-Ti	σ/\sqrt{N}	N-Ni	σ/\sqrt{N}
54132	5	0.08	1	...	1	...	3	0.12	4	0.02
54148	5	0.03	2	0.06	2	0.09	5	0.04	5	0.06
54154	3	0.05	2	0.14	2	0.31	3	0.08
55028	5	0.06	1	...	1	...	5	0.15	5	0.06
55029	5	0.04	1	4	0.07	4	0.11
55056	5	0.08	1	...	1	...	3	0.13	1	...
55063	5	0.08	1	...	2	0.21	4	0.04	4	0.06
55071	5	0.08	1	3	0.10	4	0.12
55089	5	0.07	1	...	3	0.01	2	0.07
55101	5	0.08	1	5	0.09	4	0.15
55102	5	0.05	1	4	0.12	4	0.06
55111	5	0.04	2	0.07	2	0.04	5	0.04	5	0.04
55114	5	0.08	2	0.18	2	0.15	3	0.04	4	0.04
55121	4	0.04	1	...	1	...	2	0.13	4	0.13
55122	5	0.08	2	0.02	1	...	5	0.04	2	0.21
55131	5	0.09	1	...	3	0.06	3	0.14
55142	5	0.09	1	3	0.20	3	0.09
55149	5	0.06	1	...	1	...	3	0.06	4	0.13
55152	5	0.09	1	...	2	0.21	5	0.07
55165	4	0.07	1	...	1	...	2	0.01	2	0.08
56024	5	0.03	1	...	1	...	3	0.05	4	0.03
56028	4	0.05	1	...	5	0.07	4	0.05
56040	4	0.06	1	...	5	0.09	1	...
56056	4	0.11	2	0.13	2	0.28
56070	5	0.06	1	...	2	0.11	3	0.01	5	0.10
56087	5	0.05	2	0.08	1	...	4	0.04	2	0.10
56106	5	0.04	1	...	1	...	2	0.02	2	0.10
56114	5	0.03	1	...	5	0.09	2	0.04
56118	5	0.09	1	...	1	...	3	0.14	3	0.03
56128	4	0.07	2	0.06	1	...	2	0.01
57010	5	0.04	1	...	2	0.05	6	0.04	5	0.07
57029	4	0.14	1	...	2	0.19	2	0.23
57054	5	0.03	2	0.26	2	0.13	3	0.09	5	0.08
57058	4	0.08	1	...	2	0.01	3	0.13
57067	4	0.07	1	...	3	0.08	2	0.04
57073	5	0.07	1	...	4	0.09	2	0.01
57076	5	0.07	1	...	1	...	3	0.06	5	0.06
57083	5	0.05	2	0.05	2	0.25
57085	5	0.08	2	0.08	2	0.04	2	0.19
57091	4	0.07	1	...	1	...	3	0.16	4	0.08
57114	5	0.07	1	...	2	0.00	1	...	4	0.03
57127	2	0.06	1	...	2	0.22	3	0.03
58043	5	0.03	1	...	1	...	2	0.08	3	0.13
58059	4	0.04	1	...	1	...	3	0.06
58077	2	0.23	1	...	2	0.07	2	0.23
58087	5	0.04	2	0.06	3	0.04	3	0.03

Table 6b—Continued

Star	N-Ca	σ/\sqrt{N}	N-ScI	σ/\sqrt{N}	N-ScII	σ/\sqrt{N}	N-Ti	σ/\sqrt{N}	N-Ni	σ/\sqrt{N}
59016	5	0.12	1	...	2	0.04	1	...
59024	5	0.07	3	0.08	4	0.09
59036	5	0.07	1	...	1	...	4	0.14	4	0.06
59047	5	0.04	1	...	1	...	4	0.09	4	0.05
59085	4	0.05	1	...	1	...	2	0.07	3	0.02
59089	5	0.04	1	...	1	...	5	0.04	2	0.03
59090	5	0.04	1	...	1	...	2	0.00	4	0.03
59094	4	0.01	1	...	2	0.10	3	0.06
60034	5	0.05	3	0.17
60058	4	0.10	1	2	0.20	2	0.13
60059	4	0.09	1	...	2	0.06
60064	4	0.06	1	...	2	0.01	2	0.12
60065	5	0.08	1	...	2	0.02	1	...
60066	5	0.04	1	...	1	...	2	0.06	5	0.08
60067	2	0.16	1	...	1	...	3	0.09
60069	5	0.08	2	0.24	2	0.06	3	0.05
60073	5	0.07	1	2	0.24	3	0.09
60088	5	0.07	1	...	2	0.05	4	0.05
60101	5	0.06	2	0.04	1	...	2	0.08
61015	5	0.05	2	0.11	1	...	4	0.06	5	0.05
61026	4	0.05	1	...	2	0.11
61042	5	0.06	1	...	2	0.08	5	0.05	3	0.07
61046	5	0.07	1	...	2	0.08	1	...
61050	5	0.03	1	...	1	...	5	0.04	3	0.09
61067	4	0.06	1	...	1	...	3	0.13	4	0.10
61070	5	0.07	1	...	1	...	4	0.12	4	0.08
61075	4	0.07	1	...	2	0.09
61085	5	0.06	1	...	1	...	3	0.07	5	0.07
62018	3	0.05	1
62058	5	0.04	1	...	1	...	5	0.04	3	0.08
63021	5	0.06	1	...	5	0.05	4	0.06
63027	5	0.05	2	0.01	3	0.13	3	0.11
63052	5	0.04	1	...	2	0.04	4	0.03
64023	3	0.20	1	...	2	0.25	2	0.17
64049	4	0.08	1	...	1	...	2	0.01	5	0.06
64057	4	0.11	1	...	2	0.01	4	0.05
64064	5	0.06	1	...	1	...	1	...
64067	5	0.04	1	...	1	...	1	...	2	0.13
64074	5	0.02	1	...	1	...	1	...
65042	4	0.05	1	...	1	...
65046	4	0.05	2	0.07	1	...	3	0.04
65057	3	0.12	1	...	2	0.02	4	0.07
66015	5	0.05	1	...	3	0.11	1	...
66026	5	0.05	2	0.04	2	0.01	4	0.09
66047	5	0.06	2	0.07	1	...	5	0.04	5	0.07
66054	5	0.04	1	...	1	...	4	0.06	4	0.10

Table 6b—Continued

Star	N-Ca	σ/\sqrt{N}	N-ScI	σ/\sqrt{N}	N-ScII	σ/\sqrt{N}	N-Ti	σ/\sqrt{N}	N-Ni	σ/\sqrt{N}
67049	2	0.15	1	...	3	0.19
67063	5	0.04	1	...	1	...	5	0.07	3	0.11
68044	3	0.06	2	0.06	2	0.00	1	...
69007	4	0.01	2	0.15	2	0.11	3	0.08
69012	5	0.03	1	...	2	0.04	3	0.03	5	0.02
69027	4	0.05	1	...	1	...	3	0.14	4	0.13
70032	5	0.06	1	...	3	0.07	4	0.06
70035	5	0.04	1	...	1	...	2	0.03	5	0.05
70041	5	0.06	1	...	2	0.03	2	0.13
70049	4	0.06	1	...	1	...	2	0.17	1	...
71013	3	0.17	1	...	1
73025	5	0.07	1	...	1	...	3	0.06	4	0.07
75021	5	0.07	2	0.01	3	0.11	3	0.08
76027	5	0.04	1	...	3	0.03	5	0.03
76038	5	0.06	1	4	0.05	5	0.06
77025	5	0.03	1	...	4	0.07	5	0.05
77030	5	0.05	1	...	1	...	3	0.12	1	...
80026	2	0.02	1	...	2	0.02	2	...
80029	5	0.04	1	...	5	0.05	5	0.09
81018	5	0.04	2	0.11	4	0.03	2	0.05
81019	5	0.05	1	...	1	...	4	0.04	2	0.01
81028	4	0.04	1	...	2	0.02	2	0.10
82015	4	0.05	1	...	2	0.05	2	0.12
82029	3	0.05	1	...	1
85027	5	0.04	1	4	0.03	5	0.04
85031	4	0.05	1	...	2	0.03	2	0.11
89009	5	0.04	2	0.15	2	0.06	2	0.01

Table 7. Abundance Sensitivity to Model Atmosphere Parameters

Ion	$T_{\text{eff}} \pm 100$ (K)	$\log g \pm 0.30$ (cgs)	$[\text{M}/\text{H}] \pm 0.30$ (dex)	$v_t \pm 0.30$ (km s $^{-1}$)
$T_{\text{eff}}=4200, \log g=0.75, [\text{Fe}/\text{H}]=-2.00, v_t=2.00$				
Fe I	± 0.13	∓ 0.01	∓ 0.03	∓ 0.10
Fe II	∓ 0.10	± 0.13	± 0.08	∓ 0.03
O I	± 0.03	± 0.11	± 0.08	∓ 0.03
Na I	± 0.09	∓ 0.04	∓ 0.05	± 0.00
Al I	± 0.07	∓ 0.02	∓ 0.03	∓ 0.02
Si I	∓ 0.01	± 0.02	± 0.02	∓ 0.01
Ca I	± 0.14	∓ 0.05	∓ 0.06	∓ 0.10
Sc I	± 0.26	∓ 0.01	∓ 0.06	± 0.00
Sc II	∓ 0.02	± 0.11	± 0.09	∓ 0.05
Ti I	± 0.20	∓ 0.04	∓ 0.07	∓ 0.03
Ni I	± 0.09	± 0.00	± 0.00	∓ 0.03
La II	± 0.00	± 0.15	± 0.00	± 0.00
Eu II	∓ 0.01	± 0.12	± 0.09	∓ 0.01
$T_{\text{eff}}=4200, \log g=1.00, [\text{Fe}/\text{H}]=-1.50, v_t=2.00$				
Fe I	± 0.09	± 0.02	± 0.02	∓ 0.12
Fe II	∓ 0.13	± 0.12	± 0.13	∓ 0.03
O I	± 0.02	± 0.12	± 0.10	∓ 0.03
Na I	± 0.09	∓ 0.02	∓ 0.03	∓ 0.01
Al I	± 0.10	± 0.00	∓ 0.13	± 0.00
Si I	∓ 0.05	± 0.03	± 0.05	∓ 0.03
Ca I	± 0.13	∓ 0.04	∓ 0.04	∓ 0.14
Sc I	± 0.24	± 0.03	∓ 0.04	∓ 0.03
Sc II	∓ 0.03	± 0.10	± 0.11	∓ 0.05
Ti I	± 0.19	∓ 0.01	∓ 0.05	∓ 0.05
Ni I	± 0.06	± 0.04	± 0.04	∓ 0.04
La II	± 0.00	± 0.10	± 0.08	± 0.00
Eu II	∓ 0.02	± 0.12	± 0.11	± 0.00
$T_{\text{eff}}=4200, \log g=1.25, [\text{Fe}/\text{H}]=-1.00, v_t=2.00$				
Fe I	± 0.03	± 0.09	± 0.07	∓ 0.14

Table 7—Continued

Ion	$T_{\text{eff}} \pm 100$ (K)	$\log g \pm 0.30$ (cgs)	$[\text{M}/\text{H}] \pm 0.30$ (dex)	$v_t \pm 0.30$ (km s $^{-1}$)
Fe II	±0.17	±0.27	±0.18	±0.03
O I	±0.05	±0.18	±0.13	±0.01
Na I	±0.10	±0.02	±0.02	±0.03
Al I	±0.03	±0.03	±0.14	±0.07
Si I	±0.09	±0.13	±0.09	±0.03
Ca I	±0.13	±0.04	±0.01	±0.19
Sc I	±0.23	±0.02	±0.02	±0.13
Sc II	±0.00	±0.17	±0.13	±0.03
Ti I	±0.18	±0.01	±0.02	±0.07
Ni I	±0.02	±0.11	±0.09	±0.05
La II	±0.05	±0.16	±0.13	±0.03
Eu II	±0.01	±0.17	±0.14	±0.02
$T_{\text{eff}}=4200, \log g=1.50, [\text{Fe}/\text{H}]=-0.50, v_t=2.00$				
Fe I	±0.00	±0.07	±0.06	±0.17
Fe II	±0.19	±0.19	±0.12	±0.04
O I	±0.00	±0.10	±0.08	±0.05
Na I	±0.10	±0.03	±0.02	±0.14
Al I	±0.11	±0.05	±0.08	±0.02
Si I	±0.11	±0.08	±0.06	±0.07
Ca I	±0.14	±0.06	±0.03	±0.16
Sc I	±0.21	±0.04	±0.04	±0.17
Sc II	±0.01	±0.14	±0.12	±0.01
Ti I	±0.17	±0.04	±0.01	±0.17
Ni I	±0.01	±0.10	±0.07	±0.10
La II	±0.04	±0.14	±0.11	±0.01
Eu II	±0.01	±0.13	±0.12	±0.00
$T_{\text{eff}}=4600, \log g=1.50, [\text{Fe}/\text{H}]=-2.00, v_t=1.60$				
Fe I	±0.13	±0.02	±0.03	±0.03
Fe II	±0.04	±0.13	±0.06	±0.01
O I	±0.03	±0.12	±0.10	±0.00

Table 7—Continued

Ion	$T_{\text{eff}} \pm 100$ (K)	$\log g \pm 0.30$ (cgs)	$[\text{M}/\text{H}] \pm 0.30$ (dex)	$v_t \pm 0.30$ (km s $^{-1}$)
Na I	± 0.07	∓ 0.02	∓ 0.02	± 0.00
Al I	± 0.06	∓ 0.02	∓ 0.02	± 0.00
Si I	± 0.03	± 0.01	± 0.00	∓ 0.01
Ca I	± 0.10	∓ 0.03	∓ 0.03	∓ 0.06
Sc I	± 0.18	∓ 0.04	∓ 0.05	± 0.00
Sc II	± 0.02	± 0.12	± 0.07	∓ 0.01
Ti I	± 0.14	∓ 0.03	∓ 0.04	∓ 0.01
Ni I	± 0.10	∓ 0.01	∓ 0.02	∓ 0.01
La II	± 0.04	± 0.12	± 0.08	± 0.00
Eu II	± 0.02	± 0.12	± 0.08	± 0.00
$T_{\text{eff}}=4600, \log g=1.75, [\text{Fe}/\text{H}]=-1.50, v_t=1.60$				
Fe I	± 0.13	∓ 0.01	∓ 0.03	∓ 0.08
Fe II	∓ 0.07	± 0.14	± 0.08	∓ 0.03
O I	± 0.01	± 0.13	± 0.13	± 0.00
Na I	± 0.07	∓ 0.02	∓ 0.02	∓ 0.01
Al I	± 0.07	∓ 0.02	∓ 0.02	∓ 0.01
Si I	± 0.02	± 0.03	± 0.02	∓ 0.01
Ca I	± 0.11	∓ 0.03	∓ 0.04	∓ 0.09
Sc I	± 0.19	∓ 0.03	∓ 0.05	± 0.00
Sc II	∓ 0.01	± 0.12	± 0.09	∓ 0.03
Ti I	± 0.15	∓ 0.03	∓ 0.05	∓ 0.03
Ni I	± 0.10	± 0.01	± 0.00	∓ 0.01
La II	± 0.02	± 0.13	± 0.09	∓ 0.03
Eu II	± 0.00	± 0.13	± 0.10	± 0.00
$T_{\text{eff}}=4600, \log g=2.00, [\text{Fe}/\text{H}]=-1.00, v_t=1.60$				
Fe I	± 0.11	± 0.01	± 0.00	∓ 0.13
Fe II	∓ 0.10	± 0.12	± 0.11	∓ 0.05
O I	∓ 0.04	± 0.12	± 0.17	∓ 0.01
Na I	± 0.08	∓ 0.01	∓ 0.02	∓ 0.03
Al I	± 0.06	∓ 0.01	∓ 0.02	∓ 0.02

Table 7—Continued

Ion	$T_{\text{eff}} \pm 100$ (K)	$\log g \pm 0.30$ (cgs)	$[M/H] \pm 0.30$ (dex)	$v_t \pm 0.30$ (km s ⁻¹)
Si I	±0.02	±0.03	±0.05	±0.04
Ca I	±0.12	±0.04	±0.02	±0.13
Sc I	±0.20	±0.00	±0.04	±0.01
Sc II	±0.02	±0.12	±0.11	±0.04
Ti I	±0.16	±0.00	±0.04	±0.05
Ni I	±0.07	±0.04	±0.03	±0.04
La II	±0.01	±0.12	±0.11	±0.05
Eu II	±0.01	±0.13	±0.11	±0.01
$T_{\text{eff}}=4600, \log g=2.25, [Fe/H]=-0.50, v_t=1.60$				
Fe I	±0.08	±0.03	±0.03	±0.17
Fe II	±0.11	±0.17	±0.15	±0.07
O I	±0.04	±0.12	±0.18	±0.01
Na I	±0.09	±0.03	±0.01	±0.10
Al I	±0.07	±0.01	±0.01	±0.04
Si I	±0.05	±0.05	±0.07	±0.07
Ca I	±0.12	±0.04	±0.01	±0.16
Sc I	±0.20	±0.00	±0.05	±0.04
Sc II	±0.02	±0.13	±0.12	±0.06
Ti I	±0.17	±0.00	±0.03	±0.09
Ni I	±0.04	±0.06	±0.05	±0.08
La II	±0.01	±0.13	±0.11	±0.08
Eu II	±0.02	±0.14	±0.12	±0.03

Table 8. Literature References for Figures 15–18

Object	Reference
Thin/Thick Disk	Bensby et al. (2003)
Thin/Thick Disk	Bensby et al. (2005)
Thin/Thick Disk	Edvardsson et al. (1993)
Thin/Thick Disk	Fulbright (2000)
Thin/Thick Disk	Fulbright et al. (2007)
Thin/Thick Disk	Reddy et al. (2003)
Thin/Thick Disk	Reddy et al. (2006)
Thin/Thick Disk	Simmerer et al. (2004)
Halo	Barbuy (1988)
Halo	Fulbright et al. (2000)
Halo	Reddy et al. (2006)
Halo	Simmerer et al. (2004)
Halo	Tomkin et al. (1992)
Bulge	Fulbright et al. (2007)
Bulge	Lecureur et al. (2007)
Bulge	McWilliam & Rich (1994)
Dwarf Galaxies	Sbordone et al. (2007)
Dwarf Galaxies	Shetrone et al. (2001)
Dwarf Galaxies	Shetrone et al. (2003)
Globular Cluster (NGC 104)	Carretta et al. (2009a)
...	Carretta et al. (2009b)
Globular Cluster (NGC 288)	Carretta et al. (2009a)
...	Carretta et al. (2009b)
...	Shetrone & Keane (2000)
Globular Cluster (NGC 362)	Shetrone & Keane (2000)
Globular Cluster (NGC 1904 – M79)	Carretta et al. (2009a)
...	Carretta et al. (2009b)
Globular Cluster (NGC 2808)	Carretta et al. (2009b)
Globular Cluster (NGC 3201)	Carretta et al. (2009a)
...	Carretta et al. (2009b)
Globular Cluster (NGC 4590 – M61)	Carretta et al. (2009a)

Table 8—Continued

Object	Reference
...	Carretta et al. (2009b)
...	Lee et al. (2005b)
Globular Cluster (NGC 5904 – M5)	Carretta et al. (2009a)
...	Carretta et al. (2009b)
...	Ivans et al. (2001)
Globular Cluster (NGC 6093 – M80)	Cavallo et al. (2004)
Globular Cluster (NGC 6121 – M4)	Carretta et al. (2009a)
...	Carretta et al. (2009b)
...	Ivans et al. (1999)
Globular Cluster (NGC 6171 – M107)	Carretta et al. (2009a)
...	Carretta et al. (2009b)
Globular Cluster (NGC 6205 – M13)	Johnson et al. (2005)
...	Sneden et al. (2004)
Globular Cluster (NGC 6218 – M12)	Carretta et al. (2009b)
Globular Cluster (NGC 6254 – M10)	Carretta et al. (2009a)
...	Carretta et al. (2009b)
Globular Cluster (NGC 6388)	Carretta et al. (2009a)
Globular Cluster (NGC 6397)	Carretta et al. (2009a)
...	Carretta et al. (2009b)
Globular Cluster (NGC 6752)	Carretta et al. (2009b)
Globular Cluster (NGC 6809 – M55)	Carretta et al. (2009a)
...	Carretta et al. (2009b)
Globular Cluster (NGC 6838 – M71)	Carretta et al. (2009a)
...	Carretta et al. (2009b)
...	Ramírez & Cohen (2002)
Globular Cluster (NGC 7078 – M15)	Carretta et al. (2009a)
...	Carretta et al. (2009b)
...	Sneden et al. (1997)
Globular Cluster (NGC 7099 – M30)	Carretta et al. (2009a)
...	Carretta et al. (2009b)

